© 2002 ASM International. All Rights Reserved.
Superalloys: A Technical Guide (#06128G)

SUPERALLOYS
A Technical Guide

Second Edition

Matthew J. Donachie
Stephen J. Donachie



The Materials Information Society

Materials Park, OH 44073-0002
www.asminternational.org

© 2002 ASM International. All Rights Reserved.
Superalloys: A Technical Guide (#06128G)
www.asminternational.org

Copyright © 2002
by
ASM International®
All rights reserved

No part of this book may be reproduced, stored in a retrieval system, or transmitted, in any form or by any means, electronic, mechanical, photocopying, recording, or otherwise, without the written permission of the copyright owner.

First printing, March 2002

Great care is taken in the compilation and production of this book, but it should be made clear that NO WARRANTIES, EXPRESS OR IMPLIED, INCLUDING, WITHOUT LIMITATION, WARRANTIES OF MERCHANTABILITY OR FITNESS FOR A PARTICULAR PURPOSE, ARE GIVEN IN CONNECTION WITH THIS PUBLICATION. Although this information is believed to be accurate by ASM, ASM cannot guarantee that favorable results will be obtained from the use of this publication alone. This publication is intended for use by persons having technical skill, at their sole discretion and risk. Since the conditions of product or material use are outside of ASM's control, ASM assumes no liability or obligation in connection with any use of this information. No claim of any kind, whether as to products or information in this publication, and whether or not based on negligence, shall be greater in amount than the purchase price of this product or publication in respect of which damages are claimed. THE REMEDY HEREBY PROVIDED SHALL BE THE EXCLUSIVE AND SOLE REMEDY OF BUYER, AND IN NO EVENT SHALL EITHER PARTY BE LIABLE FOR SPECIAL, INDIRECT OR CONSEQUENTIAL DAMAGES WHETHER OR NOT CAUSED BY OR RESULTING FROM THE NEGLIGENCE OF SUCH PARTY. As with any material, evaluation of the material under end-use conditions prior to specification is essential. Therefore, specific testing under actual conditions is recommended.

Nothing contained in this book shall be construed as a grant of any right of manufacture, sale, use, or reproduction, in connection with any method, process, apparatus, product, composition, or system, whether or not covered by letters patent, copyright, or trademark, and nothing contained in this book shall be construed as a defense against any alleged infringement of letters patent, copyright, or trademark, or as a defense against liability for such infringement.

Comments, criticisms, and suggestions are invited, and should be forwarded to ASM International.

Prepared under the direction of the ASM International Technical Books Committee (2001–2002), Charles A. Parker, Chair

ASM International staff who worked on this project included Veronica Flint, Manager of Book Acquisitions; Bonnie Sanders, Manager of Production; Jill Kinson, Production Project Manager; and Scott Henry, Assistant Director of Reference Publications.

Library of Congress Cataloging-in-Publication Data

Donachie, Matthew J.
Superalloys : a technical guide / M. Donachie, Jr., S. Donachie.—2nd ed.
p. cm.
Includes bibliographical references and index.
ISBN 0-87170-749-7
1. Heat resistant alloys. I. Donachie, S. (Steve) II. Title.
TN700 .D66 2002
620.1′617—dc21
2001055227

ISBN: 0-87170-749-7
SAN: 204-7586

ASM International®
Materials Park, OH 44073-0002
www.asminternational.org

Printed in the United States of America

© 2002 ASM International. All Rights Reserved.
Superalloys: A Technical Guide (#06128G)

Contents

Dedication ..... **vii**

Preface ..... **ix**

Chapter 1: Superalloys for High Temperatures—a Primer **1**
How and When to Use This Chapter 1
Some History 1
What Are Superalloys and What Can You Do to Them? 2
A Short Review of the High-Temperature Strength of Metals 2
Basic Metallurgy of Superalloys 2
Some Superalloy Characteristics and Facts 8
Applications 8
What to Look for in This Book 9

Chapter 2: Selection of Superalloys **11**
Overview 11
Wrought versus Cast Superalloys 15
The Properties of Superalloys 18
Selecting Superalloys 22

Chapter 3: Understanding Superalloy Metallurgy **25**
Groups, Crystal Structures, and Phases 25
Introduction to the Alloy Groups 26
Alloy Elements and Microstructural Effects in Superalloys 29
Microstructure 30
Superalloy Strengthening 32
Function of Processing in Microstructure Development 38

Chapter 4: Melting and Conversion **42**
Solidification of Superalloys 42
Electric Arc Furnace (EAF)/Argon Oxygen Decarburization (AOD) Overview 44
Electric Arc Furnace/Argon Oxygen Decarburization Operation 46
Vacuum Induction Melting (VIM) Overview 50
Vacuum Induction Melting Operation 51
Consumable Remelt Overview 56
Electrode Quality 58
Vacuum Arc Remelting Operation 58
Melt-Related Defects in VAR 64
Electroslag Remelting Operation 66
Melt-Related Defects in ESR 71
Triple-Melted Products 71
Ingot Conversion and Mill Products 72

© 2002 ASM International. All Rights Reserved.
Superalloys: A Technical Guide (#06128G)

Chapter 5: Investment Casting 79
Introduction 79
Investment Casting Practice 80
Investment-Cast Components 84
Investment Casting Problems 85
Superalloy Castings 89

Chapter 6: Forging and Forming 91
Forging and Related Processes 91
Forging Basics 92
Forging Considerations 93
The Forging Process 94
Practical Forging Considerations 101
Forming of Superalloys 106
Practical Forming of Superalloys 108
Formability Processes 110
Some Additional Aspects of Forming: Iron-Nickel and Nickel-Base Superalloys 111
Some Additional Aspects of Forming: Carbide-Hardened Cobalt-Base Superalloys 113
Superplastic Forming/Forging 113

Chapter 7: Powder Metallurgy Processing 117
Powder Superalloys Overview 117
Powder Metallurgy Powder Production Techniques 120
Powder Metallurgy Powder Consolidation Techniques 124
Powder-Based Disk Components 125
Other Powder-Based Superalloy Components 129

Chapter 8: Heat Treating 135
Introduction 135
Heat Treatment Types 137
Heat Treatment Procedures 139
Surface Attack and Contamination 142
Protective Atmospheres 143
Furnace Equipment 144
Practical Heat Treatment of Superalloys 145

Chapter 9: Joining Technology and Practice 149
Introduction 149
Joining the Alloy Classes 150
Joint Integrity and Design 151
Cracking and Soundness of Fusion-Welded Superalloys 152
Preweld and Postweld Heat Treatments for Fusion Welding 160
Welding Specifications 161
Fusion Welding Practice for Superalloys 161
Practical Aspects of Superalloy Fusion Welding 163
Superalloy Fusion Welding Details 165
Superalloy Solid-State Joining 173
Superplastic Forming/Bonding of Components 175
Brazing 175
Brazing Processes 178
Brazing Superalloys 181
Transient Liquid Phase (TLP, Pratt & Whitney) Bonding 183
Some Superalloy Joining Illustrations 186

© 2002 ASM International. All Rights Reserved.
Superalloys: A Technical Guide (#06128G)

Chapter 10: Machining 189
Introduction 189
Overview of Superalloy Machining 189
Specific Machining Operations 194

Chapter 11: Cleaning and Finishing 203
Introduction 203
Metallic Contamination Removal 204
Tarnish Removal 205
Oxide and Scale Removal 205
Finishing Processes 209
Cleaning and Finishing Problems and Solutions 210

Chapter 12: Structure/Property Relationships 211
Introduction 211
General Aspects of Precipitation Hardening in Superalloys 213
Grain-Boundary Carbides in Nickel-Base Superalloys 218
Grain-Boundary Carbides in Other Superalloys 222
Carbide Precipitation—General Hardening 222
IN-718 and the Role of δ Phase in Strengthening 225
Cast and Wrought Superalloy Commentary 226
Wrought Superalloys—Physical, Tensile, and Creep-Rupture Properties 241
Wrought Superalloys—Fatigue and Fracture Properties 250
Cast Superalloys—Physical, Tensile, and Creep-Rupture Properties 258

Chapter 13: Corrosion and Protection of Superalloys 287
Overview 287
Oxidation/Corrosion Testing of Superalloys and Their Coatings 289
Degradation by Gaseous Oxidation or Mixed Gases 294
Hot Corrosion 298
Coatings for Superalloy Protection 309
Diffused Aluminide Coatings 311
Overlay Coatings 316
Thermal Barrier Coatings 319
Coating Comparisons 321

Chapter 14: Failure and Refurbishment 323
Overview 323
Overheating and Microstructural Stability 324
Microstructural Degradation 327
Failures of Superalloy Components 330
Damage Recovery, Refurbishment, and Repair 334

Chapter 15: Superalloys—Retrospect and Future Prospects 339
The 20th Century 339
The 21st Century 345

Appendix A: Source Information 353
Some Superalloy Information/Product Sources 353
Sources for Collected Property Data on Superalloys 354

Appendix B: Some Additional Microstructural Information 357
Introduction 357
Topological Close-Packed Phase Formation 357

Appendix C: Other Sources 365

Subject Index 371

Alloy Index 409

© 2002 ASM International. All Rights Reserved.
Superalloys: A Technical Guide (#06128G)
www.asminternational.org

Dedication

We wish to dedicate this book to our parents, Viola and Matthew Donachie, and our wives, Cynthia and Martha.

Our father was an outstanding self-taught metallurgist. He worked as an electrician in the steel mills in Motherwell, Scotland, for a short time before emigrating to the United States. ''Scottie'' to his friends, ''Steve'' to his family, and ''Matthew'' to later life acquaintances only, was a long time ASMer and introduced us to the art and science of the metallurgy field. Many an hour was spent by us at Steve's labs in Holyoke, MA as we grew through elementary, junior high, and high school. Metallography was an art to be learned at the master's knee. Photography was a passion. All sorts of improvisations were made in the lab to produce the most wondrous metallurgical results. A patient and thorough man, Steve was most responsible for each of us in turn to choose to become a metallurgist and, eventually, to go on to receive our doctorates in the field.

Vi was responsible for our education for a many a year because Steve was away for weeks at a time during the war years of the 1940s. She made certain that we accomplished our studies and encouraged us at all times. Little did we realize the depths of her own talent until we finally were off to college and discovered that Vi had become a painter on canvas, an architect of elegant enamelware, a ceramist, a weaver of some note, and an occasional judge at competitions. She presided over the Holyoke Woman's Club and, at another time, over the Home Information Center. Yes, we remembered that she crocheted and occasionally knitted when we were younger, and her avid reading and breadth of knowledge of current affairs were remarkable. Still, Vi submerged most of her talents until later years to bring all her children to college and beyond. She was quite a remarkable woman!

The patience and character of many women are legendary, and we would like to hold out the examples of our wives, Cynthia (Steve's wife) and Martha (Matt's wife), who have put up with the workaholic nature of our lives for decades. As we have worked at various tasks over the years, they understood and helped to make it easier for us to complete those tasks. Many an evening was spent without our presence, yet they both have encouraged us. It is to them that we also dedicate this book.

With the help and encouragement of our parents and wives, we learned and, hopefully, practiced intellectual investigation and ethical exploration and exposition of knowledge in our chosen areas of metallurgy. We are truly indebted to all for the ways they have influenced our lives.

''How happy is he born and taught
That serveth not another's will
Whose armour is his honest thought
And simple truth his utmost skill!''

Sir H. Wotton in *The Golden Treasury,* F. T. Palgrave, 1861

Steve
Matt

© 2002 ASM International. All Rights Reserved.
Superalloys: A Technical Guide (#06128G)

Preface

The superalloys are, indeed, super. For over 6 decades now, they have provided the most reliable and cost effective means of achieving high operating temperature and stress conditions in aircraft and, now, industrial gas turbines. They have resisted all efforts to reduce their importance and decrease the volume of use. Instead, superalloys continue in wide use in the gas turbine field and may well begin to see even more volume of use in other fields. Superalloys now find application in such diverse fields as oil equipment and biomedical implants. As we move through the first decade of the twenty-first century, superalloys seem secure. To be sure, advances in alloy chemistry are not so easy to achieve any more, but it is being done. Surface modification, partly through the application of coating technology, has extended the useful temperature range of alloys concurrent with the introduction of directional structures and then single crystals of superalloys. Melting technology is ''head and shoulders'' above that of just 15 years ago!

In the late 40s and 50s, there were some conferences and a few published books catering to the developing field of superalloys. At Special Metals, a new generation of processing was dawning as vacuum melting of commercial alloys became a reality. By the mid 60s, the majority of the alloys in use today, except for the directionally solidified ones, existed. The 60s saw the zenith of superalloy development as columnar grain alloys and single crystals were made feasible, and many polycrystalline alloys were brought to commercial reality. Papers on superalloys at the ASM and AIME meetings became fairly routine. At the end of the decade, an important conference was set into being by a dedicated group of metallurgists representing ASM, AIME, and ASME. The first International Conference on Superalloys was not originally intended to be the nucleus of a long running forum, but it did indeed become that. The conference, known as the Seven Springs Conference after the original and only conference location, has continued from 1968 into the twenty-first century. Some other conferences have been initiated and prospered as well. Some conferences cover only specific alloys; e.g. Inconel 718 and related alloys are the subjects of a continuing series of conference.

ASM was an early leader in the presentation of books on high-temperature behavior of metals. In 1979, ASM published *Source Book on Materials at Elevated Temperatures*, in 1984, the *Superalloys Source Book*, and in 1988, the first edition of *Superalloys: A Technical Guide*. Other books on high temperature behavior/properties have been published as well by ASM. The continued success of superalloy technology has encouraged us to undertake a total revision of *Superalloys: A Technical Guide*. The new Second Edition contains much more information than the previous edition and has been modified in layout to better accommodate the technical information provided. The text has been completely revised and expanded from that of the previous edition with many additional figures and new and revised tables.

Virtually all technical aspects of superalloys are covered in this edition. The book is not intended to be exhaustive in every respect, but we believe that the

© 2002 ASM International. All Rights Reserved.
Superalloys: A Technical Guide (#06128G)

reader will find it to be most comprehensive. Chapter 4 in particular is probably the most complete and up-to-date presentation on alloy melting available. Selection of alloys is covered with many suggestions to lead the reader to ask appropriate questions either of her/himself or others in the application or development of superalloys. Furthermore, the relation of properties and microstructure is covered in more detail than in previous books. The Guide has been reviewed for accuracy, but it is possible that errors will have occurred. The writers would appreciate receiving either corrections or suggestions (or both) from readers.

If you are new to the use of superalloys, we would strongly suggest starting with Chapter 1. ''Superalloys for High Temperatures—A Primer'' will suit the needs of readers who want just a brief introduction to superalloys and cannot spend more time on the subject. If you are knowledgeable in metallurgy but have limited knowledge of superalloys, you might wish to start with Chapter 3, ''Understanding Superalloy Metallurgy,'' before proceeding to one of the specialized chapters for more in-depth information. It is most likely that your immediate needs can be satisfied by perusing this book. However, on completing appropriate chapters, you may wish to pursue reading from one of the references listed in Appendix B.

The writers wish to thank all those who contributed to this book, including the many contributors to other ASM books and the *ASM Handbook* series. We extend our special thanks to John Marcin and Joe Goebel who extensively reviewed Chapters 5 and 13 respectively. This book is the product of the authors' experience in superalloys, totaling close to 60 years between them, the authors' personal biases, their technical files, and the extensive resources of ASM International. We particularly would like to thank Veronica Flint, retired from ASM International, for her encouragement to pursue this work and for her perseverance over the several years as the material made its way into electronic and now hard copy form. Veronica Flint and Matt have worked on several past ASM books. It was always been a pleasure to work with Veronica and was especially so on this significant update of an important technical field. The successful publication of this Second Edition is a tribute once more to the dedication of ASM International to providing the greatest access to materials information for the widest possible audience.

MJD
mattd@monad.net
SJD
sdonachie@specialmetals.com
October 2001

ASM International is the society for materials engineers and scientists, a worldwide network dedicated to advancing industry, technology, and applications of metals and materials.

ASM International, Materials Park, Ohio, USA
www.asminternational.org

This publication is copyright © ASM International®. All rights reserved.

Publication title	Product code
Superalloys: A Technical Guide	06128G

To order products from ASM International:

Online Visit www.asminternational.org/bookstore

Telephone 1-800-336-5152 (US) or 1-440-338-5151 (Outside US)

Fax 1-440-338-4634

Mail Customer Service, ASM International
9639 Kinsman Rd, Materials Park, Ohio 44073-0002, USA

Email CustomerService@asminternational.org

In Europe American Technical Publishers Ltd.
27-29 Knowl Piece, Wilbury Way, Hitchin Hertfordshire SG4 0SX, United Kingdom
Telephone: 01462 437933 (account holders), 01462 431525 (credit card)
www.ameritech.co.uk

In Japan Neutrino Inc.
Takahashi Bldg., 44-3 Fuda 1-chome, Chofu-Shi, Tokyo 182 Japan
Telephone: 81 (0) 424 84 5550

Terms of Use. This publication is being made available in PDF format as a benefit to members and customers of ASM International. You may download and print a copy of this publication for your personal use only. Other use and distribution is prohibited without the express written permission of ASM International.

No warranties, express or implied, including, without limitation, warranties of merchantability or fitness for a particular purpose, are given in connection with this publication. Although this information is believed to be accurate by ASM, ASM cannot guarantee that favorable results will be obtained from the use of this publication alone. This publication is intended for use by persons having technical skill, at their sole discretion and risk. Since the conditions of product or material use are outside of ASM's control, ASM assumes no liability or obligation in connection with any use of this information. As with any material, evaluation of the material under end-use conditions prior to specification is essential. Therefore, specific testing under actual conditions is recommended.

Nothing contained in this publication shall be construed as a grant of any right of manufacture, sale, use, or reproduction, in connection with any method, process, apparatus, product, composition, or system, whether or not covered by letters patent, copyright, or trademark, and nothing contained in this publication shall be construed as a defense against any alleged infringement of letters patent, copyright, or trademark, or as a defense against liability for such infringement.

Superalloys: A Technical Guide, Second Edition
Matthew J. Donachie, Stephen J. Donachie, p 1-9
DOI:10.1361/stgs2002p001

Copyright © 2002 ASM International®
All rights reserved.
www.asminternational.org

Chapter 1

Superalloys for High Temperatures—a Primer

How and When to Use This Chapter

It is always difficult to locate concise but precise information on a subject. Executives and managers, particularly in industries using few superalloys, often need just basic information with the least extraneous or amplifying data. Purchasing agents or communications experts need a modest knowledge base to do their jobs more appropriately. The engineer may need more detail but still just a quick refresher about alloy types and design to start. The ability to lay hands on enough practical information to solve problems or answer questions about the superalloys is the basis for this book. The ability to know enough to ask questions and/or delve further into the superalloy field is the basis for this chapter!

The primer provided in this chapter supports such needs as those described previously by providing a concise overview of the major topics considered in the book, starting with a little history and then a statement about the nature of superalloys. This primer introduces the reader simply and directly to the wide variety of topics that must be considered in the application of superalloys. As for the book, whether the user is familiar with basic superalloy metallurgy or is a complete novice, this book provides a single-volume approach to the subject of superalloys. Theory is kept to a minimum, with practical knowledge stressed.

If you are new to the subject, start with this primer; it may be all that you need. If you are somewhat or strongly knowledgeable in the field, check the table of contents and index for valuable insights into what you can find in each succeeding chapter.

Some History

Designers have long had a need for stronger, more corrosion-resistant materials for high-temperature applications. The stainless steels, developed and applied in the second and third decades of the 20th century, served as a starting point for the satisfaction of high-temperature engineering requirements. They soon were found to be limited in their strength capabilities. The metallurgical community responded to increased needs by making what might be termed ‘‘super-alloys’’ of stainless varieties. Of course, it was not long before the hyphen was dropped and the improved iron-base materials became known as superalloys. Concurrently, with the advent of World War II, the gas turbine became a high driver for alloy invention or adaptation. Although patents for aluminum and titanium additions to Nichrome-type alloys were issued in the 1920s, the superalloy industry emerged with the adaption of a cobalt alloy (Vitallium, also known as Haynes Stellite 31) used in dentistry to satisfy high-temperature strength requirements of aircraft engines. Some nickel-chromium alloys (the Inconels and Nimonics), based more or less, one might say, on toaster wire (Nichrome, a nickel-chromium alloy developed in the first decade of the 20th century) were also available. So, the race was on to make superior

metal alloys available for the insatiable thirst of the designer for more high-temperature strength capability. It continues yet!

What Are Superalloys and What Can You Do to Them?

Superalloys are nickel-, iron-nickel-, and cobalt-base alloys generally used at temperatures above about 1000 °F (540 °C). The iron-nickel-base superalloys such as the popular alloy IN-718 are an extension of stainless steel technology and generally are wrought. Cobalt-base and nickel-base superalloys may be wrought or cast, depending on the application/composition involved.

A large number of alloys have been invented and studied; many have been patented. However, the many alloys have been winnowed down over the years; only a few are extensively used. Alloy use is a function of industry (gas turbines, steam turbines, etc.). Not all alloys can be mentioned; examples of older and newer alloys are used to demonstrate the physical metallurgy response of superalloy systems (see Chapters 3 and 12). Figure 1.1 compares stress-rupture behavior of the three alloy classes (iron-nickel-, nickel-, and cobalt-base). A representative list of superalloys and compositions, emphasizing alloys developed in the United States, is given in Tables 1.1 and 1.2.

Appropriate compositions of superalloys can be forged, rolled to sheet, or otherwise produced in a variety of shapes. The more highly alloyed compositions normally are processed as castings. Fabricated structures can be built up by welding or brazing, but many highly alloyed compositions containing a large amount of hardening phase are difficult to weld. Properties can be controlled by adjustments in composition and by processing (including heat treatment), and excellent elevated-temperature strengths are available in finished products.

A Short Review of the High-Temperature Strength of Metals

At ordinary temperatures, the strengths of most metals are measured in terms of short-time properties such as yield strength or ultimate strength. However, when temperatures rise, particularly to temperatures (on an absolute temperature scale) of about 50% of the melting point/range for an alloy, strengths must be reckoned in terms of the time over which they are measured. Thus, if a metal is subjected to a load considerably less than the load (stress) that would break it at room temperature, but is at a high temperature, then the metal will begin to extend with time at load.

This time-dependent extension is called creep and, if allowed to continue long enough, will lead to fracture (or rupture, as it is called). Thus the creep strength of a metal or its rupture strength (technically called creep-rupture strength but more commonly called stress-rupture strength) or both are necessary components of understanding its mechanical behavior just as much as are the customary yield and ultimate strengths. Similarly, the fatigue (cyclic) capability will be reduced. So, to fully validate the capability of a metal alloy, dependent on application temperature and load, it may be necessary to provide yield and ultimate strengths, creep strengths, stress-rupture strengths, and appropriate fatigue strengths. Related mechanical properties such as dynamic modulus, crack growth rates, and fracture toughness also may be required. Appropriate physical properties such as thermal expansion coefficient, density, and so on complete the property list.

Basic Metallurgy of Superalloys

Iron, nickel, and cobalt are generally face-centered cubic (fcc-austenitic) in crystal structure when they are the basis for superalloys. However, the normal room-temperature structures of iron and cobalt elemental metals are not fcc. Both iron and cobalt undergo transformations and become fcc at high temperatures or in the presence of other elements alloyed with iron and cobalt. Nickel, on the other hand, is fcc at all temperatures. In superalloys based on iron and cobalt, the fcc forms of these elements thus are generally stabilized by alloy element additions, particularly nickel, to provide the best properties.

The upper limit of use for superalloys is not restricted by the occurrence of any allotropic phase transformation reactions but is a function of incipient melting temperatures of alloys and dissolution of strengthening

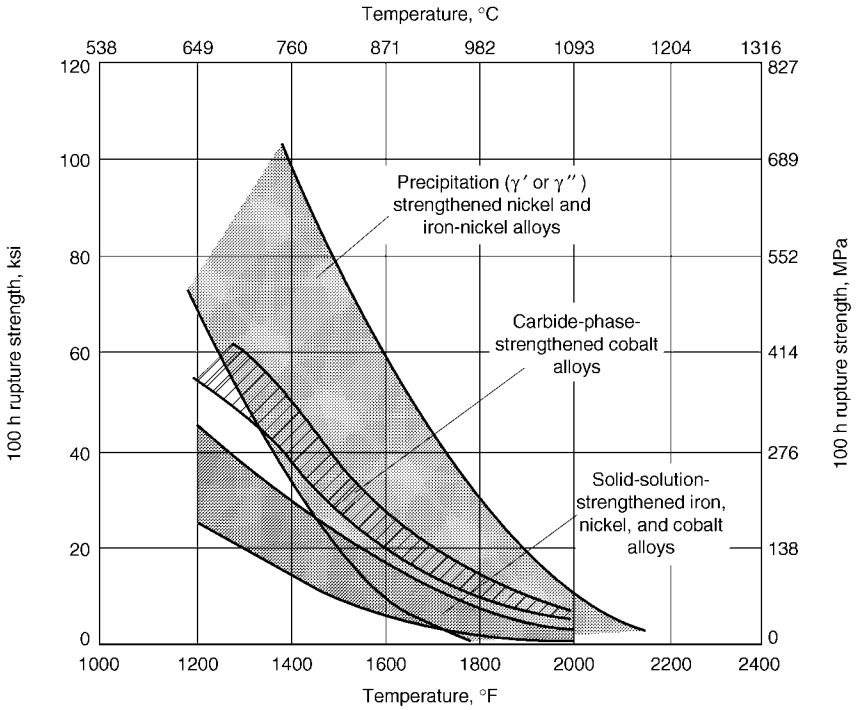


Fig. 1.1 Stress-rupture strengths of superalloys

phases. Incipient melting is the melting that occurs in some part of the alloy that, when solidified, is not at equilibrium composition and thus melts at a lower temperature than that at which it might otherwise melt. All alloys have a melting range, so melting is not at a specific temperature even if there is no nonequilibrium segregation of alloy elements. Superalloys are strengthened not only by the basic nature of the fcc matrix and its chemistry but also by the presence of special strengthening phases, usually precipitates. Working (mechanical deformation, often cold) of a superalloy can also increase strength, but that strength may not endure at high temperatures.

Some tendency toward transformation of the fcc phase to stable lower-temperature phases occasionally occurs in cobalt-base superalloys. The austenitic fcc matrices of superalloys have extended solubility for some alloying additions, excellent ductility, and (iron-nickel- and nickel-base superalloys) favorable characteristics for precipitation of uniquely effective strengthening phases.

Pure iron has a density of 0.284 lb/in.^{3} (7.87 g/cm^3), and pure nickel and cobalt have densities of about 0.322 lb/in.^{3} (8.9 g/cm^3). Iron-nickel-base superalloys have densities of about 0.285 to 0.300 lb/in.^{3} (7.9 to 8.3 g/cm^3); cobalt-base superalloys, about 0.300 to 0.340 lb/in.^{3} (8.3 to 9.4 g/cm^3); and nickel-base superalloys, about 0.282 to 0.322 lb/in.^{3} (7.8 to 8.9 g/cm^3). Superalloy density is influenced by alloying additions: aluminum, titanium, and chromium reduce density, whereas tungsten, rhenium, and tantalum increase it. The corrosion resistance of superalloys depends primarily on the alloying elements added, particularly chromium and aluminum, and the environment experienced.

The melting temperatures of the pure elements are as follows: nickel, 2647 °F (1453 °C); cobalt, 2723 °F (1495 °C); and iron, 2798 °F (1537 °C). Incipient (lowest) melting temperatures and melting ranges of superalloys are functions of composition and prior processing. Generally, incipient melting temperatures are greater for cobalt-base than for nickel- or iron-nickel-base superalloys. Nickel-base superalloys may show incipient melting at temperatures as low as 2200 °F (1204 °C). Advanced nickel-base single-crystal superalloys having limited amounts of

Table 1.1 Nominal compositions of wrought superalloys

Alloy	Composition, %										
	Cr	Ni	Co	Mo	W	Nb	Ti	Al	Fe	C	Other
Solid-solution alloys											
Iron-nickel-base											
Alloy N-155 (Multimet)	21.0	20.0	20.0	3.00	2.5	1.0	. . .	. . .	32.2	0.15	0.15 N, 0.2 La, 0.02 Zr
Haynes 556	22.0	21.0	20.0	3.0	2.5	0.1	. . .	0.3	29.0	0.10	0.50 Ta, 0.02 La, 0.002 Zr
I9-9 DL	19.0	9.0	. . .	1.25	1.25	0.4	0.3	. . .	66.8	0.30	1.10 Mn, 0.60 Si
Incoloy 800	21.0	32.5	. . .	. . .	. . .	. . .	0.38	0.38	45.7	0.05	. . .
Incoloy 800H	21.0	33.0	. . .	. . .	. . .	. . .	. . .	. . .	45.8	0.08	. . .
Incoloy 800HT	21.0	32.5	. . .	. . .	. . .	. . .	0.4	0.4	46.0	0.08	0.8 Mn, 0.5 Si, 0.4 Cu
Incoloy 801	20.5	32.0	. . .	. . .	. . .	. . .	1.13	. . .	46.3	0.05	. . .
Incoloy 802	21.0	32.5	. . .	. . .	. . .	. . .	0.75	0.58	44.8	0.35	. . .
Nickel-base											
Haynes 214	16.0	76.5	. . .	. . .	. . .	. . .	. . .	4.5	3.0	0.03	. . .
Haynes 230	22.0	55.0	5.0 max	2.0	14.0	. . .	. . .	0.35	3.0 max	0.10	0.015 max B, 0.02 La
Inconel 600	15.5	76.0	. . .	. . .	. . .	. . .	. . .	. . .	8.0	0.08	0.25 Cu
Inconel 601	23.0	60.5	. . .	. . .	. . .	. . .	. . .	1.35	14.1	0.05	0.5 Cu
Inconel 617	22.0	55.0	12.5	9.0	. . .	. . .	. . .	1.0	. . .	0.07	. . .
Inconel 625	21.5	61.0	. . .	9.0	. . .	3.6	0.2	0.2	2.5	0.05	. . .
RA333	25.0	45.0	3.0	3.0	3.0	. . .	. . .	. . .	18.0	0.05	. . .
Hastelloy B	1.0 max	63.0	2.5 max	28.0	. . .	. . .	. . .	. . .	5.0	0.05 max	0.03 V
Hastelloy N	7.0	72.0	. . .	16.0	. . .	. . .	0.5 max	. . .	5.0 max	0.06	. . .
Hastelloy S	15.5	67.0	. . .	15.5	. . .	. . .	. . .	0.2	1.0	0.02 max	0.02 La
Hastelloy W	5.0	61.0	2.5 max	24.5	. . .	. . .	. . .	. . .	5.5	0.12 max	0.6 V
Hastelloy X	22.0	49.0	1.5 max	9.0	0.6	. . .	. . .	2.0	15.8	0.15	. . .
Hastelloy C-276	15.5	59.0	. . .	16.0	3.7	. . .	. . .	. . .	5.0	0.02 max	. . .
Haynes HR-120	25.0	37.0	3.0	2.5	2.5	0.7	. . .	0.1	33.0	0.05	0.7 Mn, 0.6 Si, 0.2 N, 0.004 B
Haynes HR-160	28.0	37.0	29.0	. . .	. . .	. . .	. . .	. . .	2.0	0.05	2.75 Si, 0.5 Mn
Nimonic 75	19.5	75.0	. . .	. . .	. . .	. . .	0.4	0.15	2.5	0.12	0.25 max Cu
Nimonic 86	25.0	65.0	. . .	10.0	. . .	. . .	. . .	. . .	. . .	0.05	0.03 Ce, 0.015 Mg
Cobalt-base											
Haynes 25 (L605)	20.0	10.0	50.0	. . .	15.0	. . .	. . .	. . .	3.0	0.10	1.5 Mn
Haynes 188	22.0	22.0	37.0	. . .	14.5	. . .	. . .	. . .	3.0 max	0.10	0.90 La
Alloy S-816	20.0	20.0	42.0	4.0	4.0	4.0	. . .	. . .	4.0	0.38	. . .
MP35-N	20.0	35.0	35.0	10.0	. . .	. . .	. . .	. . .	. . .	. . .	. . .
MP159	19.0	25.0	36.0	7.0	. . .	0.6	3.0	0.2	9.0	. . .	. . .
Stellite B	30.0	1.0	61.5	. . .	4.5	. . .	. . .	. . .	1.0	1.0	. . .
UMCo-50	28.0	. . .	49.0	. . .	. . .	. . .	. . .	. . .	21.0	0.12	. . .
Precipitation-hardening alloys											
Iron-nickel-base											
A-286	15.0	26.0	. . .	1.25	. . .	. . .	2.0	0.2	55.2	0.04	0.005 B, 0.3 V
Discaloy	14.0	26.0	. . .	3.0	. . .	. . .	1.7	0.25	55.0	0.06	. . .
Incoloy 903	0.1 max	38.0	15.0	0.1	. . .	3.0	1.4	0.7	41.0	0.04	. . .
Pyromet CTX-1	0.1 max	37.7	16.0	0.1	. . .	3.0	1.7	1.0	39.0	0.03	. . .
Incoloy 907	. . .	38.4	13.0	. . .	. . .	4.7	1.5	0.03	42.0	0.01	0.15 Si
Incoloy 909	. . .	38.0	13.0	. . .	. . .	4.7	1.5	0.03	42.0	0.01	0.4 Si
Incoloy 925	20.5	44.0	. . .	2.8	. . .	. . .	2.1	0.2	29	0.01	1.8 Cu

(continued)

Table 1.1 (continued)

Alloy	Composition, %										
	Cr	Ni	Co	Mo	W	Nb	Ti	Al	Fe	C	Other
Precipitation-hardening alloys (continued)											
Iron-nickel-base (continued)											
V-57	14.8	27.0	. . .	1.25	. . .	. . .	3.0	0.25	48.6	0.08 max	0.01 B, 0.5 max V
W-545	13.5	26.0	. . .	1.5	. . .	. . .	2.85	0.2	55.8	0.08 max	0.05 B
Nickel-base											
Astroloy	15.0	56.5	15.0	5.25	. . .	. . .	3.5	4.4	<0.3	0.06	0.03 B, 0.06 Zr
Custom Age 625 PLUS	21.0	61.0	. . .	8.0	. . .	3.4	1.3	0.2	5.0	0.01	. . .
Haynes 242	8.0	62.5	2.5 max	25.0	. . .	. . .	. . .	0.5 max	2.0 max	0.10 max	0.006 max B
Haynes 263	20.0	52.0	. . .	6.0	. . .	. . .	2.4	0.6	0.7	0.06	0.6 Mn, 0.4 Si, 0.2 Cu
Haynes R-41	19.0	52.0	11.0	10.0	. . .	. . .	3.1	1.5	5.0	0.09	0.5 Si, 0.1 Mn, 0.006 B
Inconel 100	10.0	60.0	15.0	3.0	. . .	. . .	4.7	5.5	<0.6	0.15	1.0 V, 0.06 Zr, 0.015 B
IN-100	10	60	15	3	. . .	. . .	4.7	5.5	<0.6	0.15	0.06 Zr, 1.0 V
Inconel 102	15.0	67.0	. . .	2.9	3.0	2.9	0.5	0.5	7.0	0.06	0.005 B, 0.02 Mg, 0.03 Zr
Incoloy 901	12.5	42.5	. . .	6.0	. . .	. . .	2.7	. . .	36.2	0.10 max	. . .
Inconel 702	15.5	79.5	. . .	. . .	. . .	. . .	0.6	3.2	1.0	0.05	0.5 Mn, 0.2 Cu, 0.4 Si
Inconel 706	16.0	41.5	. . .	. . .	. . .	. . .	1.75	0.2	37.5	0.03	2.9 (Nb + Ta), 0.15 max Cu
Inconel 718	19.0	52.5	. . .	3.0	. . .	5.1	0.9	0.5	18.5	0.08 max	0.15 max Cu
Inconel 721	16.0	71.0	. . .	. . .	. . .	. . .	3.0	. . .	6.5	0.4	2.2 Mn, 0.1 Cu
Inconel 722	15.5	75.0	. . .	. . .	. . .	. . .	2.4	0.7	7.0	0.04	0.5 Mn, 0.2 Cu, 0.4 Si
Inconel 725	21.0	57.0	. . .	8.0	. . .	3.5	1.5	0.35 max	9.0	0.03 max	. . .
Inconel 751	15.5	72.5	. . .	. . .	. . .	1.0	2.3	1.2	7.0	0.05	0.25 max Cu
Inconel X-750	15.5	73.0	. . .	. . .	. . .	1.0	2.5	0.7	7.0	0.04	0.25 max Cu
M-252	19.0	56.5	10.0	10.0	. . .	. . .	2.6	1.0	<0.75	0.15	0.005 B
MERL-76	12.4	54.4	18.6	3.3	. . .	1.4	4.3	5.1	. . .	0.02	0.35 Hf, 0.06 Zr
Nimonic 80A	19.5	73.0	1.0	. . .	. . .	. . .	2.25	1.4	1.5	0.05	0.10 max Cu
Nimonic 90	19.5	55.5	18.0	. . .	. . .	. . .	2.4	1.4	1.5	0.06	. . .
Nimonic 95	19.5	53.5	18.0	. . .	. . .	. . .	2.9	2.0	5.0 max	0.15 max	+B, +Zr
Nimonic 100	11.0	56.0	20.0	5.0	. . .	. . .	1.5	5.0	2.0 max	0.30 max	+B, +Zr
Nimonic 105	15.0	54.0	20.0	5.0	. . .	. . .	1.2	4.7	. . .	0.08	0.005 B
Nimonic 115	15.0	55.0	15.0	4.0	. . .	. . .	4.0	5.0	1.0	0.20	0.04 Zr
C-263	20.0	51.0	20.0	5.9	. . .	. . .	2.1	0.45	0.7 max	0.06	. . .
Pyromet 860	13.0	44.0	4.0	6.0	. . .	. . .	3.0	1.0	28.9	0.05	0.01 B
Pyromet 31	22.7	55.5	. . .	2.0	. . .	1.1	2.5	1.5	14.5	0.04	0.005 B
Refractaloy 26	18.0	38.0	20.0	3.2	. . .	. . .	2.6	0.2	16.0	0.03	0.015 B
Rene 41	19.0	55.0	11.0	10.0	. . .	. . .	3.1	1.5	<0.3	0.09	0.01 B
Rene 88	16	56.4	13.0	4	4	0.7	3.7	2.1	. . .	0.03	0.03 Zr
Rene 95	14.0	61.0	8.0	3.5	3.5	3.5	2.5	3.5	<0.3	0.16	0.01 B, 0.05 Zr
Rene 100	9.5	61.0	15.0	3.0	. . .	. . .	4.2	5.5	1.0 max	0.16	0.015 B, 0.06 Zr, 1.0 V
Udimet 500	19.0	48.0	19.0	4.0	. . .	. . .	3.0	3.0	4.0 max	0.08	0.005 B
Udimet 520	19.0	57.0	12.0	6.0	1.0	. . .	3.0	2.0	. . .	0.08	0.005 B
Udimet 630	17.0	50.0	. . .	3.0	3.0	6.5	1.0	0.7	18.0	0.04	0.004 B
Udimet 700	15.0	53.0	18.5	5.0	. . .	. . .	3.4	4.3	<1.0	0.07	0.03 B
Udimet 710	18.0	55.0	14.8	3.0	1.5	. . .	5.0	2.5	. . .	0.07	0.01 B
Udimet 720	18	55	14.8	3	1.25	. . .	5	2.5	. . .	0.035	0.03 Zr
Udimet 720LI	16	57	15.0	3	1.25	. . .	5	2.5	. . .	0.025	0.03 Zr
Unitemp AF2-1DA	12.0	59.0	10.0	3.0	6.0	. . .	3.0	4.6	<0.5	0.35	1.5 Ta. 0.015 B, 0.1 Zr
Waspaloy	19.5	57.0	13.5	4.3	. . .	. . .	3.0	1.4	2.0 max	0.07	0.006 B, 0.09 Zr

Table 1.2 Nominal compositions of cast superalloys

Alloy designation	Nominal composition, %												
	C	Ni	Cr	Co	Mo	Fe	Al	B	Ti	Ta	W	Zr	Other
Nickel-base													
B-1900	0.1	64	8	10	6	...	6	0.015	1	4(a)	...	0.10	...
CMSX-2	...	66.2	8	4.6	0.6	...	56	...	1	6	8	6	...
CMSX-4	...	bal	6.5	9	0.6	...	5.6	...	1.0	6.5	6	...	
CMSX-6	...	bal	10	5	3	...	4.8	...	4.7	2	...	...	
CMSX-10	...	bal	1.8–4.0	1.5–9.0	0.25–2.0	...	5.0–7.0	...	0.1–1.2	7.0–10.0	3.5–7.5	...	
Hastelloy X	0.1	50	21	1	9	18	...	...	...	...	1	...	...
Inconel 100	0.18	60.5	10	15	3	...	5.5	0.01	5	...	...	0.06	1 V
Inconel 713C	0.12	74	12.5	...	4.2	...	6	0.012	0.8	1.75	...	0.1	0.9 Nb
Inconel 713LC	0.05	75	12	...	4.5	...	6	0.01	0.6	4	...	0.1	...
Inconel 738	0.17	61.5	16	8.5	1.75	...	3.4	0.01	3.4	...	2.6	0.1	2 Nb
Inconel 792	0.2	60	13	9	2.0	...	3.2	0.02	4.2	...	4	0.1	2 Nb
Inconel 718	0.04	53	19	...	3	18	0.5	...	0.9	...	...	...	0.1 Cu, 5 Nb
X-750	0.04	73	15	...	...	7	0.7	...	2.5	...	...	...	0.25 Cu, 0.9 Nb
M-252	0.15	56	20	10	10	...	1	0.005	2.6	...	...	...	...
MAR-M 200	0.15	59	9	10	...	1	5	0.015	2	...	12.5	0.05	1 Nb(b)
MAR-M 246	0.15	60	9	10	2.5	...	5.5	0.015	1.5	1.5	10	0.05	...
MAR-M 247	0.15	59	8.25	10	0.7	0.5	5.5	0.015	1	3	10	0.05	1.5 Hf
PWA 1480	...	bal	10	5.0	...	...	5.0	...	1.5	12	4.0	...	...
PWA 1484	...	bal	5	10	2	...	5.6	...	...	9	6	...	
Rene 41	0.09	55	19	11.0	10.0	...	1.5	0.01	3.1	...	...	...	...
Rene 77	0.07	58	15	15	4.2	...	4.3	0.015	3.3	...	...	0.04	...
Rene 80	0.17	60	14	9.5	4	...	3	0.015	5	...	4	0.03	...
Rene 80 Hf	0.08	60	14	9.5	4	...	3	0.015	4.8	...	4	0.02	0.75 Hf
Rene 100	0.18	61	9.5	15	3	...	5.5	0.015	4.2	...	...	0.06	1 V

(continued)

(a) B-1900 + Hf also contains 1.5% Hf. (b) MAR-M 200 + Hf also contains 1.5% Hf. (c) Designated R' 162 in U.S. patent 5,270,123. Also contains 0.02–0.07% C, 0.003–0.01% B, 0–0.3% Y, and 0–6% Ru.

Table 1.2 (continued)

Alloy designation	Nominal composition, %												
	C	Ni	Cr	Co	Mo	Fe	Al	B	Ti	Ta	W	Zr	Other
Nickel-base (continued)													
Rene N4	0.06	62	9.8	7.5	1.5	. . .	4.2	0.004	3.5	4.8	6	. . .	0.5 Nb, 0.15 Hf
RR 2000	. . .	bal	10	15	3	. . .	5.5	. . .	4.0	. . .	. . .	. . .	
SRR 99	. . .	bal	8	5	. . .	. . .	5.5	. . .	2.2	3	10	. . .	
Rene N5	. . .	bal	7	8	2	. . .	6.2	. . .	. . .	7	5	. . .	
Rene N6(c)	. . .	bal	4.25–6	10–15	0.5–2	. . .	5–6.25	. . .	. . .	7–9.25	5–6.5	. . .	
Udimet 500	0.1	53	18	17	4	2	3	. . .	3	. . .	. . .	. . .	. . .
Udimet 700	0.1	53.5	15	18.5	5.25	. . .	4.25	0.03	3.5	. . .	. . .	. . .	. . .
Udimet 710	0.13	55	18	15	3	. . .	2.5	. . .	5	. . .	1.5	0.08	. . .
Waspaloy	0.07	57.5	19.5	13.5	4.2	1	1.2	0.005	3	. . .	. . .	0.09	. . .
WAX-20(DS)	0.20	72	. . .	. . .	. . .	. . .	6.5	. . .	. . .	. . .	20	1.5	. . .
Cobalt-base													
AiResist 13	0.45	. . .	21	62	. . .	. . .	3.4	. . .	. . .	2	11	. . .	0.1 Y
AiResist 213	0.20	0.5	20	64	. . .	0.5	3.5	. . .	. . .	6.5	4.5	0.1	0.1 Y
AiResist 215	0.35	0.5	19	63	. . .	0.5	4.3	. . .	. . .	7.5	4.5	0.1	0.1 Y
FSX-414	0.25	10	29	52.5	. . .	1	. . .	0.010	. . .	. . .	7.5	. . .	. . .
Haynes 21	0.25	3	27	64	. . .	1	. . .	. . .	. . .	. . .	. . .	. . .	5 Mo
Haynes 25; L-605	0.1	10	20	54	. . .	1	. . .	. . .	. . .	. . .	15	. . .	. . .
J-1650	0.20	27	19	36	. . .	. . .	. . .	0.02	3.8	2	12	. . .	. . .
MAR-M 302	0.85	. . .	21.5	58	. . .	0.5	. . .	0.005	. . .	9	10	0.2	. . .
MAR-M 322	1.0	. . .	21.5	60.5	. . .	0.5	. . .	. . .	0.75	4.5	9	2	. . .
MAR-M 509	0.6	10	23.5	54.5	. . .	. . .	. . .	. . .	0.2	3.5	7	0.5	. . .
MAR-M 918	0.05	20	20	52	. . .	. . .	. . .	. . .	. . .	7.5	. . .	0.1	. . .
NASA Co-W-Re	0.40	. . .	3	67.5	. . .	. . .	. . .	. . .	1	. . .	25	1	2 Re
S-816	0.4	20	20	42	. . .	4	. . .	. . .	. . .	. . .	4	. . .	4 Mo, 4 Nb, 1.2 Mn, 0.4 Si
V-36	0.27	20	25	42	. . .	3	. . .	. . .	. . .	. . .	2	. . .	4 Mo, 2 Nb, 1 Mn, 0.4 Si
Wi-52	0.45	. . .	21	63.5	. . .	2	. . .	. . .	. . .	. . .	11	. . .	2 Nb + Ta
X-40 (Stellite alloy 31)	0.50	10	22	57.5	. . .	1.5	. . .	. . .	. . .	. . .	7.5	. . .	0.5 Mn, 0.5 Si

(a) B-1900 + Hf also contains 1.5% Hf. (b) MAR-M 200 + Hf also contains 1.5% Hf. (c) Designated R' 162 in U.S. patent 5,270,123. Also contains 0.02–0.07% C, 0.003–0.01% B, 0–0.3% Y, and 0–6% Ru.

melting-point depressants tend to have incipient melting temperatures equal to or in excess of those of cobalt-base superalloys.

Some Superalloy Characteristics and Facts

- When temperatures go above about 1000 °F (540 °C), ordinary steels and titanium alloys are no longer strong enough for application. Steels also may suffer from enhanced corrosion attack.
- When the highest temperatures (below the melting temperatures, which are about 2200 to 2500 °F (1204 to 1371 °C) for most alloys) must be achieved and strength is the consideration, then nickel-base superalloys are the materials of choice.
- Nickel-base superalloys can be used to a higher fraction of their melting points than just about any other commercially available materials. Refractory metals have higher melting points than superalloys but do not have the same desirable characteristics as superalloys and are much less widely used.
- Cobalt-base superalloys may be used in lieu of nickel-base superalloys, dependent on actual strength needs and the type of corrosive attack expected.
- At lower temperatures, and dependent on the type of strength needs for an application, iron-nickel-base superalloys find more use than cobalt- or nickel-base superalloys.
- Superalloy strength properties are directly related not only to the chemistry of the alloy but also to melting procedures, forging and working processes, casting techniques, and, above all, to heat treatment following forming, forging or casting.
- Iron-nickel-base (sometimes designated nickel-iron-base) superalloys such as IN-718 are less expensive than nickel-base or cobalt-base superalloys.
- Most wrought superalloys have fairly high levels of the metal chromium to provide corrosion resistance. In the cast alloys, chromium was high to start but was significantly reduced over the years in order to accommodate other alloy elements that increased the elevated temperature strength of superalloys. In the superalloys based on nickel, the aluminum content of the alloys increased as chromium decreased. Thus, the oxidation resistance of nickel superalloys remained similar to original levels or even increased. However, resistance to other types of corrosion attack decreased.
- Superalloys have great oxidation resistance, in many instances, but not enough corrosion resistance. For many applications at the highest temperatures, above about 1400 °F (760 °C), as in aircraft turbines, superalloys must be coated. For very long-time applications at temperatures at or above about 1200 °F (649 °C), as in land-based gas turbines, superalloys may have to be coated.
- Coating technology is an integral part of superalloy development and application. Lack of a coating means much less ability to use superalloys for extended times at elevated temperatures.
- Many alloy elements are added to superalloys in minuscule to major amounts, particularly in the nickel-base alloys. Controlled alloy elements could be as many as 14 or so in some alloys.
- Nickel and cobalt as well as chromium, tungsten, molybdenum, rhenium, hafnium, and other elements used in superalloys are often expensive and strategic elements that may vary considerably in price and availability over time.

Applications

The high-temperature applications of superalloys are extensive, including components for aircraft, chemical plant equipment, and petrochemical equipment. Figure 1.2 shows the F119 engine, which is the latest in a series of military engines to power high-performance aircraft. The gas temperatures in these engines in the hot sections (rear areas of the engine) may rise to levels far above 2000 °F (1093 °C). Cooling techniques reduce the actual component metal temperatures to lower levels, and superalloys that can operate at these temperatures are the major components of the hot sections of such engines.

The significance of superalloys in today's commerce is typified by the fact that, whereas in 1950 only about 10% of the total weight of an aircraft gas turbine engine was made of superalloys, by 1985 this figure had risen to about 50%. Table 1.3 lists some current applications of superalloys. It will be noted, however, that not all applications re-

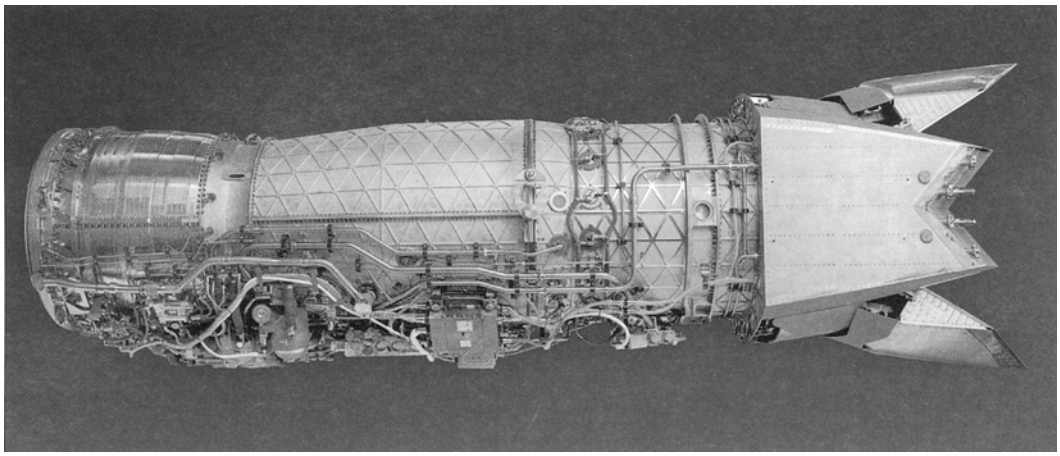


Fig. 1.2 F119 gas turbine engine—a major user of superalloys

Table 1.3 Some Applications of Superalloys

Aircraft/industrial gas turbine components:
Disks
Bolts
Shafts
Cases
Blades
Vanes
Combustors
Afterburners
Thrust reversers
Steam turbine power plant components:
Bolts
Blades
Stack-gas reheaters
Selected automotive components, such as:
Turbochargers
Exhaust valves
Metal processing, such as in:
Hot work tools and dies
Casting dies
Medical components, such as in:
Dentistry
Prosthetic devices
Space vehicle components, such as:
Aerodynamically heated skins
Rocket-engine parts
Heat treating equipment:
Trays
Fixtures
Conveyor belts
Nuclear power systems:
Control-rod drive mechanisms
Valve stems
Springs
Ducting
Chemical and petrochemical industries:
Bolts
Valves
Reaction vessels
Piping
Pumps

Adapted from *Titanium: A Technical Guide*, 1st ed.

quire elevated-temperature strength capability. Their high strength coupled with corrosion resistance have made certain superalloys standard materials for biomedical devices. Superalloys also find use in cryogenic applications.

What to Look for in This Book

The text provides those who desire it a very complete understanding of superalloys. The chapters ''Selection of Superalloys,'' ''Understanding Superalloy Metallurgy,'' ''Structure/Property Relationships,'' plus ''Corrosion and Protection of Superalloys'' enhance ability to make design decisions on superalloy use.

For those involved in processing the superalloys, virtually all process operations are included, starting with a very comprehensive look at the initial formulation of superalloys in the chapter ''Melting and Conversion.'' Subsequently, the gamut of operations is covered from casting to machining and finishing.

If you are experiencing problems with superalloys, reference to the chapters mentioned in the first paragraph of this section is in order. If failures are occurring, check the chapter ''Failure and Refurbishment.''

For those desiring a little retrospective look at the current state of superalloy applications and potential future directions, the chapter ''Superalloys—Retrospect and Future Prospects'' may be of interest.

Superalloys: A Technical Guide, Second Edition
Matthew J. Donachie, Stephen J. Donachie, p 11-24
DOI:10.1361/stgs2002p011
Copyright © 2002 ASM International®
All rights reserved.
www.asminternational.org

Chapter 2

Selection of Superalloys

Overview

General Considerations. Selection implies data. Appendix A contains a list with names and Web sites (where available) of organizations that may produce superalloys, superalloy components, or data/information on them. The first thing that should be noted for those persons selecting superalloys is that data, at least validated mechanical property data, may be hard to gather. Some archival collections of tabulated data on superalloys have been made. Computer-based data collections have been produced. Unfortunately, there is little likelihood that these collections can serve as much more than a starting point.

The subject of design allowables and validated property data is much too large to cover in this book. However, one might be advised when looking at data to remember that many data sets are made available by the ''seller'' and you, the reader, may be the ''buyer.'' Sellers and buyers tend to have different interpretations of facts or, sometimes, a convenient way of discarding unpleasant or surprising facts.

Actual plotted data may be more difficult to acquire than tabular data. Tables 2.1 to 2.4 provide some tabular data on tensile properties and stress-rupture properties of selected superalloys. Figure 1.1 may be consulted again for a general overview on stress-rupture property capability, while Fig. 2.1 gives information for some specific alloys, but hardly enough to cover the vast spectrum of superalloys invented and large number marketed.

Most data compilations depend on manufacturer's data, with some additional access to published information from technical papers. Except for mill products such as sheet and bar, it is almost never true that the same nominal composition when tested at various laboratories is ever in exactly the same condition. As is shown in this book, microstructure (read ''condition'') is the single most important factor in defining mechanical properties of superalloys. Varying microstructures can mean varying test results. Needless to say, even with identical microstructures, nominal test conditions, and nominal chemistries, there is a random statistical nature to results. The tracking of data on any one alloy is a laborious task. Consequently, most data compilations consist of an uncritical presentation of data derived from manufacturers and the literature. Caveat emptor!

Superalloy Forms. Superalloys are available in cast (usually heat treated or otherwise processed) or wrought (often heat treated or otherwise processed) forms. Cast products may include ingot for subsequent remelting or wrought processing (e.g., forging), or the products may be in the approximate shape of the component desired. Wrought products often are in an intermediate approximation of the shape desired or are mill products, including bar, sheet, wire, plate, and so on.

One of the major thrusts of superalloy metallurgy at the end of the 20th century was the production of net shape or near-net shape wrought products. (Cast net shapes have been available via investment casting processes for decades.) To this end, enhanced understanding of cold and hot working processes using computer algorithms and/or the application of new technologies such as

Table 2.1 Effect of temperature on the short-time mechanical properties of selected wrought superalloys

		Ultimate tensile strength at:						Yield strength at 0.2% offset at:						Tensile elongation, % at:		
		21 °C (70 °F)		540 °C (1000 °F)		760 °C (1400 °F)		21 °C (70 °F)		540 °C (1000 °F)		760 °C (1400 °F)		21 °C (70 °F)	540 °C (1000 °F)	760 °C (1400 °F)
Alloy	Form	MPa	ksi	MPa	ksi	MPa	ksi	MPa	ksi	MPa	ksi	MPa	ksi			
Nickel-base																
Astroloy	Bar	1415	205	1240	180	1160	168	1050	152	965	140	910	132	16	16	21
Cabot 214	...	915	133	715	104	560	84	560	81	510	74	495	72	38	19	9
D-979	Bar	1410	204	1295	188	720	104	1005	146	925	134	655	95	15	15	17
Hastelloy C-22	Sheet	800	116	625	91	525	76	405	59	275	40	240	35	57	61	63
Hastelloy G-30	Sheet	690	100	490	71	...	...	315	46	170	25	...	...	64	75	...
Hastelloy S	Bar	845	130	775	112	575	84	455	65	340	49	310	45	49	50	70
Hastelloy X	Sheet	785	114	650	94	435	63	360	52	290	42	260	38	43	45	37
Haynes 230	(a)	870	126	720	105	575	84	390	57	275	40	285	41	48	56	46
Inconel 587	Bar	1180	171	1035	150	830	120	705	102	620	90	605	88	28	22	20
Inconel 597	Bar	1220	177	1140	165	930	135	760	110	720	104	665	96	15	15	16
Inconel 600	Bar	660	96	560	81	260	38	285	41	220	32	180	26	45	41	70
Inconel 601	Sheet	740	107	725	105	290	42	455	66	350	51	220	32	40	34	78
Inconel 617	Bar	740	107	580	84	440	64	295	43	200	29	180	26	70	68	84
Inconel 617	Sheet	770	112	590	86	470	68	345	50	230	33	230	33	55	62	59
Inconel 625	Bar	965	140	910	132	550	80	490	71	415	60	415	60	50	50	45
Inconel 706	Bar	1310	190	1145	166	725	105	1005	146	910	132	660	96	20	19	32
Inconel 718	Bar	1435	208	1275	185	950	138	1185	172	1065	154	740	107	21	18	25
Inconel 718 Direct Age	Bar	1530	222	1350	196	...	...	1365	198	1180	171	...	...	16	15	...
Inconel 718 Super	Bar	1350	196	1200	174	...	...	1105	160	1020	148	...	...	16	18	...
Inconel X750	Bar	1200	174	1050	152	...	...	815	118	725	105	...	...	27	26	...
M-252	Bar	1240	180	1230	178	945	137	840	122	765	111	720	104	16	15	10
Nimonic 75	Bar	745	108	675	98	310	45	285	41	200	29	160	23	40	40	67
Nimonic 80A	Bar	1000	145	875	127	600	87	620	90	530	77	505	73	39	37	17
Nimonic 90	Bar	1235	179	1075	156	655	95	810	117	725	105	540	78	33	28	12
Nimonic 105	Bar	1180	171	1130	164	930	135	830	120	775	112	740	107	16	22	25
Nimonic 115	Bar	1240	180	1090	158	1085	157	865	125	795	115	800	116	27	18	24
Nimonic 263	Sheet	970	141	800	116	650	94	580	84	485	70	460	67	39	42	21
Nimonic 942	Bar	1405	204	1300	189	900	131	1060	154	970	141	860	125	37	26	42
Nimonic PE 11	Bar	1080	157	1000	145	760	110	720	105	690	100	560	81	30	30	18
Nimonic PE 16	Bar	885	128	740	107	510	74	530	77	485	70	370	54	37	26	42
Nimonic PK 33	Sheet	1180	171	1000	145	885	128	780	113	725	105	670	97	30	30	18
Pyromet 860	Bar	1295	188	1255	182	910	132	835	121	840	122	835	121	22	15	18
Rene 41	Bar	1420	206	1400	203	1105	160	1060	154	1020	147	940	136	14	14	11
Rene 95	Bar	1620	235	1550	224	1170	170	1310	190	1255	182	1100	160	15	12	15
Udimet 400	Bar	1310	190	1185	172	...	...	930	135	830	120	...	...	30	26	...

(continued)

(a) Cold-rolled and solution-annealed sheet, 1.2 to 1.6 mm (0.048 to 0.063 in.) thick. (b) Annealed. (c) Precipitation hardened. (d) Work strengthened and aged

Table 2.1 (continued)

Alloy	Form	Ultimate tensile strength at: 21 °C (70 °F) MPa	ksi	540 °C (1000 °F) MPa	ksi	760 °C (1400 °F) MPa	ksi	Yield strength at 0.2% offset at: 21 °C (70 °F) MPa	ksi	540 °C (1000 °F) MPa	ksi	760 °C (1400 °F) MPa	ksi	Tensile elongation, % at: 21 °C (70 °F)	540 °C (1000 °F)	760 °C (1400 °F)
Nickel-base (continued)																
Udimet 500	Bar	1310	190	1240	180	1040	151	840	122	795	115	730	106	32	28	39
Udimet 520	Bar	1310	190	1240	180	725	105	860	125	825	130	725	105	21	20	15
Udimet 630	Bar	1520	220	1380	200	965	140	1310	190	1170	170	860	125	15	15	5
Udimet 700	Bar	1410	204	1275	185	1035	150	965	140	895	130	825	120	17	16	20
Udimet 710	Bar	1185	172	1150	167	1020	148	910	132	850	123	815	118	7	10	25
Udimet 720	Bar	1570	228	...	...	1455	211	1195	173	...	...	1050	152	13	...	9
Unitemp AF2-1DA6	Bar	1560	226	1480	215	1290	187	1015	147	1040	151	995	144	20	19	16
Waspaloy	Bar	1275	185	1170	170	650	94	795	115	725	105	675	98	25	23	28
Iron-base																
A-286	Bar	1005	146	905	131	440	64	725	105	605	88	430	62	25	19	19
Alloy 901	Bar	1205	175	1030	149	725	105	895	130	780	113	635	92	14	14	19
Discaloy	Bar	1000	145	865	125	485	70	730	106	650	94	430	62	19	16	...
Haynes 556	Sheet	815	118	645	93	470	69	410	60	240	35	220	32	48	54	49
Incoloy 800	Bar	595	86	510	74	235	34	250	36	180	26	150	22	44	38	83
Incoloy 801	Bar	785	114	660	96	325	47	385	56	310	45	290	42	30	28	55
Incoloy 802	Bar	690	100	600	87	400	58	290	42	195	28	200	29	44	39	15
Incoloy 807	Bar	655	95	470	68	350	51	380	55	255	37	225	32.5	48	40	34
Incoloy 825(b)	...	690	100	~590	~86	~275	~40	310	45	~234	~34	180	~26	45	~44	~86
Incoloy 903	Bar	1310	190	...	...	...	...	1105	160	...	...	...	...	14	...	...
Incoloy 907(c)	...	~1365	~198	~1205	~175	~655	~95	1110	161	~960	~139	~565	~82	~12	~11	~20
Incoloy 909	Bar	1310	190	1160	168	615	89	1020	148	945	137	540	78	16	14	34
N-155	Bar	815	118	650	94	428	62	400	58	340	49	250	36	40	33	32
V-57	Bar	1170	170	1000	145	620	90	830	120	760	110	485	70	26	19	34
19-9 DL	...	815	118	615	89	...	...	570	83	395	57	...	...	43	30	...
16-25-6	...	980	142	...	...	415	60	770	112	...	...	345	50	23	...	11
Cobalt-base																
AirResist 213	...	1120	162	...	...	485	70	625	91	...	...	385	56	14	...	47
Elgiloy	...	690(e)–2480(d)	100(e)–360(d)	...	...	...	...	480(e)–2000(d)	70–290	...	...	...	...	34	...	...
Haynes 188	Sheet	960	139	740	107	635	92	485	70	305	44	290	42	56	70	43
L-605	Sheet	1005	146	800	116	455	66	460	67	250	36	260	38	64	59	12
MAR-M918	Sheet	895	130	...	...	...	...	895	130	...	...	...	...	48	...	...
MP35N	Bar	2025	294	...	...	...	...	1620	235	...	...	...	...	10	...	...
MP159	Bar	1895	275	1565	227	...	...	1825	265	1495	217	...	...	8	8	...
Stellite 6B	Sheet	1010	146	...	...	...	...	635	92	...	...	...	...	11	...	...
Haynes 150	...	925	134	...	...	...	...	317	46	...	...	...	...	8	...	...

(a) Cold-rolled and solution-annealed sheet, 1.2 to 1.6 mm (0.048 to 0.063 in.) thick. (b) Annealed. (c) Precipitation hardened. (d) Work strengthened and aged

Table 2.2 Effect of temperature on 1000 h stress-rupture strengths of selected wrought superalloys

		Rupture strength at:							
		650 °C (1200 °F)		760 °C (1400 °F)		870 °C (1600 °F)		980 °C (1800 °F)	
Alloy	Form	MPa	ksi	MPa	ksi	MPa	ksi	MPa	ksi
Nickel-base									
Astroloy	Bar	770	112	425	62	170	25	55	8
Cabot 214	...	...	...	...	..	30	4	15	2
D-979	Bar	515	75	250	36	70	10	...	...
Hastelloy S	Bar	...	...	90	13	25	4	...	...
Hastelloy X	Sheet	215	31	105	15	40	6	15	2
Haynes 230	...	...	...	125	18	55	8	15	2
Inconel 587	Bar	...	...	285	41	...	...	...	...
Inconel 597	Bar	...	...	340	49	...	...	...	...
Inconel 600	Bar	...	...	...	...	30	4	15	2
Inconel 601	Sheet	195	28	60	9	30	4	15	2
Inconel 617	Bar	360	52	165	24	60	9	30	4
Inconel 617	Sheet	...	...	160	23	60	9	30	4
Inconel 625	Bar	370	54	160	23	50	7	20	3
Inconel 706	Bar	580	84	...	...	...	...	...	...
Inconel 718	Bar	595	86	195	28	...	...	...	...
Inconel 718 Direct Age	Bar	405	59	...	...	...	...	...	...
Inconel 718 Super	Bar	600	87	...	...	...	...	...	...
Inconel X750	Bar	470	68	...	...	50	7	...	...
M-252	Bar	565	82	270	39	95	14	...	...
Nimonic 75	Bar	170	25	50	7	5	1	...	...
Nimonic 80A	Bar	420	61	160	23	...	...	...	...
Nimonic 90	Bar	455	66	205	30	60	9	...	...
Nimonic 105	Bar	...	...	330	48	130	19	30	4
Nimonic 115	Bar	...	...	420	61	185	27	70	10
Nimonic 942	Bar	520	75	270	39	...	...	...	...
Nimonic PE.11	Bar	335	49	145	21	...	...	...	...
Nimonic PE.16	Bar	345	50	150	22	...	...	...	...
Nimonic PK.33	Sheet	655	95	310	45	90	13	...	...
Pyromet 860	Bar	545	79	250	36	...	...	...	...
Rene 41	Bar	705	102	345	50	115	17	...	...
Rene 95	Bar	860	125	...	...	...	...	...	...
Udimet 400	Bar	600	87	305	44	110	16	...	...
Udimet 500	Bar	760	110	325	47	125	18	...	...
Udimet 520	Bar	585	85	345	50	150	22	...	...
Udimet 700	Bar	705	102	425	62	200	29	55	8
Udimet 710	Bar	870	126	460	67	200	29	70	10
Udimet 720	Bar	670	97	...	...	...	...	...	...
Unitemp AF2-1DA6	Bar	885	128	360	52	...	...	...	...
Waspaloy	Bar	615	89	290	42	110	16	...	...
Iron-base									
A286	Bar	315	46	105	15	...	...	...	...
Alloy 901	Sheet	525	76	205	30	...	...	...	...
Discaloy	Bar	275	40	60	9	...	...	...	...
Haynes 556	Sheet	275	40	125	18	55	8	20	3
Incoloy 800	Bar	165	24	66	9.5	30	4.4	13	1.9
Incoloy 801	Bar	...	...	...	...	...	...	...	...
Incoloy 802	Bar	170	25	110	16	69	10	24	3.5
Incoloy 807	Bar	...	...	105	15	43	6.2	19	2.7
Incoloy 903	Bar	510	74	...	...	...	...	...	...
Incoloy 909	Bar	345	50	...	...	...	...	...	...
N-155	Bar	295	43	140	20	70	10	20	3
V-57	Bar	485	70	...	...	...	...	...	...
Cobalt-base									
Haynes 188	Sheet	...	...	165	24	70	10	30	4
L-605	Sheet	270	39	165	24	75	11	30	4
MAR-M918	Sheet	...	...	60	9	20	3	5	1
Haynes 150	...	...	...	40(a)	5.8	...	...	...	...

(a) At 815 °C (1500 °F)

hot isostatic pressing or spray forming have been successful in enabling designers to count on wrought products with shapes much closer to the final desired shape. Costs of actually producing certain net shape wrought products have gone up, but less metal is used with a consequent overall cost savings.

Service Temperatures for Superalloys. The superalloys, as has been noted, consist of alloys of iron-nickel-, nickel-, and cobalt-base that are destined generally for use above about 1000 °F (540 °C) and below the melting points of the alloys, which usually are at or above about 2200 °F (1204 °C). Some superalloys also find use in space applications where subzero and cryogenic temperatures are an issue. The bulk of this text presumes that the application will be at elevated temperature. Cryogenic applications are covered in Chapter 12.

Wrought nickel- and iron-nickel-base alloys, in general, have temperature limitations of about 1500 °F (816 °C). Above that temperature, cast alloys generally are used. The majority of superalloys are strengthened by the production of secondary phases (precipitates), and the upper temperature limit for alloy use is governed by the base (nickel- or iron-nickel-base), the volume/type of precipitate, and the form (cast or wrought). Chapter 3 provides detailed information about the metallurgy of all superalloy types.

It is commonly understood in the superalloy industry that certain alloy types are used for specific temperatures of application. For example, most wrought nickel- and iron-nickel-base superalloys are used only to about 1200 to 1300 °F (649 to 704 °C). The range of such alloys actually starts below 1000 °F (540 °C), frequently as low as 800 °F (427 °C), and the wrought alloys are particularly useful in gas turbines when titanium alloys might be inappropriate. Cast alloys are used across the temperature range but particularly at the highest temperatures, especially as in gas turbine engines.

Superalloys usually are processed to optimize one property in preference to others. The same composition, if used in cast and wrought state, may have different heat treatments applied to the different product forms. Even when a superalloy is used in the same product form, process treatments may be used to optimize one property over others. For example, an alloy such as Waspaloy was being produced in wrought form for gas turbine disks. By adjustment of processing conditions, principally heat treatment, substantial yield strength improvements (a desirable effect) were achieved in the wrought product at the expense of creep-rupture strength.

Wrought versus Cast Superalloys

Wrought Superalloys. A wrought alloy generally is one that started from cast billets but has been deformed and reheated numerous times to reach its final state. Wrought alloys are more homogenous than cast alloys, which usually have segregation caused by the solidification process. Segregation is a natural consequence of solidification of alloys but may be more severe in some cases than in others.

Wrought alloys generally are considered more ductile than cast alloys. Thus, mill product shapes such as bar are wrought products because they can be made best by working, which generates the optimal ductility for processing and for subsequent use. Forgings obviously are also wrought products and take advantage of the superior ductility of wrought material to produce certain larger shapes, such as gas turbine disks.

Not all alloy compositions can be made in wrought form. Some alloys can only be fabricated and used in cast form. Some very difficult to work (wrought) alloys can be processed by powder metallurgy (P/M), usually to prepare them for final forging. In the intermediate-temperature application areas of gas turbines, where massive disks are frequently necessary, standard wrought or wrought P/M disks routinely are employed. Powder metallurgy processing has been employed to directly produce component blanks for final machining but such processing is rare.

Cast Superalloys. Cast alloys are found in the hot section areas of gas turbines, especially as airfoils, that is, blades and vanes. Most castings are polycrystalline (PC) equiaxed, but others are directionally solidified (DS). The PC castings contain many grains that may vary in size from one component to another. Directionally solidified castings may have a multiplicity of grains all aligned parallel to each other (usually parallel to the longitudinal or airfoil axis of a turbine

Table 2.3 Effect of temperature on the short-time mechanical properties of selected cast superalloys

	Ultimate tensile strength at:						0.2% yield strength at:						Tensile elongation, % at:		
	21 °C (70 °F)		538 °C (1000 °F)		1093 °C (2000 °F)		21 °C (70 °F)		538 °C (1000 °F)		1093 °C (2000 °F)		21 °C	538 °C	1093 °C
Alloy	MPa	ksi	MPa	ksi	MPa	ksi	MPa	ksi	MPa	ksi	MPa	ksi	(70 °F)	(1000 °F)	(2000 °F)
Nickel-base															
IN-713 C	850	123	860	125	...	...	740	107	705	102	...	...	8	10	...
IN-713 LC	895	130	895	130	...	...	750	109	760	110	...	...	15	11	...
B-1900	970	141	1005	146	270	38	825	120	870	126	195	28	8	7	11
IN-625	710	103	510	74	...	...	350	51	235	34	...	...	48	50	...
IN-718	1090	158	...	...	...	...	915	133	...	...	...	...	11	...	...
IN-100	1018	147	1090	150	(380)	(55)	850	123	885	128	(240)	(35)	9	9	...
IN-162	1005	146	1020	148	...	...	815	118	795	115	...	...	7	6.5	...
IN-731	835	121	...	...	275	40	725	105	...	...	170	25	6.5	...	...
IN-738	1095	159	...	...	...	...	950	138	...	...	...	...	...	...	...
IN-792	1170	170	...	...	...	...	1060	154	...	...	...	...	4	...	...
M-22	730	106	780	113	...	...	685	99	730	106	...	...	5.5	4.5	...
MAR-M200	930	135	945	137	325	47	840	122	880	123	...	...	7	5	...
MAR-M246	965	140	1000	145	345	50	860	125	860	125	...	...	5	5	...
MAR-M247	965	140	1035	150	...	...	815	118	825	120	...	...	7	...	
MAR-M421	1085	157	995	147	...	...	930	135	815	118	...	...	4.5	3	...
MAR-M432	1240	180	1105	160	...	...	1070	155	910	132	...	...	6	...	...
MC-102	675	98	655	95	...	...	605	88	540	78	...	...	5	9	...
Nimocast 75	500	72	...	...	...	...	179	26	...	...	...	...	39	...	...
Nimocast 80	730	106	...	...	...	...	520	75	...	...	...	...	15	...	...
Nimocast 90	700	102	595	86	...	...	520	75	420	61	...	...	14	15	...
Nimocast 242	460	67	...	...	...	...	300	44	...	...	...	...	8	...	...
Nimocast 263	730	106	...	...	...	...	510	74	...	...	...	...	18	...	...
Rene 77	...	...	...	...	...	...	...	...	...	...	...	...	...	...	...
Rene 80	...	...	...	...	...	...	...	...	...	...	...	...	...	...	...

(continued)

(a) Single crystal [001]. (b) At 760 °C (1400 °F). (c) At 980 °C (1800 °F). (d) RR-7080. (e) MM 004. (f) M 005. (g) MM 006. (h) MM 009. (i) Data from Vol 3, 9th ed., *Metals Handbook*, 1980. (j) At 650 °C (1200 °F). Source: Nickel Development Institute, except as noted

Table 2.3 (continued)

Alloy	Ultimate tensile strength at: 21 °C (70 °F) MPa	ksi	538 °C (1000 °F) MPa	ksi	1093 °C (2000 °F) MPa	ksi	0.2% yield strength at: 21 °C (70 °F) MPa	ksi	538 °C (1000 °F) MPa	ksi	1093 °C (2000 °F) MPa	ksi	Tensile elongation, % at: 21 °C (70 °F)	538 °C (1000 °F)	1093 °C (2000 °F)
Nickel-base (continued)															
Udimet 500	930	135	895	130	...	...	815	118	725	105	...	...	13	13	...
Udimet 710	1075	156	...	...	240	35	895	130	...	...	170	25	8	...	...
CMSX-2(a)	1185	172	1295(b)	188(b)	...	...	1135	165	1245(b)	181(b)	...	...	10	17(b)	...
GMR-235	710	103	...	...	...	...	640	93	...	...	...	...	3	...	18(b)
IN-939	1050	152	915(b)	133(b)	325(c)	47(c)	800	116	635(b)	92(b)	205(c)	30(c)	5	7(b)	25(b)
MM 002(d)	1035	150	1035(b)	150(b)	550(c)	80(c)	825	120	860(b)	125(b)	345(c)	50(c)	7	5(b)	12(b)
IN-713 Hf(e)	1000	145	895(b)	130(b)	380(c)	55(c)	760	110	620(b)	90(b)	240(c)	35(c)	11	6(b)	20(b)
Rene 125 Hf(f)	1070	155	1070(b)	155(b)	550(c)	80(c)	825	120	860(b)	125(b)	345(c)	50(c)	5	5(b)	12(b)
MAR-M 246 Hf(g)	1105	160	1070(b)	155(b)	565(c)	82(c)	860	125	860(b)	125(b)	345(c)	50(c)	6	7(b)	14(b)
MAR-M 200 Hf(h)	1035	150	1035(b)	150(b)	540(c)	78(c)	825	120	860(b)	125(b)	345(c)	50(c)	5	5(b)	10(b)
PWA-1480(a)	...	...	1130(b)	164(b)	685(c)	99(c)	895	130	905(b)	131(b)	495(c)	72(c)	4	8(b)	20(b)
SEL	1020	148	875(b)	127(b)	...	...	905	131	795(b)	115(b)	...	...	6	7(b)	...
UDM 56	945	137	945(b)	137(b)	...	...	850	123	725(b)	105(b)	...	...	3	5(b)	...
SEL-15	1060	154	1090(b)	158(b)	...	...	895	130	815(b)	118(b)	...	...	9	5(b)	...
Cobalt-base															
AiResist 13(i)	600	87	420(b)	61(b)	...	...	530	77	330(b)	48(b)	...	...	1.5	4.5(b)	...
AiResist 215(i)	690	100	570(j)	83(j)	...	...	485	70	315(j)	46(j)	...	...	4	12(j)	...
FSX-414	...	...	...	...	...	...	...	...	...	...	...	...	...	...	...
Haynes 1002	770	112	560	81	115	17	470	68	345	50	95	14	6	8	28
MAR-M 302	930	135	795	115	150	22	690	100	505	73	150	22	2	...	21
MAR-M 322(i)	830	120	595(b)	86(b)	...	...	630	91	345(b)	50(b)	...	...	4	6.5(b)	...
MAR-M 509	785	114	570	83	...	...	570	83	400	58	...	...	4	6	...
WI-52	750	109	745	108	160	23	585	85	440	64	105	15	5	7	35
X-40	745	108	550	80	...	...	525	76	275	40	...	...	9	17	...

(a) Single crystal [001]. (b) At 760 °C (1400 °F). (c) At 980 °C (1800 °F). (d) RR-7080. (e) MM 004. (f) M 005. (g) MM 006. (h) MM 009. (i) Data from Vol 3, 9th ed., *Metals Handbook*, 1980. (j) At 650 °C (1200 °F). Source: Nickel Development Institute, except as noted

Table 2.4 Effect of temperature on stress-rupture strengths of selected wrought superalloys

	Rupture strength at:					
	815 °C (1500 °F)		870 °C (1600 °F)		980 °C (1800 °F)	
Alloy	100 h MPa (ksi)	1000 h MPa (ksi)	100 h MPa (ksi)	1000 h MPa (ksi)	100 h MPa (ksi)	1000 h MPa (ksi)
Nickel-base						
IN-713 LC	425 (62)	325 (47)	295 (43)	240 (35)	140 (20)	105 (15)
IN-713 C	370 (54)	305 (44)	305 (44)	215 (31)	130 (19)	70 (10)
IN-738 C	470 (68)	345 (50)	330 (38)	235 (34)	130 (19)	90 (13)
IN-738 LC	430 (62)	315 (46)	295 (43)	215 (31)	140 (20)	90 (13)
IN-100	455 (66)	365 (53)	360 (52)	260 (38)	160 (23)	90 (13)
MAR-M 247 (MM 0011)	585 (85)	415 (60)	455 (66)	290 (42)	185 (27)	125 (18)
MAR-M 246	525 (76)	435 (62)	440 (63)	290 (42)	195 (28)	125 (18)
MAR-M 246 Hf(MM 006)	530 (77)	425 (62)	425 (62)	285 (41)	205 (30)	130 (19)
MAR-M 200	495 (72)	415 (60)	385 (56)	295 (43)	170 (25)	125 (18)
MAR-M 200 Hf(MM 009)	. . .	. . .	. . .	305 (44)	. . .	125 (18)
B-1900	510 (74)	380 (55)	385 (56)	250 (36)	180 (26)	110 (16)
Rene 77	. . .	. . .	310 (45)	215 (31.5)	130 (19)	62 (9.0)
Rene 80	. . .	. . .	350 (51)	240 (35)	160 (23)	105 (15)
IN-625	130 (19)	110 (16)	97 (14)	76 (11)	34 (5)	28 (4)
IN-162	505 (73)	370 (54)	340 (49)	255 (37)	165 (24)	110 (16)
IN-731	505 (73)	365 (53)	. . .	. . .	165 (24)	105 (15)
IN-792	515 (75)	380 (55)	365 (53)	260 (38)	165 (24)	105 (15)
M-22	515 (75)	385 (56)	395 (57)	285 (41)	200 (29)	130 (19)
MAR-M 421	450 (65)	305 (44)	310 (46)	215 (31)	125 (18)	83 (12)
MAR-M 432	435 (63)	330 (48)	295 (40)	215 (31)	140 (20)	97 (14)
MC-102	195 (28)	145 (21)	145 (21)	105 (15)	. . .	. . .
Nimocast 90	160 (23)	110 (17)	125 (18)	83 (12)	. . .	. . .
Nimocast 242	110 (16)	83 (12)	90 (13)	59 (8.6)	45 (6.5)	. . .
Udimet 500	330 (48)	240 (35)	230 (33)	165 (24)	90 (13)	. . .
Udimet 710	420 (61)	325 (47)	305 (44)	215 (31)	150 (22)	76 (11)
CMSX-2	. . .	. . .	. . .	345 (50)	. . .	170 (25)
GMR-235	. . .	. . .	. . .	180 (26)	. . .	75 (11)
IN-939	. . .	. . .	. . .	195 (28)	. . .	60 (9)
MM 002	. . .	. . .	. . .	305 (44)	. . .	125 (18)
IN-713 Hf(MM 004)	. . .	. . .	. . .	205 (30)	. . .	90 (13)
Rene 125 Hf(MM 005)	. . .	. . .	. . .	305 (44)	. . .	115 (17)
SEL-15	. . .	. . .	. . .	295 (43)	. . .	75 (11)
UDM 56	. . .	. . .	. . .	270 (39)	. . .	125 (18)
Cobalt-base						
HS-21	150 (22)	95 (14)	115 (17)	90 (13)	60 (9)	50 (7)
X-40 (HS-31)	180 (26)	140 (20)	130 (19)	105 (15)	75 (11)	55 (8)
MAR-M 509	270 (39)	225 (33)	200 (29)	140 (20)	115 (17)	90 (13)
FSX-414	150 (22)	115 (17)	110 (16)	85 (12)	55 (8)	35 (5)
WI-52	. . .	195 (28)	175 (25)	150 (22)	90 (13)	70 (10)

blade or vane component) and are known as columnar grain directionally solidified (CGDS) parts. On the other hand, a DS casting may have only one grain (single-crystal directionally solidified, or SCDS) with a specified crystal axis parallel to the airfoil major axis.

Castings are intrinsically stronger than forgings at elevated temperature. The coarse grain size of PC castings, as compared to finer-grained forgings, favors strength at high temperatures. In addition, casting compositions can be tailored effectively for high-temperature strength, inasmuch as forgeability characteristics are not applicable. For example, the highest creep-rupture strength at elevated temperatures can be achieved in nickel-base superalloy castings for high-stress, high-temperature turbine blade applications. The fine-grain structure of forgings, on the other hand, favors higher yield strengths and better low-cycle fatigue (LCF) strengths at low-to-intermediate temperatures, thus, the use of forgings in disk applications.

The Properties of Superalloys

General Comments. Strengthening in superalloys is by solid-solution hardening (substituted atoms interfere with deformation),

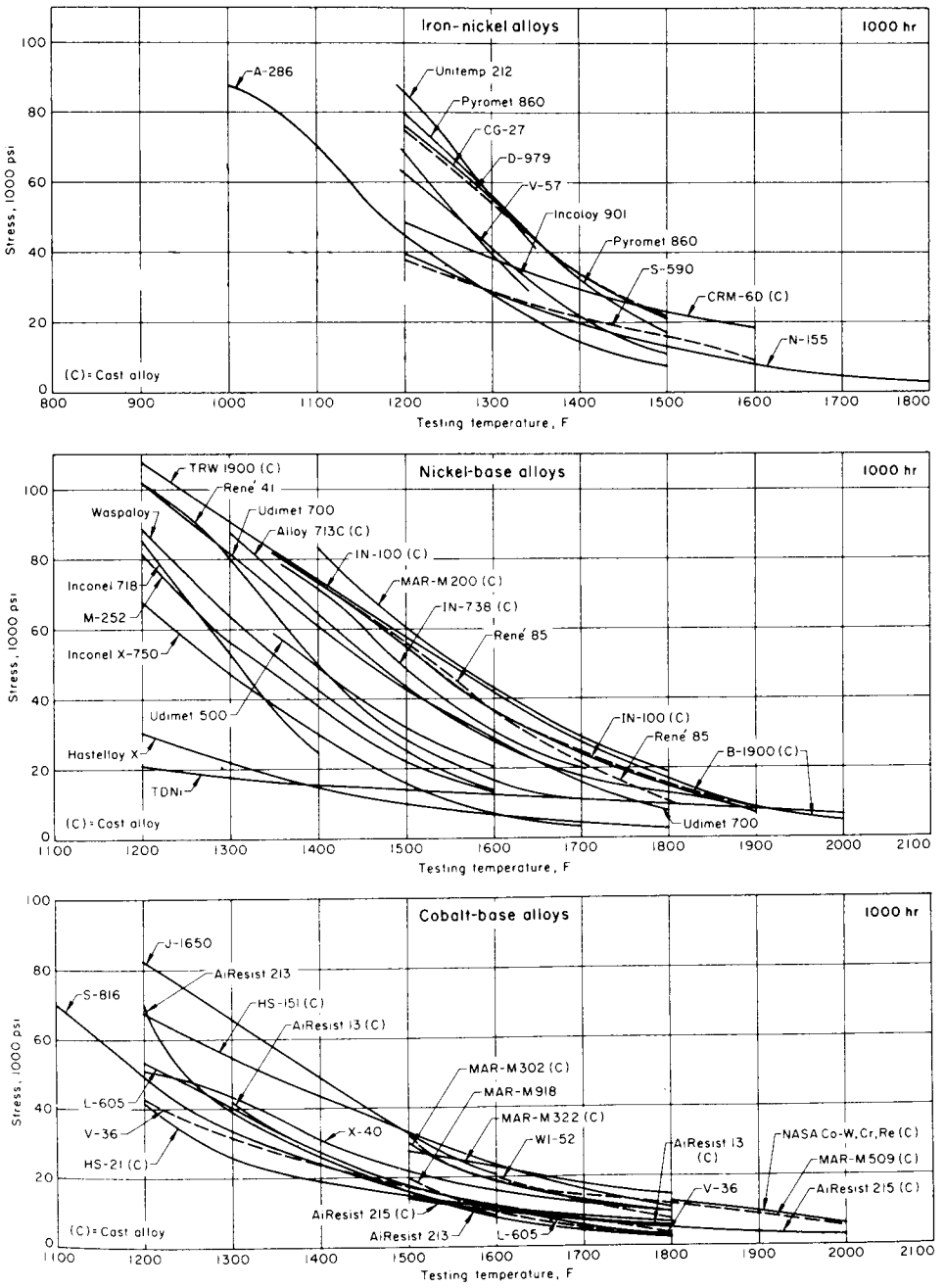


Fig. 2.1 Effect of temperature on 1000 h stress-rupture strength of a variety of superalloys plotted by alloy type

work hardening (energy is stored by deformation), and precipitation hardening (precipitates interfere with deformation). Carbide production (a favorable distribution of secondary phases interferes with deformation) also produces strength, particularly in cobalt-base superalloys. Strength is a relative term, defined by the type of strength needed. Thus, many applications require tensile yield or ultimate strengths (short-term properties), while others require creep-rupture strength (long-time property). Generally, the creep-

rupture strengths of the iron-nickel-base alloys and the nickel-base solid-solution-strengthened alloys are considerably lower than those of the nickel-base precipitation-strengthened and carbide-hardened cobalt-base alloys at temperatures above about 1200 °F (649 °C).

Modern Superalloys. Early iron-nickel-base superalloys, such as 16-25-6 alloy containing 16% Cr, 25% Ni, and 6% Mo, and the first Nimonic and Inconel series of nickel-base superalloys were essentially solid-solution strengthened. Subsequent iron-nickel- and nickel-base superalloys, containing small amounts (2 to 3%) of aluminum and titanium, achieved increased high-temperature strength through precipitation of an aluminum-titanium strengthening phase (γ'). Later nickel-base superalloys were able to accommodate larger amounts of aluminum (up to 6% or so), and much higher levels of high-temperature hardening were achieved with the higher volume fraction (V_f)γ' available. The highest hardener-content nickel-base superalloys became available as cast alloys, many today being made as CGDS and SCDS parts.

Some high hardener-content superalloys ($V_f\gamma'$ greater than about 40%) have been produced in wrought condition by P/M techniques. The iron-nickel-base superalloys peaked out in the 20+% V_f range of hardening γ' phases and do not compete with wrought nickel-base superalloys in the high end of the intermediate-temperature range today. Even alloys of near 40% $V_f\gamma'$ (e.g., Astroloy) no longer dominate the high intermediate-temperature range. P/M high $V_f\gamma'$ (~50%) alloys are the principal ones used today in the high intermediate-temperature range when wrought alloys are called out in design.

Because of a melting-point advantage, the PC cast cobalt-base superalloys are usually stronger than the nickel-base superalloys at temperatures above 2000 °F (1093 °C). This is not an absolute fact, because SCDS cast nickel-base alloys are capable of operation above 2000 °F (1093 °C) and have supplanted cobalt-base alloys in many instances. Cast cobalt-base alloys, characterized by a face-centered cubic (fcc, austenitic) solid-solution matrix and containing complex carbides, have had a successful history as airfoils for gas turbine engines (most as turbine vanes but some as turbine blades). Wrought cobalt-base alloys have found use as combustor parts in gas turbines.

Mechanical Properties and the Application of Superalloys. Because strength is a function of time, expected service time for an application as well as temperature influences the selection of a specific superalloy. The deterioration rate of some alloys with time is less than that for other alloys. For example, although oxide-dispersion-strengthened (ODS) nickel-base superalloys generally are not as strong as precipitation-strengthened nickel-base superalloys, they have a much flatter rate of creep-rupture strength reduction with time than the precipitation-strengthened alloys. Consequently, when superior resistance to strength degradation is required, and initial strength is acceptable, an ODS alloy might last longer than a standard precipitation-strengthened alloy.

For those interested in property comparisons, Tables 2.2 and 2.3 may afford an opportunity to plot data and make a visual observation of the relative merits of the tensile behavior of some alloys or alloy types. A visual picture also can be obtained for rupture behavior of a few alloys, including some no longer active, by referring to Figs. 2.2 and

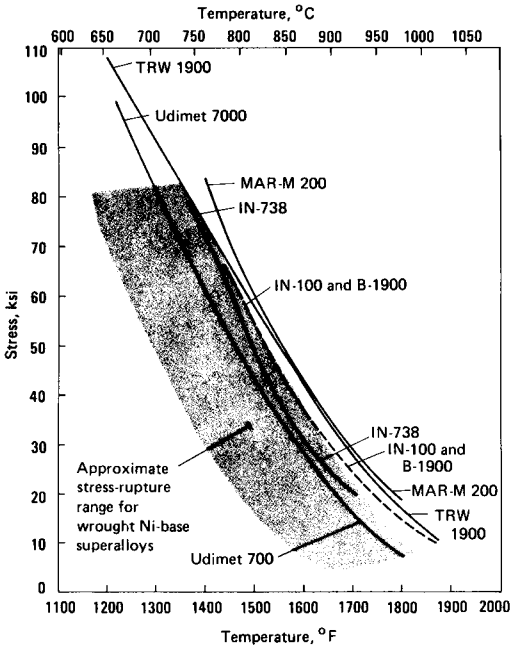


Fig. 2.2 Stress-rupture (1000 h) strengths vs. temperature for some nickel-base superalloys

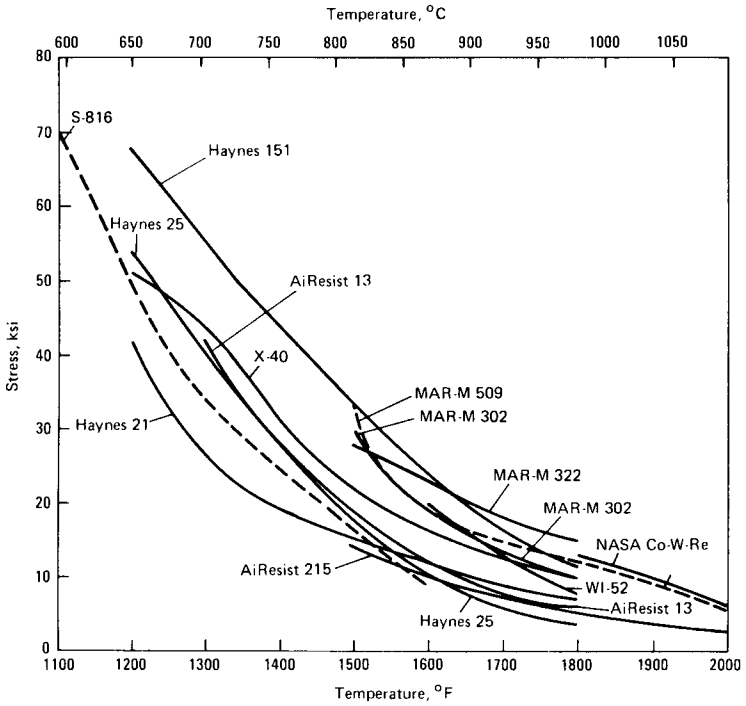


Fig. 2.3 Stress-rupture (1000 h) strengths vs. temperature for some cobalt-base superalloys

2.3. The figures show rupture strengths versus temperature for some alloys in the nickel-base and cobalt-base alloy types, respectively. Figure 2.1 does the same for all three types of superalloys. A modified version of Fig. 1.1 is given as Fig. 2.4, which adds the capability of an ODS alloy to the comparison.

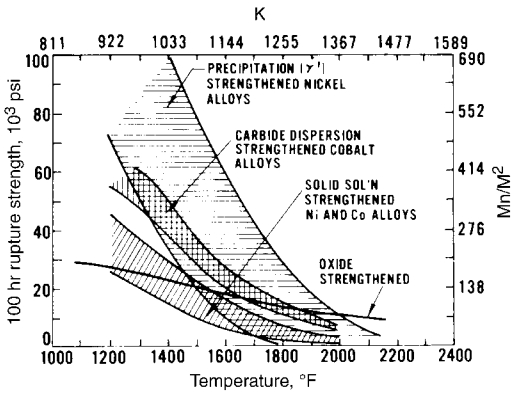


Fig. 2.4 Stress-rupture strengths of conventional superalloys, with oxide-dispersion-strengthened behavior illustrated for comparison

It should be noted that, while tensile and stress-rupture data sets are available for a wide range of alloys, creep-rupture data sets are virtually nonexistent. Many designs are concerned with the creep behavior of an alloy. Some concern themselves with creep rate; other designs with time to a fixed percent creep. An alloy that may have a longer rupture life and, hence, a greater stress-rupture capability, may for certain parts of its creep range be inferior to another alloy or another form of an alloy. Columnar grain directional solidification of an alloy can produce situations where the low-strain creep strength of a PC version of an alloy can exceed that of the CGDS version. For more on the properties of superalloys, see Chapter 12.

The superalloys are relatively ductile, although the ductilities of cobalt-base superalloys generally are less than those of iron-nickel- and nickel-base superalloys. Iron-nickel- and nickel-base superalloys are readily available in extruded, forged, or rolled form; the higher-strength alloys generally are found only in the cast condition. Hot deformation is the preferred forming pro-

cess, cold forming usually being restricted to thin sections (sheet). Cold rolling may be used to increase short-time strength properties for applications at temperatures below the lower-temperature level of about 1000 °F (540 °C) established in this chapter for superalloy use.

Superalloys typically have moduli of elasticity in the vicinity of 30×10^6 psi (207 GPa), although moduli of specific PC alloys can vary from 25 to 35×10^6 psi (172 to 241 GPa) at room temperature depending on the alloy system. Processing that leads to directional grain or crystal orientation can result in moduli of about 18 to 45×10^6 psi (about 124 to 310 GPa) depending on the relation of grain or crystal orientation to testing direction. The lower moduli result from DS processes.

Physical Properties and Density. The physical properties, electrical conductivity, specific heat, thermal conductivity, and thermal expansion sometimes tend to be low (relative to other metal systems). These properties are influenced by the nature of the base metals (transition elements) and the presence of refractory-metal additions. As noted in Chapter 1, iron-nickel-base superalloys can have densities of about 0.285 to 0.300 lb/in.^{3} (7.9 to 8.3 g/cm^3); cobalt-base superalloys, about 0.300 to 0.340 lb/in.^{3} (8.3 to 9.4 g/cm^3); and nickel-base superalloys, about 0.282 to 0.322 lb/in.^{3} (7.8 to 8.9 g/cm^3). Density can be important in aircraft gas turbines where increased density can result in increased stress on mating components. Increases achieved in alloy capability can be negated if a large density increase results as well. Modern cast nickel-base superalloys tend to have densities in the high end of the density range.

Selecting Superalloys

Intermediate-Temperature Applications—Wrought Alloys. Intermediate temperatures imply a range from about 1000 up to about 1400 °F (540 up to 760 °C). If alloys to be used are intended for massive applications, such as turbine disks, high tensile yield and ultimate strength are desired. Good tensile ductility is important, and good mechanical LCF behavior with acceptable crack propagation rates at expected load are a must. If an alloy is to be used as sheet, then good formability is a must, coupled with good weldability. Massive parts, such as disks, can benefit from good forgeability, but such a quality does not exist when high tensile strengths are required. Powder metallurgy processing enables production of forged components not otherwise processable.

Inspectability of sonic-finished shapes is crucial. Cost is a very important factor, but one that may have to be subverted to properties and processing if a desired component is to be made. Of course, use of special processing techniques such as P/M may enable a part to be formed that could not be made in any other way, and so, a high cost may be worth paying.

The essence of superalloy selection for intermediate-temperature applications is that there are standard alloys of capability similar to Waspaloy and down that can be procured and forged by conventional means. Similarly, sheet alloys are available that can be manipulated in conventional ways. For the higher-strength applications, there are no easy off-the-shelf technologies or alloys that can just be picked from a catalog and put to work. Selection of alloys is a preliminary step that must be expanded upon to get data and components in a reasonable time frame at acceptable costs.

High-Temperature Applications—Cast Alloys. High temperature can be considered to be about 1500 °F (816 °C) and up to the melting point of an alloy. Gas turbine airfoils experience temperatures in this range. If alloys are to be used for turbine airfoils, high creep and creep-rupture strengths are required. To maximize strength, the alloys for the most demanding applications in high-pressure turbine (HPT) sections should be SCDS materials. In addition to maximizing creep-rupture strength, thermal mechanical fatigue (TMF) strength is optimized by the reduction in modulus achieved by orienting a particular direction of the superalloy crystal parallel to the airfoil axis. An alloy for the most stringent turbine airfoil applications will have a high melting point, good-to-excellent oxidation resistance, high creep-rupture and TMF strength, the ability to accept a coating, and good LCF strength at temperatures where the airfoil attachment is made to a disk. These latter temperatures are about 1400 °F (760 °C) or somewhat less.

Single-crystal directionally solidified processing will also ensure that thin section properties are optimized. As section thickness is reduced, for a fixed load, a superalloy ruptures in less time than a standard thick test bar would fail. The order of property reduction is PC equiaxed = most, CGDS = less, and SCDS = least.

For turbine vanes where no centrifugal load exists, airfoils may be made from PC equiaxed high-strength cast cobalt-base alloys instead of DS processed nickel-base alloys. High incipient melting temperature is desired for first-stage turbine vanes. A special type of superalloy, an ODS alloy, has been used for turbine vanes in some applications. MA-754 relies on yttria dispersed in a corrosion-resistant nickel-chromium matrix to provide adequate creep-rupture capability. Oxide-dispersion-strengthened alloys are not common. MA-6000 is another such alloy that may have enough strength for a high-pressure turbine blade in aircraft gas turbines.

A problem with PC equiaxed airfoils is that the thermal-mechanical stresses are much higher than on CGDS or SCDS parts, owing to the higher modulus of PC equiaxed parts. The modulus of the CGDS and SCDS parts may be only 60% of the value for the PC equiaxed nickel-base cast alloys. In the most demanding conditions, TMF problems must be minimized by using DS-produced oriented grain or crystal structures to reduce stresses.

For low-pressure turbine (LPT) airfoils, alloys such as the IN-100 (Rene 100) or IN-792 and Rene 80 PC equiaxed alloys previously used for HPT airfoils may be chosen. If temperatures or stress conditions are sufficiently relaxed, IN-713, U-700, or similar first-generation PC equiaxed cast materials may suffice.

An Example of Gas Turbine Disks. A schematic of a typical gas turbine is shown in Fig. 2.5. Note that the hot sections occur near the rear of the engine. Typical gas turbine parts made from superalloys consist of the following components.

A power train in which there are:

- Shafts (which are turned by)
- Disks or wheels (attached to the shafts)
- Blades or buckets (attached to the disks)
- Vanes or stators (attached to the engine frame)

Combustion systems for burning fuel in:

- Burner cans or combusters (attached to the engine frame—may contain multiple parts)

Consider a disk for the hot section (HPT and LPT, respectively) of a gas turbine. A disk is a component attached to a shaft and that turns the shaft or is turned by it, dependent on location in an engine. The disks being considered here would turn the shafts. An HPT disk has blades attached, and gas pressure on the blades rotates the disk/shaft and powers a section of the high-pressure compressor (HPC). The various requirements that might have to be met in the choice of material for an HPT disk for a gas turbine engine, are:

Probable primary design criteria

- Yield
- Burst
- Creep
- Low-cycle fatigue
- Crack growth rate

Probable secondary design criteria

- Fabricability
- Cost
- High-cycle fatigue
- Stress corrosion
- Fracture toughness

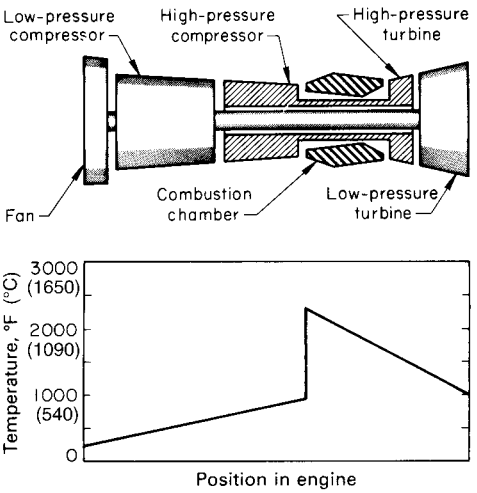


Fig. 2.5 Schematic of gas turbine engine showing principal sections and the general operating temperatures related to section position

An alloy with the best ductility and uniformity of properties is indicated for the disk because of the criticality of the application. (A disk fracture is a major event, leading to potential aircraft failure.) Wrought alloys have better ductility and higher tensile properties than cast alloys, as noted earlier.

High yield and ultimate strengths are required to resist the high centrifugal forces caused by rapid rotation and the mass of the disk and its attached blades. At the same time, mechanical and thermal cycling on loading produce fatigue conditions in the disk. This fatigue is LCF and is found at the high-stress, low-cycle ranges of load application. The material selected may have to operate in the range of 1000 to 1400 °F (540 to 760 °C). Steels are out of the question, as are titanium alloys. Wrought iron-nickel-base alloys are a possibility, as are wrought or P/M nickel-base alloys. Cast alloys are not a satisfactory choice, owing to reduced ductility, lower strengths, and greater inhomogeneity and defect possibilities.

By checking the available yield and ultimate strengths, numerous alloys might be suggested, and many have been used. However, brute strength and LCF capability are not the only requirements. Creep becomes a concern at the rims of the disks as the temperatures approach 1400 °F (760 °C). Thus, iron-nickel-base superalloys, which are good to about 1200 °F (649 °C), will compete for the lower-temperature disks, but nickel-base superalloys are required for the higher-temperature disks, because nickel-base superalloys have superior creep (and rupture) resistance. On the other hand, the iron-nickel-base superalloys are easier to forge than the nickel-base superalloys. Cobalt-base superalloys are not in contention here, because their much lower strength capability is not even close to the strength requirements for turbine disk applications.

An additional factor in the selection of an alloy for this disk application becomes the cost and availability of material. An example is the prevalence of IN-718 as the standard low intermediate-temperature turbine disk in aircraft gas turbine engines. Up until about 1975, IN-718 had wide acceptance but not necessarily better properties overall than some competitive materials. However, the alloy has less nickel in it than other alloys and does not contain cobalt. Thus, it was cheaper to make and somewhat more readily available than other competitive alloys at that time. When a cobalt shortage and attendant high alloy prices occurred in the latter part of the 1970s, more designers switched to IN-718. Of course, the more IN-718 that was desired, the more that manufacturers made, and so IN-718 became the premier wrought iron-nickel-base superalloy, in fact, the premier wrought superalloy in the world. Cost and availability, accompanied by excellent strength properties to about 1200 °F (649 °C), have made IN-718 the world standard for use as gas turbine disks.

To summarize the selection process, an alloy with maximum designer confidence in homogeneity and ductility was desired, and wrought alloys fit the bill; forgeability of IN-718 was good. Yield and ultimate strengths plus LCF resistance were quite satisfactory; creep resistance was adequate to the desired maximum application temperature. The alloy was available, had fewer strategic elements, and cost less than competitor alloys. Consequently, IN-718 is the alloy of choice for a majority of gas turbine disks.

Superalloys: A Technical Guide, Second Edition
Matthew J. Donachie, Stephen J. Donachie, p 25-39
DOI:10.1361/stgs2002p025

Copyright © 2002 ASM International®
All rights reserved.
www.asminternational.org

Chapter 3

Understanding Superalloy Metallurgy

Groups, Crystal Structures, and Phases

Superalloy Groups. As noted earlier, there are three groups of superalloys (iron-nickel-, nickel-, and cobalt-base), which are further subdivided into cast and wrought (where wrought includes powder metallurgy processing) macrostructures. In addition to macrostructure, there are crystal structure (on an atomic level) and microstructure (visible under the microscope). Metals tend to have relatively simple crystal structures.

Crystal Structures. When hard sphere models representing the crystal structures of most metals are constructed, the atom positions (seen as the hard spheres in the example of Fig. 3.1) are set in a few basic alignments. Face-centered cubic (fcc), body-centered cubic (bcc), and hexagonal close-packed (hcp) more or less cover the gamut of common metal crystal structures. If body-centered tetragonal (bct) is added to the list, then the superalloys have been covered fairly well, except for delta phase and the complex phases such as sigma (σ). There is no special need to describe the crystal structure of all phases. Sometimes, when more than one element is present (as in an alloy), a structure may be ordered. The nature of order is that specific crystallographic locations are now required for given elements. For example, if a material has a secondary phase such as Ni_3Al, the Ni_3Al will be ordered. That is, the fcc crystal structure will now have nickel atoms at the face positions and aluminum atoms at the corners. Figure 3.2 shows ordering. Ordering is very important in the strengthening of superalloys.

Phases in Superalloys. Superalloys consist of the austenitic fcc matrix phase γ plus a variety of secondary phases. Secondary phases of value in controlling properties are the fcc carbides MC, $M_{23}C_6$, M_6C, and M_7C_3 (rare) in virtually all superalloy types; gamma prime (γ′) fcc ordered $Ni_3(Al,Ti)$; gamma double prime (γ″) bct ordered Ni_3Nb; eta (η) hexagonal ordered Ni_3Ti; and the delta (δ) orthorhombic Ni_3Nb intermetallic compounds in nickel- and iron-nickel-base superalloys. The γ′, γ″, and η phases also are known as geometrically close-packed (gcp) phases. In addition to grain size and morphology, (plus occasional cold work) it is the production and control (manipulation) of the various phases that give superalloys their unique characteristics.

The superalloys derive their strength mostly from solid-solution hardeners and precipitated phases. Principal strengthening precipitate phases are γ′ and γ″, which are found in iron-nickel- and nickel-base superalloys. Carbides may provide limited strengthening directly (e.g., through dispersion hardening) or, more commonly, indirectly (e.g., by stabilizing grain boundaries against excessive shear). Carbides are found in all three superalloy groups. The δ and η phases are useful (along with γ′) in control of structure of wrought iron-nickel- and nickel-base superalloys during processing. The extent to which they contribute directly to strengthening de-

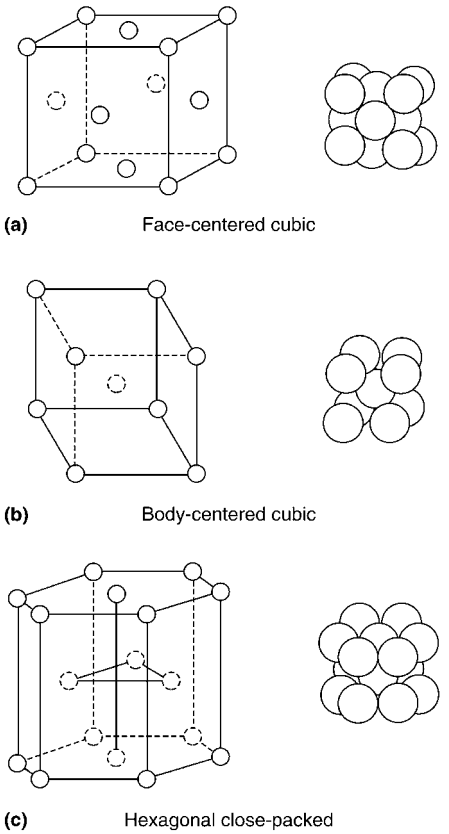


Fig. 3.1 Line sketches (left) and hard sphere atomic models (right) of crystal structures

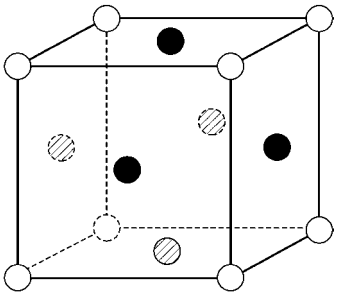


Fig. 3.2 Line sketch of an ordered fcc crystal structure of γ' phase. ● (solid circles) = nickel atoms, shared with adjacent cube. ○ (open circles) = aluminum or titanium atoms, shared with eight cubes at each corner. --- (dotted lines) show hidden atoms. Nickel atoms are always on faces; titanium or aluminum atoms are always at cube corners, in contrast to disordered structures where atoms may occupy any given location.

pends on the alloy and its processing. In addition to those elements that produce solid-solution hardening and/or promote carbide and γ' formation, other elements (e.g., boron, zirconium, and hafnium) are added to enhance mechanical or chemical properties. These minor elements are not customarily found in most cobalt-base alloys. Some carbide- and γ'-forming elements may contribute significantly to chemical properties as well. Borides may form in the iron-nickel- and nickel-base superalloys.

Detrimental phases also form in the superalloys. Among these phases are σ, μ, and Laves. These phases are so-called topologically close-packed (tcp) phases and may not be of concern in trace amounts, but are invariably detrimental when more than trace amounts are present.

Table 3.1 summarizes data on the commonly encountered phases in iron-nickel- and nickel-base superalloys. Additional tabular information on phases is provided in Tables 3.2, 3.3, and Appendix B.

Introduction to the Alloy Groups

Iron-Nickel-Base Superalloys. The most important class of iron-nickel-base superalloys includes those alloys that are strengthened by intermetallic compound precipitation in an fcc matrix. The most common precipitate is γ', typified by A-286, V-57, or Incoloy 901. Some alloys, such as Inconel (IN) 718, which precipitate γ' and γ'', were classed as iron-nickel-base but now are considered to be nickel-base (sometimes nickel-iron-base is used). Other iron-nickel-base superalloys consist of modified stainless steels primarily strengthened by solid-solution hardening. Alloys in this last category vary from 19-9DL (18-8 stainless with slight chromium and nickel adjustments, additional solution hardeners, and higher carbon) to Incoloy 800H (21% Cr, high nickel with small additions of titanium and aluminum, which produces some γ' phase). At the current time iron-nickel-base superalloys invariably are used in the wrought condition.

Nickel-Base Superalloys. Although there are solid-solution-hardened nickel-base su-

Table 3.1 Phases observed in superalloys

Phase	Crystal structure	Lattice parameter, nm	Formula	Comments
γ'	fcc (ordered $L1_2$)	0.3561 for pure Ni_3A1 to 0.3568 for $Ni_3(A1_{0.5}Ti_{0.5})$	Ni_3A1Ni_3(A1, Ti)	Principal strengthening phase in many nickel- and nickel-iron-base superalloys; crystal lattice varies slightly in size (0 to 0.5%) from that of austenite matrix; shape varies from spherical to cubic; size varies with exposure time and temperature. Gamma prime is spherical in iron-nickel-base and in some of the older nickel-base alloys, such as Nimonic 80A and Waspaloy. In the more recently developed nickel-base alloys, γ' is generally cuboidal. Experiments have shown that variations in molybdenum content and in the aluminum/titanium ratio can change the morphology of γ'. With increasing γ/γ' mismatch, the shape changes in the following order: spherical, globular, blocky, cuboidal. When the γ/γ' lattice mismatch is high, extended exposure above 700 °C (1290 °F) causes undesirable η (Ni_3Ti) or δ (Ni_3Nb) phases to form.
η	hcp ($D0_{24}$)	a_0 = 0.5093 c_0 = 0.8276	Ni_3Ti (no solubility for other elements)	Found in iron-nickel-, cobalt-, and nickel-base superalloys with high titanium/aluminum ratios after extended exposure; may form intergranularly in a cellular form or intragranularly as acicular platelets in a Widmanstätten pattern
γ''	bct (ordered $D0_{22}$)	a_0 = 0.3624 c_0 = 0.7406	Ni_3Nb	Principal strengthening phase in Inconel 718; γ'' precipitates are coherent disk-shaped particles that form on the {100} planes (avg diam approximately 600 Å, thickness approximately 50 to 90 Å). Bright-field transmission electron microscopy (TEM) examination is unsatisfactory for resolving γ'' due to the high density of the precipitates and the strong contrast from the coherency strain field around the precipitates. However, dark-field TEM examination provides excellent imaging of the γ'' by selective imaging of precipitates that produce specific superlattice reflections. In addition, γ'' can be separated from γ' using the dark-field mode, because the γ'' dark-field image is substantially brighter than that of γ'.
Ni_3Nb (δ)	Orthorhombic (ordered Cu_3Ti)	a_0 = 0.5106–0.511 b_0 = 0.421–0.4251 c_0 = 0.452–0.4556	Ni_3Nb	Observed in overaged Inconel 718; has an acicular shape when formed between 815 and 980 °C (1500 and 1800 °F); forms by cellular reaction at low aging temperatures and by intragranular precipitation at high aging temperatures
MC	Cubic	a_0 = 0.430–0.470	TiC NbC HfC	Titanium carbide has some solubility for nitrogen, zirconium, and molybdenum; composition is variable; appears as globular, irregularly shaped particles that are gray to lavender; ''M'' elements can be titanium, tantalum, niobium, hafnium, thorium, or zirconium.
$M_{23}C_6$	fcc	a_0 = 1.050–1.070 (varies with composition)	$Cr_{23}C_6$ $(Cr, Fe, W, Mo)_{23}C_6$	Form of precipitation is important; it can precipitate as films, globules, platelets, lamellae, and cells; usually forms at grain boundaries; ''M'' element is usually chromium, but nickel-cobalt, iron, molybdenum, and tungsten can substitute.
M_6C	fcc	a_0 = 1.085–1.175	Fe_3Mo_3C Fe_3W_3C-Fe_4W_2C Fe_3Nb_3C Nb_3Co_3C Ta_3Co_3C	Randomly distributed carbide; may appear pinkish: ''M'' elements are generally molybdenum or tungsten; there is some solubility for chromium, nickel, niobium, tantalum, and cobalt.
M_7C_3	Hexagonal	a_0 = 1.398 c_0 = 0.4523	Cr_7C_3	Generally observed as a blocky intergranular shape; observed in alloys such as Nimonic 80A after exposure above 1000 °C (1830 °F), and in some cobalt-base alloys

(continued)

Table 3.1 (continued)

Phase	Crystal structure	Lattice parameter, nm	Formula	Comments
M_3B_2	Tetragonal	a_0 = 0.560–0.620 c_0 = 0.300–0.330	Ta_3B_2 V_3B_2 Nb_3B_2 (Mo, Ti, Cr, Ni, Fe)$_3B_2$ Mo_2FeB_2	Observed in iron-nickel- and nickel-base alloys with about 0.03% B or greater; borides appear similar to carbides, but are not attacked by perferential carbide etchants; ''M'' elements can be molybdenum, tantalum, niobium, nickel, iron, or vanadium.
MN	Cubic	a_0 = 0.4240	TiN (Ti, Nb, Zr)N (Ti, Nb, Zr)(C, N) ZrN NbN	Nitrides are observed in alloys containing titanium, niobium or zirconium; they are insoluble at temperatures below the melting point; easily recognized as-polished, having square to rectangular shapes and ranging from yellow to orange
μ	Rhombohedral	a_0 = 0.475 c_0 = 2.577	Co_2W_6 (Fe, Co)$_7$(Mo, W)$_6$	Generally observed in alloys with high levels of molybdenum or tungsten; appears as coarse, irregular Widmanstätten platelets; forms at high temperatures
Laves	Hexagonal	a_0 = 0.475–0.495 c_0 = 0.770–0.815	Fe_2Nb Fe_2Ti Fe_2Mo Co_2Ta Co_2Ti	Most common in iron-base and cobalt-base superalloys; usually appears as irregularly shaped globules, often elongated, or as platelets after extended high-temperature exposure
σ	Tetragonal	a_0 = 0.880–0.910 c_0 = 0.450–0.480	FeCr FeCrMo CrFeMoNi CrCo CrNiMo	Most often observed in iron-nickel- and cobalt-base superalloys, less commonly in nickel-base alloys; appears as irregularly shaped globules, often elongated; forms after extended exposure between 540 and 980 °C (1005 to 1795 °F)

peralloys, the most important class of nickel-base superalloys is that strengthened by intermetallic compound precipitation in an austenitic fcc matrix. For alloys with titanium and aluminum, the strengthening precipitate is γ′. Such alloys are typified by the wrought alloys Waspaloy, Astroloy, U-700, and U-720, or the cast alloys Rene 80, Mar-M-247, and IN-713. For niobium-strengthened nickel-base superalloys, the strengthening precipitate is γ″. These γ″-hardened alloys are typified by IN-718. Some nickel-base alloys may contain niobium plus titanium and/or aluminum and use both γ′ and γ″ precipitates in strengthening. Alloys of this type are IN-706 and IN-909. These three alloys (IN-718, IN-706, and IN-909) may sometimes be found listed as iron-nickel-base (or nickel-iron-base) superalloys.

The class of nickel-base superalloys that is essentially solid-solution strengthened is typified by such alloys as Hastelloy X and IN-625. The solid-solution-strengthened nickel-base alloys may derive some additional strengthening from carbide and/or intermetallic compound precipitation.

A third class of nickel-base superalloys includes oxide-dispersion-strengthened (ODS) alloys such as IN-MA-754 and IN-MA-6000E, which are strengthened by dispersion of inert particles such as yttria, coupled in some cases with γ′ precipitation (MA-6000E).

Nickel-base superalloys are used in both cast and wrought forms, although special processing (powder metallurgy/isothermal forging) frequently is used to produce wrought versions of the more highly alloyed compositions (Rene 95, Astroloy, and IN-100). An additional dimension of nickel-base superalloys has been the introduction of morphological (grain-aspect ratio and orientation) control as a means of improving properties. In fact, in some instances, grain boundaries have been removed (see discussion of investment casting in Chapter 5). Wrought powder metallurgy alloys of the ODS class and cast alloys such as MAR-M-247 have demonstrated property improvements, owing to control of grain morphology by directional recrystallization or directional solidification.

Table 3.2 Compositional ranges of major alloying additions in superalloys

Element	Range, %	
	Fe-Ni- and Ni-base	Co-base
Cr	5–25	19–30
Mo, W	0–12	0–11
Al	0–6	0–4.5
Ti	0–6	0–4
Co	0–20	. . .
Ni	. . .	0–22
Nb	0–5	0–4
Ta	0–12	0–9
Re	0–6	0–2

Cobalt-Base Superalloys. The cobalt-base superalloys are invariably strengthened by a combination of carbides and solid-solution hardeners. The essential distinction in these alloys is between cast and wrought structures. Cast alloys are typified by X-40 and wrought alloys by L-605 (HA-25). No intermetallic compound possessing the same degree of utility as the γ' precipitate in nickel- or iron-nickel-base superalloys has been found to be operative over a wide range in cobalt-base systems.

Alloy Elements and Microstructural Effects in Superalloys

Introduction. Properties in superalloys usually are developed (for a given composition) by a combination of cast/wrought processing followed by heat treatment. Chemistry is very important in providing for the level of strength and corrosion properties that may be achieved. However, the processing steps are the key to achieving optimal properties in superalloys.

Grain structure is developed by processing. Microstructural changes are invariably produced by dissolving all or most of the carbides and other intermetallic precipitate phases (e.g., γ' or δ) and then causing their redistribution in an appropriate form. Grain size in castings is a direct function of the casting process and, except for polycrystalline alloys, is not capable of being varied much. Wrought alloy grain sizes can be varied over a wider range. Wrought alloy grain sizes tend to be smaller than grain sizes in cast alloys, as noted previously. Microstructure includes not only grain size and morphology but also the type and distribution of secondary phases in the superalloy austenitic matrix.

Major Elements in Superalloys. Superalloys contain a variety of elements in a large number of combinations to produce desired effects. Table 3.2 lists common ranges for major alloy element additions while Table 3.3 lists the role of some alloy elements in su-

Table 3.3 Role of alloying elements in superalloys

Effect(a)	Iron-base	Cobalt-base	Nickel-base
Solid-solution strengtheners	Cr, Mo	Nb, Cr, Mo, Ni, W, Ta	Co, Cr, Fe, Mo, W, Ta, Re
fcc matrix stabilizers	C, W, Ni	Ni	. . .
Carbide form:			
MC	Ti	Ti	W, Ta, Ti, Mo, Nb, Hf
M_7C_3	. . .	Cr	Cr
$M_{23}C_6$	Cr	Cr	Cr, Mo, W
M_6C	Mo	Mo, W	Mo, W, Nb
Carbonitrides: M(CN)	C, N	C, N	C, N
Promotes general precipitation of carbides	P	. . .	. . .
Forms γ' Ni_3(Al, Ti)	Al, Ni, Ti	. . .	Al, Ti
Retards formation of hexagonal η (Ni_3Ti)	Al, Zr	. . .	. . .
Raises solvus temperature of γ'	. . .	. . .	Co
Hardening precipitates and/or intermetallics	Al, Ti, Nb	Al, Mo, Ti(b), W, Ta	Al, Ti, Nb
Oxidation resistance	Cr	Al, Cr	Al, Cr, Y, La, Ce
Improve hot corrosion resistance	La, Y	La, Y, Th	La, Th
Sulfidation resistance	Cr	Cr	Cr, Co, Si
Improves creep properties	B	. . .	B, Ta
Increases rupture strength	B	B, Zr	B(c)
Grain-boundary refiners	. . .	. . .	B, C, Zr, Hf
Facilitates working	. . .	Ni_3Ti	. . .
Retard γ' coarsening	. . .	. . .	Re

(a) Not all these effects necessarily occur in a given alloy. (b) Hardening by precipitation of Ni_3Ti also occurs if sufficient Ni is present. (c) If present in large amounts, borides are formed.

peralloys. Some elements go into solid solution to provide one or more of the following: strength (molybdenum, tantalum, tungsten, and rhenium); oxidation resistance (chromium and aluminum); hot corrosion resistance (titanium); phase stability (nickel); and increased volume fractions (V_f) of favorable secondary precipitates (cobalt). Other elements are added to form hardening precipitates such as γ' (aluminum and titanium) and γ'' (niobium). A major addition to nickel-base superalloy chemistry in recent years has been the element rhenium, which has extended the temperature capability of the columnar grain directionally solidified (CGDS) and single-crystal directionally solidified (SCDS) casting alloys. Rhenium appears to produce these improvements by significantly reducing the coarsening rate for γ'.

Beneficial Minor Elements in Superalloys. Minor elements (carbon and boron) are added to form carbides and borides; these and other elements (e.g., magnesium) are added for purposes of tramp-element control. Some elements (boron, zirconium, and hafnium) also are added to promote grain-boundary effects other than precipitation or carbide formation. Lanthanum has been added to some alloys to promote oxidation resistance, and yttrium has been added to coatings to enhance coating life.

Elements Causing Brittle Phase Formation. Many elements (cobalt, molybdenum, tungsten, rhenium, chromium, etc.), although added for their favorable alloying qualities, can participate, in some circumstances, in undesirable tcp phase formation (σ, μ, Laves, etc.). The tcp phases usually have low ductility (are brittle) and cause loss of mechanical (and sometimes corrosion) properties when present in anything more than trace amounts.

Detrimental Tramp Elements in Superalloys. Elements such as silicon, phosphorus, sulfur, lead, bismuth, tellurium, selenium, and silver, often in amounts as low as the parts-per-million level, have been associated with property-level reductions in superalloys, but they are not visible optically or with an electron microscope. Microprobe and Auger spectroscopic analyses have determined that grain boundaries can be decorated with tramp elements at high local concentrations. Elements such as magnesium tend to tie up and remove some detrimental elements such as sulfur in the form of a compound, and titanium tends to tie up the element nitrogen as TiN. In such cases, these and other similar compounds often are visible in the microstructure.

Elements Producing Oxidation and Hot Corrosion Resistance. All true superalloys contain some chromium plus other elements to promote resistance to environmental degradation. The role of chromium is to promote Cr_2O_3 formation on the external surface of an alloy. When sufficient aluminum is present, formation of the more protective oxide, Al_2O_3, is promoted when oxidation occurs. A chromium content of 6 to 22 wt% generally is common in nickel-base superalloys, whereas a level of 20 to 30 wt% Cr is characteristic of cobalt-base superalloys, and a level of 15 to 25 wt% Cr is found in iron-nickel-base superalloys. Amounts of aluminum up to about 6 wt% may be present in nickel-base superalloys. Chromium is the principal element needed for hot corrosion resistance, but titanium and, perhaps, other elements may supplement the chromium effects.

Alloying Element Summary. The major alloying elements that may be present in nickel-base superalloys are illustrated in Fig. 3.3. The height of the element blocks indicates the amounts that may be present.

Microstructure

Introduction. The evolution of microstructure has been much more pronounced in the iron-nickel-base and nickel-base superalloys than in cobalt-base alloys. Some of the elements mentioned previously produce readily discernible changes in microstructure; other elements produce more subtle microstructural effects. The precise microstructural effects produced are functions of processing and heat treatment. The most obvious microstruc-

tural effects involve precipitation of gcp phases such as γ', formation of carbides, and formation of tcp phases such as σ.

Summary of Phases in Iron Nickel- and Nickel-Base Superalloys. The major phases and form of occurrence in iron-nickel- and nickel-base alloys are:

- γ matrix, in which the continuous matrix is an fcc nickel-base nonmagnetic phase that usually contains a high percentage of solid-solution elements such as cobalt, iron, chromium, molybdenum, and tungsten. All nickel-base alloys contain this phase as the matrix.
- γ' formed from aluminum and titanium, which react with nickel to precipitate a phase coherent with the austenitic gamma matrix. Other elements, notably niobium, tantalum, and chromium, also enter γ'. This is the principal high-temperature strengthening phase. It appears as spheres or cuboids when properly formed.
- γ' films along grain boundaries in some wrought and cast alloys; produced by heat treatments and service exposure. These films may be beneficial for creep-rupture properties.
- γ' in rafts (elongated γ' in the grain) may be produced by initial heat treatment or by extended service operation. These rafts may be useful for increasing creep-rupture properties.
- γ'', in which nickel and niobium combine in the presence of iron to form bct Ni_3Nb, which is coherent with the gamma matrix, while inducing large mismatch strains (of the order of 2.9%). This phase provides very high strength at low-to-intermediate temperatures, but it is unstable at temperatures above about 1200 °F (649 °C). This precipitate is found in only a few nickel-(nickel-iron-) base alloys.
- Carbides, where carbon in amounts of about 0.02 to 0.2 wt% combines with reactive elements, such as titanium, tantalum, hafnium, and niobium, to form metal carbides. There are several carbide phases. During heat treatment and service, MC carbides tend to decompose and generate other carbides, such as $M_{23}C_6$ and/or M_6C, which tend to form at grain boundaries. Carbides in nominal solid-solution alloys may form after extended service exposures.
- Borides, where a relatively low density of boride particles may be formed when bo-

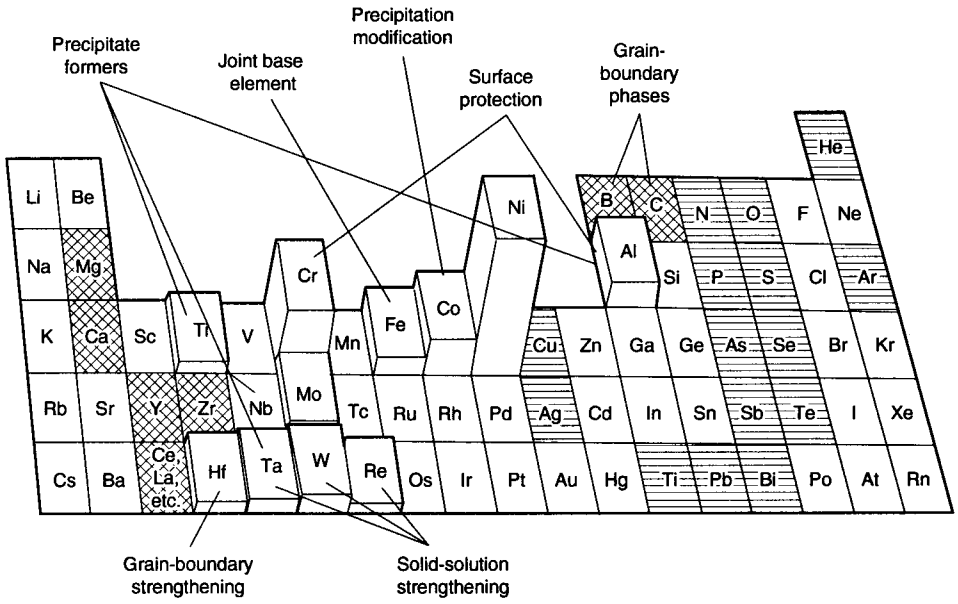


Fig. 3.3 Alloying elements used in nickel-base superalloys. Beneficial minor elements are marked with cross-hatch, while detrimental tramp elements are marked with horizontal line hatch.

ron segregates to grain boundaries. There are several boride phases. Generally, boride phases in minute amounts are favorable for creep-rupture properties.
- tcp phases, which are usually platelike or needlelike phases such as σ and Laves that may form for some compositions and under certain conditions. These phases can cause lowered rupture strength and ductility. The likelihood of their presence increases as the solute segregation of the ingot increases.

How Microstructures Evolved. Microstructural phase morphology can vary widely, for example, script versus blocky carbides, cuboidal versus spheroidal γ′, cellular versus uniform precipitation, acicular versus blocky σ, and discrete γ′ versus γ′ envelopes (films). Initial microstructures of all superalloys contained some amount of carbide, dependent on the carbon content of the material, with cobalt alloys showing substantial amounts of carbide phases. However, except for modifications in the amount of carbides, cobalt alloy microstructures have not evolved much over the years.

In the iron-nickel-base and nickel-base precipitation-hardened superalloys (which appeared after the development of solution-hardened superalloys), small amounts of titanium-rich γ′ caused precipitation hardening, and microstructural change was initiated. The product in early alloys was, in reality, metastable γ′, which was spheroidal in nature but unstable and could transform to η. As alloy development proceeded, changes in chemistry led to modification of γ′. Coupled with the modification of carbide content and morphology and the introduction of favorable minor elements, the microstructure of nickel-base superalloys was considerably altered.

Although γ′ in early superalloys was spheroidal, as wrought nickel-base superalloys became more complex, the γ′ in the microstructure became more cuboidal. This structure resulted from the need to pack more and more γ′ into a given volume. When cast nickel-base superalloys became available in the mid-1950s and became necessary for design applications (after 1960), V_f of γ′ approached and exceeded 50% and sometimes reached over 60%. Misfit of γ′ changed with this chemical progression so as to make possible the closeness of packing needed to accommodate the V_f of γ′ that strengthens the current nickel-base superalloys.

Typical Microstructures. Typical operating microstructures of representative superalloys are shown in Fig. 3.4. Macrostructures are shown for a polycrystalline (PC) cast cobalt and a PC cast nickel superalloy and indicate the carbide phases that are usually seen. At higher magnifications, cuboidal γ′ is visible in both wrought and cast nickel-base superalloys, as are grain boundaries decorated with phases (mostly carbides). In the cast nickel-base superalloys at moderate magnification, eutectic γ′ nodules may be found. These modules are really a γ-γ′ eutectic solidification product. They are mentioned again in Chapter 12. Typical precipitation-hardened nickel-base superalloy microstructures as they evolved from spheroidal to cuboidal γ′ are sketched in Fig. 3.5. Some additional microstructures are shown in Appendix B.

Superalloy Strengthening

Precipitates and Strength. Precipitates strengthen an alloy by impeding the deformation process that takes place under load. Some principal hardening precipitate characteristics that act to obstruct deformation are:

- Degree of mismatch between precipitate and matrix. The optimal situation is for matrix and precipitate to have the same crystal structure and almost the same size of crystal lattice. It is possible to pack more precipitate in the matrix gamma phase this way. Mismatches in iron-nickel-base and nickel-base superalloys range from 0 to +/− about 1%.
- Precipitate order. The introduction of preferred positions (ordering) for individual atoms increases the amount of energy required to pass deformation elements (dislocations) through a precipitate. The ordered precipitates possess an energy (antiphase domain boundary or APB) rep-

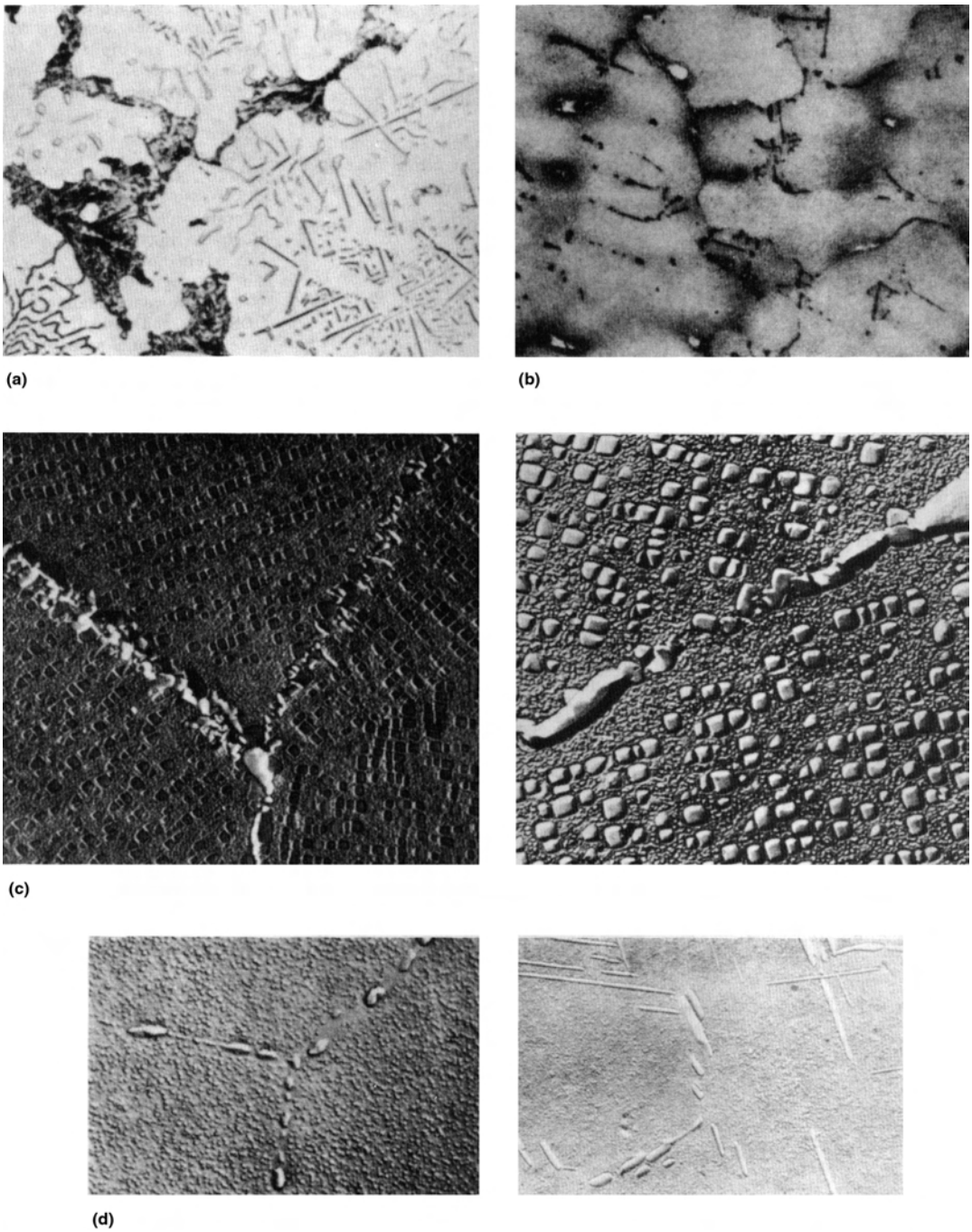


Fig. 3.4 Typical operating microstructures of representative superalloys. (a) Cast cobalt-base alloy. 250×. (b) Cast nickel-base alloy. 100×. (c) Wrought (left, 3300×) and cast (right, 5000×) nickel-base alloys. (d) Two wrought iron-nickel-base alloys (left, 17,000×); IN-718 (right, 3300×) currently is more commonly called a nickel-iron or nickel-base alloy. Note script carbides in (a) and (b) as well as eutectic carbide-cobalt grain-boundary structures in (a), spheroidal and cuboidal γ' as well as grain-boundary carbides in (c), and spheroidal γ' as well as grain-boundary carbides or grain-boundary and intragranular δ phases in (d). γ'' not obvious but present in (d) (right)

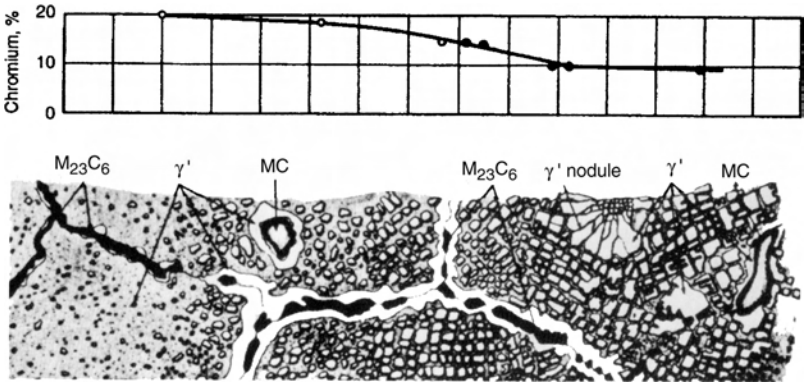


Fig. 3.5 Qualitative description of the evolution of microstructure and the change in chromium content for nickel-base superalloys

resenting the extra energy associated with ordered atom positions versus normal disordered or random positions. Higher APB energies require correspondingly more force for deformation to occur.

- Precipitate size. When the size is too low, dislocations may pass through the crystal too easily. When size is too large, dislocations will bow and strength may be lower than optimal. Optimal size is a function of the property being measured. In creep rupture, a single size is most desirable but is only achievable in specially processed CGDS or SCDS nickel-base superalloys. For wrought superalloys, a two-size precipitate structure may be more desirable, because it minimizes tendencies to notch sensitivity. A single size of γ′ produced at a low aging temperature after an incomplete solution of γ′ may promote higher tensile strengths at the expense of reduced creep-rupture capability.

The principal precipitate phase in superalloys is γ′. The γ′ phase is an ordered ($L1_2$) intermetallic fcc phase having the basic composition $Ni_3(Al, Ti)$. Alloying elements affect γ′ mismatch with the matrix phase, γ′ APB energy, as well as γ′ morphology and γ′ stability. A γ′-related phase, η, is an ordered ($D0_{24}$) hexagonal phase of composition Ni_3Ti that may exist in a metastable form as a titanium-rich γ′ before transforming to η. Other types of intermetallic phases, such as δ orthorhombic Ni_3Nb, or γ″ bct-ordered ($D0_{22}$) Ni_3Nb strengthening precipitate, have been observed and contribute significantly to iron-nickel- and nickel-base superalloy strength.

Gamma Prime. Gamma prime is an intermetallic compound of nominal composition Ni_3Al with titanium and other elements dissolved in it, as noted earlier. It is stable over a relatively narrow range of compositions but possesses remarkable properties that enable it to provide high-temperature strength to iron-nickel- and nickel-base superalloys. It precipitated as spheroidal particles in early nickel-base alloys, which tended to have a low V_f of particles (see Fig. 3.6a). Later, cuboidal precipitates were noted in alloys with higher aluminum and titanium contents (Fig. 3.6b). The change in morphology is related to a matrix-precipitate mismatch. It has been noted that γ′ tends to occur as spheres for 0 to +/−0.2% mismatches, becomes cuboidal for mismatches of about +/−0.5 to 1%, and is platelike at mismatches above about +/−1.25%.

In cast alloys, a γ-γ′ eutectic will form and may persist after heat treatment. In addition, during heat treatment or service operation, γ′ envelopes or films may form in the grain boundary around the $M_{23}C_6$ that is precipitated there or around MC that are decomposing.

Gamma Double Prime. Gamma double prime is a coherent precipitate of composi-

tion Ni_3Nb and precipitates in nickel- (nickel-iron-) base superalloys such as IN-706 and IN-718. In the absence of iron, or under certain temperature and time conditions, δ precipitate of the same Ni_3Nb composition forms instead. The latter is invariably incoherent and does not confer strength when present in large quantities. However, small amounts of δ can be used to control and refine grain size, resulting in improved tensile properties, fatigue resistance, and creep rupture ductility. Careful heat treatment is required to ensure precipitation of γ″ instead of δ. The γ″ often precipitates together with γ′ in IN-718, but γ″ is the principal strengthening phase under such circumstances.

Carbides. Carbides are also an important constituent of superalloys, at least those alloys that are not in single-crystal form. The carbides are particularly essential in the grain boundaries of PC cast alloys for production of desired strength and ductility characteristics. Carbide levels in wrought alloys always have been below those in cast alloys, but some carbide has been deemed desirable for optimal strength properties to be achieved. As cleanliness of superalloys has increased, the carbide levels in wrought alloys have been lowered. Carbides, at least large ones, have become a limiting fracture mechanics criteria for modern wrought superalloy application.

Carbides may provide some degree of matrix strengthening, particularly in cobalt-base superalloys, and are necessary for grain-size control in some wrought alloys. Some carbides are virtually unaffected by heat treatment while others require such a step in order to be present. Various types of carbides are possible, depending on alloy composition and processing. As noted previously, some of the important types are MC, M_6C, $M_{23}C_6$, and M_7C_3, where M stands for one or more types of metal atom. In many cases, the carbides exist jointly. However, they usually are formed by sequential reactions in the solid state following breakdown of the MC, which normally is formed in the molten state. Generally, MC is a high-temperature carbide, and $M_{23}C_6$ and M_7C_3 are lower-temperature carbides. M_6C is intermediate in temperature of formation. MC carbides form from the melt and are created either by that reaction or the precipitation from supersaturated solid solutions at high temperatures, in excess of 1900 °F (1038 °C). The $M_{23}C_6$ carbides are favored by exposure temperatures of about 1400 to 1500 °F (790 to 816 °C). M_6C carbides gen-

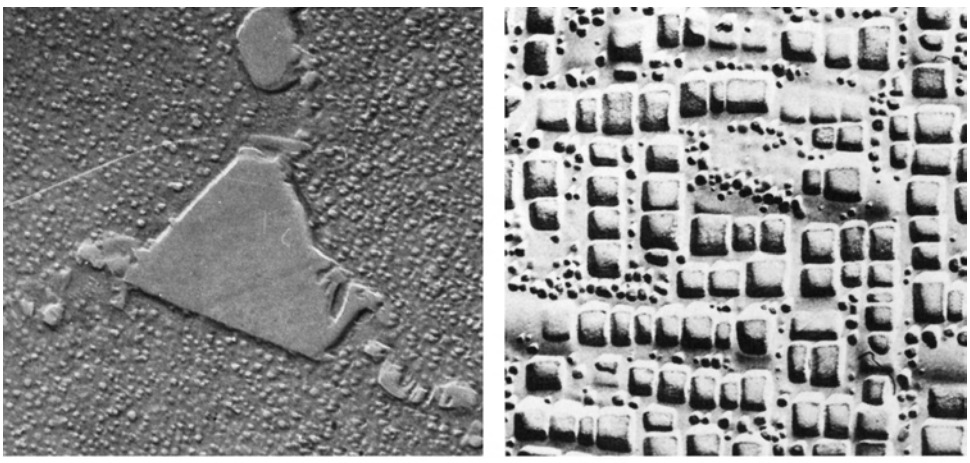


Fig. 3.6 Microstructure of (a) fully heat treated Nimonic 80, showing a grain boundary $M_{23}C_6$ carbide and uniformly dispersed spheroidal γ′ in a γ matrix and (b) cuboidal γ′ in fully heat treated U-700. Original magnification 6000×

erally are formed from about 1500 to 1800 °F (816 to 982 °C), perhaps as high as 1900 °F (1038 °C).

The carbides encountered in superalloys serve three principal functions. First, grain-boundary carbides, when properly formed, strengthen the grain boundary, prevent or retard grain-boundary sliding, and permit stress relaxation. Second, if fine carbides are precipitated in the matrix, strengthening results. (This is important in cobalt-base alloys that cannot be strengthened by γ'). Third, carbides can tie up certain elements that would otherwise promote phase instability during service.

The MC carbide usually exhibits a coarse, random, globular, or blocky microstructure (Fig. 3.7a) or a script morphology in the microstructure (more visible at lower magnifications). The carbide $M_{23}C_6$ is found primarily at grain boundaries (Fig. 3.7b) and usually occurs as irregular, discontinuous, rounded, or blocky particles, although plates and regular geometric forms have been observed.

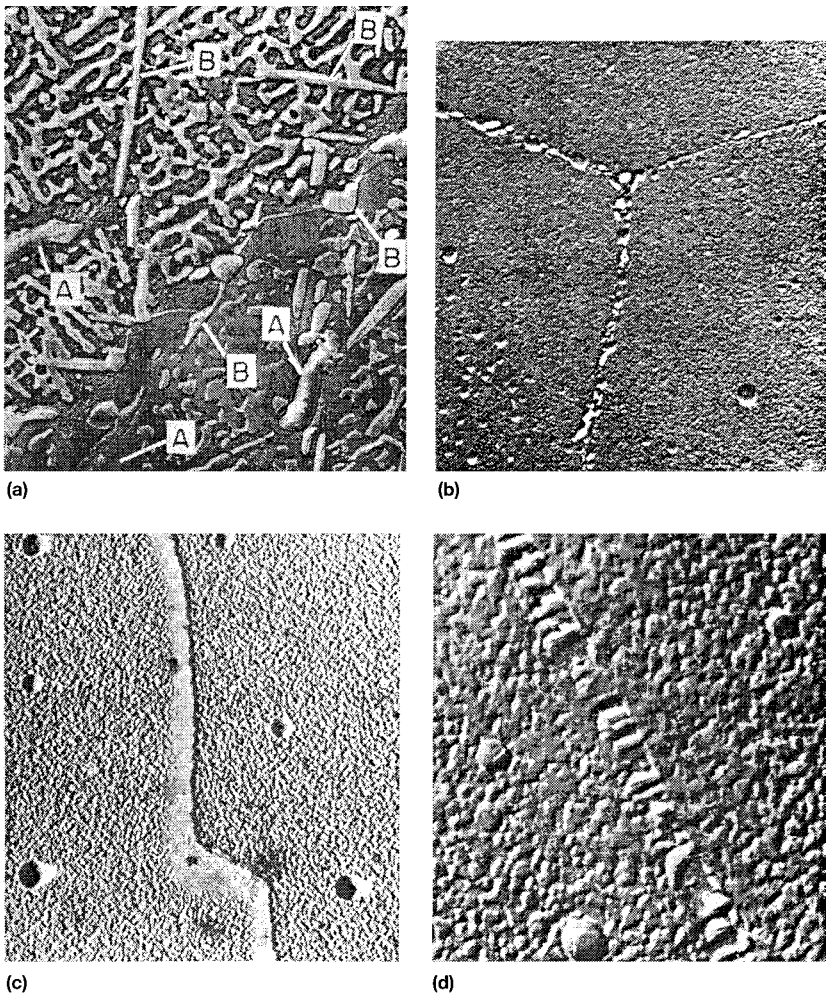


Fig. 3.7 Carbides in microstructures of nickel-base superalloys. (a) Fully heat treated and operated B-1900 showing MC (arrows A) and M_6C (arrows B) carbides, (b) fully heat treated Waspaloy showing globular $M_{23}C_6$ carbides in grain boundary, (c) Waspaloy showing MC film in grain boundary, (d) Waspaloy showing cellular zipperlike $M_{23}C_6$ at grain boundary. Original magnifications: (a) = 2000×, (b) = 3000×, (c) = 5000×, (d) = 20,000×

The M_6C carbide also can precipitate in blocky form in grain boundaries and, less often, in a Widmanstätten intragranular morphology (Fig. 3.7a). Continuous grain-boundary $M_{23}C_6$ and Widmanstätten M_6C or cellular, discontinuous (zipperlike) grain-boundary $M_{23}C_6$, caused by an improper choice of processing or heat treatment temperatures, are to be avoided for best ductility and rupture life. Undesirable continuous grain-boundary MC films are shown in Fig. 3.7(c), and undesirable cellular $M_{23}C_6$ is shown in Fig, 3.7(d).

MC carbides, fcc in structure, usually form in superalloys during freezing. They are distributed heterogeneously through the alloy, both in intergranular and transgranular positions, often interdendritically. Little or no orientation relation with the alloy matrix has been noted. MC carbides are a major source of carbon for subsequent phase reactions during processing, heat treatment, and service.

MC, for example, TiC and HfC, are among the more stable compounds in nature. The preferred order of formation (in order of decreasing stability) in superalloys for these carbides is HfC, TaC, NbC, and TiC. In these carbides, M atoms can readily substitute for each other, as in (Ti, Nb)C. However, the less reactive elements, principally molybdenum and tungsten, can also substitute in these carbides. For example, (Ti, Mo)C is found in U-500, M-252, and Rene 77.

Recent alloys with high niobium and tantalum contents contain MC carbides that do not break down easily during processing or solution treatment in the range of 2190 to 2300 °F (1200 to 1260 °C).

$M_{23}C_6$, for example, $Cr_{23}C_6$, readily forms in alloys with moderate-to-high chromium content. They form during lower-temperature heat treatment and service, that is, about 1400 to 1500 °F (760 to 816 °C) although it is thought that they may form as high as 1800 °F (982 °C) both from the degeneration of MC carbide and from available soluble residual carbon in the alloy matrix. Although usually seen at grain boundaries (Fig. 3.7b), they occasionally occur along twin bands, stacking faults, and at twin ends.

The M_6C carbides have a complex cubic structure. They form when the molybdenum and/or tungsten content is more than 6 to 8 at.%, typically in the temperature range of 1500 to 1800 °F (815 to 980 °C). The M_6C forms with $M_{23}C_6$ in Rene 80, Rene 41, and AF 1753. Because M_6C carbides are stable at higher temperature levels than are $M_{23}C_6$ carbides, M_6C is the carbide more commercially important as a grain-boundary precipitate for controlling grain size during the processing of wrought alloys.

The M_7C_3 Carbides. Although M_7C_3 is not widely observed in superalloys, it is present in some cobalt-base alloys and in Nimonic 80A, a nickel-chromium-titanium-aluminum superalloy, when heated above 1830 °F (999 °C). Additions of such elements as cobalt, molybdenum, tungsten, or niobium to nickel-base alloys prevents formation of M_7C_3. Massive Cr_7C_3 is formed in Nimonic 80A in the grain boundaries after heating to 1975 °F (1080 °C). Subsequent aging at 1300 °F (704 °C) to precipitate γ' impedes precipitation of $M_{23}C_6$ due to the previously formed Cr_7C_3, which generally exhibits a blocky shape when present at grain boundaries.

Borides and Other Beneficial Minor Elements (Other Than Carbon). Small additions of minor elements, particularly zirconium and boron, are essential to improved creep-rupture resistance of superalloys. Although limited information has been generated on M_xZr_y compounds, it is known that borides form in nickel-base superalloys and probably in iron-nickel-base ones as well. Borides are hard particles, blocky to half-moon in appearance, that are observed at grain boundaries, but not in the volume with which carbides appear. The boride commonly found in superalloys is of the form M_3B_2, with a tetragonal unit cell. MB_{12} is also known but has been little investigated.

Hafnium plays a role as a ''minor'' element in that its use results in decidedly improved ductility of grain-boundary regions. Magnesium assists as well, apparently by combining with sulfur, which is very detrimental to the ductility of iron-nickel- and nickel-base alloys.

Function of Processing in Microstructure Development

Introduction. Superalloy processing is considered to be the art/science of rendering the superalloy material into its final form. Processing and alloying elements are interdependent. The general microstructural changes brought about by processing result from the overall alloy composition plus the processing sequence. Microstructures are not only a function of chemistry but also a function of melting, working, and heat treatment. Processing, from melting to casting or wrought product to heat treatment, is an integral part of superalloy production. Heat treatment is the most commonly known of the process steps, because it generally is the

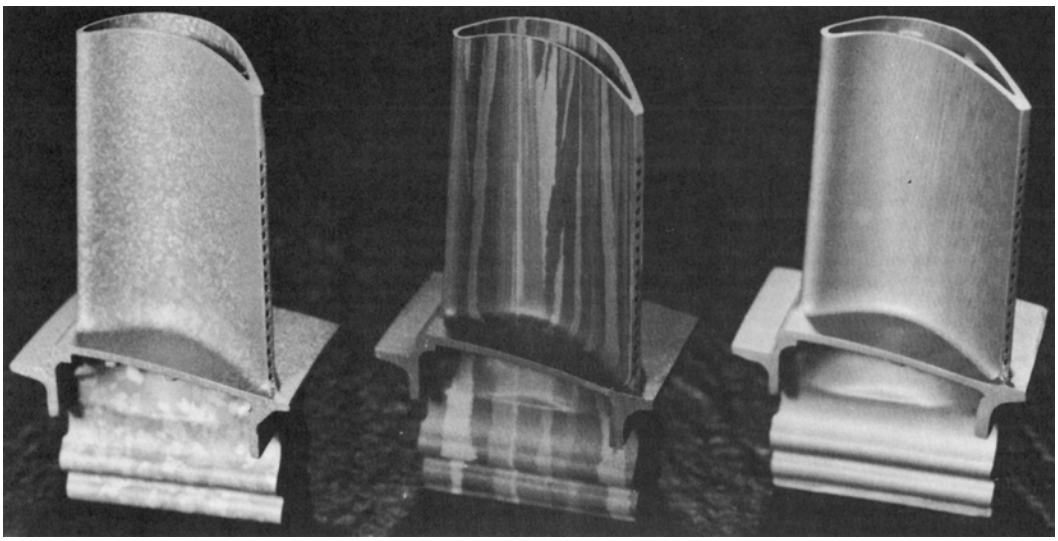


Fig. 3.8 Macrostructure of three turbine blades: polycrystalline (left), columnar grain directionally solidified (center), and single crystal directionally solidified (right)

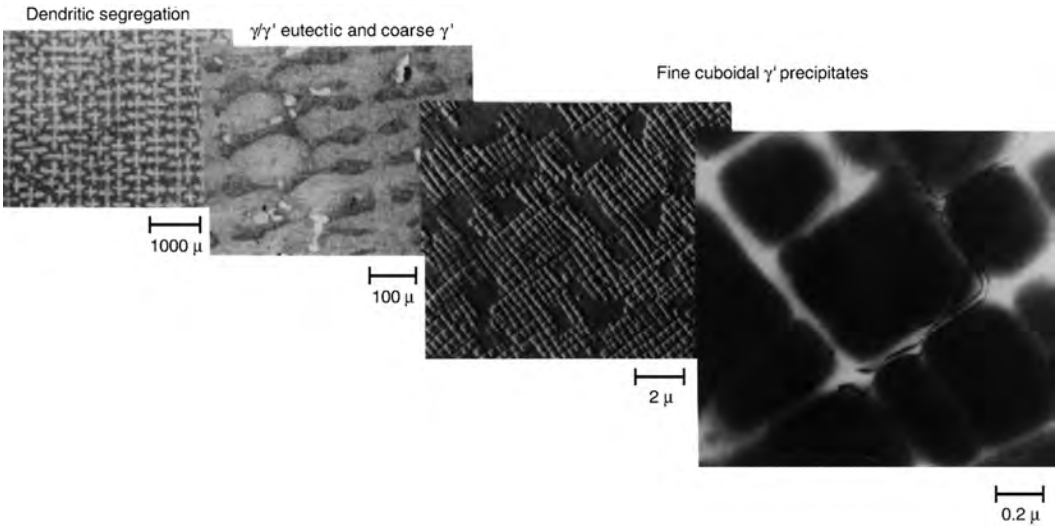


Fig. 3.9 Range from macrostructure to electron microstructure for a single-crystal nickel-base superalloy

final processing step bringing about the desired properties, particularly the properties of the precipitation-hardened alloys. The effects of processing are discussed in more detail in the appropriate chapters.

Processing and Microstructure. The three most significant process-related microstructural variables, other than those resulting from composition/heat treatment interactions, are the size, shape, and orientation (in anisotropic structures) of the grains. As previously indicated, grain size varies considerably from cast to wrought structure, generally being significantly smaller for the latter. Special processing—for example, directional solidification or directional recrystallization—can effect changes not only in grain size but also in grain shape and orientation, which significantly alter mechanical and physical properties. Figure 3.8 shows the macrostructure of the three grain conditions available in cast superalloys. Note the many grains of the PC blade and the coarse elongated grains of the CGDS turbine blade. The SCDS blade shows no grain boundaries, because it is a single grain. However, there is structure to be seen in the single-crystal blade, as noted for the sequential magnification microstructure of the single crystal shown in Fig. 3.9. Dendrites from solidification are visible at lower magnification, as are some γ-γ' eutectic and coarse γ'. Eventually, the uniform cuboidal γ' is seen at the higher magnifications. The fine cuboidal precipitates shown in Fig. 3.9 are the desired goal for most cast superalloys but are not necessarily the desired object for all γ' hardened superalloys.

Structure/property relationships are covered in more detail in Chapter 12. References for additional reading in the area and in other aspects of superalloys are given in Appendix C.

Superalloys: A Technical Guide, Second Edition
Matthew J. Donachie, Stephen J. Donachie, p 41-77
DOI:10.1361/stgs2002p041

Copyright © 2002 ASM International®
All rights reserved.
www.asminternational.org

Chapter 4

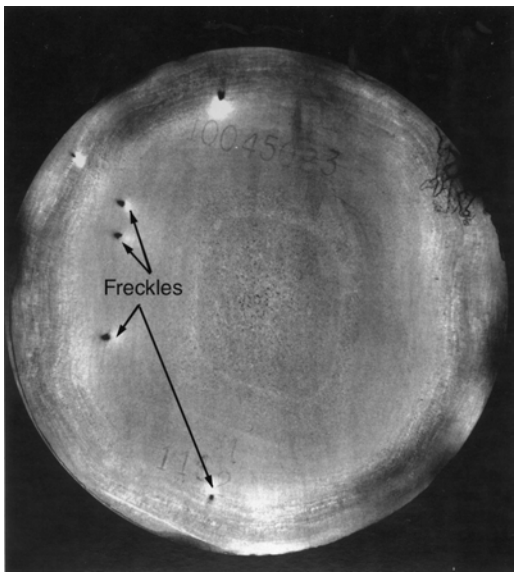
Melting and Conversion

Solidification of Superalloys

Introduction. The solidification of superalloys is governed, as is the solidification of all metals, by the laws of the phase diagram. However, the kinetics of the solidification process determine the microstructure that actually is formed. When solidification occurs, solvent-lean alloy forms first and then grows, usually by dendritic solidification, in the directions of heat and alloy gradients. Most superalloys are far more difficult to solidify in a controlled fashion than ordinary alloys of such metals as copper, aluminum, or steel.

What makes the solidification of superalloys outstandingly different from less sophisticated alloys is that the solute contents of these alloys are very high. Thus, for most superalloys it is necessary that they be solidified under controlled conditions. When solidification rates are too slow, the solute rejected from the first dendrites formed (primary dendrites) may form continuous channels of very high solute content. When these channels solidify (as ''freckles''), they are too concentrated in solute to be dissolved by subsequent heat treatment, and thus form continuous hard defects. Figure 4.1 shows a transverse slice through an IN-718 freckle structure and the analysis associated with the freckles. Laves phases and carbides are hard particles, which form in these heavy solute concentration regions and are highly detrimental to fatigue life. Freckled structures must be avoided in any superalloy that is intended for service where fatigue life is an important design criterion.

Freckle Formation. The effect of the phase diagram on solute rejection in IN-718 is shown in Fig. 4.2(a), which is a pseudobinary phase diagram for this alloy. Figure 4.2(b) shows the dendritic structure of IN-718 in the as-cast condition. A trace for niobium (per-



Compositions of a freckle and surrounding matrix area in weight percent

Element	Inside freckle	Outside freckle
Al	0.43	0.67
Si	0.16	0.12
Ti	1.33	0.97
Cr	17.36	18.58
Fe	15.23	17.62
Ni	52.55	53.19
Nb	9.43	5.46
Mo	3.51	3.38

Fig. 4.1 Freckles in IN-718 nickel-base superalloy billet forged from vacuum arc remelted ingot in which control of melt conditions was lost. Note: Composition of freckle vs. matrix was by microprobe and does not show carbon, which would be elevated in the freckles.

pendicular to the primary dendrite axis) is shown as Fig. 4.2(c). This series of figures illustrates that the primary dendrite structure is nominally 3% Nb, whereas the nominal Nb content of IN-718 is about 5%. The primary dendrites reject solute into the interdendritic liquid and, as seen in the niobium trace, the niobium content in the liquid may reach about 9%. (For IN-718, the other major element rejected into the interdendritic region is

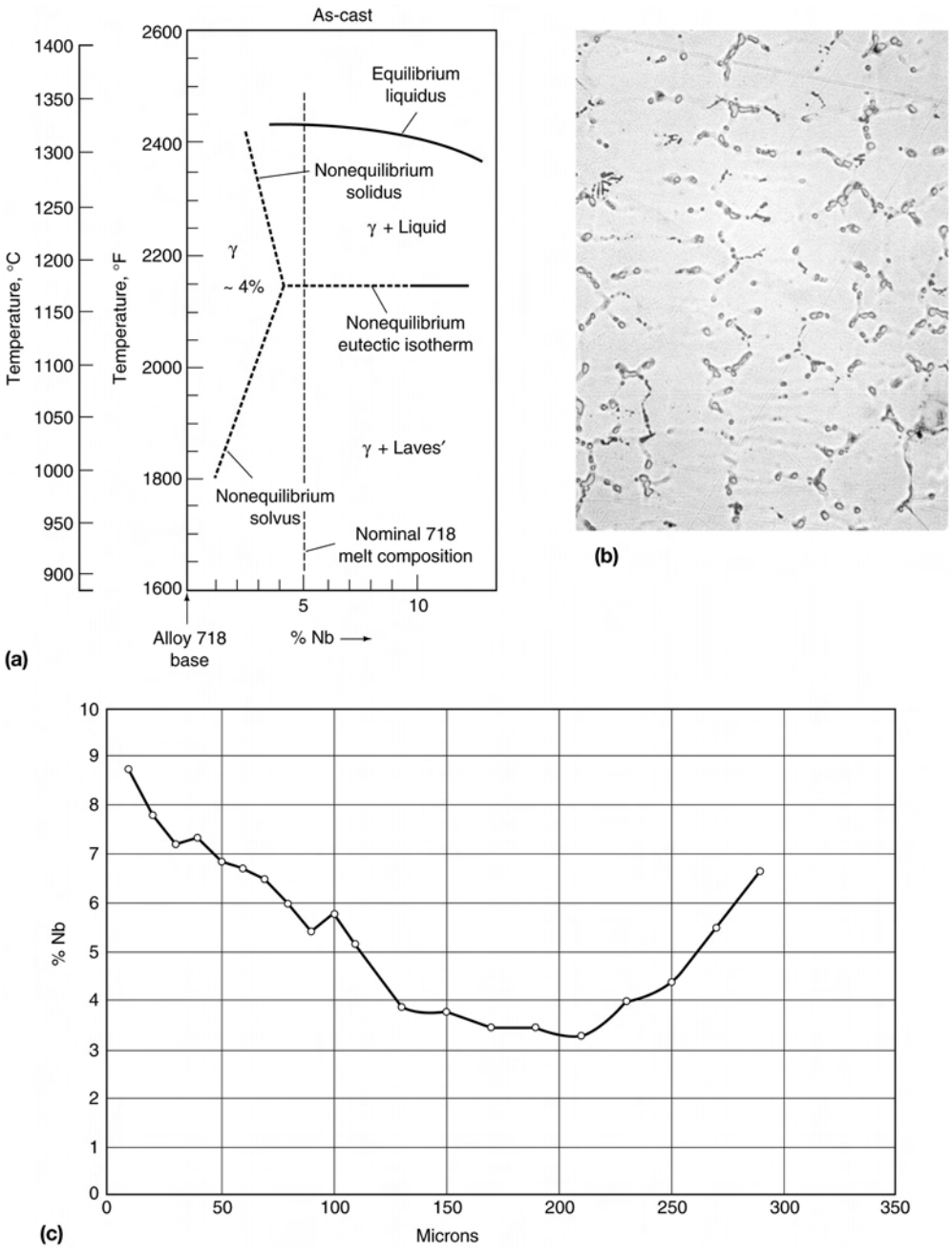


Fig. 4.2 IN-718 nickel-base superalloy showing (a) pseudobinary phase diagram for niobium, (b) dendritic ingot structure produced by vacuum arc remelting (VAR), and (c) niobium distribution in trace perpendicular to dendrite

carbon.) The low niobium primary dendrites grow into the solidifying metal in a direction perpendicular to the solidification front. This region of solid dendrites and liquid interdendritic regions has a temperature gradient defined by the width of this ''mushy'' zone and the liquidus and solidus temperatures. The size of the dendrites in the mushy zone is related to the local solidification time (LST). Local solidification time is defined as:

$$\text{LST} = T_L - T_S/G \cdot R$$

where T_L is the liquidus temperature (° C), T_S is the solidus temperature (° C), G is the temperature gradient (° C/cm), and R is the solidification rate (cm/min).

Increasing heat extraction or decreasing heat input (rate of molten metal introduction to the ingot) increases both G and R. This decreases LST, and, as is intuitively obvious, increasing heat extraction or decreasing heat input thus decreases dendrite size.

When the solidification conditions become sufficiently slow (high LST) that the dendrites and the separation between them becomes large, the interdendritic regions may combine into a continuous channel of liquid. The channel remelts some of the primary dendrites and becomes several dendrites in diameter. This makes the feature visible at 1× magnification; that is, it becomes a macroscopic feature, while the normal interdendritic segregation is a microscopic feature. A critical characteristic of the large channel is that it becomes self-perpetuating.

Several theories have been proposed to explain the self-perpetuating nature of a freckle. They may be divided into two classes: those that assume that the interdendritic liquid is of lower density than the density of the liquid found in the region just above the liquidus (presumably alloys strengthened primarily with titanium and aluminum), and those that assume that the interdendritic liquid is of greater density than the liquid in the region just above the liquidus (presumably alloys strengthened with niobium). Low-density freckle formation tends to take the form of vertical channels at slight angles to the longitudinal axis of the ingot. High-density freckle formation favors the formation of radial freckles, which follow the shape of the boundary between the liquid plus solid/solid zone (but do not necessarily form on the boundary). Alloys forming high-density interdendritic liquids also may form vertical freckles. The theories have an underlying weakness, in that there is no large database concerning the densities of the compositions that are produced in interdendritic liquids in superalloys.

Conditions for Freckle Formation. Freckles occur in regions with high LSTs, that is, in large ingots, solidifying slowly and thus with large mushy zones (low $G \cdot R$). In general, the more highly alloyed the material, the thinner the mushy zone must be to avoid the formation of freckles. The mushy zone thickness is affected by both melt rate and ingot diameter. This relationship is shown for IN-718 in Fig. 4.3. (Fig. 4.3 is a calculation from a solidification modeling program.) It is seen that, for a given ingot diameter, increasing melt rate increases mushy zone thickness and thus favors freckle formation. Also evident from Fig. 4.3 is that increasing ingot diameter, which decreases cooling rate, also increases mushy zone thickness. The use of LST measurement and mushy zone thickness calculation cannot yet be used to predict freckle formation. It can be used to evaluate the qualitative effect of changing solidification conditions. With regard to changes in alloy content, it may be generalized that those elements (titanium and niobium) that contribute greatly to effective precipitate formation in nickel- and nickel-iron-base superalloys also segregate positively. Furthermore, the

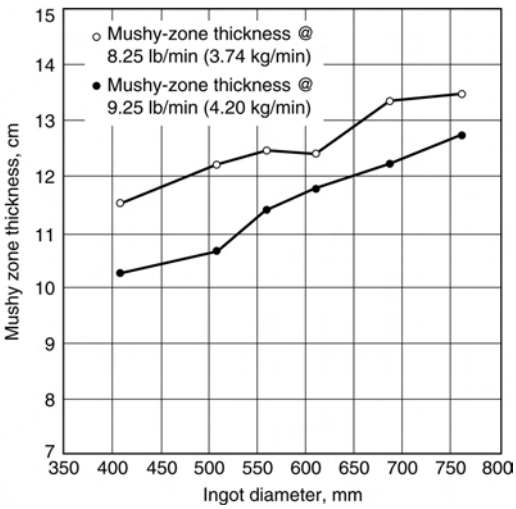


Fig. 4.3 Mushy-zone thickness vs. ingot diameter

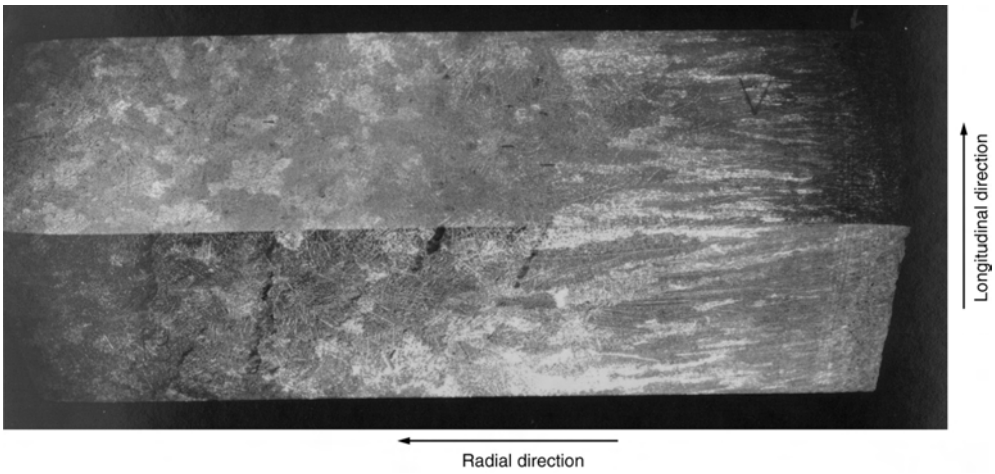


Fig. 4.4 Section from static-cast Waspaloy electrode showing both longitudinal and transverse planes. Note the circular appearance of freckles on the transverse plane and the obvious "channel" nature of the freckles in the longitudinal plane.

segregated regions are different in density from the matrix; thus, increasing hardener content in a superalloy increases the tendency to freckle.

Figure 4.4 shows a section from a statically cast ingot of Waspaloy (see Consumable Remelt Overview for definition of static casting). In this figure, the channellike nature of the freckle is seen when viewed in the longitudinal direction. When viewed from the transverse direction, the channels are seen as dark, etching round spots, thus the common name of freckles. For most commercially useful wrought superalloys, the solidification conditions of static casting will produce freckles. Thus, these alloys are normally static cast as electrodes, which are consumably remelted under controlled conditions. The consumable remelt processes, vacuum arc remelting (VAR) and electroslag remelting (ESR), can greatly reduce LST by enhanced cooling and by limiting the amount of alloy that is molten at a given time (melt rate). Unfortunately, the electric currents used in consumable remelting processes generate magnetic fields. These magnetic fields affect the flow of the interdendritic liquid, further complicating prediction and control of freckle generation. Additionally, while the formation of features related to positive segregation may be suppressed, the nature of the remelting process is such that features that are solute-lean may be introduced into the final ingot. These features are discussed in the sections on consumable remelting.

As is discussed in the subsequent sections of this chapter, melting methods for specific alloys are selected primarily on three criteria: economics, melt segregation requirements, and degree of chemistry control required. Table 4.1 lists common melting combinations for some frequently used superalloys.

Electric Arc Furnace (EAF)/Argon Oxygen Decarburization (AOD) Overview

Introduction. The EAF/AOD process was originally developed in the 1960s for efficient melting of high-chromium ferrous alloys, that is, stainless steels (steels containing 11.5% Cr or greater). Many superalloys are, in effect, specialized stainless steels. Others, while being nickel-base superalloys that contain high chromium, may be melted in a similar manner to stainless steels. As for most melting processes, the charge of material assembled for the melt is the most costly item in the process. It is a particular advantage of the EAF/AOD process that the raw material that may be used in the process is the least costly of that used in any superalloy melting process. Scrap may be used without requiring premelt preparation. To a limited degree, ox-

Table 4.1 Common melt methods for selected superalloys

Alloy	Melt method
600	EAF/AOD + ESR
625	EAF/AOD + ESR
	VIM + ESR
	VIM + VAR
706	VIM + ESR
	VIM + VAR
	VIM + ESR + VAR
718	VIM + ESR
	VIM + VAR
	VIM + ESR + VAR
925	EAF/AOD + ESR
A-286	EAF/AOD + ESR
	VIM + ESR
	VIM + VAR
C-276	EAF/AOD + ESR
Hast. X	EAF/AOD + ESR

Note: EAF, electric arc furnace; AOD, argon oxygen decarburization; ESR, electroslag remelting; VIM, vacuum induction melting; VAR, vacuum arc remelting

ides of expensive raw materials (such as niobium and molybdenum) may be used to replace more costly elemental material. Thus, EAF/AOD is the lowest-cost melting process for superalloys.

Electric Arc Furnace/Argon Oxygen Decarburization Process Description. As may be deduced by the dual nature of the process name, there are two pieces of equipment involved in the process: an electric arc furnace and an argon oxygen decarburizing vessel. The assembled charge is placed into the EAF. The arc furnace power is provided through large carbon electrodes, which protrude into the furnace through the furnace roof and may be extended into or withdrawn from the charge. To begin the melt, the electrodes are extended into the charge, and a current is passed from the electrodes through the charge to the base of the furnace. As the electrodes are gradually withdrawn, an arc is established between the charge and the electrode. This arc provides the power for the initial melt-in of the charge.

After melt-in of the charge, lime (CaO) is introduced to provide a slag that will reduce the sulfur level of the melt. Additionally, oxygen is introduced into the melt by insertion of a pressurized oxygen lance underneath the liquid surface. The reaction of oxygen with carbon, silicon, and aluminum removes most of these elements into the slag, while the heat of the exothermic reaction maintains the desired melt temperature. This process of removing the undesired elements from the melt is known as the reduction phase of the melt. It is a notable feature of the EAF/AOD process that after the initial melt-down, temperatures are maintained in both pieces of equipment by the oxidation of reactive elements in the melt, not by use of external power. When necessary, cooling is accomplished by the addition of solid scrap to the melt.

This process generates large amounts of slag, both from oxidation and desulfurization. The slag is removed manually from the melt by scraping the metal surface so as to draw the slag through an opening at the back of the arc furnace and collect it in a ladle below the opening. After deslagging, a chemistry sample is obtained for the heat. Adjustments to the heat chemistry will be made on the basis of the sample analysis. To maintain temperature during this period, aluminum may be added to the heat and then removed completely by an oxygen ''blow.''

When the desired chemistry is obtained, the charge in the arc furnace is poured from the front of the furnace into a transfer ladle. The transfer ladle is brought to the second piece of equipment involved in this process, the AOD vessel. The molten charge is transferred to the AOD vessel. The AOD vessel has no independent power supply. It is, however, set up with tuyeres in the bottom of the vessel to bottom-inject selected mixtures of oxygen and argon into the charge. The degree of oxidation is decreased by increasing argon content (reduced partial pressure of oxygen) until, thermodynamically, chromium metal becomes more stable than chromium oxide, and oxidized chromium is recovered from the slag. Similarly to the blown arc furnace, aluminum may be added to the melt and preferentially oxidized so that the aluminum reduction increases the temperature of the melt.

When the recovery process has neared completion, final chemistry trim additions are made, based on the results of a chemistry sample, and the heat is manually deslagged and poured into a teeming vessel. The teeming vessel, most commonly equipped with a moveable stopper plug in the vessel bottom, is used to introduce the metal into molds. Molds may be direct poured through the top of the mold, or more commonly, the melt is poured into a central sprue that feeds a number of molds that are filled from the bottom

up. Round electrodes and rectangular slab molds are most commonly used in superalloy production. The product may be hot-worked directly or, depending on the alloy solidification characteristics, consumably remelted to obtain a less segregated structure than that obtainable through direct casting.

Electric Arc Furnace/Argon Oxygen Decarburization Operation

Alloy Composition and Charge Assembly. There are several significant characteristics of the EAF/AOD process that dictate which superalloys are commonly melted by this process.

First, if the product is to be used in the AOD-cast condition, then alloy selection is driven by the composition of the superalloy and the solidification characteristics of this composition. The product from an AOD vessel is generally static cast. The segregation structures of the product must be acceptable in the final form of the product. This means that the solute content of the superalloy must be low or not segregate strongly. Exceptions to this would be for alloys that segregate moderately but that have applications where the presence of the segregate is not detrimental to the performance of the superalloy.

Second, if the product does not require the extremely low gas contents or chemical control that are typical of vacuum primary melt processes, then the superalloy may be EAF/AOD melted, cast as electrode, and consumably remelted.

The foremost reasons for using EAF/AOD in preference to vacuum processes are the inherently lower cost of the raw materials used in the charge and the reduced melting times. As previously noted, superalloys may be regarded as a specialized stainless steel. Chromium is a major addition to most superalloys. The refining of chromium is difficult, with the cost increasing as both iron and carbon are removed. The ability of the EAF/AOD process to reduce carbon levels while recovering most of the chromium addition allows high-carbon ferrochrome to be used in place of low-carbon ferrochrome or even elemental chromium. (In 2000 prices, the respective cost differences are approximately $0.40/lb Cr, $0.60/lb Cr, and $4.00/lb Cr.) Excess carbon is simply consumed as fuel for the process. Similarly, scrap alloy to be used in the melt does not have to be degreased or otherwise specially prepared, because carbonaceous contamination is removed during the process. The elimination of costs for scrap preparation is again a cost saving.

The recycling of scrap is a significant feature of the superalloy industry. Internal scrap losses/recycling may range between 25 to 50% in producing mill products. Many major components are machined into their final shapes from these mill products, with large losses of material to machining chips. The ability of EAF/AOD to forego the removal of oil and grease from these chips is a major saving. Additionally, as EAF/AOD removes elements with high free energies of formation for oxides, alloy scrap of compatible but not necessarily identical alloys may be used, thus increasing the supply of scrap while reducing the overall inventory of scrap that needs to be maintained. The down-side of this process is that superalloys containing high levels of elements with high free energy of formation of oxides are generally difficult to control in EAF/AOD for both tight composition ranges and freedom from oxide inclusions.

Just as raw materials that are high in carbon may be used for EAF/AOD, so may materials that are high in sulfur. Sulfur is another element that is costly to remove from ores. Thus, high-sulfur charge material is less costly than low-sulfur material. The ability of the EAF/AOD process to intimately mix sulfur-reducing compounds (such as lime) into the liquid ensures that reduction of the sulfur into the slag will occur.

Charging the EAF. Computer programs are generally used to select the initial charge materials from the available inventory. The form of material and the nature of the arc furnace into which it will be charged dictates a specific loading order for charging the selected material. Generally, the charge is loaded into several bottom-opening containers. Each container may, in its turn, be located over the arc furnace, the bottom opened, and the contents dropped into the furnace. The impact of large scrap pieces on the refractory bottom of the arc furnace may severely damage that refractory and reduce furnace lining life. Thus, lighter scrap pieces, such as machining chips, are generally added to the arc furnace first, so as to provide a cushion upon which sub-

sequent larger pieces may be charged. The last material added to the top of the charge is also of lighter form. This is done so that when the carbon electrodes are driven into the charge to initiate melting, they will be submerged in the charge material. This allows the arc to be drawn through the charge metal and not to the lining or roof of the arc furnace. Again, the purpose is protection of the refractory lining.

The Electric Arc Furnace. A popular design of EAF is illustrated schematically in Fig. 4.5. The capacity of the AOD furnace must be matched with that of the companion AOD vessel. Successful EAF/AOD operations for superalloys may be as small as 20,000 lbs (9,000 kg) but are commonly in the 80,000 lb (36,000 kg) range. The furnace is a round, steel, water-cooled shell lined with refractory brick. The choice of brick is dictated by the alloys being melted and the furnace design. The economics of melting are that a furnace lining for a medium-sized arc furnace (40,000 lb, or 18,000 kg, capacity) may cost in the order of $10,000.

The bottom of the furnace is fixed, but the top may be swung in the horizontal plane entirely clear of the furnace shell so that the charge may be added. The furnace top has three carbon electrodes that protrude through the roof and may be extended or retracted. The front of the furnace has a pour spout, while 180° away there is an opening in the shell wall through which slag may be removed during the melt. The furnace is generally located in a pit, so that the pour lip and the slag removal openings are at floor level for the furnace crew. The pit allows the placement of transfer vessels and deslagging vessels next to the pour lip and the deslag opening, but at levels so that the tops of these vessels are slightly below the openings from which they will be receiving metal or slag from the furnace. The entire furnace is mounted on trunions so that the furnace may be tilted up to 90° forward to empty the molten metal charge into the teeming vessel. The backward tilt for deslagging is normally less than 20°.

Initially, because of the low apparent densities of charge material, not all the charge may be added to the furnace. After that portion of the charge that is feasible is added to the furnace, the cover is relocated on the furnace, the electrodes are lowered into the charge, and the arcs are struck between the charge and the electrodes. Initially, the arc is maintained at lower voltages. As melting be-

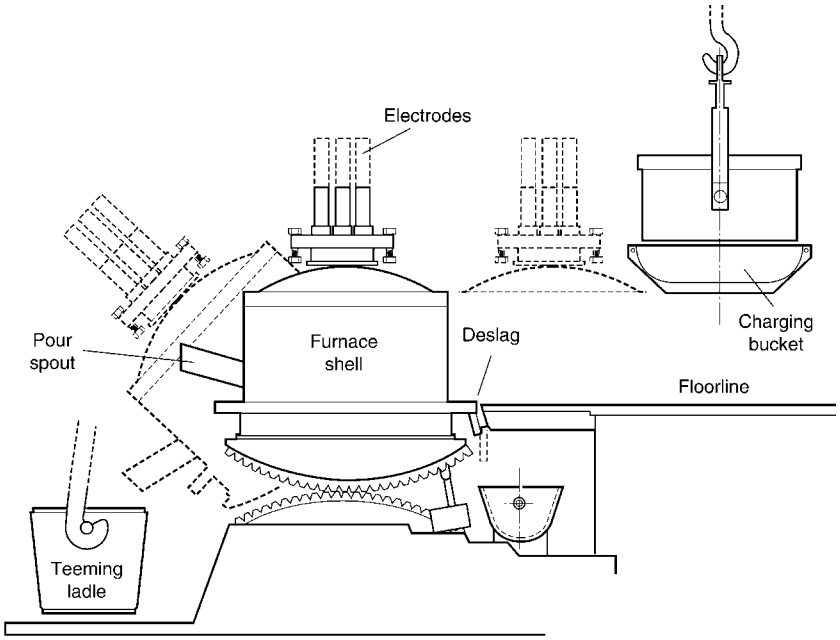


Fig. 4.5 Schematic of electric arc furnace

gins and the electrodes move lower into the charge (bore in), the voltage is gradually increased to attain longer arc length and more efficient melting. Melting continues until the entire charge is molten. At this point, the initial charge volume is reduced to that of the molten metal, and the furnace may be opened and the remaining portions of the charge added (the recharge). This additional charge is melted by the arcs until the entire bath is molten. Further heating of the melt may now be done by blowing the heat with an oxygen/argon mix injected through a hand-held lance. The oxides generated may be very aggressive in attacking the refractory lining of the furnace. In fact, general erosion of the refractory occurs in every melt. However, to protect against severe localized attack at the melt line, lime is usually added to the charge. As slag is formed in the arc furnace, it is removed manually. The furnace is tilted backward and the slag is raked off the top of the melt, drawn through the slag removal opening, and falls into the vessel placed there to receive it. This process may be repeated as necessary, depending on the charge.

After the major portion of the slag has been formed and removed, a ladle sample is taken to determine the chemistry of the melt. Based on that chemistry, further blowing may be conducted, or small levels of alloying addition may be made to attain the chemistry desired prior to transfer to the AOD vessel. Typical melt times for the EAF portion of the EAF/AOD process are in the order of 3 h.

When the arc furnace charge has been melted, adjusted to the desired temperature, and deslagged, it is poured into a transfer vessel. Generally, a transfer ladle (a refractory-lined vessel with a pour lip) is positioned in front of the arc furnace, and the furnace is rotated to pour the contents of the furnace into the vessel. The vessel may be lined with MgO so as to modify the nature of the lime-based slag. Unless the composition of the slag is properly maintained, it may become liquid and mix with the molten metal rather than remain solid and float to the top of the melt. To avoid temperature loss during transfer, the vessel is usually preheated. The transfer ladle is moved to the AOD vessel and its contents poured into that vessel.

The AOD Vessel. Figure 4.6 illustrates, schematically, an AOD vessel. The vessel, like the EAF, is steel walled and refractory lined. The general shape is that of a concrete mixer, that is, a container with a generally rounded bottom, a conical top, and mounted on trunions so that it may be tipped in the vertical plane. The size, of course, is matched to the arc furnace and may hold upward of 80,000 lb (36,000 kg) of molten metal. The essential feature of the AOD vessel is that in the bottom of the vessel are several tuyeres for the injection of an argon-oxygen gas mix. The tuyeres consist of concentric tubes, the center of which injects the argon-oxygen mix into the vessel. The outer tube carries inert gas only (usually additional argon) to cool the reaction occurring at the end of the center tube.

The refractory lining of the AOD vessel is similar in composition to that of the EAF furnace and also erodes during the processing, contributing oxides to the slag formed during the process. Control of the basicity of the slag formed is, again, a key item in ensuring that selective attack of the refractory by the slag does not occur.

In the AOD vessel, the first operation is to decarburize the melt. If the melt were blown through the tuyeres with pure oxygen, the result would be not only decarburization but a conversion of much of the chromium alloy content into chromium oxide. The economic feasibility of the decarburization reaction is related to the discovery that reduction of the ox-

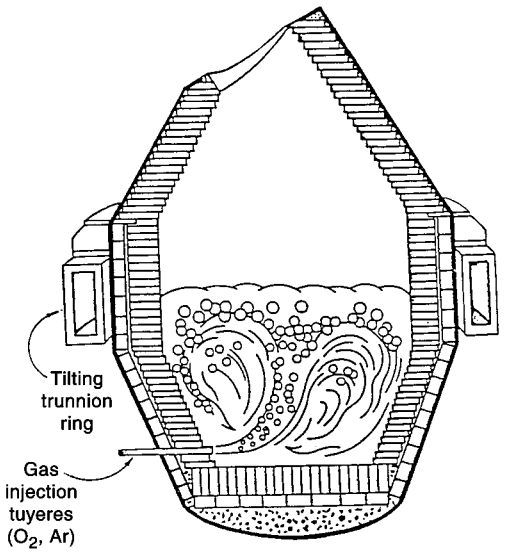


Fig. 4.6 Schematic of argon oxygen decarburizing vessel

ygen partial pressure over the melt by inert argon greatly decreased the amount of chromium oxidized. When carbon levels are high, a typical ratio used of argon to oxygen is 3 to 1. As the carbon content is reduced, the proportion of argon may be increased. By the time that decarburization is complete, the ratio of argon to oxygen may be as high as 6 to 1.

The decarburization reaction heats the bath, as does the small amount of chromium oxidation that occurs. Silicon also will be removed, but the heat of reaction is low, so there is little contribution to heating the charge. It is important to remember that the AOD vessel contains no external heating sources. The temperature is raised by the exothermic reactions. Should the charge need to be cooled, this is accomplished by adding solid scrap to the charge. It is economically important that the charge temperature be kept uniform, because the percentage of valuable alloying elements (principally chromium but also niobium) that becomes slag is affected by the charge temperature. Overheating the charge, followed by cooling, and then followed by heating again is time-consuming and detrimental to the full recovery of the elements that have partitioned to the slag.

During the decarburization cycle, lime is added to the charge. The lime is very thoroughly mixed into the liquid charge during blowing, leading to a high degree of desulfurization of the charge. The CaS formed in this reaction becomes part of the slag. When a chemistry control sample shows that the desired degree of decarburization has been obtained, the melting operation enters the recovery phase. In this phase, the slag is reacted with cheap elements (principally silicon and/or aluminum mixed with lime) that will preferentially form oxides compared to chromium and niobium. This causes the reduction of these expensive elements in the charge and their return into the melt. Very sophisticated programs exist to use the known composition from the sample taken from the transfer ladle plus the amount of oxygen blown through the charge to predict the amount of oxidized chromium and niobium to be recovered. The correct amount of reduction mix may be added accordingly.

When reduction is complete (often confirmed by yet another chemistry sample), the charge is deslagged manually, by scraping the slag from the surface of the molten charge and out the tilted top of the cone. Final trim additions are made to bring the charge to its desired composition, and the AOD vessel is rotated to decant the molten charge into a teeming ladle.

Teeming. The teeming ladle and charge are transferred to the area where the heat is to be tapped. Figure 4.7 shows a schematic for a bottom-pour mold setup. The heat is tapped by the opening of a bottom plug in the teeming ladle. As the heat enters the central pouring sprue or ''trumpet,'' a stream of argon may be flowed alongside it to provide shrouding against oxygen and nitrogen pickup from the atmosphere. The trumpet feeds a number of runners located radially around it. The runners feed the molten metal into the bottom of the molds. Mold powders or fluxes are added to the advancing metal front to improve surface quality by providing thermal insulation from the mold surface. At the end of the pour, exothermic compounds may be added to the top of the mold to insulate the top of the solidifying electrode and

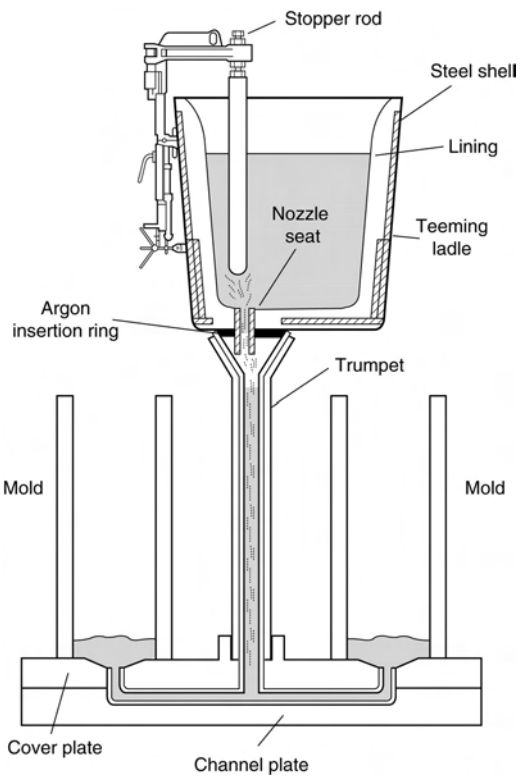


Fig. 4.7 Schematic of bottom-pour teeming in EAF/AOD melting

provide a degree of hot topping, where the molten metal will fill the shrinkage occurring upon solidification lower in the electrode.

Argon oxygen decarburized electrodes also may be top poured, but the need to continually close the teeming ladle tap, transfer the ladle, and reinitiate argon shrouding produces variable conditions from electrode to electrode. Should difficulty in closing the nozzle be experienced during top pour, then a safety problem arises. Thus, bottom pouring is the more generally used process.

Vacuum Induction Melting (VIM) Overview

Introduction. Compared to air-melting processes, VIM of superalloys provides a considerable reduction in oxygen and nitrogen contents. Accordingly, with fewer oxides and nitrides formed, the microcleanliness of vacuum-melted superalloys is greatly improved compared to air (EAF/AOD)-melted superalloys. Additionally, high-vapor-pressure elements (specifically lead and bismuth) that may enter the scrap circuit during the manufacture of superalloy components are reduced during the melting process. Accordingly, the vacuum-melted superalloys (compared to EAF/AOD-melted alloys) are improved in fatigue and stress-rupture properties. Control of alloying elements also may be achieved to much tighter levels than in EAF/AOD products.

Vacuum melting, however, is more costly than EAF/AOD melting. The EAF/AOD process allows compositional modification (reduction of carbon, titanium, sulfur, silicon, aluminum, etc.). In vacuum melting, the charge remains very close in composition to the nominal chemistry of the initial charge made to the furnace. Minor reductions in carbon content may occur, and most VIM operations now include a deliberate desulfurization step. However, the composition is substantially fixed by choice of the initial charge materials, and these materials are inevitably higher-priced than those that are used in arc-AOD.

Vacuum Induction Melting Process Description. The charge generally consists of three portions: a virgin portion, which consists of material that has never been vacuum melted; a refractory portion, which consists of those virgin elements that are strong oxide formers and have the tendency to increase the solubility of oxides and nitrides in the virgin charge; and a revert (or scrap) portion, which consists of both internal and external scrap that previously has been vacuum melted. Vacuum-melted scrap has already had its gas content reduced to levels consistent with vacuum production. Scrap, however, has the possibility of having become contaminated during the production process, and care (expense) must be taken in the segregation and preparation of scrap materials for vacuum melting.

The virgin portion of the charge is placed into the VIM furnace first. This may be done by opening the furnace or, more commonly, by charging the furnace through hoppers lowered through a large vacuum lock (bulk charger) located over the crucible. The furnace is capable of quickly pumping down to or maintaining vacuum levels below 100 μm (and often into the <10 μm) range. The virgin material is melted by application of current to the induction coils surrounding the refractory crucible. When the virgin material has been completely melted (all molten), it outgasses. The outgassing is monitored until it is complete. At that point, the reactive and revert additions may be made, bringing the charge to its planned weight.

A ladle sample is taken after all additions are complete. Based on the analysis of this sample, trim additions are made to bring the melt into a very precise compositional range. Because there are no ongoing chemical changes in the melting, as there are in EAF/AOD, the compositional requirements of a melt may be met as closely as allowed by the reproducibility of chemical analysis. After the trim additions have been made, the temperature of the heat is brought precisely to the desired point, and the heat is poured into molds.

The heat, although produced in vacuum, will still have generated significant amounts of slag from the products of deoxidation, desulfurization, and the deterioration of the refractory crucible lining. The heat is poured so as to decant the molten metal from under the slag. Generally, the refractory pouring system used to conduct the molten metal to the molds also is provided with a series of dams and weirs to trap slag that may have

been entrained into the pour stream. Finally, the pouring system itself generally ends in a refractory tub (a tundish) that contains a considerable volume of metal and allows residence time for entrained slag to float to the top of the tundish and be removed from the pour stream. The pour stream exits the bottom of the tundish. The pour time is regulated by tundish nozzle diameter and pour temperature.

Vacuum-induction-melted superalloys intended for wrought applications are seldom used in the as-cast condition. The vast majority of the ingots cast are intended for consumable remelting operations in order to improve the structure of the material and/or enhance the cleanliness further than may repeatedly be accomplished in VIM. Thus, VIM molds tend to be either tall, cylindrical molds that will be remelted into rounds in VAR or ESR, or to be rectangular (slab) molds destined for remelting by ESR. In all cases, the industry terminology is not to refer to these cast pieces as ''ingot'' but as ''electrode,'' emphasizing their intended use as intermediate stock in a multiple-melting process.

Vacuum Induction Melting Operation

Vacuum Induction Melting Charge. The VIM charge is calculated to a specific chemistry aim. The calculation involves the use of three different types of materials plus a correction factor. The first types of materials are those described as virgin. Generally, this consists of elemental materials from refineries. These materials may contain significant amounts of dissolved oxygen and nitrogen. The oxygen will be reduced in the subsequent melting operation. Nitrogen reduction, while occurring in VIM, proceeds at such a slow rate that, as a practical matter, nitrogen reduction must be accomplished by selection of low-nitrogen raw materials. The significant distinction between virgin and other charge materials is not that they are the products of a refinery, but that they have never had their gas levels reduced by vacuum melting.

Based on this definition of virgin material, there is an economically important type of material produced through the EAF/AOD process that must be classified as virgin. This is the product of the reclamation of high-alloy-content grinding swarf, furnace skulls, and any other manufacturing by-products containing superalloy but which are too fine or too contaminated with grinding material or slag to be used as direct charge materials into the VIM. Such material is processed by EAF/AOD melting to produce a material that will be low in carbon and reactive elements. This new material, although made from vacuum-melted scrap, will be high in oxygen and must be treated as a virgin material despite its origin as scrap from vacuum-melted material.

The second type of material is that known as reactive. Reactive materials are generally elemental materials and are technically virgin. However, these materials (commonly, titanium and aluminum) are such strong oxide and nitride formers that they increase the solubility of these gases in the virgin portion of the charge. They are thus weighed out and maintained separately from the nominal virgin charge and will be added to the melt only after degassing of the virgin charge is complete.

The third type of material is revert. Because of the relatively low efficiencies of manufacturing processes in producing superalloy components, a great amount of scrap is produced during manufacture. The reclamation of this scrap, both internal (at the melters) and external (during fabrication of the component), forms a major economic segment of the superalloy business. Large pieces of scrap (process crops) are produced during the melting processes and in subsequent forming to mill products. These solid pieces may be directly charged back into a VIM process, provided that the melting facility has in place a system to track identification and composition of these pieces.

The other large source of revert superalloy is chips from machining processes. The chips, in addition to being carefully segregated, must be crushed for effective packing into charge containers and degreased to remove the cutting fluids from the machining process. Many machining processes use low-melting-point metal mounting material to hold the piece for machining. These fixturing metals are highly alloyed with lead and bismuth, and machining into them produces

contamination of the superalloy chips with these elements that are so detrimental to superalloy performance. Chip-lot chemistry is traditionally certified by the melting and analysis of a small sample from each processed (sorted, crushed, and degreased) batch of chips. Because contamination of chips is in the form of particulate, which may be segregated within the batch, such samples are highly inaccurate with regard to predicting absolute amounts of lead and bismuth in the chips. Fortunately, when the level of these contaminants is low, they are removed to insignificant levels by the vacuum-melting process. However, severe contamination will not be completely removed unless it is detected and normal processing times are greatly extended, an action which may be economically impractical.

Revert need not be precisely the same composition as the heat being assembled in the charge make-up process. Compatible revert is any material that can be used in the melting of another (different) alloy by the simple adjustment of the weight of virgin material additions in the charge so as to compensate for the compositional differences.

The remaining factor in calculating the VIM charge is to have established guidelines concerning the amount of material from the preceding heat that will be picked up during the melting process. When a VIM heat is poured, a significant amount of material is left on the walls of the crucible. The subsequent heat remelts this material, and its composition must be compatible with the new heat. Thus, the choice of compositions in sequencing melts throughout a VIM campaign must be carefully considered. A correction factor for this compositional modification must be applied to each heat during charge calculation. Like the correction for using compatible revert, this correction factor will be reflected in the amount and types of virgin material selected for the charge. Under some circumstances, melting of a heat of a different composition will require the running of a wash heat to prepare the melting crucible for the new chemistry. Wash heats are generally composed of the unalloyed element that is the major component of the next heat.

Vacuum Induction Furnace. The furnace itself is simply a steel shell connected to high-speed vacuum systems. Furnaces may be top- or side-opening, and there is a moderate degree of variety in VIM furnace design. The heart of the furnace is the crucible. The crucible is generally of a size (10,000 to 50,000 lb, or 4500 to 22,750 kg capacity) that the refractory lining is not made as a single piece, but is built up from refractory brick. (Smaller furnaces, used for production of master melt, may use single-piece crucibles.) There are usually two layers of brick. The backup lining protects the induction coil in the event of a failure of the outer or working lining. The working lining is the primary interface with the metal and is replaced when erosion of the lining becomes excessive. A different factor that may limit refractory life is the expansion of the refractory during the repeated melting cycles. Most commercially available refractory brick is incompletely sintered and expands during use, causing loss of crucible integrity. The characteristics of the chosen brick, with regard to resistance to erosion and expansion, control the life of the working lining and thus the length of a VIM campaign.

Outside of the refractory is a set of induction coils, made from copper tubing and cooled by water flowing through the tubing. The passage of current through the coils creates a magnetic field that induces a current in the charge. When the heating of the charge material is sufficient that the charge has become all molten, these magnetic fields cause stirring of the liquid charge. The optimal induction coil frequency for heating the charge varies with the charge shape, size, and melt status (liquid or solid). Older equipment used a single frequency, but newer power supplies are able to be operated at variable frequencies and are adjusted throughout the melt to obtain the most rapid heating/melting conditions. In some VIM furnaces, the coils are installed in sections. By use of only certain sections of the coil stack, a liquid charge can be stirred without imparting sufficient energy to the charge so as to cause further heating. Figure 4.8 illustrates the construction of a VIM crucible.

In most VIM furnaces there is a vacuum lock bulk charger located directly over the crucible. Charge material may be added to the heat through the bulk charger while melting is in process in the crucible. The material to be added is placed in bottom-opening buckets, placed in the bulk charger, and the charger is evacuated. The valve iso-

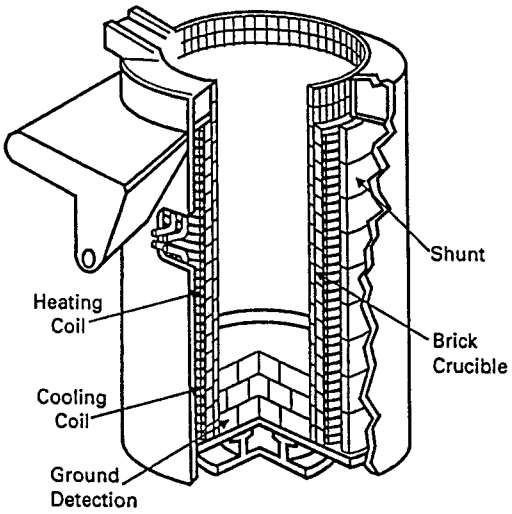


Fig. 4.8 Schematic of vacuum induction melting crucible (shell, coil stack, backup lining, and working lining)

lating the charger from the melt chamber is opened, and the bucket is lowered to a point close to the crucible top and the bottom opened so as to drop the charge material into the crucible. In constant operation, if a furnace is not to be opened to the atmosphere, all charge material for a heat will be added by this process.

Older VIM furnaces may have been designed as single-chamber furnaces wherein the molds into which the charge is to be poured are put inside the furnace at the beginning of the melt. (A single-chamber furnace must thus be opened after each heat to extract the molds and put in the new molds.) Most furnaces have some system of large vacuum locks for transferring the prepared molds into the melt chamber. In some furnaces there is a separate chamber for the molds. (These are double-chamber furnaces.) In either type of furnace, the prepared molds thus may be moved into the pour position at some time much later than the initiation of the charging/melting cycle of the furnace. When the molds are in position and vacuum in both the mold and melt chambers is equal, the valve separating the chambers may be opened. A schematic of a top-opening, double-chamber VIM furnace is shown as Fig. 4.9.

Pouring Systems. Systems that transfer molten metal are referred to as launders. Launders are refractory-lined steel troughs and are used in VIM furnaces with separate melt and mold chambers. The refractory may

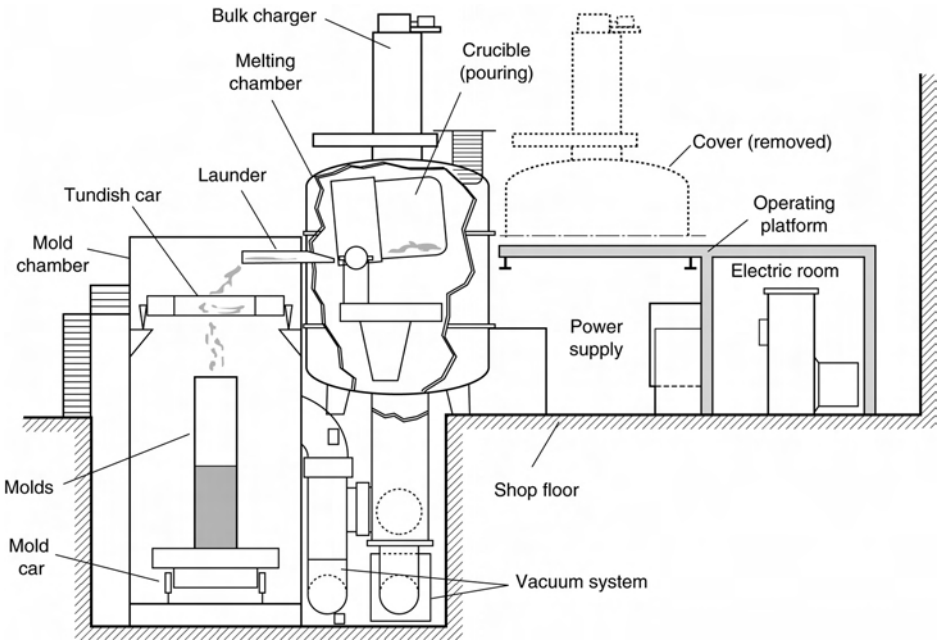


Fig. 4.9 Schematic of double-chamber VIM

be brick or, because the launder size is not excessive, cast and sintered as single pieces of refractory. Launders often incorporate projections (dams and weirs) into the line of flow of the molten metal to help prevent the transfer of slag into the molds during pouring. (Dams are the projections rising from the bottom of a launder. The weirs are the projections coming down into the top of the pour stream.)

Final removal of entrained melt slag is accomplished by the use of a tundish. The tundish is a ceramic bricked or cast tub into which the metal flows after leaving the launder. (Some systems are designed to pour directly from the crucible into the tundish.) A typical tundish design has significant depth and provides a low-velocity flow path from the point of entry of the metal to the bottom-installed nozzle through which the metal exits into the molds. Dams and weirs may also be used in the tundish to collect slag particles. (The bottom-projecting dams direct metal flow to the top of the tundish as a flotation aid for the slag particles.) An important feature of the tundish is the nominal residence time of the metal in the tundish, because this controls the extent to which entrained slag will float to the top of the tundish and be removed from the pour. The height of metal in the tundish is kept constant by regulating the metal pour rate from the crucible into the launder. The combination of metal temperature and fixed height of liquid head in the tundish make the flow (pour rate) out of the tundish nozzle a fixed rate.

The molds are commonly made from ferrous materials, generally cast iron but with forged steel molds becoming increasingly more common. The trade-off between mold life and cost dictates the choice for many producers. The primary mechanism of mold failure is from thermal fatigue (heat checking of the mold interior surfaces). The resistance of the forged molds to failure by this mechanism is greater than that of cast molds. However, molds are often lost to other factors, such as a misaligned pour stream impacting the mold wall, in which case the lower cost of cast molds becomes a factor. Mold walls may be straight, but it is not uncommon for them to have a slight taper to aid in the extraction of the solidified electrode from the mold. The shrinkage of the cast electrode from the mold wall is generally sufficient that little or no force is necessary to remove the solid electrode from the mold.

Vacuum Induction Melting Furnace Operation. The following sequence represents a nominal VIM cycle for the production of a heat in a two-chamber furnace. Most VIM operations will follow this general sequence, while specific practices, particularly with regard to vacuum measurements, will differ in detail.

At the completion of the preceding heat, the melt chamber is isolated from the mold chamber. The absolute vacuum level of the melt chamber is noted and a base leak-up rate is taken. Leak-up rates are taken by blanking off all of the vacuum ports to the melt chamber and measuring the deterioration of vacuum level in the furnace as a function of time. A common time period for this measurement is three minutes. The rate of deterioration is a measurement of the inherent vacuum integrity of the furnace. This cannot be measured by vacuum alone, because the large pumping capacities of the pumps used in VIM are able to achieve low vacuum pressures despite significant leakage into the furnace. However, prevalent thought is that continuously drawing air into the vacuum furnace and across the melt is bad practice.

Immediately after ensuring that the furnace is vacuum-tight, the addition of the virgin portion of the heat will begin through the bulk charger. Full melting power will be applied, and melting will begin while the containers are being added. When all of the virgin portion of the charge has been added and the charge has become all molten, the temperature of the melt will be controlled to a set refining temperature and a leak-up rate taken. This leak-up rate will be significantly higher than the base rate for the furnace, because outgassing of the virgin material will be taking place. The outgassing is a response of the gas in solution in the melt to the low partial pressures of gases in the vacuum chamber. (Note that the amount of gas in solution in the liquid metal is also a function of the metal temperature.) Some degassing is accomplished because carbon in the charge will form CO with the oxygen and also be evolved from the melt. The progress of degassing is followed by measuring the leak-up rate at set time intervals. When a constant leak-up rate is obtained, this indi-

cates that degassing (refining) of the melt is complete.

Temperature control during this process is monitored by the use of optical pyrometers. It should be noted that to use an optical pyrometer, one does not have to obtain a highly accurate absolute value. Rather, by reducing the metal temperature to a point where the melt surface just begins to freeze over and obtaining a pyrometer reading, a relative value is obtained for the all-molten temperature. Subsequent temperature control may be made by reference to the number of degrees of superheat required above the all-molten temperature.

The addition of the revert portion of the charge may begin after the outgassing is complete. The refractory elements, or a portion of the refractory elements, may now be added as well. The addition of aluminum serves to further lower the oxygen content of the melt by reacting to form alumina and floating to the top of the melt. At some point in this cycle (after deoxidation has been completed), it is common to add calcium to the melt to desulfurize the material. Commonly, either a nickel-calcium addition alloy, lime, or a combination of both is used. Much of the CaS formed may be incorporated into the oxide (slag) cover on the melt, although some of the sulfide may adhere to the refractory walls of the crucible. Heats must contain a minimum aluminum content to ensure that the CaS sticks to the crucible wall and does not revert back into the heat or subsequent heats as sulfur.

It should be noted that the initial use of VIM for superalloy melting envisioned the melting of pure metals in a vacuum environment without the use of slag-forming elements. The recognition of the role of sulfur in degrading high-temperature properties of some superalloys has led to the need to both reduce sulfur content and to modify the chemical nature of the remaining sulfur in order to improve the consistency of mechanical properties. Thus, modern VIM heats all contain substantial slag forming components as well as oxide components floating on the top of the molten charge. Care must be taken to avoid incorporating these components into the cast electrodes.

When all revert, sulfur control, and refractory additions have been made and the charge is all-molten and thoroughly stirred, a sample taker is inserted through a small vacuum lock and into the melt. This dip sample is analyzed to determine the elemental additions that must be made to bring the melt into the desired chemistry range. The trim additions are made and mixed into the melt. A second dip sample may be made to confirm the chemistry if the level of trim additions necessary was deemed to be unusually large. Coincident with this, the molds for the heat will have been assembled, run into the mold chamber, the chamber pumped down, the launder pass-through valve opened, and the launder extended into position in the mold chamber. The tundish will also be moved into position (the tundish is often preheated).

At this time (just prior to pour), the melt temperature is recontrolled by optical pyrometer and then the optical reading confirmed by immersion of a consumable thermocouple. The pour temperature is important, because this controls the viscosity of the melt and thus the pour rate through the tundish nozzle. While pour temperatures must be sufficiently high to avoid freeze-off in the tundish nozzle, they should be as low as possible to reduce the solubility of TiN in the melt.

Often, a final addition of magnesium (as nickel-magnesium) is made to the melt. This is to ensure that the remaining sulfur in the melt will be present in final wrought form as MgS. MgS tends to form spherical particles in the solid (whereas other sulfides may form grain-boundary films) and greatly improves the consistency of elevated-temperature ductility in some alloys. Because of the high vapor pressure of magnesium, it cannot be retained in the melt under vacuum or even partial vacuum and is vaporized from the melt during the time preceding pouring and during the pouring process. Argon is often added to the melt chamber at fractions of atmospheric pressure to control the vaporization. The condensation of magnesium dust in the melt chamber presents a safety hazard throughout the industry, because the dust is pyrophoric. When exposed to air in situ, it will burn. If stirred up into a dust cloud, it may ignite explosively.

Prior to the pour, a final dip sample is collected. The chemical analysis of record will be made from this sample. The pour is accomplished by tilting the crucible to pour liquid metal into the launder. The metal is decanted out from under the slag cover on the

melt. The flow rate is initially fast, to fill the tundish so that full effectiveness of the tundish in floating out entrained oxides is attained. When the tundish is filled to its desired level, the crucible tilt is reduced to maintain that level. It is not uncommon to begin the pour with the tundish located over a front overflow mold so that metal cast prior to the tundish operating at full efficiency is not incorporated into the electrodes. As each electrode mold is filled, the next mold is indexed under the pour stream (the pour stream is generally continuous). The final material in the crucible is drained out into a back overflow mold to both accommodate any overcharge of metal beyond the mold capacity and to ensure that the last metal poured, which may have high slag entrainment, is not incorporated into an electrode.

While the melt cycle begins for the next heat, the cast electrodes are held in place for a time sufficient to solidify them, and then stripped from the molds. For many alloys, it is necessary that the newly stripped electrodes be annealed prior to use in a consumable remelt practice, and thus the electrodes may be transferred directly to an annealing furnace.

Being a static cast product, the structure of the electrode will contain a high degree of positive segregation and thus require controlled remelting to generate a more desirable cast structure. As electrode solidification initiates at the mold wall and progressed into the center, the centerline of the electrode will usually contain a high degree of porosity. This is known as the secondary pipe cavity. The volume change upon solidification will also have caused a major shrinkage (primary pipe cavity) on the top of the electrode. The primary shrinkage may be eliminated through the use of hot tops. Hot tops are ceramic insulating sleeves that allow the top of the electrode to remain molten for longer than the regions below the hot top. Thus, the molten metal may drain more thoroughly into the pipe near the electrode top. When the hot top is cut from the electrode, the primary shrinkage cavity is removed. The loss of the material remaining in the hot top is small. It is important to recognize that the hot top generally cannot fill all of the secondary shrinkage of an electrode due to the extremely long length-to-diameter ratios involved in the cast electrodes. A typical ratio would be 9 to 1 for a nominal 17 in. (43 cm) diameter electrode cast in a 150 in. (3.8 m) long mold.

Consumable Remelt Overview

Introduction. Static casting is the process of pouring a large volume of molten metal into a mold and controlling its solidification by mold design and metal feed so as to eliminate porosity. However, for large castings, the solidification rate is generally so slow that for superalloys, positive segregation defects will be formed (as discussed in the section on solidification). Thus, the production of superalloys by EAF/AOD or by VIM is generally by static casting the alloy into electrodes for subsequent remelting under controlled conditions.

There are two commonly used remelting processes, VAR and ESR. In both processes, the electrode is located in a water-cooled crucible. The working face of the electrode is heated to the melting point, so that drops of liquid metal fall from the face and are collected in the crucible and rapidly solidified. As the electrode is consumed by the advance of the melting face, it is fed into the crucible to maintain a uniform distance between the melting face and the solidifying pool of molten metal.

While having these broad characteristics in common, the methods by which the electrode face is melted are drastically different. The different melting methods have implications regarding the magnitude of cooling rates obtained and the nature of defects created by the remelting process itself.

Vacuum Arc Remelting Process Description. In VAR, the electrode is remelted in a vacuum chamber, of which the water-cooled crucible is an integral part. A direct electric current (dc) is passed through the electrode to the bottom of the crucible (the stool) and the electrode withdrawn, so that an arc is formed between the stool and the electrode face. The heat generated by this arc melts the face of the electrode, and metal transfer onto the stool begins as the molten metal drips onto the stool and is solidified. As the volume of metal on the stool (the ingot) builds up, an equilibrium state is reached in which there is a solid ingot, a mushy zone of both liquid and solid above that, and then a zone that is totally liquid. Because the heat extraction in

the steady-state condition of melting is fastest through the sidewalls and slower down the ingot and through the stool, the mushy zones and liquid zones are shallower near the sidewalls and deeper in the ingot center. As noted in the section on solidification, the thickness and growth angles of the mushy zone determine if the interdendritic liquid regions will coalesce to form positive segregation channel defects.

The thickness of the mushy zone at the center of a VAR ingot is controlled by the efficiency of heat extraction, the size (diameter) of the crucible, and the melt rate of the electrode face. The melt rate is controlled by the magnitude of current passed through the electrode. Other factors that are controlled so as to positively affect the solidifying structure are the distance of the melting face above the molten pool (arc gap) and the clearance of the sides of the electrode from the crucible (annulus).

It should be recognized that, when the electrode face becomes molten, the metal droplets are immediately transferred by gravity into the molten pool. Thus, VAR is a process in which it is inherently impossible to superheat the metal. This, coupled with the very high heat-extractive capability of the process, makes VAR the choice for economic manufacture of the largest-diameter ingots of segregation-prone superalloys. Additionally, the exposure of small volumes of molten metal to high vacuum is capable of removing detrimental high-vapor-pressure elements, such as lead and bismuth, that may not have been completely removed in VIM. Unfortunately, beneficial high-vapor-pressure elements such as magnesium are also reduced greatly in concentration.

Vacuum arc remelting ingots, however, are not guaranteed to be defect-free. The nature of the arc that provides the heat for the process is such that a different type of defect becomes inherent in the product. These defects, which are solute-lean (negative segregation), are not inherently as detrimental to the properties of a component as are defects resulting from positive segregation. For the most part, these defects also occur in discrete regions, as opposed to continuous channel defects, and their presence may be considered and accommodated in component design.

Electroslag Remelting Process Description. Electroslag remelting is not performed in vacuum. The heat source that causes melting from the working face of the electrode is a molten slag composed of CaF_2 plus oxide additions. The process is an alternating current (ac) process, and the current is passed through the electrode, then a slag cover, through the solidifying ingot, and through the stool. The molten slag provides the heat source for melting the electrode face. However, while the VAR molten drops pass through vacuum, the drops from ESR pass through slag. The exposure of the molten metal, both while it is gathering into droplets on the electrode face and as it is passing through the slag, allows reaction with the slag to occur. The reaction reduces oxides incorporated in the cast electrode while also greatly reducing the sulfur content through reaction with the CaF_2. Beneficial high-vapor-pressure elements such as magnesium are not reduced to the extent that they are in VAR. Electroslag remelting produces a cleaner, lower-sulfur ingot than does VAR.

The depth of immersion of the electrode into the slag, which is very shallow, is the analogous control to arc gap in VAR. Similarly, the choice of electrode diameter and crucible diameter determine the annulus, which is also an important control factor. Like VAR, melt rate is determined by power input, with melt current being the parameter varied to control the melt rate. Unlike VAR, ESR has incorporated a high volume of molten material (the slag) into the process. Thus, where VAR is a process with low thermal inertia, the ESR process has a high thermal inertia and does not respond as rapidly to changes in power input.

Because of the presence of the slag as a heat source in the solidification of an ingot, the fundamental relationship between mushy-zone thickness and distance from the side of the water-cooled crucible is changed. To a first approximation, it is generally stated that ESR pools are both deeper and steeper than VAR pools at corresponding melt rates and crucible diameters. This means that ESR is inherently more sensitive to the formation of positive segregation than is VAR. An alternative statement of the same phenomenon is that the maximum size of ESR ingot that can be produced free of positive segregation is smaller than the size that would be produced by VAR.

An additional benefit for ESR is the ability to melt simple shapes. Much of the volume

of superalloy that is used in sheet or plate form is from electrodes that are cast as rectangular cross-section slabs and melted into larger slab molds in ESR. VAR product is always round.

Electrode Quality

Composition. A common factor affecting consumable remelt quality for both ESR and VAR is the quality of the electrode. Electrode quality is affected by composition, cleanliness (low oxide and nitride content), and soundness (freedom from porosity and cracks). The most important characteristic of an electrode is composition. With the exception of reductions in volatile elements, VAR does not change the composition of the electrode. (For high-nitrogen electrodes, some reduction of nitrogen is accomplished by flotation of nitrides. As the solubility levels of TiN in the alloy are approached, this mechanism is no longer effective.) Electroslag remelting reduces sulfur content but may also cause minor changes in composition through reaction of titanium, aluminum, zirconium, and silicon with components of the slag. These changes are predictable in a mature process. Thus, there is no practical way to achieve composition modification once the master heat has been cast, but departure from normal practice in ESR may change titanium, aluminum, zirconium, or silicon content.

Cleanliness. The cleanliness of the cast electrode with regard to entrained oxide and nitride is an important characteristic for VAR electrodes. The introduction of a high volume of oxide or nitride onto the molten pool in VAR may degrade the efficiency of melting of the arc as well as disturb the electrical characteristics measured to maintain control of the arc gap. This is not a problem in electrodes to be melted by ESR.

Porosity. The porosity (secondary shrinkage) of an electrode may be of some concern in VAR. Vacuum arc remelting of electrodes with centerline porosity results in the preferred melting of the face in the porosity area. Thus, the melt face is no longer flat. The effect of this with regard to gap control during melting has not been quantified. A secondary problem connected with centerline porosity is the concern that projecting dendrites in this region may become detached from the electrode and fall, unmelted, into the molten pool. Then they may be incorporated into the structure without being remelted. The composition of such a region thus will be that of a primary dendrite (alloy-lean) rather than representative of the bulk composition. Theoretically, these concerns might also apply to ESR processes, but the necessity for melted or unmelted material to pass through the slag makes ESR products inherently less sensitive to electrode porosity.

Cracking. The final electrode characteristic affecting remelt quality is the freedom of the electrode from transverse cracking. In highly alloyed superalloys, the thermal stresses generated upon cooling of electrodes or upon heating in the remelt process may be sufficient to form transverse cracks. When the melt front of either VAR or ESR approaches such a crack, the heat transfer up the electrode is diminished, because of the thermal barrier presented by the crack. Thus, the material in front of the crack becomes hotter than would occur under equilibrium conditions and will tend to melt at a faster rate. After the melt front has gone through the crack, it encounters cold material, and the melt rate will tend to drop. In both VAR and ESR, the result is that the controls respond with changes in applied power to try to keep the melt rate constant. This, however, is seldom accomplished without some discernable disruption to the continuous nature of the growth of the solidification front. The only defense against these melt rate excursions (MREs, also called ''events'') is to produce an electrode free of cracks. In the future, it is hoped that more sophisticated melting controls will be able to detect the melt rate changes earlier and thus compensate for them more efficiently.

Vacuum Arc Remelting Operation

The VAR Furnace. Figure 4.10 illustrates, schematically, the construction of a VAR furnace. The VAR crucible is immersed in a tank of cooling water. Often, a tube is used to further enclose the crucible and limit the thickness of the water stream moving past the crucible surface. This increases the water velocity and thus increases heat removal from the crucible surface. Such tubes are called water guides. The crucible base (stool) has

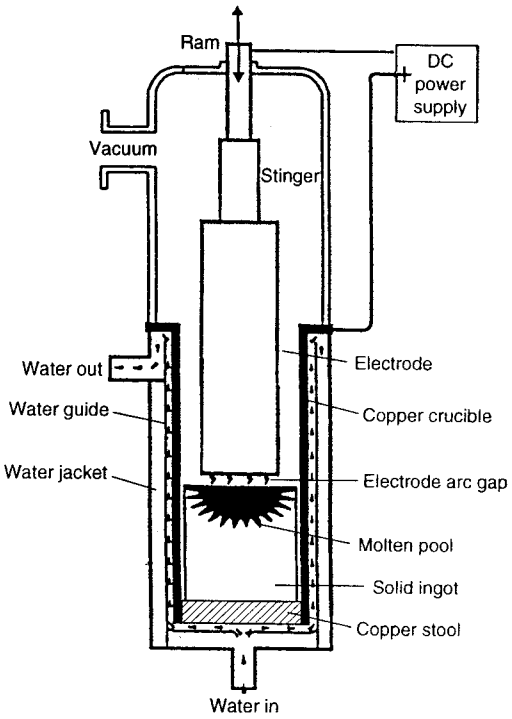


Fig. 4.10 Schematic of VAR furnace

provision for the inlet of a gas (usually helium). When an ingot is solidifying in the crucible, it pulls away from the crucible wall as it cools. This reduces heat conduction to the crucible wall. To maintain the highest possible heat removal from the solidifying ingot, a high-heat-capacity gas such as helium is introduced into the gap that is formed by the ingot shrinkage.

The top of the crucible mates with the VAR head. The head contains the vacuum ports and the ram, which drives the electrode into the crucible as it is consumed. The power supply is dc. Most VAR furnaces have two melting stations (crucible setups). While an electrode is melting in one station, the next station is prepared for melting. When one melt is finished, the VAR head is rotated in the horizontal plane to be located over the second crucible/electrode setup. The electrode is attached to the ram through a stinger, which is welded to the electrode. The ram in newer designs is capable of X-Y movement. In VAR, this is not movement in the horizontal plane, which would allow centering of the stinger/electrode assembly in the crucible. It is actually angulation of the ram from the vertical, so that if the stinger is not perfectly parallel with the electrode, then the ram may be angled to make the electrode parallel to the crucible sides. The VAR head mates to the crucible flange through an O-ring seal.

Vacuum Arc Remelting Furnace Operation. Electrode preparation is an important part of high-quality VAR operation. Oxides are not desired on a VAR electrode, because they add a source of oxide particles to the system, and many oxides are unstable at high temperatures in vacuum. Ionized volatile components from oxides create conditions under which the arc becomes unstable and causes a lack of control over the consistency of the remelt process. Thus, it is common practice to grind all electrode surfaces free of oxide.

In general, the stinger is welded to the electrode externally from the furnace. Preference for electrode orientation (stinger welded to electrode top or to electrode bottom) varies from producer to producer, with the choice being made primarily for operational reasons, rather than for quality effects. The furnace is pumped down and leak checked (leak-up rate measurement). Vacuum levels vary from producer to producer but are in the range of 0.1 to 10 μm. The only known effect of higher vacuum is to improve resistance of the arc to occurrences of instability.

The arc is struck between the electrode and the stool, and melt power (current) is stepped up to either the desired steady-state level or beyond (high-amp start-up). High-amp start-ups are often used to develop the steady-state pool shape as rapidly as possible. Pool shape in the start-up region is drastically different from regions higher in the ingot because of the additional heat-extractive contribution of the stool.

Vacuum Arc Remelting Control. The three major parameters defining the melt process are ingot and electrode diameter, arc gap, and melt rate. The choice of ingot and electrode diameter defines the clearance (annulus) between the crucible and the electrode. Insufficient clearance, either through a poor choice of annulus or through an off-center set-up, will lead to excessive current loss from the electrode to the crucible wall, rather than through the arc to the ingot. The choice of ingot diameter controls the amount of possible heat extraction and dictates the choice of melt rate so as to avoid positive segregation

defects in the ingot. These choices, of course, are long-term choices dictated in the purchase of VIM molds and VAR crucibles. They are not controllable (except for alignment) in the day-to-day melting process.

The arc gap is the nominal distance of the melting electrode surface above the molten pool at the top of the solidifying ingot. While often shown in schematics as a large distance, the commercially useful gaps range from a minimum of about 0.1 to a maximum of 0.5 in. (2.5 to 12.5 mm). When one considers that the nominal diameter of a molten metal drip from the electrode melt surface is 0.75 to 1.0 in. (18.8 to 25.4 mm), then it is obvious that the arc gap is not the precise clearance implied by schematics.

Vacuum arc remelting is a dc system, and the arc gap may be considered as the resistance in this circuit. As the melt current is held constant, any increase or decrease in the resistance of the circuit (change in arc gap) is seen as a change in voltage. Early VAR controls actually did measure these changes in voltage as a means for maintaining a uniform arc gap throughout the melt. Modern systems control the arc gap by measurement of drip short frequency (DSF). Figure 4.11 illustrates the change in melt voltage across an arc gap measured in 0.001 s time intervals. When a drip (drop) of molten metal is formed on the melting electrode surface, there is a point in time at which it is in contact with both the electrode and the molten pool. This causes a sudden decrease in voltage (an electrical short) across the arc gap. The duration of the short is measured in milliseconds. Control systems measure the number of drips of a given duration.

It has been demonstrated that the frequency of drip shorts (usually in drips/min) is related to the width of the arc gap. The relationship is not linear over the whole range of melt conditions that may be experienced but does allow useful measurement and control of the arc gap in the ranges that are currently used commercially. The higher the DSF, the smaller the arc gap. Making the gap smaller increases the duration of a short and thus increases the number of shorts counted. The relationship between arc gap and DSF also changes with changes in the melt current. At higher currents (higher melt rate), the drips are larger but less frequent. Thus, as

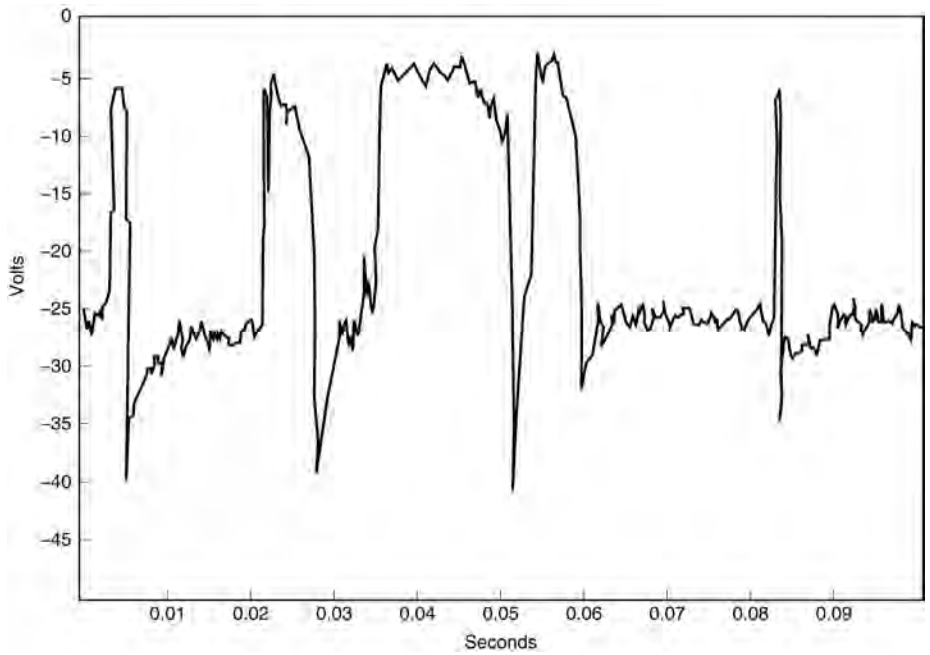


Fig. 4.11 High-speed data collection from VAR process illustrating the variations in time duration of negative voltage spikes (drip shorts)

illustrated in Fig. 4.12, raising the current requires a reduction in DSF to maintain equivalent arc gap.

Drip short frequency is measured over a period of time, usually fractions of a minute. Individual DSF values vary widely. Thus, control signals for the ram drive (electrode feed speed) are fluctuating. Normally, the ram is in continuous motion. The response to changes in DSF is to increase or to decrease the ram speed. Monitoring of the consistency of the ARC gap may be accomplished by computing a rolling average or by simple observation of the width of the band generated in recording each individual DSF measurement.

The electrode melt rate is the other important parameter to be controlled. The melt rate is dependent on the melt current. Many producers choose to select a given melt amperage and hold it constant. Other producers use load cells built into the VAR furnace to measure electrode weight and thus, the change in weight. The change in weight is used to calculate a melt rate, and the applied current is varied to attempt to maintain uniform melt rate. Similarly to DSF measurement, individual melt rate measurements will vary widely depending on the time frame chosen for the measurement. Melt rates are generally calculated using rolling averages. A common averaging time is 20 minutes.

Load cells are subject to the generation of false signals. Load cell design and maintenance are important factors in maintaining the quality of material melted in melt rate control. In addition to attention to detail in the design and maintenance of the load cells, it is possible to restrict the response of the system to perceived rapid changes in melt rate, so that false load cell signals do not generate an unnecessary change in the melt current, which would cause a real change in the equilibrium size and shape of the melt pool.

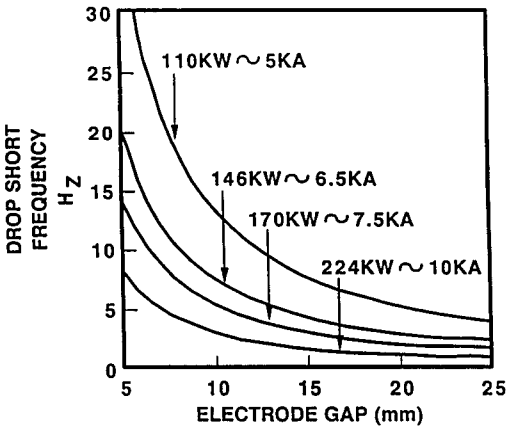


Fig. 4.12 Drip short frequency vs. arc gap as a function of melt current

Figure 4.13 shows a nominal representation, for a hypothetical melt, of some of the major control parameters measured during VAR. The melt begins with a high-amperage start-up (in amperage control) and, at the completion of the start-up, is placed into melt rate control. Note that the changes in voltage and DSF are not independent changes but are the result of the deliberate change in amperage. The voltage and amperage traces show a large number of spikes. This is a normal VAR characteristic. Much-larger spikes, either in magnitude or duration, might indicate a departure of the melt from the intended conditions.

At the end of the melt, if the electrode were completely consumed or the power was just abruptly shut off, the large molten pool would solidify, with the formation of a shrinkage cavity several hundred pounds deep into the ingot. This cavity would have to be removed during subsequent processing. To minimize the amount of material that must be cropped because of the end of melt shrinkage, it is common to step down the melt current as the end of melt approaches and to leave a small amount of electrode (a nominal 1 in., or 25.4 mm, of electrode length) unmelted. This ''biscuit'' allows continued heat to be put into the solidifying ingot at levels that are below those that would melt the biscuit but that serve to shrink the molten pool before final solidification and formation of the shrinkage cavity. Because the shrinkage cavity is always removed by cropping, this process is an economic issue, not a quality issue.

Vacuum Arc Remelting Control Anomalies. Variations in the traces of VAR parameters may indicate changes in melt conditions that will be detrimental to the quality of the solidification structure. Two of the more easily recognized problems are dead shorts and MREs.

Dead shorts occur when the electrode is driven into the top of the molten pool, causing direct transfer of the melt current to the solidifying ingot. Such a problem might be

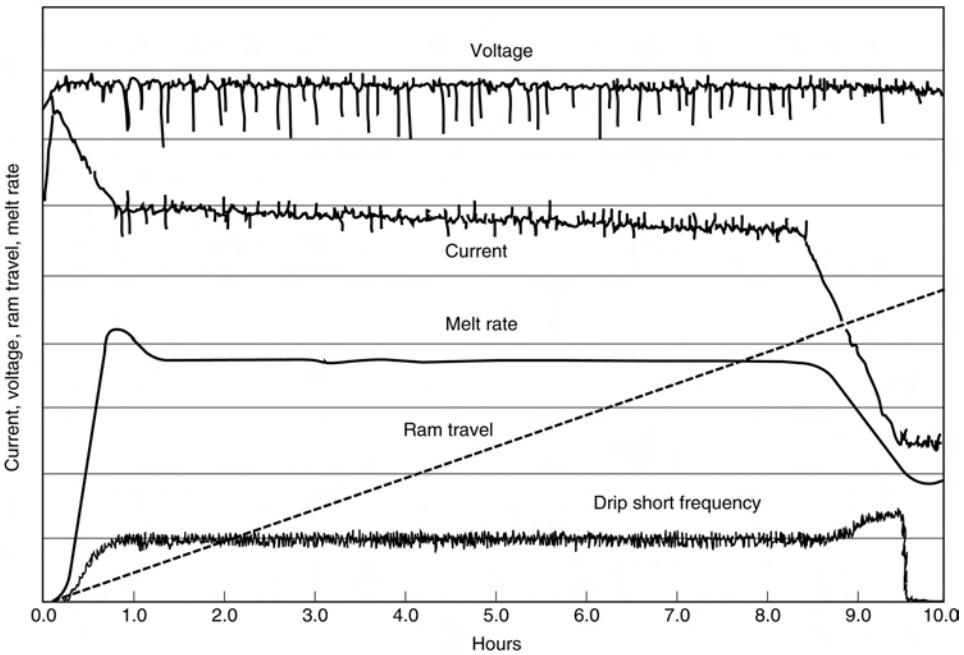


Fig. 4.13 Melt trace for VAR process showing variation in drip short frequency, melt current, melt rate, ram travel, and voltage during the melt

caused by an unusually shaped primary shrinkage cavity in the electrode. If the normal ram drive programming cannot accommodate the unusual shape, the electrode may be driven into the pool. This will show on the recorded parameters as a sudden reduction of voltage to zero and an immediate ram back-out from the dead short situation. Drip short frequency, of course, would also go to zero while the electrode face was in contact with the pool. (This would not show as zero DSF, because DSF is measured over a time period.) Dead shorts will cause a major change in solidification characteristics in the molten pool in that region.

Another cause of multiple dead shorts is the presence of high volumes of oxides and nitrides in the VAR electrode. If the oxide-nitride volume being melted onto the molten pool surface exceeds the capability of the process to sweep the ''dirt'' to the side and incorporate it into the ingot surface, then the ability to sustain an arc will be deteriorated. Melt rate will drop, and the ram travel, unable to react rapidly to sudden changes in arc gap, will drive the electrode into the pool, causing a short. This may happen repetitively as the ram backs out of the pool and then advances into it again.

Transverse cracks in the electrode cause MREs, the most readily definable VAR chart anomaly. Electrodes may develop transverse internal cracks due to thermal stresses. This may happen in the cooling of the electrode, or, often, due to the thermal stresses generated as the VAR melt front moves up the electrode. When the melt front approaches a transverse crack, heat transfer across the crack is diminished, and the material below the crack becomes hotter than normal. Thus, the melt rate begins to increase. The ram speed, which responds to a decreasing DSF, does not respond fast enough to maintain arc gap, thus the arc gap increases. This decrease may be observed on the chart. Similarly, the voltage responds to the larger gap, and the voltage on the VAR chart is seen to increase. Because the melt rate is increasing, the melt current drops rapidly to attempt to bring the melt rate back into control. Thus, the first part of an MRE may be seen as an increase in melt rate, increase in ram speed, decrease in DSF, an increase in voltage, and a decrease in amperage.

When the melt front progresses through the crack, the process reverses. The metal behind the crack is relatively cold, and melt current is low. The melt rate thus begins to drop rap-

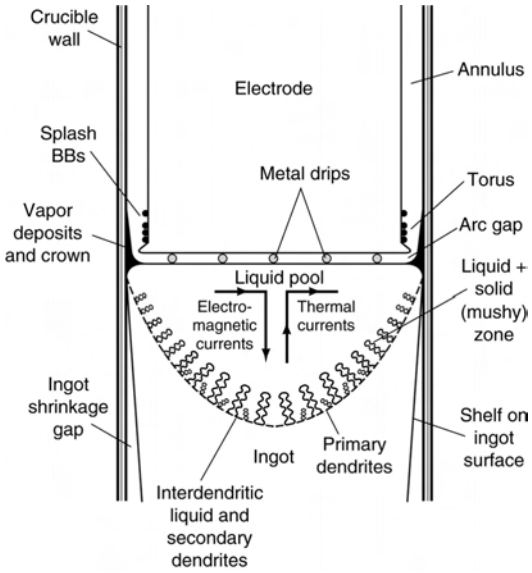


Fig. 4.14 Longitudinal schematic of the structure developed in a VAR ingot during melting

idly, the arc gap begins to close, and thus voltage decreases and DSF increases. Ram speed also slows, and the melt current increases. This region of an MRE is generally larger than the region of increased melt rate, and the structures generated are those that are typical of the cessation or drastic reduction of melting.

Vacuum Arc Remelting Pool Details. Figure 4.14 schematically illustrates the features of a molten pool in a VAR ingot. The relative sizes of annulus and arc gap are not to scale. The most important feature shown is the depth of the molten pool. It generally is assumed that the depth of the liquid zone is representative of the depth of the liquid + solid zone. (It will be recalled that the depth and angle of the liquid + solid zone controls freckle formation for any given alloy.) The size (depth) and shape of that zone might be thought, for a given crucible diameter, to have a direct relationship with heat input (melt rate) and heat extraction (water cooling). As is shown in Fig. 4.15 (a composite graph from several independent sources), the melt rate is directly proportional to the applied melt current. However, as seen in Fig. 4.16, the relationship between pool depth and melt current is direct but is divided into two separate regions. The reason for this is indicated by the two lines in Fig. 4.14, which indicate the direction of liquid metal flow in the VAR pool. Competing currents are generated by the tendency of lower-density hot metal to rise along the ingot centerline (thermal buoyancy stirring) versus the tendency of electromagnetic fields (Lorentz stirring) to drive liquid metal from the edge of the crucible to the center of the crucible and down the centerline. Figure 4.16 is divided into two regimes, because the inflection point (nominally 6600 amperes for 20 in., or 51 cm, IN-718 ingot) marks where Lorentz stirring becomes stronger than thermal buoyancy stir-

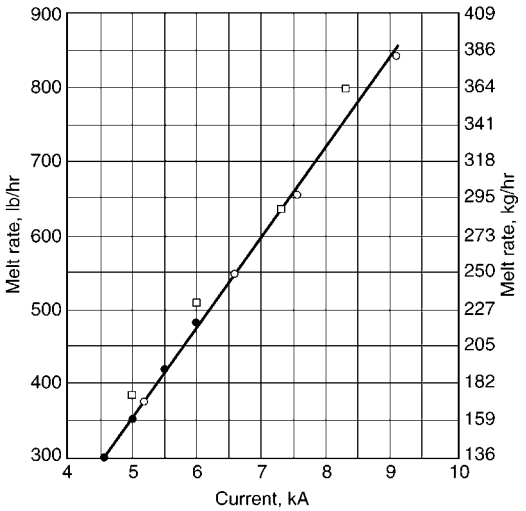


Fig. 4.15 Melt rate vs. VAR melt current (20 in. ingot)

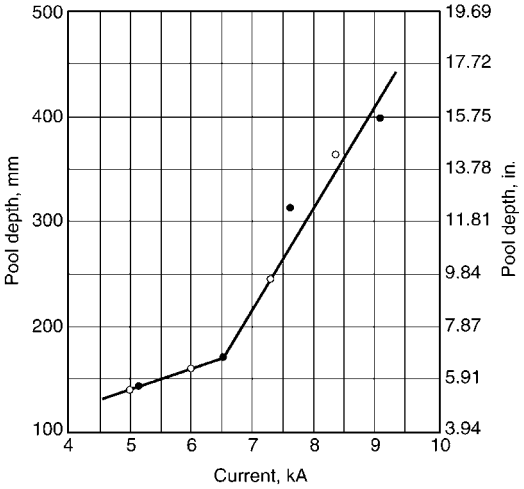


Fig. 4.16 Vacuum arc remelting pool depth vs. melt current

ring. The apparent depth of the molten pool is altered not because there is a change in the volume of molten metal, but because the centerline stirring at higher amperages causes the pool to depart from a nominal U-shape and become deeper in the center. Thus, high VAR amperages not only produce deeper pools, but also alter the angle of the liquid + solid zone, with respect to the ingot axis.

In addition to deepening the molten pool and increasing the angle of the liquid + solid zone, melting at a current where Lorentz stirring is dominant has an additional ramification. At low currents, oxides and nitrides in the electrode are melted out, drop onto the molten pool surface, and are swept to the sides of the electrode. When melting at high currents, these particles may not migrate to the edge of the ingot but may be incorporated to some extent in the general structure of the ingot, perhaps with a concentration along the centerline. It is thus considered inadvisable to melt superalloys at VAR currents in the Lorentz-dominated region.

The edge of a VAR ingot is the first metal to solidify. It is thus, as dictated by the phase rule, alloy-lean. It is present as a skin around VAR ingots and is known as ''shelf.'' The shelf, in addition to being alloy-lean, contains both the oxides and nitrides collected from the melt pool surface as well as portions of the vapor deposits and splash BBs that have been deposited on the crucible wall above the advancing molten pool. This material can sometimes be carried through onto the surfaces of finished forging billet if material removal in peeling the forged billet is insufficient. Figure 4.17 illustrates a forged IN-718 ingot prior to peeling the billet surface. The extent of penetration of the shelf into the forged billet is evident from the extent of the white etching edge regions.

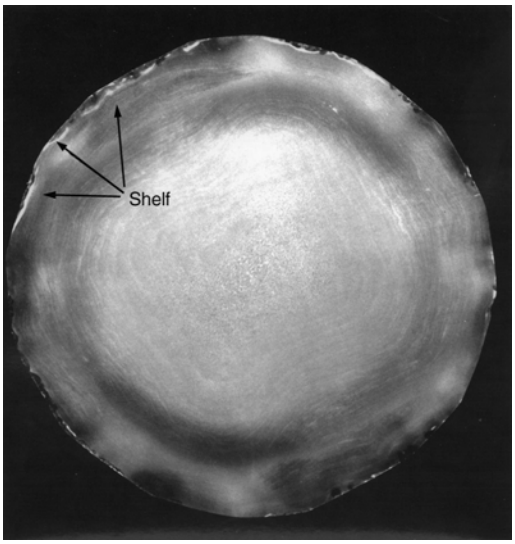


Fig. 4.17 Transverse billet section of IN-718 nickel-base superalloy macroetched to show VAR shelf location and depth at billet surface

Melt-Related Defects in VAR

Discrete White Spots. Under ideal conditions, the arc is distributed uniformly across the surface of the molten pool. (This is called a diffuse arc.) However, the introduction of conductive ionic species into the melt or increases in the resistance (arc gap) in the system may cause the arc to become locally concentrated (constricted arc). Constricted arcs do not dwell in one place on the molten pool surface, but move about the surface. When constricted arcs undercut the crown/shelf (Fig. 4.14), small pieces of the shelf may fall into the molten pool. These pieces move by gravity down the pool profile. They do not readily remelt into the pool, because they have a higher melting point than the pool in general. Ultimately, they are not dissolved and are incorporated into the ingot as regions of low solute content, containing stringers of oxide and nitride. When detected in the final product, they are seen as light etching defects containing stringers of oxide and nitride and are known popularly as ''dirty white spots.'' More correctly, these regions are called discrete white spots, in keeping with their nature as a distinct but isolated structure within the ingot matrix. Theoretically, a piece of shelf, free of oxides and nitrides, might be undercut and form a discrete white spot that is not dirty. Figure 4.18 shows macro- and micrographs of a discrete white spot containing ''dirt'' stringers.

Often, because of the lack of solute, the grain size in discrete white spots will be larger than that of the matrix. When present, dirt stringers act as stress raisers. Thus, discrete white spots, which have a high probability of being large-grain and dirty, are acknowledged to be detrimental to properties in superalloys. Unfortunately, although best

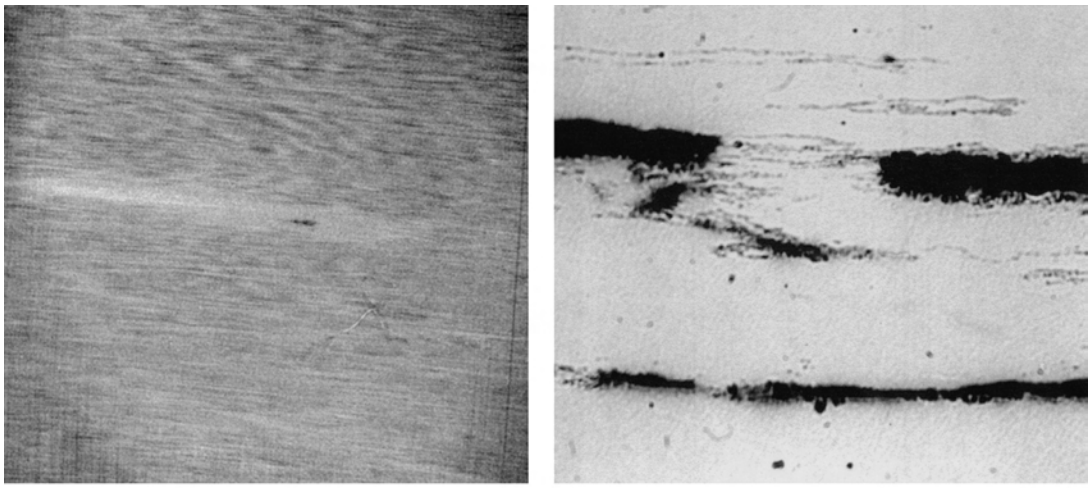


Fig. 4.18 Longitudinal section taken from sonic defect in IN-718 nickel-base superalloy (a) macroetched to show white spot and crack associated with the defect and (b) micrograph of same location showing oxide and nitride stringers associated with the discrete white spot

practice for electrode preparation and for VAR melting may minimize the frequency of occurrence of discrete white spots, there is no way to guarantee their elimination in VAR products. The probability of their occurrence in the final component must be considered in the design of the component.

Solidification White Spots. Because discrete white spots cannot be prevented from forming in VAR products, it is prudent to inspect critical components for the presence of these defects. Currently, there is no method of detecting a subsurface defect except to the extent that, combined with forging deformation, a crack may be generated that will be detectable by ultrasonic inspection. Macroetching of the surface of critical components is a common method for detection of discrete white spots and any other melt-related structure. In considering the results of macroetching, the method by which contrast is obtained between the white spot and the matrix must be considered. For example, in IN-718, the contrast is not directly due to the niobium differences between the two regions. Rather, most macroetches attack the precipitating delta phase in IN-718. Thus, contrast is seen in IN-718 because of differences in volume of precipitated delta between the two regions. When forged under conditions that minimize delta formation (coarse-grain forging), a macroetched component will show much less contrast between niobium-rich and niobium-lean regions. Conversely, a sample of IN-718 heat treated to maximize delta formation may be uniformly attacked despite the presence of niobium gradients. However, the fabrication temperatures for most components are such that solute-lean regions will show as light (white) etching features.

A problem in inspecting macroetched superalloy components for harmful light etching features is that superalloy ingots are not completely homogenous. As an example, Fig. 4.19 shows the same slice of forged VAR IN-718 in two different heat treated conditions. In the first condition, delta precipitation is very high, a high degree of attack by the etchant is obtained, and no contrast is evident. When heat treated at 1825 °F (996 °C), close to the delta solvus temperature, much of the delta in the niobium-lean regions is dissolved and contrast is enhanced. The structure then is shown to consist of concentric rings of alloy (niobium)-lean and alloy-rich material. These concentric rings are the inherent solidification structure of a VAR ingot. Fortunately, most fabrication of IN-718 is conducted in the temperature region close to the delta solvus, and light etching features may be detected on the component structure.

A continuing problem in macroetch inspection is that many of the features detected are related to the inherent ring solidification

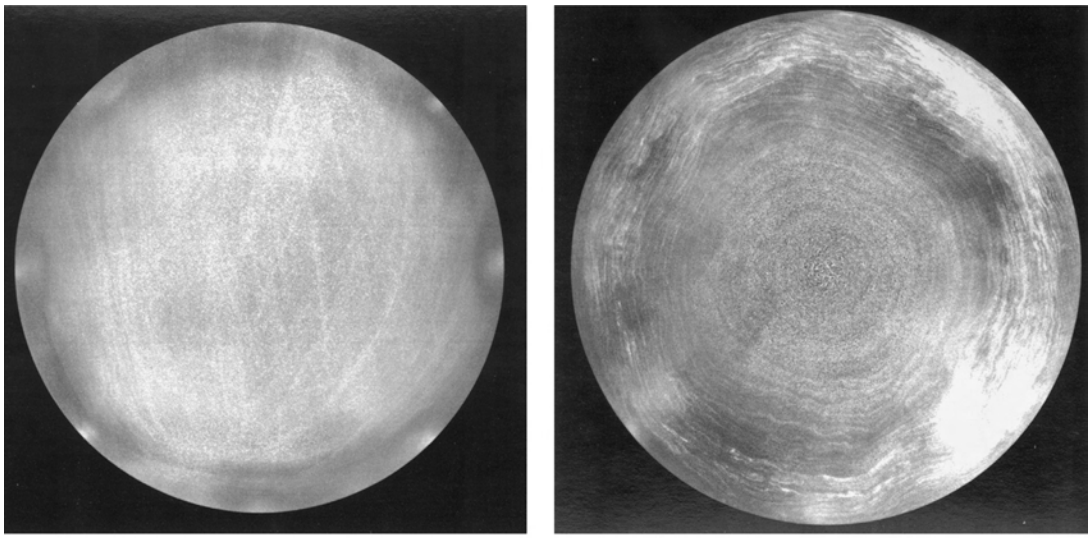


Fig. 4.19 Transverse billet section of IN-718 nickel-base superalloy showing niobium distribution in homogenized and forged product (a) heat treated to maximize delta precipitation and macroetched, showing lack of contrast in section, and (b) same section heat treated to exceed the local minimum delta solvus and macroetched

structure of VAR ingots. These regions may simply be wider-than-normal spots in the ring structure or may be reactions to events such as local supercooling caused by the melt-in of splash BBs (see Fig. 4.14). Discontinuities in the ring and reaction with splash BBs become more prevalent as the molten pool becomes shallower. Thus, in the start-up regions of VAR ingots, where equilibrium pool depth has not been achieved and stool cooling is still very strong, there may be a very high frequency of these light etching features. Figure 4.20 shows a macroslice of forged VAR IN-718 taken from the start-up region. The light etching features have been named ''solidification white spots.'' Generally, the only effect of one of these features will be to allow localized grain growth if the forging temperature exceeds the localized decrease in the precipitate solvus temperature. Oxide-nitride stringers are not present in solidification white spots.

Unfortunately, the detection of any light etching defect on the surface of a critical component will be cause for the removal of that component from the production line and critical examination of the features to determine the suitability of the component for its application. While the presence of oxide-nitride stringers is an obvious cause for rejection of the component, most manufacturers have also developed standards for acceptance or rejection of localized grain-size variation. Thus, while solidification white spots are not immediately rejected as are discrete white spots, efforts are necessary to minimize their formation and inclusion in the VAR product to reduce inspection costs. Generally, these measures include taking crops from the bottom of the ingot to ensure that the start-up region material is not included in the final product. Using high melt rate in the initial start-up reduces the size of the start-up region. Higher melt rates also increase the molten pool depth and thus decrease the occurrence of localized reductions in solidification rate in the ring structure. Other factors related to VAR control, such as the annulus, are also known to affect the frequency of formation of solidification white spots.

Electroslag Remelting Operation

The ESR Furnace. Figure 4.21 illustrates, schematically, the construction of an ESR furnace. The ESR crucible is normally self-contained, unlike the VAR crucible, in that the inside and outside shells through which the cooling water runs are assembled as a sin-

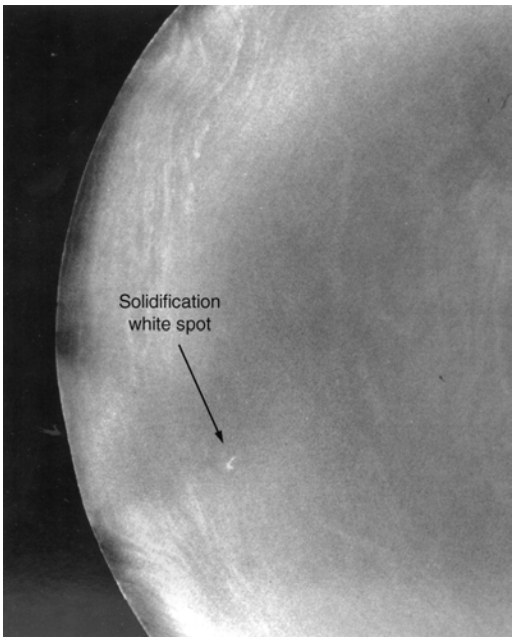


Fig. 4.20 Transverse billet section of IN-718 nickel-base superalloy, macroetched to show solidification white spots resulting from too low a VAR melt rate

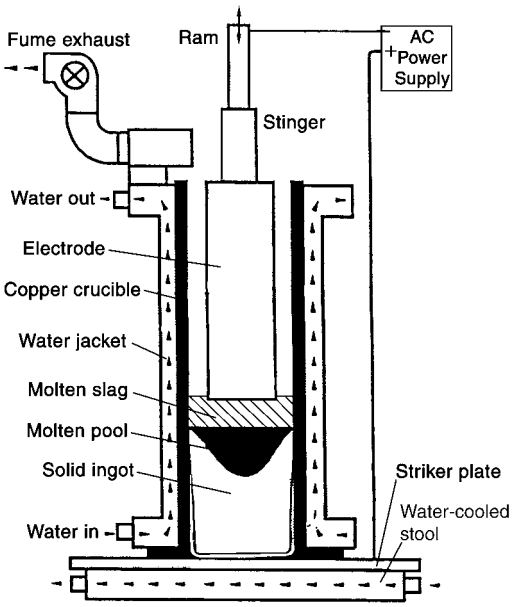


Fig. 4.21 Schematic of electroslag remelting

gle piece. A water-cooled stool is assembled to the shell to form the bottom of the crucible. A starter or striker plate is usually enclosed in the junction between the crucible shell and the crucible stool. For crucibles to be used with hot slag starts, the crucible may contain an opening at the bottom (a ''mouse hole'') through which the molten flux will be introduced. Unlike the VAR furnace, the top of the crucible does not mate to the rest of the furnace but operates exposed to air.

The top of the ESR furnace contains the ram drive and load cells. It is connected electrically to the crucible stool through, most commonly, four vertical bus bars located at 90° intervals around the crucible. The ESR head commonly is able to be translated in the horizontal direction by an X-Y drive, which allows centering of the electrode in the crucible prior to the start of the melt. (Note that X-Y capability is inherently different in ESR compared to VAR.) The power supply is most often AC. Most ESR furnaces have two melting stations (crucible setups). While an electrode is melting in one station, the next station is prepared for melting. When one melt is finished, the ESR head is rotated in the horizontal plane to be located over the second crucible/electrode stinger setup (the electrode is attached to the ram through a stinger, which is welded to the electrode). Melting is then ready to begin.

Electroslag Remelting Furnace Operation. Unlike VAR, electrode preparation is not a critical part of quality ESR operation. Oxides on an electrode surface are incorporated into the slag. Thus, electrodes for ESR are generally not ground. An exception to this is for production of premium-quality material where the end-user specifications require grinding to ensure the removal of potential iron-mold pullout on the electrode surface. Also, the shrinkage cavity at the top of the electrode is not a problem, if the electrode is melted top down. Thus, electrodes for ESR are not commonly hot topped in VIM or cropped prior to melting.

The ESR stinger is welded to the electrode externally from the furnace. The stinger is often tubular, because only the periphery of the electrode is involved in the welding process. The electrode is placed into the crucible and connected to the head. The X-Y drive is used to center the electrode in the crucible. (Note that the X-Y drive may compensate for welding of the stinger off-center but cannot compensate for an angle between the stinger axis and the electrode axis.)

There are two possible start-up scenarios, cold start and hot start. In cold start, the slag and small particles of the alloy to be melted (usually machining chips) are placed on the starter plate. The electrode is touched into the slag-alloy mix and backed out to establish an arc. High melt power is used in this start-up phase. The arc melts down both the slag and the metal particles, at which point the electrode becomes immersed in the slag and the melt process shifts to melting of the electrode surface by the slag. It is necessary that the start-up power be sufficiently high that actual welding (melt-in) occurs between the embryonic ingot and the starter plate. This is required so that the electrical conduction path will be predominantly through the electrode, then the slag to the ingot, from the ingot through the starter plate, and then to the stool.

In hot slag starts, the slag is melted externally by electric arc in graphite crucibles. The molten slag is introduced, generally through a bottom mouse hole, into the crucible. The electrode is lowered into the slag, and melting commences. Although high initial melt power is not required to melt slag and metal starter material, a high-power profile start-up is generally used to ensure the melt-in of the ingot to the starter plate (to ensure good electrical conduction paths).

High-power start-ups also compensate, as they do in VAR, for the extra cooling effect of the proximity of the ingot to the stool and help develop steady-state melt conditions at an earlier time in the melt.

Electroslag Remelting Control. The three major parameters defining a melt process are:

- Ingot and electrode diameter (as in VAR)
- Electrode immersion depth in the slag (analogous to arc gap in VAR)
- Melt rate

The choice of ingot and electrode diameter defines the clearance (annulus) between the crucible and the electrode. Insufficient clearance is generally regarded as a problem in processes using cold slag starts, in that the slag-chip mix may get hung up in the annulus. However, a tight annulus may result in more uniform heat distribution across the molten pool. There is no published information to support either viewpoint. Thus, annulus becomes, much more than in VAR, a parameter dictated by the individual producer's philosophy.

Electrode immersion is generally thought of as a depth of penetration of the electrode into the slag. There is no definitive method for measuring the immersion, but observation of interrupted melts suggests that the meniscus of slag reaching up the side of the electrode will generally not exceed 0.25 in. (6.4 mm). Thus, schematics of the ESR process are misleading when they imply significant immersion into the molten slag. However, the degree of immersion, as affected by the ram drive, can produce drastically different electrical signals. The quality of the melt has been found to be responsive to these signals. Thus, while there is no realistic understanding of what depth of immersion means physically, the parameter that controls it can be demonstrated to have a significant effect on melt quality.

ESR is an AC process, and the electrode immersion plus the thickness of the slag cap may be considered as the resistance (impedance) in this circuit. Changing the weight of slag in the system or the slag composition changes the impedance of the circuit and thus changes the amperage and voltage required to maintain a given power input (for constant melt rate). The slag cap thickness is the primary driver, while electrode immersion may account for 10%–20% of the total impedance. Measurement of the changes in this resistance or of the corresponding changes in voltage may be used to control the immersion of the electrode in the slag. This suggests that the voltage and impedance changes associated with electrode immersion are actually the impedance of the circuit associated with the interfacial resistance between the electrode melt surface and the slag surface. It thus should be realized that, in ESR of superalloys, the electrode immersion is always extremely shallow, and, in fact, the most common electrode positioning is that of ''skittering'' on the top of the molten slag cap. The degree of this skittering is commonly controlled by the repetitive change in voltage in the process (volt swing).

The electrode melt rate is the other important parameter to be controlled. The melt rate is dependent on the melt current. Although some VAR processes are run in constant current rather than in melt rate control, ESR processes are exclusively melt rate control. Melt

rates are generally calculated using rolling averages. A common averaging time is 20 minutes. Load cells are subject to the generation of false signals and to errors in the absolute value. Thus, load cell design and maintenance are important factors in maintaining the quality of ESR. In ESR, the melt current responds to changes in the melt rate and attempts to hold the melt rate constant at the set point. Because of the presence of the slag, which must be heated or cooled, in the system, the response time of ESR to the melt current change is much slower than that of VAR.

A fourth factor controlling melt quality and unique to ESR is the choice of slag and the volume of slag used. The resistance of the slag cap depends on both the resistivity of the slag and the thickness of the slag cap through which the melt current must travel. An additional consideration is the degree of chemical reactivity of the slag with elemental components of the electrode.

Figure 4.22 shows a nominal representation, for a hypothetical melt, of some of the major control parameters measured during ESR. The melt begins with a high-amp start-up in amperage control and, at the completion of the start-up, is placed into melt rate control. Note that the change in voltage is the result of the deliberate change in amperage. As in VAR, at the end of the melt, if the electrode were completely consumed or the power was just abruptly shut off, the large molten pool would solidify, with the formation of a shrinkage cavity several hundred pounds deep into the ingot. This cavity would have to be removed during subsequent processing. To minimize the amount of material that must be cropped because of the end of melt shrinkage, it is common to step down the melt current as the end of melt approaches and leave a small amount of electrode (a nominal 1 in., or 25.4 mm, of electrode length) unmelted. Unlike VAR, this biscuit is generally not used to put electrical power into the melt. Rather, it simply prevents radiation loss from the slag. Because of the presence of the slag as a heat source at the top of the ingot, ESR hot topping practices are not as extended as are those for VAR.

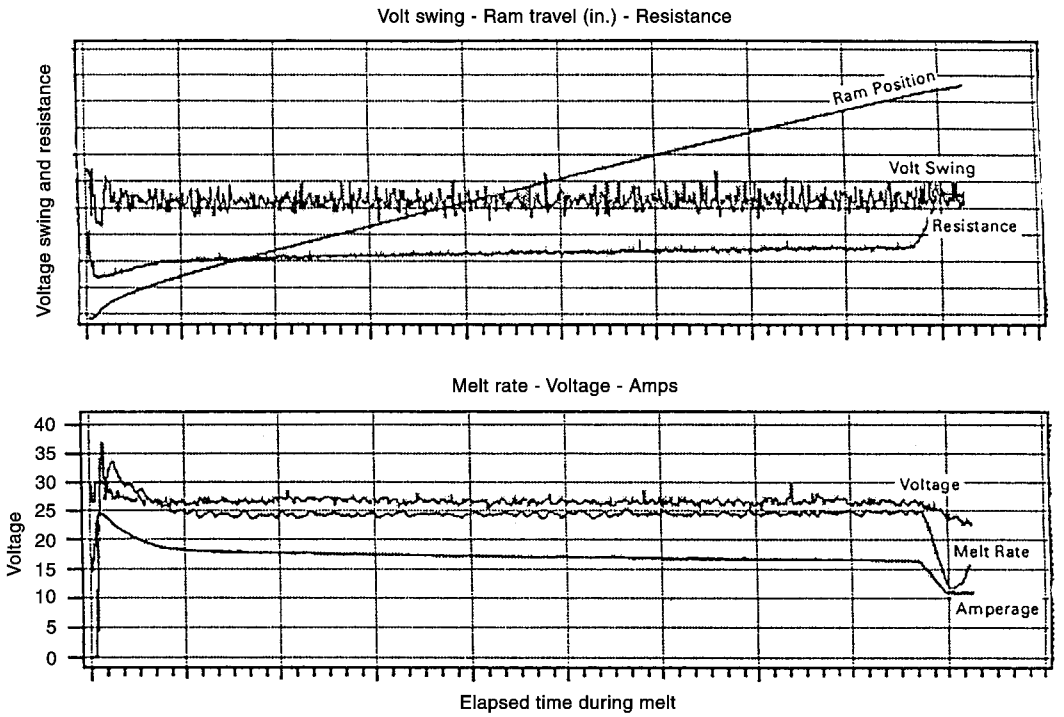


Fig. 4.22 Melt trace for ESR showing variation of melt current, melt rate, ram travel, slag resistance, voltage, and volt swing

Slag Choices. All ESR slags contain CaF_2 as the primary constituent. Oxides may be added to the slag to raise the resistivity (so as to make melting more efficient electrically) or to modify the slag chemistry with regard to its reactivity with the metal being melted. There is a universal designation system for slags in which the percentage of constituents is listed in the order $CaF_2/MgF_2/CaO/MgO/Al_2O_3$. Thus, a common base slag such as $60\%CaF_2/20\%CaO/20\%Al_2O_3$ should be referred to as 60/0/20/0/20. Unfortunately, the system is seldom adhered to in the industrial world, and 0s are often omitted. Thus, the previously mentioned slag is generally referred to as 60/20/20.

Titanium and zirconium are superalloy elements that often interact with the slag during ESR. Many proprietary slags contain additions of TiO_2 and/or ZrO_2 to prevent excessive loss of these elements into the slag during melting. The loss is due to exchange with any oxide in the slag that is less stable than the element in the electrode. A common problem with titanium-bearing superalloys is that commercially available CaF_2 contains SiO_2. During ESR, the SiO_2 is converted to silicon, which is picked up by the metal. Thus, the slag is enriched in TiO_2, which reduces the titanium content of the metal. This reaction generally results in a titanium gradient in the ingot, because the SiO_2 content is consumed early in the melt and no longer plays a part in the reaction after the first few hours of melting. When ESR slag is recycled, it is already depleted in SiO_2, and this reaction no longer occurs. The slag always tries to move to chemical equilibrium with the molten metal at the operating temperature of the slag. Thus, repetitive recycle of slag with a given alloy composition produces a slag that is naturally buffered against causing elemental loss from the electrode during ESR. Unfortunately, slag loss (left as a skin on the electrode during the process) generally keeps recovery levels of the slag below 100%, so some fresh slag is always needed in the ESR process.

Electroslag Remelting Pool Details. Figure 4.23 schematically illustrates the features of a molten pool in an ESR ingot. As in the VAR pool schematic, the relative sizes of annulus and immersion are not to scale. The most important feature shown is the depth of the molten pool. (It will be recalled that the depth and angle of the liquid + solid zone controls freckle formation for any given alloy.) Compared to VAR, very few studies have been done on the nature of the molten pool in ESR. The pool differs fundamentally from a VAR pool in that the molten slag cap provides a source of heat to the system, and the slag skin on the solidifying ingot provides insulation, reducing heat extraction. Consequently, for comparable melt rates and crucible diameters, an ESR ingot will have a deeper, steeper-sided pool. Thus, compared to VAR, ESR ingots have traditionally been regarded as being more prone to the formation of positive segregation effects.

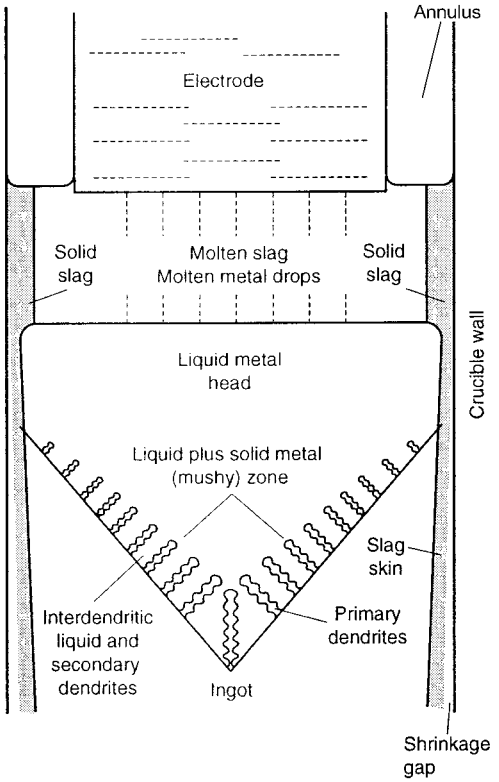


Fig. 4.23 Longitudinal schematic of the structure developed in an ESR ingot during melting

It must be supposed that thermal gradients, similar to those in a VAR pool, are also present in the ESR pool. However, the nature of the electromagnetic currents has not been identified, to date, in any publications. While the shape of an ESR pool may inherently be more prone to positive segregation, that shape may be altered by judicious choice of

melting parameters. It is possible to produce a U-shaped pool in ESR that is very similar to that in VAR. For alloy systems that are highly alloyed but have only moderate freckle-forming tendencies, such as Waspaloy, ESR processes can be made sufficiently robust that they can be used for critical rotating components without undue concern for the presence of positive segregation effects.

Melt-Related Defects in ESR

Introduction. In Fig. 4.23, the schematic for the edge of a solidifying ingot indicates a processing advantage for ESR that has made it desirable to develop this process for use in critical components. The insulating nature of the slag creates conditions at the edge of the ingot that do not produce shelf. Thus, with no arc instabilities of concern and no shelf to be undercut, the formation of discrete white spots in ESR product could only occur by some infrequent occurrence, such as drop-in of pieces from an unsound electrode.

Positive Segregation. Alloys that have high-density interdendritic liquids may form unique structures in ESR. The high-density liquid tends to flow downhill toward the center of the ingot. Although channel defects may not be formed, large pools of high-solute alloy may be formed. These regions may form in widely separated parts of an ingot and be separated by ''normal'' material. Because of the greater number of variables inherent in ESR, the underlying causes for such segregation have not been determined. The nature of these areas and their effect on properties have not been reported.

Electroslag Remelting Ingot Surface. The interaction of the molten metal with the slag cap should be understood, with regard to obtaining good surface on ESR ingots. As shown in Fig. 4.23, the molten slag solidifies against the water-cooled crucible side just as the molten metal would. The molten metal pool, in addition to being V-shaped (containing the mushy zone), also contains a fully molten straight-sided component or metal head. The metal head remelts some of the solidified slag on the crucible wall, so a thinner slag layer is then contained between the ingot and the crucible wall. Should this slag skin be locally penetrated by the metal head, a thin stream of metal will be driven through the hole. Such a metal fin or bleedout is illustrated in Fig. 4.24. Note that the penetration of the slag is through a circular region that is essentially the size of a dime. The molten metal not only moves down the ingot surface in response to gravity, but is forced upward from the penetration due to the combined hydrostatic pressure of the molten metal head and the molten slag cap. Bleedout formation is sensitive to melting conditions and slag composition. While there is no published association of bleedouts with detrimental structure, there is an economic factor involved, in that an ingot with bleedouts will require grinding prior to forging or other hot working.

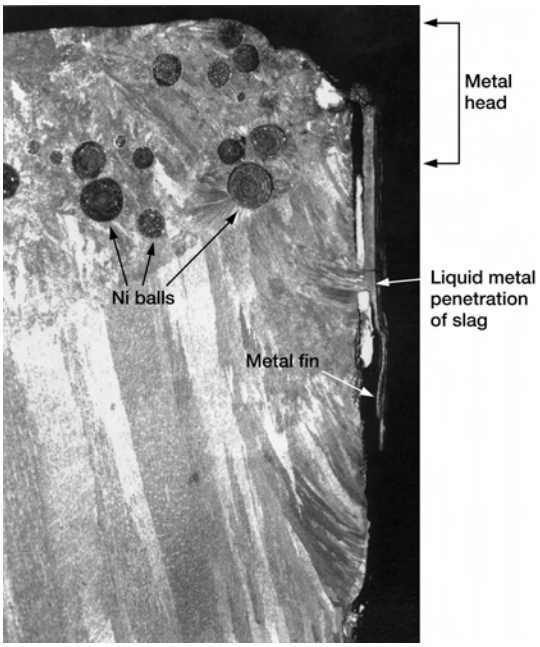


Fig. 4.24 Longitudinal section through a metal fin formed by a bleedout on the surface of an ESR ingot. Note: The circular, dark etching features are nickel balls introduced in an experiment to delineate the shape of the molten pool. They are not related to the bleedout mechanism.

Triple-Melted Products

Background. Several producers of critical rotating components in the gas turbine industry have adopted the use of a hybrid secondary melt process: VIM to ensure an initial

electrode with low oxygen and precise chemistry, followed by ESR. The ESR electrode will be clean and sound but may contain freckles. The final segregation-free structure is obtained through the application of a third melting process (VAR) to the ESR ingot.

Triple Melt Ingot Processing. The ESR ingot (sometimes referred to as an ''ingode,'' because it is an ingot for remelting as an electrode) may be processed in one of two ways. The most direct process is to simply VAR the ingode. This process (melt-melt-melt) requires a size progression through VIM, ESR, and VAR, which makes the VAR diameter one that is capable of producing structure free of positive segregation. For IN-718, a typical sequence of diameters for the VIM, ESR, and VAR, respectively, would be 14, 17, and 20 in. (35.6, 43.2, and 50.8 cm). The weight of electrode going into the final VAR process is thus restricted by the practical length/diameter of a 14 in. (35.6 cm) VIM electrode (6500 lb, or 2950 kg).

If a larger VIM electrode diameter (10,000 lb, or 4950 kg) is used, then a larger ESR ingot may be produced. To achieve the desired ingode diameter for VAR, the larger ESR ingot is forged back to the desired size, ground to clean off the forging scale, and the ends cropped square. This process is designated melt-melt-forge-melt, with diameters after VIM, ESR, forge, and VAR, respectively, being 17, 20, 17, and 20 in. (43.2, 50.8, 43.2, and 50.8 cm). This melt-melt-forge-melt practice is more time-consuming but may be justified by the inherently higher yields associated with larger ingots. Also, very large components may require input weights only obtainable by a melt-melt-forge-melt process.

The clean, sound ingode (from either process method) is remelted by VAR. The improved cleanliness and soundness of the electrode facilitates VAR control. The products, referred to as Triple Melt, have a much-reduced frequency of dirty white spot occurrence compared to Double-Melt (VIM + VAR) product. Also, at larger diameters, the sound electrode facilitates control to avoid formation of positive segregation. However, even in Triple Melt, discrete white spots and solidification white spots will occur, and their presence must be considered in the component design.

Ingot Conversion and Mill Products

Introduction. Primary hot working operations for superalloys are directed toward converting cast ingots into mill products. Mill products fall into two classes: long products (billet and bar) and flat products (plate and sheet).

As a result of the melting process, all superalloys will be segregated, to a greater or lesser degree, during solidification. Simple compositions may become homogeneous simply from the exposure to high temperature during hot working. More complex compositions may need deliberate high temperature, extended time exposure (homogenization) prior to hot working to level the compositional gradients created in the ingot. Figure 4.25 schematically illustrates the major operations used for ingot breakdown. These are cogging (forging), rolling, or extrusion. Extrusion differs from cogging or rolling in that all the deformation occurs in one pass. In the process of working superalloys, many different thermal-mechanical cycles of heating and deformation occur. Furthermore, intermediate ingot conditioning may be necessary.

Because superalloys are process-history sensitive, these thermal-mechanical processing cycles can have an important effect on the final properties of a given alloy component. Admittedly, the final processing steps (forging or rolling and subsequent heat treatment) after ingot breakdown are the primary generators of structure and, hence, properties. However, all steps in the movement from ingot to final wrought product contribute to the ultimate result.

Some mill products, principally long products, may undergo further hot working (generally, forging) to shape them into a final component. Because of factors such as possible low forging temperature, inhomogeneous deformation, die chill, friction, and so

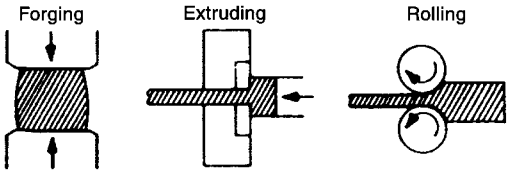


Fig. 4.25 Schematic illustration of major operations used for ingot breakdown

on, the forged microstructure in regions of a component can contain remnants of the as-cogged microstructure. Isothermal (superplastic) forging (see Chapter 6) is helpful in minimizing such effects. However, as fatigue properties have become increasingly important for forgings, stricter grain size, microstructural uniformity, and quality requirements have been imposed—sometimes by specification, and sometimes by recommended or approved practices agreed to by customer and supplier. The many improvements in melting technology as well as the introduction of improved and automated equipment for ingot breakdown have enhanced grain size control, microstructure, and quality in billet or mill product produced from ingots. In addition to controls on the interior structure of an ingot/billet during breakdown, improved surface finish has been sought to provide for better sonic inspectability.

Homogenization of Solute Distribution in Ingots. The problem of nonuniform solute distribution in the interdendritic regions of cast ingots must be considered during the conversion process. For low-solute-content alloys, the heating sequences used on converting the as-cast ingot to a wrought product will serve to produce an adequately (chemically) uniform structure. However, for highly alloyed materials, such as Waspaloy, IN-718, and U-720, extended times at temperatures far in excess of the forging temperature are required to homogenize the cast product. In some alloys, these temperatures may deliberately exceed the melting point of some of the interdendritic regions. Homogenization temperatures of 2200 °F (1204 °C) are not unusual, while times at these temperatures will not untypically reach four days. Despite extended times at high temperatures, some solute gradients may not be completely leveled. Figure 4.26 shows the niobium distribution in a well-homogenized ingot of IN-718 after forging to billet. The difference between the maximum and minimum values is 0.7% Nb.

In wrought compositions, the carbon content generally is much lower than found in similar alloy versions employed for investment casting. Thus, the as-cast ingot structure for a wrought alloy composition does not contain an appreciable number of carbides. The carbon is concentrated in the interdendritic regions and reacts to form carbides during the homogenization treatment. The temperature at which the carbides are first

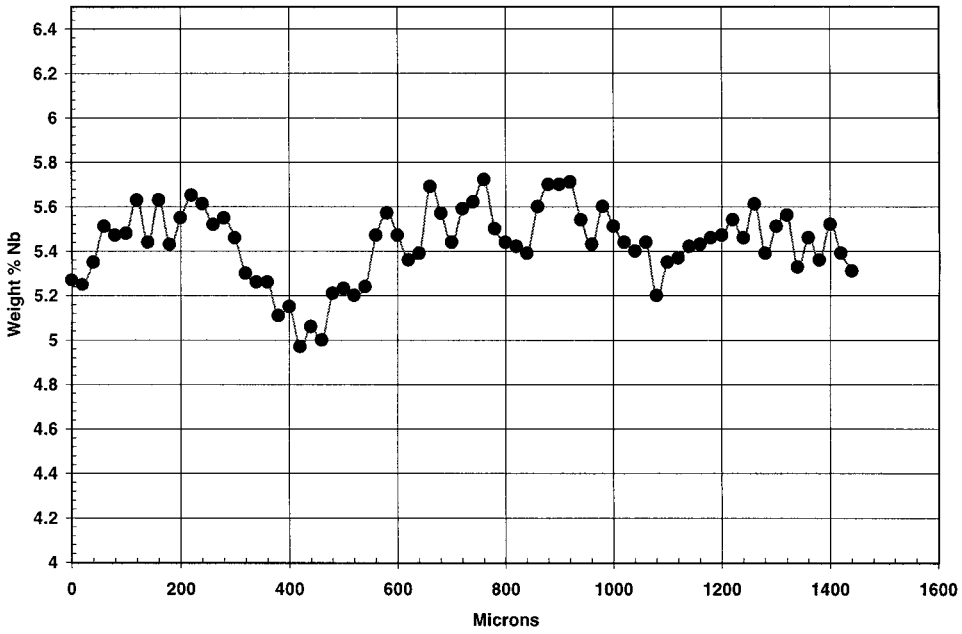


Fig. 4.26 Niobium distribution in a transverse trace of IN-718 homogenized and forged to 10 in. (25 cm) billet

formed is the primary factor controlling the individual carbide size. Subsequent exposure to very high temperatures and times may cause carbides to coarsen, but gross coarsening is not encountered until the melting point (solidus) of the alloy is approached. The region of formation of the carbides is the former interdendritic region. Thus, upon subsequent working, the carbides appear as localized stringers, where the spacing between the stringers is related to the earlier interdendritic distance.

A second phenomenon to be noted as occurring during homogenization is the generation of porosity in the ingot. Many superalloys demonstrate strong Kirkendall effects (atoms of differing elements move at different rates and atom-sized voids left behind can coalesce) between the interdendritic region and the dendritic matrix. Thus, homogenized ingots typically contain high levels of porosity. The mechanical working of these ingots must be sufficient to close up the porosity. Insufficient deformation or the creation of dead zones during conversion may result in residual porosity being present in the mill product.

Cogging. The multiple-pass conversion of ingot to a smaller cross section/longer length is called cogging. Cogging involves hot working the ingot with a large forging press. (Rolling may be used to the same effect, although this is technically referred to as blooming.) The purpose of the cogging operations is to break down the as-cast microstructure by repeated working and reheating of the material. The cogging process refines grain structure. In recent years, the need for improved inspectability of billet and bar has led to a desire to control the grain size in the ingot/billet as it is reduced and/or upset to appropriate sizes for either mill product or forging operations.

It has been suggested that cogging has some similarities with the radial forging processes such as rotary forging. However, the radial strain distributions near the periphery of cogged ingots differ from that produced by radial forging.

For press cogging, several points have been made relative to the process:

- The press must have enough capacity and speed to create the necessary cogging force in as short a time as possible, to minimize surface contact chilling. The force generated must be sufficient to cause strain at the interior of the ingot.
- Tool radii must be carefully designed and maintained to prevent lapping.
- A square-rectangle-square cogging sequence is desired if a round product cannot be produced.
- High-strength superalloy dies are preferred, to minimize tool erosion.
- A high-quality starting surface for an ingot will maximize cogging results.
- Automation is highly desirable.

Defects in the ingot can cause difficulties, but these are not described here. The preceding sections have fully developed the melting processes that lead to modern high-quality ingots, which minimize the probability of defects that will cause rupture or cracking during the cogging process. However, satisfactory cogging or, for that matter, subsequent forging of components should not be interpreted to mean that chemistry defects do not exist. In VAR ingots white spots do exist and can have an effect on final component capability, but yet not cause any problems in cogging.

At one time, most billet was cogged to square or round-cornered square; some was cogged to octagons or round. Subsequent forging is more difficult for square/rectangular product. A round cogged product may be preferred. Another aspect of cogging was the inability of the whole of an ingot to be deformed at one time during one thermal-mechanical cycle. Deformation and reduction might be accomplished first at one end only of an ingot, while the opposite end received several reheats with no introduction of strain energy. The cycle might then be repeated on the opposite end.

Ingots are generally transferred straight from homogenization into the forging furnace and allowed to equilibrate. It is a feature of most cogging operations that, for economic reasons, the ingot is never reheated sufficiently long to attain the actual temperature of the furnace throughout its cross section. Thus, cogging generally occurs at a lower temperature than the furnace temperature and on a steadily falling temperature curve. Temperature loss is accentuated as smaller cogged section size is reached. Actual billet

temperatures must be sufficient to cause recrystallization of the alloy. The selection of reheat furnace temperature and soak-time windows are chosen to compensate for this practice.

Automated equipment such as GFM rotary forging machines can reproducibly convert a long length of reasonably sized ingots to billet. Billet cogging is receiving increasing attention, particularly with regard to process modeling. However, the literature on cogging (and extrusion, rolling, wire drawing, etc.) of superalloys is quite limited.

Cogging of IN-718. IN-718 is a high-strength, intermediate-temperature-of-operation nickel-base superalloy. As noted elsewhere, it is the most-used superalloy and finds service in both military and commercial aircraft gas turbines, land-based gas turbines, and in critical components of space shuttle engines. Generally, the as-cast homogenized microstructure consists of very large grains that must be broken down into a uniform fine grain structure. Cogging traditionally is a process of working the sides of a square ingot down the length of the ingot by a series of short press strokes that introduce the necessary strain. Each working pass reduces the diameter by a discrete amount.

Owing to the large cross sections of today's ingots, in the order of 300 in.^{2} (1935 cm^2) or more, it is difficult to get complete strain penetration in any single press stroke. Thus, when a length of the ingot has been worked, the process must be repeated, and so on to complete the necessary size reduction and grain-size refinement. Thus, as indicated previously, IN-718 is cogged in a sequence that starts with press forging and ends with reheating in the furnace for the next forging sequence. Furnace temperature for cogging is varied as the section size is reduced. Initially, the furnace may be set to 2050 °F (1121 °C); however, as the section size decreases, the furnace temperature is lowered to below the δ solvus, which is about 1850 °F (1010 °C). This temperature reduction allows spheroidized δ phase to form at grain boundaries and restrict subsequent grain growth during cogging. The final cogging operation is to round up the forged product so that subsequent machining

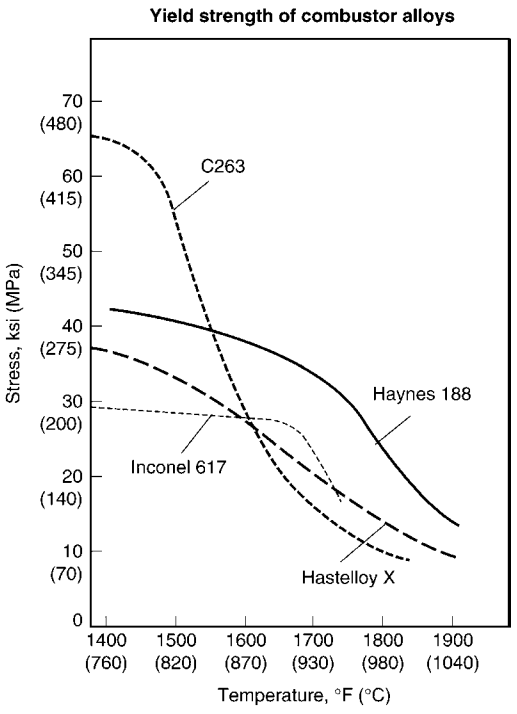


Fig. 4.27 Yield strength vs. temperature of sheet superalloys for combustor applications

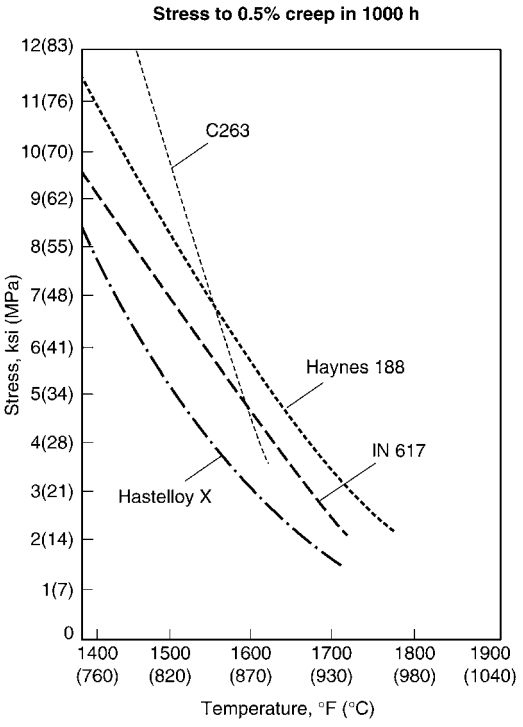


Fig. 4.28 Creep strength (0.5%) vs. temperature of sheet superalloys for combustor applications

Table 4.2 List of components and application reason for HA-188 in the F-100 engine

Component	Principal reason for selection
Combustor inner wall	Creep life and low cycle fatigue strength
Combustor outer wall	Creep-buckling resistance
Augmentor (afterburner) rear liner	Creep-buckling and oxidation resistance
Flameholders	Thermal fatigue and oxidation resistance
Nozzle convergent liner	High-temperature strength

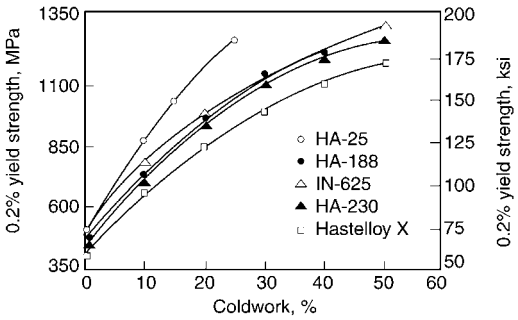


Fig. 4.29 Room-temperature 0.2% yield strength vs. cold work for various sheet superalloys

(peeling) of the product will produce a shape amenable to automated ultrasonic inspection.

Extrusion. Extrusion finds use for powder consolidation, and most powder metallurgy components start from extruded powder billets. Extrusion also is used for the production of seamless tubing. Extrusion was used at one time for alloys such as Astroloy to convert ingot to billet. As is the case with cogging, extrusion could benefit from newer techniques of modeling; however, superalloy extrusion does not offer many product opportunities and is a relatively standard procedure where used on superalloys today. Extrusion can be used to produce shaped products, including such mill products as bar stock.

Extrusion of alloys such as U-700 entails encasing the ingot in a mild steel or stainless steel can. This step is necessary to prevent chilling and resultant surface cracking from contact with the container and die. An added effect is that the can protects the tooling. If alloys with a wider hot working range than U-700 are used, canning may not be required. However, special die and liner materials may be necessary. Adequate lubrication is a must in all instances, and high-pressure-capability extrusion presses are necessary.

Extruded bar product may be used for the production of wrought turbine airfoils, but most hot section airfoil components are now cast.

Rolling. Superalloys, particularly nickel-base superalloys, are the most difficult materials to roll. Primary rolling of these materials usually is done at temperatures near the melting point and on very rugged mills designed to withstand the high stresses encountered in the working of these alloys. Nickel-base superalloys have narrow working-temperature ranges. Mill products consist of bar, sheet, and shapes. At one time, bar stock was used for the production of gas turbine hot section airfoils. U-700, for example, was used in wrought form for such components. Forging or roll forming of alloys was employed in blade production. Some high-strength alloys such as B-1910 (wrought variant of B-1900) were successfully demonstrated as blades but were bypassed, owing to the switch to cast high-pressure turbine airfoils.

Sheet and other semifinished mill products, such as round, rectangular, and shaped bar, are produced by rolling. Many reheats may be necessary, and frequent conditioning of surfaces may be required. In some instances, it may be necessary to encase the material to be rolled.

Sheet product finds use in gas turbine applications where formability and high-temperature oxidation resistance and strength are required. In particular, for combustors or burner cans in gas turbines, nickel-base and cobalt-base sheet products excel. Some alloys

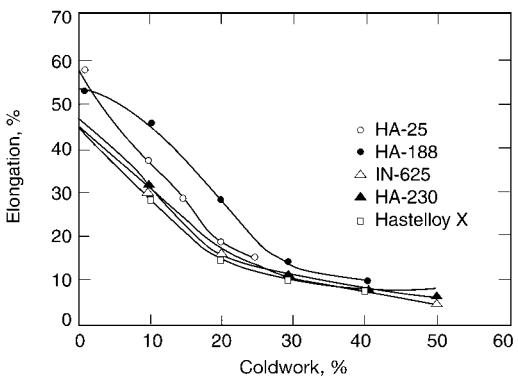


Fig. 4.30 Room-temperature tensile elongation vs. cold work for various sheet superalloys

considered or used over the years include Hastelloy X, HA-188, C-263, and IN-617. Figures 4.27 and 4.28 provide a comparison of these four alloys. Hastelloy X is the least expensive of these materials, being a nickel-base alloy with a substantial iron content. HA-188 is a cobalt-base superalloy that has found major use as a higher-temperature alternative to Hastelloy X. HA-188 has found use in the hot section of the F-100 engine that powers the F-15 fighter aircraft. Table 4.2 lists some applications of HA-188 in the F-100.

Mill Product Availability. Dependent on alloy composition, rod and bar are available in a wide variety of alloy/size combinations. Plate and sheet are produced, and seamless tube is available. Sheet up to 8 ft (2.45 m) has been produced. Strip in some alloys can be available in coil weights to as much as 8000 lb (3636 kg). Wire is available in straight or coiled lengths.

Not all wrought superalloys are available or needed in mill product form. Current alloys manufactured as mill products may include:

- Cobalt-base superalloys such as HA-188, HA-25 (L-605), HA-31
- Nickel-base superalloys such as Rene 41, HA-214, Waspaloy, IN-625, IN-718, U-720, Hastelloy X, IN-617, C-263, and IN-X750
- Iron-nickel-base superalloys such as A-286

Although ingot breakdown requires hot deformation, some mill products may be finished by cold working. In general, cold-worked structures are not satisfactory for most high-temperature applications. However, for instances when superalloys are used at lower temperatures, cold-worked structures can have substantially increased short-time strength properties with reduced ductility or toughness (see Fig. 4.29 and 4.30).

Superalloys: A Technical Guide, Second Edition
Matthew J. Donachie, Stephen J. Donachie, p 79-90
DOI:10.1361/stgs2002p079
Copyright © 2002 ASM International®
All rights reserved.
www.asminternational.org

Chapter 5

Investment Casting

Introduction

What Is Investment Casting? In investment casting, a ceramic slurry is applied around a disposable pattern, usually wax, and allowed to harden to form a disposable casting mold (shell). The disposable pattern is typically removed by steam, leaving a hollow cavity inside the ceramic shell into which molten metal can be poured. Molten superalloy metal is poured into the mold and allowed to solidify under various practices. When no special heat control or other metal solidification control is exercised, the casting that is produced is polycrystalline (PC). If special techniques are used in conjunction with directional heat removal (directional solidification, or DS), columnar grain (CG) or single crystal (SC) products result. The term ''disposable'' in investment casting means that the pattern is destroyed during its removal from the mold and that the mold is destroyed to recover the casting.

Application To Superalloys. Investment cast superalloys are usually nickel-base and cobalt-base. Polycrystalline casting technology for superalloys has been thriving for 60 years, since the cobalt alloys were adapted to the gas turbine engine. In the latter half of the past century, investment casting became the only way to produce required parts from modern high-strength nickel-base superalloys that operate in the gas paths of turbines.

A significant advance in control was the development of a CG structure produced by directional solidification (CGDS). Single crystals of nickel-base superalloys have been produced by directional solidification (SCDS) as well. Directional solidification casting technology has become a commonly accepted production process for nickel-base superalloys. Columnar grain directionally solidified structures have been produced by promoting unidirectional heat flow within the furnace during the solidification cycle. Substantial property improvements have resulted for many alloys. A logical extension of CG technology is the production of SC hot section aircraft gas turbine components. Directional casting to create a SC article provides composition flexibility and opens the possibility of additional alloy development for high-strength nickel-base superalloys. Although initially restricted to relatively small turbine airfoil components of aircraft gas turbines, CGDS and SC processing has been extended to produce airfoils for large industrial gas turbines.

Although cobalt-base superalloys can be directionally solidified in CG structures, they are invariably cast as PC parts. Single-crystal manufacture of cobalt-base superalloys may be possible but has not been reported. It is doubtful that sufficiently significant property benefits would result from SC or CG cobalt-base superalloys to warrant the expense of such processing.

Dimensional tolerances for superalloy investment castings are generally 0.003 in. (0.075 mm), with section thicknesses as low as 0.05 in. (1.25 mm) or less, and excellent surface finishes can be obtained. Nickel-base superalloy castings are produced by investment casting under vacuum, while most cobalt-base superalloys are produced by investment casting in air. Improvements in properties have been made not only through control of composition, but also through

more precise control of microstructure. The absence of grain boundaries in SC alloys permits elements such as carbon, zirconium, and boron to be deleted from the composition. The resulting increase in melting point in turn provides improved flexibility in alloy composition and heat treatment.

Investment casting permits intricate internal cooling passages and reentrant angles to be achieved and produces a near-net shape of very precise dimensions. Most investment castings are small, random-grain-oriented PC articles ranging in weight from less than a pound to a few pounds, with some castings over 100 lb (45 kg). CG and SC parts are being cast regularly in lower weights with some as large as 10 to 20 lb (4.5 to 9.0 kg). Cobalt-base and high V_f γ' nickel-base superalloys plus IN-718 γ''-hardened nickel-iron-base superalloys are processed to complex final shapes by investment casting. Iron-nickel-base superalloys are not customarily investment cast. Investment-cast superalloys are predominantly used in the aircraft gas turbine field, although there is a modest market for other products. Most investment-cast superalloys are intended for hot section gas path applications where temperatures are above about 1500 °F (816 °C).

As noted, a wide range of alloys are cast as smaller parts in PC, CG, or SC form. However, while smaller components (a few pounds or so) dominate the unit volume of the investment-cast superalloy business, large investment castings have significant impact on a cast-metal weight basis. Large superalloy castings are being made in configurations up to several feet in diameter and hundreds of pounds in weight. A cast alloy commonly used to obtain the economic benefits of large sections is IN-718.

Investment Casting Practice

Source Stock for Investment Casting. Nickel-base and some cobalt-base superalloy remelting stock for investment casting is produced by vacuum induction melting (VIM). Vacuum induction melted heats of superalloys intended for the investment casting process are much smaller in mass than the VIM heats used to produce stock for wrought alloy processing. Heat sizes are more likely to be in the 4000 to 5000 lb (1815 to 2270 kg) range at best. Controls are similar to those used for VIM product intended for wrought superalloys.

Superalloys are reheated in VIM or other controlled-environment furnaces for subsequent casting into parts. All superalloys can be melted in high-frequency induction furnaces, in vacuum (VIM), or another atmosphere. Initial melting also can be done in consumable arc, electron beam, or other furnaces with appropriate atmosphere control. Superalloys that contain appreciable amounts of aluminum, titanium, or other reactive metals are melted by induction or electron beam processes under vacuum or a protective atmosphere prior to casting.

The Basics. There are two distinct processes for making investment casting molds: the solid investment (solid mold) process and the ceramic shell process. The ceramic shell process has become the predominant technique for engineering applications, displacing the solid investment process. The basic steps in this process are illustrated in Fig. 5.1. A fine refractory aggregate is combined with a silicate binder to produce the shell into which the molten superalloy is cast. The resulting castings usually have very fine surface finish and very accurate dimensions.

Pattern Materials. Cast articles are made by creating a pattern of the article in wax or plastic. The pattern is duplicated as many times as necessary, typically using conventionally machined injection tooling. Pattern materials for investment casting can be loosely grouped into waxes and plastics. Waxes are more commonly used. Plastic patterns (usually polystyrene) are frequently used in conjunction with relatively thin ceramic shell molds.

Modern gas turbine applications require complex cooling passages in what were once solid airfoil shapes. Hollow castings with complex internal features are made by first creating a ceramic positive replica of the internal hollow passage through injection of a ceramic slurry into a die cavity, forming a ceramic core. This core is then placed into the wax injection die, which contains the external pattern of the desired component (e.g., turbine blade), and then wax fills the die, encapsulating the core with wax. The result is a wax pattern that, at the wax interfaces with the air or the ceramic core, has the form desired for the finished part. Figure 5.2 shows

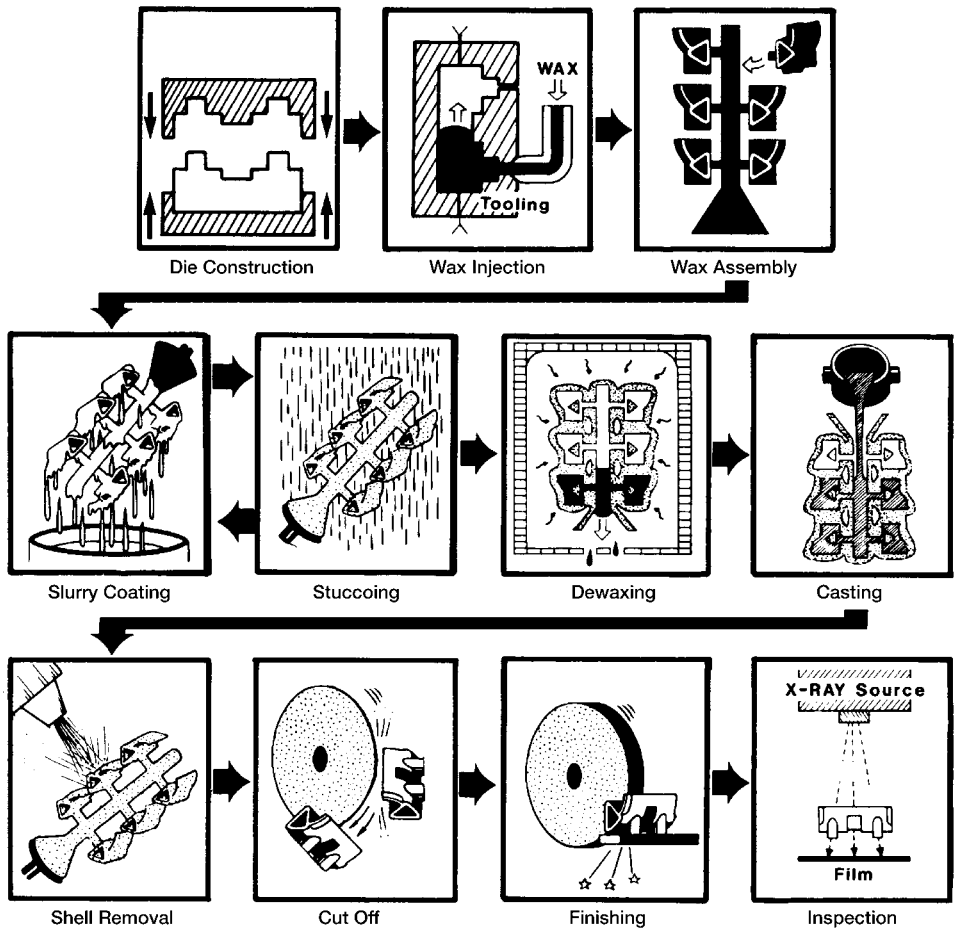


Fig. 5.1 Schematic illustration of the investment casting process

a cast turbine blade with convex wall removed, revealing the complex internal structure produced with the aid of a core of the design shown next to the blade.

Making the Mold. An appropriate number of wax patterns are attached to a ''tree'' complete with the usual casting devices of pouring cup, sprue, risers, and so on to channel metal from the pourcup into the part geometry. The resulting tree is invested (coated) with ceramic of various sizes by dipping the assembled tree in a slurry, applying ceramic granules, and then drying the assembly under controlled conditions. The investing process is carried out for as many times as needed to build up a satisfactory ceramic coating. The invested tree is dried and the wax is burned out. Then the investment is fired at a higher temperature to achieve maximum strength through sintering. This process results in a mold tree with a series of individual article molds attached to it. The ceramic cores have become embedded in the ceramic that forms the shell, and the result is an integral ceramic form into which molten metal can be poured. This resulting mold is now ready for use.

Mold Requirements. Many alloys are investment cast, including VIM superalloys. These metals are melted and poured into the mold and solidified under conditions according to whether the product is to be large or small, PC, CG, or SC. The mold is the key to generating a satisfactory part. The ceramic of the mold must not be attacked significantly by the molten metal (i.e., no mold-metal reaction). However, the ceramic should be capable of dissolution in an appropriate base (e.g., KOH) to clean passages or external surfaces with no metal deformation by mechanical processing.

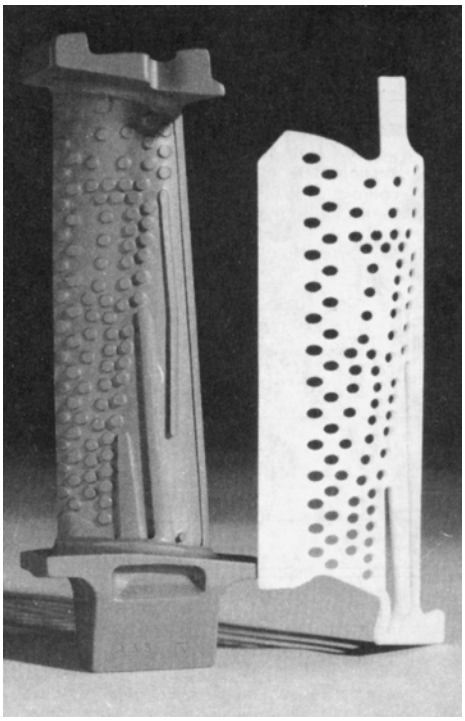


Fig. 5.2 Investment-cast turbine blade with convex wall removed showing complex internal arrangement produced by the core standing alongside the blade

The shell must be strong enough to resist deformation but thin enough to let heat of solidification be transferred away by conduction and radiation. Mold design, including the dimensions of the article to be produced, is a critical part of the investment casting process. A skilled designer must be able to predict the shrinkage of a molten mass to very precise limits. In parts where the minimum dimensions may be as thin as 0.020 in. (0.058 cm) or as large as a yard (meter) or more in diameter, the mold design process is particularly challenging.

Grain size in PC parts is controlled by an appropriate primary dip coat in the investment, along with manipulation of the mold-metal pour temperatures and use of selective mold insulation to adjust heat flow. An example is the microcast-X method, which makes fine-grained (ASTM 5 to 3) PC superalloys by using a very low superheat (low pour temperature) and a heated mold.

Grain control (generally, orientation) in CGDS or SCDS products is achieved by use of special furnaces that provide appropriate thermal gradients and by selective filters and/or starter nucleation sites. Cores in DS parts may need to be modified in chemistry, because the long time of solidification exposes them to more heat and increases the possibility of warping. Grain size cannot be significantly altered, owing to the directional nature of the solidification process and the need to avoid any nucleation events that might introduce spurious grains.

Shell Preparation. The ceramic shell must be prepared for the casting operation. After dipping, any support fixtures used for dipping are removed. The shell is then dewaxed by using a high-pressure steam autoclave, which rapidly flashes out the wax. The shell is then fired at high temperature to sinter the ceramic particles together via the vitrification of the silicate binder. The shell is then cleaned and inspected.

Postcast Processing. After casting, the expendable ceramic shell is removed and the parts are cut from the tree. As noted earlier, if the castings possess internal ceramic cores for internal feature fabrication, this core is removed using caustic chemicals. The positive core, when removed, gives rise to the negative cavity possessing complex internal features. Most castings are typically heat treated to homogenize the metallurgical structure and precipitate strengthening phases to optimize mechanical properties. The castings are then inspected via x-ray (internal defects), fluorescent penetrant inspection (external defects), chemical grain etch (crystal integrity), ultrasonic inspection (wall thickness for hollow parts), and dimensional inspection.

Details of the Shell Mold Investment Casting Process. The modern shell mold investment casting process consists of a number of steps, as previously indicated schematically (Fig. 5.1):

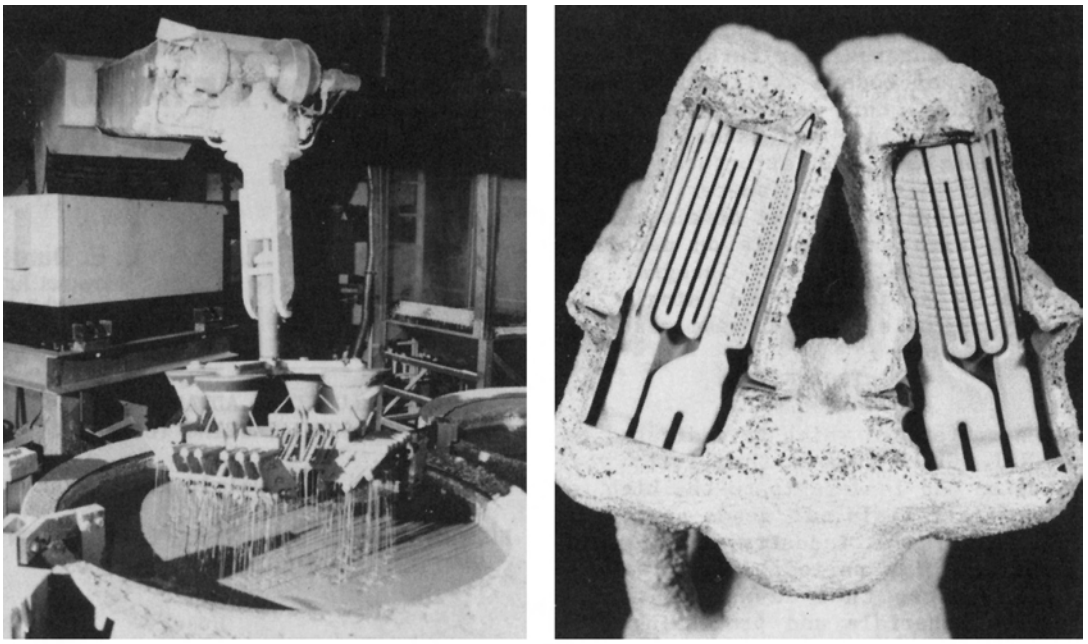
- Construct a die or tool that has at least one internal cavity that corresponds to the external geometry of the article to be produced. One must allow for shrinkage, and more than one cavity might be constructed in the tool.
- Set, in the tool, an appropriate core to form the internal geometry of the article to be produced.
- Inject an appropriate pattern material (usually wax) into the tool to produce a pat-

tern. Many duplicates of the pattern usually will be produced.
- Join one or more of the patterns together on a tree, with wax runners and so on, with the desired gating arrangement to form a wax assembly or cluster.
- Invest the wax cluster in various ceramics, using slurries of the same. This amounts to alternately subjecting the wax assembly to different ceramic slurries, followed by periods of drying, until a sufficient (thickness/strength) green shell has been built up. The first application is the face coat, which significantly affects the grain size (PC cast alloys) and surface finish of the cast parts. Subsequent to the slurry coat(s), coarser ceramic stucco is built up. At the present time, the procedure is automated, but for many years, all dipping processes were by hand. See Fig. 5.3 for a view of the automated dipping of investment casting molds and a cutaway view of the shell showing the intricacy of the airfoil to be produced.
- Remove all or most of the pattern, often using a steam autoclave (this process allows the reclamation of the wax pattern material as well), then heat to elevated temperature in a furnace to complete pattern removal by burnout. This process fires the green shell or prefires it before the shell is transferred to a higher-temperature furnace for final firing of the ceramic to produce a cured and strong shell.
- Place the mold in a can, often surrounded by insulating ceramic, and then in a furnace for preheating before pouring.
- Pour liquid superalloy into the mold, often through a dross filter. Solidify the mold either by conventional heat transfer (yielding a PC part) or by directional heat transfer processes (DS), leading to a CG or SC part dependent on the use of selectors to get a single grain or just a water-cooled copper plate to initiate directional growth.
- Remove the mold from the casting furnace and from the can. Break out the raw casting from the mold, usually removing the ceramic shell by mechanical means or a combination of mechanical and chemical means (caustic solution in an autoclave at elevated temperature).
- Cut the sprues, gates, and risers from the article and eliminate any residual gate material.
- Possibly solution heat treat the article at this point, especially if it is a DS product that might have unfavorable recrystallized surface grains created by a combination of stress from mechanical processing and the temperatures of solution heat treatment.
- Clean and finish the article surfaces using methods that may include grinding, polishing, blasting, and/or media finishing.
- Inspect the part to standards set by the caster and by the consumer. Inspection consists of all or most of the following: visual, fluorescent penetration, radiography, ultrasonic (for wall thickness in hollow parts), and dimensional gaging. If the article is DS, then crystallographic orientation of the article or the orientation differences of grains or subgrains may be checked by x-ray diffraction.

Polycrystalline Castings to Directional Solidification. The production of PC castings involves all of the steps noted previously but no special control over the heat transfer or grain nucleation processes. For PC castings, modifications to mold design and inoculants were introduced with success in the control of grain size. Certain heat transfer adjustments were made as well; however, no heat transfer gradient control was used.

The adaptation of DS, a very old process to investment casting, was done by creating and maintaining an environment where the heat of solidification had to be transferred out effectively along a line parallel to the growing component, that is, the airfoil axis. A chill was introduced and heat was supplied radially to create the necessary conditions. Multiple grains formed on the chill plate and grew perpendicular to it along the axis of heat flow. An article was produced that had elongated (columnar) grains with individual grain sizes actually larger in transverse section than the grains of PC castings. There were many beneficial aspects of the production of CGDS articles, and these are discussed in Chapter 12.

It was a short step to the concept of introducing a seed on, or a grain filter above, the chill plate to let only a single orientation of grain grow into the article. Columnar grain directionally solidified alloys have many parallel grains, and the relative orientation of one to another varies. By insertion of a grain filter, SCDS articles were produced. The first



(a) (b)

Fig. 5.3 (a) Automated dipping of investment casting molds, (b) cutaway view of shell mold for an air-cooled gas turbine blade

articles were from the identical compositions used for CGDS. Because of the absence of grain boundaries, grain boundary hardeners were no longer needed. Thus, subsequent articles were produced from new compositions tailored to take advantage of SCDS technology.

Figure 5.4 shows a schematic of the DS process as well as schematics for CGDS and SCDS processing. Figure 5.5 shows a traditional production casting furnace that is easily adapted to DS processing.

Investment-Cast Components

Polycrystalline Articles. Early investment-cast articles were small in size and were cast from cobalt-base alloys. Air-melted material was used, and dross was a problem. Grain control was limited. As knowledge progressed and vacuum melting was developed for the superalloy business, nickel-base alloys with their titanium and aluminum content began to be produced. As indicated elsewhere, solid parts were made first, but then hollow and, finally, complex hollow hardware began to appear. Figures 5.6 through 5.11 show, respectively, the following PC articles:

- Polycrystalline cast cobalt-base turbine guide vanes and segments
- Cast turbine airfoils and other high-integrity investment-cast gas turbine components
- Polycrystalline cast hollow nickel-base turbine blade of simple cooling geometry shown with cross sections of some other cooling configurations
- Cutaway view of PC cast complex nickel-base turbine blade
- Typical large structural casting
- Investment-cast polycrystalline integral nozzles and integral rotors for a gas turbine engine

The components in Fig. 5.10 and 5.11 are most interesting, because they show the movement to larger cast components as well as the intent to use PC-cast nickel-base superalloys in integral blade-disk rotating components. Also, note the complexity of the geometry of the parts in Fig. 5.11.

Directional Grain-Structured Articles. Directional solidification of nickel-base super-

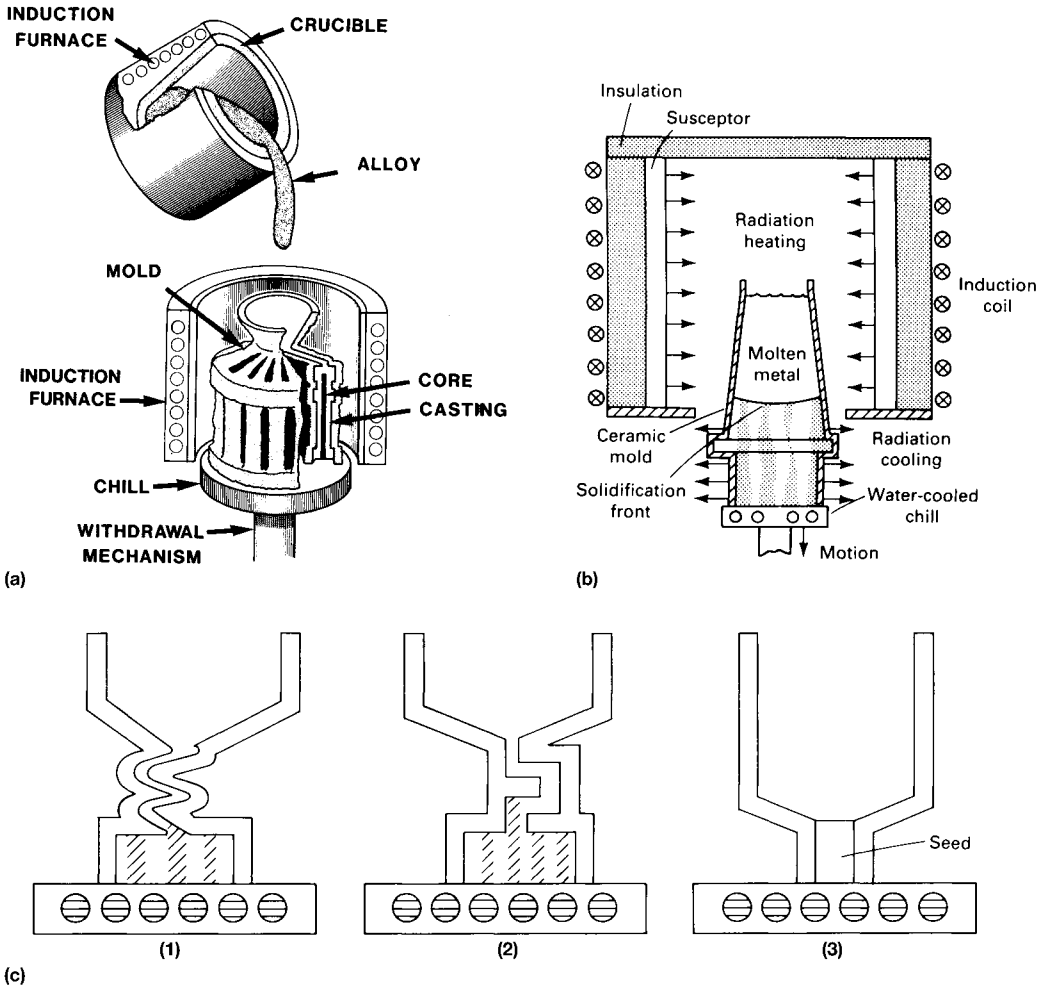


Fig. 5.4 (a) Schematic of typical directional solidification (DS) practice, (b) schematic cutaway showing cooling and metal growth in a columnar grain DS process, and (c) schematic of methods used in single-crystal DS process. (1) Use of helical mold section, (2) use of a right-angle mold section, and (3) seeding

alloys as pseudoairfoil structures was demonstrated in the late 1950s at the research laboratories of the General Electric Company but was initially brought to commercial availability by Pratt & Whitney in consort with the major investment casting companies. Early work produced columnar grain structures. The significance of this work was that it showed that a somewhat more expensive casting process than that used for producing PC articles could be used to achieve maximum capability in an existing superalloy, which was not being used owing to ductility problems. Subsequently, not only were complex cored CGDS airfoils produced, but also, SC articles were produced by DS processing. Figure 5.12 illustrates the evolution of grain structure from PC to SCDS, with both turbine vanes and blades being shown. Figure 5.13 shows some of the DS processing gas turbine airfoil products, while Fig. 5.14 provides a sketch illustrating the selection process for investment-cast DS products leading to CGDS or SCDS parts.

Investment Casting Problems

Some Problem Areas. Dimensional discrepancies, inclusions, porosity, coarse grain size, surface attack in core leaching, core shift and resulting undersized wall thickness,

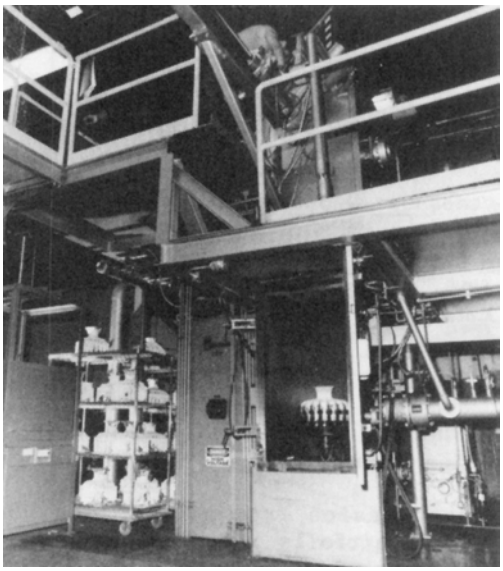


Fig. 5.5 Traditional production investment casting furnace

and core warping are a few of the problems encountered in investment casting of superalloys. These problems reduce casting yield and cause potential property-level reductions if not properly controlled.

Directional solidification adds additional problems to those normally encountered in superalloy casting. Increased tendencies for inclusions (owing to the use of hafnium to enhance transverse ductility), separately nucleated grains, grain misorientation, and the

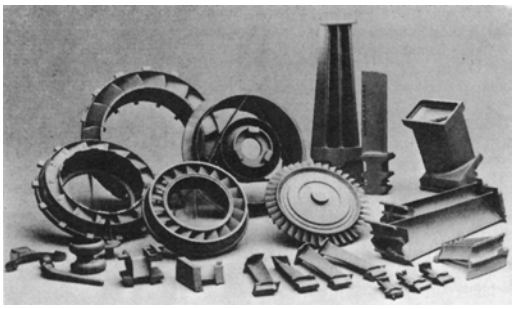


Fig. 5.7 Cast turbine airfoils and other high-integrity investment-cast gas turbine components

tendency for freckle grains (grain nucleation caused by inverse segregation due to dendrite erosion) are causes for casting rejects in CGDS product. Freckles, slivers, low angle boundaries, and spurious solidification-nucleated grains are casting problems in SC production. In both CGDS and SC alloys, surface recrystallization induced by surface strains and excess temperatures in postcast processing can be a cause for casting rejection. Recrystallization poses one of the major difficulties in postcast processing of DS cast nickel-base superalloys, especially for SCDS-cast airfoil components.

Avoidance of Problems. Inclusions are controlled by melting technology and the use of filters to eliminate dross. Selective surface attack is controlled by modifying the autoclave leaching processes. In the past several decades, improved shell and core materials

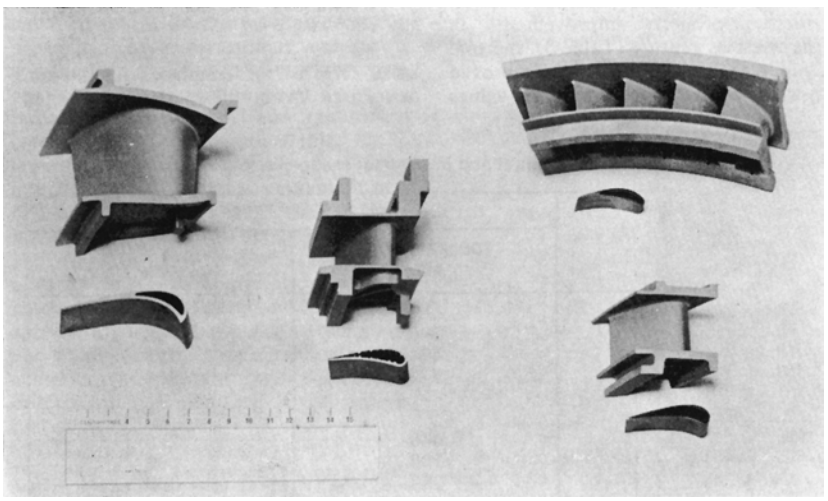


Fig. 5.6 Polycrystalline cast cobalt-base turbine guide vanes and segments

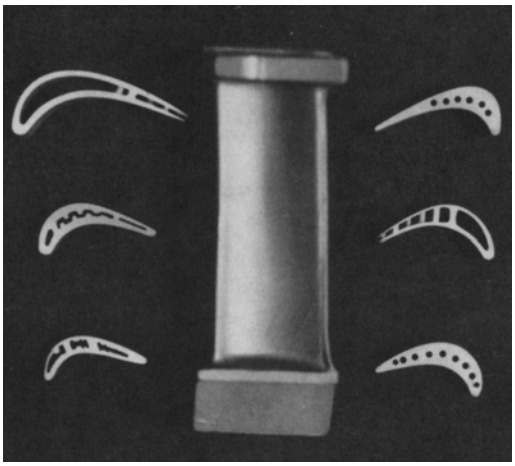


Fig. 5.8 Polycrystalline cast hollow nickel-base turbine blade of simple cooling geometry shown with cross sections of some other cooling configurations

and casting mold design plus control of grain size and inclusions have led to improvements in casting yield and, occasionally, improvements in cast part strength. Casting porosity has been a problem in parts having large cross sections and in certain small parts made of some high-V_f γ' alloys. Hot isostatic pressing (HIP) techniques used for powder processing have been applied successfully in many instances to eliminate nonsurface-connected porosity, particularly in large castings of iron-nickel- and nickel-base superalloys. Improved fatigue and creep life generally result (Fig. 5.15), because casting quality is improved by HIP. (See Chapter 12 for more on this subject.) Hot isostatic pressing has been applied not only to PC alloys but also, occasionally, to SCDS turbine airfoils.

Figure 5.16 shows recrystallization phenomena on a turbine airfoil after solution heat treatment. There are several possible sources for the recrystallization-inducing plastic deformation that occurs during manufacturing and processing of newly cast parts as well as during service and refurbishment procedures. They include contraction stresses during mold cooling, ceramic knock-off, mechanical core removal, stamping of identification marks, grinding on the component airfoil surface or the attachments, impact damage, mechanical removal of coatings or coating residues, and so on. It is necessary to avoid the inadvertent creation of stress if recrystallization is to be prevented. Most process specifications for DS-cast alloys provide guidance on such potential stress-inducing operations. Often the process specifications are tailored to a given manufacturer's operating preferences.

Improved Castings through Modeling and Prototyping Technology. Improvements in mold design and casting temperature control have been developed through computer mod-

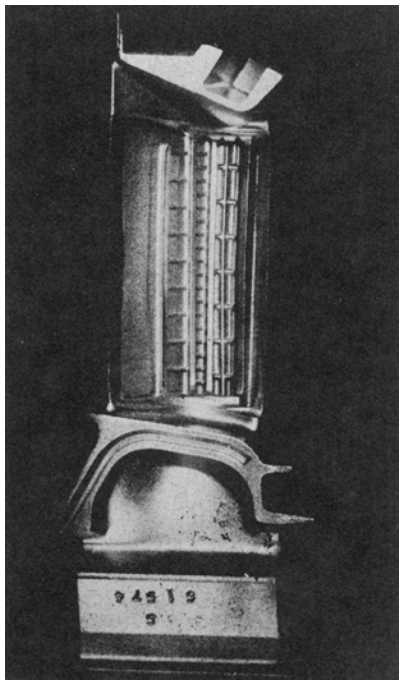


Fig. 5.9 Cutaway view of PC cast complex nickel-base turbine blade

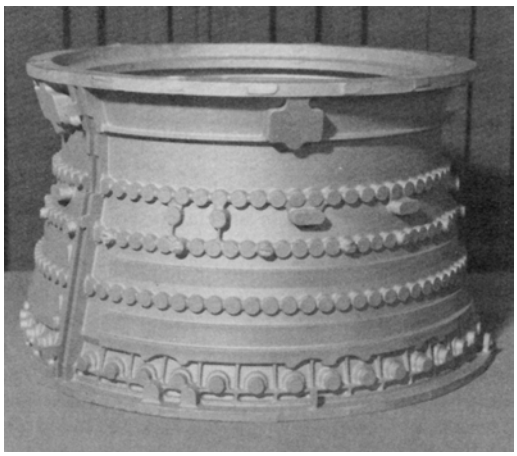


Fig. 5.10 Typical large structural casting

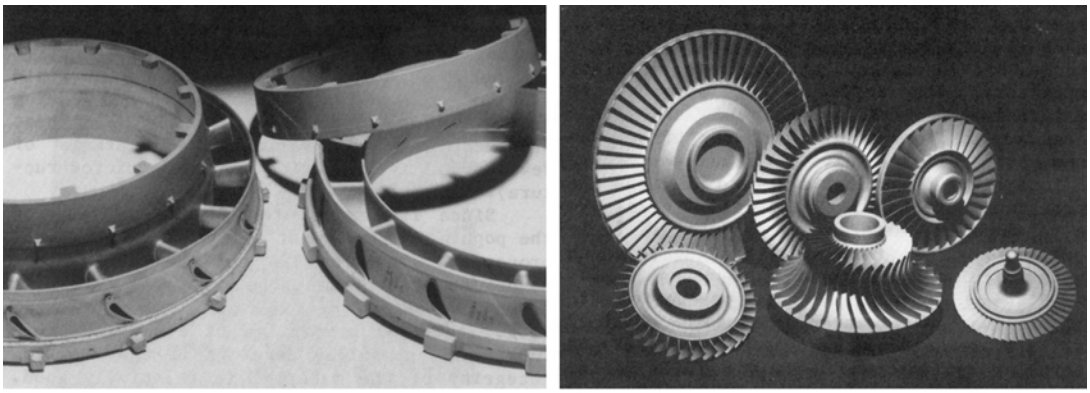


Fig. 5.11 Investment-cast gas turbine engine. (a) Polycrystalline integral nozzles, and (b) integral rotors

eling of the casting process. Modeling requires knowledge and/or development of algorithms to represent the thermal and mechanical processes occurring during the heat up, introduction of molten metal (pouring), and metal solidification sequences of the casting process. The vast computer power now available enables improved and rapid modeling of a given article and casting process. Results are encouraging, but it should be noted that, while the modeling concepts (algorithms) are well developed, there is a gross lack of data on physical properties of molten and solid metal superalloys with which to ''feed'' the model. There is still much opportunity for advancement in this area.

A new technology known as rapid prototyping has enabled significant changes in the casting industry by eliminating the need for many of the investment casting process steps. This elimination has led to significant cost and lead-time reduction for development hardware. Processes such as stereolithography, selective laser sintering, and other three-dimensional (3-D) printing technology can provide casting patterns without the use of costly conventional wax or ceramic injection dies. Special machines can take a 3-D computer-aided design (CAD), convert the design into cross-sectional layers, and build a 3-D representation of the CAD geometry in plastic, wax, or polymer. Some processes can directly build, from three-dimensional CAD

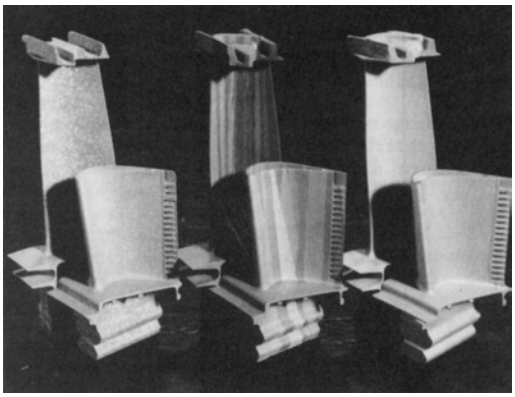


Fig. 5.12 Evolution of grain structure as seen in a polycrystalline, columnar grain directionally soldified, and single crystal directionally solidified blade

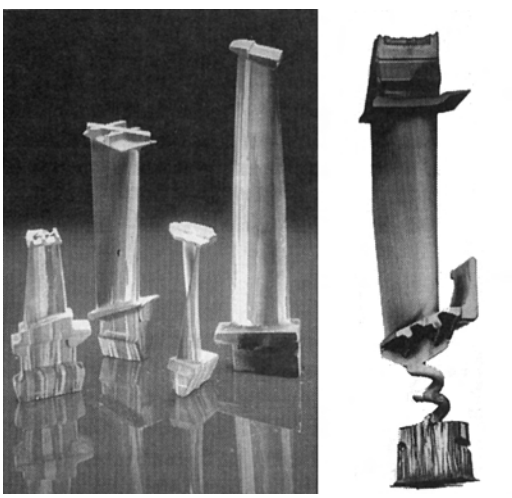


Fig. 5.13 Turbine airfoil components produced by directional casting in (left) CGDS form, and (right) SCDS form

geometry, 3-D ceramic shells into which metal can be poured. Other technologies focused on direct metal fabrication from three-dimensional CAD geometry are being developed. These technologies have revolutionized the industry in allowing faster development through low-cost iterative design so that design concepts can be transitioned to production rapidly.

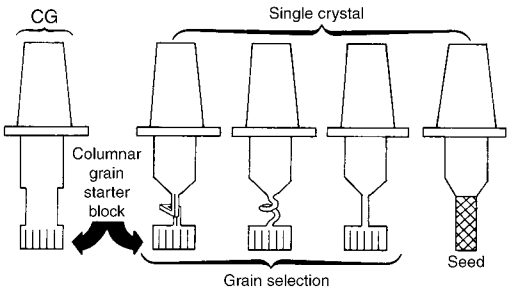


Fig. 5.14 Schematic of the selection process used to produce CGDS or SCDS turbine airfoils

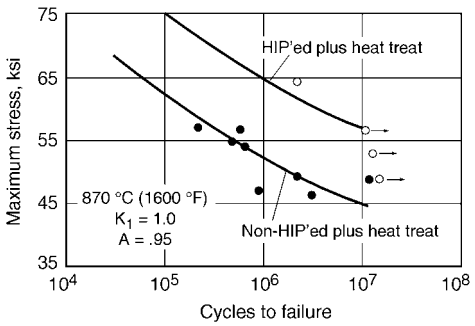


Fig. 5.15 Graph showing that HIP used to close casting pores can have a beneficial effect on high-cycle fatigue strength. Alloy is Rene 80 nickel-base superalloy

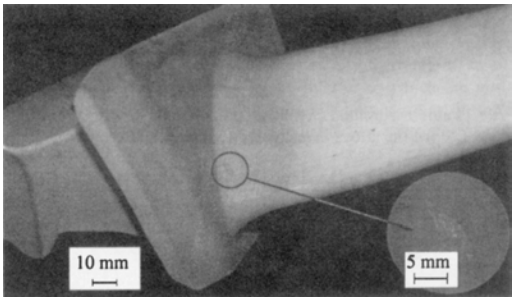


Fig. 5.16 Recrystallization phenomena on a turbine airfoil after solution heat treatment

Superalloy Castings

General Comments. Use of precision investment castings in aircraft gas turbines, particularly for turbine airfoils, has been the single most important driving force in the growth of the investment casting industry. Castings are intrinsically stronger than forgings at elevated temperatures. The coarse grain size of castings as compared to fine-grain forgings favors strength at very high temperatures. Additionally, casting compositions can be effectively tailored for high-temperature strength, because forgeability characteristics are not applicable. Although cast cobalt-base airfoils were in use for low-pressure turbine parts in the mid-1950s, forged nickel-base investment cast airfoils were in use for the high-pressure turbine. However, when aircraft engine operating temperatures increased markedly, castings replaced forged airfoils to provide satisfactory service durability. Initial cast airfoils were solid, but further temperature increases led to use of air-cooled cast airfoil designs. For the air cooling process to be advantageous, complex casting designs were required. The resulting alloy and investment process development, which led to complex internal passages in turbine airfoils, has been remarkable. Polycrystalline investment-cast alloys made way for DS alloys, and CGDS and SCDS alloys are now commonplace in the gas turbine industry.

Polycrystalline Investment Casting. Nickel-base and cobalt-base alloy castings generally are made by the investment casting process, as noted earlier. Cobalt-base alloys usually are melted and cast in air, although some of the more advanced alloys such as MAR-M 509 must be melted and cast under vacuum. In the past, most nickel-base and cobalt-base castings were small, about 2 lb (1 kg) or less. However, with improved casting procedures and weld repair processes, in conjunction with the advent of HIP, large, complex investment-cast parts have been replacing forgings and weldments in aircraft engines. These investment-cast parts may attain dimensions as large or larger than about 60 in. (150 cm) in diameter. See Chapter 12 for more information on HIP use as a tool to improve casting quality by sealing internal porosity.

Extensive use of PC nickel alloy castings essentially began with Inconel 713 and con-

tinued with the invention and adaptation of IN-100 and B-1900 to aircraft gas turbines. Alloys currently are available that can be used at temperatures up to over 1900 °F (1038 °C).

Directional Investment Casting. Only nickel-base superalloys are DS processed. Alloy master melt (heat) preparation follows the same procedures as for PC alloys, although there may be chemistry steps that differ from heats for PC casting. Cast part sizes for airfoils are comparable to those for PC parts, but DS processing is not viable or reasonable, from a technical design standpoint, for large castings such as cases for gas turbine engines. Turbine airfoils as large as a half-yard (half-meter) or more have been cast as CG or SC parts for commercial large gas turbines.

Columnar grain directional solidification began commercially with PWA 664, which was a DS processed version of the alloy MAR-M-200, a very strong but not too ductile alloy when cast as a PC article. PWA 664 was made viable by the addition of hafnium as an alloying element to prevent columnar grain MAR-M-200 from coming apart on transverse grain boundaries. The resulting alloy was designated PWA 1422.

Single-crystal directional solidification began with a SC version of MAR-M-200, but commercial application did not begin until the development of PWA 1480. Dependent on how one counts, Monocrystalloy (single-crystal MAR-M-200) might be deemed the first-generation SC alloy. PWA 1480 represents a second generation and PWA 1484 a third generation. Some may consider PWA 1480 the first-generation and PWA 1484 the second-generation SC alloy. Other SC alloys have been invented, patented, and are in use by the major aircraft engine manufacturers and by several producers of small gas turbine engines.

Superalloys: A Technical Guide, Second Edition
Matthew J. Donachie, Stephen J. Donachie, p 91-115
DOI:10.1361/stgs2002p091
Copyright © 2002 ASM International®
All rights reserved.
www.asminternational.org

Chapter 6

Forging and Forming

Forging and Related Processes

Introduction. With the development of the gas turbine engine, there came a demand for alloys not only with superior high-temperature strength but also with the capability of being fabricated to unique shapes. In the early days, superalloys, based on the cast cobalt dental alloy Vitallium, became the materials of choice for gas turbine engine airfoils. Some cobalt-base and nickel-base alloys became available as sheet to operate at temperatures then in effect. Gas turbines were the principal driver for superalloy development, and the systems of the time were geared for wrought products.

Cobalt-Base versus Iron-Nickel- and Nickel-Base Superalloys. Cast cobalt-base superalloys such as Vitallium were interesting and extremely useful in components where the highest strengths were needed in the early years of the gas turbine. However, cast alloys were not considered suitable for a wide range of applications. It was thought that cast alloys were intrinsically less ductile than wrought alloys, and design engineers were worried about having adequate ductility available for design. Consequently, wrought superalloys became of more interest for the new high-temperature applications that developed with the gas turbine. This decision was based on some factual data that indicated lower ductility for cast alloys and general engineering design concepts based on wrought alloys with good fabricability and ductility.

Early wrought superalloys were customarily the alloys of iron-nickel- or nickel-base. Thus, where possible (especially for design-critical applications), these alloys tended to be the alloys of choice, not cobalt-base alloys. However, for some years, cobalt alloys remained the choice for such applications as gas turbine airfoils and any other part that could be cast and that did not require a lot of ductility. Alloy development changed this aspect somewhat, allowing wrought cobalt alloys to be produced, but principally as sheet. For massive wrought parts such as gas turbine disks, the iron-nickel- and nickel-base alloys became, and remain today, the materials of choice.

As the market for high-temperature alloys developed, increased-strength wrought disks were made, usually by forging of iron-nickel- and nickel-base superalloys; barstock of the same alloy types was produced for further forging or rolling to shapes such as turbine airfoils. The iron-nickel- and nickel-base precipitation-hardened alloys thrived. Sheet products made from Inconel, Nimonic 75, Inconel X (Inconel X-750), Hastelloy X, and the cobalt alloy Haynes Alloy 25 (also known as L-605) made their way into the pipeline. Eventually, superalloys such as HA-188 (cobalt-base) and C-263 (nickel-base) made their way into the sheet alloy field. Wrought alloys such as A-286, IN-901, various Nimonic compositions, Waspaloy, and Astroloy were applied as forged gas turbine disks and, in some instances, as forged blades in gas turbines. Cast cobalt alloys still maintained an edge for certain applications, but wrought-processed precipitation-hardened superalloys were in great demand, and still are, for a variety of gas turbine applications. A knowledge of the general forging processes and their ability to control not just shape but microstructure and properties is vital to the uti-

lization of superalloys in most high-temperature applications.

Wrought Processing Operations. Generically, wrought processing usually involves the introduction of heat and deformation to solid metal to shape it and to impart desirable properties. In the process of working superalloys, many different thermal-mechanical cycles of heating and deformation occur with the input (by working) and removal (by recrystallization) of strain. Because superalloys are process-history sensitive, these thermal-mechanical processing cycles can have an important effect on the final properties of a given alloy component. Cold deformation of large shapes is not normally feasible with superalloys, although sheet may be cold rolled to impart favorable properties.

Forging is one wrought process, but there are others. Not all forging processes are alike. This chapter focuses on wrought processing by forging, but the control of microstructure, shape and properties by rolling, extrusion, and so on is vitally important and has the same technical basis. Melting technology and the primary conversion process of cogging are playing an ever-increasing role in the control of microstructure and properties of wrought superalloys. Metal suppliers are being required to supply ever more tightly controlled microstructures to the forging manufacturers. Microstructural development and maintenance of that structure is, with modern practice, highly dependent on the billet structure present at the start of the forging cycle.

Forming, while related to forging, usually does not require finished components to possess as much ductility, strength, or toughness as forged parts. Much less information is available on forming as a manufacturing process for superalloys. It is rare that a forming process is used to control and/or develop microstructure in superalloys.

Forging of Superalloys. The earliest superalloys were not overly difficult to forge, but it was quickly found that, in general, superalloys, because of their greater strength at elevated temperatures, were more difficult to forge than most other metals. This became especially true when precipitation-hardenable superalloys began to dominate the market. Early iron-nickel-base superalloys were little but extensions of stainless steel technology. However, with the introduction of precipitation hardening, elevated temperature strengths rose markedly, and the stiffness/strength of these new superalloys made them difficult to forge.

It is true that some of the iron-base superalloys, such as A-286, are similar to austenitic stainless steels in forgeability, but superalloys generally are more difficult to forge than stainless steels. Some superalloy compositions eventually became so intrinsically strong at elevated forging temperatures that they could not be shaped by conventional forging techniques. In these instances, the alloys were used either in the cast condition or in wrought shapes made by powder metallurgy processing. (See the section on superplastic forming/forging as well as Chapter 7.)

Forging Basics

The Aims of Forging. Regardless of the method used, the forging of superalloys generally should be done as part of total thermomechanical processing. In other words, shaping should not be the only factor in forging. Work energy can be introduced and managed via temperature and deformation controls to impart the most useful or desired design qualities in a component. This discussion assumes that forging intends to create both shape and properties.

In some cases, forgings are deliberately processed for better tensile properties, stress-rupture behavior, creep strength, or low-cycle fatigue life. Therefore, the objectives for the forging cycle may be:

- Uniform grain refinement
- Control of second-phase morphology
- Controlled grain flow
- Structurally sound components

Fine grain size is not necessarily a desired outcome for all alloys. The objectives are to optimize properties (as defined by the component specification) in all sections of the component. This may require generating a grain size that is within a defined size range. The soundness and uniformity of the forging also must be ensured. Most forgings are inspected by ultrasonic testing, macroetch, and mechanical test of integral coupons. In order to impart optimal work during each stage, it may even be necessary to include redundant work if work penetration in the subsequent

processing sequence is not likely to be uniform. The forging process today does not operate as a stand-alone function as it did at the start of the superalloy age.

Controlling the Deformation Process. Recrystallization must be achieved in each operation to obtain the desired grain size and flow characteristics in a forged superalloy. Recrystallization also helps to eliminate the grain- and twin-boundary carbides that tend to develop during static heating or cooling. Nonuniform distribution of inhomogeneities will likely lead to problems. Up to 80% of metal reduction accompanying recrystallization is usually completed over falling temperatures; the remaining 20% can be as warm work at lower temperatures for additional strengthening. However, the range of applications for superalloy forgings is so diversified that in some circumstances, the aim of the forging process may be to produce a duplex, not a single, grain size in the finished component.

During the latter quarter of the last century, a trend developed to lower the strain rate and to heat the dies. Faster strain rates lead to frictional heat buildup, nonuniform recrystallization, and metallurgical instabilities, and are also likely to cause radial-type ruptures, especially in high γ' alloys. Superalloys can be forged by a variety of methods, and two or more of these methods are often used in sequence. A particular outcome of lower strain rate was the introduction of isothermal superplastic forging/forming or, at least, isothermal forging (see later section).

Forging Considerations

Rating Forging Capability. Customary forging temperatures for alloys and relative forgeability/formability comparisons of alloys are needed for product and manufacturing design. Forgeability ratings have been developed and are meant to be objective but remain somewhat subjective; thus they are presented in relative form. Traditionally, forgeability has meant the ability to deform a material to the shape of a die without introducing surface ruptures or internal defects. This rating is inherently related to the flow stress and ductility of alloys over the range of working temperatures. For components with demanding grain size requirements, the actual forging temperature ranges may be within a very limited temperature region of the range defined in traditional forgeability ratings.

Forgeability ratings and customary forging temperatures of the most commonly forged superalloys are listed in Table 6.1. In the forgeability ratings listed, alloy A-286 is assigned an arbitrary value of 1, because it is one of the most forgeable of the superalloys. The other alloys listed are assigned values that are multiples of 1, depending on their forgeability. As the arbitrary number increases, forgeability decreases. In establishing forgeability ratings, the power required is a minor consideration. Forgeability is determined more by the ease with which a given shape can be formed. Alloys that are difficult to forge generally require more blows and, consequently, more operations than the more easily forgeable alloys.

Table 6.1 Forging temperatures and relative forgeability ratings for some wrought superalloys

	Forging temperature(a)				
	Upset and breakdown		Finish forging		
Alloy	°C	°F	°C	°F	Forgeability rating(b)
Iron-base alloys					
A-286	1095	2000	1035	1900	1
V-57	1095	2000	1035	1900	1
16-25-6	1095	2000	1095	2000	1
Nickel-base alloys					
Alloy R-235	1205	2200	1205	2200	3
Astroloy	1120	2050	1120	2050	5
Hastelloy W	1205	2200	1035	1900	4
Hastelloy X	1175	2150	1175	2150	3
Inconel 600	1150	2100	1035	1900	1
Inconel 700	1120	2050	1105	2025	4
Inconel 718	1095	2000	1035	1900	2
Inconel X-750	1175	2150	1120	2050	2
Inconel 751	1150	2100	1150	2100	3
Incoloy 901	1150	2100	1095	2000	2
M-252	1150	2100	1095	2000	3
Rene 41	1150	2100	1120	2050	3
U-500	1175	2150	1175	2150	4
U-700	1120	2050	1120	2050	5
Waspaloy	1160	2125	1035	1900	3
Cobalt-base alloys					
J-1570	1175	2150	1175	2150	2
J-1650	1150	2100	1150	2100	2
HS-25 (L-605)	1230	2250	1230	2250	3
S-816	1150	2100	1150	2100	4
Haynes 188	1205	2200	1205	2200	3

(a) Lower temperatures are often used for specific forgings when structural uniformity is a requirement. (b) Based on the considerations discussed in text. As the rating increases, forgeability decreases.

Various factors go into making up the forgeability ratings for superalloys. Rate of die deterioration is important. For a given shape/volume, if die deterioration increases more rapidly and the number (percent) of rejected forgings plus the number of blows required to produce a given shape increases, then the forgeability is clearly decreasing. These factors are considered in establishing the ratings given in Table 6.1. The values of 1 to 5 in Table 6.1 are based on the difficulties that are encountered in the finishing forging operation.

Alloys processed by superplastic forging are not assigned forgeability values of the customary type. The principal reason that such alloys are being isothermally or superplastically forged is that their forgeability numbers in conventional means are off the scale.

The forging temperatures given in Table 6.1 are the temperatures of the billet surface as it is removed from the furnace. Forging should begin immediately, with a loss in temperature of no more than 75 °F (42 °C). Forging can be continued until the stock has cooled 200 °F (110 °C), or more for some alloys, below the temperatures given in Table 6.1, without damage to the workpiece. However, because greater pressures are required, forging is seldom done at temperatures substantially lower than those given in Table 6.1.

The three critical factors in any method of superalloy forging are dimensional reduction (strain), rate of dimensional reduction (strain rate), and temperature of the workpiece at any time during forging. The relationships between all three factors versus degree of recrystallization must be known before a forging process can be designed for a given component. These relationships recognize three distinct types of recrystallization: dynamic, meta-dynamic, and static.

Dynamic recrystallization occurs instantaneously during the application of strain to the material. There are critical temperature and strain rate combinations for dynamic recrystallization to occur. There is also a critical strain for dynamic recrystallization to proceed to completion (100% recrystallized grain).

Meta-dynamic recrystallization occurs when the metal is still hot at the end of deformation. It occurs in material that has been strained but did not dynamically recrystallize. Residual heat, influenced by the cooling rate from the deformation temperature is thus a critical parameter in determining the extent of meta-dynamic recrystallization that will occur.

Static recrystallization occurs in the absence of deformation. Thus, it is primarily a factor in grain growth during pre-heating of the forging increments and in subsequent heat treatment of the component.

Forging Methods. Forged superalloy components are produced by:

- Die forging
- Upsetting
- Extrusion forging
- Roll forging
- Swaging (or versions using proprietary rotary forging machines)
- Ring rolling
- Two or more of these methods used in sequence

The die forging categories can be subdivided into:

- Open-die forgings
- Open-die forgings formed with the aid of plugs and rings to impart certain shapes
- Closed-die blocker-type forgings
- Closed-die finish forgings

Which type is produced depends on complexity of shape and tolerances required. For example, as shown in Table 6.2, closed-die finish forgings have much thinner ribs and webs, tighter radii, and closer tolerances than blocker forgings.

The Forging Process

The Process Area. Forging requires a source of force and of heat. As such, forging operations can cover a substantial area in a manufacturing facility. Hydraulic press forges are common force sources, as are mechanical screw-driven machines. Some drop forge machines may exist but are not used to produce high-strength components that require great control of load, strain rate, and temperature. Rapid load application is probably best done with a hydraulic machine. Heat sources generally must be located in close proximity to the forging presses in order to minimize heat loss.

Table 6.2 Design guides for some conventional superalloy forgings

Alloy	Type of forging	Min web thickness, in. (mm)	Min rib width, in. (mm)	Thickness tolerance, in. (mm)	Min corner radii, in. (mm)	Min fillet radii, in. (mm)
A-286, Inco 901, Hastelloy X, Waspaloy, Udimet 630, TD-Nickel(a)	Blocker	0.75–1.25 (19.1–31.8)	0.75–1.00 (19.1–25.4)	0.18–0.25 (4.6–6.4)	0.62 (15.8)	0.75–1.25 (19.1–31.8)
	Finish	0.50–1.00 (12.7–25.4)	0.62–0.78 (15.8–19.8)	0.12–0.18 (3.0–4.6)	0.50 (12.7)	0.62–1.00 (15.8–25.4)
Inco 718, Rene 41, X-1900(a)	Blocker	1.00–1.50 (25.4–38.1)	1.00–1.25 (25.4–31.8)	0.20–0.25 (5.1–6.4)	0.75 (19.1)	1.00–2.00 (25.4–50.8)
	Finish	0.75–1.25 (19.1–31.8)	0.78–1.00 (19.8–25.4)	0.15–0.20 (3.8–5.1)	0.62 (15.8)	0.75–1.50 (19.1–38.1)
Astroloy, B-1900(a)	Blocker	1.50–2.50 (38.1–63.5)	1.25–1.50 (31.8–38.1)	0.25–0.30 (6.4–7.6)	1.00 (25.4)	1.25–2.50 (31.8–63.5)
	Finish	1.00–1.50 (25.4–38.1)	1.00–1.25 (25.4–31.8)	0.18–0.25 (4.6–6.4)	0.75 (19.1)	1.00–2.00 (25.4–50.8)

Note: For forgings over 400 in.^{2} (258,064 mm^2) in plan area. For forgings of 100 to 400 in.^{2} (64,516 to 258,064 mm^2) plan area, design allowables can be reduced 25%. For forgings under 100 in.^{2} (64,516 mm^2), design allowables can be reduced 50%. Recommended draft angles are 5 to 7 degrees. Machining allowance for finish forgings is 0.15 to 0.25 in. (3.81 to 6.35 mm). Some shapes can require higher minimum allowables than shown above. (a) Based on limited data

Isothermal or superplastic forging relies on an in situ furnace arrangement to retain the correct temperature for forging. In all other instances, the workpiece is removed from a furnace and taken to the press. This requires manipulators of some sort, as very high temperatures are encountered, often with large metal masses. The part is forged for as many strokes as permitted, considering the allowable temperature drop or component dimensional reduction. The component is then returned to the furnace for in-process heating, if it is to be forged again. If no further forging is contemplated, normal practice would be to cool to room temperature. For furnace information, see Chapter 8.

Forging the Superalloys. Forging may be accomplished with one or a group of dies and in closed or open dies, as noted. Closed dies better define the final shape of the forging. Some dies may be just flat platens that are used to transfer the load needed to change a dimension. The more complex the dies, the more expensive they become. Also, the more complex the dies, the more difficult it becomes to extract heat. Die design is a significant part of the superalloy forging process, just as it is for investment-cast parts. Forging dies, moreover, can be expensive. Costs in the multihundreds of thousands of dollars can be incurred for the die set to make a single part. Die design is not to be taken lightly. A change in die design, a flaw in the design, or a failure of a die can be extremely costly.

Open-die forging (hand or flat-die forging) frequently is used to produce preforms for relatively large parts, such as disks and shafts for gas turbines. Many such preforms are completed in closed dies. Open-die forging is seldom used for producing forgings weighing less than 20 lb (9 kg).

Closed-die forging is used widely for forging superalloys. The procedures, however, are generally different from those used for forging similar shapes from carbon or low-alloy steels. For example, preforms made by open-die forging, upsetting, ring rolling, or extruding are used to a greater extent for closed-die forging of superalloys than for steel. Because of the greater difficulties in forging superalloys, compared with forging similar sizes and shapes from steel, diemaking is also different.

Upset forging is the most common superalloy forging operation. It is normally the operation used to produce preforms for gas turbine disks (by closed die), casings (by ring rolling) and airfoils. In upset forging of superalloys, the maximum unsupported length (L) of upset is about three diameters (d), or ($L/d < 3/1$).

Extrusion also is used to produce preforms for subsequent forging in closed dies. Whether the preform is produced by extruding a slug or by forming an upset on the end of a smaller cross section depends mainly on the equipment available.

Roll forging sometimes is used to produce preforms for subsequent forging in closed dies. The rolling techniques for preforming of superalloys are basically the same as those for preforming steel. Roll forging saves ma-

terial and decreases the number of closed-die operations required.

Ring rolling produces hollow-centered, round forgings. This forging process is often applied to gas turbine casings. It is also used to make preforms for subsequent die forging. The final ring-rolled components contain much greater amounts of deformation than do die forgings. The general method used for superalloys is essentially the same as that used for steel. Superalloys with forgeability ratings of 1 or 2 (Table 6.1) can be ring rolled with the same procedures as those used for carbon and low-alloy steels. Alloys with forgeability ratings of 3, 4, and 5 require more steps in ring rolling and supplemental heating with auxiliary torches. Interior and pressure (exterior) rollers generally are required to transmit the force.

Rotary forging occurs in what is essentially a giant swaging machine. It has found much use in forging of shafts and shaft/disk combinations for aircraft gas turbines.

Forging a Small Aircraft Gas Turbine (AGT) Disk. Figure 6.1 shows the starting billet material for a series of planned Waspaloy nickel-base superalloy forgings for a small AGT disk. Figure 6.2 shows a set of forging mults after being open-die forged to ''pancakes.'' The parts shown are about 3.5 in. (~9 cm) thick and about 26 in. (~66 cm) in diameter. After further forging with a closed die, the part looks as shown in Fig. 6.3, where the dimensions now are 33 in. (~84 cm) in diameter, 2.75 in. (~7 cm) thick at the rim, and 1.74 in. (~4.5 cm) thick at the center. By use of appropriate temperatures and forging strain cycles, forged parts such as the sonic-machined disk or the integral disk-shaft (both shown in Fig. 6.4) were manufactured for gas turbine operations.

The components shown in Fig. 6.4 weighed 100 lb (~45.5 kg) and 20 lb (~9 kg), respectively, for the disk and integral disk-shaft. These weights were common for the gas turbines of the 1960s. As aircraft gas turbines have grown in size, component weights have grown, and the necessary increment weights of an alloy to be cut from a billet and forged have grown accordingly. Increments from which forging are made now commonly weigh over 1000 lb (455 kg). With greater use of superalloys in land-based gas turbines, very large forging weights are now at issue with forging increments of greater than 10,000 lb (~4550 kg) being routinely manufactured.

Deformation and Metal Removal in an AGT Disk Forging. Figure 6.5 schematically illustrates the steps in the production of a

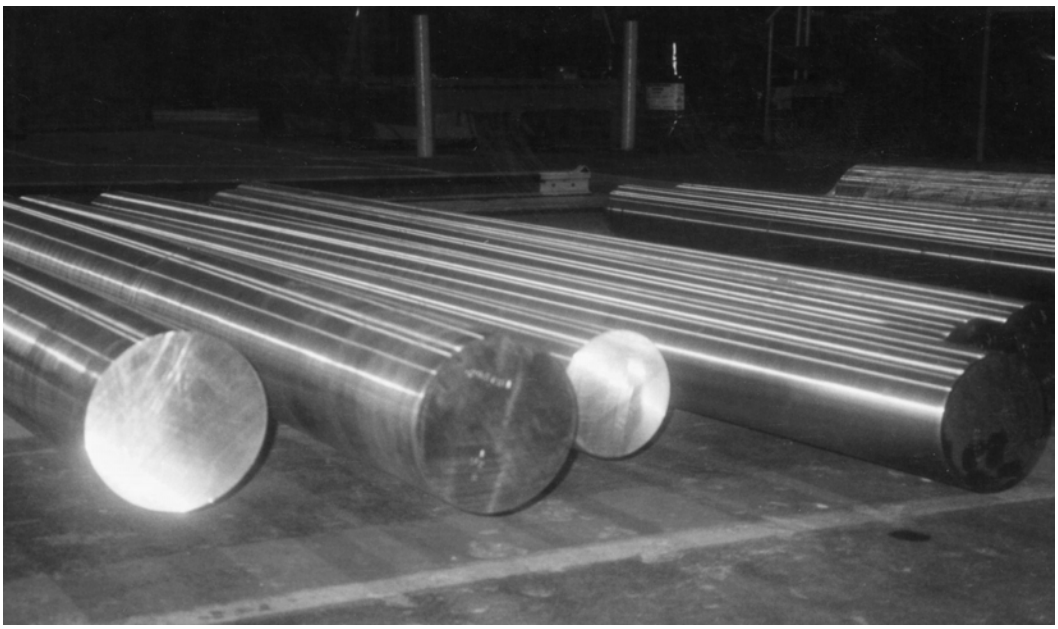


Fig. 6.1 Waspaloy nickel-base superalloy billets prior to cutting into multiple pieces (mults) for forging



Fig. 6.2 Open-die "pancake" forgings of Waspaloy nickel-base superalloy

simple AGT disk. The schematic is overlaid with grid lines representing the strain that occurs in each region during the indicated forging operation.

The first operation is an upsetting operation and would be performed on a forging increment cut from a billet of known grain size. (Where applicable, the solvus temperatures for intermetallics are considered in setting forging temperatures.) The increment is pancaked, generally in a single operation but sometimes in multiple operations. Note the reduced distortion in the ''dead zone'' regions near the original contact points of the increment with the die surfaces. This is due to a combination of reduced temperatures from contact with the die (die chill) and the frictional resistance to metal flow at the die-increment interface. Figure 6.6 shows a macroetched cross section of a forged pancake in which the dead zone can be detected as the



Fig. 6.3 Closed-die forged Waspaloy nickel-base superalloy forging produced from "pancake" in Fig. 6.2

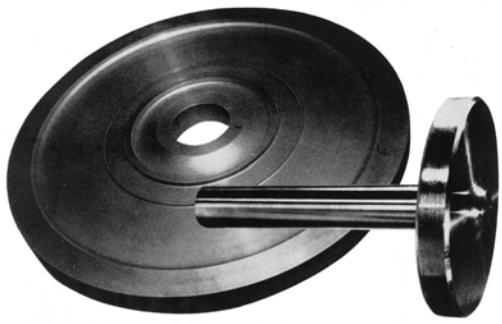


Fig. 6.4 Astroloy nickel-base superalloy forged components: disk and integral disk-shaft

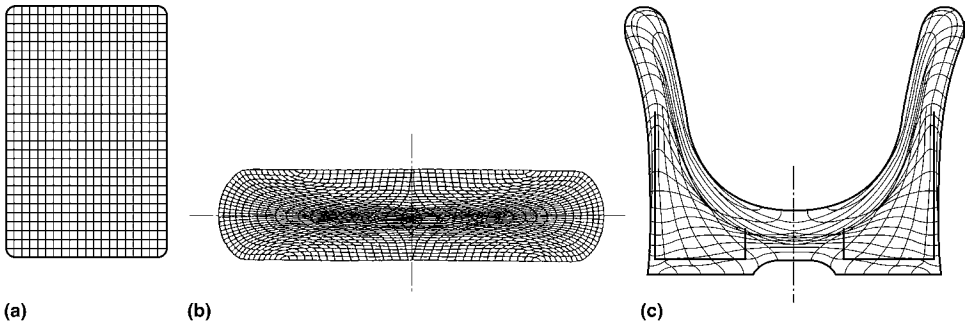


Fig. 6.5 Schematic illustration of strain introduced in regions of a forging during the steps required for production of a simple aircraft gas turbine disk. (a) The increment to be forged, overlaid with grid lines, (b) after upset to a "pancake," and (c) final forged shape

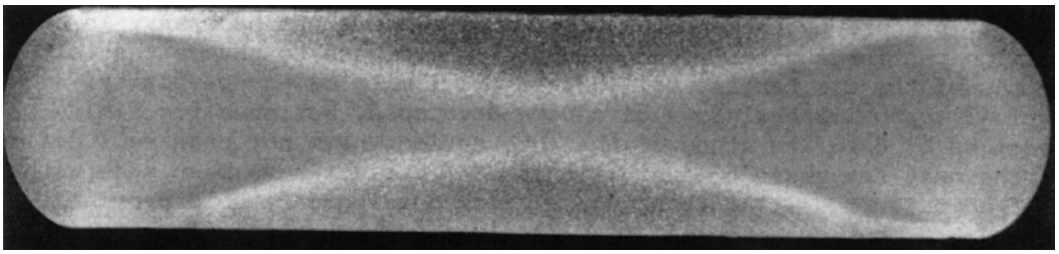


Fig. 6.6 Microstructure of cross section through a forged IN-718 "pancake" showing dead zone as darker-appearing etched layers in the regions adjoining the top and bottom surfaces of the pancake

darker-appearing etched layers in the regions adjoining the top and bottom surfaces of the pancake.

The pancake is inspected and, if necessary, cracks from the upsetting operation are ground out. The pancake is re-heated and forged to a final shape. In the case of the illustration, the shape is a very simple cross section. Shape changes can be more dramatic than those changes shown in Fig. 6.5. Cooling practice from the forging operation may have an effect on the structures developed in the final part.

The part is then machined to a sonic shape by the forger and tested by both ultrasonic inspection and macroetch. An integral test coupon will have been forged as part of the component. The coupon is removed from the component, machined, and tested for conformance to the specification mechanical test requirements of the component. In many forge houses, it is no longer necessary to perform a mechanical test on each component. Test results are taken from a statistical sampling. As long as the results remain in statistical control, it has been claimed that the forging parameters are under control and it is not necessary to test each part individually.

Figure 6.7 shows the relationships between forged shape, sonic shape, and final component as machined by the engine manufacturer.

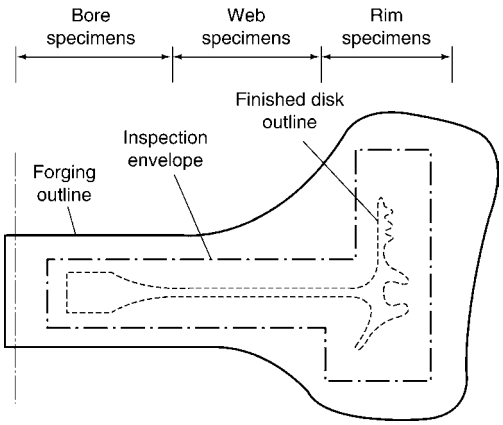


Fig. 6.7 Sketch showing outline of final forged component (disk), sonic inspection envelope, and finished disk

Forging as a Science. Modern forging technology not only uses a great deal of isothermal forging to reduce forging loads and improve die fill, but also uses an increasing array of automated controls and process modeling. It is important to recognize that, with the availability of modern computing power, it is possible to model the strain, strain rates, and temperatures during the forging process and thus predict with good accuracy the resulting microstructure in various sections of the component. Forging is no longer an art —it is a science. We have come a long way from the early forging processes where chainfalls, push rods, and operator force manipulated the product in the forging press. Figure 6.8 shows a turbine shaft of A-286 iron-nickel-base superalloy being forged circa 1960.

Forged turbine blades were the norm for many years for AGTs and are used in land-based gas turbines. Precision forging was introduced in the early stages of application for AGT components, which were relatively small. Figure 6.9 shows the results of typical steps in the forging of a turbine blade. The high cost of nickel-base superalloys means that forged turbine blades and other components should be produced only by manufacturing methods that maximize material use and minimize postforge machining. In early gas turbine engines, nickel-base superalloys were forged oversize and machined to final dimensions. As forging technology allowed, enhanced-precision, oversize turbine blades were replaced with precision-forged blades. Figure 6.10 visually demonstrates the difference between oversize and precision-forged blades and contrasts them with the final machined component. Precision-forged airfoils now are routinely produced.



Fig. 6.8 Forging a turbine shaft of A-286 iron-nickel-base superalloy

Precision forging also is used in the production of disk components. The much larger size and the large size of the billet make it difficult to get the same degree of control in disks as in airfoils. Near-net shape production is possible using powder methods (see Chapter 7) and superplastic isothermal forging (see subsequent information). The results have been quite satisfactory, with improved properties possible and sharp reductions in machining cost and in metal scrap.

Some Forging Problems. Problems with forgings can arise from many sources. Poor grain size control, grain size banded areas, poor carbide or second-phase morphology/distribution, internal cracking, and surface cracking are among the sources for rejection of forged parts. Figures 6.11 and 6.12 show some surface and peripheral cracking that occurred in a nickel-base superalloy during forging. These problems undoubtedly arose from some combination of too low a forge temperature, too great a reduction, or local chilling.

Figure 6.13 shows changes in microstructure of IN-718 that may be caused by unintended temperature variation within a forging. Lower-temperature forging areas retain unrecrystallized grain from the original billet.

Figure 6.14 shows the effect of too high a forging temperature for IN-718. In this case, the forging temperature has slightly exceeded the δ solvus temperature in a niobium-lean region of the billet. (See Fig. 4.26 under the section ''Homogenization of Solute Distribution in Ingots'' in Chapter 4.) Without sufficient δ phase present, the grain size has grown in the niobium-lean region. The alternating ringlike niobium-rich/niobium-lean nature of the solidification process accounts for this region appearing as a band.

Process Modeling. The forging industry has incorporated numerous technological innovations during the last two decades. The use of computer-aided design, manufacture, and engineering is particularly significant in the forging of heat-resistant alloys because of

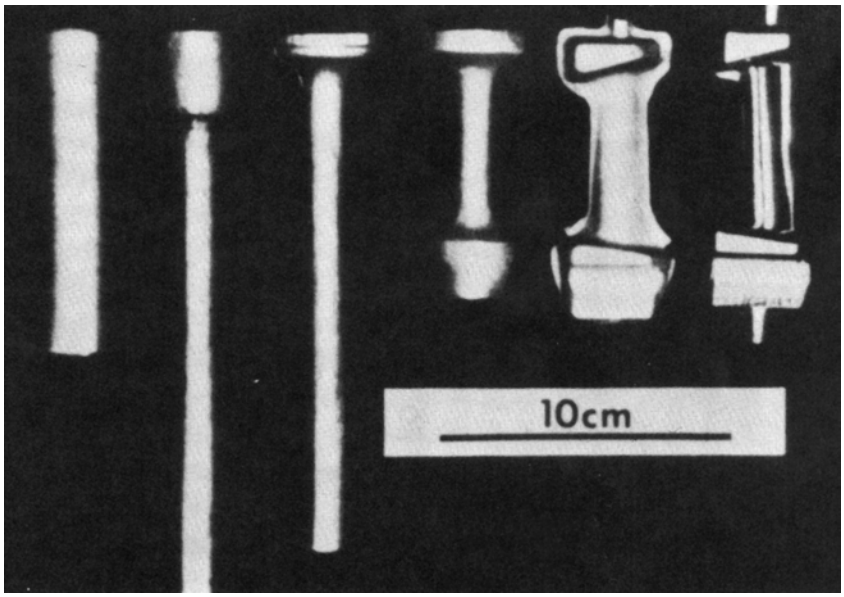


Fig. 6.9 Results of typical steps in the forging of a nickel-base superalloy turbine blade

the premium placed on higher quality and lower cost. On one hand, the thrust of alloy development has been to increase the service temperature, which means lower forgeability of the alloys. On the other hand, near-net shape manufacturing demands even closer control on the final shape. Machining of these alloys is difficult and expensive and can sometimes amount to 40% of the cost of production. The complexity of these demands makes computers more relevant to the portion of the forging industry concerned with heat-resistant alloys. Process modeling has become a very important adjunct to the forging business. Given accurate materials data and proper assumptions, computers can analyze and simulate the forging process, predict material flow, optimize the energy consump-

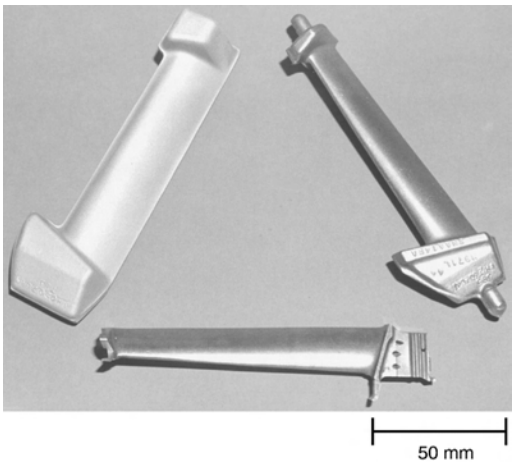


Fig. 6.10 Left to right: oversize, precision-forged, and final machined blades showing size variations



Fig. 6.11 Surface cracking caused by poor forging practice



Fig. 6.12 Peripheral cracking caused by poor forging practice

tion, and perform design and manufacturing functions.

Isothermal Forging and Hot-Die Forging. Single-temperature forging, whether by so-called isothermal processing or by the use of hot dies and some temperature drop, has been very effective for enhanced processing of superalloys. This technology offers a number of advantages:

- Closer tolerances than those possible in conventional forging processes can be achieved, resulting in reduced material and machining costs.
- Because die chilling is not a problem in isothermal or hot-die forging, lower strain rates (hydraulic presses) can be used.
- Lower strain rates are associated with reduced flow stress of the work material, so forging pressure and thus energy costs are reduced.
- Larger parts can be forged in existing hydraulic presses.

Practical Forging Considerations

Ingot Composition and Microstructure Control Is Critical. Starting stock for superalloy forgings is produced by various procedures, as described in Chapter 4. The cast ingots usually are converted to billets prior to forging. Workability in forging is affected by composition and by microstructure. After forging, optimal properties generally are achieved by precipitation hardening. Solid-solution strengthening and work hardening often contribute to strengthening, dependent on the alloy base and type. Cleaner, less-segregated heats of the most precise chemistry are always desired. The less-segregated heats are less susceptible to hot cracking during forging. Hot cracking can be a critical problem in alloys such as U-500, Rene 41, and Astroloy because of their narrow hot-working temperature ranges. Ingot (billet) microstructure plays a vital role in ensuring that the billet can be forged successfully and the properties can be achieved. As demands for larger components continue to be made, there is a continuing pressure on superalloy melters to create larger and larger billets. Of course, the forgers wish to retain the desirable microstructures of the much smaller billets, for example, those less than 10 in. (25.4 cm) in diameter, which were characteristic of the early vacuum arc and electroslag remelting processed superalloys of the 1960s.

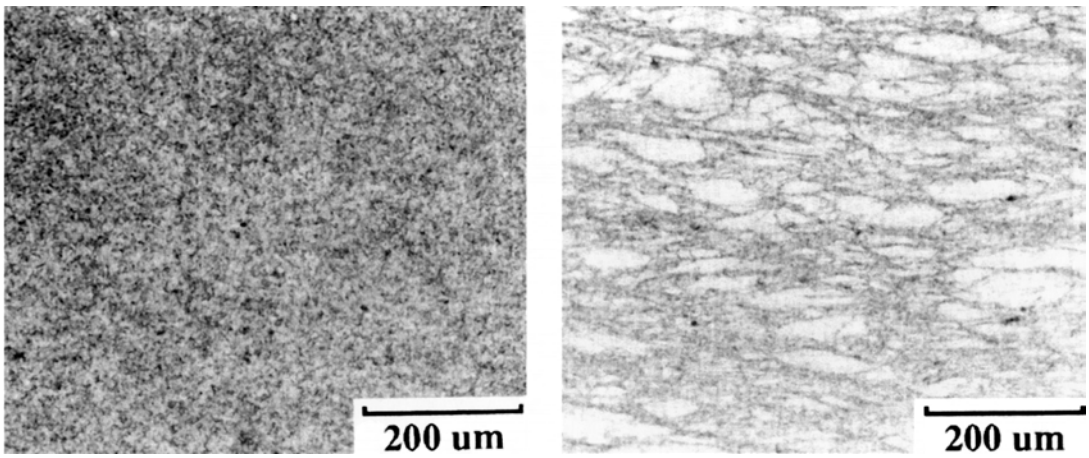


Fig. 6.13 IN-718 microstructure showing changes caused by unintended forging-temperature variations. Desired microstructure of completely recrystallized grains (left) vs. microstructure with many unrecrystallized grains (right)

In superalloys, high sulfur levels may constrict the favorable processing range, while addition elements such as magnesium may counteract the effect of sulfur and expand the process range. Superalloys such as IN-100 may have forging temperatures that vary, dependent on whether or not isothermal/superplastic forging is used. Grain refinement requirements also may affect the forging process. Powder metallurgy processing (see Chapter 7) plays a very important role in the processing of the high-strength wrought superalloys such as IN-100 and Rene 95.

Hot working of superalloys is a never-ending battle against:

- Limited working-temperature ranges
- Possible incipient melting
- Possible stringers, porosity, or undesirable second phases
- Loss of grain size control in (localized) solute-lean regions

Without proper attention to forging conditions, unfavorable microstructure, such as carbide films (refer to Fig. 3.7c), may be formed on grain boundaries at some stages in wrought processing. Such structures will restrict the range of processing conditions.

Aspects of Forgeability and Forging Reductions. Although more complete forgeability ratings and forging temperatures are given in Table 6.1, a short version of forgeability ratings (on a basis of resistance to cracking in forging) plus a single forging temperature are given in Table 6.3 for some of the more popular superalloys. Reference to Table 6.1 is preferred, but a glance at the short form of Table 6.3 may provide some quick insight into the possibility of forging a given alloy.

Forgeability not only governs the complexity of shape and tolerances that can be obtained, but also the amount of processing required during forging. Reduced forgeability means more in-process anneals and probably more conditioning of forged product before the next forging step. Some alloys can be reduced more than others before requiring annealing and/or special conditioning. For example, in initial upsetting, more forgeable superalloys (e.g., A-286, U-630, IN-718 and Hastelloy X) can be reduced 50 to 60% per pass, while maximum reduction rates of only 25 to 40% are common for Astroloy and Rene 41.

Process Control and Modeling Required. Because of their rather narrow hot-working range, the forging of superalloys requires accurate temperature control and other processing precautions. Some alloys need ceramics, metal coatings, insulating cloth, and/or oil-impregnated cloth to maintain proper temperatures and suitable lubrication. Others may best be processed with refractory metal dies in isothermal conditions. Compounding the problem is the fact that metallurgical characteristics sometimes call for other than optimal forging temperatures. Mechanical property capability is generated by the finish microstructure of forged precipitation-hardened superalloys. Sometimes the forging process temperatures, and so on are spelled out in specifications.

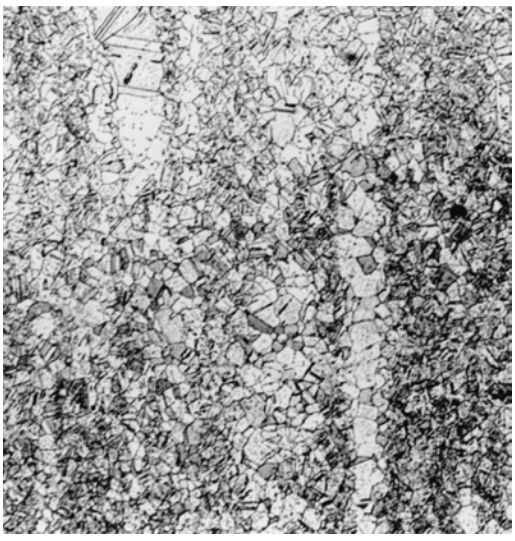


Fig. 6.14 IN-718 microstructure showing grain-size bands caused by too high a forging temperature

Table 6.3 Condensed forgeability ratings and forgeability temperatures guide for superalloys

	Forging temperature		
Alloy	°C	°F	Forgeability
A-286	1065	1950	Excellent
Inconel 901	1095	2000	Good to excellent
Hastelloy X	1095	2000	Excellent
Waspaloy	1080	1975	Good
Inconel 718	1065	1950	Excellent
Astroloy	1095	2000	Fair to good

In the earlier years of the industry, forging was an art form. However, at the turn of the 21st century, temperature, strain, and strain-rate conditions are being modeled with good accuracy. Such efforts are necessary, because adjustments in temperature and deformation can dramatically affect the grain size and final mechanical properties of forged superalloys. Perhaps the best illustration of that is the recognition that IN-718 may be forged to three distinctly different structures with significantly different properties.

Standard forged IN-718 is forged above the δ solvus. Completely recrystallized structures in the range of ASTM 4–6 are obtained. The component is strengthened by solution treatment above the solvus and use of a two-step age-hardening treatment.

Fine grain IN-718 may have initial forging operations performed above the δ solvus and final operations done just slightly below the δ solvus. This produces a grain size of about ASTM 8. The component is strengthened by solution treatment below the δ solvus and a two-step age-hardening treatment. Forgeability (with respect to die fill and resistance to cracking) is reduced compared to standard forged IN-718, owing to forging temperature restrictions.

Direct-age forged IN-718 is forged similarly to fine grain IN-718 or may be forged completely subsolvus. Grain sizes in the range of ASTM 10 can be obtained. Additionally, the component is not solution treated prior to the two-step age-hardening treatment. The amount of niobium in solution (and thus the amount available for precipitation hardening) plus the amount and morphology of the δ out of solution (pinning grain boundaries) are highly dependent on both the final forging temperature and the cooling sequence from that operation.

Also, because superalloys are inherently stiff, stock displacement during hot working is difficult yet proper stock distribution prior to finish forging is vitally important. Process modeling may help. Other precautions necessary to ensure sound forgings include intermittent penetrant inspection during forging to ensure freedom from surface defects (standard practice for the less forgeable alloys) and the use of oil and graphite mixtures for lubrication. If sulfur-bearing lubricants are used, reheating must be avoided, and clean-up after forging is necessary. In addition, heat must be maintained for a sufficient time during forging to ensure grain refinement, and forging dies must be kept in top condition.

Iron-Nickel-Base Superalloys. The iron-nickel base superalloys can be forged into a great variety of shapes with substantial reductions, approaching the forgeability of type 304 stainless steel. However, temperature has an important effect on forgeability. The optimal temperature range for forging A-286 and similar iron-nickel-base superalloys is narrow. On the basis of forging pressure, A-286 is considerably more difficult to forge than a plain carbon steel, even though A-286 is among the most forgeable of the superalloys (Table 6.1). However, A-286 requires only about half the specific energy that Rene 41 requires for the same upset reduction and the same forging temperature.

Nickel-Base Superalloys. To improve the high-temperature strength of the forgeable nickel-base superalloys, titanium and aluminum contents were increased and chromium content reduced as superalloys were developed in the latter half of the 20th century. As high-temperature strength was increased, forgeability decreased. This fact is clear from Table 6.4, where the alloys are presented in decreasing order of forgeability, which aligns with increasing amounts of hardeners (combined titanium and aluminum).

The Astroloy composition exhibits about the highest elevated-temperature strength possible, while maintaining forgeability by conventional means. The introduction of vacuum melting is the principal reason that titanium and aluminum levels could rise to the levels at which they presently stand. However, at these levels, the alloys likely would not be forgeable if the additional benefits of vacuum melting were not obtained. The reduction in the levels of oxygen and nitrogen

Table 6.4 Relationship of forgeability and hardener content of some wrought nickel-base superalloys

Alloy	Ti + Al, %	Cr, %
Waspaloy	4.4	19.5
Rene	4.5	19
U-500	6	18
Astroloy	7.5	15

Note: Alloys are listed in order of increasing high-temperature strength and decreasing forgeability.

eliminated most of the oxides and nitrides that contributed to poor forgeability in earlier wrought precipitation-hardened nickel-base superalloys. Because of this reduction, alloys with such excellent high-temperature strength as Astroloy could be forged.

As shown in Table 6.1, all but one of the nickel alloys are less forgeable than the iron-nickel-base superalloys. Almost all require more force to produce a given shape. Astroloy is the most difficult of the nickel-base alloys to forge conventionally. For a given percentage of upset reduction at a forging temperature of 2000 °F (1093 °C), this alloy requires about twice the specific energy needed for the iron-base alloy A-286. In the forgeability ratings listed in Table 6.1, Astroloy has about one-fifth the forgeability of Inconel 600. However, these ratings reflect only a relative ability to withstand deformation without failure; they do not indicate the energy or pressure needed for forging, nor can the ratings be related to low-alloy steels and other alloys that are considerably more forgeable.

Forging of nickel-base superalloys (and iron-nickel-base superalloys, too) requires close control over both metallurgical and operational conditions. Particular attention must be given to control of the workpiece temperature. Recording usually is required for data on transfer time, soaking time, finishing temperature, and percentage reduction. Critical parts are numbered, and precise records are kept. These records are useful in determining the cause of defective forgings, and they permit metallurgical analysis so that defects can be avoided in future products.

Nickel-base alloys are sensitive to minor variations in composition, which can cause large variations in forgeability, grain size, and final properties. In one instance, wide heat-to-heat variations in grain size occurred in parts forged from Incoloy 901 in the same sets of dies. For some parts, optimal forging temperatures had to be determined for each incoming heat of material, by making sample forgings and examining them after heat treatment for variations in grain size and other properties. Improved ingot metallurgy is making the forging operation more consistent and easier to monitor, and wide variations in product structure are less frequent than in former years.

One last note on the forging of nickel-base alloys is that the forging techniques developed for one shape usually must be modified when another shape is forged from the same alloy. Therefore, development time is often needed to establish suitable forging and heat treating cycles. This is especially true for stronger, more advanced alloys such as Waspaloy and Astroloy and applies as well to the powder-processed alloys such as IN-100 and Rene 95.

Cobalt-Base Superalloys. Many of the cobalt-base alloys cannot be forged successfully, because they contain more carbon than iron-base alloys and, therefore, greater quantities of hard carbides, which impair forgeability. The cobalt-base alloys listed in Table 6.1 are forgeable. The strength of these alloys at elevated temperatures, including the temperatures at which they are forged, is considerably higher than for iron-base alloys. Consequently, the pressures required to forge them are several times greater than those required for iron-base alloys.

Even when forged at their maximum forging temperature, the cobalt-base alloys S-816 and HS-25 work harden; thus, forging pressure must be increased as greater reductions are taken. Accordingly, these alloys generally require frequent reheating during forging to promote recrystallization and to lower the forging pressure for succeeding steps.

Forging conditions (temperature and reduction) have a significant effect on the grain size of cobalt-base alloys. Because low ductility, notch brittleness, and low fatigue strength are associated with coarse grains, close control of forging and of final heat treatment is important. Cobalt-base alloys are susceptible to grain growth when heated above about 2150 °F (1175 °C). They heat slowly and require a long soaking time for temperature uniformity. Forging temperatures and reductions, therefore, depend on the forging operation and the part design.

These alloys usually are forged with small reductions during initial breakdown operations. The reductions are selected to impart sufficient strain to the metal so that recrystallization (and usually grain refinement) will occur during subsequent reheating. Because the cross section of a partly forged section has been reduced, less time is required to reach temperature uniformity in reheating. Consequently, because reheating time is shorter, the reheating

temperature may sometimes be increased 50 to 150 °F (28 to 84 °C) above the initial forging temperature without damaging effects. However, if the part receives only small reductions in subsequent forging steps, forging should be continued at the lower temperatures. These small reductions, in turn, must be in excess of about 5 to 15% to prevent abnormal grain growth during subsequent annealing. The forging temperatures given in Table 6.1 are usually satisfactory.

Grain Refinement—Controlling Structure with Precipitated Phases. In order to refine grain structure (to improve low-cycle fatigue resistance and/or stress-rupture resistance) it is common, in forgings, to process precipitation-hardening superalloys within a more restricted temperature range than is given in Table 6.3. The temperature range is restricted so that not all of the precipitating elements are in solution during forging, thus causing pinning of grain boundaries and restriction of grain growth. The forging conditions must be chosen and controlled so that sufficient strain and temperature are used to allow recrystallization while not allowing the temperature to exceed the solution temperature for the precipitate. The grain structure obtained by such processing must be retained during heat treatment of the forging by either direct aging of the forged structure or aging after a pseudo-solution heat treatment that does not exceed the true solution temperature of all of the precipitate.

A principal use of such processing is in the production of direct-aged IN-718, the most dominant wrought superalloy. As luck would have it, the alloy also has a much wider processing window than conventional γ′-hardened superalloys. The major strengthening phase in IN-718 is not γ′ but γ″. Both phases will dissolve upon heating to high temperatures. The stable precipitate phase in IN-718 is δ, another variant of Ni_3Nb. Figure 6.15 shows a time-temperature-transformation (TTT) diagram for the precipitates in IN-718. Note that the TTT diagram does not address the relative volume of each precipitate. The shape of the TTT curve (specifically the δ solvus temperature) is modestly affected by niobium content in the alloy. Thus, because all IN-718 retains some degree of niobium-rich and niobium-lean bands, *the minimum local solvus temperature must be considered in establishing forging temperatures.*

For IN-718, the volume of γ″ and δ greatly exceed the volume of γ′. At low temperatures, the metastable precipitates γ′ and γ″ predominate. At temperatures above 1700 °F (927 °C), the dominant phase is δ. At temperatures about 1700 °F (927 °C), the δ phase

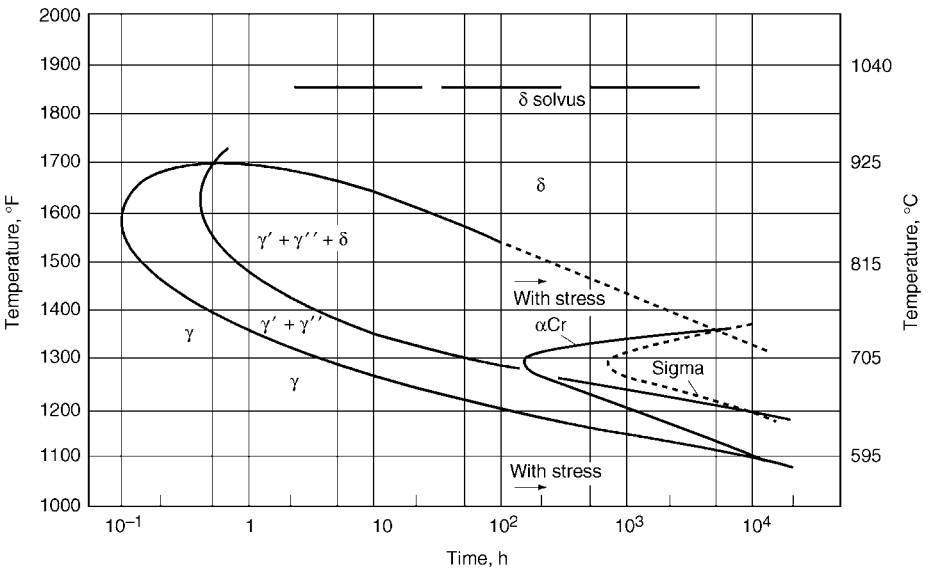


Fig. 6.15 Time-temperature-transformation diagram for IN-718

forms in a needlelike Widmanstätten structure. As the temperature is increased, the morphology of the δ phase becomes more blocky. When δ phase is subjected to strain at higher temperatures, 1800 to 1850 °F (982 to 1010 °C), the δ phase is spheroidized. As the temperature is increased, the volume of stable precipitate is decreased, with complete solution occurring at the δ solvus temperature. Thus, hot working in the range 1800 to 1850 °F (982 to 1010 °C) causes the formation of a small volume of spheroidized δ phase that pins grain-boundary growth. The greater percentage of niobium is retained in solution and is available to form the strengthening γ″ precipitate upon subsequent direct heat treatment (aging) of the forged part.

Forming of Superalloys

Introduction. Forming refers to the plastic deformation of relatively thin pieces (sheet, plate) of superalloys to produce bends and/or shapes with curved surfaces. Forming processes include:

- Drawing
- Spinning
- Stretch forming
- Press-brake forming

Formability and degree of work hardening (hardness or strength versus cold reduction) are interrelated. The greater the work hardening (slope of stress versus strain curve, the more difficult is further working (forming). The differences in composition of various superalloys cause differences in their formability. Figure 6.16 compares the degree of work hardening (hardness increase with cold reduction) of several lower-strength nickel-base superalloys to that experienced in a cobalt-base superalloy (HA-188), a precipitation-hardened iron-nickel-base alloy (A-286), American Iron and Steel Institute (AISI) type 304 stainless steel, and a low-carbon ferritic steel. It is quite obvious that superalloys will be considerably more difficult to form than low-carbon steel.

Cold forming is preferred for superalloys, especially in thin sheets. Most of these alloys can be hot formed effectively only in a narrow temperature range, between about 1700 and 2300 °F (927 and 1260 °C). Cold-forming with intermediate annealing between operations is usually preferred to hot forming.

Although forging is frequently used to develop macrostructures and post-heat-treating microstructures for optimal properties in precipitation-hardened superalloys, forming has no similar aim. The intent of forming is to achieve a form, not to produce a special structural effect after the forming operation (and attendant in-process and postprocess heat treatments) is completed.

The Role of Alloy Elements in Formability. Alloys such as cobalt-base alloys HA-25 and HA-188, which contain the greatest amount of cobalt, require a greater magnitude of force to form than iron-nickel- or nickel-base alloys. Most alloys that contain substantial amounts of molybdenum or tungsten for strengthening, such as HA-230 or Rene 41, are harder to form than alloys containing lesser amounts of these elements.

Alloys that contain aluminum and titanium are strengthened by precipitation of the γ′ phase. The $V_f\gamma'$ depends strongly on the amounts of aluminum and titanium present, and on overall composition. Alloys that might be formed and contain γ′ include Nimonic 80A, Waspaloy, and HA-214. These alloys typically contain 15, 20, and 33% $V_f\gamma'$, respectively. Many precipitation-hardened alloys require complex production steps to produce satisfactory components. As the $V_f\gamma'$ increases, the precipitation-hardened superalloys become extremely difficult to form.

Most of the iron-nickel- and nickel-base alloys contain less than 0.15% C; more carbon than this causes excessive carbide precipitation, which can severely reduce ductility. Cobalt-base alloys invariably contain greater than 0.15% C and so may have more limited ductilities in some instances than the preceding precipitation-hardened alloys. Small amounts of boron are used in some of the heat treatable nickel-base alloys, such as Rene 41 and U-700, to optimize carbide precipitation at grain boundaries; too much boron, however, also can cause cracking during forming.

Silicon content should be below 0.60% and preferably less than 0.30%. More than 0.60% Si causes cracking of cold-drawn alloys and may cause weld cracking in others. Silicon at levels of less than 0.30% usually does not contribute to difficulties in forming. When

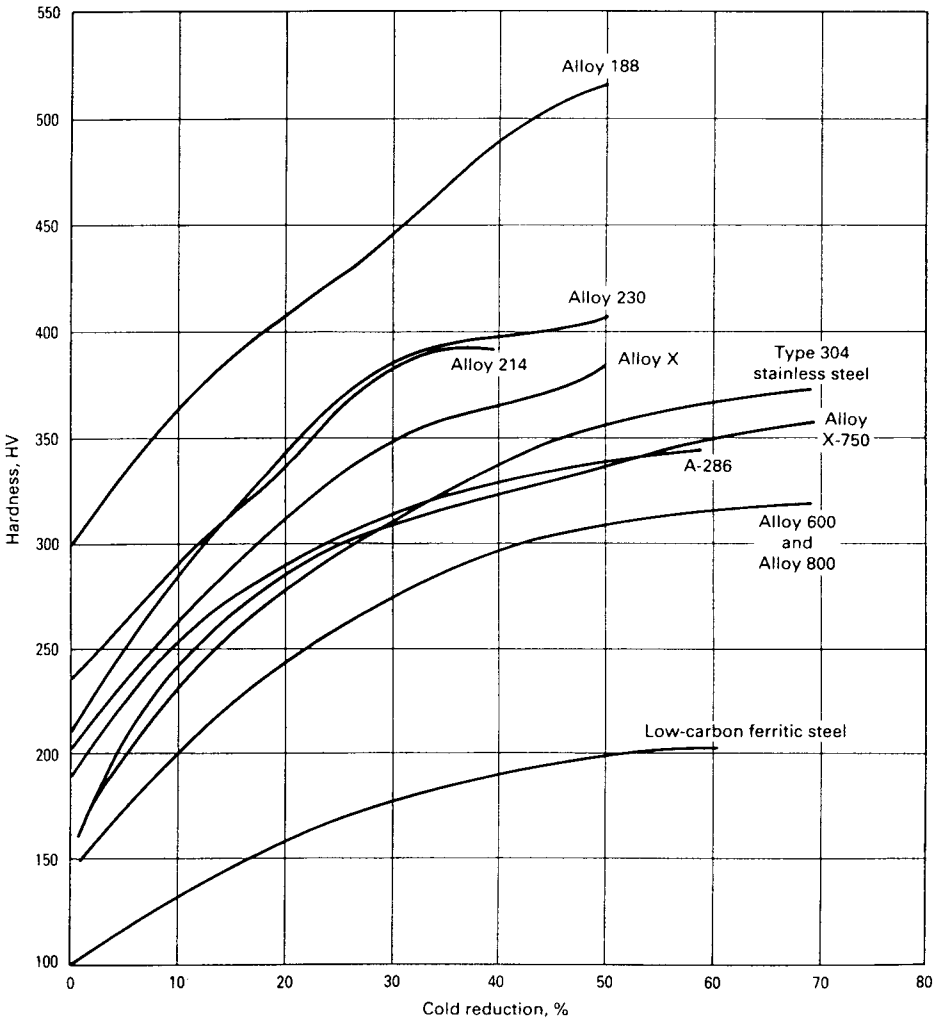


Fig. 6.16 Effect of cold reduction on the hardness of several superalloys and steels

hot forming is performed, sulfur can cause hot shortness of nickel-base alloys.

Effect of Alloy Condition on Formability. In order to produce the fine grain structure that is best for cold forming, heat-resistant alloys must be cold worked (reduced) beyond a critical percentage reduction and then annealed. The critical amount of cold work varies with the alloy and with the annealing temperature, but is usually 8 to 10%. Reheating metal that is only slightly cold worked can result in abnormal grain growth, which can cause orange peel or alligator-hide effects in subsequent forming.

For example, a Hastelloy X component, partly formed, stress relieved, and then given the final form, had severe orange peel on much of its surface. The partial forming resulted in only about 5% cold working, and during stress relief, an abnormally coarse grain structure developed. The difficulty was corrected by making certain that the metal was stretched 10% or more before it was stress relieved. In addition, the solution consisted of stress relieving at the lowest temperature and shortest time that could be used, because higher temperatures and longer times increased grain growth.

Severely cold-formed parts should be fully annealed after final forming. If annealing causes distortion, the work can be formed within 10% of the intended shape, annealed, pickled, and then given the final forming.

Practical Forming of Superalloys

Rating Formability. Formability refers to the ease with which sheet metal can be formed. As is the case for forgeability, material formability is difficult to measure. There is no single index for predicting specific material formability for all processing conditions. The deformation modes in the forming of most sheet metal components are complex and consist of bending, unbending, stretching, and deep drawing.

Material chemistry, macrostructure and microstructure, the forming process, and the final article shape all interact in the forming event and therefore should be considered simultaneously. This requirement makes material formability an elusive factor to quantify. Forming technology depends a great deal on practical experience. Material characteristics such as tensile ductility, strain-hardening exponent, and anisotropy parameters can act as guides to the nature of formability and can be used for comparing materials.

In any forming operation, the useful ductility of material is that amount up to the point of necking. Greater ductility at peak load and a large separation between yield and tensile strengths are desirable. A measure of stretchability is provided by the strain-hardening exponent (*n*-value).

The rolling and rerolling of a metal during its manufacture may cause alignment of individual grains. This usually imparts anisotropic plastic properties to the sheet. Recrystallization during annealing may tend to restore isotropy. The plastic-strain ratio, *r*, (the ratio of the width strain to thickness strain in a uniaxial tensile test) is a measure of normal anisotropy, that is, the variation of properties in the plane of the sheet relative to those perpendicular to the sheet surface. A material with a high *r*-value resists localized necking in the thickness direction; therefore, deep drawability is high. There are various correlations between deep drawability and *r*-value. Planar anisotropy causes uneven flow of metal, resulting in ''earing'' of drawn cups. Some typical forming characteristics of several superalloys are given in Table 6.5.

Forming limit curves are increasingly being used to predict the formability of materials. The forming limit curve is an experimental construction for combinations of strain paths that describes the strain to necking (or fracture).

Heat Treating of Precipitation-Hardened Alloys for Formability. Solution-annealed products are usually soft enough to permit mild forming. If the solution-annealed alloy is not soft enough for the forming operation, an annealing treatment must be used that will remove the effects of cold work and dissolve the age-hardening and other secondary phases. Some control of grain size is sacrificed, but if cooling from the annealing temperature is very rapid, the age-hardening elements will be retained in solution. Further stress-relief annealing after forming can be done at a lower temperature to decrease the risk of abnormal grain growth.

Several lower-temperature in-process anneals may be required in severe forming of precipitation-hardened alloys, but the high-temperature anneal need not be repeated. Care needs to be taken to minimize formation

Table 6.5 Forming characteristics of some superalloys

		Thickness		Anisotropy		Olsen cup depth		Ericksen cup depth	
Alloy	UNS No.	mm	in.	*r*	Δr	mm	in.	mm	in.
Alloy 80A	N07080	0.9	0.035	0.91	−0.02	...	...	12.5	0.492
Alloy 263	N07263	0.9	0.035	0.86	0.01	...	...	12.8	0.504
Alloy P16	...	0.9	0.035	0.98	−0.40	...	...	10.5	0.413
Alloy 188	R30188	1.2	0.047	0.94	0.13	...	...	12.6	0.496
Alloy 188	R30188	0.63	0.025	0.95	−0.024	12.5	0.492	...	...
Alloy 230	...	0.76	0.030	0.93	−0.059	11.0	0.433	...	...
Alloy 625	N06625	0.61	0.024	0.97	−0.139	11.7	0.461	...	...
Alloy X	N06002	0.61	0.024	0.95	−0.105	10.2	0.402	...	...

of precipitation-hardening phases or additional carbides prior to completion of the forming process. Intermediate annealing should be performed at a temperature that produces optimal ductility for the specific metal, as shown in the following example.

Example: Change in Heat Treatment to Eliminate Cracking in an Age-Hardening Alloy. A large manifold was made by welding together two drawn halves into a doughnut shape. Each half was drawn to a depth of 5 in. (127 mm) from 0.25 in. (3.5 mm) thick Rene 41 that had been solution treated at 2150 °F (1175 °C) and water quenched.

Drawing of the plate stock on a 7000 lbf (31,000 N) drop hammer produced severe work hardening, and cracking occurred frequently. To eliminate the cracking, forming was done in three steps, and the parts were annealed at 1975 °F (1080 °C) before the second and the third step. The forming characteristics of the Rene 41 plate were greatly improved by modifying the solution treatment.

The revised treatment consisted of first soaking the alloy at 1000 °F (540 °C), transferring it to a gantry furnace, and holding it at 1975 °F (1080 °C) for 30 min. The work was then lowered rapidly through the bottom of the furnace into a salt bath at 400 to 500 °F (205 to 260 °C). Thus, the elapsed time between leaving the high-temperature zone and entering the quench was kept to 4 or 5 s. The alloy was in the precipitation range, 1100 to 1850 °F (595 to 1010 °C), for a minimum time, and minimum hardness (16 to 21 HRC) was obtained. The salt bath provided a more uniform quench and a more ductile alloy than the original water quench. The better ductility of the alloy allowed forming of the manifold halves in two operations.

Effect of Rolling Direction on Formability. Depending on the size, amount, and dispersion of secondary phases, the precipitation-hardenable alloys show greater directional effects (Fig. 6.17) than alloys that are not precipitation hardenable. However, vacuum melting and solution annealing serve to reduce directional effects (anisotropy), although the mechanism for a vacuum-melting benefit is unclear.

As shown by data for press-brake bending in Fig. 6.17, directional effects contribute erratically to cracking and surface defects. The following example shows how directionality

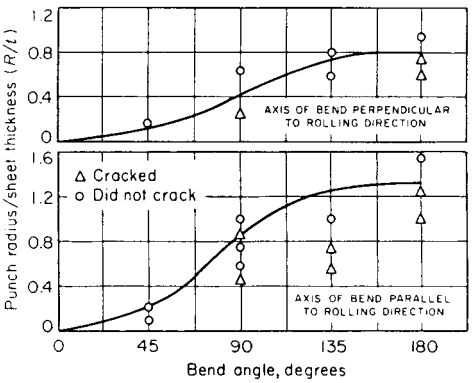


Fig. 6.17 Effect of forming direction relative to rolling direction on formability of Rene 41 nickel-base superalloy sheet in press-brake bending. Sheet thickness 0.02 to 0.187 in. (0.5 to 4.75 mm)

seriously affected the forming characteristics of iron-nickel-base superalloy A-286.

Example: Effect of Directionality in Bulging A-286. A contoured exhaust cone (Fig. 6.18a) was made by cutting a flat blank from mill-annealed A-286 sheet, rolling and welding a cone from the blank, and then bulging the cone into final shape. Developed blanks for two cones were cut from one sheared rectangle (Fig. 6.18b) with little waste of stock. Several lots of A-286 produced good parts, but one lot of material cracked in bulging. As shown in Fig. 6.18(a), cracks occurred in the cone adjacent to the weld at the location where the forming stresses were perpendicular to the rolling direction, which was also the direction of minimum elongation.

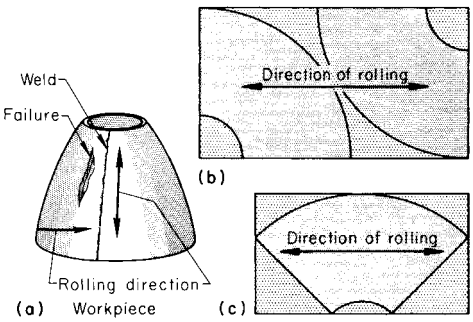


Fig. 6.18 A-286 iron-nickel base superalloy exhaust cone, (a) showing crack location after bulge forming, (b) and (c) showing layouts used in cutting cone blanks from 0.04 to 0.05 in. (1 to 1.3 mm) sheet

The good and inferior lots of A-286 were compared as to elongation with and across the rolling direction, and the inferior lot showed substantially greater difference in elongation between the two test directions. Annealing the welded cones before bulging reduced the number of cracked cones, but not by a satisfactory percentage. A higher percentage of acceptable cones resulted when the blanks were cut with their edges oriented to the rolling direction, as shown in Fig. 6.18(c). Cones made from these blanks had less abrupt change in the forming direction relative to rolling direction on each side of the weld, and the forming stresses were never perpendicular to the rolling direction; however, there was more scrap material from cutting the blank. When a revision of production techniques at the mill reduced the elongation difference in the two directions of stress, it was possible to use the more economical blank layout shown in Fig. 6.18(b).

Effect of Speed on Formability. The speed at which a metal is deformed affects its formability. In general, each metal has a critical speed of forming. In some cases, the ductility increases until this critical speed is reached, after which it decreases sharply with increasing speed. A plateau of maximum strain where ductility is greatest may be reached. This plateau seems to be broad for most superalloys. The breadth of the plateau depends on the use of biaxial or triaxial loading of the material during forming. Table 6.6 gives optimal speeds for three superalloys and three forming operations.

Formability and Processes

Methods. Few applications in forming superalloys involve quantities that warrant the use of high-production methods and tools. Usually, only a few to a few hundred parts are needed. Therefore, methods that require a minimum of tooling, such as press-brake forming, drop hammer forming, spinning, and explosive forming, have been used more than other methods. Presses or other machines are the same as those used for forming steel, but more power is needed to form superalloys because of their higher strength. The power required to form a given workpiece is from 50 to 100% more for superalloys than for low-carbon steel.

Safety in Explosive Forming. Operations involving explosives and pressure vessels are governed by state, county, and municipal regulations. The requirements and restrictions of these regulations should be taken into account in tool design and operational setup for explosive forming, which occasionally may be used for superalloys.

Tools. Tools used for forming superalloys are usually the same as those used for forming stainless steel in similar quantities. Clearance between punch and die is generally the same as that for stainless steel. Superalloys also resemble stainless steels in that they are likely to adhere to dies or mandrels, resulting in galling or tearing of the dies and workpieces. Steel dies, punches, or mandrels can be plated with approximately 0.2 to 0.5 mils (5 to 13 pm) of chromium in order to minimize adherence. However, small production quantities seldom justify this practice. Cast iron has proved adequate and nongalling for many low-production rate forming tools. If a heat-treatable grade of iron is used, areas in which high wear is anticipated can be locally hardened.

Lubrication. Some lubrication is usually required for optimal results in drawing, stretch forming, or spinning. Lubrication is seldom needed for the press-brake forming of V-bends, but will greatly improve results if a square punch is used. Mild forming operations, for example, those no more severe than

Table 6.6 Recommended forming speeds for three superalloys

		Forming speed for:					
		Tensile forming		Bulge forming		Draw forming	
Alloy	UNS No.	m/s	ft/s	m/s	ft/s	m/s	ft/s
A-286	S66286	15 to >84	100 to >425	0 to >213	0 to >700	0–236	0–775
Alloy 41	N07041	0 to >107	0 to >350	0 to >213	0 to >700	0–229	0–750
Alloy 25	...	30 to >130	50 to >275	...	...	198–251	650–825

a 10% reduction, can usually be accomplished successfully with unpigmented mineral oils and greases. Polar lubricants, such as lard oil, castor oil, and sperm oil, are preferred for mild forming. They will usually produce acceptable results and are easily removed. For more severe forming, metallic soaps or extreme-pressure (EP) lubricants, such as chlorinated, sulfochlorinated, or sulfurized oils or waxes, are recommended. They can be pigmented with a material such as mica for extremely severe forming.

Lubricants that contain white lead, zinc compounds, or molybdenum disulfide are not recommended for superalloy forming, because they are too difficult to remove before annealing or before high-temperature service. At high temperatures, any sulfur or lead on the surface of the alloys can be harmful. Sulfurized or sulfochlorinated oils can be used if the work is carefully cleaned afterward in a degreaser or an alkaline cleaner. Work that has been formed in zinc alloy dies should be flash pickled in nitric acid before heat treatment to prevent the possibility of liquid metal embrittlement by zinc.

Lubricants used for spinning operations must cling tenaciously; otherwise, they will be thrown off the workpiece by centrifugal force. Metallic soap or wax applied to the workpiece before spinning is usually satisfactory. In power spinning, a coolant should also be used during the process.

Occasionally, it is advantageous to use two kinds of lubricant in the same operation. In one stretch-forming application, the strain at the middle of the work was 3 to 4%, but near the ends, where the metal pulled tangential to the die, the strain was 10 to 12%. A light coat of thin oil was adequate for most of the work, but an EP lubricant was used at the ends.

Some Additional Aspects of Forming: Iron-Nickel and Nickel-Base Superalloys

Forming Practice for Iron-Base Superalloys. Alloy A-286 has work-hardening characteristics similar to those of type 304 stainless steel (Fig. 6.16) but has slightly lower formability. Most other iron-nickel-base superalloys are somewhat less formable than A-286. Typical forming practice is suggested by the following examples.

Example: Forming an A-286 Tube by Spinning. The tube shown at the top of Fig. 6.19 was backward spun from a roll forging that had been solution annealed at 1800 °F (982 °C). A starting groove had been machined into the tube in a previous operation. Spinning was performed in three passes on a machine capable of spinning a part 42 in. (1065 mm) in diameter and 50 in. (1270 mm) in length. Backward spinning was used in preference to forward spinning because:

- The finished component was longer than the mandrel.
- Forward spinning would have required a change in component design to permit hooking over the mandrel.
- Backward spinning is faster than forward spinning.

It was convenient to leave flanges at both ends and to trim these off later. The flanges prevented bell-mouthing and permitted trimming of the portions likely to have small radial cracks.

Example: N-155 Exit Nozzle Produced by Tube Spinning and Explosive Forming. The exit nozzle shown in Fig. 6.20 was produced from fully annealed 0.135 in. (3.4 mm) thick N-155 sheet. The sheet was rolled into a cylinder, with grain direction at right angles to the long axis, and was gas tungsten arc welded. The weld was ground flush on both

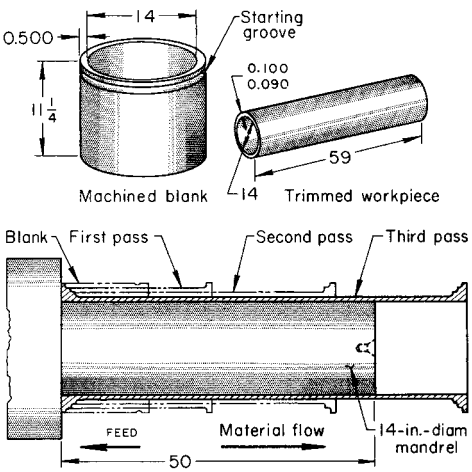


Fig. 6.19 Backward spinning of A-286 iron-nickel-base superalloy roll-forged tube. (Dimensions in inches)

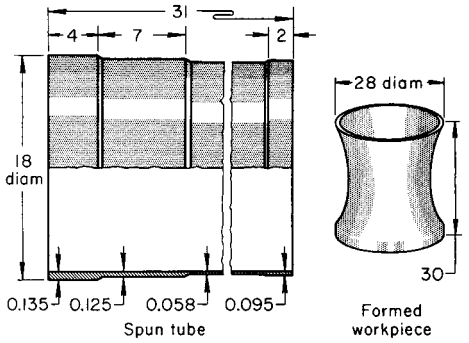


Fig. 6.20 Exit nozzle of N-155 produced by tube spinning and subsequent explosive forming. (Dimensions in inches)

the inside and outside, after which the cylinder was tube spun to the various wall thicknesses shown in Fig. 6.20. The component was then placed in a die and explosively formed to the shape shown at right in Fig. 6.20. The underwater explosive-forming technique was used, with a vacuum of 0.03 atm (3 KPa) between the workpiece and the die. The first shot of explosive charge produced approximately 90% of the final shape. A second shot, using the same size charge, completed the workpiece, after which it was annealed.

Forming Practice for Nickel-Base Superalloys. Two types of annealing treatments are used to soften the precipitation-hardenable nickel-base superalloys for forming. Type used is based on the ductility required for forming and, if subsequent welding is required, on the avoidance of adverse metallurgical effects during and after welding.

A high-temperature anneal is used to obtain maximum ductility and/or when no welding will be done on the formed part. A lower-temperature anneal, resulting in some sacrifice in ductility, is used when the formed part will be welded. For example, solution annealing of Rene 41 at 2150 °F (1175 °C) followed by quenching in water gives maximum ductility. However, parts formed from sheet annealed in this way should not be welded. During welding or subsequent heat treatment, they are likely to crack at a brittle carbide network developed in the grain boundaries. A lower annealing temperature, preferably 1950 to 1975 °F (1066 to 1080 °C), results in less sensitization during welding and decreases the likelihood of grain-boundary cracking. Formability is reduced by 10 to 20%, but is adequate for most forming operations.

Typical practice for forming nickel-base alloys is described in the following examples.

Example: Forming and Slotting Hastelloy X. Multiple flutes for a component were finish formed and slotted one at a time with hand indexing in a mechanical press. Slots were required to be within 0.02 in. (0.5 mm) of true position. The work metal was 0.04 to 0.044 in. (1 to 1.1 mm) Hastelloy X sheet. Before the mechanical press operations, the sheet had been formed by a rubber-diaphragm process, electrolytically cleaned, annealed to 74.5 to 81.5 HR3OT, pickled, restruck in the forming press, and trimmed. The flutes were partially formed in this series of operations.

In choosing a method of finish forming, it was decided that the only way to form the flutes to the required shape was to use a solid tool. The rubber-diaphragm forming process, however, was the best way to form the main contours of the part. The flutes could not be fully formed by a conventional die alone, because the percentage elongation exceeded the limits for Hastelloy X, which were 38 to 42% elongation in 2 in. (50 mm).

By making use of the natural tendency of the superalloy blank to form wrinkles, the flutes were preformed during rubber-diaphragm forming, but pressures were only enough to form them 75% complete. However, this forming lowered the amount of elongation needed in the final die-forming operation, and definite locations for flutes were provided; therefore, each flute could be produced in one stroke of the mechanical press. The tooling consisted of a die and a cam-actuated punch of high-carbon high-chromium tool steel hardened to 58 to 60 HRC, as well as die inserts, stripper, and cam sections of lower-alloy air-hardening tool steel. The punch pierced the slot and flattened the bulge above the flute. The stripper formed the flute when struck by the punch holder.

Example: Explosive Forming of IN-718. Fully annealed IN-718 sheet was used to make the flame deflector shown in Fig. 6.21. The sheet was rolled onto a cylinder, with the grain direction at right angles to the long axis. A 4.5 in. (115 mm) outside diameter by 32 in. (815 mm) long tube was gas tungsten arc welded from the cylinder using Rene 41

filler rod. The weld was made flush on the inside, and the outside was ground flush to +0.005 in. (+0.13 mm). The tube was spun to the dimensions shown in Fig. 6.21, fully annealed at 1750 °F (954 °C), and grit blasted. An outstanding characteristic of this alloy is its slow response to age hardening, which enables it to be welded and annealed with no spontaneous hardening unless cooled slowly. Explosive forming of the flame deflector was accomplished by three successive charges in a split die, and the component was fully annealed after explosive forming.

Some Additional Aspects of Forming: Carbide-Hardened Cobalt-Base Superalloys

General. Forming the cobalt-base alloys requires more force than many of the iron-nickel- and nickel-base alloys that are formed. The cobalt-base alloys such as HA-25, with lower nickel content, are more difficult to form than the higher-cobalt content alloys. The practice used in forming HA-25 parts is suggested in the following example.

Example: Explosive Forming of HA-25. Figure 6.22 shows the setup used for the explosive forming of a tail-pipe ball from HA-25 sheet. The sheet was gas tungsten arc welded (butt) into a cylinder, and the shape was formed by three explosive charges. No annealing was done between welding and the first two shots of explosive forming, but after the first two shots, the component was withdrawn from the die, annealed at 2150 °F (1175 °C), and descaled. The component was returned to the die for further forming. The third explosive charge used about 25% more explosive. Tolerance on diameters was maintained within ±0.01 in. (±0.25 mm). Explosive forming was preferred over forming on an expanding mandrel. This preference was because the mandrel left flats on the wall of the workpiece and explosive forming did not.

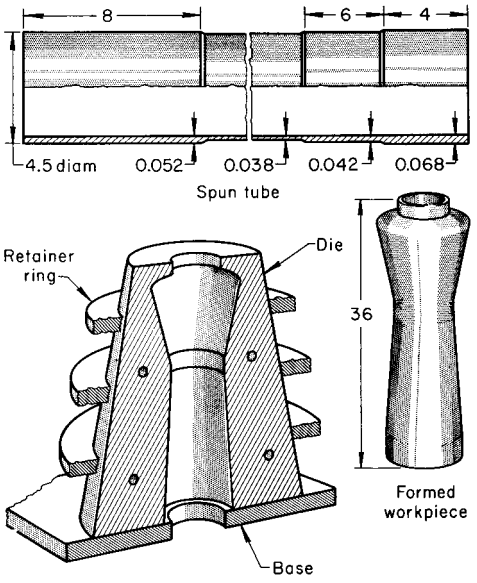


Fig. 6.21 Flame deflector of IN-718 produced from sheet by explosive forming with three successive charges. (Dimensions in inches)

Superplastic Forming/Forging

General. One of the major advances in forging and forming in the latter half of the 20th century was the recognition of the phenomenon of superplasticity and its adaptation to commercial forging and forming practices. IN-718 is one of many alloys now available in fine-grained controlled-composition sheet. With the appropriate conditions, fine-grained alloys can be superplastically shaped at isothermal temperatures. In the case of superplastic forming (SPF), the IN-718 is referred to as IN-718 SPF. The sheet is available with grain size that is sufficiently stable at the processing temperature of 1800 °F (982 °C) or less to ensure adequate time for SPF (note Fig. 6.23 for grain growth characteristics).

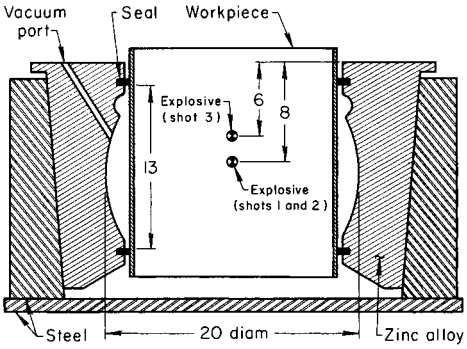


Fig. 6.22 Welded cylinder of HA-25 in position for explosive forming. (Dimensions in inches)

Forming. The SPF process lets strains of up to 250% be generated in superalloys that normally could not support strains of much over 50% before requiring annealing. The secret to superplastic deformation is the fine grain size and the maintenance of a low strain rate in the forming process, as well as a constant temperature. The superplastic behavior of IN-718, for example, allows the production of larger, more complex and detailed parts. Figure 6.24 shows a few articles made for gas turbine trials. One problem with SPF (of IN-718, at least) was the inability to reach specification mechanical properties after postprocessing heat treatment. Hot isostatic pressing was used to upgrade the stress-rupture capability of IN-718.

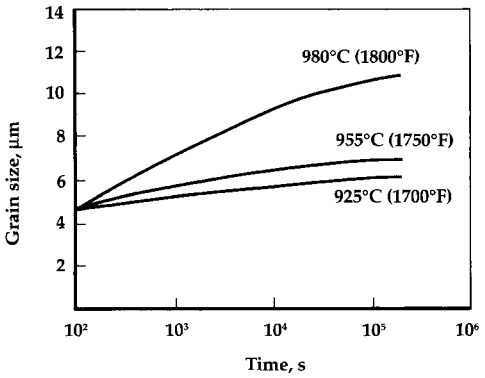


Fig. 6.23 Grain growth vs. time for IN-718 SPF

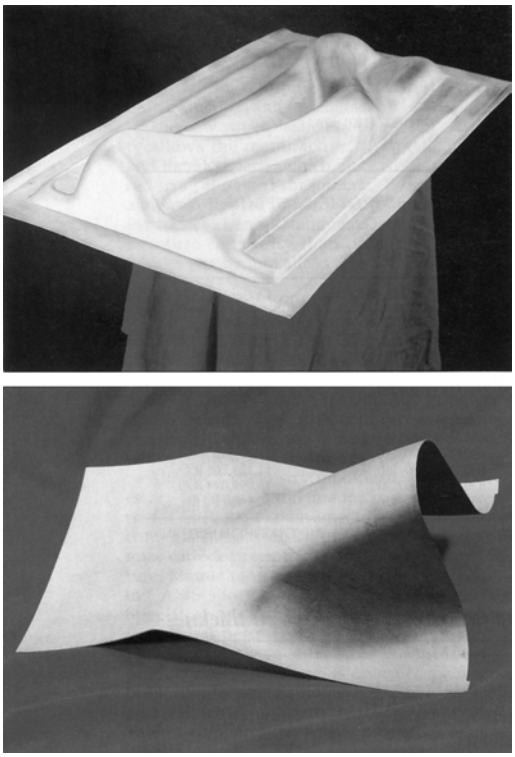


Fig. 6.24 Potential components for gas turbine applications, superplastically formed of IN-718. Noise suppressor assembly (top) and exhaust mixer nozzle component (bottom)

Forging. As for superplastic forging, the subject is one that is not directly treated but rather revolves around isothermal forging and ''Gatorizing'' processes, which are proprietary in many instances. Superplastic forging by the Gatorizing process was invented in the mid-1960s, and various patents were issued. The ability to do such superplastic-type processing has resided in the ability to get appropriate alloys into the proper microstructural condition to respond superplastically to applied forces. Most, if not all, nickel-base superalloys forged this way are extruded or powder processed to get homogenous, fine-grain billets for forging.

Refractory metal dies and inert atmospheres (principally for die life) are required, and times of forging are relatively long. On the other hand, die filling is excellent when compared to conventional closed-die forging of the strongest nickel-base disk alloys used in gas turbines. Conventional closed-die forging became a very difficult process when alloys of the level of Astroloy/U-700 began to



Fig. 6.25 Machined flat disk for aircraft gas turbine

be specified for gas turbine high-pressure turbine section disks. When the next level of strength (IN-100, Rene 95, etc.) was sought, it became virtually an economic and technical impossibility to produce acceptible disks. Concurrently, gas turbine engine sizes were going up, and disks were getting much larger. Powder processing to directly produce disks was tried but was discarded for various reasons (see Chapter 7). However, the powder process was successfully used as the precursor method to get preforms for subsequent superplastic or near-superplastic processing of ultrahigh-strength nickel-base alloys for massive gas turbine disks. A machined typical flat gas turbine disk is shown in Fig. 6.25.

Mention should be made here of the turn of events in the superalloy large-structure forging activity. In the early days, attention was focused on achieving shapes/sizes. Then attention shifted to the control of properties by control of the microstructure of the components, which meant using appropriate forging and heat treating sequences, possibly with several temperatures during the forging process. Now events have come full circle, and the objective is usually to do the deformation processing with a single temperature and concentrate on die filling. The properties are achieved from optimized billet structure and by appropriate postdeformation processing.

Superalloys: A Technical Guide, Second Edition
Matthew J. Donachie, Stephen J. Donachie, p 117-134
DOI:10.1361/stgs2002p117
Copyright © 2002 ASM International®
All rights reserved.
www.asminternational.org

Chapter 7

Powder Metallurgy Processing

Powder Superalloys Overview

Introduction. Powder metallurgy (P/M) techniques are being used extensively in superalloy production. Under normal circumstances, they are applied only to nickel-base superalloys. The applications are principally for high-strength gas turbine disk alloy compositions, such as IN-100 or Rene 95, which are difficult or impractical to forge by conventional methods. A limited use exists for oxide-dispersion-strengthened (ODS) alloys in airfoils.

Powder metallurgy of conventional γ'-hardened alloys offers the advantage of creating homogeneous, fine-grained billets or preforms from highly alloyed nickel-base alloys. Conventional ingot metallurgy processes generally cannot compete with powder in the areas of homogeneity and fine grain size. Some powder processes may be capable of creating a final product by application of rapid prototyping along the lines referred to for castings in Chapter 5.

Use of near-net shape processes has lowered costs by reducing the input weight of critical raw materials and the amount of secondary machining operations. Powder metallurgy processing also allows closer control of microstructure within a part than is possible in cast and ingot metallurgy wrought products. Figure 7.1 provides an illustration of the potential for raw material input reduction for a specific gas turbine part (compressor disk) when produced by conventional ingot metallurgy, hot isostatic pressing (HIP) plus forging, and direct HIP to produce a near-net shape part. Actual raw material savings will depend on the P/M route chosen and the complexity of the component being produced. Dollar savings will reflect:

- Increased alloy cost in powder versus cost as ingot
- Increased powder handling and consolidation costs versus ingot handling and forging costs
- Reduced machining costs for P/M product versus ingot metallurgy product
- Decreased metal input weight

It is significant to note from Fig. 7.1 that the P/M processes required markedly fewer processing steps, and that direct HIP (as-HIP) reduced the material input weight from 210 to 40 lb (95 to 18 kg). However, despite the reduced volume of raw material and reduced machining costs, the costs of P/M parts generally exceed the cost of conventional ingot metallurgy parts. Thus, P/M generally is used only where the component can not be made by ingot metallurgy or where a property advantage is gained over parts made by ingot methods.

Historical Background. The development of superalloys has been driven by the need for increasingly higher strength at higher temperatures for advanced aircraft engines. As the strength of these materials increased, hot workability decreased. The advent of vacuum melting enabled the introduction of higher retained levels of the precipitation-hardening elements, aluminum and titanium. Concurrently, extraneous second phases and inclusions were reduced. The latter effect promoted increased forgeability in the existing alloys, but the higher hardening element levels led to reduced forgeability by conventional means. Additional problems were en-

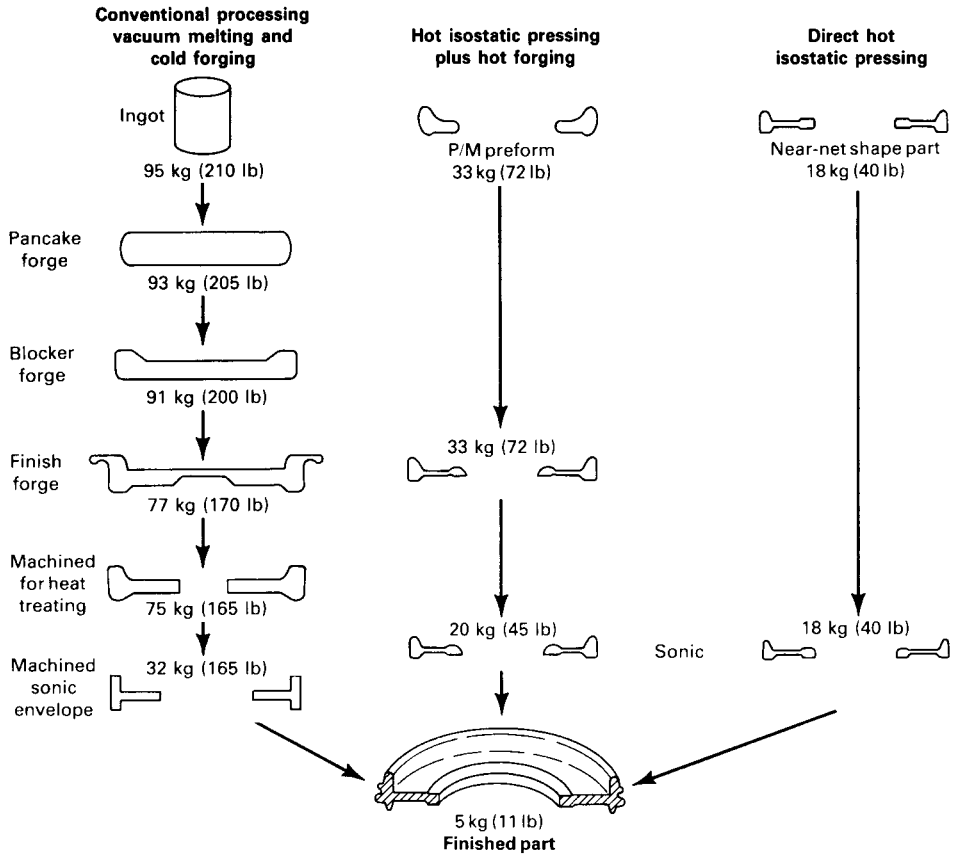


Fig. 7.1 Possible processing sequences for a gas turbine compressor disk illustrating the input weight reductions possible with P/M superalloy technology

countered as the result of increased segregation associated with more complex alloying and the need for larger ingots for larger turbine disks. The development of Astroloy put nickel-base superalloys at the limits of conventional forging techniques. By superb application of metallurgical knowledge and practical forging know-how, Astroloy was made into disks for gas turbine applications. However, the forging process was more costly than with earlier alloys and the results prone to more scatter than desired. A solution to these problems was to minimize segregation through rapid solidification of the metal by atomization to powder and consolidation by P/M methods that do not melt the powder particles but still attain full density.

In the 1950s, P/M was adapted to produce the oxide-dispersion-hardened alloy, TD-nickel, a thoria-hardened version of pure nickel. The P/M process (with oxide-type hardening) was tried for other compositions with varying success and by the 1960s was being tried (without oxide hardening) for γ'-hardened airfoil alloys. The results for γ'-hardened airfoil alloys were not promising, owing to the retention of prior particle boundaries in the product. Moreover, the finer grain size of a powder product was not amenable to the level of creep-rupture strengths required of airfoils. Furthermore, the cast superalloys could be made hollow (to conserve weight) and cast with simple internal passages for cooling. Consequently, P/M technology languished for a few years, despite some continued interest in the ODS alloys as sheet for combustors or in small bulk form for combustor nozzle applications.

However, when improved forgeability was seen as the only way to get good wrought disk components of high-strength alloys, the process was revisited. Initially, prior particle

boundaries (PPB) were found to be outlined by carbide particles. This resulted in unacceptable properties for the P/M parts. The PPB problem was solved through the development of low-carbon alloys, for example, low-carbon (LC) Astroloy.

Improved powder-making techniques were developed and consolidation processes were adapted so as to produce the kinds of wrought powder disk components now in use in the aircraft gas turbine field. Many compositions of the best-known P/M superalloys are basically similar to the cast alloys but are manufactured similarly to wrought alloys. The important P/M superalloys (IN-100, Rene 95, and Astroloy) were adapted in the P/M process by reducing their carbon content and by adding stable carbide formers to eliminate the problem of PPB carbides. To facilitate HIP, alloy compositions also were modified to increase the temperature gap between the γ' solvus (above which HIP has to be carried out for increasing grain size) and the solidus temperature (where melting occurs).

Initial P/M superalloy compositions were modifications of existing alloys, such as Astroloy and, later, IN-100 and Rene 95. Several of these alloys had been produced with extreme difficulty via the ingot metallurgy manufacturing process for use in aircraft engines. IN-100 was not successful, but the P/M process changed the situation. The three alloys were made available for application by use of P/M processing and are still among the most widely used P/M superalloys.

Adoption of P/M techniques was not without incident, and, although direct powder consolidation was favored for economic reasons, it became desirable, for quality reasons, to do some degree of forging on all powder nickel-base disks. Current technology favors:

- Powder production by gas atomization (in vacuum/inert gas)
- Powder consolidation by HIP or extrusion to form billet
- Component production by isothermal or superplastic forging to shape/dimensions

The first aircraft gas turbine to employ widespread use of a P/M extruded and isothermally forged nickel-base superalloy turbine was the Pratt & Whitney F100. It began operational service on the F-15 Eagle fighter in 1974. As-HIP Astroloy found use in many Pratt & Whitney military and commercial gas turbines. In addition to the widespread use of extruded and isothermally forged components, more than 100,000 as-hot isostatically pressed P/M superalloy components are flying in a variety of military and commercial engines. Currently, most aircraft gas turbine P/M disks are produced via extrusion and isothermal forging. When used, a typical aircraft engine may require anywhere from 1500 to 4500 lb (680 to 2040 kg) of nickel-base superalloy powder isothermal forgings.

Powder Metallurgy Superalloys Today. Superalloy components made by P/M techniques are being used in advanced turbine engines. The important aspects of the P/M process, as applied to gas turbine engine hardware, are:

- Ability to produce near-net shapes, with reduced material weight and reduced machining (but at a higher input material cost—the reduced machining costs are about offset by the higher cost of powder)
- Improved property uniformity and alloy-development flexibility, due to the elimination of macrosegregation and the development of finer grain size
- Reduced energy requirements and shorter delivery time, because the P/M process requires fewer steps than conventional ingot technology

One of the more interesting developments using nickel-base superalloys was the Allied Signal dual-alloy turbine wheel concept for aircraft auxiliary power units. This design, which began development around 1980, used a HIP-bonded, cast MAR-M-247 blade ring to an as-HIP low-carbon Astroloy hub. This procedure provides an assembly with a fine-grained, fatigue-resistant hub and an investment-cast, creep-resistant blade ring. By the turn of the 21st century, more than 1000 assemblies of this P/M component on the GTCP 331 auxiliary power unit (APU) engine had accumulated more than 12 million cycles without failure. Based on this experience, other turbine applications have either been introduced or are being designed and certified. Nearly 10,000 as-HIP turbine disks with integral or inserted blades are also in use in other APU applications, and this use continues to increase.

With segregation essentially eliminated, alloy designers were able to develop a number of new P/M alloys, such as AF 115, AF 2-

Table 7.1 Composition of some P/M superalloys

	Composition, wt%													
Alloy	C	Cr	Mo	W	Ta	Ti	Nb	Co	Al	Hf	Zr	B	Ni	Other
Rene 95	0.07	13.0	3.5	3.5	...	2.5	3.5	8.0	3.5	...	0.05	0.01	bal	...
IN-100	0.07	12.5	3.2	...	...	4.3	...	18.5	5.0	...	0.04	0.02	bal	0.75V
LC Astroloy	0.04	15.0	5.0	...	...	3.5	...	17.0	4.0	...	0.04	0.025	bal	...
N 18	0.02	11.5	6.5	...	...	4.3	...	15.5	4.3	0.5	...	0.015	bal	...
Rene 88DT	0.03	16.0	4.0	4.0	...	3.7	0.7	13.0	2.1	...	0.03	0.015	bal	...
Udimet 720	0.025	16.0	3.0	1.25	...	5.0	...	14.7	2.0	...	0.03	0.020	bal	...
IN-706	0.02	16.0	...	...	...	1.7	3.0	...	0.15	...	...	...	bal	38Fe
IN-718	0.02	18.0	3.0	...	...	0.9	5.0	...	0.45	...	...	0.004	bal	18Fe
AF 115	0.05	10.5	2.8	6.0	...	3.9	1.7	15.0	3.8	2.0	...	...	bal	...
AF 2-1DA-6	0.04	12.0	2.75	6.5	1.5	2.8	...	10.0	4.6	...	0.10	0.015	bal	...
PA101	0.10	12.5	...	4.0	4.0	4.0	...	9.0	3.5	1.0	...	...	bal	...
MERL 76	0.02	12.4	3.2	...	...	4.3	1.4	18.5	5.0	0.4	0.06	0.02	bal	...
TMP-3	0.07	10.8	3.1	3.4	...	2.8	3.9	6.9	3.9	...	0.05	0.01	bal	...
SR3	0.03	13.0	5.1	...	...	4.9	1.6	12.0	2.6	0.2	0.03	0.015	bal	...
KM4	0.03	12.0	4.0	...	...	4.0	2.0	18.0	4.0	...	0.03	0.03	bal	...

Table 7.2 Engine systems using forged P/M superalloys

Engine	Number produced through 1996
GE T700	9674
GE F404/414	3077
GE F110	2259
GE 90	38
PW F100	6496
PW 2000	951
PW 4000	1819

1DA, and so on, with exceptionally high strength for application in gas turbines. Unfortunately the defect tolerance of these alloys was generally not acceptable. Defect tolerance is the ability of a material to resist the growth of a crack initiated by a defect in the microstructure. Consequently, P/M superalloy development began to center on somewhat lower strength but highly defect-tolerant compositions, such as Rene 88DT and Udimet 720.

Table 7.1 summarizes the chemistry of some P/M superalloys. Table 7.2 lists engine systems using forged P/M superalloys. Table 7.3 summarizes the early applications of P/M superalloys in terms of components, engine use, and reasons for using P/M technology. Table 7.4 lists the large number of alloys and platforms that have been using as-HIP (not forged) P/M superalloys.

Powder Metallurgy Powder Production Techniques

Introduction. Virtually all powder used to produce P/M superalloys is prealloyed, meaning that the powder is made from the

Table 7.3 Aerospace applications of P/M superalloys

				Reason for using P/M technology	
P/M superalloy	Component	Engine	Aircraft/ manufacturer	Cost reduction	Improved properties
IN-100	Turbine disks, seals, spacers	F100	Pratt & Whitney	X	X
Rene 95	Turbine disks, cooling plate	T700	Helicopter/G.E.	...	...
	Turbine disks, compressor shaft	F404	F-18 Fighter	X	...
	Vane	F404	G.E.	...	...
	High-pressure turbine blade retainer, disks, forward outer seals	F101	...	X	...
Astroloy	High-pressure turbine disks	JTSD-17R Turbofan	...	X	...
Merl 76	Turbine disks	Turbofan	...	X	X
Inconel MA-754	Turbine nozzle vane	F404	F-18 Fighter	...	X
	High- and low-pressure turbine vanes	Selected engines	...	...	X
Stellite 31	Turbine blade dampers	TF 30-P100	USAF F-111F	X	...
Inconel MA-6000E	Turbine blades	TFE 731	...	...	X

Table 7.4 Engines and airframe systems using as-HIP powder metallurgy superalloys

G.E. Aircraft Engines		CFM International		Allied Signal	
Turbine	**Airframe**	**Turbine**	**Airframe**	**Turbine**	**Airframe**
CF6-80C2/E1	B-747-400, 767AWACS	CFM56-3B1/B2	B-737-300	GTC-131-3[A]	B-2
F108-CF-100	KC-135-R	CFM56-3B2/3C	B-737-400	GTC-131-9[D]	MD-90
F110-GE-100	F-16 C/D/G	CFM56-3B4	B-737-500	GTC-131-9[B]	B-737-X
F110-GE-129	F-16-D/G	CFM56-5A1	A-320-100/-200	GTC-131-9[A]	Airbus A319, A320, A321
F110-GE-400	F-14B	CFM56-5A/5B	A-319	GTCP-331-200	B-757/B-767 B-747-200B
F118-GE-100	B-2	CFM56-5B 1/B2	A-321-100	GTCP-331-250	A300, A310, C17A
F404-GE-400/402	F/A-18 C/D	CFM56-5C2/C4	A-340-200/300	GTCP-331-350	Airbus A330, A340
F404-GE-400/402	F-117A	CFM56-7	B-737-700	GTCP-331-350	B-777
T700-GE-401	Bell AH 1W	CFM56-8	B-737-600/800	RE-220	Gulfstream V Global Express CRJ-700
T700-GE-401	Sikorsky SH-60B/F	. . .	. . .	. . .	. . .
T700-GE-700	Sikorsky UH-60A/L	. . .	. . .	. . .	. . .

Table 7.5 Powder production methods

Step	Inert gas atomization(a)	Soluble gas process	Rotating electrode process(b)	Plasma rotating electrode process	Centrifugal atomization with forced convective cooling (RSR)(c)
Melting 1	VIM; ceramic crucible	VIM; ceramic crucible	VIM, VAR, ESR	VIM, VAR, ESR	VIM; ceramic crucible
Melting 2	. . .	. . .	Argon arc	Plasma	. . .
Melt disintegration system/ environment	Nozzle; argon stream	Expansion of dissolved hydrogen against vacuum and Ar + H_2 mixture	Rotating consumable electrode; argon or helium	Rotating consumable electrode; argon	Rotating disk; forced helium convective cooling

(a) VIM, vacuum induction melting. (b) VAR, vacuum arc remelting; ESR, electroslag remelting. (c) RSR, rapid solidification rate

molten state and each powder particle is essentially a mini-ingot with the same composition as the molten alloy.

An important prerequisite for making P/M superalloys that possess reliable properties is the use of clean powders. Years of intensive work were spent in identifying and controlling the problems related to unclean powders. Today, argon and vacuum (also known as soluble gas process) atomization, as well as atomization by the rotating electrode process, are known to be suitable for producing powders with the required low oxygen content and low degree of contamination.

Various means of producing superalloy powders are summarized in Table 7.5. All produce spherical powders and generally involve only one of the following atomization processes:

- Inert gas atomization
- Soluble gas atomization
- Centrifugal atomization

The principal commercial powder-making processes are gas atomization and vacuum atomization.

Inert Gas Atomization. The most common technique of producing superalloy powders is inert gas atomization (Fig. 7.2). Master melt of an alloy is made, typically, by vacuum induction melting (VIM) in order to minimize oxygen and nitrogen contents, then cast as ingots. Master melt is remelted, generally by VIM, but also by electron beam, plasma or conventional arc heating. Atomization then is carried out by pouring the master melt through a refractory orifice. A high-pressure inert gas stream (typically argon) breaks up the alloy into liquid droplets, which are solidified at a rate of about 1.8×10^2 F/s (10^2 K/s).

The spherical powder is collected at the outlet of the atomization chamber. The maximum particle diameter resulting from this process depends on the surface tension, viscosity, and density of the melt, as well as the

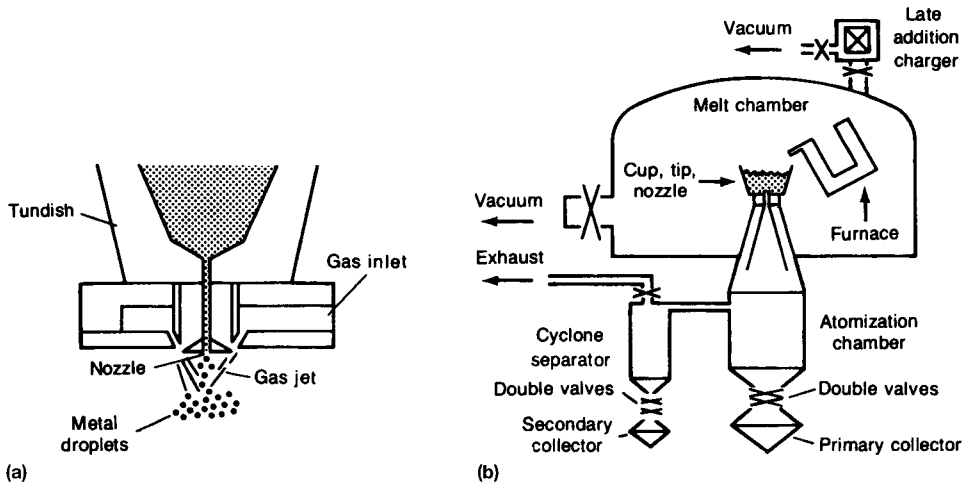


Fig. 7.2 Gas atomization system for producing superalloy powder. (a) Nozzle detail (b) system

velocity of the atomizing gas. The principal factor is gas velocity. A distribution of particle sizes is achieved, and this distribution is invariably skewed. Powders desired may lie in a given range, for example, 100 to 240 mesh, or be characterized as being ''less than'' a certain maximum size, for example, less than 100 mesh. Oxygen contents are of the order of 100 ppm, depending on particle size. Powder is classified by size and by sieving them under inert gas. Generally, spherical fine particles are desired for further processing in superalloy applications. Unfortunately, decreasing particle size means decreasing yield from each atomizing run! Consequently, finer mesh sizes are more expensive.

Powder characteristics are a function of the powder distribution achieved by the powder manufacturing process and the subset or fraction of the powder selected for the component manufacturing step. Although all particles may be more or less spherical, it is easier to pack a more diverse powder size distribution than a narrow size distribution. Impurities may be a function of powder size, but a more important factor is that sizes and numbers of inclusions, such as oxides and ceramic particles, are directly related to the maximum permitted size in a powder distribution. All other factors remaining the same, the smaller the maximum powder particle size (the smaller the classifying screen size), the smaller the maximum inclusion size.

Maximum inclusion size is not the same as maximum permitted particle size. It has been shown that some particles (powder or inclusions) of elliptical or rod shape always have a finite probability of dropping through the sieve used for sizing. The possible size of an inclusion is surprisingly large for some powders.

Vacuum (Soluble Gas) Atomization. Another important powder production method, the vacuum or soluble gas process, is based on the rapid expansion of gas-saturated molten metal. The process uses two vertical chambers connected by a transfer tube. The metal is vacuum induction melted in the lower chamber and then the lower chamber is pressurized with gas (normally hydrogen). The molten metal is forced upward through the transfer tube. A fine spray of molten droplets forms as the dissolved gas is suddenly released in the vacuum chamber (Fig. 7.3). The droplets solidify at a rate of about 1.8×10^3 F/s (10^3 K/s), and the cooled powder is collected under vacuum in another chamber, which is sealed and backfilled with an inert gas. This method is capable of atomizing up to 2200 lb (1000 kg) of superalloy in one heat and produces spherical powder that can be made very fine (Fig. 7.4). This method has been successfully employed for LC Astroloy, MERL 76, and IN-100.

Centrifugal Atomization. The third method of powder preparation is based on centrifugal atomization. This process usually is performed under vacuum or in a protective atmosphere. One example of this method is the rotating electrode process (REP) used in

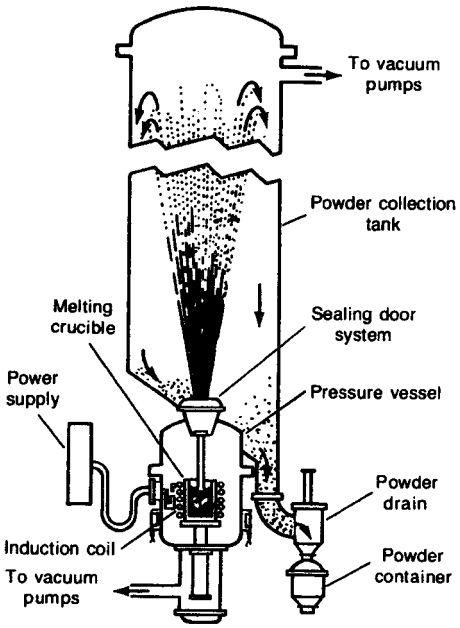


Fig. 7.3 Soluble gas atomization system for producing superalloy powder

the early production of IN-100 and Rene 95 powder. In this process, a bar of the desired composition, 0.6 to 3 in. (15 to 75 mm) in diameter, serves as a consumable electrode. The face of this positive electrode, which is rotated at high speed, is melted by a direct current electric arc between the consumable electrode and a stationary tungsten negative electrode (Fig. 7.5). Centrifugal force causes

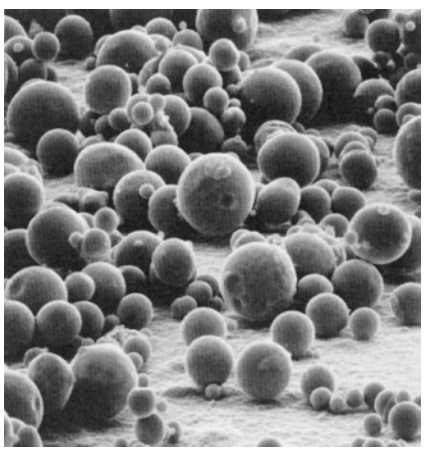


Fig. 7.4 Scanning electron micrograph of soluble-gas-atomized nickel-base superalloy powder

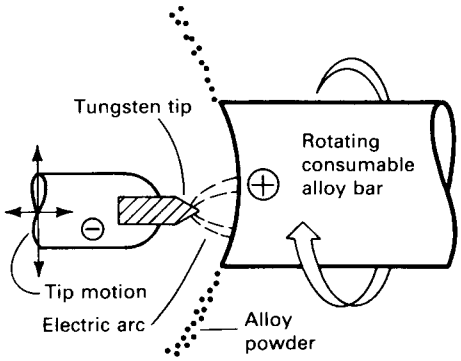


Fig. 7.5 Schematic of rotating electrode process

spherical molten droplets to fly off the rotating electrode. These droplets freeze and are collected at the bottom of the tank, which is filled with helium or argon. A major advantage of this process is the elimination of ceramic inclusions and the lack of any increase in the gas content of the powder relative to that of the alloy electrode.

A variant on the REP process is the plasma rotating electrode process (PREP). Instead of an arc from a tungsten electrode, a plasma arc is used to melt the superalloy electrode surface. Cooling rates are higher, up to 10^5 K/s for IN-100 powder. On average, particle sizes are nearly twice as large in these processes as in gas atomization. Neither REP nor PREP processes are currently in active production for superalloys.

Powder Evaluation and Preparation. Following powder production, the powders are screened to remove oversized particles and so meet the specification limits for powder mesh size. Then powder lots are blended. The necessity for blending is multifold. First, some powder lots or remaining portions thereof may be of insufficient weight to produce the desired component. Second, by averaging the powder over large weights, the risk of an individual lot being excluded because it fails to meet standards is reduced.

All powder handling is performed in such a way as to minimize the possibility of introducing foreign material into the powder. This involves the use of specially designed stainless steel containers, valves, and inert handling of powder in clean rooms. Of course, powder will need to be screened to get the desired powder size required by specification. Powder normally also is screened to mini-

mize the inclusion size in the final part. Depending on the application, powder sizes ranging from −60 to −325 mesh (−250 to −45 μm) are typically used. The smaller the particle size (larger mesh number), the smaller the probable inclusion size. Prior to being loaded into containers for consolidation, superalloy powders are evaluated for cleanliness by techniques such as water elutriation, which separates nonmetallic inclusions from the powder for counting, sizing, and identification. Specifications allow, for example, only powder blends with less than 20 particle/kg to be processed. For some as-HIP parts, low-cycle fatigue (LCF) testing of consolidated powder blends has been required.

A consolidated sample of powder can be evaluated by conducting large bar (e.g., 0.500 in. diameter × 2.0 in. gage section, or 1.27 mm diameter × 5.08 mm gage section) fatigue tests. In the use of such testing, cleanliness is evaluated on the basis of fatigue life and fracture origin. Figure 7.6 shows how the cyclic fatigue behavior of a P/M nickel-base superalloy (Astroloy) is affected by a reduction of mesh size, leading to reduced maximum inclusion size.

Powder Metallurgy Powder Consolidation Techniques

Introduction. Superalloy powders are consolidated principally by making preforms or billets using:

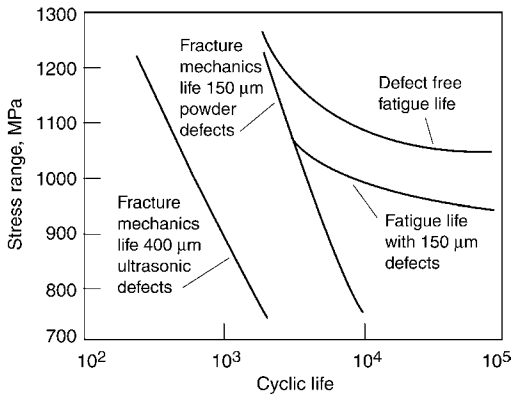


Fig. 7.6 Cyclic fatigue behavior of nickel-base superalloy (Astroloy) as affected by reduction in maximum powder defect size

- Extrusion
- HIP
- Combination of HIP and extrusion

An alternative consolidation process with some promise is the spray forming of superalloy components. The Osprey process, or variants thereof, can create a built-up article by repetitive spraying of powder onto an appropriate mandrel. It is unlikely that such an article would be used in critical applications without subsequent HIP or deformation processing.

Consolidation to Billet or Preform. A key feature of any consolidation process is the necessity to minimize contamination of the powder, especially from adsorbed surface gases and organic material mixed in with the powder. Containers for consolidation are made from stainless steel or mild steel. Exhaustive procedures are used to ensure that the containers are clean before powder loading. A final filter is commonly used to rescreen the powder when it enters the container as a final in-process control to ensure that no oversized particles are in the consolidated part. At some point in the processing, the powder is subjected to a vacuum and heated to remove air and adsorbed moisture. This can be accomplished during loading or after loading the powder into a container. In the former case, powder is loaded from an evacuated container into an evacuated consolidation container, and then the container is sealed. In the latter case, powder is loaded in air into a consolidation container, which is subsequently cold and hot outgassed and then sealed. Preferably, powders are packed into sheet metal containers under dynamic vacuum (either warm or cold). Various combinations or modifications of these two outgassing techniques are used by different manufacturers.

After the evacuated container is sealed, it is heated to the desired temperature and compacted, either isostatically under gas pressure or in a closed die.

Hot Isostatic Pressing. Hot isostatic pressing has been used both to produce shapes directly for final machining and to consolidate billets for subsequent forging. In HIP, powder-filled stainless steel containers are designed and produced to a size and dimension such that a desired component or billet shape will result during the HIP procedure. The

powder containers can be simple geometric shapes or complex near-net shapes. The containers are placed in an autoclave that is subsequently heated and pressurized. Generally, components with maximum diameters to about 4 ft (1.3 m) are able to be inserted into an autoclave. Superalloys are normally HIPed to full density at temperatures ranging from 2000 to 2200 °F (1093 to 1204 °C) under a pressure of 15 ksi (103 MPa). One advantage of HIP is that a fully dense product can be obtained without retained PPB. Grain size control during HIP is achieved by choosing a HIP temperature either above or below the γ' solvus. Grain size achieved during HIP will increase significantly if the HIP temperature exceeds the γ' solvus. An example of an as-HIP turbine disk including near-net sonic shape and the resulting finished product is shown in Fig. 7.7.

Extrusion. For extrusion of preconsolidated billet, the powder may be preconsolidated by HIP, a separate forging press, or in the extrusion press against a blank die. Extrusion ratios for solid billet are normally at least 3 to 1. Loose powder can be packed into symmetrical stainless steel cans instead of shaped containers, and then subjected to high temperature and pressure by extrusion. The extrusion of loose powder requires a specialized container with a nose plug designed to protect the evacuation stem on the container from rupturing prior to entering the extrusion die. Extrusion ratios used for direct extrusion of powder are at least 7 to 1. In the extrusion process, pressure forces the metal (container and powder) through an orifice sufficiently small as to get good amounts of plastic deformation and resultant powder bonding, producing a high-density compact. Essentially 100% density is achieved, and the resulting billet can be cut to mults for final processing. Typical extrusion temperatures for P/M superalloys range from 1900 to 2150 °F (1040 to 1175 °C).

Spray Forming. The ''spraying'' of powder superalloys in vacuum or inert atmosphere onto a mandrel in such a way as to create an approximate or exact shape and dimension of the component desired is known as spray forming. Spray forming actually involves atomizing a stream of molten metal into droplets and collecting the droplets, an approximately 50/50 mixture of liquid and solid, on a substrate before they fully solidify. The process is capable of producing various shapes, such as billet, tubes, disks, and sheet, in steels and corrosion-resistant alloys but generally has not been qualified for superalloys, at least for critical rotating parts.

Spray-formed preforms can have a density up to about 99.8% of theoretical, but the material is normally HIP and/or hot worked after spray forming to fully densify the compact and to improve properties. Compared to conventional P/M, the advantage of the process is the potential of lower cost, because powder handling, canning, and the initial consolidation step are eliminated. Disadvantages of the process are a coarser structure and the inability to control inclusion size through particle sizing. The process was originally developed by Osprey Metals. It has been claimed that Osprey-consolidated parts may be used with or without further deformation processing; however, deformation processing would be desirable. (See subsequent comments about deformation and defect detection.)

Other Consolidation Processes. The consolidation by atmospheric pressure (CAP) process and the fluid die process exist. Neither technique requires an expensive HIP unit. The CAP process resembles a vacuum sintering process, assisted by low pressure exerted on the surface of a shaped glass container. The fluid die process incorporates a cavity surrounded by a dense, incompressible mass of material. The higher mass of these containers, compared to the mass of sheet containers, allows greater vibration during filling and sealing, ensuring more complete filling and uniform tap density. The outer material softens appreciably at the compaction temperature, allowing pressure to be transmitted to the powder. Conventional die forging equipment is used to transmit pressure and is capable of much higher ram pressures than those possible with HIP autoclaves; full consolidation occurs in less than 1 s.

Powder-Based Disk Components

General. The precursor to final component shape is likely to be a billet but may be a preform of substantially the shape of the desired component. Billet origin, before the (often isothermal) powder forging operation to produce configurations desired for final machining, may be either extruded or HIPed

compacts. Although virtually every P/M consolidation technique has been applied to superalloys, production of superalloy disks is usually accomplished by HIP and related processes or by extrusion plus isothermal forging. Full density can be achieved by these processes.

A benefit of the P/M process is that the consolidated products often are superplastic and amenable to isothermal forging. Thus, force requirements can be greatly reduced, and near-net forgings can be made. Superplastic P/M superalloys are normally isothermally forged at low strain rates to take advantage of the reduced force requirements and to produce desired close-tolerance forgings. Near-net shapes are also made by HIP.

Although P/M alloys cost more than conventional wrought alloys, they have allowed designers to design to higher creep strength and tensile capability while maintaining the expected cyclic life of components. The value added to the system in terms of the performance benefit gained by the system operating temperature and weight reduction more than balances any increased cost of P/M application.

Both P/M isothermal forging and direct-HIP powder metallurgy methods permit the manufacture of so-called near-net shape parts with attendant improved material use and reduced machining costs. Hot compaction of billets by extrusion leads to improved forgeability through very fine grain size, improved hot ductility, and superplasticity in compacts. Compaction by HIP provides similar benefits to those of extrusion, although the grain sizes of HIP billets may be coarser than those of extruded powder billets.

Conventional high-strain forging is difficult to accomplish in P/M superalloy compositions, owing to the high strength and cracking tendencies of these materials. However, recent work has shown that the high strain-rate formability of Udimet 720 can be markedly improved by HIP at a temperature slightly below the solidus of the alloy. The improvement is attributed to the elimination of grain boundaries, which are coincident with PPBs. As a result, conventional forging and ring rolling of P/M billet is deemed practical. Powder metallurgy forging also exploits the improved forgeability deriving from the higher incipient melting temperature and reduced grain size of P/M material.

As suggested previously, there are concerns in some applications that a direct-HIP near-net shape may contain unrecognized defects that would inhibit satisfactory application of a component. Forged precompacted powder billets and/or preforms provide the degree of deformation and consequent mechanical properties that some designers prefer. While direct isothermal powder superalloy forging might be preferred for cost reasons, the use of powder billets and/or preforms ensures that full densification has been achieved and that reasonable amounts of deformation energy have been applied to the metal before the final shape is produced. The deformation processing is thought to enhance the detectability of subsurface imperfections that otherwise would limit the fracture mechanics life of the article. In short, if a component were going to have a defect, many would argue that the defect would be exposed as a result of deformation processing.

Component Production. Powder preforms or billets are turned into components, using the following established techniques:

- Isothermal forging of P/M superalloy billets or preforms
- Direct HIPing of powder to final component

A principal objective of P/M superalloy component production is the achievement of high mechanical properties in components such as gas turbine disks, which are in the order of several feet (~0.6 m) in diameter and up to about 0.5 ft (~0.15 m) thick. Volume and shape of the component to be produced can be critical to container-filling capability and to subsequent consolidation. As volume, particularly thickness, increases, it becomes proportionately harder to create a disk with uniform properties. This is a result of the geometrical limitations of powder filling, the difficulties of getting uniform deformation into the powder preform, and the subsequent wide variation in temperature and cooling rate in large components during heat treatment.

Depending on the application for a superalloy part, the powder consolidation process can be controlled to yield either a fine or a coarse grain size. Fine grain size is preferred for intermediate temperatures of up to about 1200 to 1300 °F (649 to 704 °C), which might be used for turbine disks be-

cause of the higher tensile strength and ductility of fine-grained superalloys at these temperatures. For high-temperature blade and vane applications, however, a large grain size (ASTM 1 to 2) provides superior creep strength.

Inspection. It is important to note that gas turbine disks are inspected extensively prior to completion of manufacturing and release to service. Sonic inspection is one of the processes used to validate the integrity of a forged or as-HIP disk. Note the sonic shape shown in Fig. 7.7 and that it consists of flat, parallel surfaces to make sonic inspection more accurate.

The uniform grain size and lack of segregation in P/M material generally improves forgeability, machinability, and ultrasonic inspectability. The ultrasonic inspectability (background noise level) of P/M alloys, due to their homogeneity, is superior to most conventional cast plus wrought superalloys. As a result, smaller flaws can be detected in the P/M superalloys.

Powder Metallurgy Disk Alloys. Aircraft gas turbine disks, designed to operate at about 1200 °F (649 °C) in current high-performance engines, require forgeable alloys with:

- High yield strength (to maximize LCF resistance and resistance to short-time deformation)
- High ultimate strength (to tolerate overspeed without burst)
- High creep resistance and good damage tolerance in fatigue (the crack growth rate must be kept low even under conditions of environmental attack and hold times under stress)

Powder metallurgy superalloys combine the highest yield and tensile strengths with good creep- and stress-rupture properties and excellent LCF and crack propagation characteristics. Several P/M superalloys have replaced ingot metallurgy forged alloys as turbine disks. These alloys include:

- LC Astroloy
- MERL 76
- IN-100
- Rene 95
- Rene 88DT

As previously noted, Table 7.1 gives compositions of some of the dozens of superalloys evaluated for disk applications. In general, the strength of these alloys is a direct function of their γ' or γ'' content. Powder

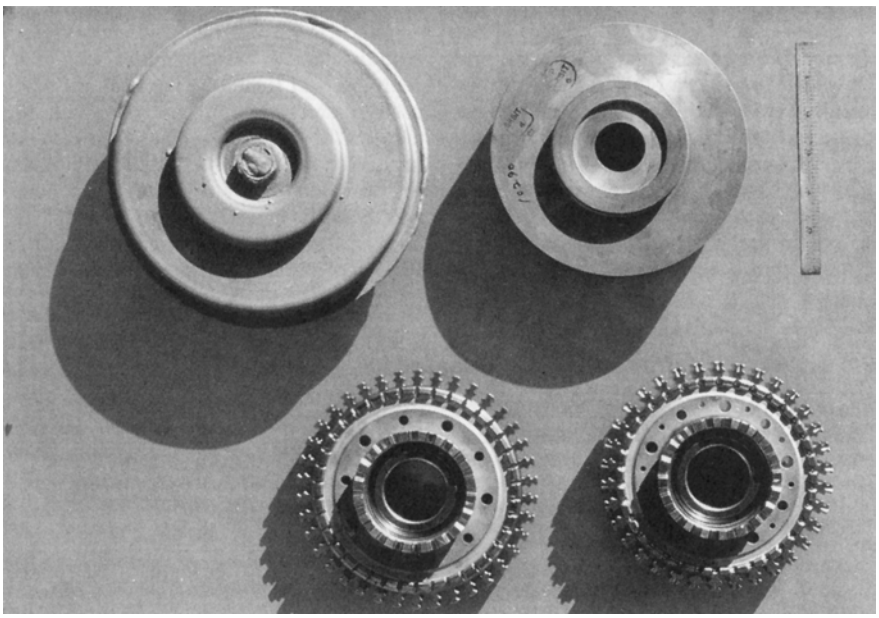


Fig. 7.7 As-HIP Rene 95 turbine disks. As-HIP shape (upper left), sonic shape (upper right), finished machined disks (bottom)

processing permits the attainment of a fine grain size, which lends the alloys their superplastic forming capability (as in the Pratt & Whitney Gatorizing process). The alloys are characterized by a high homogeneous concentration of both solid-solution strengthening elements and the γ'- and γ''-forming elements aluminum, titanium, and niobium. These factors (high levels of strengtheners) would limit forgeability of conventionally cast and wrought alloys but are easily overcome in powder metal products.

Defects and Problems in P/M Superalloy Products. Over the years of the development and application of nickel-base superalloy powder disks, defects have been a major concern. Several problems arise directly from powder techniques:

- Increased residual gas content
- Carbon contamination
- Ceramic inclusions
- Formation of PPB oxide and/or carbide films

The oxide inclusions from the ceramic nozzle or carbides from the alloy chemistry were (and are) sources of concern to designers. Furthermore, incomplete powder bonding and less than 100% densification must be avoided. P/M processing can result in porosity formed between prior particles. A very different origin of porosity is inert argon gas that can be trapped in hollow powder particles from atomization as well as trapped in the powder during compaction and consolidation. The gas entrapped in consolidation may come from the hollow argon-atomized powder particles, from container leakage, or from insufficient evacuation and purging of containers before consolidation.

A turbine disk is a heavy component rotating at high speeds, and the energy that can be released if one breaks is substantial. In an aircraft gas turbine, the damage from a broken airfoil may be economically great, but public safety is rarely at risk. However, if a disk fractures and separates from the engine, major structural damage occurs, and loss of the aircraft may follow. For larger disks found in land-based gas turbines, the damage to property could be even more extensive. Thus, it is axiomatic that disks must not break.

Any disk, whether from a cast ingot or one from powder, in origin, may have a ''defect'' from the designer's point of view. The aim of P/M not only is to make possible a component from a superalloy that cannot be produced (as a disk) by conventional deformation processing techniques, but also to ensure that the maximum potential defect size is acceptable to designers. Various defects have been evaluated, and solutions to their potential appearance or harm have been found. Table 7.6 lists types of defects and solutions to minimizing their occurrence. Although not specifically listed as a solution to a problem, it is important to stress again that smaller particle fractions of powders generally have smaller maximum metallic or ceramic (oxide, carbide) inclusion sizes. The downside of the smaller powder size, again, is increased cost.

Some claim is made that spray-formed powder preforms are less prone to gas entrapment, owing to the nature of the build-up process as opposed to the confinement and

Table 7.6 Minimizing common defects in P/M superalloys

Defect	Minimized by
Ceramic inclusions	• Screening • ''Rafting'' and removal of low-density ceramic defects during melting • Cyclone separation and other techniques that take advantage of density differences
Metallic inclusions	• Adequate cleaning of atomization facility at start-up and during changeover of alloy compositions
Voids and pores	• Removal of hollow powder particles • Hot or cold outgassing of powder during can filling • Leak testing of containers
Prior particle boundary contamination	• Ultralow-carbon compositions • Addition of strong carbide formers, e.g., Hf, Nb, and Ta • Modification of heating schedules before and during consolidation • Maximizing deformation of powder particles during consolidation • Postconsolidation working, e.g., isostatic forging

Compiled from information in *Superalloys, Supercomposites, and Superceramics,* J.K. Tien and T. Caulfield, Ed., Academic Press, New York, 1989

pressing arrangement characteristic of more conventional techniques. This may be true, but there are offsetting possibilities, including greater possibility of contamination from the atmosphere and less densification in spraying when no pressure is applied to cause sintering/bonding of the individual powder particles. One technique to reduce porosity in powder spraying has been to use nitrogen atomization. Preform porosity was reduced significantly by a switch from argon to nitrogen. Unfortunately, there also was an increase in the number of micrometer-sized carbonitride agglomerates from the process. It was suggested that the small size of the additional carbonitrides produced by nitrogen atomization did not have a significant effect on LCF. The use of nitrogen usually requires slight modifications in composition, such as lower carbon content, to accommodate the nitrogen increase associated with the atomization process.

Other Powder-Based Superalloy Components

General. As mentioned earlier, P/M has been applied to create dispersion-strengthened nickel-base alloys as sheet product and then as turbine airfoils. TD Nickel and its analogs, such as TD Nichrome and other variants, relied on a dispersion of oxides (sometimes carbides) in a suitable matrix. The matrix of these ODS superalloys usually was nickel or nickel-chromium, occasionally iron, and rarely cobalt. Although at first aimed commercially at sheet applications of non-γ'-hardened alloys, work was done as well (with powder techniques) on γ'-hardened nickel-base superalloys. The intent was to add dispersion-hardening capability to turbine blade/vane airfoil alloys as well as sheet alloys. The attempts to marry ODS and γ' hardening in the 1950s and 1960s were largely unsuccessful, but the ODS alloys, TD Nickel and TD Nichrome, did achieve some measure of commercial application.

In addition to the technical difficulties of producing a sufficiently fine oxide dispersion in superalloys, there was concern over the use of thoria (ThO_2) as the dispersant, because thoria is mildly radioactive. Thoria was replaced by yttria (Y_2O_3), and the application of oxide dispersions to superalloys was enhanced with the introduction of mechanical alloying (MA). Mechanical alloying now is the principal technique for introducing the requisite oxide/strain energy combination to achieve maximum properties in ODS superalloys, both in those with and without γ' hardening. Oxide-dispersion-strengthened alloys can benefit from aligned crystal growth in the same manner as can directionally cast alloys, and directional recrystallization has been used in ODS alloys to produce favorable polycrystalline grain orientations with elongated (high-aspect-ratio) grains parallel to the major loading axis.

Despite widespread acceptance of P/M superalloys in gas turbine disks, P/M techniques have not found much success in the production of standard γ'-hardened nickel-base superalloys for applications such as sheet or turbine airfoils. Oxide dispersion strengthening has some viability for such applications. Conventional P/M superalloys have found use in biomedical applications and in some small components used at high temperatures.

Mechanically Alloyed Superalloys. The MA process was developed to introduce a fine inert oxide dispersion into matrices that contain desirable alloying elements, such as nickel (matrix) and chromium for corrosion resistance. Mechanical alloying provides a means for producing P/M dispersion-strengthened alloys of varying compositions with unique sets of properties. Commercial alloy compositions, which are listed in Table 7.7, are based on either nickel-chromium or iron-chromium matrices. Some noncommercial ODS alloys used more conventional γ'-hardened superalloy bases. Among the more common ODS alloys are alloy MA-754, alloy MA-758, and alloy MA-956.

Table 7.7 Nominal composition of selected mechanically alloyed materials

Alloy designation	Ni	Fe	Cr	Al	Ti	W	Mo	Ta	Y_2O_3	C	B	Zr
MA-754	bal	...	20	0.3	0.5	...	...	...	0.6	0.05	...	...
MA-758	bal	...	30	0.3	0.5	...	...	...	0.6	0.05	...	...
MA-956	...	bal	20	4.5	0.5	...	...	...	0.5	0.05	...	...

Mechanical Alloying to Produce Powder. What sets MA apart from other P/M superalloy processes is the unique manner in which the particles are produced and the deformation that is imparted to the particles. The intent, generally, is to introduce a ceramic dispersoid (usually an oxide) into the superalloy matrix. Conventional powders are essentially solidified cast ingots on a microscale. It is difficult, if not impossible, to get a random dispersion of particles introduced into the melt to be carried over to the powder. Consequently, conventional P/M would require that superalloy powders be mixed with the dispersant and then consolidated. This procedure does not result in adequate random dispersions or sufficient strengthening.

The MA process induces deformation to get the intimate mixing and attachment of the constituents of the powder. Mechanical alloying is a deformation process and may be defined further as a method for producing composite metal powders with a controlled microstructure. The MA process involves repeated fracturing and rewelding of a mixture of powder particles in a ball mill charge. On a commercial scale, the process is carried out in horizontal ball mills. During each collision of the balls, many powder particles are trapped and plastically deformed. The process is illustrated schematically in Fig. 7.8.

The production of mechanically alloyed ODS alloys requires the development of a uniform distribution of submicron refractory oxide particles in a highly alloyed matrix. Elemental materials and master alloy plus dispersoid are part of the attritor charge. A typical powder mixture may consist of fine (4 to 7 μm) nickel powder, −150 μm chromium powder, and −150 μm master alloy (nickel-titanium-aluminum). The master alloy may contain a wide range of elements selected for their roles as alloying constituents or for gettering of contaminants. About 2 vol% of very fine yttria (250 Å or 25 nm) is added to form the dispersoid. The yttria becomes entrapped along the weld interfaces between fragments in the composite metal powders.

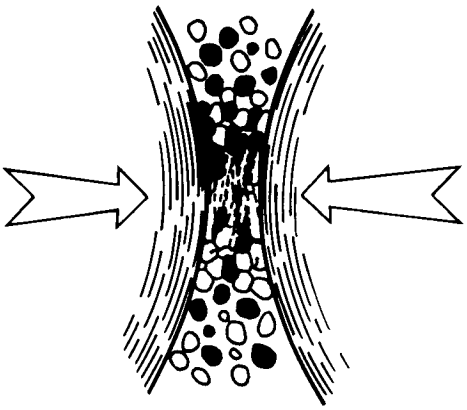


Fig. 7.8 Sketch showing formation of mechanically alloyed superalloy powder particles in a ball mill

Sufficient deformation occurs in each collision to rupture any absorbed surface-contaminant film and expose clean metal surfaces. Cold welds are formed where metal particles overlay, producing composite metal particles. At the same time, other powder particles are fractured. Figure 7.8 shows two metallic constituents, indicated by light and dark particles, although in a commercial alloy there may be several constituents (Fig. 7.9). As the process progresses, most of the particles become microcomposites, similar to the one produced in the collision illustrated in Fig. 7.8. The cold welding, which increases the size of the particles involved, and the fracturing of the particles, which reduces particle size, reach a steady-state balance, resulting in a relatively coarse and stable overall particle size. The internal structure of the particles, however, is continually refined by the repeated plastic deformation.

Consolidation to Produce MA Components. The production of powder containing a uniform dispersion of fine refractory oxide particles in a superalloy matrix is only the first step in achieving the full potential of ODS alloys. The powder must be consolidated and worked under conditions that develop coarse grains during a secondary recrystallization heat treatment. Consequently, MA powder is consolidated and then heat treated to optimize grain structure and properties. After MA, the powder generally is put into low-carbon steel tubes and extruded to full density. A schematic illustration of the complete MA powder production and consolidation process is given in Fig. 7.10. Extrusion temperature and reduction are critical, because the final microstructure of the product is affected by these quantities,

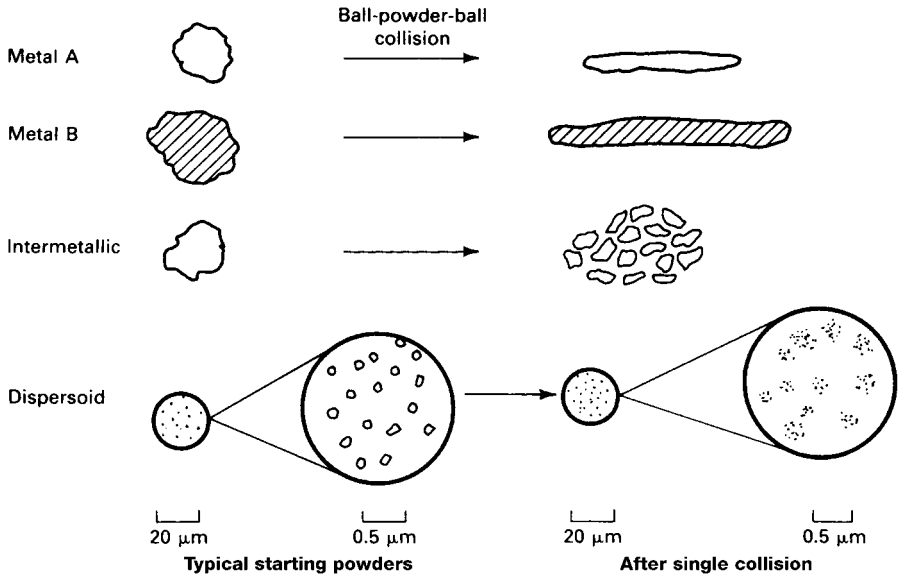


Fig. 7.9 Representative constitutents of starting powders used in mechanical alloying, showing deformation characteristics during attritor ball milling

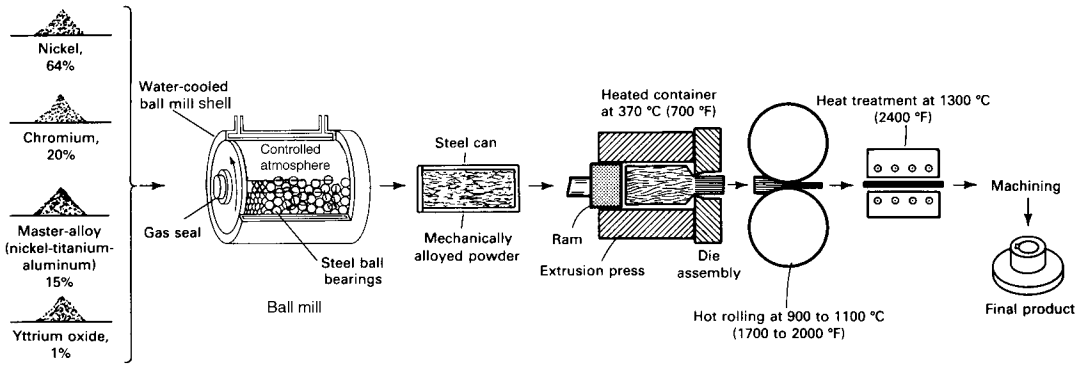


Fig. 7.10 Schematic of thermomechanical processing sequence in the production of consolidated mechanically alloyed superalloy components

and the ability to control this microstructure is important. For nickel-base alloys, reduction ratios of 13 to 1 and temperatures of 1950 to 2050 °F (1065 to 1120 °C) are typical.

The extruded stock, now fully consolidated, is then hot rolled into mill shapes. For rolling, as with extrusion, the thermomechanical treatment followed during deformation is critical to the final microstructure and properties of the product. For iron- and nickel-base superalloys, rolling temperatures are normally between 1750 and 1950 °F (950 and 1065 °C), with rolling resulting in highly directional working of the product. An alternate consolidation method is HIP followed by hot-working. Currently this process is in use for production of MA-754 plate.

MA-754 forged vanes (static airfoils) have been in commercial use for years, but for a material such as MA-754 to be used as an airfoil, the bar stock (or forging) is recrystallized at 2372 °F (1300 °C) to produce a crystallographically oriented microstructure. The large, elongated grain structure that results from this heat treatment maximizes longitudinal elevated-temperature properties, much as the elongated grain structure of columnar

grain directional solidification enhances the properties of cast superalloy airfoils. The resulting DR alloys have exceptional strength at very high temperatures.

Mechanically Alloyed Product Availability. Mechanically alloyed material is available as mill products or custom forgings. The mill product forms of mechanically alloyed ODS alloys vary (Table 7.8), depending on factors such as ease of fabrication and applicable forming methods. Common forms include bar, plate, and sheet.

All of the alloys are available as bars, and much of the data reported in the literature refer to bar properties. All of the bar products can be precision forged. Plate is readily amenable to a variety of hot forming operations, including hot shear spinning. Optimal formability and minimum flow stress are obtained when the plate is in the fine-grain (unrecrystallized) condition. The standard grain-coarsening anneal is then applied to the formed component. The only alloy currently available in sheet form is MA-956. MA-956 also has been produced in a number of other forms, including pipe, thin-wall tube, and fine wire, for special applications. MA-754 has been produced as hot rolled wire. In addition, although not a mill product per se, both seamless and flat butt-welded rings have been made from MA-754 and MA-758. MA-956, which is readily cold rolled to standard sheet tolerance, is commercially available in gages down to thicknesses of 0.010 in. (0.25 mm) and widths up to 24 in. (610 mm). A wide variety of components have been cold formed from MA-956 sheet by standard metal-forming operations. Experience has shown that warming to about 200 °F (95 °C) is necessary to prevent cracking, because this alloy undergoes a ductile-to-brittle transition in the vicinity of room temperature.

Alloy MA-754 was the first mechanically alloyed ODS superalloy to be produced on a large scale. This material is basically a Ni-2OCr alloy strengthened by about 1 vol% Y_2O_3 (see Table 7.7). It is comparable to thoria-dispersed TD NiCr (an earlier ODS alloy strengthened by thoria), but it has a nonradioactive dispersoid.

Alloy MA-758 is a higher-chromium version of MA-754. This alloy was developed for applications in which the higher chromium content is needed for greater oxidation resistance. The mechanical properties of this alloy are similar to those of MA-754, when identical product forms and grain structures are compared.

Alloy MA-956 is a ferritic iron-chromium-aluminum alloy, dispersion strengthened with yttrium aluminates formed by the addition of about 1 vol% Y_2O_3. Because of its generally good hot and cold fabricability, MA-956 has been produced in the widest range of product forms of any mechanically alloyed ODS alloy (see Table 7.8). In sheet form, this alloy is produced by a sequence of hot and cold working, which yields large pancake-shaped grains following heat treatment. This grain structure ensures excellent isotropic properties in the plane of the sheet.

Applications for MA Alloys. Mechanically alloyed ODS alloys were used first in aircraft gas turbine engines and later in industrial turbines. Components include vane airfoils and platforms, nozzles, and combustor/augmentor assemblies. As experience was gained with production, fabrication, and use of the alloys, this knowledge was applied to the manufacture of component parts in numerous indus-

Table 7.8 Available product forms for mechanically alloyed oxide-dispersion-strengthened alloys

Product form	Alloy MA-956	Alloy MA-754	Alloy MA-758
Hot finished rounds	X	X	X
Hot finished flats	X	X	X
Extruded rounds	X	X	X
Extruded section	X	X	...
Extruded tube	X	...	...
Hot rolled plate	X	X	X
Hot rolled sheet	X	...	...
Cold rolled sheet	X	...	...
Cold drawn round	X	...	...
Cold drawn tube	X	...	...
Hot rolled wire	X	...	...
Cold drawn wire	X	...	...

tries. These include diesel engine glow plugs, heat treatment fixtures (including shields, baskets, trays, mesh belts, and skid rails for steel plate and billet heating furnaces), burner hardware for coal- and oil-fired power stations, gas sampling tubes, thermocouple tubes, and a wide variety of components used in the production or handling of molten glass.

Because of its high long-time elevated-temperature strength, alloy MA-754 has been extensively used for aircraft gas turbine vanes and high-temperature test fixtures. Alloy MA-758 has found applications in the thermal processing industry and the glass processing industry. Alloy MA-956 is used in the heat treatment industry for furnace fixturing, racks, baskets, and burner nozzles. It also is used in advanced aerospace sheet and bar components, where good oxidation and sulfidation resistance are required in addition to high-temperature strength properties.

Biomedical Applications of P/M Superalloys. Aerospace components are not the only application for P/M superalloys. Because the cobalt-based alloys used in orthopedics are difficult to machine, near-net shape capability is desirable. Both casting and P/M processes have the ability to produce near-net shapes. However, the inherent ductility and toughness of wrought products (P/M or conventional forged) is to be preferred in the demanding environment of the human body.

Although many orthopedic implants are made by casting, P/M techniques are used to make some implants. Fully dense implants are made by HIP of prealloyed powders to provide materials with excellent mechanical properties. Figure 7.11 shows hip and knee joints, which constitute the most common total joint replacements. The major implants produced by HIP are total hip replacements made from a cobalt-chromium-molybdenum alloy that meets the composition requirements of ASTM F 799.

Requirements for powders used in implant production include compositional control, consistent tap densities (to ensure consistency of final part dimensions when working with fixed-mold cavity dimensions), and a high degree of powder cleanliness. The standards of aerospace P/M are applied to powders used in biomedical applications. Currently, all P/M-processed orthopedic implants have been made with powders produced by inert gas atomization.

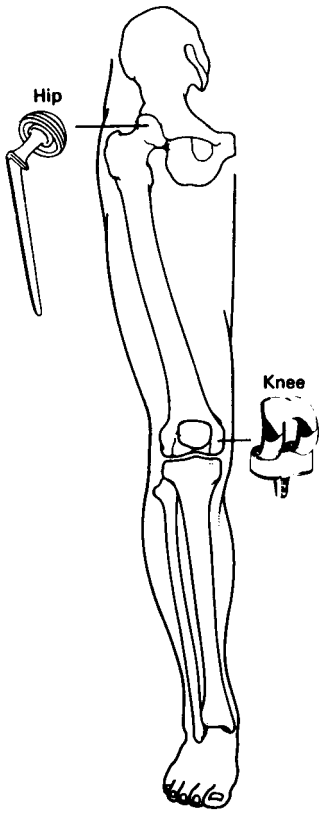


Fig. 7.11 Sketch showing location and shape of some conventional orthopedic implants made of P/M cobalt-base superalloys

Other P/M Applications. The shaft and disk of the back section of the compressor in F-404 turbofan engines were made of HIP Rene 95. Rene 95 P/M superalloy parts produced as near-net shapes by direct HIP were cost-effective due to improved material use and significant reduction in machining requirements.

Powder Metallurgy Cobalt-Base Superalloys. Cobalt-base superalloys produced by P/M processing are generally not used in heat-resistant applications. They are more commonly used in corrosion-resistant applications (e.g., Co-Cr-Mo alloys used for orthopedic implants, mentioned previously) and wear-resistant applications (e.g., cutting tools and hardfacing alloys), although cobalt hardfacing alloys also provide high-temperature corrosion resistance. The powder pro-

cessing of cobalt-base alloys is similar to that of nickel-base P/M alloys (i.e., spherical powders produced by gas atomization are consolidated by HIP).

A P/M turbine blade damper made of Stellite 31 is being used in the TF3O-P100 engine. Compacts were cold pressed in rigid tooling on a 10 ton (89 kN) hydraulic press and vacuum sintered to high density. A total of 68 of these 0.2 oz (6 g) parts are used in the first-stage rotor assembly of the jet engine. Powder processing proved to be more economical than precision casting, because minimal grinding was required to achieve the final dimensional tolerances. The near-net shape capability of P/M processing resulted in a significant cost advantage for this part.

Superalloys: A Technical Guide, Second Edition
Matthew J. Donachie, Stephen J. Donachie, p 135-147
DOI:10.1361/stgs2002p135
Copyright © 2002 ASM International®
All rights reserved.
www.asminternational.org

Chapter 8

Heat Treating

Introduction

Why Heat Treat? All superalloys, whether precipitation hardened or not, generally require the application of heat for some period of time for purposes of preparing solid material for a subsequent processing step (ingot cogging, component forging, etc.). In addition, some chemical processing, such as coating, requires that heat and resultant high temperatures be applied to cause the chemical changes to occur. In order to effect microstructural changes in alloys, heat invariably is required. Thus, heat treatment is the logical consequence of the processing requirements for superalloys as well as the logical precursor for the generation of optimal properties for many superalloy applications.

What Is Heat Treatment? Strictly speaking, heat treatment is any application, for any amount of time, of a temperature sufficiently high as to accomplish one of the following:

- Reduce stresses
- Allow atom movements to redistribute existing alloy elements
- Promote grain growth
- Promote new recrystallized grain formation
- Dissolve phases
- Produce new phases, owing to precipitation from solid solution
- Cause alloy surface chemistry to change by introduction of foreign atoms
- Cause new phases to form by introduction of foreign atoms

Some Common Heat Treatments for Superalloys. Heat treatments are routinely given to superalloys to develop properties or complete a chemical process treatment. The most common heat treatments are:

- Stress relieving
- In-process annealing
- Full annealing
- Solution annealing
- Coating diffusion
- Precipitation (age) hardening

Some Nonobvious Heat Treatments. It might seem fairly obvious, by the definition of heat treatment, that superalloys regularly undergo many other heat treatment steps during processing. Surprisingly, some superalloy users do not note the obvious and assume that the only heat treatments are those common ones listed previously. In other words, if a temperature cycle is not called for in an alloy specification, then it is not a heat treatment. A few examples of treatments that are often overlooked by people charged with the application of superalloys (mostly precipitation-hardened iron-nickel- and nickel-base superalloys) are:

- Applying a thermal shock test to an airfoil
- Heating an alloy during pack coating
- Welding an alloy
- Brazing an alloy
- Reheating an alloy for rewelding for the second or third time
- Reheating a brazed component to rebraze
- Process reheating without full anneal during hot working
- Cooling to room temperature from an in-process anneal without deformation of the component

Illustration. The reason for mentioning the preceding overlooked treatments is that the property data for design are usually generated on superalloys to which only the heat treatments that follow the stated alloy specification heat treat requirements have been applied.

Example: Cast Nickel-Base Superalloy. A hypothetical cast nickel-base superalloy or alloy-component combination might have specifications that call for:

- Solution heat treat at 2250 °F (1232 °C) for 1 h, air cool or faster
- Heat at 1975 °F (1080 °C) for 2 h, air cool or faster
- Heat at 1600 °F (871 °C) for 12 h, cool to room temperature

The preceding heat treatment is, therefore, what might be applied (by a person who receives an unprocessed metal casting) to material to be tested for generation of property data. (The subject of casting source, size, and so on is another issue and is covered in Chapter 12.) However, a knowledgeable observer might have followed the manufacturing process of the actual part from raw casting to finished part and observed the following heat treat steps:

- Ramp up in stages of temperature to 2250 °F (1232 °C)
- Solution heat treat at 2250 °F (1232 °C), air cool or faster
- Heat at 1550 °F (843 °C) for 12 h in pack-coating container, cool slowly
- Heat at 1975 °F (1080 °C) for 2 h, air cool or faster
- Heat at 1600 °F (871 °C) for 12 h, cool to room temperature

The above is a simple example, and time-temperature combinations are not meant to directly correspond to any particular cast nickel-base superalloy. However, the picture is clear. Ramping up in stages may add some significant high-temperature exposure to the superalloy component. Heating at 1550 °F (843 °C) for 12 h is an additional heat treatment, by the definition at the start of this Chapter. Tests on material that does not fully represent the actual heat treat conditions for application run the risk of leaving open the possibility of some unwelcome surprises arising in alloy service at a later date.

If a precipitation-hardened superalloy component is heated to a high temperature, particularly above about 1000 °F (540 °C), then it is being heat treated. Even solution-hardened alloys or carbide-strengthened alloys such as the cobalt-base superalloys can be heat treated by exposure above 1000 °F (540 °C). Because stress relief heat treatments often take place at temperatures considerably over 1000 °F (540 °C), even the role of stress relief on materials properties always should be considered in the development of property data on superalloys. Similarly, other heat treatment steps should be evaluated for influence on component design and subsequent service.

The structure and properties achieved by a specific heat treatment are affected by the section size of the part being heat treated. Thus, most heat treaters have adopted conventions for defining the amount of time that a part will be in a furnace prior to ''beginning'' the required heat treatment (e.g., 15 min exposure prior to considering the part as being ''at temperature''). As *the total thermal* cycle experienced by the part determines the microstructure and properties, the applicability of a selected convention to a given alloy and section thickness should be demonstrated.

Example: Heat Treating IN-718. An IN-718 part was required to be solution treated near the delta solvus but still in the delta precipitation region (2 h at 1750 °F), air cooled and then reheated another 2 h at 1750 °F and again air cooled. In an effort ''to be sure to conform to the specification'' (the 2 h requirement) the heat treater held the part in the furnace for 2 h prior to beginning the count for the required 2 h at temperature (a total time of 4 h in the furnace for each heat treatment, that is, the part had a total of 8 h exposure in a 1750 °F furnace). The result was that massive acicular delta formed in the high Nb rings typical of IN-718 (Fig. 4.19 and 4.26) and the batch of parts was rejected for excessive delta. Although the heat treatment ''conformed,'' the total cycle was unsuitable for the material.

If there is an interest in fully defining an alloy for a particular application, at least consider the possibility that nonobvious heat treatments may be affecting properties. A decision may be made to evaluate only the basic alloy specification heat treatments anyway, but do so after rationalizing the question of whether or not there may be surprises later.

Table 8.1 Typical stress relieving and annealing cycles for wrought heat-resisting alloys

Alloy	Stress relieving			Annealing(a)		
	Temperature		Holding time per inch of section, h	Temperature		Holding time per inch of section, h
	°C	°F		°C	°F	
Iron-base and iron-nickel-chromium alloys						
19-9 DL	675(b)	1250(b)	4	980	1800	1
A-286	(c)	(c)	. . .	980	1800	1
Discaloy	(c)	(c)	. . .	1035	1900	1
Nickel-base alloys						
Astroloy	(c)	(c)	. . .	1135	2075	4
Hastelloy X	(c)	(c)	. . .	1175	2150	1
Incoloy 800	870	1600	1½	980	1800	¼
Incoloy 800H	. . .	. . .	. . .	1175	2150	. . .
Incoloy 825	. . .	. . .	. . .	980	1800	. . .
Incoloy 901	(c)	(c)	. . .	1095	2000	2
Inconel 600	900	1650	1	1010	1850	¼(d)
Inconel 601	. . .	. . .	. . .	980	1800	. . .
Inconel 625	870	1600	1	980	1800	1
Inconel 690	. . .	. . .	. . .	1040	1900	½
Inconel 718	(c)	(c)	. . .	955	1750	1
Inconel X-750	880(e)	1625(e)	. . .	1035	1900	½
Nimonic 80A	(c)	(c)	. . .	1080	1975	2
Nimonic 90	(c)	(c)	. . .	1080	1975	2
Rene 41	(c)	(c)	. . .	1080	1975	2
Udimet 500	(c)	(c)	. . .	1080	1975	4
Udimet 700	(c)	(c)	. . .	1135	2075	4
Waspaloy	(c)	(c)	. . .	1010	1850	4
Cobalt-chromium-nickel-base alloys						
L-605 (HS-25)	(f)	(f)	. . .	1230	2250	1
N-155 (HS-95)	(f)	(f)	. . .	1230	2150	. . .
S-816	(f)	(f)	. . .	1205	2200	1

(a) Minimum hardness is achieved by cooling rapidly from the annealing temperature, to prevent precipitation of hardening phases. Water quenching is preferred, and is usually necessary for heavy sections; air cooling is preferred for heavy sections of Waspaloy, Udimet 500, Udimet 700, and Inconel X-750, because water quenching causes cracking. However, for complex shapes subject to excessive distortion, oil quenching is often adequate and more practical. Rapid air cooling usually is adequate for parts formed from strip or sheet. Rapid cooling from the annealing or solution treating temperature does not suppress the aging reaction of some alloys, such as Astroloy; these alloys become harder and stronger. (b) Nominal temperature; 650 to 705 °C (1200 to 1300 °F) is permissable. (c) Full annealing is recommended, because intermediate temperatures cause aging. (d) Short time is required for prevention of grain coarsening. (e) Used only for stress equalizing of warm worked grades. (f) Full annealing is recommended if further fabrication is performed; otherwise, material can be stress relieved at approximately 55 °C (100 °F) below annealing temperature.

Heat Treatment Types

Stress Relieving. Stress relieving of superalloys frequently entails a compromise: the desirability of maximum relief of residual stress must be weighed against possible effects deleterious to high-temperature properties and corrosion resistance. Wrought alloys may be age hardenable or solution or carbide strengthened. True stress relieving of wrought material usually is confined to alloys that are not age hardenable. Wrought alloys are often more apt to be stress relieved than are cast alloys, because there are fewer cast alloys either solution or carbide strengthened. Most use of castings in current practice is for nickel-base superalloys which are age hardenable and cannot be given high-temperature exposures without changing alloy properties.

The time and temperature cycles for stress relief may vary considerably, depending on the metallurgical characteristics of the alloy and on the type and magnitude of residual stresses developed by previous fabricating processes. Stress-relieving temperatures are usually below the annealing or recrystallization temperatures. Typical cycles for some wrought superalloys are listed in Table 8.1; temperatures at least 45 °F (25 °C) higher or lower than those listed are usually satisfactory.

Some superalloy castings are placed in service in the as-cast condition. However, some castings may be stress relieved:

- When they are not precipitation (age) hardened
- When they are of an extremely complex shape that might crack during the initial heating-up period in service
- When their dimensional tolerances are stringent
- After they have been welded

It is important to note that stress-relief heat treatments are not normal practice with cast nickel-base superalloys.

It is not possible to tabulate the stress-relief cycles for cast alloys, because they are particularly dependent on chemistry, geometry, and prior processing. For many alloys, stress-relief cycles can be developed by empirical studies of stress decay with time and temperature, as determined by nondestructive means such as x-ray diffraction. This is not an effective technique for superalloys, where extensive material testing of critical properties and subsequent data analysis must be performed to determine the efficacy of a given cycle. Particular care must be given to evaluate the effects of stress relief on such time-dependent effects as low-cycle fatigue, crack growth, and creep rupture.

In-process annealing or stress relief of weldments should immediately follow welding of precipitation-hardenable alloys where highly restrained joints are involved. If the configuration of the weldment does not permit high-temperature annealing, aging can be used for stress relieving the joints.

Full Annealing. When applied to superalloys, annealing implies full annealing, that is, complete recrystallization and the attainment of maximum softness. The practice is really only applicable to wrought alloys of the nonhardening type. For a majority of the hardenable alloys, annealing cycles are the same as those used for solution treating. However, the two treatments serve different purposes.

Solution treating has the intent to dissolve second phases for subsequent reprecipitation. Annealing is used mainly to increase ductility (and reduce hardness) to facilitate forming or machining, prepare for welding, relieve stresses after welding, produce specific microstructures, or soften age-hardened structures by re-solution of second phases. Annealing may be used to homogenize a cast ingot.

Annealing practices vary considerably among different organizations. Representative annealing temperatures, holding times, and cooling procedures for wrought superalloys are given in Table 8.1. Experience with specific parts for known requirements often indicates advantageous modifications of temperature, time, or cooling method.

In-Process Annealing. Most wrought superalloys can be cold formed but are more difficult to form than austenitic stainless steels. Severe cold forming may require several intermediate (in-process) annealing operations. Full annealing must be followed by fast cooling. Even during hot work to break down an ingot to a more desirable size and macro/microstructure, superalloys begin to store energy and need to be reheated for subsequent deformation processes. The same requirement for hot-working operations applies when final mill products are made. Similarly, when forged articles are being produced in a multistep sequence, in-process anneals are required. An exception is the isothermal/superplastic deformation (forging) of superalloys that is done for some applications. When heat is supplied to maintain constant temperature in such isothermal processes, no in-process anneals are used.

Reheating for hot working thus is an in-process annealing practice whose aim is to promote adequate formability of the metal being deformed. Temperatures vary widely, depending on alloy and working practice. Control of temperature can be critical to resultant properties, because varying degrees of recrystallization may be desired. In most standard operations, heating or reheating for hot working is a full annealing step, with recrystallization and dissolution of all or most secondary phases. Occasionally, when final application products are being shaped (e.g., forging of a gas turbine disk), reheating for hot working is restricted to temperatures that do not dissolve all secondary phases, so that the remaining phases can be used to limit grain growth.

Cold working is usually performed on alloys in the solution-treated condition rather than the worked condition or precipitation-hardened condition. The cold-working procedure is carried out in this manner because of the markedly lower strength and increased ductility of the material (see Fig. 8.1). In addition to effects on strength and ductility, the cold-working process can affect mechanical

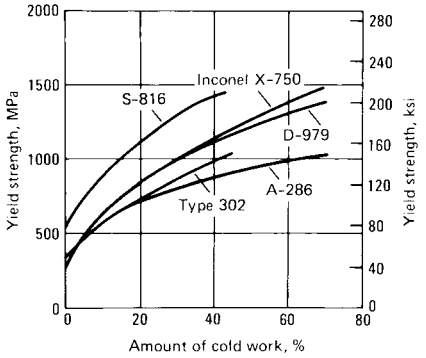


Fig. 8.1 Effect of cold work on room-temperature yield strength of some superalloys and a stainless steel

properties through its influence on grain growth during subsequent in-process or solution heat treatments and the reaction kinetics of aging.

Solution Annealing. Solution treating is intended to dissolve second phases to produce maximum corrosion resistance or to prepare an alloy for subsequent aging. Additionally, it will homogenize microstructure prior to aging and/or fully recrystallize a wrought structure for maximum ductility. Actual production solution treating may not fully dissolve all second phases in precipitation-hardened alloys. Typical solution treating cycles are given in Tables 8.2 and 8.3.

Precipitation treatments are intended to bring out desirable strengthening precipitates and control other secondary phases, including carbides and detrimental topologically close-packed (tcp) phases. Precipitation treatments also can serve to stress relieve articles. Typical precipitation (aging) cycles are given in Tables 8.2 and 8.3.

Heat Treatment Procedures

Quenching. The purpose of quenching heat-resisting alloys is to maintain, at room temperature, the supersaturated solid solution obtained during solution treating of precipitation-hardening alloys. Quenching permits a finer γ' particle size to be achieved upon subsequent aging. Cooling methods commonly used include oil and water quenching as well as various forms of air or inert gas cooling. Some common cooling methods are indicated in Table 8.2 for wrought alloys and in Table 8.3 for casting alloys. The essence of quenching is to retain hardening elements (aluminum, titanium, and niobium) in solution as much as possible to permit the development of an optimal γ' or γ'' plus γ' distribution during one or more precipitation heat treatments. Solid-solution and carbide-hardened alloys are not quenched. Internal stresses resulting from quenching can accelerate overaging in some age-hardenable alloys.

Solution or Full Annealing Processes. The purpose of these treatments is to do one of the following:

- Fully recrystallize an alloy
- Homogenize an alloy
- Dissolve all or nearly all phases in the face-centered cubic matrix structure

The first step in heat treating precipitation-hardened superalloys is usually solution treatment. In some wrought alloys, the solution treating temperature will depend on the properties desired. A higher temperature is specified for optimal creep-rupture properties; a lower temperature is used for optimal short-time tensile properties at elevated temperature, improved fatigue resistance (via finer grain size), or improved resistance to notch rupture sensitivity. The higher solution treating temperature will result in some grain growth (in wrought alloys) and more extensive dissolution of carbides.

Obviously, high temperatures are needed for full annealing or solution treating. In some instances, these temperatures may range from about 1800 up to 2250 °F (982 to 1232 °C) or even to 2400 °F (1316 °C) for single-crystal superalloys. Temperatures above 2200 °F (1204 °C) become increasingly more difficult to attain in a cost-effective manner. Also, when heating at the highest temperatures (and sometimes at the lower annealing temperatures), care must be taken to avoid melting (incipient melting) caused by equilibrium and nonequilibrium alloy element segregation during prior solidification. This is a problem with large castings and cast shapes, such as turbine airfoils. Residual segregation is not as severe a problem with wrought alloys, which have been homogenized by deformation and application of heat.

Precipitation (Aging) Processes. Precipitation treatments strengthen age-hardenable alloys by causing the precipitation of one or more phases (γ' and γ'') from the supersaturated matrix that is developed by solution

Table 8.2 Typical solution treating and aging cycles for wrought heat-resisting alloys

	Solution treating				Aging			
	Temperature				Temperature			
Alloy	°C	°F	Time, h	Cooling procedure	°C	°F	Time, h	Cooling procedure
Iron-base alloys								
A-286	980	1800	1	Oil quench	720	1325	16	Air cool
Discaloy	1010	1850	2	Oil quench	730	1350	20	Air cool
					650	1200	20	Air cool
N-155	1175	2150	1	Water quench	815	1500	4	Air cool
Nickel-base alloys								
Astroloy	1175	2150	4	Air cool	845	1550	24	Air cool
	1080	1975	4	Air cool	760	1400	16	Air cool
Hastelloy S	1065	1950	½	Rapid quench	...	...	...	...
Hastelloy X	1175	2150	1	(a)	...	...	...	...
Inconel 901	1095	2000	2	Water quench	790	1450	2	Air cool
					720	1325	24	Air cool
Inconel 600	1120	2050	2	Air cool	...	...	...	...
Inconel 601	1150	2100	1	Air cool	...	...	...	...
Inconel 617	1175	2150	2	(a)	...	...	...	...
Inconel 625	1150	2100	2	(a)	...	...	...	...
Inconel 706	925–1010	1700–1850	...	...	845	1550	3	Air cool
					720	1325	8	Furnace cool
					620	1150	8	Air cool
	925–1010	1700–1850	...	...	730	1350	8	Furnace cool
					620	1150	8	Air cool
Inconel 718	980	1800	1	Air cool	720	1325	8	Furnace cool
					620	1150	8	Air cool
Inconel X-750 (AMS 5667)	855	1625	24	Air cool	705	1300	20	Air cool
Inconel X-750 (AMS 5668)	1150	2100	2	Air cool	845	1550	24	Air cool
					705	1300	20	Air cool
Nimonic 80A	1080	1975	8	Air cool	705	1300	16	Air cool
Nimonic 90	1080	1975	8	Air cool	705	1300	16	Air cool
Rene 41	1065	1950	½	Air cool	760	1400	16	Air cool
Udimet 500	1080	1975	4	Air cool	845	1550	24	Air cool
					760	1400	16	Air cool
Udimet 700	1175	2150	4	Air cool	845	1550	24	Air cool
	1080	1975	4	Air cool	760	1400	16	Air cool
Waspaloy	1080	1975	4	Air cool	845	1550	24	Air cool
					760	1400	16	Air cool
Cobalt-base alloys								
Haynes 25; L-605	1230	2250	1	Rapid air cool	(b)	(b)	...	...
Haynes 188	1175	2150	½	Rapid air cool	...	...	...	...
Haynes 556	1175	2150	½	Rapid air cool	...	...	...	...
S-816	1175	2150	1	(a)	760	1400	12	Air cool

Note: Alternate treatments may be used to improve specific properties. (a) To provide an adequate quench after solution treating, it is necessary to cool below about 540 °C (1000 °F) rapidly enough to prevent precipitation in the intermediate temperature range. For sheet metal parts of most alloys, rapid air cooling will suffice. Oil or water quenching is frequently required for heavier sections that are not subject to cracking. (b) Aging occurs in service at elevated temperatures.

treating and retained by rapid cooling from the solution treating temperature. The precipitation temperatures determine not only the type but also the size distribution of precipitate. Precipitation heat treatments are invariably at a constant temperature, which may range from as low as 1150 °F (621 °C) to as high as 1900 °F (1038 °C). Multiple precipitation treatments are common in wrought alloys but uncommon in cast alloys.

Factors that influence the selection or number of aging steps and precipitation time and temperature include:

- Type and number of precipitating phases available
- Anticipated service temperature
- Desired precipitate size
- The combination of strength and ductility desired
- Heat treatment of similar alloys

The size distribution and, perhaps, the type of precipitate are affected by aging temperature. When more than one phase is capable of precipitating from the alloy matrix, judicious selection of a single aging temperature

Table 8.3 Typical solution treating and aging cycles for some cast precipitation-hardened nickel-base superalloys

Alloy	Heat treatment (temperature/duration in h/cooling)
Polycrystalline (conventional) castings	
B-1900/B-1900 + Hf	1080 °C (1975 °F)/4/AC + 900 °C (1650 °F)/10/AC
IN-100	1080 °C (1975 °F)/4/AC + 870 °C (1600 °F)/12/AC
IN-713	As-cast
IN-718	1095 °C (2000 °F)/1/AC + 955 °C (1750 °F)/1/AC + 720 °C (1325 °F)/8/FC + 620 °C (1150 °F)/8/AC
IN-718 with hot isostatic pressing (HIP)	1150 °C (2100 °F)/4/FC + 1190 °C (2175 °F)/4/15 ksi (HIP) + 870 °C (1600 °F)/10/AC + 955 °C (1750 °F)/1/AC + 730 °C (1350 °F)/8/FC + 665 °C (1225 °F)/8/AC
IN-738	1120 °C (2050 °F)/2/AC + 845 °C (1550 °F)/24/AC
IN-792	1120 °C (2050 °F)/4/RAC + 1080 °C (1975 °F)/4/AC + 845 °C (1550 °F)/24/AC
IN-939	1160 °C (2120 °F)/4/RAC + 1000 °C (1830 °F)/6/RAC + 900 °C (1650 °F)/24/AC + 700 °C (1290 °F)/16/AC
MAR-M-246 + Hf	1220 °C (2230 °F)/2/AC + 870 °C (1600 °F)/24/AC
MAR-M-247	1080 °C (1975 °F)/4/AC + 870 °C (1600 °F)/20/AC
Rene 41	1065 °C (1950 °F)/3/AC + 1120 °C (2050 °F)/0.5/AC + 900 °C (1650 °F)/4/AC
Rene 77	1163 °C (2125 °F)/4/AC + 1080 °C (1975 °F)/4/AC + 925 °C (1700 °F)/24/AC + 760 °C (1400 °F)/16/AC
Rene 80	1220 °C (2225 °F)/2/GFQ + 1095 °C (2000 °F)/4/GFQ + 1050 °C (1925 °F)/4/AC + 845 °C (1550 °F)/16/AC
Udimet 500	1150 °C (2100 °F)/4/AC + 1080 °C (1975 °F)/4/AC + 760 °C (1400 °F)/16/AC
Udimet 700	1175 °C (2150 °F)/4/AC + 1080 °C (1975 °F)/4/AC + 845 °C (1550 °F)/24/AC + 760 °C (1400 °F)/16/AC
Waspaloy	1080 °C (1975 °F)/4/AC + 845 °C (1550 °F)/4/AC + 760 °C (1400 °F)/16/AC
Directionally-solidified (DS) castings	
DS MAR-M-247	1230 °C (2250 °F)/2/GFQ + 980 °C (1800 °F)/5/AC + 870 °C (1600 °F)/20/AC
DS MAR-M-200 + Hf	1230 °C (2250 °F)/4/GFQ + 1080 °C (1975 °F)/4/AC + 870 °C (1600 °F)/32/AC
DS Rene 80H	1190 °C (2175 °F)/2/GFQ + 1080 °C (1975 °F)/4/AC + 870 °C (1600 °F)/16/AC
Single-crystal castings	
CMSX-2	1315 °C (2400 °F)/3/GFQ + 980 °C (1800 °F)/5/AC + 870 °C (1600 °F)/20/AC
PWA 1480	1290 °C (2350 °F)/4/GFQ + 1080 °C (1975 °F)/4/AC + 870 °C (1600 °F)/32/AC
Rene N4	1270 °C (2320 °F)/2/GFQ + 1080 °C (1975 °F)/4/AC + 900 °C (1650 °F)/16/AC

AC, air cooling; FC, furnace cooling; GFQ, gas furnace quench; RAC, rapid air cooling

may result in obtaining optimal amounts of multiple precipitating phases. Alternatively, a double-aging treatment that produces different sizes and types of precipitate at different temperatures may be employed. Double-aging or even quadruple-aging treatments have been used. Aging treatments usually are sequentially lower, for example, for a wrought nickel-base superalloy such as Waspaloy, an intermediate age at 1550 °F (843 °C) followed by a lower temperature age at 1400 °F (760 °C) would be the rule.

So-called primary strengthening precipitates (γ' and γ'', sometimes η) are not the only phases precipitating during aging heat treatments. Carbides and, under unfavorable conditions, tcp phases such as σ also can form during aging. A principal reason for two-step aging sequences, in addition to γ' or γ'' control, is the need to precipitate or control grain-boundary carbide morphology. For all γ' dispersions, particularly in wrought alloys, care must be taken to ensure the correct carbide distribution.

In some instances, especially where more than two aging temperatures are used, so-called yo-yo heat treatments have been employed. A yo-yo aging process involves first a lower-temperature exposure followed by a slightly higher-temperature exposure. A pro-

cess for a wrought alloy might involve, for instance, 1600 °F (871 °C) followed by 1800 °F (982 °C), then 1200 °F (649 °C) followed by 1400 °F (760 °C). Note that these are not specific temperatures for any particular alloy but are intended to show the type of complex precipitation treatments that have evolved for certain alloys.

Example of Double-Aging Sequence. U-500 is double aged for stabilization of grain-boundary carbides. U-500 is typical of wrought precipitation-hardened superalloys that contain MC and $M_{23}C_6$ carbides and are strengthened by γ'. For a good balance of tensile strength and stress-rupture life, the alloy is:

- Solution heat treated at 1800 °F (982 °C) for 4 h (air cooled)
- Stabilized at 1550 °F (843 °C) for 24 h (air cooled)
- Aged at 1400 °F (760 °C) for 16 h (air cooled)

The solution exposure dissolves all phases except MC carbides, and γ' precipitates nucleate during cooling from the solution temperature. The stabilization at 1550 °F (843 °C) precipitates discrete $M_{23}C_6$ at grain boundaries as well as more γ'. Final aging increases the volume fraction, and possibly the number, of γ' precipitates. The grain-boundary $M_{23}C_6$ increases stress-rupture life, as long as it is not a continuous carbide film, which would markedly decrease rupture ductility.

Surface Attack and Contamination

Introduction. Although superalloys offer resistance to surface degradation during elevated-temperature service, heat treatment temperatures (particularly solution treatment) can degrade surface characteristics. The potential forms of surface degradation include oxidation, carbon pickup, alloy depletion, and contamination.

Precipitation-hardenable superalloys usually have good oxidation resistance in oxidizing atmospheres within their normal range of service temperatures. These temperatures may be at or above their aging temperatures, which are in the range of about 1400 to 1800 °F (760 to 982 °C), depending on the alloy. Some superalloys may require coatings in service owing to reduced levels of chromium and more aggressive environments than earlier superalloys faced. This is particularly true for gas turbine airfoil alloys.

Alloy Depletion. In addition to oxidation, exposure to high-temperature environments can cause changes in the composition of the alloy near the surface. Because certain elements are preferentially consumed by the scale layer, the bulk composition can become depleted. For example, boron oxidation leads to deboronization of wrought alloys. Some alloys can be very susceptible to deboronization. This process can affect the properties of the surface layers and can be of considerable concern, for instance, in sheet products.

Intergranular Attack. At temperatures used for solution treating, many superalloys are susceptible to selective surface attack. A common form is intergranular oxidation. Intergranular oxidation is measured optically as depth of intergranular penetration. Figure 8.2 shows the depth of intergranular oxidation that occurred in Rene 41 heated in air. Sometimes, surface attack can be of a carbide, such as shown in Fig. 8.3. The result is the same: a notch (either in the grain boundary or in a grain) is created, and the potential for component failure is increased. Generally, finish surfaces are not exposed to air during heat treatment, and oxidation occurs only in service operation. In service, coatings are frequently applied to protect the surface, dependent on temperature and gaseous environment.

The principal mode of intergranular attack involves not only the preferential oxidation

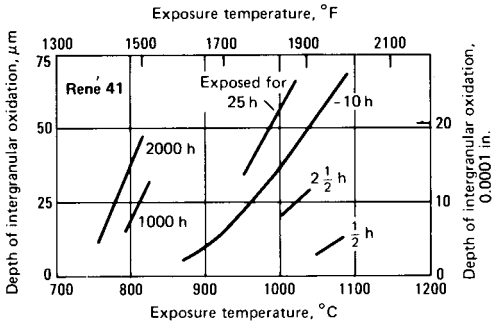


Fig. 8.2 Effect of time and temperature on oxidation of Rene 41 precipitation-hardened nickel-base alloy

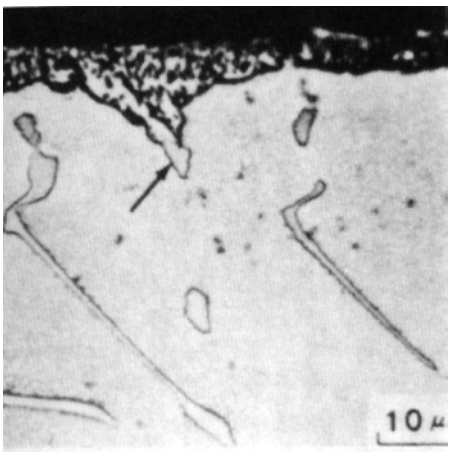


Fig. 8.3 Oxidized carbide in precipitation-hardened nickel-base alloy

of chromium but also the attack of aluminum and titanium, the constituents of γ' and η hardening phases. Attack of the minor elements zirconium and boron also takes place, along the grain boundaries. In relation to intergranular oxidation, aluminum is preferable to titanium as a hardening element, because aluminum oxide provides a denser and less permeable barrier to the diffusion of oxygen. Molybdenum increases susceptibility to intergranular attack in age-hardenable alloys.

Surface Contamination. Carbon pickup can occur if the solution treating atmosphere has a carburizing potential. For instance, the carbon content of the surface of A-286 alloy has been observed to increase from 0.05 to 0.30%. The added carbon forms a stable carbide (TiC), thus removing titanium from solid solution and preventing normal precipitation hardening in the surface layers. TiN can be formed in the same manner, as a result of nitrogen contamination. The pickup of nitrogen after annealing in that gas is shown in Fig. 8.4.

Miscellaneous Contaminants. All exposed surfaces of heat-resisting alloy parts should be kept free of dirt, fingerprints, oil, grease, forming compounds, lubricants, and scale. Lubricants or fuel oils that contain sulfur-bearing compounds are particularly active in corroding the metal surface of superalloys containing nickel and chromium. Attack occurs by first forming Cr_2S_3 and then, as the attack progresses, also forming a Ni-Ni_3S_2 eutectic, particularly at low pressures of less than 10^{-4} torr in vacuum. The Ni-Ni_3S_2 eutectic melts at 1190 °F (645 °C).

Scale and slag from furnace hearths are another source of contamination. Contact with steel scale, slag, and furnace spallings should be avoided; low-melting constituents can form on the metal surface and promote corrosion.

Protective Atmospheres

Introduction. Protective atmospheres are used in annealing or solution treating if heavy oxidation cannot be tolerated.

Solution Treatment or Annealing Atmospheres. If oxidation can be tolerated in wrought alloys (because of subsequent stock removal) or oxidation is negligible for the temperature-time conditions involved (particularly in some cast alloys or wrought sheet alloys used for combustion application), superalloys can be annealed or solution treated in air or in some of the normal mixtures of air and combustion products found in gas-fired furnaces. Such atmospheres include:

- Exothermic
- Endothermic
- Dry hydrogen
- Dry argon
- Vacuum

Exothermic Atmosphere. A lean and dilute exothermic atmosphere is relatively safe and economical. The surface scale formed in such

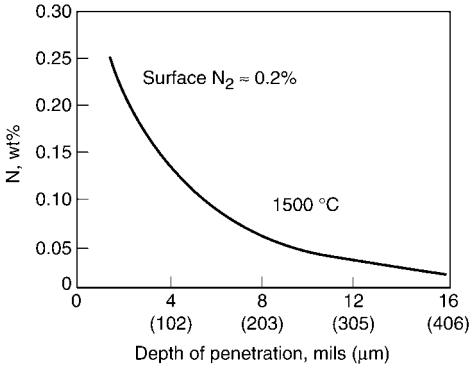


Fig. 8.4 Nitrogen content vs. depth for Inconel nickel-base superalloy heated at 816 °C (1500 °F) in nitrogen

an atmosphere can be removed by pickling or by salt bath descaling and pickling. Such an atmosphere, formed by burning fuel gas with air, contains about 85% N, 10% CO_2, 1.5% CO, 1.5% H_2, and 2% water vapor. This atmosphere will produce a scale rich in chromium oxides.

Endothermic Atmospheres. Endothermic atmospheres prepared by reacting fuel gas with air in the presence of a catalyst are not recommended because of their carburizing potential. Similarly, the endothermic mixture of nitrogen and hydrogen formed by dissociating ammonia is not used because of the probability of nitriding. Under appropriate conditions, nitrogen can be formed for significant depths below the surface of a superalloy (note Fig. 8.4).

Dry Hydrogen. Dry hydrogen of dew point −60 °F (−50 °C) or lower, is used in preference to dissociated ammonia for bright annealing of superalloys. If the hydrogen is prepared by catalytic gas reactions instead of by electrolysis, residual hydrocarbons, such as methane, should be limited to about 50 ppm to prevent carburizing. Hydrogen is not recommended for bright annealing of alloys containing significant amounts of elements (such as aluminum or titanium) that form stable oxides not reducible at normal heat treating temperatures and dew points. Hydrogen is not recommended for annealing or solution treating alloys that contain boron, because of the danger of deboronization through formation of boron hydrides.

Dry Argon. Dry argon of dew point −60 °F (−50 °C) or lower, should be used if no oxidation can be tolerated. It is mandatory that this type of atmosphere be used in a sealed retort or sealed furnace chamber. If the argon has a slightly higher dew point, but not over −40 °F (−40 °C), oxidation will be limited to a thin surface film that can usually be tolerated. A purge of at least ten times the volume of the retort is recommended before the retort is placed in the furnace. To prevent the formation of an oxide film, the argon must be kept flowing continually during and after the treatment, until the workpieces have cooled nearly to room temperature.

Superalloys containing stable-oxide formers such as aluminum and titanium, with or without boron, must be bright annealed in a vacuum or in a chemically inert gas such as argon, as described previously.

Vacuum Atmosphere. Vacuum atmosphere, generally below 2×10^{-3} torr (20 μm), is commonly used for superalloys above 1500 °F (815 °C). It is particularly desirable when parts are at or close to final dimensions. Precipitation-hardenable alloys containing stable oxide formers such as aluminum and titanium must be bright annealed in vacuum or inert gas.

Atmospheres for Precipitation Treatment. Air is the most common aging atmosphere. The smooth, tight oxide layer that is formed is usually unobjectionable on the finished product. However, if this oxide layer must be minimized, a lean exothermic gas (air-gas ratio about 10 to 1) can be employed. It will not entirely prevent oxidation, but the oxide layer will be very light. The use of gases containing hydrogen and carbon monoxide for aging cycles is dangerous because of the explosion hazard at temperatures below 1400 °F (760 °C).

Furnace Equipment

Furnaces. Basic equipment considerations seldom differ from those influencing the selection of furnaces for heat treating stainless steel. In general, the temperature-control limits are ±25 °F (±14 °C), and temperatures may range up to about 2350 °F (1290 °C). Generally, superalloy component heat treatment is a batch process. Batch heating for annealing or solution treating may be done in box furnaces for nonprecipitation-hardened superalloys. Box furnaces may have provisions for purging, preheating, and quenching, if the high-temperature compartment is supplemented by other chambers.

Some processing may be done by continuous processing furnaces, such as belt conveyor furnaces. Belt conveyor furnaces, although widely used for production annealing, are less gas tight than roller hearth furnaces. Consequently, atmosphere costs for a belt conveyor furnace are likely to be higher than for a roller hearth furnace of the same volume.

Often, vacuum furnaces are used for heat treating superalloys. Heating of furnaces may be accomplished by resistance elements or by induction. Vacuum furnace design also dictates a batch operation. If components are vacuum solution treated or annealed, cooling

from the solution or annealing temperatures can be accomplished in a vacuum retort pressurized with an inert gas that provides conductive cooling after heating is discontinued.

Aging of superalloys, commonly in the range of 1150 to as high as 1900 °F (621 to 1038 °C), is usually done in box furnaces, with or without protective atmospheres. The usual operating-temperature tolerance is ±25 °F (±14 °C) for wrought alloys and ±15 °F (±8 °C) for casting alloys. Continuous furnaces are seldom used, because of the long aging cycles. Salt baths are not recommended, because reaction could occur between chloride in the bath and the alloy surface during the long-time immersion that would be required for aging.

Fixturing. Fixtures for holding finished parts or assemblies during heat treatment may be of either the support type or the restraint type. For alloys that must be cooled rapidly from the solution treating temperature, the best practice is to employ minimum fixturing during solution treating and quenching and to control dimensional relations by the use of restraining fixtures during aging.

Support fixtures are used when restraint is not required or when the part itself provides sufficient self-restraint. A support fixture also functions as an aid in handling parts and helps the part to support its own weight. Long, narrow pieces, such as tubes or bolts, are most easily fixtured by hanging vertically. Components such as rings, cylinders, and beams that have a large, flat surface can be placed on a flat furnace tray or plate. For components of slightly asymmetrical shape, special supports can be built up from a flat tray. If these supports are fabricated by welding, they must be stress relieved prior to use.

Asymmetrical components can be supported in several ways. One method is to lay the part on a tray of sand, making certain that most of the bottom area is well supported. Alluvial garnet sand is most commonly used as the supporting medium. Another method of support is the use of a ceramic casting formed to the shape of the part. However, this method is costly and subject to size limitations. Turbine blades and asymmetrical ducting are examples of components that can be supported either in a sand tray or by ceramic castings.

Restraint fixtures are generally more complicated than support fixtures and may require machined grooves, lugs or clamps to hold parts to a given shape. To maintain symmetry and roundness in an A-286 frame assembly during aging, the assembly was processed on a flat plate into which grooves had been machined. These grooves accepted the rims on the outer and inner shrouds and held them in restraint during heat treatment. To prevent the center hub from rising or dropping in relation to the outer shroud, both the hub and the shroud were clamped to the grooved plate fixture.

It is possible to perform some straightening of parts in aging fixtures of the type described previously. A slightly distorted part can be forced into the fixture and clamped. Some stress relieving will occur along with aging. However, fixtures for hot sizing are not always successful for superalloys, because of the high creep strength of these alloys at the aging temperature.

The use of threaded fasteners for clamping is not recommended, because they are difficult to remove after heat treatment. A slotted bar held in place by wedges is preferred. Usually, the coefficient of expansion of both the fixture and part should be nearly the same. However, in some applications, the fixture is purposely made from a material having different expansion characteristics, in order to apply pressure to the part as the temperature increases.

Although not normally considered in heat treatment practice, the degree of contact of the heat treated article with fixturing may be important when long heat treat times are used. A component resting in sand or with ceramic fixturing attached may experience reductions in the heat flux in the contact areas and may either heat or cool too slowly.

Practical Heat Treatment of Superalloys

General. The strengthening of superalloys usually requires solution treating and aging. It should be noted that cooling rate from the solution temperature is critical for some alloys (see typical cycles for wrought alloys in Table 8.2, and for casting alloys in Table 8.3). Heat-up rate may be important as well, especially for solution treatment of cast alloy articles.

Manufacturing Economics. Solid-solution- and carbide-hardened superalloys, such as Hastelloy X or the cobalt-base superalloys, generally have minimal unique aspects with respect to heat treatment, other than melting point constraints. Various heat treatment temperatures and times have been tried, but significant property effect differences are not produced by most adjustments in stress relief, mill anneal, or full anneal time-temperature conditions. Other than the fact that some cobalt-base superalloys have higher melting points than solid-solution-hardened nickel- and iron-nickel-base superalloys, a few temperature cycles probably can encompass heat treatment schedules for all of the solution- or carbide-hardened superalloys. Consequently, economic improvement by consolidation of heat treatment cycles and standardization of times is not often an issue in wrought solid-solution hardened superalloy manufacture.

For wrought precipitation-hardened alloys, the situation is somewhat different, and for cast precipitation-hardened superalloys, it may be significantly different. Complex heat treatment cycles (often including coating diffusion cycles) have been developed over the years to wring out the optimal property values from these cast superalloys. Unfortunately, the process of development has led to the proliferation of heat treatments.

Every alloy has its own unique heat treatment schedule that leads to optimal properties. While it is undeniable that optimal properties may be produced by tailoring heat treatment schedules, it also is true that production costs can be adversely affected by this kind of situation. In particular, with precipitation heat treatment temperatures ranging from about 1600 to 1800 °F (871 to 982 °C) and times from about 4 to 32 h, manufacturing operations were impeded from efficient operation by the need to continually adjust heat treatment conditions for each new alloy/component that came through the production line. Precipitation heat treatments were identified as a principal cause of economic problems in manufacturing.

Consequently, great efforts were expended to revise the precipitation heat treatment sequences to reduce the number of aging temperatures and times. Future design of alloys or attempts to apply existing alloys must recognize the need to try to make selection of aging cycles compatible with an organization's available furnaces. Exceptions must arise and, indeed, there is no one standard aging cycle adaptable to all cast superalloys. Meanwhile, the number of varied aging cycles has been significantly reduced over the latter part of the 20th century. No similar reduction has been achieved in solution treating cycles, owing to the wide range of (incipient) melting points. Coating diffusion cycles consistently have remained at one or two temperature levels over the years. So, the heat treatment economic adjustments in cast superalloy processing have come at the expense of an optimized precipitation heat treatment schedule.

Heating/Cooling Rates and Wrought Alloys. A major function of the solution annealing treatment is to fully recrystallize warm- or cold-worked wrought structure and to develop the required grain size. Aspects such as heating rate and time at temperature are important considerations. Rapid heating to temperature is usually desirable to help minimize carbide precipitation and to preserve the stored energy from cold or warm work required to provide recrystallization and/or grain growth during the solution treatment itself.

Time-at-temperature considerations for solution heat treatments are similar to those for full or in-process (mill) annealing, although slightly longer exposures are generally indicated to ensure full dissolution of secondary carbides. For minimum-temperature solution treatments, heavier sections should generally be exposed at temperature for about 10 to 30 min, and thinner sections should be exposed for somewhat shorter times. Solution treatments at the high end of the prescribed temperature range can be shorter, similar to mill annealing. Although very massive parts, such as forgings, may benefit from somewhat longer times at temperature, in no case should any component be exposed to solution treatment temperatures for excessive periods (such as overnight). Long exposures at solution treatment temperatures can result in partial dissolution of primary carbides, with consequent grain growth or other adverse effects.

The effects of cooling rate on alloy properties following solution heat treatment can be much more pronounced than those related to in-process or full annealing. Because the solution treatment places the alloy in a state of greater supersaturation relative to carbon, the propensity for carbide precipitation upon

cooling is significantly increased over that for mill annealing. It is therefore even more important to cool from the solution treatment temperature as fast as possible, bearing in mind the constraints of the equipment and the need to avoid component distortion due to thermal stresses.

Heating/Cooling Rates and Cast Superalloys. Incipient melting on heating for solution treatment is a distinct possibility with some cast alloys. By adjusting the heat-up rate so as to ramp temperatures upward slowly, it may be possible to homogenize lower melting areas during heat up in cast alloys. The result can be that the incipient melting temperature may be driven higher, allowing a corresponding increase in the allowable solution temperature.

Heat treatment of cast superalloys in the traditional sense was not employed until the mid-1960s. Before the use of shell molds, the heavy-walled investment mold dictated a slow cooling rate, with its associated aging effect on the casting. Investment-cast alloys using shell molds at first were aged without any solution treatment. As faster cooling rates with shell molds developed, the aging response varied with section size and the many possible casting variables. Furthermore, the introduction of coating diffusion cycles at temperatures significantly above the normal aging temperatures affected the microstructure of as-cast alloys. Consequently, solution treatments were adopted for cast nickel-base superalloys.

Solution Treating Combined with Brazing. Unlike full annealing or in-process (mill) annealing, which is usually performed as a manufacturing step itself, solution treating may sometimes be combined with another operation, which imposes significant constraints on both heating and cooling practices. A good example of this is vacuum brazing. Often performed as the final manufacturing step in the fabrication of components, such a process precludes subsequent solution treatment by virtue of the limits imposed by the melting point of the brazing compound. Therefore, the actual brazing temperatures are sometimes adjusted to allow simultaneous solution heat treating of the component.

Unfortunately, the nature of vacuum brazing furnace equipment specifically, and vacuum furnace equipment in general, is such that relatively slow heating and cooling rates are standard. In these circumstances, even with the benefit of advanced forced-gas cooling equipment, the structure and properties of alloy components are likely to be less optimal than those achievable with solution treatments performed in other types of equipment.

Alternate Heat Treatments for Specific Properties. In some instances, the solution treating temperature employed will depend on the properties desired. This is indicated in Table 8.2 for alloys A-286, Inconel 718, Rene 41, Udimet 700, and Waspaloy. A higher temperature is specified for optimal creep and creep-rupture properties; a lower temperature is specified for optimal short-time tensile properties at elevated temperature. The principal objective is to put γ'-type phases into solution and dissolve some carbides. The higher solution treating temperature will result in some grain growth and more extensive solution of carbides in wrought alloys. After aging, the resulting microstructure of these wrought alloys consists of large grains that contain the principal aging phases and of a heavy concentration of carbides in the grain boundaries. The lower solution treating temperature dissolves the principal aging phases without grain growth or significant high-temperature carbide solution. See Chapter 12 for a further discussion of alloy-microstructure-property relationships.

Superalloys: A Technical Guide, Second Edition
Matthew J. Donachie, Stephen J. Donachie, p 149-187
DOI:10.1361/stgs2002p149
Copyright © 2002 ASM International®
All rights reserved.
www.asminternational.org

Chapter 9

Joining Technology and Practice

Introduction

General Aspects. This chapter is about the joining of superalloys by nonmechanical means. As such, it is concerned with the broad categories of fusion welding, solid-state welding, and brazing, as applied to superalloys of all types. Fusion welding is the principal joining technique.

Superalloys, except those with high aluminum and titanium contents, are welded with little difficulty. Nickel-base superalloys, for example, IN-718, that have a slow aging reaction also are welded without problems. Most welding concern is focused on the high-strength γ'-hardened nickel superalloys, which are the high precipitation-hardener-(aluminum + titanium) content alloys. The procedures used in welding superalloys depend, to some extent, on the mechanism by which they are strengthened for high-temperature service, that is, whether primarily solid-solution strengthening or primarily precipitation strengthening is employed.

Concepts of Welding. Fusion welding relies on melting and solidification of either base alloys of the components to be joined or base alloys plus a filler that may have:

- The same nominal composition of the base alloys (assuming that joining is of components of the same composition)
- A composition compatible with the chemistry of the components being joined both environmentally (corrosion, oxidation, etc.) and mechanically (acceptable yield, tensile, and other mechanical properties), but not necessarily the composition of any of the components being joined.

Fusion welding effects a metallurgical bond/joint between/among the respective components. However, it introduces a cast structure of variable size and properties that depends on the metals being welded and the precise welding technique used.

Solid-state welding creates the same result as fusion welding, without producing the formerly melted area. This concept is vitally important, because cast structures (result of fusion welding) are not desirable in many instances of superalloy operation. There are many solid-state processes and intermediate layers may be used to bring about successful bonding (in the case of diffusion bonds). Intermediate layers are essential to most diffusion bonding operations. The interlayer may be different from any of the basis metals/alloys.

Brazing relies on the melting and subsequent solidification of an interlayer (braze metal) without any melting of the basis metals.

Joining Superalloys. The design engineer who wishes to use a fusion-welded structure for demanding service faces a challenging dilemma. The materials involved and the deposited weld metal must exhibit sufficient ductility to withstand the severe thermal cycle imposed by fusion welding. Many applications demand that specimens taken from a qualification-welded assembly be capable of passing $2t$ 180° side-bend testing (where t is the material thickness). This test requires 20% elongation of the outer fibers of the bend specimen. After welding, some applications for which a weldment is designed may demand different properties of the weld joint from those exhibited by the bare metals.

Most solid-solution (nonprecipitation-hardening) superalloys have sufficient ductility to meet the preceding fusion welding requirements. The weld fabrication of these materials is straightforward, in that they usually do not require special preheat or postheat. Furthermore, interpass temperature control during welding normally is not critical. On the other hand, the defining characteristic of many iron-nickel- and nickel-base superalloys is the existence of a precipitate phase, which is dispersed in a matrix. The precipitation-hardenable superalloys are different from the former alloys, in that they generate a second phase when exposed to temperatures for specified times in a particular range. The second phase is customarily produced by heat treatment and can be dramatically affected by other processing or service temperature exposure.

The precipitation-hardened alloys distinguish themselves by exhibiting superior mechanical properties after being precipitation treated (aged). Fusion leads to dissolution of the hardening phases and their reprecipitation in less desirable physical form in the matrix. The matrix, if previously wrought, is now cast. The essence of employing joining processes on precipitation-hardened superalloys, particularly nickel-base superalloys, is to find a way to keep the high strength associated with γ' hardening (or the long-term strength associated with oxide dispersion strengthening, or ODS) from being lost because of the welding process. The precipitation-hardened materials are usually fusion welded in the annealed (or solution annealed) condition and are subsequently heat treated to precipitate the second phase as a final or near-final production step.

Solid-state welding processes that produce limited width joints have been applied to the precipitation-hardened alloys, in some instances. Processes such as inertia bonding and diffusion bonding have found some use but are not as widely applied as fusion welding. Solid-state joining of precipitation-hardened superalloys may eliminate the need to age after joining.

In cobalt-base superalloys, a carbide dispersion accounts for much of the hardening. During fusion welding, cobalt-base superalloys are much less at risk for the loss of hardening by solution and/or growth of the carbide phases than are the iron-nickel- and nickel-base precipitation-hardened alloys. Changes in cobalt-base superalloy structure can occur, nevertheless, and additional carbide precipitation can cause high hardening rates, while grain growth can lead to changes in ductility and strength.

While joining superalloys in air is feasible, the nature of the γ'-hardened superalloys is that some aluminum and titanium may be lost from the matrix, the volume fraction (V_f) γ' will be reduced, and/or distribution of the γ' phase will be distorted by the joining process. Shielding gases or vacuum are used to protect bonds in most γ'-hardened superalloys.

The highest-strength joints are produced by true metallurgical bonds created by fusion or solid-state welding. However, use of brazing, which does not produce melting of the base metals being joined, is a viable procedure for joining some superalloys. In general, the concepts of weldability apply to brazing. Owing to lack of melting of the base metals, cracking caused by incipient melting is not a problem.

If brazing is carried out under thermal conditions similar to those of welding, then similar property results should be expected. A principal concern for brazing is the melting temperature of the braze metal (filler) and its strength. The braze filler melting temperature will affect the heat treatment that the base metal receives from the brazing process. In some instances, if the braze temperature is compatible with the planned aging temperature, a concurrent aging may be deliberately produced during brazing. The strength of a brazed component is determined by the strength of its braze filler metal.

Joining the Alloy Classes

Solid-Solution-Hardened Wrought Superalloys. These materials have good weldability and are often used in the as-welded condition. The alloys are usually formed by additions to nickel of chromium, cobalt, molybdenum, iron, and sometimes small amounts of aluminum, silicon, and niobium. Under moderate loading, alloys of this group can be used up to temperatures approaching 2100 °F (1150 °C). Typical applications are welded containers and fixtures for thermal processing, and headers and manifolds for chemical and petrochemical processing.

The potential problem in welding these materials is base metal grain size. As grain

size increases, weldability decreases. In some applications, a minimum grain size in the base metal is specified for maximum creep resistance. As grain size increases, ductility of a metal decreases and weldability may be reduced. A compromise is to limit welding processes for coarser grain metals to those methods that use low heat input.

Carbide-Hardened Wrought (and Cast) Cobalt-Base Superalloys. These alloys do not precipitate γ' phase. However, they contain generous additions of carbide-forming elements, such as chromium, niobium, and a supersaturated amount of carbon. They enjoy reasonably good weldability in the wrought or as-cast condition, but usually require special precautions for welding after they have been in service, owing to the further precipitation of carbides.

Cast alloys such as WI-52 and wrought alloys such as Haynes 188 are welded extensively. Filler metals generally are less highly alloyed cobalt-base alloy wire, although parent rod or wire (the same composition as the alloy being welded) has been used. Gas turbine vanes that crack in service are repair welded using the preceding techniques, for example, WI-52 vanes using Haynes 25 filler rod and 1000 °F (540 °C) preheat. Indeed, good weldability is an important reason for the selection of cobalt superalloys for this application.

Precipitation-Hardenable Wrought Superalloys. Precipitation-hardened nickel-base and iron-nickel-base superalloys are considerably less weldable than cobalt-base superalloys. Because of the presence of the strengthening phase, when fusion welded, these alloys tend to be susceptible to hot cracking (weld cracking) and postweld heat treatment (PWHT) cracking, sometimes called strain-age cracking (see subsequent sections). These materials are characterized by their distinctively high strength at room temperature through about 1300 °F (705 °C). They range in alloy content from iron-nickel-base A-286 alloy thru the nickel-iron-base alloy IN-718 to the nickel-base alloys of the Waspaloy type. These alloys may have good weldability in the annealed condition, dependent on actual composition. Most are formed, machined, and welded in the annealed condition. They then are reannealed after welding and aged to obtain the desired properties. Alternate joining of superalloys, particularly the iron-nickel- and nickel-base superalloys, is done to some degree by solid-state joining processes. By far, the most joining is done by fusion welding.

The postweld processing of these precipitation-hardenable materials after fusion welding may be considerably difficult, owing to a tendency to cracking. The susceptibility to hot cracking is directly related to the aluminum and titanium contents.

Joint Integrity and Design

Design Aspects. The principal concerns for joining superalloys are to:

- Retain all or most of the strength of the base alloys
- Prevent or minimize joint cracking
- Keep the join line thin and positioned in the lowest-stressed location of the welded assembly

Joining of superalloys may range from the joining of disks to the bonding of paired turbine vanes, from the development of a case structure by buildup from sheet and forged components to the welding-on of cast bosses, to a case or application of a hard facing to turbine tips for wear resistance.

The design of fabricated structures is influenced by the application requirements and the characteristics and mechanical properties of a joint produced by a particular joining process. For example, physical characteristics of the weld joint, including undercut or underfill in fusion welds, upset in solid-state welds, and weld distortion, are important considerations. These characteristics affect not only the physical dimensions of the component but also joint mechanical properties. Obviously, mechanical properties, as influenced by the integrity and metallurgical structure of the joint, are the principal considerations in joint design.

In many applications, it is necessary to design components made of different materials. The process of making such assemblies often requires the welding of dissimilar metals, the welding of diffusion-bonded materials, and sometimes weld overlay cladding and even thermal spraying. These types of unusual welding and spraying applications require special knowledge and treatments that may

have been developed specifically for each material.

Designers of fabricated structures must consider both joining process applicability and the physical characteristics and mechanical properties of the joints. From a joining process standpoint, an efficient design will use a process optimally suited to a particular material thickness and joint configuration. Process suitability must consider component size and shape. For example, will the component fit in an available electron beam welding (EBW) chamber or brazing furnace? If necessary, can the entire part be suitably protected from the atmosphere during a diffusion bonding or a fusion welding process? What is the cost of producing the joint (including both capital equipment and operating costs) and of postjoining processing requirements, such as PWHT? What is the likelihood of such behavior as low fusion-zone ductility or low toughness in rapidly cooled welds, or poor axial fatigue behavior when defects occur?

Integrity. It is not intended to suggest that assemblies are the only joined parts, but, generally speaking, it is assemblies that go into initial service. However, repair welding or brazing of cracked but nonseparated parts is common, even in production—sometimes on newly cast, large nonrotating components for gas turbines. Repair welding also can be used to fill surface porosity in large cast structures.

It was not unusual, before the widespread introduction of IN-718 into gas turbines, to have sheet metal components or other nonrotating structures of precipitation-hardened superalloys crack upon welding and rewelding. Occasionally, a part might have been welded and rewelded as many as five or more times before clearing the production line! Clearly, the integrity of a part that cracks on so many rewelds is of concern not only from the production cost standpoint but also from a potential service cracking standpoint. On the other hand, if, after final heat treatments, no cracking was observed, experience suggests that such welds were satisfactory.

Finally, in the service life of nearly every welded structure and in components that have never been welded, there arises a need for alteration or repair. In many cases, it becomes necessary to splice new materials into old. Most of the iron-nickel- and nickel-base superalloys require special conditioning before repair welding. Cobalt-base alloys are less demanding.

Cracking and Soundness of Fusion-Welded Superalloys

Introduction. Hot cracking (Fig. 9.1) may occur in the weld heat-affected zone (HAZ) or in the weld metal of precipitation-hardened nickel-base and iron-nickel-base superalloys. Hot cracking occurs to varying degrees, depending on the amount of weldment restraint, the welding conditions, and other factors, including alloy composition. Hot cracking is not unique to superalloys, and the causes and cures of hot cracking in superalloys are not generically different from those of other materials.

Weld metal cracks are usually resolved by good welding practices, including:

- Proper design
- Cleanliness
- Correct choice of filler metal

Another form of weld-related cracking is PWHT cracking, sometimes called postweld strain-age cracking. The terminology ''PWHT'' is used in this book. Postweld heat treat cracking has occurred with virtually all precipitation-hardened superalloys. It differs from hot cracking, and the cracks are most

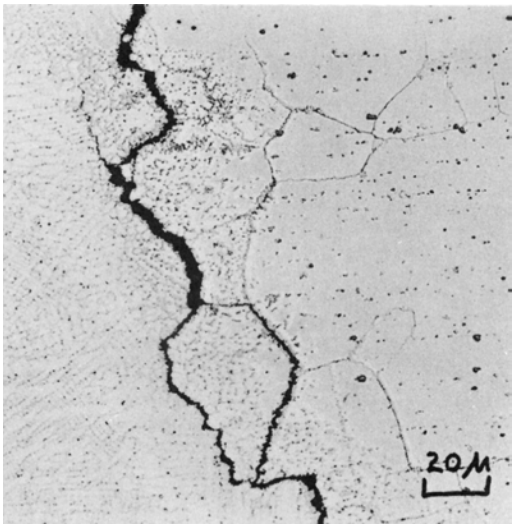


Fig. 9.1 Hot crack in heat-affected zone of U-700 nickel-base superalloy after fusion melting

commonly found in the HAZ. Their crack length (Fig. 9.2) is greater than crack length in hot cracking and they frequently extend through the weld metal or for substantial distances in the base (parent) metal itself. Postweld heat treat cracks occur, as the name implies, during heat treatment aimed at:

- Reestablishing properties of the weldment itself
- Providing stress relief to the weldments and base metal

Cracking is probably associated with the reduced ductility caused by precipitates such as γ' and η, by secondary topologically close-packed (tcp) or carbide phases (in nickel-base superalloys), or by excess carbide precipitation in cobalt-base alloys. Some alloys, such as A-286 iron-nickel-base superalloy, are inherently difficult to weld, despite having only moderate levels of γ' hardeners. There is some evidence that high-titanium alloys may be more difficult to weld than alloys of similar $V_f\gamma'$ that rely on high aluminum-titanium ratios for their strength capabilities.

Verification of Crack-Free Welded Assemblies. Visible surface cracking is a concern, but may be found by standard fluorescent penetrant inspection (F.P.I.) procedures. A principal concern for welding superalloys is that cracking or microfissuring may take place below the surface and be undetectable by standard liquid penetrant methods. Furthermore, microfissuring probably will be below the detectable limits for x-ray or other nondestructive inspection methods. Weld techniques for superalloys, therefore, must address the likelihood of limited inspectability.



Fig. 9.2 Example of postweld heat treat cracking in a Waspaloy nickel-base precipitation-hardened superalloy weld test (restrained patch) specimen

Because microfissures can occur in the subsurface of the weld and be difficult to detect, fatigue strength can be drastically reduced. However, standard tensile and stress-rupture strengths may be affected minimally by microfissuring. Unless fatigue tests are run, microfissures must normally be detected by metallographic examination. Once a standard joining practice is developed for a given weld technique + alloy + component, it is common to assume that adherence to the standard practice will guarantee absence of subsurface cracking in superalloy welded components.

Postweld Heat Treat Cracking. Cracking is sometimes found in age-hardenable alloys that are slowly cooled. Cracking frequency increases when these alloys are reheated through the hardening temperature range in the presence of residual or applied stress in a constrained condition. The rate of alloy hardening by precipitation of γ' is of primary importance relative to the heating or cooling rate through the hardening temperature range. For cracking to occur, the thermal cycles must allow sufficient hardening for the imposed stress to cause cracking. Of equal importance is the imposed stress, which must be sufficient in magnitude to initiate cracking. When these two phenomena occur simultaneously, they can result in severe PWHT cracking.

Postweld heat treat cracking occurs in precipitation-hardenable alloys when cold-work stresses, weld-induced residual stresses, and the stress imparted by aging exceed the yield strength (and available ductility) of the material. The result is an instantaneous, catastrophic failure by cracking (Fig. 9.3).

The root of the PWHT strain-age cracking problem, from the metallurgical viewpoint, thus is γ'-type compound precipitation. The nominal composition of γ' is Ni_3Al. However, the precise composition is more complex, as noted previously. Alloys whose γ' is formed predominantly by nickel-aluminum-titanium age more rapidly than those using niobium to form γ' and γ''. As a result, the



Fig. 9.3 Postweld strain-age cracking in nickel-base superalloy X-750. Alloy was welded in the age-hardened condition and re-aged at 705 °C (1300 °F)

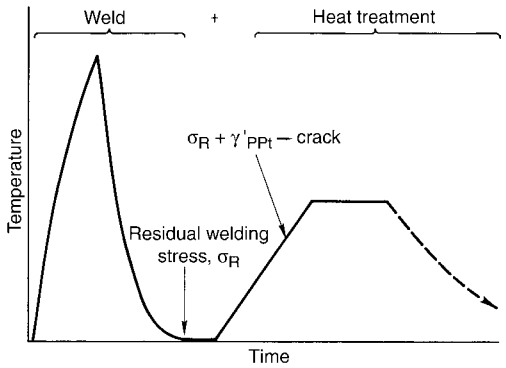


Fig. 9.4 Schematic sequence of events leading to postweld heat treat cracking.

former alloys superalloys, are more prone to PWHT than the niobium-containing superalloys (IN-718 and IN-706).

As noted in Chapter 8, a typical heat treatment for a precipitation-hardened alloy is to solution the alloy, quench it, reheat it to age it at one temperature, quench or rapid cool, and then reheat again to a second age temperature. This is an oversimplification but conveys the message that, during and after the joining process, superalloy parts or workpieces can be heated and cooled several times in and through the temperature range where precipitation of the hardening γ' phase takes place.

Figure 9.4 shows schematically how PWHT cracking occurs. During welding, the peak temperature reached in the weld and the HAZ results in high residual stresses being retained after the weld has solidified. When the part is placed in a furnace for PWHT, two things occur. First, the residual stresses relax, but, simultaneously, the stress-relief temperature is in the region for precipitation of γ', and so the part is undergoing a further strengthening reaction. The strengthening is accompanied by a reduction in ductility. The stress relief is slow, compared to the buildup of stresses from aging and the concurrent ductility reduction. The part cracks. The greater the γ' hardener, the greater the tendency to cracking.

After welding a part or assembly, the residual stress is relieved, and the maximum strength is obtained by a solution anneal and aging heat treatment. Problems arise when a welded superalloy structure is heated through the aging temperature range on its way to/from the solution temperature. Strain aging after welding is dependent on both the rate as well as the magnitude of γ' precipitation. Titanium and aluminum are the γ' strengtheners in precipitation-hardened superalloys (except for niobium in IN-718 and IN-706). When the (Al + Ti) level exceeds some critical value, PWHT (strain-age) cracking becomes a significant problem. Figure 9.5 shows a plot of weldability as a function of the (Ti + Al) content, a number that will reflect the expected level of γ' precipitates.

Little welding is performed in the aged condition if a weldment is to be reheat treated or put into elevated-temperature service, because the preaged structure may have a greater tendency to PWHT cracking. Solution annealing a superalloy before welding can strongly reduce its tendency to PWHT cracking. However, even if one solution treats and fast air cools a precipitation-hardened alloy, the tensile ductility may be too low to effectively preclude PWHT cracking. In order to truly soften and make a precipitation-hard-

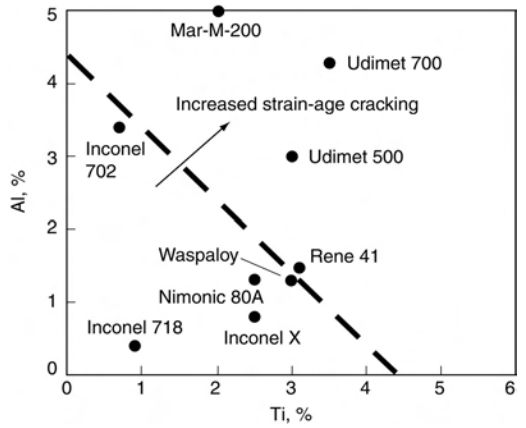


Fig. 9.5 Diagram showing the effect of aluminum and titanium hardener content on the tendency to welding problems with nickel-base superalloys

ened alloy more ductile, a different kind of heat treatment is required.

The base metal of a precipitation-hardened superalloy can be protected effectively against PWHT cracking by welding in the overaged condition. This prevents aging during reheating but means that the alloy will have below-normal strength upon completion of the welding and PWHT. Figure 9.6 shows that U-700 nickel-base superalloy in the solution-treated condition (no age) will crack severely in PWHT in a relatively low-restraint weldment. On the other hand, if the same alloy is overaged and slow cooled prior to welding, it achieves a substantial improvement in PWHT cracking resistance. Although not fully understood, another method to reduce PWHT cracking is the use of vacuum or inert atmospheres in PWHT.

Alloys IN-718 and IN-706, fortunately, do not undergo PWHT cracking. The age hardening develops via the Ni_3Nb, γ'', precipitate, but the γ'' precipitate is formed at a much slower rate than that at which γ' forms in γ'-hardened superalloys. This allows alloys such as IN-718 to be heated into the solution temperature range without suffering significant aging and the resultant PWHT (strain-age) cracking. Figure 9.7 compares the aging rates of several γ' alloys with those of IN-718, which is strengthened with the γ'' precipitate. Hardening is retarded in γ''-hardened alloys such as IN-718, and these alloys offer great

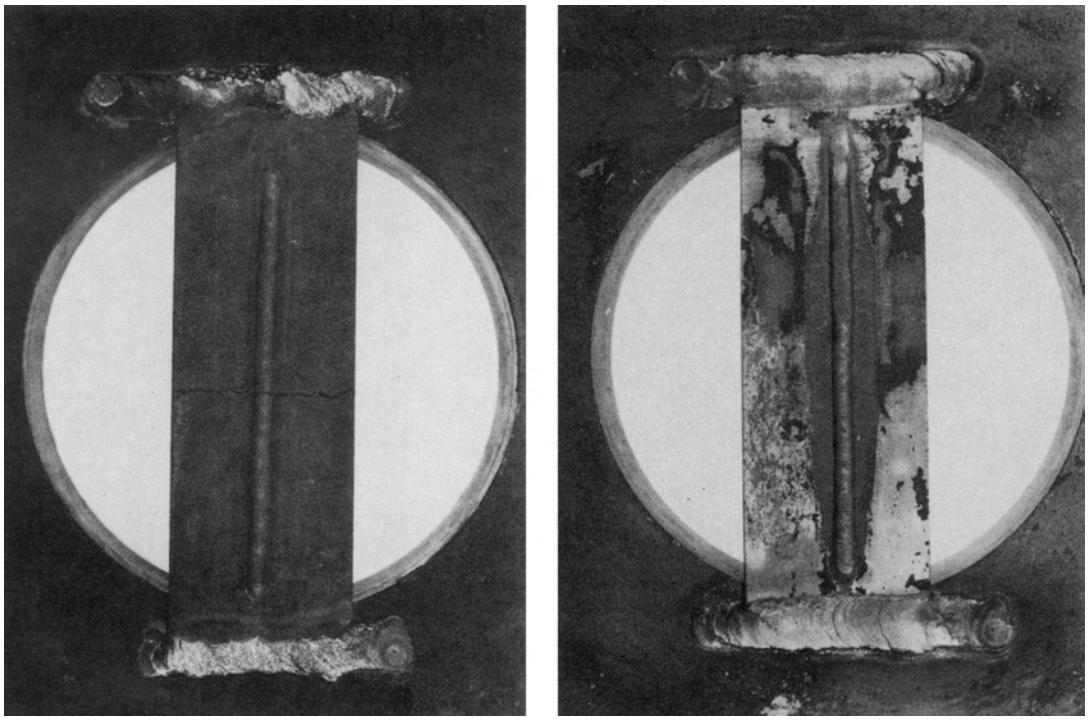


Fig. 9.6 Minipatch welding tests on U-700 nickel-base superalloy showing the benefit of overaging on postweld heat treatment cracking, (left) solution heat treated, (right) overage heat treated

latitude in methods for heating and cooling parts.

Welded structures that require corrosion resistance but not high strength often will not need PWHT and can thus avoid PWHT cracking. However, if they are placed in service at elevated temperature, they may still crack during the initial heat-up cycle.

Postweld Heat Treatment Cracking Susceptibility Curves. The circular patch test is a high-restraint weld test that can be used to evaluate the sensitivity of an alloy to PWHT cracking. The test, when used with thermal treatments, can be used to produce crack-susceptibility C-curves. These are so named because of the characteristic ''C'' shape of the temperature-time space that separates the cracked from the uncracked behavior of this rate process. Figure 9.8 shows that, for a given C-curve behavior, different heating rates can produce cracked or uncracked parts. Figure 9.9 shows that alloy chemistry variations can affect the crack sensitivity of a given alloy.

Hot Cracking—Predominantly in the HAZ. Hot cracking occurs due to the effects of the thermal cycle of welding. Rapid heating and cooling occur in the areas adjacent to the weld. The effects of such rapid thermal cycles on the metals are what create the HAZ microstructures, illustrated by Fig. 9.10 for U-700, a very difficult-to-weld nickel-base superalloy. Incipient (local) melting can be caused by the welding process. Incipient melting at grain boundaries can lead to reduced ductility and subsequent cracking. Unfortunately, one cannot protect against hot cracking in a manner similar to protecting against PWHT. A fusion welding process invariably produces a HAZ thermal cycle, which puts some of the age-hardening constituents into solution. During slow cooling or reheating, these constituents can reprecipitate, age harden the alloy, and produce a crack-susceptible condition in the HAZ. This can occur regardless of the PWHT.

Peak temperatures as high as 1800 °F (982 °C) cause no noticeable changes in the HAZ microstructures. Relative to Fig. 9.10, however, there is some dissolution of γ' at 1900 °F (1038 °C), and this continues to 2100 °F (1149 °C). The result is further dissolution of the coarse, blocky γ'. Also visible at 2100 °F (1149 °C) is a phase reaction beginning at a grain boundary. At 2150 °F (1175 °C) (no mi-

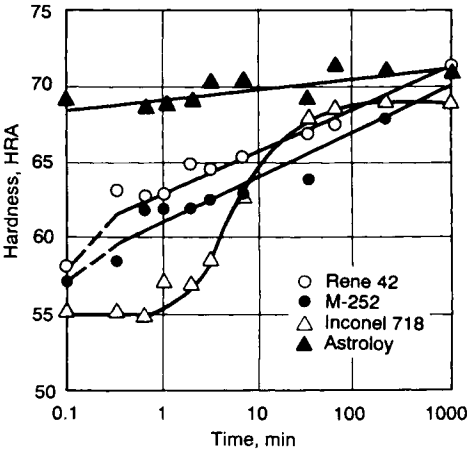


Fig. 9.7 Aging curves showing hardness vs. time for selected nickel-base superalloys. Note the slow initial kinetics for IN-718.

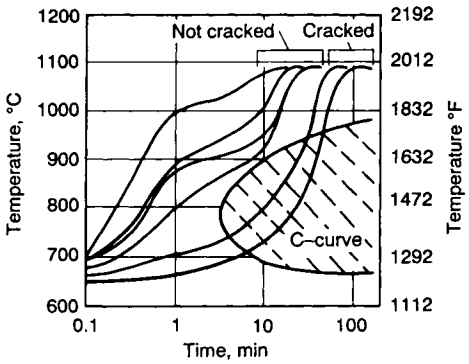


Fig. 9.8 Effect of heating rate on the cracking tendency of Rene 41 nickel-base superalloy during postweld heat treatment after receiving preweld solution anneal

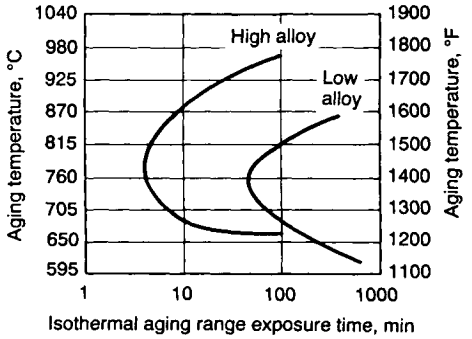


Fig. 9.9 Effect of alloy composition on cracking tendency of Rene 41 nickel-base superalloy. Showing effects of high alloy vs. low alloy concentrations of iron, silicon, manganese, and sulfur in the alloy

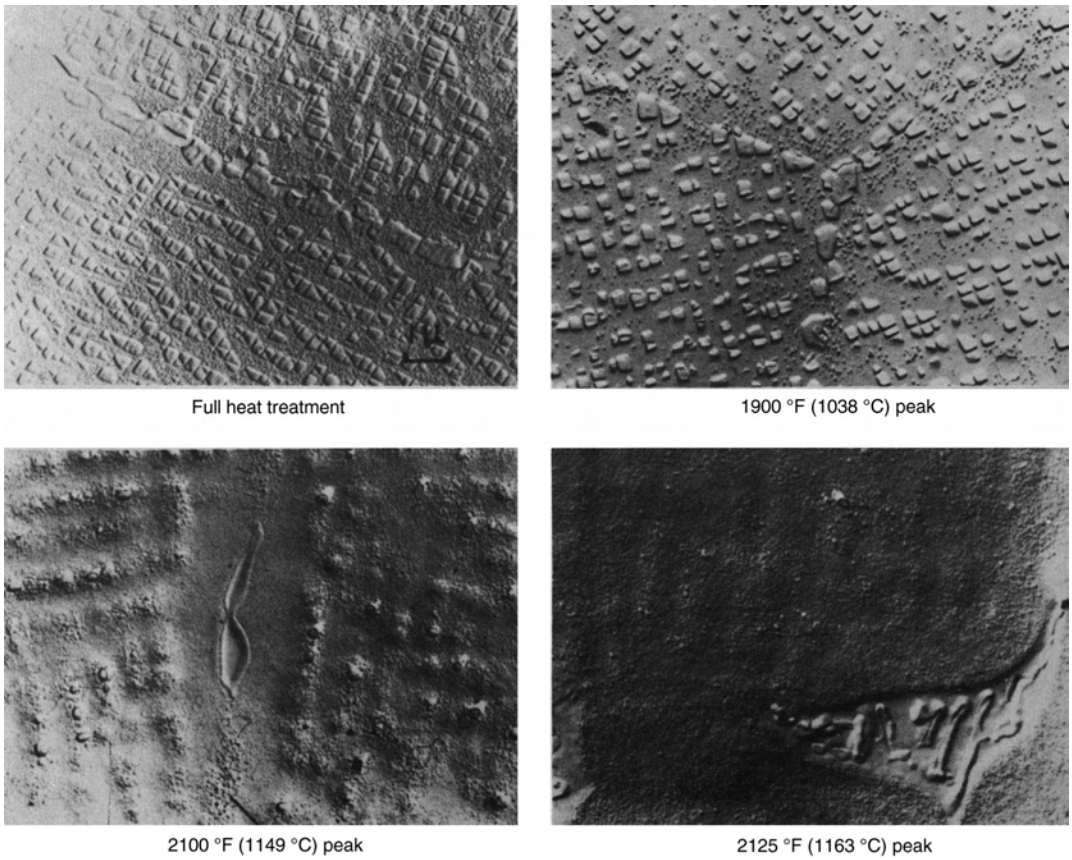


Fig. 9.10 Microstructures produced in U-700 nickel-base superalloy to simulate portions of the heat-affected zone corresponding to the peak welding temperature

crograph shown), the grain-boundary reaction is readily identified as incipient melting (local melting) phenomena. The presence of incipient melting creates the necessary low ductility and low strength condition, and the thermal and mechanical strains of the welding process or subsequent heating provide the strains that lead to failure.

A composite micrograph (Fig. 9.11) of the HAZ of a welded U-700 alloy, with enlargement to show detail, can be used to illustrate the hot HAZ cracking problem. It is obvious that the predominant amount of cracking happens in the region where a small amount of melting has occurred. The region of partial melting, unfortunately, corresponds to the location where the localized strains that occur adjacent to the weld are greatest. The cracking usually does not occur in the weld metal where the amount of melting is greater or in the HAZ where it does not melt.

Liquation Cracking in the HAZ. Phases, such as MC carbides and Laves phases, that form during solidification have the potential to initiate melting in the HAZ during welding and spread along the grain boundaries (Fig. 9.12). The melting, often termed ''liquation,'' occurs because of a reaction between the dissolving precipitate and the matrix. When this melting is accompanied by sufficient thermal stress, cracks can form along the HAZ grain boundaries and extend into the fusion zone. Such cracking may be termed ''liquation cracking,'' ''hot cracking,'' or ''microfissuring.'' A number of alloy systems are known to experience liquation cracking; some are listed in Table 9.1

Liquid metal is invariably associated with the HAZ in superalloys, because the HAZ stretches from the base metal to the edge of the fusion zone and will include all or part of the partly solidified (or partly melted)

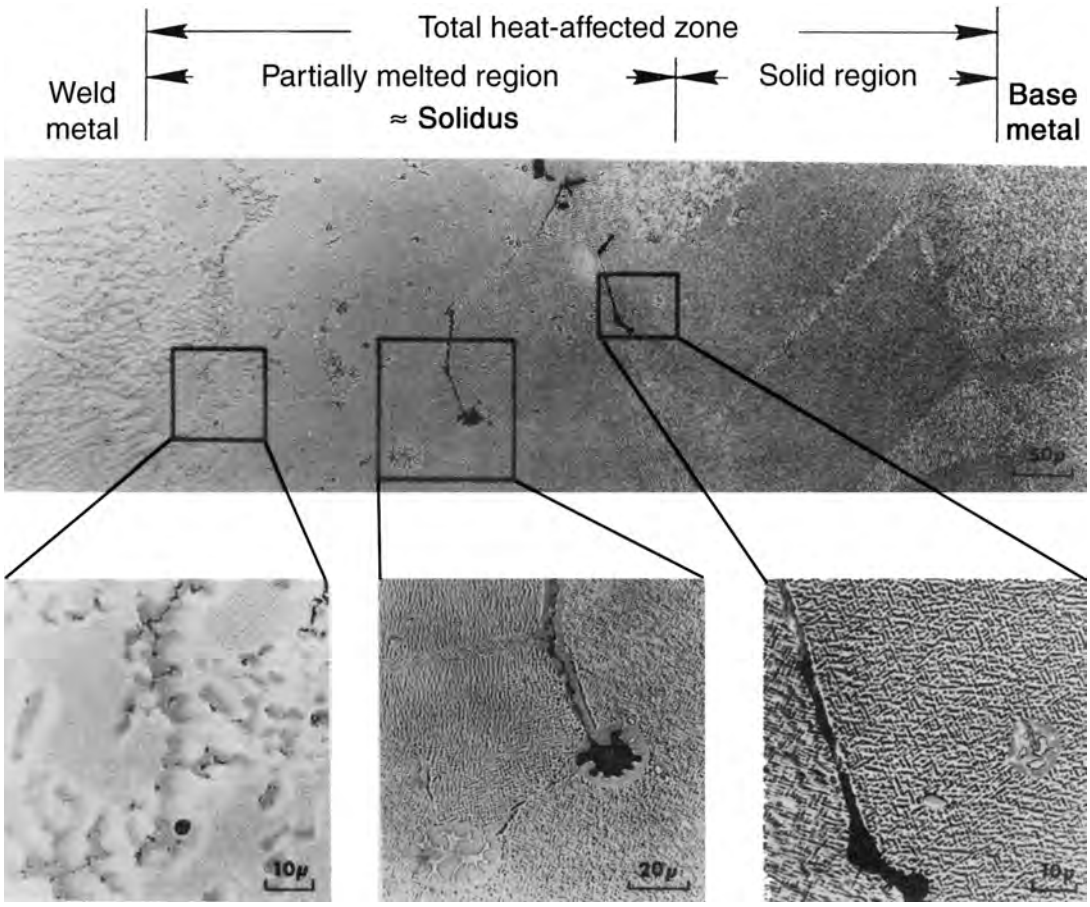


Fig. 9.11 Composite micrograph of U-700 nickel-base superalloy showing location of extended heat-affected zone, noting partly melted regions and showing some hot cracking defects

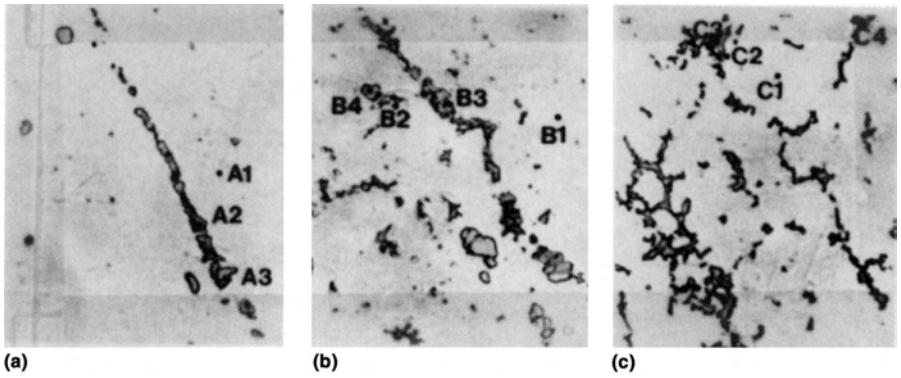


Fig. 9.12 Liquation of a NbC stringer in IN-718 nickel-base superalloy. (a) Stringer before onset of liquation, (b) initial stages of liquation, (c) movement of stringer liquation into grain boundaries of alloy

Table 9.1 Some superalloy systems showing liquation

Alloy system	Liquating phase
Hastelloy X	M_6C
Inconel 600	Cr_7C_3; Ti(Cn)
A-286	TiC or Ti(CN)

mushy zone. It can be concluded that many superalloys, if welded, will contain a HAZ during welding that has a mushy zone full of intergranular liquid. The mushy-zone liquid generally does not contribute to poor weldability, because during the normal course of solidification, it is always open to the fusion zone. The fusion zone acts as a source of liquid to backfill or heal shrinkage or cracks that might otherwise form.

Grain Size, Precipitates, and Liquation Cracking. A large grain size promotes liquation cracking, as shown in Fig. 9.13. Liquation cracking is sensitive to the amount and location of second-phase precipitates as well. The size of precipitates in the HAZ, as well as the location relative to the position of grain boundaries, changes during the welding thermal cycle. Precipitates tend to dissolve during the thermal cycle.

Effect of Contaminants on Weld Soundness. Superalloys must be clean and free of machining oils and other contaminants if welds free of defects are to be achieved. Introducing contaminants to the fusion zone can lead to fissuring and porosity. The presence of low-melting elements and alloys in the HAZ can lead to fissuring by liquation cracking. Some elements that have been identified in alloy chemistries as potential sources of liquation cracking are sulfur, phosphorus, lead, and boron. The first three elements are known impurities, but the fourth is a deliberate additive to enhance the creep-rupture strength of alloys. Other impurity elements of concern have been oxygen and nitrogen. It has been suggested that if the impurity level restrictions shown in Table 9.2 are observed, increased liquation cracking will not be observed.

The problem of cracking due to low-melting-point contaminants also has been noted with the presence of copper, brass, and lead externally introduced to a metal. The low-melting material becomes liquid in the HAZ as the arc passes and the liquid penetrates the grain boundary, perhaps in the manner of liquid metal embrittlement reactions. This grain-boundary penetration reduces the strength of the boundary and, coupled with yield-strength-level stress, leads to microfissuring. Thus, care must be taken when using copper chills and tooling not to deposit the copper on the surface of the base material. Lead can cause weld metal fissuring if introduced even in minute quantities to the fusion zone. Unfortunately, lead/brass/copper hammers are commonly used in shops to ''adjust'' the position of metal parts in the tooling. Instances have been noted where this practice resulted in weld HAZ and/or weld fusion zone fissuring.

Most of the high-temperature alloys have excellent oxidation resistance, because they develop a tightly adhering refractory oxide on the surface of the material. This is a highly useful property, from an application standpoint, but it can lead to problems such as trapped oxide in the weld metal and lack-of-fusion defects at the weld metal/parent metal interface if the surface of the material to be welded is not free of oxide. The oxide cannot be removed by simple wire brushing —the metal surface may appear to be clean after brushing, but the oxide has only been

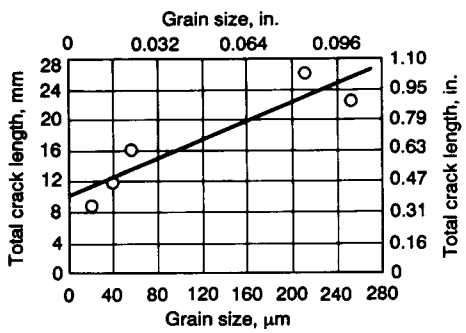


Fig. 9.13 Total crack length of microfissures in IN-718 plotted against grain size, showing that increased grain size leads to more cracking (microfissuring)

Table 9.2 Suggested impurity limits permitted to avoid liquation-type hot cracking in superalloys

Element	Composition, wt% (maximum)
Sulfur	0.015
Phosphorus	0.015
Silicon	0.02
Oxygen	0.005
Nitrogen	0.005

polished. An aggressive abrasive grinding operation is needed to positively remove the oxide. Less-than-ideal inert gas protection can allow the formation of an oxide film on the surface of the deposited weld metal. Care needs to be taken to remove this oxide before multipass welding to avoid the problems of entrapped oxide and lack-of-fusion defects.

Reducing Susceptibility to Liquation Cracking. Welding parameters and fabrication sequence often can be adjusted to reduce the possibility of liquation cracking. In addition, there are several metallurgical conditions that minimize HAZ liquation cracking:

- Grain size should be minimized.
- Impurity content should be minimized.
- If precipitates are desired for grain size control, solidification precipitates such as MC carbides should be used.
- The amount of precipitate that liquates should be minimized. If a particularly difficult cracking problem cannot be resolved any other way, then increasing the amount of precipitate may produce enough liquation to initiate backfilling from the mushy zone and promote healing of cracks.
- Welding should take place when the alloy has undergone some combination of heat treatment to produce the solutioned and/or homogenized conditions, followed by rapid cooling (direct quenching should be avoided). These heat treatments minimize impurity concentration on the grain boundaries.

Preweld and Postweld Heat Treatments for Fusion Welding

Cold-Worked Alloys. Strain-strengthened (cold-worked or work-hardened) alloys usually are welded in the combined hot-cold-worked condition. The metal in the HAZ is essentially solution treated by the welding heat, resulting in a decrease in hardness and strength. Although work-strain-strengthened alloys frequently are preheated for welding, the preweld heat treatments must be done in a limited temperature range to avoid annealing the metal. This same restriction on heat treating temperature applies to postweld treatments of these alloys.

Solid-solution-strengthened alloys generally are welded in the solution-treated condition and are used without PWHT. These alloys have a small zone of grain growth adjacent to the weld, but this does not appreciably reduce weld strength.

Solid-solution-strengthened alloys normally do not require PWHT to achieve or restore optimal mechanical properties. Postweld heat treatment is sometimes used to provide stress relief. Complete stress relief can be achieved with full solution anneal, which also gives the alloy an optimal metallurgical condition. Solution annealing will eliminate any prior cold work by recrystallization and will dissolve secondary $M_{23}C_6$-type carbides that may have formed upon cooling during welding. Typical solution annealing temperatures for some solid-solution-strengthened alloys are given in Table 9.3. The time required can range from a few minutes to about an hour, followed by rapid quenching in water or air. A popular calculated time is 140 s/mm (1h/in.) of cross-section thickness.

In cases where stress relief is needed and a fine grain size is required, mill annealing is effective. The mill annealing heat treatment is similar to solution annealing. However, the lower temperatures involved are not sufficient to dissolve secondary carbides that may have precipitated intergranularly during welding. The mill annealing treatment may not develop the stress-rupture properties in the weldment to their full potential. Examples of minimum mill annealing temperatures are given in Table 9.3.

Precipitation-Hardened Superalloys. The precipitation-strengthened alloys are typically used in the solution treated and aged condition. Solution treatment can be per-

Table 9.3 Typical solution annealing and mill annealing temperatures for solid-solution-strengthened alloys

	Solution annealing temperature range		Minimum temperature for mill annealing	
Alloy	°C	°F	°C	°F
Hastelloy X	1165–1190	2125–2175	1010	1850
Hastelloy S	1050–1135	1925–2075	955	1750
Alloy 625	1095–1205	2000–2200	925	1700
RA333	1175–1205	2150–2200	1040	1900
Inconel 617	1165–1190	2125–2175	1040	1900
Haynes 230	1165–1245	2125–2275	1120	2050
Haynes 188	1165–1190	2125–2175	1120	2050
Haynes 25 (L-605)	1175–1230	2150–2250	1040	1900

formed either above or below the γ' solvus temperature, depending on the desired microstructure. In wrought material, aging results in a homogeneous distribution of γ' and intergranular, secondary-type carbides. That distribution may not be the case in cast alloys. In any event, the γ' distribution in weld metal may or may not be homogeneous because of the segregational effects of weld solidification.

Precipitation-strengthened alloys may be welded in the solution-treated condition, because greater ductility of the base metal in this condition permits some relaxation of the stresses associated with welding. However, note the comments made earlier under the section ''Postweld Heat Treat Cracking'' concerning welding in the overaged condition instead of the solution-annealed condition.

Postweld heat treatment of precipitation-hardened alloys generally includes a re-solution treatment and an aging treatment.

Welding Specifications

The American Welding Society (AWS) has published specifications related to welding and brazing. Government and industry have developed numerous additional specifications related to the joining of superalloys. These specifications may be quite general or very specific, often describing in detail the fabrication or weld repair of an individual component. While there is a continuing trend to standardization of specifications, unique specification requirements could be encountered by designers planning to use certain superalloys. This situation may be characteristic of the more technologically sophisticated alloys used in high-performance applications.

Most superalloy primary users, such as the gas turbine manufacturers, have specifications related not only to production welding, but also to repair and refurbishment of superalloys. Repair and refurbishment have become increasingly important as the cost of materials and components for gas turbines has increased. Joining techniques often play a prominent role in the process of returning components to service. In any industry, the integrity of repair and refurbishment processes is a prime concern, but in some industries it is a critical aspect of customer service and a corresponding financial profit center. Specifications are vitally important in the initial production of components and even more so for aftermarket situations. Control by specification can ensure the integrity of a joining process. Although there is a common thread to the needs for repair and refurbishment joining specifications, the diversity of metals and philosophies of joining make the likelihood of common repair and refurbishment specifications slim.

Fusion Welding Practice for Superalloys

General. Superalloys can be welded by the following fusion welding techniques:

- Gas tungsten arc welding (GTAW)
- Gas metal arc welding (GMAW)
- Shielded metal arc welding (SMAW)
- Submerged arc welding (SAW)
- Plasma arc welding (PAW)
- Electron beam welding (EBW)
- Laser beam welding (LBW)
- Resistance spot welding (RSW)
- Resistance seam welding (RSEW)

Procedures and equipment are generally similar to those used for welding austenitic stainless steel. Electron beam welding involves an evacuated chamber to permit electrons to be generated and delivered to the workpiece, or it involves production of the electrons in vacuum but delivery through an inert gas shielding setup to the workpiece in nonvacuum EBW. All processes except some versions of EBW can be done in air. Protection of the weld zone can be provided by localized inert gas shielding or appropriate electrode coatings that produce slag and/or a protective gas.

Complete enclosure in a protective chamber of the high-vacuum environment associated with the traditional EBW process inherently provides the best atmospheric protection, but at a higher cost and with less flexibility. In addition to proper shielding from the atmosphere, welded component cleanliness (including filler metals) is necessary to avoid weld contamination. The automatic welding of extremely large components may prove difficult, particularly with the EBW process.

In addition to their role in PWHT cracking, residual stresses in welds can greatly influence the performance of a fabricated aerospace component by degrading fatigue properties. Distortion can cause difficulties in the final assembly and operation of high-tolerance aerospace systems. Thus, the use of high-energy-density welding processes to produce full-penetration, single-pass autogenous welds rather than multiple conventional arc welding may be desirable to minimize these difficulties.

Arc Processes. An arc, struck between an electrode and the workpiece, is the most common method of heating for fusion welding. Heat generated by the arc melts the filler metal (sometimes the filler is the electrode, as in GMAW) and the base metals. A molten pool is produced, invariably under the protection of a slag gas or inert gas blanket. The pool solidifies as the heat source retreats from the area, and a solidified weld nugget is formed. A HAZ is generated from the interface of the previously molten metal to a distance in the metal being joined where the temperature reached in the welding process becomes sufficiently low that no metallurgical changes occur.

Superalloys can be welded by all the arc welding processes. Gas tungsten arc welding is widely used, especially for joining thin sections. In general, SMAW and GMAW are used in joining sections more than 0.250 in. (6.4 mm) thick, where the heat input does not adversely affect the weld metal or the base metal. Submerged arc welding generally is used only in high-volume production welding of sections more than 1 in. (25.4 mm) thick. Shielded metal arc welding is widely used for joining solid-solution nickel-base superalloys but is rarely used for joining precipitation-strengthened superalloys. It is a process in which the heat for welding is generated by an arc established between a flux-covered consumable electrode and a workpiece. The electrode tip, molten weld pool, arc, and adjacent areas of the workpiece are protected from atmospheric contamination by a gaseous shield obtained from the combustion and decomposition of the electrode covering. Additional shielding is provided for the molten metal in the weld pool by a covering of molten flux or slag. Filler metal is supplied by the core of the consumable electrode and from metal powder mixed with the electrode covering of certain electrodes. Shielded metal arc welding is often referred to as arc welding with stick electrodes, manual metal arc welding, or stick welding. Direct current electrode positive generally is used to obtain optimal mechanical properties.

Resistance Welding Processes. Resistance welding, which is another fusion welding process, occurs when heat is generated by resistance to electrical current at two surfaces in contact with each other. When heat is generated, the metal melts in the vicinity of the current flow. Pressure keeps the faces together. When the current is interrupted, a solidified weld nugget is formed. The nugget is contained within the metal being joined and does not reach an external surface. Resistance welding is fast. When done locally, a spot results, hence ''spot'' welding. When spots overlap, the result is ''seam'' welding.

Electron Beam Welding. Electron beam welding is a high-energy-density fusion welding process that works by bombarding the joint to be welded with an intense beam of high-voltage electrons. The electron energy is converted to thermal energy as the electrons impact and penetrate into the workpiece. This process causes the weld-seam interface surfaces to melt and produces the weld joint coalescence desired.

Originally, EBW generally was performed only under high-vacuum (1×10^{-4} torr, or lower) conditions. Currently, there are three distinct modes of EBW employed:

- High-vacuum, where the workpiece is at a high vacuum ranging from 10^{-6} to 10^{-3} torr
- Medium-vacuum, where the workpiece may be in a ''soft'' or ''partial'' vacuum ranging from 10^{-3} to 25 torr
- Nonvacuum, which is also referred to as atmospheric EBW, where the workpiece is at atmospheric pressure in air or protective gas

In all EBW applications, the electron beam gun region is maintained at a pressure of $l0^{-4}$ torr or lower.

Laser Beam Welding. Laser beam welding is a fusion welding process that produces coalescence of materials with the heat obtained from the application of a concentrated coherent light beam impinging on the surfaces to be welded. The word ''laser'' is an acronym for ''light amplification by stimulated emis-

sion of radiation.'' The laser is a unique source of thermal energy, precisely controllable in intensity and position. For welding, the beam must be focused by optical elements (mirrors or lenses) to a small spot size to produce a high-power density. This controlled power density melts the metal and, in the case of deep penetration welds, vaporizes some of it. When solidification occurs, a fusion zone, or weld joint, results. A laser beam can be transmitted through the air for appreciable distances without serious power attenuation or degradation.

More on Causes and Prevention of Weld Defects in Fusion Welding. Weld defects such as cracks, porosity, inclusions, and incomplete fusion usually are unacceptable in weldments made of superalloys. Nondestructive inspection is used on almost all completed weldments; destructive inspection generally is limited to test samples. Various types of leak tests are used on weldments that are to be subjected to pressure in service.

''Porosity'' is the term used to describe gas pockets or voids in the weld metal. Voids in welds can occur when gases have been trapped in a groove or between two pieces of metal being welded. When welding a lining in a thick-walled vessel or when welding one tube inside another, entrapped gas can cause a void if it does not have an easy escape path. Typical causes of porosity from arc welding include improper shielding, moisture, incorrect amperage, and excessive arc length. Dry electrodes are essential. When high amperage or a long arc length is used, deoxidizers that help prevent porosity can be totally consumed when transferring across the arc.

Cold shuts and surface pits in a weld are possible evidence of a subsurface crack or of porosity that has emerged at the surface. Also, there may be lack of fusion between successive layers of weld metal or between adjacent weld beads. Cold shuts can occur between the weld metal and the base metal when hot metal runs ahead onto a cold metal surface and does not fuse properly. Cold shuts should be removed by grinding, because they are linear discontinuities that may prevent successful weld qualification bend tests, compromise strength, and contribute to crevice corrosion problems. Both visual and liquid penetrant inspection are used to locate cold shuts and surface pits.

Inclusions are usually slag, oxides, or other nonmetallic solids entrapped in the weld metal between adjacent beads or between the weld and parent metal. Excessive weld pool agitation, downhill welding, and undercutting can lead to slag entrapment. These conditions can usually be prevented by good weld practice and proper weld design.

Cracks and fissures are another set of defects that affect properties. These defects have been covered previously in discussions of hot cracking and PWHT cracking. To elaborate on the cracking potential, it should be noted that several additional possibilities exist for cracking beyond those discussed previously. Centerline longitudinal cracking is caused by concave beads or a very deep, narrow weld bead. Crater cracking occurs when the arc is extinguished over a relatively large weld pool. The resulting concave crater is prone to shrinkage cracking. Bridging cracks occur in highly stressed joints where good penetration is not achieved at the arc initiation point.

Overheating during arc welding can cause hot short cracking in the weld metal or the base metal and excessive carbide precipitation at grain boundaries in the HAZ. This can be avoided by using the recommended amperage ranges, maintaining a short arc length, and not weaving the electrode excessively.

Cracks of any type and size usually cannot be tolerated. If a material proves to be crack sensitive, base-metal cracking can be minimized by reducing heat input and depositing small beads, which result in lowered residual stresses. Other procedures have been discussed previously in this chapter.

Practical Aspects of Superalloy Fusion Welding

General. Gas tungsten arc welding is the most common welding technique for superalloys. The data in Table 9.4 are intended to serve as starting points for the establishment of machine settings for GTAW. These conditions are, in general, suitable for welding iron-nickel-, nickel- and cobalt-base superalloys when making butt, corner, or T-joints, using an appropriate groove design based on stock thickness and application. An increase in welding current of 10 to 20 A may be

Table 9.4 Conditions for gas tungsten arc welding of superalloys

Base-metal thickness, in. (mm)	Diameter of filler metal(a), in. (mm)	Electrode diameter(b), in. (mm)	Shielding gas		Welding current(c), A
			Gas	Flow rate, ft^3/h (L/M)	
0.010 (0.254)	0.020 (0.508)	0.040–0.060 (1.02–1.52)	Ar	12–15 (5.7–7.1)	10–15
0.020 (0.508)	0.030 (0.762)	0.060 (1.52)	Ar	12–15 (5.7–7.1)	15–25
0.030 (0.762)	0.030; 0.045 (0.762; 1.14)	0.060 (1.52)	Ar	12–15 (5.7–7.1)	25–35
0.045 (1.14)	0.045 (1.14)	0.060 (1.52)	Ar	12–15 (5.7–7.1)	40–50
0.050 (1.27)	0.045 (1.14)	0.060 (1.52)	Ar	12–15 (5.7–7.1)	45–55
0.060 (1.52)	0.045 (1.14)	0.060 (1.52)	Ar	12–15 (5.7–7.1)	55–65
0.080 (2.03)	0.060 (1.52)	0.060 (1.52)	Ar	12–15 (5.7–7.1)	75–85
0.100 (2.54)	0.060; 0.090 (1.52; 2.29)	0.093 (2.36)	Ar or He	12–20 (5.7–9.4)	95–105
0.125 (3.18)	0.060; 0.090 (1.52; 2.29)	0.093 (2.36)	Ar or He	12–20 (5.7–9.4)	110–135
0.250 (6.35)	0.060; 0.090 (1.52; 2.29)	0.093 (2.36)	Ar or He	12–20 (5.7–9.4)	130–200

The data in this table are intended to serve as starting points for the establishment of optimal machine settings for welding workpieces on which previous experience is lacking. The data are subject to adjustment as necessary to meet the special requirements of individual applications. Torch nozzle diameter was 7/16 in. (11 mm); nozzle had a gas lens. (a) Minimum wire diameters were applicable. (b) EWTh-2 electrodes. (c) Direct current electrode negative with high-frequency arc starting. An increase of 10 to 20 A may be needed for melt-through T-joints.

needed for melt-through T-joints. Generally, the interpass temperature should range from 200 to 350 °F (93 to 177 °C), depending on the alloy. Oscillation of the welding torch may help to prevent cracking by changing the solidification pattern. This may also improve the appearance of the weld.

Welding Fixtures. Fixtures used in arc welding superalloys are generally similar to those used on other metals. Chill bars are often used to cool the weld area rapidly. Backing bars, inserts, and facing plates that are in contact with the workpieces on either the root or the face side of the welds should be located so as not to contaminate the weld metal or base metal, or cause gas or flux entrapment. These accessories are usually made of copper.

Hold-down bars and backing bars extend the full length of the weld. The backing bars usually contain passages to facilitate inert gas shielding. When grooved backing bars are used, the grooves should be shallow to minimize melt-through and to limit the height of the root reinforcement. Grooves in backing bars should have rounded corners, causing them to be elliptical in shape, to prevent entrapment of slag.

Cobalt-Base Superalloys. Cobalt-base superalloys are available in both cast and wrought forms. Generally, the cast alloys are somewhat more difficult to weld than the wrought alloys, but they are still very weldable. Where the application requires very high reliability of welds, only GTAW and GMAW are recommended; otherwise, SMAW is used if the thickness of the parts is appropriate. Cobalt-base superalloy sheet also can be welded successfully by resistance techniques. Electron beam welding and PAW can be used on cobalt-base superalloys, but usually are not required in most applications, because alloys of this class are so readily weldable. Appropriate preheat techniques are needed in GMAW and GTAW to eliminate tendencies to hot cracking.

Iron-Nickel- and Nickel-Base Superalloys. Nickel and iron-nickel superalloys are available in cast and wrought form. Wrought forms are those most commonly welded. Welded assemblies have been produced by GMAW, GTAW, EBW, laser, and PAW techniques. Filler metals, when used, usually are weaker, more ductile austenitic alloys so as to minimize hot cracking. Occasionally, base-metal compositions are employed as fillers. Such welding is generally restricted to the low $V_f\gamma'$ alloys, usually in the wrought condition. Cast alloys of high $V_f\gamma'$ have not been welded successfully on a consistent basis when filler metal is required, as in weld repair of service parts. However, EBW can be used to make structural joints in such alloys. In addition to being weldable by the usual fusion welding techniques mentioned previously, nickel and iron-nickel alloys can be resistance welded when in sheet form.

Frequently, a root pass is made by GTAW and the subsequent passes by GMAW. Submerged arc welding can be used on certain alloys, but the welding flux must be carefully selected to obtain adequate protection and

provide correct elemental additions to the weld pool. The welding conditions chosen must avoid excessive heat input. When welding metal more than 3 in. (7.6 cm) thick, shrinkage stresses decrease ductility slightly, and a postweld stress-relieving treatment may be necessary. The manufacturer of the alloy should be consulted for specific details.

The solid-solution superalloys are readily welded in the annealed condition. No heat treatment is needed after welding to improve corrosion resistance, and generally the alloys do not become embrittled after long exposure at temperatures up to about 1500 °F (815 °C). Table 9.4 lists general conditions for GTAW of nickel-based superalloys.

Because of their γ'-strengthening mechanisms and capabilities, some nickel and iron-nickel superalloys are welded in the solution heat treated condition, as noted previously. Special preweld heat treatments have been used for some alloys. Weld techniques for superalloys must address not only hot cracking but PWHT cracking, as noted earlier. This is of particular interest in terms of the microfissuring (microcracking) phenomenon that sometimes occurs.

In addition to being weldable by the usual fusion welding techniques, some iron-nickel-base and nickel-base superalloys can be resistance welded when in sheet form.

Further Comments on Preweld and Postweld Heat and Mechanical Treatments. The solid-solution (nonprecipitation-hardened) superalloys are welded in both the annealed and moderately cold-worked condition. Weldments made of solid-solution alloys can be used as welded or after stress relieving, depending on the alloy and application. Stress relieving in the range from 800 to 1600 °F (427 to 871 °C), depending on the alloy and its condition, can be used to reduce or remove stresses in work-hardened solid-solution alloys without producing a recrystallized grain structure. A low-temperature stress-equalizing heat treatment of 600 to 800 °F (316 to 427 °C) can be used to redistribute stresses without appreciably decreasing the mechanical strength produced by the previous cold working.

Usually, preheating nickel-base superalloys is neither needed nor recommended. A postweld thermal or mechanical treatment is sometimes needed, especially for the precipitation-hardened alloys, to redistribute and relieve residual stresses resulting from weld-shrinkage strains.

The precipitation-hardenable alloys often are welded in the solution-treated condition, although test data indicate that welding Rene 41 in the overaged condition can help prevent strain-age cracking. If a high degree of deformation should occur during preweld forming, or if the alloy has a high work-hardening rate, process annealing on the formed workpieces, before welding, may be required. Precipitation-hardenable alloys are given a solution treatment after welding to relieve residual stresses, and then they are hardened by an aging heat treatment. If the normal aging time or temperature is exceeded, overaging occurs; loss of strength and increase in ductility can result.

Superalloy Fusion Welding Details

General. Although the general aspects of fusion welding have been discussed previously, the following sections provide some more detailed aspects of fusion welding processes as applied to superalloys.

Aspects of Gas Tungsten Arc Welding. All superalloys are weldable by GTAW. This process is widely used for welding thin sections and for applications where a flux residue would be undesirable. Thin sections of aluminum-containing, precipitation-hardening alloys are frequently joined without filler metal. The addition of filler metal is usually recommended for solid-solution alloys. Direct current electrode negative (DCEN) is recommended for both manual and automatic GTAW. Alternating current can be used for automatic current if the arc length can be closely controlled. Solid-solution-hardened alloys are easier to weld than precipitation-hardened or carbide-hardened alloys.

The welding arc is started by a high-frequency current. Extensions on the workpiece (start-up and run-off pads that are machined off before the weldment is put into service) frequently are used to ensure full-penetration welds and to minimize cracks in the weld metal caused by starts and stops. Heat input is kept as low as possible to minimize annealing and grain growth in the HAZ. General conditions for GTAW of nickel-base alloys are summarized in Table 9.4.

Joint Design for GTAW. The same nominal joint designs are used for GTAW and SMAW. Joint design for GMAW requires special consideration but is basically the same as GTAW with adjustments to dimensions. Unless it has been proven satisfactory by experience, a joint design that has been developed for another metal should not be used for nickel-base superalloys.

For joint design with some iron-nickel-base superalloys, designs similar to stainless steel can be used. For other applications, design must be similar to that for nickel-base superalloys. Nickel-base weld metal does not flow as readily or penetrate as deeply as steel weld metal does. Therefore, joints in nickel-base superalloys must be more open to allow placement of weld metal, and lands should be thinner to accommodate lower penetration. Excessive puddling and heat input have a detrimental effect, because loss of residual deoxidizers may result. Use of the single- and double-bevel T-joint may not be suitable in some cases because of lack of joint accessibility.

When no filler metal is used, the sections to be joined must be held tightly together (zero root opening) to promote proper fusion. Because nickel-base alloys are more viscous in the molten condition than steel, when a V-, U-, or J-groove design is used, a slightly larger bevel angle than is needed for steel is used to ensure complete penetration. When welding iron-nickel- (chromium) base alloys, V-grooves should be beveled to a 75 to 80° groove angle; U-grooves are beveled to a 30° groove angle, with a 0.187 to 0.312 in. (4.5 to 8 mm) radius. A J-groove should have a 15° bevel angle with a radius of at least 0.375 in. (9.5 mm); a 0.250 in. (6.4 mm) radius is preferred. T-joints between members of different thicknesses should have bevel or J-grooves.

A square-groove butt joint in metal up to 0.125 in. (3.2 mm) thick can be made by welding on one side only, using the proper root opening to provide full penetration. A backing strip usually is needed to produce good back reinforcement. Although a square-groove butt joint can be made in metal up to 0.250 in. (6.4 mm) thick, provided that a backing weld is used, metal thicker than 0.125 in. (3.2 mm) should preferably be beveled and welded from both sides. When this is not practical, the root opening should be increased and a backing strip should be used to ensure full penetration. When butt welding two pieces of different thicknesses, the heavier section should be machined to the thickness of the thinner section at the joint for ease of welding and for better stress distribution. Nonuniform penetration can result in undesirable crevices and voids in the underside of the joint and can create stress raisers that act as focal points for mechanical failure in service.

When pipe or tubing is used to carry corrosive materials, backing rings should be avoided if they cannot be removed after welding. Crevices between the backing ring and the tube are highly susceptible to localized corrosion.

When a product made of a precipitation-hardenable nickel-base alloy cannot be heat treated after welding (because of size or shape), the following technique can be used. Connecting pieces made of a solid-solution alloy, or one that is unaffected by the welding heat, are welded on the joint side of each component of the product, and the components plus connecting pieces are given an aging heat treatment. Welding of the final product is done at the connecting pieces. The composition and location of the connecting pieces must be carefully selected so that welds are made in noncritical locations and so that service performance of the weldment is not adversely affected. This approach is often used for vessels that cannot be stress relieved after welding and is often referred to as ‘‘safe ending.’’

Corner and lap joints should be avoided if service temperatures are high or if service conditions involve thermal or mechanical cycling. When corner joints are used, a full-thickness weld must be made. Usually, a fillet weld on the root side also is required. Joint design often affects selection of the welding process and procedure. For example, when joining thin-walled tubes to tube sheets and tubes to flanged connections, and when welding bellows joints of various types, differential melting, caused by the varying heat transfer capability of different base-metal thicknesses, may require special welding techniques. Sometimes, differential melting can be prevented by machining the thicker member to the same thickness as that of the thinner member, or by suitable preheating of the thicker member. Directing the heat of

welding to the thicker member is also beneficial. When these methods cannot be applied, a combination welding procedure may be successful.

Shielding Gases for GTAW. Argon, helium, or a mixture of argon and helium is used as shielding gas. The arc characteristics and heat pattern are affected by the choice of shielding gas. This choice should be based on welding trials for the particular production operation. Argon is normally used for manual welding; helium has shown some advantages over argon for machine welding thin sections without the addition of filler metal.

Welding-grade argon and helium should be used; oxygen, carbon dioxide, or nitrogen in the shielding gas are not used, because they reduce the service life of the tungsten electrode (in GTAW) and can cause porosity in certain alloys. An addition of about 5% H_2 to argon acts as a reducing agent and is sometimes beneficial when the work metal has not been thoroughly cleaned. However, argon with 5% H_2 should be used only for first-pass or single-pass welding, because porosity can result if this mixture is used for subsequent passes in multiple-pass welding.

Filler Metals for GTAW. Filler metals may be used with any superalloy. Filler metals used with nickel-base superalloys usually have the same general composition as the alloy being welded. However, because of high arc currents and high welding temperatures, compositions of filler metals are often modified to resist porosity and hot cracking of the weld metal. Tack welding and root-pass welding without filler metal are permissible for some alloys. However, care must be taken to avoid centerline splitting and crater cracking when no filler metal is used. To minimize cracking, concave welds should be avoided. Table 9.5 gives the compositions of filler metals commonly used in GTAW; several of these filler metals are used for welding metals other than nickel-base alloys.

For welding the precipitation-hardenable nickel-base superalloys, either a precipitation-hardenable or a solid-solution filler metal may be used, depending on service requirements. Maximum mechanical properties, particularly in thick metal, are obtained when precipitation-hardenable filler metals are used, because most of the weld deposit then is composed of hardenable filler metal. The solid-solution filler metals produce welds with lower mechanical properties, but they can be used where maximum strength is not needed. For example, consider welding IN-718 using filler metal of either Rene 41, Inconel 718, GMR 235, Hastelloy S (AMS 5838), or Inconel 82. Weld specimens using the first three filler metals (precipitation hardenable) give tensile properties similar to those of the base metal, but Hastelloy S and Inconel 82 filler metals (solid solution) give tensile properties about one-third lower than those of the base metal.

Filler metal of the ERNiCr-3 classification (Table 9.5) is used for welding iron-nickel-(chromium-) base alloys to each other and to dissimilar metals, for high-temperature service, and for nuclear applications. Filler metal of the ERNiCrFe-5 classification is used to weld nickel- (chromium-) iron-base alloys and Inconel 600. The niobium-plus-tantalum content of these filler metals minimizes hot cracking in the weld when high stress is developed, such as when welding thick metal.

Filler metal of the ERNiCrFe-6 classification is used for welding some combinations of dissimilar metals. The deposited weld metal responds to age-hardening treatments. The age-hardening response of this filler material is slight and does not exclude its use in the temperature range of 1000 to 1500 °F (540 to 816 °C).

Filler metal of the ERNiCrFe-7 classification contains aluminum, titanium, niobium, and tantalum and is used for welding the precipitation-hardenable alloys. The deposited filler metal responds to aging treatments. The weldment must be stress relieved prior to aging. Filler metals of the ERNiCrMo-3, ERNiCrMo-4, and ERNiCrMo-7 classifications are intended for welding the nickel-chromium-molybdenum alloys. Aerospace Material Specification (AMS) 5838 (Hastelloy S) is used for welding a variety of nickel-chromium, nickel-chromium-molybdenum, and cobalt- and iron-nickel base alloys. It is well suited for dissimilar welding and exhibits excellent high-temperature stability.

The filler metals listed in Table 9.5 by trade name have no applicable AWS classifications, but most have AMS designations that are given in the table. These filler metals are primarily used for welding alloys of the same composition, although they are sometimes used for welding alloys of a different

Table 9.5 Compositions of filler metals and electrode wires for arc welding of superalloys

AWS classification or trade name	Composition, %													
	C	Mn	Fe	S	Si	Cu	Ni(a)	Co	Al	Ti	Cr	Nb + Ta	Mo	Other
Nickel-based bare electrodes for GTAW and GMAW														
ERNiCr-3	0.10	2.5–3.5	3.0	0.015	0.50	0.50	67 min	(b)	. . .	0.75	18.0–22.0	2.0–3.0(c)	. . .	0.50
ERNiCrFe-5	0.08	1.0	6.0–10.0	0.015	0.35	0.50	70 min	. . .	. . .	. . .	14.0–17.0	1.5–3.0	. . .	1.0
ERNiCrFe-6	0.08	2.0–2.7	10.0	0.015	0.35	0.50	67 min	. . .	. . .	2.5–3.5	14.0–17.0	. . .	. . .	0.50
ERNiCrFe-7	0.08	1.0	5.0–9.0	0.01	0.50	0.50	70 min	. . .	0.40–1.00	2.00–2.75	14.0–17.0	0.70–1.20	. . .	0.50
ERNiCrMo-3	0.10	0.5	5.0	0.015	0.5	. . .	bal	1.0	0.4	0.4	20.0–23.0	3.15–4.15	8.0–10.0	. . .
GMR 235	0.16	0.25	9.0–11.0	0.03	0.6	. . .	bal	2.5	1.75–2.25	2.25–2.75	14.0–17.0	. . .	4.5–6.5	0.009 B
ERNiCrMo-2	0.05–0.15	1.0	17.0–20.0	0.03	1.0	. . .	bal	0.5–2.5	. . .	. . .	20.5–23.0	. . .	8.0–10.0	0.2–1.0 W
Hastelloy S	0.01	0.2	1.0	0.005	0.20	. . .	67	. . .	0.2	. . .	15.5	. . .	15.5	0.009 B, 0.02 La
ERNiCrMo-7	0.007	0.50	1.5	0.005	0.04	. . .	65	1.0	. . .	. . .	16	. . .	15.5	. . .
Haynes 556	0.10	1.5	. . .	0.005	0.40	. . .	20	20	0.3	. . .	22	0.1	3	0.9 Ta, 0.2 N, 2.5 W
ERNiCrMo-4	0.01	0.5	5.5	0.005	0.04	. . .	62	1.2	. . .	. . .	16	. . .	16	3.5 W, 0.35 V
Inconel 601	0.05	0.5	14.1	0.007	0.25	0.25	60.5	. . .	1.35	. . .	23.0	. . .	. . .	. . .
Inconel 617	0.07	0.02	0.4	0.005	0.14	. . .	54	12.5	1.0	0.24	22	. . .	9	. . .
Inconel 718	0.08	0.35	bal	0.015	0.35	0.3	50–55	1.0	0.2–0.8	0.65–1.15	17.0–21.0	4.75–5.5	2.8–5.5	(d)
Rene 41 (AMS 5800)	0.12	0.1	5.0	0.015	0.5	. . .	bal	10.0–12.0	1.4–1.6	3.0–3.3	18.0–20.0	. . .	9.0–10.5	(e)
Waspaloy (AMS 5828C)	0.07	0.10	0.75	. . .	0.1	. . .	bal	13.5	1.4	3.0	19.75	. . .	4.45	(f)
Nickel-based covered electrodes for SMAW														
ENiCrFe-1	0.08	1.5	11.0	0.015	0.75	0.50	68 min(a)	. . .	. . .	. . .	13.0–17.0	1.5–4.0	. . .	0.50
ENiCrFe-2	0.10	1.0–3.5	6.0–12.0	0.020	0.75	0.50	bal	. . .	. . .	. . .	13.0–17.0	0.5–3.0	0.5–2.5	0.50
ENiCrFe-3	0.10	5.0–9.5	6.0–10.0	0.015	1.0	0.50	bal	(g)	. . .	1.0	13.0–17.0	1.0–2.5(h)	. . .	0.50
ENiMo-1	0.12	1.0	4.0–7.0	0.030	1.0	. . .	bal	2.5	. . .	. . .	1.0	. . .	26.0–30.0	(j)
ENiMo-3	0.12	1.0	4.0–7.0	0.030	1.0	. . .	bal	2.5	. . .	. . .	2.5–5.5	. . .	23.0–27.0	(j)
ENiCrMo-3	0.10	0.5	5.0	0.015	0.50	. . .	bal	1.0(a)	0.40	0.40	20.0–23.0	3.15–4.15	8.0–10.0	. . .
ENiCrMo-2	0.10	0.5	18.5	0.005	0.5	. . .	47	1.5	. . .	. . .	22	. . .	9	0.005 B
ENiCrMo-7	0.007	0.5	1.5	0.005	0.10	. . .	65	1.0	. . .	. . .	16	. . .	15.5	. . .
ENiCrMo-4	0.01	0.5	5.5	0.005	0.04	. . .	62	1.2	. . .	. . .	16	. . .	16	3.5 W, 0.35 V
Inconel 117	0.01	0.6–1.4	1.7	0.008	0.50	0.20	52	12.0	0.2	. . .	23.5	0–0.5	9.0	. . .
Iron-nickel-chromium, iron-chromium-nickel, and cobalt-based heat-resistant alloy filler metals														
19-9 W (AMS 5782)	0.07–0.13	1.00–2.00	bal	0.030	1.00	0.50	8.00–9.50	. . .	. . .	0.10–0.30	19.0–22.0	1.00–1.30	0.35–0.65	(k)
Multimet (N-155) (AMS 5794)	0.1	1.00–2.00	bal	0.030	1.00	. . .	19.00–21.00	18.5–21.0	. . .	. . .	20.0–22.5	0.75–1.25	2.5–3.5	(m)
A-286 (AMS 5804)	0.04–0.05	1.25–1.35	bal	0.008	0.70	. . .	25	. . .	0.24–0.32	2.2	15	0.10–0.12	1.25	(n)
HS-25 or L-605 (AMS 5796)	0.10	1.5	3 max	. . .	10 max	. . .	10	bal	. . .	. . .	20	. . .	. . .	15 W
Haynes 188	0.10	0.6	1.5	0.005	0.35	. . .	22	39	. . .	. . .	22	. . .	. . .	14.5 W, 0.04 La

(a) Contains incidental cobalt. (b) Cobalt, 0.10% max, when specified. (c) Tantalum, 0.30% max, when specified. (d) Phosphorus, 0.015%; boron, 0.006%. (e) Boron, 0.01%; total of other elements, 0.003%. (f) Boron, 0.005%; zinc, 0.04%. (g) Cobalt, 0.12% max, when specified. (h) Tantalum, 0.30% max, when specified. (j) Vanadium, 0.60%; phosphorus, 0.04%; total of other elements, 0.50%. (k) Phosphorus, 0.04% max; tungsten, 1.25 to 1.75%. (m) Phosphorus, 0.040% max; tungsten, 2.00 to 3.00%. (n) Phosphorus, 0.02% max; boron, 0.0015 to 0.0022%

composition. For instance, Rene 41 and GMR 235 filler metals have been used to weld Inconel 718.

Welding Techniques with GTAW. When filler metal is used, the hot end of the wire must be kept under the shielding gas, and wire diameter should be no larger than work-metal thickness. Excessive turbulence in the molten weld pool must be avoided; otherwise, any deoxidizing elements will burn out.

To ensure a sound weld, the arc must be maintained at the shortest possible length. When no filler metal is added, arc length should not exceed 0.05 in. (1.27 mm) and preferably should be 0.02 to 0.03 in. (0.51 to 0.76 mm) long. When filler metal is added, the arc is longer, but it should be as short as possible, consistent with filler-metal diameter. Filler metals often contain elements specifically added to improve resistance to cracking and porosity. To obtain the full benefit of these elements, the finished weld should consist of about 50% filler metal.

A greater-than-normal electrode extension is needed for fillet welds and for the first few passes on heavy sections. Small-diameter filler-metal wires and more passes may be used on welds made in other than the flat position, for adequate control of weld metal. When the back sides of butt welds do not show adequate penetration, they should be ground back to sound metal, and back beads should be deposited. When possible, backing gas should be provided when welding the first side.

Aspects of Gas Metal Arc Welding. Solid-solution strengthened nickel-base alloys and, with suitable welding procedures, many precipitation-hardenable alloys can be joined by GMAW. Gas metal arc welding is best suited to the joining of thick sections of more than about 0.250 in. (6.4 mm) thick, where high filler-metal deposition rates are desirable. Gas metal arc welding is sometimes used for joining iron-nickel-base superalloys when sections are more than 0.250 in. (6.4 mm) thick, where joint design and workpiece size can compensate for the high heat input of GMAW.

Spray, pulsed arc, globular, and short circuiting metal transfer can be used. Optimal metal transfer is obtained when operating slightly above the transition from globular to spray transfer. All of these methods use electrode wire of comparatively small diameter. Incomplete fusion and oxide inclusions can occur when the short circuiting arc is used. Multiple-pass welds should be made only by highly skilled welders. Direct current electrode positive (DCEP) should be used, because the greater heating effect of reverse polarity assists in obtaining the required high melting rate.

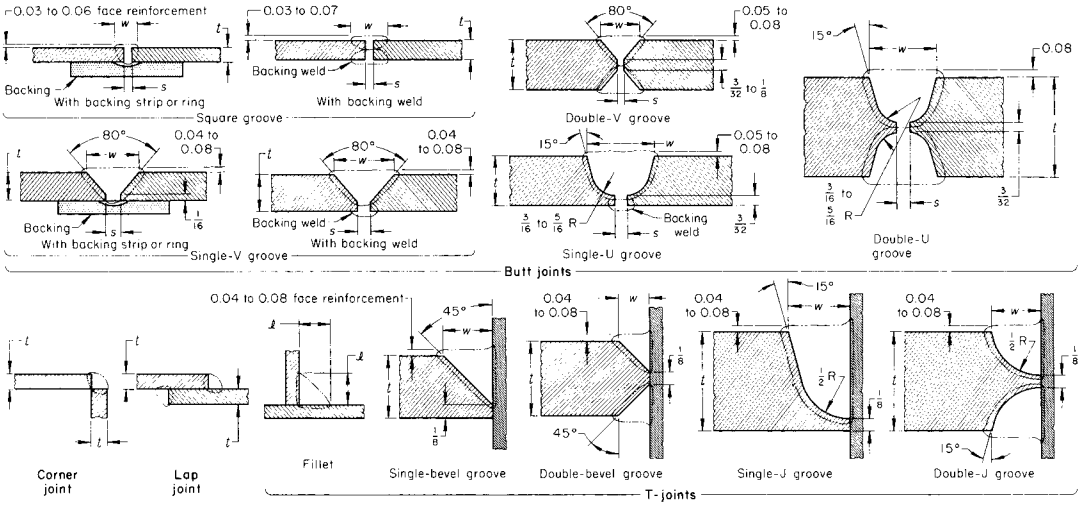
Shielding Gases for GMAW. The shielding gas for nickel-base superalloys is argon or an argon-helium mixture. Gas flow rates depend on joint design, type of metal transfer, and welding position. As the percentage of helium in an argon-helium mixture is increased, gas flow rate must be increased to give adequate protection. Pure argon is normally used for spray transfer. Other types of metal transfer commonly use argon with 25 to 30% helium added.

Joint Designs for GMAW. For U-groove designs using globular or spray metal transfer, the root radius should be decreased by about 50% and the bevel angle should be doubled, compared with those shown in Fig. 9.14. When using a short circuiting arc, the U-groove designs shown in Figure 9.14 can be used without change.

Welding Techniques for GMAW. Best results are obtained when the electrode holder is positioned at about 90° to the joint. Some inclination (up to about 15°) is permissible to permit a better view of the work, but excessive inclination can draw the surrounding atmosphere into the shielding gas, resulting in porous or heavily oxidized welds. Arc length is important. Weld spatter occurs if the arc is too short, and loss of control occurs if the arc is too long.

The manipulation and electrode holder angle used with pulsed arc welding are similar to those used with SMAW. A slight pause at the limit of the weave is required to avoid an undercut. Electrode wire compositions for GMAW are the same as those recommended for filler metals for GTAW (Table 9.5). With globular and spray transfer, wire with 0.035 in. (0.89 mm), 0.045 in. (1.14 mm), or 0.062 in. (1.57 mm) diameters are used. The short circuiting arc generally requires wire 0.045 in. (1.14 mm) or less in diameter.

General Aspects of Submerged Arc Welding. Shielded metal arc welding is widely used for joining solid-solution-strengthened nickel-base superalloys and can be used also for iron-nickel-base solid-solution-hardened



Base-metal thickness (*t*), in. (mm)	Width of groove or bead (*w*), in. (mm)	Maximum root opening (*s*), in. (mm)	Approximate amount of metal deposited, lb/ft (kg/m)	Approximate weight of electrode(a), lb/ft (kg/m)
Square-groove butt joint with backing strip or ring				
0.037 (0.940)	0.125 (3.18)	0 (0)	0.02 (0.03)	0.025 (0.037)
0.050 (1.27)	0.156 (3.97)	0 (0)	0.04 (0.06)	0.05 (0.074)
0.062 (1.57)	0.188 (4.76)	0 (0)	0.04 (0.06)	0.06 (0.089)
0.093 (2.36)	0.188–0.250 (4.76–6.35)	0.031 (0.794)	0.06 (0.09)	0.08 (0.119)
0.125 (3.18)	0.250 (6.35)	0.063 (1.59)	0.07 (0.10)	0.09 (0.134)
Square-groove butt joint with backing weld				
0.125 (3.18)	0.250 (6.35)	0.031 (0.794)	0.11 (0.16)	0.15 (0.22)
0.188 (4.76)	0.375 (9.52)	0.063 (1.59)	0.24 (0.36)	0.32 (0.48)
0.250 (6.35)	0.088 (2.24)	0.094 (2.38)	0.31 (0.46)	0.42 (0.63)
Single V-groove butt joint with backing strip or ring				
0.188 (4.76)	0.35 (8.89)	0.125 (3.18)	0.227 (0.338)	0.31 (0.46)
0.250 (6.35)	0.51 (12.95)	0.188 (4.76)	0.443 (0.659)	0.61 (0.91)
0.313 (7.94)	0.61 (15.49)	0.188 (4.76)	0.582 (0.866)	0.80 (1.19)
0.375 (9.52)	0.71 (18.03)	0.188 (4.76)	0.745 (1.11)	1.02 (1.52)
0.500 (12.7)	0.91 (23.11)	0.188 (4.76)	1.16 (2.0)	1.59 (2.37)
0.625 (15.9)	1.16 (29.46)	0.188 (4.76)	1.61 (2.40)	2.21 (3.29)
Single V-groove butt joint with backing weld				
0.250 (6.35)	0.41 (10.41)	0.094 (2.38)	0.42 (0.63)	0.58 (0.86)
0.313 (7.94)	0.51 (12.95)	0.094 (2.38)	0.54 (0.80)	0.74 (1.10)
0.375 (9.52)	0.65 (16.51)	0.125 (3.18)	0.73 (1.09)	1.00 (1.49)
0.500 (12.7)	0.85 (21.59)	0.125 (3.18)	1.21 (1.80)	1.67 (2.49)
0.625 (15.9)	1.06 (26.92)	0.125 (3.18)	1.46 (2.17)	2.00 (2.98)
Double V-groove butt joint				
0.500 (12.7)	0.40 (1.016)	0.125 (3.18)	0.89 (1.32)	1.16 (1.73)
0.625 (15.9)	0.49 (12.45)	0.125 (3.18)	1.08 (1.61)	1.48 (2.20)
0.750 (19)	0.62 (15.75)	0.125 (3.18)	1.46 (2.17)	2.00 (2.98)
1.00 (25.4)	0.81 (20.57)	0.125 (3.18)	2.42 (3.60)	3.34 (4.97)
1.25 (31.75)	1.03 (26.16)	0.125 (3.18)	2.92 (4.35)	4.00 (5.95)
Single U-groove butt joint(b)				
0.500 (12.7)	0.679 (17.2)	0.125 (3.18)	1.03 (1.53)	1.41 (2.10)
0.625 (15.9)	0.745 (18.9)	0.125 (3.18)	1.38 (2.05)	1.90 (2.83)
0.750 (19.0)	0.813 (20.7)	0.125 (3.18)	1.68 (2.50)	2.30 (3.42)
1.00 (25.4)	0.957 (24.3)	0.125 (3.18)	2.63 (3.91)	3.60 (5.36)
1.25 (31.75)	1.073 (27.25)	0.125 (3.18)	3.62 (5.39)	4.96 (7.38)
1.50 (38.1)	1.215 (30.86)	0.125 (3.18)	4.79 (7.13)	6.55 (9.75)
1.75 (44.5)	1.349 (34.26)	0.125 (3.18)	5.98 (8.90)	8.19 (12.19)
2.00 (50.8)	1.485 (37.72)	0.125 (3.18)	7.40 (11.0)	10.12 (15.06)

(continued)

(a) To obtain linear feet of weld per pound of consumable electrode, take the reciprocal of pounds per linear foot. If the underside of the first bead is chipped out and welded, add 0.21 lb/ft (0.31 kg/m) of metal deposited (equivalent to 0.29 lb/ft, or 0.43 kg/m, of consumable electrode). (b) For GMAW (except with the short circuiting arc), root radius should be one-half the value shown, and bevel angle should be twice as great.

Fig. 9.14 Joint designs and dimensions for arc welding of nickel-base and iron-nickel-base superalloys

Base-metal thickness (*t*), in. (mm)	Width of groove or bead (*w*), in. (mm)	Maximum root opening (*s*), in. (mm)	Approximate amount of metal deposited, lb/ft (kg/m)	Approximate weight of electrode(a), lb/ft (kg/m)
Double U-groove butt joint(b)				
1.00 (25.4)	0.679 (17.2)	0.125 (3.18)	2.06 (3.07)	2.82 (4.20)
1.25 (31.8)	0.745 (18.9)	0.125 (3.18)	2.76 (4.12)	3.80 (5.66)
1.50 (38.1)	0.813 (20.7)	0.125 (3.18)	3.36 (5.0)	4.60 (6.85)
2.00 (50.8)	0.957 (24.3)	0.125 (3.18)	5.26 (7.83)	7.20 (10.71)
2.50 (63.5)	1.073 (27.25)	0.125 (3.18)	7.24 (10.8)	9.92 (14.76)
Corner and lap joint				
0.062 (1.57)	. . .	. . .	0.02 (0.03)	0.04 (0.06)
0.125 (3.18)	. . .	. . .	0.05 (0.07)	0.07 (0.10)
0.188 (4.76)	. . .	. . .	0.10 (0.15)	0.14 (0.21)
0.250 (6.35)	. . .	. . .	0.19 (0.28)	0.26 (0.39)
0.375 (9.52)	. . .	. . .	0.42 (0.63)	0.57 (0.85)
0.500 (12.7)	. . .	. . .	0.74 (1.10)	1.02 (1.52)
T-joint with fillet				
. . .	. . .	0.125 (3.18)	0.03 (0.04)	0.04 (0.06)
. . .	. . .	0.188 (4.76)	0.07 (0.10)	0.10 (0.15)
. . .	. . .	0.250 (6.35)	0.12 (0.18)	0.16 (0.24)
. . .	. . .	0.313 (7.94)	0.19 (0.28)	0.26 (0.39)
. . .	. . .	0.375 (9.52)	0.27 (0.40)	0.37 (0.55)
. . .	. . .	0.50 (12.7)	0.47 (0.70)	0.64 (0.95)
. . .	. . .	0.625 (15.9)	0.74 (1.10)	1.01 (1.50)
. . .	. . .	0.750 (19)	1.07 (1.59)	1.46 (2.17)
. . .	. . .	1.00 (25.4)	1.90 (2.82)	2.60 (3.87)
Single-bevel-groove T-joint				
0.250 (6.35)	0.125 (3.18)	. . .	0.07 (0.10)	0.09 (0.013)
0.313 (7.94)	0.188 (4.76)	. . .	0.13 (0.19)	0.17 (0.25)
0.375 (9.52)	0.250 (6.35)	. . .	0.19 (0.28)	0.26 (0.39)
0.500 (12.7)	0.375 (9.52)	. . .	0.38 (0.57)	0.52 (0.77)
0.625 (15.9)	0.500 (12.7)	. . .	0.63 (0.59)	0.86 (1.28)
0.75 (19)	0.625 (15.9)	. . .	0.93 (1.38)	1.28 (1.90)
1.00 (25.4)	0.875 (22.2)	. . .	1.77 (2.63)	2.42 (3.60)
Double-bevel-groove T-joint				
0.500 (12.7)	0.188 (4.76)	. . .	0.25 (0.37)	0.34 (0.51)
0.625 (15.9)	0.250 (6.35)	. . .	0.39 (0.58)	0.54 (0.80)
0.750 (19)	0.313 (7.94)	. . .	0.56 (0.83)	0.77 (1.15)
1.00 (25.4)	0.438 (11.1)	. . .	0.99 (1.46)	1.36 (2.02)
1.25 (31.75)	0.563 (14.3)	. . .	1.54 (2.29)	2.15 (3.20)
1.50 (38.1)	0.688 (17.5)	. . .	2.21 (3.29)	3.03 (4.51)
1.75 (44.4)	0.813 (20.6)	. . .	3.00 (4.46)	4.09 (6.09)
2.00 (50.8)	0.938 (23.8)	. . .	3.90 (5.80)	5.35 (7.96)
Single J-groove T-joint				
1.00 (25.4)	0.625 (15.9)	. . .	1.78 (2.65)	2.4 (3.6)
1.25 (31.8)	0.719 (18.3)	. . .	2.50 (3.72)	3.4 (5.1)
1.50 (38.1)	0.781 (19.8)	. . .	3.23 (4.81)	4.4 (6.5)
1.75 (44.4)	0.875 (22.2)	. . .	4.09 (6.09)	5.6 (8.3)
2.00 (50.8)	0.969 (24.6)	. . .	4.93 (7.34)	6.8 (10.1)
2.25 (57.2)	1.031 (26.2)	. . .	5.80 (8.63)	8.0 (11.9)
2.50 (63.5)	1.094 (27.8)	. . .	6.94 (10.3)	9.5 (14.1)
Double J-groove T-joint				
1.00 (25.4)	0.500 (12.7)	. . .	1.48 (2.20)	2.0 (3.0)
1.25 (31.8)	0.563 (14.3)	. . .	1.90 (2.83)	2.6 (3.9)
1.50 (38.1)	0.594 (15.1)	. . .	2.56 (3.81)	3.5 (5.2)
1.75 (44.4)	0.625 (15.9)	. . .	3.11 (4.63)	4.3 (6.4)
2.00 (50.8)	0.656 (16.7)	. . .	3.81 (5.67)	5.2 (7.7)
2.25 (57.2)	0.688 (17.5)	. . .	4.51 (6.71)	6.2 (9.2)
2.50 (63.5)	0.750 (19)	. . .	5.27 (7.84)	7.2 (10.7)

(a) To obtain linear feet of weld per pound of consumable electrode, take the reciprocal of pounds per linear foot. If the underside of the first bead is chipped out and welded, add 0.21 lb/ft (0.31 kg/m) of metal deposited (equivalent to 0.29 lb/ft, or 0.43 kg/m, of consumable electrode). (b) For GMAW (except with the short circuiting arc), root radius should be one-half the value shown, and bevel angle should be twice as great.

Fig. 9.14 **(continued)** Joint designs and dimensions for arc welding of nickel-base and iron-nickel-base superalloys

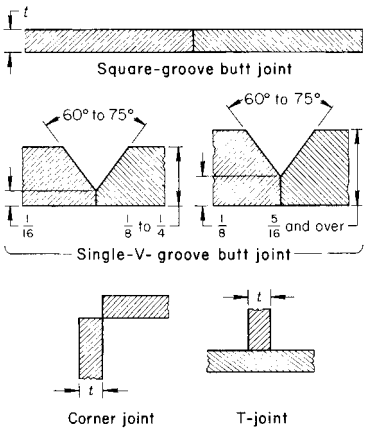
superalloys. Shielded metal arc welding is rarely used for joining precipitation-hardenable alloys. Direct current electrode positive is generally used to obtain optimal mechanical properties. Weaving is sometimes desirable, but the amount should not exceed three times the electrode diameter. Overheating can cause hot short cracking in the weld metal or the base metal and excessive carbide precipitation at grain boundaries in the HAZ. This can be avoided by using the recommended amperage ranges, maintaining a short arc length, and not weaving the electrode excessively.

Electrodes for SMAW. Electrodes are listed in Table 9.5. Electrode composition should be similar to that of the base metal with which the electrode is to be used.

Welding Conditions for SMAW. Figure 9.15 gives welding conditions for making butt, corner, and T-joints in solid-solution-strengthened superalloys by SMAW. Conditions are for nickel-base superalloys but apply as well to iron-nickel-base solid-solution-strengthened alloys.

Although the weld metal of iron-nickel base superalloys flows well, the weld metal of most nickel-base alloys does not flow readily, as previously indicated, and must be manipulated or correctly positioned. This often requires a slight weave and a short pause at the sides to allow the undercut to be filled in. When the arc is broken, it should be shortened and the travel speed increased slightly. This reduces the weld pool size. When restarting, a reverse or T-restrike should be used. The arc is struck at the leading edge of the weld crater and carried back to the rear of the crater. The travel direction is then reversed and normal weaving started. All welding slag should be removed before placing a weld in service. Catastrophic high-temperature corrosion occurs if this is not done. Adhering slag can also enhance crevice corrosion at lower temperatures. Slag should also be removed between passes to ensure high-quality, metallurgically sound welds.

More About Electron Beam Welding. Electron beam welding is high-energy-density fusion process that is accomplished by bombarding the joint to be welded with an intense (strongly focused) beam of electrons that have been accelerated up to velocities 0.3 to 0.7 times the speed of light at 25 to 200 kV, respectively. The instantaneous conversion of the kinetic energy of these electrons into thermal energy as they impact and penetrate into the workpiece on which they are impinging causes the weld-seam interface surfaces to melt and produces the weld-joint coalescence desired. Electron beam welding



Metal thickness, in. (mm)	No. of passes	Current (DCEP)(a), A	Electrode diameter(b), in. (mm)
Square-groove butt joints			
1/16 (1.59)	1	40–70	3/32 (2.38)
5/64 (1.98)	1	40–70	3/32 (2.38)
3/32 (2.38)	2	45–75	3/32 (2.38)
Single-V-groove butt joints			
1/8 (3.18)	2	40–70	3/32 (2.38)
5/32 (3.97)	2	40–70	3/32 (2.38)
3/16 (4.76)	2–3	40–70	3/32 (2.38)
1/4 (6.35)	3–4	40–130	3/32–5/32 (2.38–3.97)
3/8 (9.52)	5–6	40–130	3/32–5/16 (2.38–7.94)
1/2 (12.70)	8–10	40–130	3/32–5/16 (2.38–7.94)
Corner joints and T-joints(c)			
1/16 (0.063)	1	40–70	3/32 (2.38)
5/64 (1.98)	1	40–70	3/32 (2.38)
3/32 (2.38)	1	40–70	3/32 (2.38)
1/8 (3.18)	1	40–70	3/32 (2.38)
5/32 (3.97)	1	40–100	3/32–1/8 (2.38–3.18)
3/16 (4.76)	1	40–100	3/32–1/8 (2.38–3.18)
1/4 (6.35)	2	40–130	3/32–5/32 (2.38–3.97)
3/8 (9.52)	3	40–130	3/32–5/32 (2.38–3.97)
1/2 (12.70)	6	40–130	3/32–5/32 (2.38–3.97)

(a) Current should be within the range recommended by the electrode manufacturer. (b) Where a range is shown, the smaller diameters are used for the first pass in the bottom of the groove, and the larger diameters are used for the final passes. (c) Fillet welds

Fig. 9.15 Joint designs and dimensions for some specific configurations in SMAW of solid solution strengthened nickel- and iron-nickel-base superalloys

is used to weld any metal that can be arc welded; weld quality in most metals is equal to or superior to that produced by GTAW.

Because the total kinetic energy of the electrons can be concentrated onto a small area of the workpiece, power densities as high as 10^6 W/cm^2 can be achieved. That is higher than is possible with any other known continuous beam, including laser beams. The high-power density plus the extremely small intrinsic penetration of electrons in a solid workpiece result in almost instantaneous local melting and vaporization of the workpiece material. That characteristic distinguishes EBW from other welding methods in which the rate of melting is limited by thermal conduction.

Electron Beam Welding of Superalloys. Because of the marked differences in composition and weldability among nickel-, iron-, and cobalt-base superalloys, generalizations concerning EBW of these alloys are not useful. However, it is important to note that, if an electron beam can reach a given area of a superalloy joint, it can invariably weld the part successfully.

Solid-solution nickel-base superalloys such as Hastelloy N, Hastelloy X, and IN-625 are readily EB welded. Hastelloy B and IN-600 can be welded to type 304 stainless steel and to themselves. Precipitation-strengthened nickel-base superalloys that are rated good in weldability by the electron beam process include Inconel 700 (not U-700), IN-718, Inconel X-750, and Rene 41. IN-718 can be welded in either the annealed or the aged condition. Inconel X-750 should be welded in the annealed condition, and Rene 41 should be welded in the solution-treated condition. Other precipitation-hardened alloys that have fair weldability include casting alloys IN-713C and GMR-235 and wrought U-700 and Waspaloy.

Of the iron-nickel-base superalloys, N-155 has good electron beam weldability, and alloys 16-25-6 and A-286 are rated fair. Alloy A-286 is usually welded in the solution-treated condition; hot cracking may result if welded in the aged condition.

Of the cobalt-base alloys, HS-21 has good weldability in unrestrained joints (and is generally poor in restrained joints). Cast alloy HS-31 (X-40) has fair-to-good weldability, and alloy S-816 has fair weldability by the EBW process.

Superalloy Solid-State Joining

General. Superalloys can be joined by the following solid-state welding techniques:

- Diffusion bonding or welding (DFW)
- Friction welding (FRW)
- Inertia bonding (IB)
- Transient liquid phase bonding (TLP)

Solid-state welding (SSW) processes are those that produce coalescence and a metallurgical joint at temperatures below the melting point of the base metals being joined. These processes involve either the use of deformation, or diffusion and limited deformation, to produce high-quality joints between both similar and dissimilar materials.

Diffusion bonding, which relies on the application of pressure at the joint during the heating cycle to produce high-quality welds that match base-metal properties, has been used infrequently with superalloys. Inertia bonding, which is a form of friction welding, was used successfully to join stacks of gas turbine disks (wrought superalloys) for aircraft turbines. Friction welding also has been successfully applied to the moderate V_f γ' alloys.

Solid-state techniques such as DFW are necessary for joining ODS nickel-base superalloys, because the heat of fusion welding would completely negate the ODS effect in areas of melting and drastically reduce it in areas of long exposure to heat during a fusion welding process.

Diffusion Bonding Processes. One form of SSW, called diffusion bonding or welding, is accomplished by bringing the surfaces to be welded together (faying surfaces) under moderate pressure and elevated temperature in a controlled atmosphere, so that a coalescence of the interfaces or faying surfaces can occur. Prerequisites for accomplishing bonding include a clean and smooth surface combined with a low applied pressure and moderate-to-high temperatures. Because DFW requires heat, pressure, and a vacuum (inert gas or a reducing atmosphere), equipment is frequently custom-built by the user. The driving force for the application of diffusion welding to nickel-base superalloys stems from the relatively poor fusion weldability of precipitation-hardened superalloys and the needs of the aerospace industry to produce reliable welds for high-performance hardware. Dif-

fusion bonding could be applied to iron-nickel-base superalloys, but there is no commercial market for the product at this time.

Surface cleanliness is essential to DFW. Prior surface deformation—by scratch brushing, for example—may be beneficial. Cleanliness must be maintained up to and including the application of heat and pressure. In many instances, no intermediate layer is required to effect a satisfactory diffusion bond. In other cases, intermediate layers of foil or some sort of surface activation may be necessary to develop a sound bond. Recrystallization may occur across the bond line, but it is not necessary for achieving a full-strength joint. There is no gross deformation of the parts being joined by DFW. Stop-off may be used with this technique to prevent a specific portion of the bond line from being welded.

Under actual shop conditions, surface contaminants are invariably present, and, depending on the materials being joined, mechanisms must exist for dispersion of contaminants away from or into localized areas on the faying surface.

Diffusion bonding is usually performed at a bonding temperature equal to or greater than one-half the absolute melting temperature of the material being welded. However, the choice of joining temperature is strongly influenced by the time required for surface contaminants to diffuse away, the tendency to weld above or below a phase transformation, and the amount of load available at the faying surfaces.

Diffusion Bonding of Superalloys. Nickel-base superalloys such as U-700, IN-718, and IN-600 have been successfully diffusion welded. However, all have low carbon contents, coupled with the presence of carbide formers (chromium, titanium, and molybdenum). Because of this, organic surface contaminants can be reduced to stable carbides on the faying surfaces. Unfortunately, these materials have low interstitial solubility for oxygen, coupled with the presence of stable oxide formers (chromium, aluminum, and titanium). This phenomenon renders the base metal highly susceptible to environmental contamination. In order to achieve bonding, an interlayer is needed.

U-700, with an electroplated nickel-cobalt interlayer at the faying surface, bonded when subjected to 1 ksi (7 MPa) at 2140 °F (1172 °C) for 4 h. The resulting tensile and creep-rupture strengths were nearly equivalent to the base metal. Diffusion bonding processes require applications, at high temperatures, of moderately high pressures, with lower pressures at the highest temperatures. A long bonding time generally is required in order to guarantee the bonded joint efficiency of the components. These processes require expensive pressure equipment and consume large amounts of energy. Furthermore, there is continued concern about cleanliness (oxides, etc.) on the surfaces to be joined. Also, there is the problem of tailoring the intermediate layer to achieve a bond without the presence of brittle intermetallic compounds.

Great care must be exercised to ensure that weld surfaces are thoroughly cleaned before welding. It is also necessary to prevent recontamination during welding and to provide surface extension so that clean surfaces can come into intimate contact. Because of the previously mentioned reasons, diffusion bonding has not been widely applied to the superalloys. One limited application involved the manufacture of burner cans for the Pratt & Whitney TF30-P-100 military turbine engine. In this application, a hollow sandwich panel structure (called Finwall, Pratt & Whitney) was made by diffusion welding two Hastelloy X nickel-base superalloy facesheets to a corrugated center section.

In general, diffusion welding of the iron-base and cobalt-base superalloys has not been pursued because of the ease with which they can be fusion welded.

Friction Welding Processes. Friction welding is a process in which the heat for welding is produced by direct conversion of mechanical energy to thermal energy at the interface of the workpieces without the application of electrical energy, or heat from other sources, to the workpieces. Friction welds generally are made by holding a nonrotating workpiece in contact with a rotating workpiece under constant or gradually increasing pressure until the interface reaches welding temperature, and then stopping rotation to complete the weld. The frictional heat developed at the interface rapidly raises the temperature of the workpieces, over a very short axial distance, to values approaching, but below, the melting range; welding occurs under the influence of a pressure that is applied while the heated zone is in the plastic temperature range.

More recent technology has led to the development of linear friction welding which enables nonrotationally symmetrical parts to be joined by a solid-state method. Paired vanes, for instance, might be made with this technology.

Friction welding is classified as a SSW process, in which joining occurs at a temperature below the melting point of the work metal. If incipient melting does occur, there is no evidence in the finished weld, because the metal is worked during the welding stage.

Friction Welding of Superalloys. Most nickel-base and cobalt-base superalloys are easily friction welded to themselves and to alloy steels. The nickel-base superalloy GMR-235 can be welded to 1040 steel, IN-718 to IN-713C, and IN-713 to 8630 steel in producing jet engine parts that require high-strength bonds.

Inertion Bonding Processes. Another form of SSW, called deformation welding, is accomplished by subjecting the surfaces to be welded to extensive deformation. Melting or fusion is not associated with the process. Because diffusion welding and deformation welding both may be accomplished by the application of heat and pressure, some specific processes may share characteristics of both methods.

In the process of inertia bonding, a rotating symmetrical object (e.g., a turbine disk) is brought into contact with another nonrotating symmetrical object (e.g., another disk, a shaft, or a spacer, etc.). The rotational applied force is released, and the rotating component is forced into the other component along a centerline. The rotational energy is converted to heat energy at the interface as a linear force is applied along the rotational centerline. The rotation and friction bring the temperature to a level where a metallurgical bond is formed across the interface, but there either is no melting at the interface or any molten metal is forced out, thus achieving a solid-state bond.

Inertia Bonding of Nickel-Base Superalloys. The inertia bonding process has been applied to gas turbine engines. In principle, by bonding disks along a rotational centerline, a great deal of weight can be removed from a rotating assembly. This can be accomplished for several reasons. Many disks no longer need to have bores where they would be attached to shafts. Also, shafts only need to be stub lengths attached to ends of a bonded disk assembly instead of running much longer distances to connect disks to the appropriate compressor or turbine areas. Production applications of the inertia bonding process exist although only a limited number of large disks may have been inertia bonded. As larger and larger disks were created, larger IB machines were required, thus increasing capital costs. Precipitation-hardening alloys of the Waspaloy or Astroloy type have been joined in assemblies by use of inertia bonding.

Superplastic Forming/Bonding of Components

Superplastic forming (see schematic in Fig. 9.16) of plate and/or sheet was developed as a reduced-cost method for processing of various metals. A combination of superplastic forming and diffusion bonding has been used on some nickel-base superalloys to produce complex structures.

Brazing

General. Brazing is the melting and resolidification above about 800 °F (427 °C), in a thin gap, of an appropriate alloy chemistry to produce a metallurgical bond between two surfaces. The surfaces may be of the same or different metals. The process is akin to soldering at lower temperatures, but the strengths of brazed joints are much greater. Also, brazing does not normally use capillary attraction to draw a molten filler into the gap. Instead, a physical interlayer often is put between the bond surfaces before heating to the braze temperature.

Owing to the nature of the superalloys that need to be brazed and the necessity of keeping a clean interface for maximum strength of the brazed joints, atmosphere control is practiced. Various brazing methods have been developed, but, for superalloys, induction and furnace brazing in inert gas or vacuum atmospheres has proved to be most successful. Torch brazing is difficult and requires special precautions and techniques. Induction brazing of small, symmetrical parts is very effective, because its speed minimizes reac-

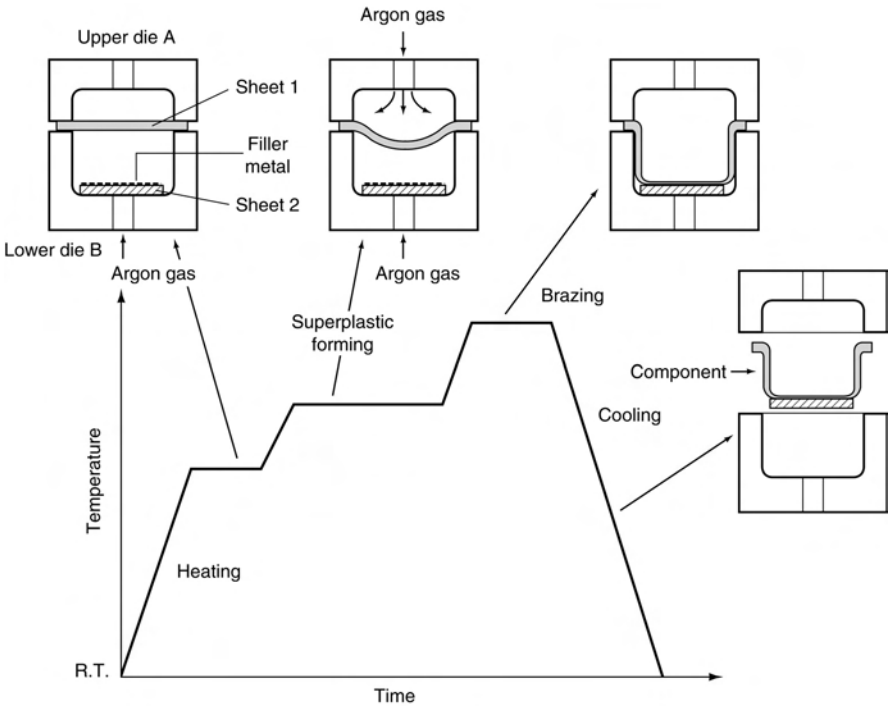


Fig. 9.16 Schematic representation of the joining of two sheets or a sheet and a plate by using superplastic behavior to form one sheet and the forming pressure to bond the sheet to the second sheet/plate by diffusion bonding or brazing

tion between braze filler metal and base metal. However, furnace brazing is favored for large parts, because uniformity of temperature throughout the heating and cooling cycle can be readily controlled.

The nature of brazing superalloys consists of selecting an appropriate braze filler plus choosing a reasonable set of brazing parameters (cleaning procedure, braze temperature, atmosphere, etc.).

Brazing Filler Metals. The AWS has classified several gold-, nickel-, and cobalt-base brazing filler metals that can be used for elevated-temperature service (Table 9.6). In addition to these brazing filler metals, there are many that are not classified by AWS. The AWS classified brazing filler metals are suitable for high-temperature service; however, if the application is for temperatures above 1800 °F (982 °C) or in severe environments, the required brazing filler metal may not be in Table 9.6.

Generally, superalloys are brazed with nickel- or cobalt-base alloys containing boron and/or silicon, which serve as melting-point depressants. In many commercial brazing filler metals, the levels are 2 to 3.5% B and 3 to 10% Si. Phosphorus is another effective melting-point depressant for nickel and is used in filler metals from 0.02 to 10%. It is also used where good flow is important in applications of low stress, where temperatures do not exceed 1400 °F (760 °C). It should be noted that excess boron, silicon, or phosphorus is detrimental to alloy properties when found in a bulk superalloy.

In addition to boron, silicon, and phosphorus, chromium is often present to provide oxidation and corrosion resistance. The amount may be as high as 20%, depending on the service conditions. Higher amounts, however, tend to lower brazement strength.

Cobalt-base filler metals are used mainly for brazing cobalt-based components, such as first-stage turbine vanes for jet engines. Most cobalt-base filler metals are proprietary. In addition to containing boron and silicon, these alloys usually contain chromium, nickel, and tungsten to provide corrosion and oxidation resistance and to improve strength and microstructural stability.

Table 9.6 American Welding Society (AWS) brazing alloys for elevated-temperature service

AWS classification	Composition, % Cr	B	Si	Fe	C	P	S	Al	Ti	Mn	Cu	Zr	Ni	Other elements total	Solidus, °F (°C)	Liquidus, °F (°C)	Brazing range, °F (°C)
Nickel-based alloy filler metals(a)																	
BNi-1	13.0–15.0	2.75–3.50	4.0–5.0	4.0–5.0	0.6–0.9	0.02	0.02	0.05	0.05	. . .	. . .	0.05	bal	0.50	1790 (977)	1900 (1038)	1950–2200 (1066–1204)
BNi-1a	13.0–15.0	2.75–3.50	4.0–5.0	4.0–5.0	0.06	0.02	0.02	0.05	0.05	. . .	. . .	0.05	bal	0.50	1790 (977)	1970 (1077)	1970–2200 (1077–1204)
BNi-2	6.0–8.0	2.75–3.50	4.0–5.0	2.5–3.5	0.06	0.02	0.02	0.05	0.05	. . .	. . .	0.05	bal	0.50	1780 (971)	1830 (999)	1850–2150 (1010–1177)
BNi-3	. . .	2.75–3.50	4.0–5.0	0.5	0.06	0.02	0.02	0.05	0.05	. . .	. . .	0.05	bal	0.50	1800 (982)	1900 (1038)	1850–2150 (1010–1177)
BNi-4	. . .	1.5–2.2	3.0–4.0	1.5	0.06	0.02	0.02	0.05	0.05	. . .	. . .	0.05	bal	0.50	1800 (982)	1950 (1066)	1850–2150 (1010–1177)
BNi-5	18.5–19.5	0.03	9.75–10.50	. . .	0.10	0.02	0.02	0.05	0.05	. . .	. . .	0.05	bal	0.50	1975 (1079)	2075 (1135)	2100–2200 (1149–1204)
BNi-6	. . .	. . .	. . .	. . .	0.10	10.0–12.0	0.02	0.05	0.05	. . .	. . .	0.05	bal	0.50	1610 (877)	1610 (877)	1700–2000 (927–1093)
BNi-7	13.0–15.0	0.01	0.10	0.2	0.08	9.7–10.5	0.02	0.05	0.05	0.04	. . .	0.05	bal	0.50	1630 (888)	1630 (888)	1700–2000 (927–1093)
BNi-8	. . .	. . .	6.0–8.0	. . .	0.10	0.02	0.02	0.05	0.05	21.5–24.5	4.0–5.0	0.05	bal	0.50	1800 (982)	1850 (1010)	1850–2000 (1010–1093)

AWS classification	Composition, % Au	Cu	Pd	Ni	Other elements total	Solidus, °F (°C)	Liquidus, °F (°C)	Brazing range, °F (°C)
BAu-1	37.0–38.0	bal	. . .	. . .	0.15	1815 (991)	1860 (1016)	1860–2000 (1016–1093)
BAu-2	79.5–80.5	bal	. . .	. . .	0.15	1635 (890)	1635 (890)	1635–1850 (890–1010)
BAu-3	34.5–35.5	bal	. . .	2.5–3.5	0.15	1785 (974)	1885 (1029)	1885–1995 (1029–1091)
BAu-4	81.5–82.5	. . .	. . .	bal	0.15	1740 (949)	1740 (949)	1740–1840 (949–1004)
BAu-5	29.5–30.5	. . .	33.5–34.5	35.5–36.5	0.15	2075 (1135)	2130 (1166)	2130–2250 (1166–1232)

AWS classification	Composition, % Cr	Ni	Si	W	Fe	B	C	P	S	Al	Ti	Zr	Co	Other elements total	Solidus, °F (°C)	Liquidus, °F (°C)	Brazing range, °F (°C)
Cobalt-based alloy filler metals																	
BCo-1	18.0–20.0	16.0–18.0	7.5–8.5	3.5–4.5	1.0	0.7–0.9	0.35–0.45	0.02	0.02	0.05	0.05	0.05	bal	0.50	2050 (1121)	2100 (1149)	2100–2250 (1149–1232)

(a) If determined, cobalt is 0.1% maximum unless otherwise specified. Source: AWS 5.8-81

Product Forms of Braze Fillers. Available forms of AWS classified and proprietary brazing filler metals include wire, foil, tape, paste, and powder. The form used is dictated frequently by the application. If the filler metal required for a specific application is only available as a dry powder, then brazing aids such as cements and pastes are available to help position the brazing filler metal.

Brazing filler-metal powders usually are atomized and sold in a range of specified particle sizes, which ensures uniform heating and melting of the brazing filler metal during the brazing cycle. These powders can be mixed with water, plasticizers, or organic cements to facilitate positioning. If the mixture must support its own weight until the brazing cycle begins, an organic binder or cement is required. These binders burn off in atmosphere brazing, and little or no residue results. When the brazing filler metal is supplied as a paste, it is simply a premixed powder and binder.

Brazing filler metals are available in the form of tapes and foils. The foils usually are made by melt spinning operations and tend to be very homogeneous microcrystalline structures. Brazing tapes are made of powder that is held together by a binder and formed into a sheet. Most foils have a high metalloid (phosphorus, silicon, boron) content, while tapes can be made from brazing filler metals that have no metalloid content. The metalloids usually are melting-point depressants and frequently form brittle phases. In some cases, where the composition is workable, such as BAu, foils can be made by cold rolling. Foil also can be produced by rolling an alloy of suitable composition into a foil before adding the metalloids. However, most of the nickel- or cobalt-base brazing filler metals require melt spinning to form foils. Tapes and foils are best suited for applications requiring a large area joint, good fit-up, or where brazing flow and wetting may be a problem.

Brazing wires of nonfabricable alloys usually are made by powder metallurgy (P/M) processes from atomized powder, and are held together by a binder or by extruding powder into wire and sintering. This form of brazing filler metal is better able to support itself than are pastes and powders of filler metal, but is not used to replace tapes or foils where precision is needed in placing the filler metal, such as for joint gaps less than 0.005 in. (0.125 mm).

Brazing Processes

Surface Cleaning and Preparation. Cleaning of all surfaces that are involved in the formation of the desired brazed joint is necessary to achieve successful and repeatable brazed joints. All obstruction to wetting, flow, and diffusivity of the thermally induced molten brazing filler metal must be removed from both surfaces to be brazed prior to fit-up assembly. The presence of contaminants on one or both surfaces to be brazed may result in void formation, restricted or misdirected filler-metal flow, and contaminants included within the solidified brazed area, which reduce mechanical properties of the resulting brazed joint. Common contaminants are oils, greases, residual zyglo fluids, pigmented markings, residual casting or coring materials, and oxides formed either through previous thermal exposures or by exposures to contaminating environments.

Chemical cleaning methods are most widely used. As part of any chemical cleaning procedure for preprocessing assemblies for brazing, a degreasing solvent to remove all oils and greases should be the first operation. This is necessary to ensure wettability of the chemicals used for cleaning. Oils and greases form a very thin film on metals, which prevents wettability by both the subsequent chemical cleaning and/or the molten filler metals. Oil and grease removers that are widely used include degreasing solutions such as stabilized perchloroethylene or stabilized trichloroethylenes. These may be used as simple manual soaks, sprays, or by suspending the parts in a hot vapor of the chemicals, commonly referred to as a vapor degreasing process. In conjunction with these processes, anodic and cathodic electrolytic cleaning also can be used. Incidentally, these types of processes are also needed in diffusion bonding operations.

A chemical cleaning procedure can be a simple single-step process or may involve multistep operations. If surfaces of the braze joint are in the machined condition, vapor degreasing may be sufficient to remove machining oils, handling oils, and zyglo penetrants to yield a sound, clean surface for

brazing. If, on the other hand, one or both of the surfaces to be brazed is not a machined surface, then additional chemical cleanings should be employed. Once vapor degreasing is accomplished, care must be taken to maintain the surface integrity of the brazed components by handling in an environmentally clean atmosphere. Additional methods of chemical cleaning to remove oxides and other adherent metallic contaminants include immersion in phosphate acid cleaners or acid pickling solutions, which are comprised of nitric, hydrochloric, or sulfuric acids or combinations of these.

Care must be taken in time of exposure for both acid cleaning and acid pickling of superalloys. Overexposure during chemical cleaning can lead to excessive metal loss, grain-boundary attack, and selective phase structure attack. As a last step in chemical cleaning, an ultrasonic cleaning in alcohol or clean hot water is recommended to ensure removal of all traces of previous cleaning solutions.

If no subsequent mechanical cleaning is used, the components to be brazed should be stored and transported to the braze preparation areas in dry, clean containers, such as plastic bags. The time between cleaning and braze application to the assembled joints should be kept as short as manufacturing processes allow.

Mechanical cleaning usually is confined to those metals with heavy, tenacious oxide films or to repair brazing on components exposed to service. Mechanical methods are standard processes—abrasive grinding, grit blasting, filing, or wire brushing (stainless steel bristles must be used). These are used not only to remove surface contaminants, but to slightly roughen or fray the surfaces to be brazed.

Care must be taken that the surfaces are not burnished and that mechanical cleaning materials are not embedded in the metals to be brazed. In grit blasting, choice of medium is critical. Wet and dry grit blasting commonly are used, but wet mediums are subject to additional cleaning requirements to remove the embedded grit. The mediums used are iron grits, silicon carbide grits, and grits comprised of brazing filler metals. Grit sizes as coarse as No. 30 (0.0232 in., or 0.59 mm) are recommended for cleaning forgings and castings. Finer grits (No. 90 and No. 100, 0.0065 and 0.0059 in., or 0.17 and 0.15 mm, respectively) are used for general blasting. All grit mediums should be changed frequently, because extensive reuse of the same medium results in loss of sharp angles or facets. Once these configurations are lost or markedly reduced in the grit medium, burnishing rather than cleaning occurs. Overused medium results in the entrapment of oxides in the metal. If possible, the angle of grit blasting should be less than 90° to the surfaces to be cleaned. This also reduces the chances of embedding the oxides or medium in the surfaces to be brazed.

Care must be taken to remove all blasting medium from the surface after mechanical cleaning, because these mediums will contaminate the braze. Iron grit may impart an iron film, which oxidizes as a rust. Aluminum oxides, if not removed, prevent wetting and flow of the brazing filler metal; thus, use of aluminum oxides is not recommended. Silicon carbide is extremely hard and has sharp facets. Consequently, it becomes embedded if an improper blasting angle is used. Blasting with a nickel brazing filler metal or similar alloy gives the best results; stainless steel blasting medium also is acceptable.

After mechanical cleaning, air blasting or ultrasonic cleaning should be used to remove all traces of loosened oxides or cleaning medium. Care must be taken to ensure maintenance of the clean surfaces and components; once cleaned, they should be assembled and brazed as soon as possible.

Certain superalloys, particularly nickel-base alloys containing high percentages of aluminum and titanium, may require a surface pretreatment to ensure maintenance of the cleaned surfaces. This surface pretreatment after cleaning is generally an electroplate of nickel, commonly referred to as nickel flashing. Thickness of the plate flashing is kept under 0.0006 in. (0.015 mm) for alloys with less than 4% titanium plus aluminum and 0.0008 to 0.0012 in. (0.020 to 0.030 mm) for alloys with greater than 4% titanium plus aluminum. This promotes wettability in the braze joint without seriously affecting the braze strength and other mechanical properties of the braze. The thickness of nickel plating may have to be increased as the brazing temperature is increased and as the time above 1800 °F (982 °C) is increased. Titanium and aluminum will diffuse to the surface of the nickel plating upon heating.

Fixturing. One prerequisite to successful brazing that is often neglected is proper fixturing. One type of fixturing is classified as cold fixturing and is used primarily for assembly purposes. In most cases, cold fixtures are made of hot and cold rolled iron, stainless alloys, nonferrous alloys, and nonmetals, such as phenolics and micarta. These fixtures are used for assembly and tack welding details; they need not be massive or heavy, but should be sturdy enough to assemble components as required by design.

Hot fixtures (fixtures used in the furnace for brazing) must have good stability at elevated temperatures and the ability to cool rapidly; metals are not stable enough to maintain tolerances during the brazing cycle. Therefore, ceramics, carbon, or graphite are used for hot fixturing. Ceramics, due to their high processing cost, are used for small fixtures and for spacer blocks to maintain gaps during brazing of small components. Graphite has been found to be the most suitable material for maintaining flatness in a high-vacuum or argon atmosphere, and it provides faster cooling because of its porosity. Graphite should be coated with an $A1_2O_3$ slurry to prevent carburization of parts during the brazing cycle. It should not be used in a pure dry hydrogen atmosphere, because it will cause carburization of the base metals by gaseous transfer. Molybdenum and tungsten may be used, but they are generally avoided because of their cost.

Controlled Atmospheres. Controlled atmospheres (including vacuum) are used to prevent the formation of oxides during brazing and to reduce the oxides present so that the brazing filler metal can wet and flow on clean base metal. Controlled atmosphere brazing is widely used for the production of high-quality joints. Large tonnages of assemblies of a wide variety of base metals are mass produced by this process.

Controlled atmospheres are not intended to perform the primary cleaning operation for the removal of oxides, coatings, grease, oil, dirt, or other foreign materials from the parts to be brazed. All parts for brazing must be subjected to appropriate prebraze cleaning operations, as dictated by the particular metals. Controlled atmospheres commonly are employed in furnace brazing; however, they also may be used with induction, resistance, infrared, laser, and electron beam brazing. In applications where a controlled atmosphere is used, postbraze cleaning generally is not necessary. In special cases, flux may be used with a controlled atmosphere:

- To prevent the formation of oxides of titanium and aluminum when brazing in a gaseous atmosphere
- To extend the useful life of the flux
- To minimize postbraze cleaning

Fluxes should not be used in a vacuum environment.

The use of controlled atmospheres inhibits the formation of oxides and scale over the whole part and permits finish machining to be done before brazing in many applications. In some applications, such as the manufacture of electronic tubes, eliminating flux is tremendously important. Some types of equipment, such as metallic muffle furnaces and vacuum systems, may be damaged or contaminated by the use of flux.

Pure dry hydrogen is used as a protective atmosphere, because it dissociates the oxides of many elements. Hydrogen with a dew point of -60 °F (-51 °C) dissociates the oxides of most elements found in superalloys, with the exception of the oxides of aluminum and titanium, which are found in most of the high-strength superalloys.

Inert gases, such as helium and argon, do not form compounds with metals. In equipment designed for brazing at ambient pressure, inert gases reduce the evaporation rate of volatile elements, in contrast to brazing in a vacuum. Inert gases permit the use of weaker retorts than required for vacuum brazing. Elements such as zinc and cadmium, however, vaporize in pure dry inert atmospheres.

An increasing amount of brazing of superalloys, particularly precipitation-hardenable alloys that contain titanium and aluminum, is done in a vacuum. Vacuum brazing in the range of 10^{-4} torr has proved adequate for brazing most of the nickel-base superalloys. By removal of gases to a suitably low pressure, including gases that are evolved during heating to brazing temperature, very clean surfaces are obtainable. A vacuum is particularly useful in the aerospace, electronic tube, and nuclear fields, where metals that react chemically with a hydrogen atmosphere are used, or where entrapped fluxes or gases are intolerable. The maximum tolerable pres-

sure for successful brazing depends on a number of factors that are primarily determined by the composition of the base metals, the brazing filler metal, and the gas that remains in the evacuated chamber.

Vacuum brazing is economical for fluxless brazing of many similar and dissimilar base-metal combinations. Vacuums are especially suited for brazing very large, continuous areas where:

- Solid or liquid fluxes cannot be removed adequately from the interfaces during brazing, and
- Gaseous atmospheres are not completely efficient because of their inability to purge occluded gases evolved at close-fitting brazing interfaces

It is interesting to note that a vacuum system evacuated to 10^{-5} torr contains only 0.00000132% residual gases, based on a starting pressure of 1 atm (760 torr). Vacuum brazing has the following advantages and disadvantages compared with other high-purity brazing atmospheres:

- Vacuum removes essentially all gases from the brazing area, thereby eliminating the necessity for purifying the supplied atmosphere. Commercial vacuum brazing generally is done at pressures varying from 10^{-5} to 10^{-1} torr, depending on the materials brazed, the filler metals being used, the area of the brazing interfaces, and the degree to which gases are expelled by the base metals during the brazing cycle.
- Certain oxides of the base metal dissociate in vacuum at brazing temperatures.
- Difficulties sometimes experienced with contamination of brazing interfaces, due to base-metal expulsion of gases, are negligible in vacuum brazing.
- Low pressure existing around the base and filler metals at elevated temperatures removes volatile impurities and gases from the metals. Frequently, the properties of base metals are improved. This characteristic is also a disadvantage when elements in the filler metal or base metals volatilize at brazing temperatures, thus changing the melting point of the filler metal or properties of the base metal. This tendency may, however, be corrected by employing partial-pressure vacuum brazing techniques.

Brazing Superalloys

General. As noted previously, superalloys are generally brazed with nickel-base or cobalt-base alloys containing boron and/or silicon, which serve as melting-point depressants. Chromium often is present to enhance oxidation and corrosion resistance. High chromium levels can lower brazement strength. Cobalt-base filler metals are used mainly for brazing cobalt-base components.

Nickel-Base Superalloys. In the selection of a brazing process for a nickel-base alloy, the characteristics of the alloy must be carefully considered. The nickel-base superalloy family includes alloys that differ significantly in physical metallurgy, such as precipitation hardened versus solid-solution strengthened, and in process history, cast versus wrought. These characteristics can have a profound effect on their brazeability.

Precipitation-hardenable alloys present several difficulties not normally encountered with solid-solution alloys. Precipitation-hardenable alloys often contain appreciable (greater than 1%) quantities of aluminum and titanium. The oxides of these elements are almost impossible to reduce in a controlled atmosphere (vacuum, hydrogen). Therefore, as previously noted, nickel plating or the use of a flux is necessary to obtain a surface that allows wetting by the filler metal.

Because the wrought forms of these alloys are hardened at temperatures of 1000 to 1500 °F (538 to 816 °C), brazing at or above these temperatures may alter the alloy properties. This frequently occurs with silver-copper (BAg) filler metals, which occasionally are used on superalloys.

Liquid metal embrittlement is another difficulty encountered in brazing of precipitation-hardenable alloys. Many nickel-, iron-, and cobalt-base alloys crack when subjected to tensile stresses in the presence of molten metals. This is usually confined to the BAg filler metals. If precipitation-hardenable alloys are brazed in the hardened condition, residual stresses are often high enough to initiate cracking.

Cleanliness, as in all metallurgical joining operations, is important when brazing nickel-

base superalloys. Cleanliness of base metal, filler metal, flux (when used for induction brazing), and purity of atmosphere should be as high as practical to achieve the required joint integrity. Elements that cause surface contamination or interfere with braze wetting or flow should be avoided in prebraze processing. All forms of surface contamination, such as oils, chemical residues, scale, or other oxide products, should be removed by using suitable cleaning procedures. The use of nickel-base filler metals offers some cost-effectiveness in this regard, because nickel-base brazes are known to be self-fluxing and thus more forgiving to slight imperfections in cleanliness.

Attempting to braze over the refractory oxides of titanium and aluminum that may be present on precipitation-hardenable nickel-base alloys must be avoided. Procedures to prevent or inhibit the formation of these oxides before and/or during brazing include special treatments of the surfaces to be joined or brazing in a highly controlled atmosphere. Surface treatments include electrolytic nickel plating and reducing the oxides to metallic form. As stated earlier, a typical practice is to nickel plate the joint surface of any alloy that contains aluminum and/or titanium. For vacuum brazing, when aluminum and titanium are present in trace amounts, use of 0.0001 to 0.0003 in. (0.0025 to 0.0076 mm) plate is considered optional. Alloys with up to 4% Al and/or titanium require 0.0004 to 0.0006 in. (0.0102 to 0.0152 mm) plate, while alloys with aluminum and/or titanium contents greater than 4% require 0.0008 to 0.0012 in. (0.0203 to 0.0305 mm) plate. When brazing in a pure dry hydrogen atmosphere, thicker plating of 0.001 to 0.0015 in. (0.025 to 0.038 mm) is desirable for alloys with high (>4%) aluminum and/or titanium contents.

Dry, oxygen-free atmospheres that are frequently used include inert gases, reducing gases, and vacuum. The brazing atmosphere, whether gaseous or vacuum, should be free from harmful constituents such as sulfur, oxygen, and water vapor. When brazing in a gaseous atmosphere, monitoring of the water vapor content of the atmosphere as a function of dew point is common practice. A dew point of −60 °F (−51 °C) is average; −80 °F (−62 °C) or below produces a better-quality braze.

During brazing, residual or applied tensile stress should be eliminated or minimized as much as possible. Also, inherent stresses present in the precipitation-hardenable alloys may lead to stress-corrosion cracking. Stress relieving or annealing prior to brazing is also recommended for all furnace, induction, or torch brazing. Brazing filler metals that melt below the annealing temperature are likely to cause stress-corrosion cracking of the base metal.

Surface Behavior of Nickel-Base Superalloys in Hydrogen and Vacuum. Aluminum and titanium, when contained in a base metal, form oxides in pure dry hydrogen unless the percentage contained is very low (approximately 0.3%) or is tied up with carbon, or as another stable compound. In a laboratory, using a vacuum atmosphere in a very clean furnace, it is claimed that aluminum and titanium oxides can be removed from the surface of the part to be brazed, leaving a clean surface for the wetting and flow of the filler metal.

In production brazing, however, furnace conditions are not as suitable, and a series of colors may be seen on the surface of the base metal, depending on the percent of titanium and/or aluminum in the base metal. Nickel-base superalloys containing very low amounts of titanium (less than 0.2%) will remain bright when processed in a good-quality atmosphere. As the percentage of titanium in the base metal is increased, the surface color of the cleanly machined base metal will vary from gray to light gold, to gold, to brown, to light purple, and finally, with high titanium contents (3 to 4%), to dark purple. With aluminum, the color fringes are gray, ranging from a very light tint to a dark gray as the percentage of aluminum in the base metal is increased.

Thermal Cycles in the Brazing of Nickel-Base Superalloys. Consideration must be given to the effect of the brazing thermal cycle on the base metal. Filler metals that are suitable for brazing nickel-base alloys may require relatively high thermal cycles. This is particularly true for the filler-metal alloy systems most frequently used in brazing of nickel-base alloys—the nickel-chromium-silicon or nickel-chromium-boron systems.

Solid-solution-strengthened nickel-base superalloys such as Inconel 600 may not be adversely affected by nickel braze filler-metal brazing temperatures of 1850 to 2250 °F

(1010 to 1232 °C). Precipitation-strengthened alloys such as IN-718, however, will display adverse property effects when exposed to brazing cycles higher than their normal solution heat treatment temperatures. Inconel 718, for example, is solution heat treated at 1750 °F (954 °C) for optimal stress-rupture life and ductility. Braze temperatures of 1850 °F (1010 °C) or above result in grain growth, producing a decrease in stress-rupture properties, which cannot be recovered by subsequent heat treatment.

Consideration of base-metal property requirements for service enables selection of an appropriate braze filler for joining a nickel-base superalloy. Lower-melting-temperature, below 1900 °F (1038 °C), braze filler metals are available within the nickel-base alloy family and within other braze filler-metal systems (see Table 9.6).

Brazing of ODS Nickel-Base Superalloys. Oxide dispersion-strengthened alloys are P/M alloys that contain stable oxide evenly distributed throughout the matrix. The oxide does not go into solution in the alloy, even at the liquidus temperature of the matrix. However, the oxide is usually rejected from the matrix upon melting of the matrix, which occurs during fusion welding, and cannot be redistributed in the matrix upon solidification. Therefore, ODS alloys are usually joined by brazing. There are two general classes of ODS alloys: the conventional (non-mechanically alloyed) and the mechanically alloyed superalloys such as MA-754. (The γ'-hardened ODS alloys saw limited use.)

Conventional ODS nickel and nickel-chromium alloys are not commercially available. However, these alloys and MA-754 were/are the easiest to braze of the nickel-base ODS superalloys. Vacuum, hydrogen, or inert atmospheres can be used for brazing. Prebraze cleaning consists of grinding or machining the faying surfaces and washing with a solvent that evaporates without leaving a residue. Generally, brazing temperatures should not exceed 2400 °F (1316 °C) unless demanded by a specific application that has been well examined and tested. The brazing filler metals for use with these ODS alloys usually are not classified by AWS. In most cases, the brazing filler metals used with these alloys have brazing temperatures in excess of 2250 °F (1232 °C). These fillers include proprietary alloys that are nickel-, cobalt-, gold-, or palladium-base.

Cobalt-Base Superalloys. The brazing of cobalt-base superalloys is readily accomplished with the same techniques used for nickel-base superalloys. Because most of the popular cobalt-base alloys do not contain appreciable amounts of aluminum or titanium, brazing atmosphere requirements are less stringent. These materials can be brazed in either a hydrogen atmosphere or a vacuum. Filler metals are usually nickel- or cobalt-base alloys or gold-palladium compositions. Silver or copper braze filler metals may not have sufficient strength and oxidation resistance in many high-temperature applications. Although cobalt-base superalloys do not contain appreciable amounts of aluminum or titanium, an electroplate or flash of nickel is often used to promote better wetting of the brazing filler metal.

Nickel-base brazing alloys, such as AWS BNi-3, have been used successfully on Haynes 25 for honeycomb structures. It has been reported that after brazing, a diffusion cycle is used to raise the braze joint remelt temperature to 2300 to 2400 °F (1260 to 1316 °C). Table 9.7 presents the effects of a high-temperature braze at 2240 °F (1227 °C) for 15 min on the mechanical properties of Haynes 25. One cobalt-base brazing filler metal (AWS BCo- 1, see Table 9.6) appears to offer a good combination of strength, oxidation resistance, and remelt temperature for use on Haynes 25 foil.

Cobalt-base superalloys, much like nickel-base alloys, can be subject to liquid metal embrittlement or stress-corrosion cracking when brazed under residual or dynamic stresses. This frequently is observed when using silver or BAg filler metals. Liquid metal embrittlement of cobalt-base superalloys by copper (BCu) filler metals occurs with or without the application of stress; therefore, BCu filler metals should be avoided when brazing cobalt-base superalloys.

Transient Liquid Phase (TLP, Pratt & Whitney) Bonding

Transient Liquid Phase Bonding Process. Transient liquid phase bonding is a kind of diffusion bonding process that relies on a transient liquid interlayer produced during the bonding process. A designed interlayer

Table 9.7 Effect of brazing on mechanical properties of Haynes 25 cobalt-base superalloy

Condition	Test temperature, °F (°C)	Ultimate strength, ksi (MPa)	0.2% offset yield strength, ksi (MPa)	Elongation, %
Tensile testing				
Mill anneal	Room	147.9 (1019.7)	69.2 (477.1)	56
After braze cycle	Room	108.3 (746.7)	69.2 (477.1)	12
Mill anneal	1500 (816)	57.4 (395.8)	30.5 (210.3)	17
After braze cycle	1500 (816)	57.0 (393.0)	33.2 (229.0)	24
Mill anneal	1800 (982)	21.0 (144.8)	18.1 (124.8)	35
After braze cycle	1800 (982)	21.5 (148.2)	18.8 (129.6)	35

Condition	Test temperature, °F (°C)	Stress, ksi (MPa)	Hours to rupture
Stress-rupture testing			
Mill anneal	1500 (816)	24.5 (168.9)	82
After braze cycle	1500 (816)	24.5 (168.9)	72.3
Mill anneal	1650 (899)	15.0 (103.4)	56
After braze cycle	1650 (899)	15.0 (103.4)	36
Mill anneal	1800 (982)	6.5 (44.8)	110
After braze cycle	1800 (982)	6.5 (44.8)	120

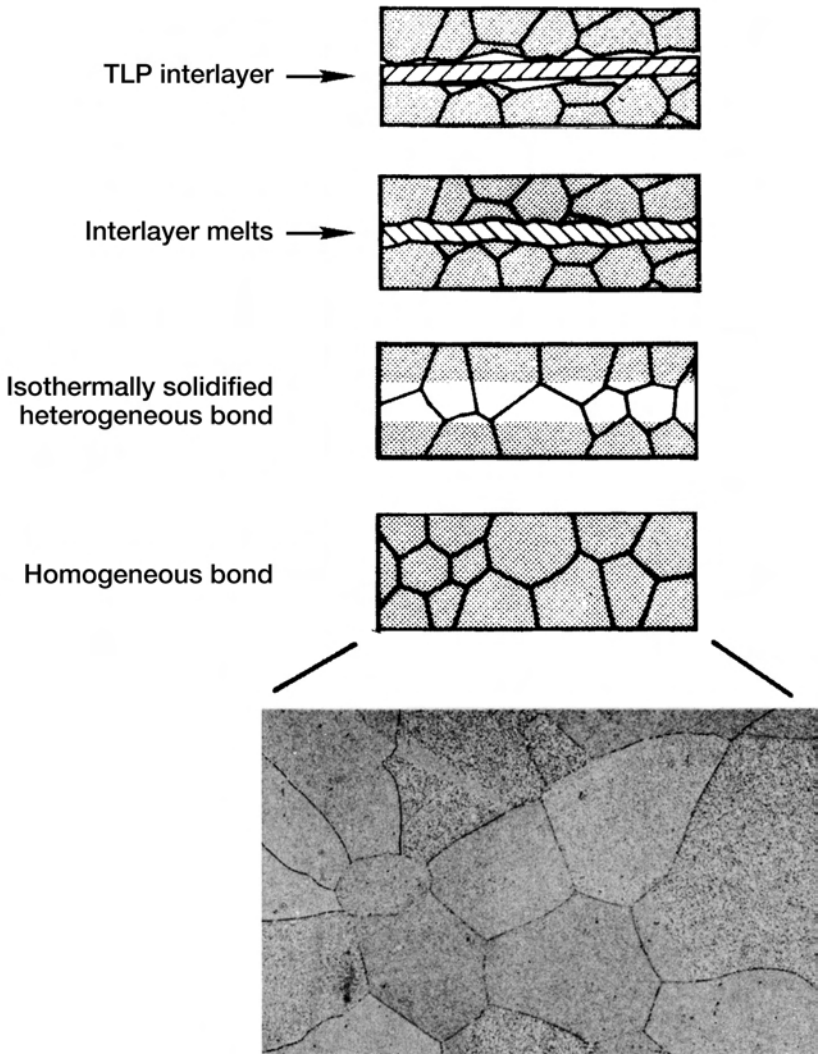


Fig. 9.17 Functional description of the TLP bonding process with micrograph showing microstructure across completed joint

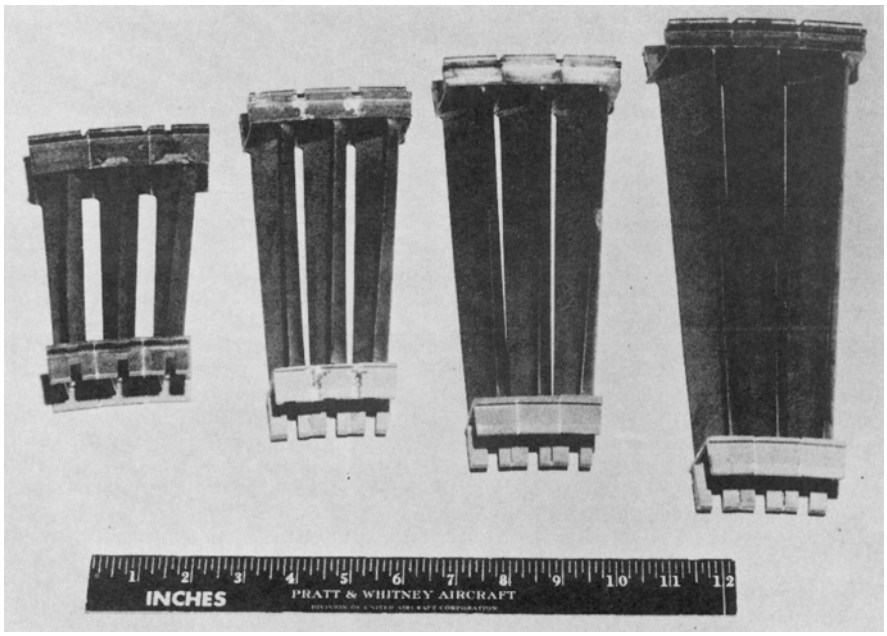
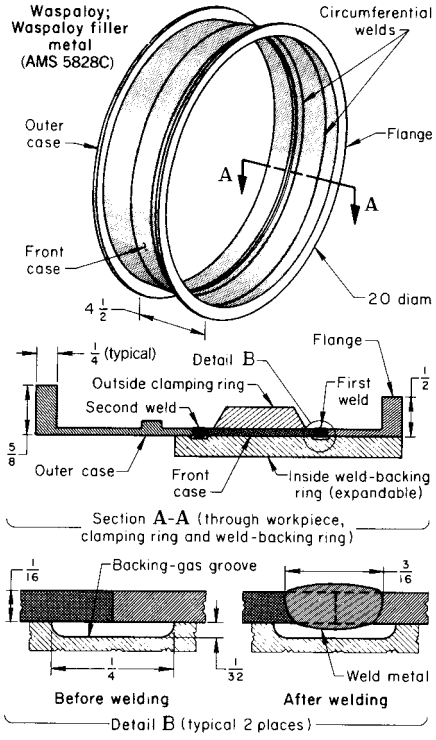


Fig. 9.18 Transient-liquid-phase-bonded low-pressure turbine vane castings for commercial aircraft gas turbine engine



Joint type	Butt
Weld type	Square-groove
Welding process	Automatic GTAW
Power supply	200 to 300 A transformer-rectifier, constant current
Torch	Mechanical, water cooled
Electrode	3/32 in. (2.38 mm) diam EWTh-2, tapered to 0.025 in. (0.635 mm) diam
Electrode extension	1/4 in. (6.35 mm)
Arc starting	High frequency
Current (DCEN):	
First weld	65–70 A
Second weld	70 A
Voltage (both welds)	9–9½ V
Welding speed:	
First weld	11 in./min (279 mm/min)
Second weld	13½ in./min (343 mm/min)
Filler metal	0.032 in. (0.813 mm) diam Waspaloy
Filler-metal feed	Constant speed, with feedback control
Filler-metal speed	20 in./min (508 mm/min)
Shielding gas (argon):	
At torch	30–35 ft^3/h (14–17 L/min)
Backing gas	8–10 ft^3/h (4–5 L/min)
Welding position	Flat
Number of passes	1

Fig. 9.19 Welding information on Waspaloy nickel-base superalloy gas turbine shroud

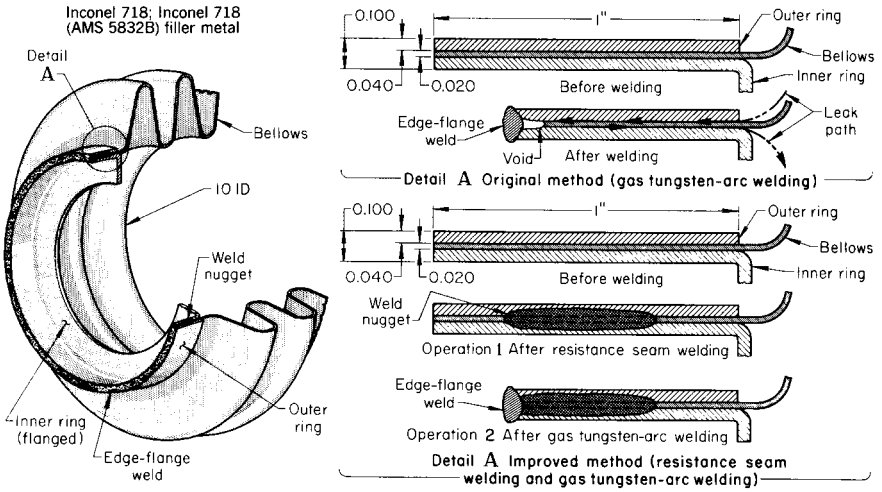
composition is applied between the two interfaces to be joined, and then, under pressure, the assembly is heated to a given temperature. The interlayer melts but does not attack the basis metals. Rather, it gradually changes its composition by diffusion of atoms to and from the basis metals to homogenize and resolidify. By suitable choice of interlayers, bonding parameters, and part design, it is possible to produce homogeneous bonds (see Fig. 9.17) that are impossible to discern both chemically and mechanically. Processing is generally in vacuum to avoid contamination problems with the surfaces to be joined.

Joining Nickel-Base Superalloys by TLP Bonding. Transient liquid phase bonding has been achieved in moderate sizes of components in nickel-base precipitation-hardened alloys of the Mar-M 200 family and the U-700 family. An example of the process is seen in Fig. 9.18, which shows TLP-bonded low-pressure turbine vane clusters produced for a commercial aircraft gas turbine engine. Although these parts were in a polycrystalline cast nickel-base superalloy, successful joints can be made in single-crystal directionally solidified parts as well. Joints also have been made in P/M superalloys, but the challenge of joining large (up to a meter or so in diameter) annulus areas on disks is one that cannot necessarily be met with consistency.

Some Superalloy Joining Illustrations

A few examples of practical superalloy joining will indicate some of the techniques and considerations applied to nickel-base superalloys intended for demanding aerospace applications.

Example: Modification of PWHT to Minimize Distortion. The gas turbine shroud



Conditions for GTAW

Joint type	Edge
Weld type	Three-member edge flange
Fixture	Rotating positioner
Power supply	300 A transformer-rectifier
Electrode	0.040 in. (1.02 mm) diam EWTh-2
Torch	300 A, water cooled
Filler metal	0.035 in. (0.889 mm) diam Inconel 718
Shielding gas	Argon at 15–18 ft^3/h (7.1–8.5 L/min)
Current	50–55 A (DCEN)
Voltage	10–12 V
Arc starting	High frequency
Arc length	0.040 in. (1.02 mm) (approx)
Welding speed	60 in./min (1524 mm/min)
Preweld cleaning	Immerse for 15 min in a solution of 30–40% HNO_3 and 2–5% HF

Fig. 9.20 Bellows joint of IN-718 nickel-base superalloy showing welding information

shown in Fig. 9.19 required two circumferential welds to join an outer case, a front case, and a flange, all made of Waspaloy. Single-pass welds were made by automatic GTAW.

Waspaloy is susceptible to PWHT cracking during service in the temperature range of 1200 to 1500 °F (649 to 816 °C). Waspaloy components, therefore, are usually solution treated prior to welding and, after welding, are again solution treated at about 1975 °F (1080 °C) for 1 h and then aged at 1400 °F (760 °C) for 16 h. In this instance, excessive distortion was encountered during solution treatment, and therefore, a modified heat treatment was developed that consisted of solution treating the components between rough and finish machining (prior to welding), stress relieving the weldments at 1600 °F (871 °C) for 1 h, then aging at 1400 °F (760 °C) for 10 h. Note: Changing the heat treatment conditions should not be done casually. It is essential that any change be done in conjunction with the customer and validated for properties by appropriate tests. It also should be noted that 1600 °F (871 °C) can cause some γ' precipitation in solution treated Waspaloy.

Joint areas were cleaned by wiping with methyl ethyl ketone, and parts were handled with gloves. The assembly was held together in a fixture with an expandable inside weld-backing ring that forced the assembly against an outside ring, as shown in Fig. 9.19. The inside ring was relieved at the roots of the joints for backing-gas flow, and the assembly was purged with argon gas for 5 min before welding was started. Welds were inspected for surface cracks before and after heat treatment by fluorescent penetrant techniques and for internal defects by x-ray radiography.

Example: Resistance Seam Welding Used with GTAW. A 10 in. (254 mm) inner diameter bellows assembly for a fuel duct for a rocket motor (Fig. 9.20) consisted of a straight section of a 0.020 in. (0.51 mm) thick bellows wall sandwiched between two 0.040 in. (1.02 mm) thick rings, all made from IN-718. A high-reliability seal weld was required. Originally, the joint was made with GTAW. The acid-cleaned assembly was mounted on a rotating turntable and welded with 0.035 in. (0.89 mm) diameter IN-718 (AMS 5832B) filler metal under argon shielding gas. When the joint was tested hydrostatically under an internal pressure of 160 psi (1103 MPa), the joint did not leak, but when it was vacuum tested with a helium mass spectrometer, significant leakage was detected.

After considerable investigation, it was determined that during welding the bellows wall melted back faster than the rings, so that weld metal was deposited at the edges of the rings only, resulting in a void that provided a leak path between the rings and the unintegrated surfaces of the bellows (see after-welding view in detail A, original method, Fig. 9.20). One small void was enough to cause a leak.

The problem was solved by RSPW and GTAW the joint. The joint was first RSPWed (see operation 1, improved method, Fig. 9.20) and then machined back to the edge of the seam weld. A gas tungsten arc edge-flange weld was deposited as before (see operation 2, improved method, Fig. 9.20). The completed combination weld was gas-tight under both methods of testing.

Superalloys: A Technical Guide, Second Edition
Matthew J. Donachie, Stephen J. Donachie, p 189-202
DOI:10.1361/stgs2002p189
Copyright © 2002 ASM International®
All rights reserved.
www.asminternational.org

Chapter 10

Machining

Introduction

General Comments. Machining is used in the manufacture of superalloy parts. Regardless of size, virtually any part needs some sort of machining done on it. Superalloys are considerably more costly to machine than conventional steels. Advances in near-net shaping with precision casting, precision forging, and powder metallurgy (P/M) processing provide important alternatives because of the difficulty and expense involved in machining superalloys. Despite these advances in near-net shape processing, machining plays a vital role in superalloy part manufacture. Much of the high machining cost is due to the fact that allowable cutting speeds for superalloys are only 5 to 10% of those used for steel.

Surface condition, particularly after machining, plays an important role in the mechanical property response of superalloys, especially under cyclic conditions. Consequently, machining processes are of concern not only with respect to ease and cost of metal removal, but also because some machining processes may significantly impact the cyclic behavior of superalloys more than others.

Methods of Machining. Most customary machining methods can be used for superalloys. The more common are:

- Turning
- Grinding
- Milling
- Broaching

Other chip-making processes used for superalloys are planing, drilling, screw machining, boring, gear cutting, and tapping. Single-point turning is the most frequently used machining process for superalloys. Conventional machining methods find much use with superalloys, because the conventional chip-making processes provide much higher metal removal rates than processes such as electrochemical machining (ECM).

Overview of Superalloy Machining

General Aspects. Superalloys generally are classified as having poor machinability. This is not surprising, because the very characteristics that render superalloys good high-temperature materials are responsible for their poor machining behavior. The iron-nickel-base superalloys, which have descended from stainless steels, usually machine more easily than the nickel-base and cobalt-base superalloys under similar conditions of heat treatment. However, the iron-base alloys do present chip-breaking problems, which often require special tool geometries.

The nickel-base and cobalt-base alloys have several characteristics in common that contribute to high machining costs. The factors affecting mechanical/machining properties of superalloys are that they:

- Retain strength at high temperatures (where common tool steels begin to soften)
- Possess unusually high dynamic shear strength
- Contain, in their microstructure, hard carbides that make superalloys abrasive

- Work harden during metal cutting
- Possess poor thermal diffusivity, which leads to high cutting tool lip temperatures
- Form a tough, continuous chip during metal cutting

Unfortunately, most of the conventional means of improving machinability are not effective with superalloys. Alloy modification and heat treatment generally are not effective as modifications are detrimental to desired mechanical properties. Hot machining holds some possibilities, but it is expensive and introduces other problems.

Use of nonconventional electrically assisted processes is another approach, but metal removal rates are very low. In addition, after the introduction of nonconventional machining methods, it was discovered that many of the conventional metal removal methods created favorable residual stresses in the surfaces of machined parts. For example, ECM of a nickel-base superalloy after conventional turning reduced the fatigue endurance stress capability by about 50% because of the removal of favorable compressive stresses. Machining method, speeds, and costs need to be balanced against the overall property advantages and/or disadvantages of a given process.

Relative Machinability. The relative machinability of several superalloys, stainless steels, refractory metals, and alloy steels is compared in Fig. 10.1 in terms of cutting speed in face milling. For the alloy steels and most of the other metals, cutters with carbide inserts were employed. For the nickel-base superalloys, the speeds shown are based on cutters with high-speed steel inserts. The slowest speeds, 20 sfm (6 m/min), were required for the three nickel-base superalloys (Rene 41, U-500, and U-700), even though the hardness of two of these was only slightly higher (and of one alloy, lower) than that of the 4340 steel (340 HB, in this comparison), which was milled at the highest speed shown, 525 sfm (160 m/min).

In addition to the large variations in machinability among different alloys, the same alloy will differ in its response to different machining operations. This is illustrated by Tables 10.1 and 10.2. In Table 10.1, the machinabilities of PH 15-7 Mo and A-286 (both precipitation-hardening iron-base alloys although only A-286 is an iron-nickel-base superalloy) are compared with that of 4130 steel, arbitrarily rated at 100% for each of the operations considered. The 4130 steel was heat treated to 15 HRC, which is equivalent to a tensile strength of 100 ksi (689 MPa). The iron-nickel-base alloys were solution treated and aged to 43 HRC, equivalent to a tensile strength of 200 ksi (1379 MPa) for PH 15-7 Mo, and to 35 HRC with a tensile strength of 163 ksi (1124 MPa) for A-286.

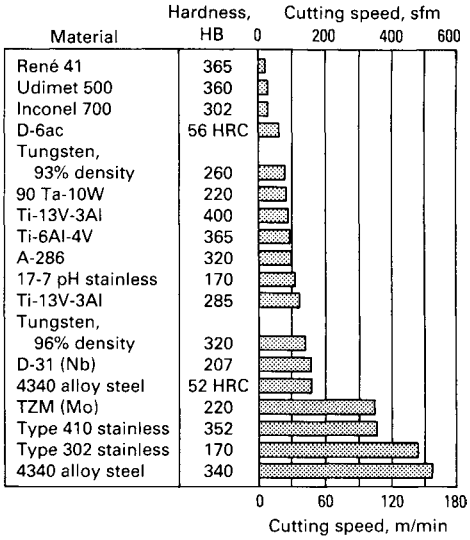


Fig. 10.1 Typical speeds for face milling of selected superalloys versus some steels, titanium, and refractory metal alloys

Table 10.1 Comparison of machining characteristics of PH 15-7 Mo (43 HRC) steel with A-286 (35 HRC) iron-nickel-base superalloy (relative to 4130 steel at 15 HRC as 100%)

	Rate of metal removal relative to 4130, %	
Operation	**PH 15-7 Mo**	**A-286**
Face milling	10.5	8.5
End milling	9.5	25.0
Straddle milling	13.9	11.5
Turning	11.5	15.6
Threading, 32–300 mm (1¼–12 in.) thread	37.7	47.0
Band sawing	26.7	28.6
Drilling, 6 mm (¼ in.) diam	14.2	3.6
Drilling, 13 mm (½ in.) diam	7.0	7.1
Reaming, 6 mm (¼ in.) diam	38.1	20.9
Reaming, 13 mm (½ in.) diam	17.4	22.4
Tapping, 6–710 mm (¼–28 in.) thread	9.8	15.2
Tapping, 13–500 mm (½–20 in.) thread	22.7	14.2
Average, all operations	**18.25**	**18.30**

Table 10.2 Comparison of machining characteristics of Inconel X-750 (15 HRC) nickel-base superalloy, Haynes 25 (24 HRC) cobalt-base superalloy, and with A-286 (35 HRC) iron-nickel-base superalloy (relative to 4130 steel at 15 HRC as 100%)

	Inconel rate of metal removal relative to 4130, %		
Operation	**X-750**	**HS-25**	**A-286**
Face milling	4.5	2.6	8.5
End milling	11.4	10.2	25.0
Straddle milling	11.6	9.6	11.5
Turning	15.2	23.2	15.6
Threading, 32–300 mm (1¼–12 in.) thread	83.0	96.0	47.0
Band sawing	22.8	19.0	28.6
Drilling, 6 mm (¼ in.) diam	10.6	12.0	3.6
Drilling, 13 mm (½ in.) diam	9.3	9.4	7.1
Reaming, 6 mm (¼ in.) diam	7.2	15.7	20.9
Reaming, 13 mm (½ in.) diam	10.0	16.7	22.4
Tapping, 6–710 mm (¼–28 in.) thread	18.9	7.4	15.2
Tapping, 13–500 mm (½–20 in.) thread	13.9	14.1	14.2
Average, all operations	**18.2**	**19.7**	**18.3**

As indicated in Table 10.1, the average rates of metal removal for the two iron-nickel-base alloys for the 12 machining operations are almost identical—18.25% for PH 15-7 Mo and 18.30% for A-286. Nevertheless, in comparing the ratings for specific machining operations, several marked differences appear. For example, although the machinability ratings for both alloys are similar in face milling and straddle milling, PH 15-7 Mo is approximately three times more difficult to machine than A-286 in end milling. Other marked differences were recorded for turning, for drilling/reaming the smaller-diameter holes, and for tapping.

Table 10.2 compares the machining characteristics of three widely used superalloys representing the three alloy classes: iron-nickel-base (A-286), nickel-base (Inconel X-750), and cobalt-base (Haynes 25). Although the average machinability ratings of the three alloys are similar, marked differences occur for several processes—for example, the threading, reaming, end milling, and drilling of 0.250 in. (6.4 mm) diameter holes.

Cutting Tool Materials. Commonly used cutting tool materials for superalloys are high-speed steels (HSS), carbides, coated carbides, boron nitride, and ceramics. Carbide tools are most common. For superalloys, high-speed cobalt tool steels are recommended for milling, drilling, tapping, and broaching. Carbides are used for turning, planing, and face milling. The most commonly used carbide is the C-2 grade (>90% tungsten carbide, balance cobalt). Modification of tungsten carbide tools with the addition of 0.5 to 4% tantalum carbide has been beneficial in improving abrasion resistance. Titanium carbide tools are not applicable for superalloys, because of the high solubility of titanium carbide in nickel and cobalt. Some common HSS and sintered carbides used for superalloy machining are listed in Tables 10.3 and 10.4, respectively.

Tool Life. In machining superalloys, the common causes of tool failure are excessive flank wear, excessive groove formation at chip edges, and the inability to meet surface finish and accuracy requirements. Other contributing factors include excessive crater depth and destruction of the cutting edge by

Table 10.3 Some high-speed tool steels for machining superalloys

	Composition, %						
Type	**C**	**W**	**Mo**	**Cr**	**V**	**Co**	**Applications**
M6	0.8	4	5	4	1.5	12	Heavy cuts, abrasion resistant
M30	0.8	2	8	4	1.25	5	Heavy cuts, abrasion resistant
M33	0.9	1.5	9.6	4	1.15	8	Heavy cuts, abrasion resistant
M34	0.9	2	8	4	2	8	Heavy cuts, abrasion resistant
M36	0.8	6	5	4	2	8	Heavy cuts, abrasion resistant
M41	1.1	6.75	3.75	4.25	2	5	Heavy cuts, abrasion resistant
M42	1.1	1.5	9.5	3.75	1.15	8	Heavy cuts, abrasion resistant
M43	1.2	2.75	8	3.75	1.6	8.25	Heavy cuts, abrasion resistant
M44	1.15	5.25	6.25	4.25	2.25	12	Heavy cuts, abrasion resistant
M46	1.25	2	8.25	4	3.2	8.25	Heavy cuts, abrasion resistant
M47	1.1	1.5	9.5	3.75	1.25	5	Heavy cuts, abrasion resistant
T4	0.75	18	. . .	4	1	5	Heavy cuts
T5	0.8	18	. . .	4	2	8	Heavy cuts, abrasion resistant
T6	0.8	20	. . .	4.5	1.5	12	Heavy cuts, hard material
T8	0.75	14	. . .	4	2	5	General purpose, hard material
T15	1.5	12	. . .	4	5	5	Extreme abrasion resistant

Table 10.4 Sintered carbides for machining superalloys

Grade	Composition, %			Transverse rupture strength	
	WC	TiC	Co	MPa	ksi
C-1	94	. . .	6	2186	317
C-2	91	. . .	9	1896	275
C-3	95.5	. . .	4.5	1379	200
C-4	97	. . .	3	1207	175
C-6	82	8	10	1482	215
C-7	80	12	8	1207	175
C-8	84	10	6	1427	207
C-50(a)	72	8	8.5	. . .	. . .

(a) Also contains 11.5% TaC

fracture, plastic flow, or melting. Surface speed is the single most important factor in determining tool life. In contrast with other workpiece materials, feed and depth of cut are also important for tool life in machining superalloys. Cutting temperatures reached for superalloys are typically 1400 to 1850 °F (760 to 1010 °C). These temperatures are sufficiently high that oxidation and diffusion become significant contributing factors to total tool wear even for the carbide tools.

Many data sets are available for typical carbide tool lives relative to cutting speeds during the turning of various superalloys. For example, A-286 (wrought iron-nickel-base superalloy) is the easiest of the superalloys to machine, with a tool life of 25 min at a cutting speed of 155 sfm (46.5 m/min).

The poorest machining characteristics are exhibited by materials such as IN-100, a cast high-strength polycrystalline (PC) nickel-base superalloy airfoil now, however, used largely as a P/M wrought product. In cast form, this alloy limits typical tool life to only 12 min at the reduced cutting speed of 30 sfm (9.2 m/min). Powder metallurgy versions of an alloy should produce better tool life, because the carbon content usually is reduced for a powder-processed wrought alloy over that same alloy in the cast version. If the P/M alloy version has previously been made by ingot metallurgy practice, the machinability may still be improved but not by as much as over the cast version. Conventional ingot metallurgy alloys do not always differ much in carbon content from the cast version (if it exists).

Because alloy and process development is proprietary within superalloy customer companies, actual machining characteristics for a widely available commercial alloy such as IN-100 could depend on relevant corporation specifications. Some corporate specifications may show greater differences in carbon content from wrought to cast versions of an alloy than do others.

If the approximate limits of superalloy machinability characteristics are defined as falling between the two extremes of turning processes on wrought A-286 and cast PC IN-100, some selected superalloys may be ranked in order of increasing ease of machining as:

- MAR-M-302 (cobalt-base)
- AF2–1DA (nickel-base)
- René 95 (nickel-base)
- U-500 (nickel-base)
- René 41 (nickel-base)
- HS-25 (cobalt-base)
- INCO 718 (nickel-base)
- Waspaloy (nickel-base)
- Incoloy 901 (nickel-base)

Similar data are available for carbide face milling, high-speed drilling, and other machining operations. The literature also provides recommendations for all machining operations for various superalloys as well as tool geometries. All data, however, are only general guides. A change in casting process from conventional to columnar grain directional solidification in a nickel-base superalloy will change the distribution and size of the carbides, owing to the differing heat transfer situations in each process type. Moreover, alloy chemistries may be changed to accommodate a different casting process. Machining of superalloys is so difficult that careful study should be undertaken for any alloy to develop a set of machining parameters that result in reasonable tool life as well as an economic analysis that covers speeds, feeds, tool materials, and cutting tool reconditioning costs.

Grinding. Grinding is characterized by very high surface speeds, high forces, and very small chip size, approximately 1% of the thickness involved in fine turning. The energy per unit volume of metal removed is high, about 30 times that for turning. Consequently, the cutting material must be very hard, refractory, and nonreactive.

It is very important that the grinding wheel cut rather than deform the metal. Increasingly

with superalloys, grinding has become a shaping technique as well as a finishing operation. Al_2O_3 abrasive, usually vitreous rather than resinoid bonded, is the primary abrasive used in grinding superalloys. Silicon carbide, diamond, and Borazon, however, have advantages for some applications.

Although grinding is used primarily to produce a finished component with good surface integrity, productivity and economy also are important factors. Wheel wear is measured by a grinding (*G*) ratio, that is, the volume of metal removed from the workpiece to the volume of the grinding wheel, that is worn away during the process. In grinding superalloys, the *G*-ratio varies from 2 to 70, whereas in grinding steel, the *G*-ratio is between 60 to 200. The approximate *G*-ratios for IN-100, HS-25, Waspaloy, IN-718, and René 41 are 4, 6, 10, 11, and 18, respectively.

Finish grinding parameters selected for good surface integrity tend to promote high wheel wear and low *G*-ratios. For rough grinding, however, conditions can be selected to give higher *G*-ratios. Rough grinding conditions should not produce grinding cracks. Wrought superalloys usually can be handled in a manner to prevent this phenomenon, but the high-strength, cast nickel-base and cobalt-base alloys are crack sensitive. Special precautions, therefore, must be taken in grinding these alloys.

Manufacturing Comparisons. Although helpful, machinability ratings based on cutting speed or metal removal rate have limited utility. Ratings that permit estimations of machining costs and shop load for production scheduling are more useful. Such manufacturing ratings reflect the consideration of noncutting time as well as cutting time. Allowance is made for such time-consuming factors as tool changes and setup adjustments (to obtain the greater rigidity needed in machining a more difficult material).

In a development program for an aerospace vehicle, simulated service tests were conducted on identical structural parts made from two nickel-base alloys (Hastelloy X and Rene 41) and a cobalt-base alloy (HS-25). Although the production of acceptable parts was the primary concern, the machining program afforded an opportunity to compile comparative information on the three alloys. Milling predominated in the machining schedule, but enough drilling, single-point cutting, shaping, and abrasive sawing operations were involved to provide a fair knowledge of the production capabilities of the three alloys in these operations.

Fittings for assembling one body joint, one wing joint, and four wing-to-body joints were produced in 14 different shapes of various degrees of complexity (see illustrations in Fig. 10.2). In all, 102 pieces were machined, 34 of each of the three alloys, in approximately 1 man-year (2119 h) of manufacturing time. Table 10.5 analyzes production time per alloy for each of the 14 parts. Table 10.6 rates

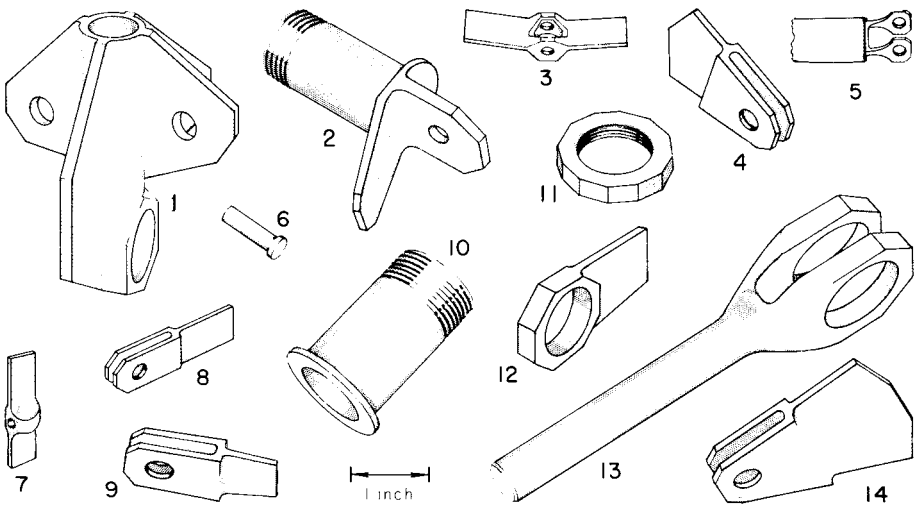


Fig. 10.2 Sketches of some parts used for machining comparisons given in Tables 10.3 and 10.4

Table 10.5 Manufacturing time required to produce the same part from Hastelloy X and Rene 41 nickel base superalloys and from HS-25 cobalt-base superalloy. Time per piece and total production time is shown. Note manufacturing ratings in Table 10.6

Part number	Production time per piece, h			Quantity machined of each alloy	Total production time, h
	Hastelloy X	Rene 41	HS-25		
1	71.8	116.5	126.0	4	1257.2
2	27.0	39.3	25.0	1	91.3
3	15.8	9.5	6.0	1	31.3
4	11.2	10.0	15.8	4	148.0
5	13.0	10.5	13.5	1	37.0
6	7.0	13.0	11.5	1	31.5
7	10.5	14.0	21.3	1	45.8
8	4.6	7.3	5.3	5	86.0
9	5.4	6.3	4.6	4	65.2
10	4.1	7.3	6.1	4	70.0
11	1.6	1.8	2.0	5	27.0
12	20.5	20.0	51.0	1	91.5
13	18.0	25.0	19.5	1	62.5
14	18.5	36.0	20.5	1	75.0
Total	**229.0**	**316.5**	**328.1**	**34**	**2119.3**

Table 10.6 Manufacturing ratings for superalloys whose production time is given in Table 10.5

Alloy	Development program		Subsequent manufacturing rating, %
	Time, h	Rating, %	
Hastelloy X	531.3	100	100
Rene 41	773.2	69	72
HS-25	814.8	65	61

the three alloys on the basis of the development program and again on the basis of subsequent manufacturing experience with the same alloys.

Specific Machining Operations

Turning. Because the superalloys retain most of their strength at cutting temperatures, more heat is generated in the shear zone, and greater tool wear occurs for a given cutting speed than with most other metals. Moreover, because the cutting of superalloys requires a larger force (about twice the force for cutting medium-carbon alloy steel in turning operations), tool geometry, tool strength, and/or rigidity of the toolholder are also important concerns.

As noted previously, carbide tools are usually used in turning heat-resistant alloys, although ceramic, coated carbide, cubic boron nitride, and HSS tools are also used. A C-2 grade is frequently selected for roughing. A C-3 grade is used in finishing. Standard carbide inserts with positive or negative rakes are suitable for the roughing and finishing of superalloys.

High-speed-steel tools are seldom used in turning superalloys, except for interrupted cuts. In such applications, HSS tools are more practical than carbide tools because of their greater shock resistance. The general-purpose, highly alloyed grades such as T15, M36, or M44 are usually selected despite higher cost. Tools of these grades have longer life than general-purpose grades such as M2 or T1.

The careful application of ceramic tools can improve productivity by allowing higher cutting speeds in the turning of superalloys. Speeds generally range from 500 to 700 sfm (150 to 200 m/mm), with feeds of about 80% those of carbide tools. Depth-of-cut notching of the tool is more pronounced when cutting superalloys with ceramic tools because of the relatively low fracture toughness of ceramics and because of the high-temperature strength of the superalloys. The tougher ceramics (SiAlON and SiC whisker-reinforced $A1_2O_3$) exhibit less depth-of-cut notching than $A1_2O_3$-TiC ceramics. These tougher ceramics are about as chemically inert as the Al_2O_3-TiC ceramics, but nevertheless they are more apt to react with iron-nickel- and cobalt-base workpieces. Consequently, SiAlON and SiC whisker-reinforced Al_2O_3 are most effective when cutting wrought nickel-base alloys. The cast nickel-base alloys, because of their grain structure, chip even the tougher ceramics.

Coated carbides yield small increases in the metal removal rate when cutting the iron-

base alloys. In general, metal removal rates can be increased only about 25%, and higher tool costs limit their application. Coated carbide tools have not yet been proven effective in significantly increasing the metal removal rates of fully aged nickel-base superalloys. The limitation is the ability of the substrates to resist deformation at substantially higher cutting temperatures, regardless of the coating materials used. Cubic boron nitride tools are used when turning the harder nickel-base (wrought and cast) and cobalt-base cast alloys.

Tool-holding devices must be given consideration equal to that of tool design when superalloys are being turned. A fivefold difference in tool life could result from variations in tool positioning, as suggested in the following example.

Example: A Mechanical Toolholder and Tool Setting Gage for a Plunge Cutting Tool. To reduce the time required for accurately positioning a brazed carbide tool used for the close-tolerance, 0.010 in. (0.25 mm) total depth plunge grooving of a 0.250 in. (6.4 mm) wide A-286 weldment flange, the mechanical holder and tool (ordinarily used for cutoff) illustrated in Fig. 10.3 were employed. A tool-setting gage of the flush-pin type helped position the tool accurately. The ease of inserting the tools, together with the positive positioning afforded by the gage, resulted in a decrease of tool-setting time from 30 min per tool to less than 5 min per tool.

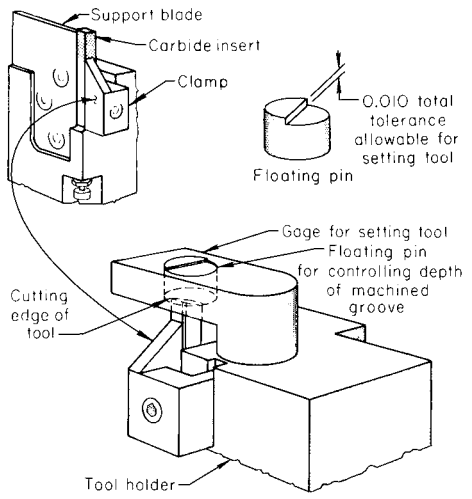


Fig. 10.3 Cuttoff tool, holder, and tool-setting guage used in plunge grooving (dimensions in inches)

Tool life also increased by 20% because of the mechanical toolholder.

Cutting Fluids for Turning. Water-soluble oils in mixtures of 1 part oil with 20 to 40 parts water are most frequently used in turning superalloys. Water-based chemical emulsions have also proved acceptable. Supplying a constant flood of cutting fluid to the cutting area is frequently more important than the composition of the fluid.

Sulfurized or chlorinated cutting oils, applied straight or diluted 1 to 1 with low-viscosity mineral oil, are used in some applications. Diluting the cutting oil with mineral oil permits better mobility (and cooling) without seriously impairing the properties of these chemically active oils. Active cutting oils are preferred to soluble oils when surface finishes are critical and when HSS cutting tools are being used. Note: If sulfurized or chlorinated oil is used as a cutting fluid, the workpieces must be thoroughly cleaned before heat treatment or high-temperature service. Serious damage to workpieces during heat treat cycles or subsequent service may result if any residue remains.

Boring and Trepanning. Superalloys are bored by methods similar to those used for turning, although the speeds and feeds must be reduced in most cases, because the same cooling and lubricating efficiency cannot be obtained as in cutting. In addition, in boring operations, the cutting tool cannot be held as rigidly as in turning. The selection and application of tool materials are similar to turning, but tool geometry varies. The end relief angle of boring tools must be varied inversely with the diameter being bored.

Trepanning has been used as a method of machining superalloys. Limited experience indicates that the speeds, feeds, and tool materials suitable for boring are satisfactory for trepanning under similar conditions. Several cast alloys have been successfully trepanned in the as-cast condition (160 to 210 HB) with cutting tools made of M2 and T5 HSS; speeds of 40 to 50 sfm (12 to 15 m/min) and feeds of 0.005 in./rev (0.13 mm/rev) were used.

Planing and Shaping. Planing has been done on some large superalloy castings, but is seldom done on wrought heat-resistant products. Workpieces are usually planed without a cutting fluid, but synthetic emulsions are sometimes used. Shaping tools with

+8° side rake, 0 to 3° back rake, 4 to 6° relief angle, and 0.045 to 0.060 in. (1.1 to 1.5 mm) nose radius are suitable for superalloys. Ram speeds must be slow; 7 to 13 sfm (2 to 4 m/min) is optimal, using a feed of 0.020 to 0.030 in./stroke (0.5 to 0.75 mm/stroke) for roughing and 0.010 to 0.015 in./stroke (0.25 to 0.40 mm/stroke) for finishing. Depths of cut range from 0.050 to 0.100 in. (1.3 to 2.5 mm) for roughing and 0.015 to 0.030 in. (0.4 to 0.75 mm) for finishing. Sulfur-free chlorinated oil applied with a brush is recommended for use as a cutting fluid in shaping.

Broaching. Although broaching is one of the more difficult machining operations, it is extensively used on superalloys, because it is often the only practical method of machining the complex contours of blades, disks (wheels), and related components of gas turbines. The successful broaching of superalloys requires careful consideration of broach design, broach material, and technique. The following points are important:

- Broach design that provides ample clearance for swarf
- Good rigidity of the machine and work combined with adequate power
- Avoidance of the tool edge rubbing against the workpiece
- Careful selection of cutting oil

Face (hook) angle, back angle, and gullet shape are important in broach design because of the behavior of superalloys in shearing and chip formation. The use of short, replaceable broach inserts can provide cost savings as well as better control of surface finish and accuracy. The pitch of the teeth should be approximately 25% more than that for broaching plain-carbon and low-alloy steels in order to provide the necessary greater chip clearance. The large pitch also will decrease the total load by reducing the number of teeth in engagement. For the same desired chip thickness, it is therefore necessary to use longer broaches or more broaches to a set. The front cutting angle (rake) can be increased by a maximum of 15°, promoting a freer chip flow and minimizing the work-hardening tendency. Rubbing contact should be avoided by providing as large a relief angle as possible, consistent with tool strength and support for the cutting edge.

Tool Modifications for Broaching. In producing gas turbine components, a change in work metal is sometimes necessary; such a change may require revisions in broach design. Improved results in broaching specific alloys and contours can be achieved by redesigning broach tools.

Example: Machining Changes Needed to Accommodate the Replacement of an Iron-Nickel-Base Superalloy, A-286, by a Nickel-Base Superalloy, Rene 41 in a Design. Redesigning a broach by increasing pitch length and land width enabled the broaching of 7½ times as many fir-tree slots (internal broaching) in Rene 41 turbine disks for a gas turbine as with the conventional design. The disks were first- and second-stage gas turbine units, requiring 119 and 109 attachment slots, respectively.

The broach of the original conventional design had been used with reasonable success on similar parts made of A-286. However, when it was tried on Rene 41 disks using the same operating conditions as for A-286, only eight slots could be obtained per broach resharpening. Not only were tools being expended by wear and excessive grinding, but tooth breakout occurred after several grinds. The revised design, with stronger teeth, enabled the broaching of 60 or more slots per broach sharpening. Use of a backoff angle of only 1° for the full-form slot shown in Fig. 10.4 extended the life of a broach to 12 or more sharpenings. Broaches were sharpened as soon as chips fused to the cutting edge and could not be brushed off freely. Broaches had smooth surfaces, 10 μin. (0.25 μm), and teeth were ground to a sharp edge (no flat land). A broaching speed of 6 sfm (1.8 m/

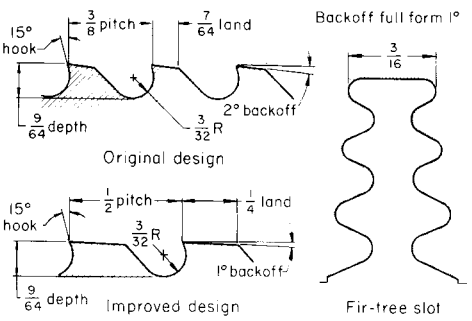


Fig. 10.4 Original (top left) tool design for A-286 iron-nickel-base superalloy and, (bottom left) improved tool design for Rene 41 to broach same slot (right) in a gas turbine (dimensions in inches)

min) yielded the best results, and the machine used had sufficient capacity to provide smooth cutting at this low speed. Grade M2 HSS was an acceptable tool material if nitrided and oxide coated by steam, but best results were obtained using T15 (65 to 67 HRC). All tools made from Tl5 were tempered three times and were oxide coated after grinding.

Example: Redesign of a Tool for Broaching X-40 Cobalt-Base Superalloy Turbine Vanes. Redesign provided improvement in both tool life and surface finish during broaching the root form in X-40 turbine vanes at low hardness (10 to 15 HRC) when tools were altered to a large 45° shear angle and a sharper positive face angle. For this soft cast alloy, chip formation was a problem when a small 5° shear angle was tried because of the probability of chipping the work at the exit of the cut. Details of the original and improved tools are given in Table 10.7. The changes in face angle and backoff clearance, and especially the increase in shear angle, almost completely eliminated chipping. The productive life of the high-speed steel broach of the original design averaged 300 pieces per setup. However, after the tooth profile was redesigned, the broach averaged 13,000 pieces per setup. The operation used rigid fixturing, pressurized cutting fluid, and a horizontal broaching machine.

High-speed steel is usually used for broaching superalloys. The more highly alloyed grades of HSS, such as T4, T5, and T6, are generally superior in terms of broach wear and life. Although acceptable results can be obtained with an M2 broach for some applications involving iron-base heat-resistant alloys (such as A-286), M3 (class 2) broaches are near the minimum in alloy content (only slightly higher than general-purpose grades) usually considered suitable for broaching heat-resistant alloys. The selection of solid broaches versus those with inserted cutting edges depends on the size and design of the broach as well as on cost. Cost is usually the deciding factor. In many applications (particularly when large broaches are being used), cost can be decreased by using HSS inserts in an alloy steel body. Assuming that the other factors are constant, whether broaches are solid or have inserts will not influence broach performance.

Table 10.7 Improved tool design for broaching a root form in gas turbine vanes of X-40 cobalt-base superalloy

Broach detail	Original	Improved
Face angle, degrees	18	12
Backoff clearance, degrees	2	4
Pitch, mm (in.)	7.1 (9/32)	8.7 (11/32)
Tooth depth, mm (in.)	6 (1/4)	4.8 (3/16)
Shear angle, degrees	5	45
Tool life, number of pieces per setup	300	13,000

Cutting Fluids for Broaching. The main difficulty in broaching superalloys usually lies in a fusion buildup on the tip of the tooth and consequent rapid wearing of the edges. A good cutting fluid can help considerably. By rapidly wetting the surfaces in contact, the cutting fluid inhibits welding between the chip and the tool edge. A flood of sulfochlorinated oil over the area being broached is preferred and, in most applications, is mandatory for acceptable results. In some applications, cutting fluids similar to thread cutting oil have been used successfully, but the use of such fluids is usually a compromise, especially when broaching nickel-base or cobalt-base superalloys.

In one instance, a change to sulfochlorinated oil improved results in broaching a 16-25-6 iron-nickel-base solid-solution-strengthened superalloy (ordinarily one of the easier-to-broach superalloys). Such oils commonly contain about 1% active sulfur, along with chlorine and synthetic additions. A plentiful supply of cutting fluid in the area being broached is of equal, if not greater, importance than fluid composition. Preferably, cutting fluid is supplied under pressure up to about 5 psi (35 kPa). To obtain the lower viscosity required for use in pressure systems, the cutting oil can be diluted with plain mineral oil. A mixture of one part concentrated cutting oil and one part mineral oil has lower viscosity than concentrated cutting oil and is adequate for most applications. Cutting fluids with viscosity higher than 300 Saybolt universal seconds (SUS) are not recommended for broaching. As noted for turning, thorough cleaning of workpieces broached with chemically active oils (sulfurized or chlorinated) is extremely important before heat treatment or high-temperature service in order to prevent damage to the workpiece.

Drilling Concepts. The superalloys can be drilled by conventional drilling methods, but

several nontraditional machining methods provide important alternatives because of the forces required in the conventional drilling of these alloys. Nontraditional drilling methods are particularly attractive when deep, small-diameter holes must be drilled in superalloys. When conventional drilling is employed, the high forces produced necessitate maximum rigidity of the machine, tools, and setup. In terms of tool design, the most important single requirement is that the drills be as short and rigid as possible within the limiting requirements of the workpiece and setup. The conventional drilling of heat-resistant alloys is performed with gun drills, twist drills, or oil-hole drills. Table 10.8 presents one concept of grouping some superalloys for convenience in comparing certain machining properties. Some inconsistencies in grouping exist as, for example, where Rene 77 (actually an electron vacancy—N_V—controlled U-700) and Astroloy performance has caused these alloys to be grouped separately. This is surprising, because Astroloy and U-700 are very close in chemistry and are often treated for discussion (when in wrought form) as a single alloy version.

Table 10.9 lists the typical applications of these drills in terms of hole size and the various superalloys as they have been grouped in Table 10.8. Gun drills have the largest range of hole size applications, while twist drills have the smallest range. Oil-hole drills are helpful in deep-hole drilling and can sometimes achieve hole depths up to 30 diameters.

Twist Drills. Stub-length screw-machine drills, type-C aircraft drills with accurately ground split points, rail drills, and extra-heavy web drills are recommended. These heavy-duty drills yield much better results for twist drills than standard jobbers-length drills because of their greater rigidity.

The crankshaft or split points, which are standard for type-C aircraft and heavy-web drills, are preferred for drilling all iron-nickel-base superalloys harder than 400 HB and other superalloys harder than 350 HB. Drills with standard chisel-edge points can be used for softer alloys. Drill wear and life can be controlled to some extent by modifying the drill point. Chipping of drill corners can be reduced by decreasing the point angle; however, severe wear at the point can be reduced by increasing the point angle to 135°. Excessive margin wear can be eliminated by using a dual-angle (118°/90°) lip. All drills should be machine ground to very close accuracy. A slight amount of runout or point eccentricity will greatly reduce drill life.

The effect of drill design modification can be seen in the case of drilling solution-treated and aged Astroloy nickel-base superalloy. Drills with split points were tested against

Table 10.8 Grouping of superalloys for reference in comparisons for nominal speeds and feeds

Group(s)	Alloys
Ni Wrt 1	Incoloy 901, Incoloy 903, Inconel 617, Inconel 625, Inconel 706, Inconel 718, Inconel X-750, Inconel 751, M252, Nimonic 75, Nimonic 80A, Waspaloy, Inconel MA 754(b)
Ni Wrt 2	Astroloy IN-102, Inconel 700, Nimonic 90, Nimonic 95, Rene 41, Rene 63, Udimet 500, Udimet 700, Udimet 710
Ni Wrt 3	Rene 95, Rene 77, Inconel MA 6000(b)
Ni Wrt 4	Hastelloy B, Hastelloy B-2, Hastelloy C, Hastelloy C-276, Hastelloy S, Hastelloy X, Inconel 600, Inconel 601, Refractoloy 26, Udimet 630
Ni Wrt 5	TD-nickel
Ni Cast 1	Hastelloy B, Hastelloy C, ASTM A297, grades HW and HX, ASTM A608 grades HW50, HX50
Ni Cast 2	B-1900, IN-100 (Rene 100), IN-738, IN-792, Inconel 713C, Inconel 718, M252, MAR-M-200, MAR-M-246, Rene 80, TRW VI A, Udimet 500, Udimet 700
Co Wrt	AiResist 213, Haynes 25 (L-605) Haynes 188, J-1570, S-816
Co Cast	AiResist 13, AiResist 215, Haynes 21, MAR-M-302, MAR-M-322, MAR-M-509, NASA Co-W-Re, WI-52
Fe Wrt	A-286, Discaloy, Incoloy 800, Incoloy 801, Incoloy 802, N-155, V-57, W-545, 16-25-6, 19-9DL, Incoloy MA 956(b)
Fe Cast 1	ASTM A297 grade HC
Fe Cast 2	ASTM 351 grades HK-30, HK-40, HT-30
Fe Cast 3	ASTM A297 grades HD, HE, HF, HH, HI, HK, HL, HN, HP, HT, HU; ASTM A608 grades HD50, HE35, HF30, HH30, HH33, HI35, HK30, HK40, HL30, HL40, HN40, HT50, HU50

(a) Ni Wrt, nickel-base wrought alloy: Ni Cast, nickel-base casting alloy: Co Wrt, cobalt-base wrought alloy: Co Cast, cobalt-base casting alloy: Fe Wrt, iron-base wrought alloy; Fe Cast, iron-base casting alloy. (b) In the tables on speeds and feeds, the mechanically alloyed products are sometimes listed separately. Otherwise the grouping and hardness of the mechanically alloyed products provides nomimal feeds and speeds.

Table 10.9 Typical range of hole sizes when drilling superalloys with gun, twist, or oil-hole drills
For holes larger than 50 mm (2 in.) in diameter, spade drills or trepanning tools are needed.

Alloy group from Table 10.8	Condition	Hardness, HB	Range of nominal hole size					
			Gun drills(a)		Twist drills(b)		Oil-hole drills(c)	
			mm	in.	mm	in.	mm	in.
Ni Wrt 1	Annealed or solution treated	200–300	1.5–50	1/16–2	3–19	1/8–3/4	3–38	1/8–1 1/2
Ni Wrt 1	Solution treated and aged	300–400	1.5–50	1/16–2	3–19	1/8–3/4	3–38	1/8–1 1/2
Ni Wrt 2	Solution treated	225–300	1.5–50	1/16–2	3–19	1/8–3/4	3–38	1/8–1 1/2
Ni Wrt 2	Solution treated and aged	300–400	1.5–50	1/16–2	3–19	1/8–3/4	3–38	1/8–1 1/2
Ni Wrt 3	Solution treated	275–390	1.5–50	1/16–2	3–19(d)	1/8–3/4(d)	3–38	1/8–1 1/2
Ni Wrt 3	Solution treated and aged	400–475	. . .	. . .	3–19(d)	1/8–3/4(d)	3–38	1/8–1 1/2
Ni Wrt 4	Annealed or solution treated	140–220	1.5–50	1/16–2	3–25	1/8–1	3–38	1/8–1 1/2
Ni Wrt 4	Cold drawn or aged	240–310	1.5–50	1/16–2	3–25	1/8–1	3–38	1/8–1 1/2
Ni Wrt 5	As-rolled	180–200	1.5–50	1/16–2	3–50	1/8–2	3–38	1/8–1 1/2
Ni Cast 1	As-cast or cast and aged	200–375	1.5–50	1/16–2	3–19	1/8–3/4	3–38	1/8–1 1/2
Ni Cast 2	As-cast or cast and aged	250–320	1.5–50	1/16–2	3–19	1/8–3/4	3–38	1/8–1 1/2
Ni Cast 2	As-cast or cast and aged	320–425	. . .	. . .	3–19(d)	1/8–3/4(d)	6–25(e)	1/4–1(e)
Co Wrt	Solution treated	180–230	1.5–50	1/16–2	3–19	1/8–3/4	3–38	1/8–1 1/2
Co Wrt	Solution treated and aged	270–320	1.5–50	1/16–2	3–19	1/8–3/4	3–38	1/8–1 1/2
Co Cast	As-cast or cast and aged	220–290	1.5–50	1/16–2	3–25	1/8–1	3–38	1/8–1 1/2
Co Cast	As-cast or cast and aged	290–425	. . .	. . .	3–19(d)	1/8–3/4(d)	6–25(e)	1/4–1(e)
Fe Wrt	Solution treated	180–230	1.5–50	1/16–2	3–25	1/8–1	3–38	1/8–1 1/2
Fe Wrt	Solution treated and aged	250–320	1.5–50	1/16–2	3–25	1/8–1	3–38	1/8–1 1/2
Fe Cast 1	Annealed	135–185	1.5–50	1/16–2	3–50	1/8–2	3–50	1/8–2
Fe Cast 2	Annealed or normalized	135–185	1.5–50	1/16–2	3–50	1/8–2	3–50	1/8–2
Fe Cast 3	As-cast	160–210	1.5–50	1/16–2	3–50	1/8–2	3–50	1/8–2
MA-754	Mechanically alloyed	277	1.5–50	1/16–2	1.5–17	1/16–11/16	1.5–38	1/16–1 1/2
MA-956	Mechanically alloyed	270	1.5–50	1/16–2	1.5–17	1/16–11/16	1.5–38	1/16–1 1/2
MA-6000	Mechanically alloyed	450	1.5–50	1/16–2	3–17(d)	1/8–11/16(d)	3–38	1/8–1 1/2

(a) Single-flute carbide gun drill. (b) HSS drills except as specified in footnotes. (c) HSS or carbide drills except as specified in footnotes. (d) Carbide twist drill. (e) Carbide drill only. Source: Metcut Research Associates Inc.

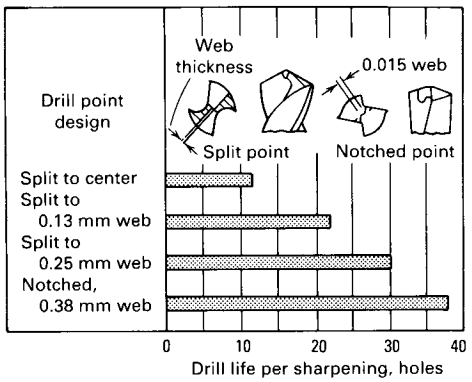


Fig. 10.5 Effect of drill-point design on life of T15 drills when drilling 0.310 in. (7.87 mm) deep holes in 0.800 in. (20 mm) thick Astroloy nickel-base superalloy

drills with notched points to determine the effect of point design on drill life. The service lives of three split points and of one notched point are plotted in Fig. 10.5. Of the split points, the least satisfactory results were obtained with a point split to center (no web thickness). Split-point designs with web thicknesses of 0.005 to 0.010 in. (0.1 to 0.25 mm) exhibited longer service lives. However, a notched point, with a 0.015 in. (0.4 mm) web, yielded the best results. All drills had 135° point angles. Additional tests confirmed the finding that a 135° point angle is superior to 118°. Clearance angles of 9 to 10° proved superior in supplementary tests to clearance angles of 7 to 8° and 11 to 120°. All drills were made of T15 HSS and were operated at 11.2 sfm (3.41 m/mm) with a feed of 0.002 in./rev (0.05 mm/rev). Cutting fluid was a sulfochlorinated concentrate of mineral and fatty oil.

High-Speed Steel Twist Drills. High-speed steel twist drills are used when drilling superalloys. In many applications, twist drills made of the general-purpose grades have proved satisfactory, as judged by the number of holes drilled and by the initial cost of the drills and the cost of resharpening. The premium grades of HSS, such as T15, M33, or M36, are preferred for drilling many of the superalloys, and their use is often mandatory for obtaining acceptable drill life.

The higher cost of the drills made from the more highly alloyed HSS (commonly about

four times the cost of their general-purpose counterparts) and the higher cost of resharpening are often warranted by increased tool life. However, a new application can usually be started with drills made of a general-purpose HSS, and a premium grade is then used only when the need for it has been established. Various surface treatments such as nitriding also can be applied to HSS drills to improve drill life.

Gun Drills. Gun drills are recommended for the deep-hole drilling (depths greater than 3 diameters) of larger diameters (up to 2 in., or 50 mm) or in the more difficult-to-machine alloys, such as:

- Wrought nickel-base precipitation-hardened alloys of the type Rene 95, Rene 77, and Astroloy
- Cast nickel-base precipitation-hardened alloys of the type IN-100 (Rene 100), Rene 80, and MAR-M-247
- Cast cobalt-base alloys of the type MAR-M-302 and MAR-M-509

This type of drill tends to steady itself, and it avoids the work hardening that occurs at the extremes of point with a standard twist drill (where the cutting speed varies from a maximum at the hole periphery to zero at the center).

Oil-Hole Drills. Oil-hole drills are used to advantage for the deep drilling of small holes, in which frequent retraction for lubrication and chip clearance might otherwise be required. Because these drills have polished flutes and chip breakers ground into the cutting edge, they provide forced lubrication at the cutting area and avoid coiled chips that might clog flutes.

Fixturing for Drilling. Because the successful drilling of most heat-resistant alloys depends on the rigidity of the workpiece, fixturing is important. When the workpiece is too thin or too weak to withstand clamping forces, special techniques must be employed, such as filling portions of the workpiece with a low-melting alloy to give it added support and rigidity. Note, again, that caution is required in the use of low-melting alloys, lest some contamination of the surface result in liquid metal embrittlement or surface attack during subsequent heat treatment or service exposure.

Tapping and Thread Milling. Machining internal threads in heat-resistant alloy workpieces is especially difficult, mainly because the surface to be threaded work hardens during the operation (drilling, reaming, or boring) that prepares the hole for threading. Therefore, the preliminary operations should be planned so that the tools continuously cut chips of substantial thickness; this is done to prevent burnishing of the workpiece. Because reamed holes are the most likely to cause difficulty in tapping (particularly in nickel-base and cobalt-base alloys), chip thickness in reaming should be no less than 0.005 in. (0.13 mm) and preferably 0.010 in. (0.25 mm) or more.

Most production problems in tapping superalloys are more readily solved by some alteration in the method of preparing the holes than by changes in the tapping operation. Subject to the limitation on chip thickness mentioned in the preceding paragraph, holes should be made to maximum rather than minimum size to reduce the amount of metal to be removed, thus prolonging tap life.

General Tapping Practice. Drill presses are ordinarily used for the tapping of superalloys, because production lots are usually small. For large production lots, the cost of tapping can be decreased by using turret lathes or automatic chucking machines. Regardless of the machine used, it should be equipped with a mechanical feed, such as lead control and, whenever possible, torque-limiting tapping heads with axial float should be used in conjunction with automatic feed. Electrodischarge machining also has been used to produce internal threads on superalloys.

For small production quantities, taps made of a general-purpose grade of HSS (such as M1) will produce satisfactory results in superalloys, but surface treatment of the taps by liquid nitriding is recommended. When larger quantities are tapped, the higher cost of taps made of one of the more highly alloyed HSS (such as M4, M36, or T15) is usually warranted.

Cutting Fluid. Sulfochlorinated oils should be used for tapping all heat-resistant alloys, and the oil should be supplied in plentiful amounts during the tapping operation. Recommended practice is to force the cutting fluid under pressure of about 5 psi (35 kPa) through a nozzle directly into the hole being tapped. If the sulfochlorinated oil is too viscous for the pressure system, it can be diluted

with a thinner mineral oil without seriously impairing its characteristics. Note that chemically active cutting fluids must be removed from the tapped holes to prevent damage to the work metal during subsequent heat treatment or high-temperature service.

Milling. Climb milling is generally preferred to conventional milling, if suitable equipment is available. Climb milling requires the ultimate in rigidity and a machine equipped with a backlash eliminator. However, cuts deeper than 0.060 in. (1.5 mm) are seldom attempted with the climb milling of superalloys, because it is virtually impossible to obtain the required rigidity.

For milling superalloys, two principles of cutter design must be given special consideration. First, tooth strength must be greater than that required for milling steel or cast iron, and second, relief angles must be large enough to prevent rubbing action and consequent work hardening of the alloy being cut. Regardless of the cutter material, inserted blades are used on nearly all but the smallest cutters, because even under the most favorable machining conditions, the life of the cutting edges is short. Mechanical methods of securing the blades in the cutter body are preferred because replacement of chipped or broken blades is easier. Cutter life can sometimes be greatly increased by small design changes.

Milling-Cutter Material. Because of the interrupted cutting action, HSS is used for cutters in most applications for milling superalloys. However, carbide is frequently more economical than HSS when milling the more difficult-to-machine alloys, such as Rene 41 and MA-6000. Small solid-carbide end mills have been successfully used in a few applications. The more highly alloyed grades of HSS usually outperform the general-purpose grades, but there is less difference in performance between the two grades in milling cutters than in some other tools used for machining superalloys.

Cutting Fluid for Milling. Sulfochlorinated oil introduced in copious amounts at the exhaust side of the cutter is the preferred condition for milling superalloys. Soluble-oil emulsions are often used, and they provide better cooling for the tools and workpieces than straight oils. However, some sacrifice in surface finish and tool life attends the use of soluble-oil emulsions compared to sulfochlorinated oils. The latter are often diluted with mineral oil (up to 50%) to obtain fluidity with no large sacrifice in ability to promote cutting action and good surface finish. Workpieces milled with sulfochlorinated or other chemically active oils must be thoroughly cleaned before being placed in service at elevated temperature.

Grinding Operations. Even when operating conditions are favorable, superalloys are more difficult and costly to grind than low-alloy steels. Because high-temperature nickel-base and cobalt-base superalloys are sensitive to the level of energy used during processing, metallurgical alterations and microcracking may occur at the surface. The altered material zones or layers can attain a substantial proportion of the thickness of thin components, resulting in a deleterious effect on the requirements for the surface being produced. These requirements include low distortion, absence of cracks, fine finish, or high fatigue strength. Therefore, parameters and conditions for the grinding of superalloys should be controlled to planned values in order to obtain high-integrity surfaces.

Grinding Fluids. Fluids are classified in four principal groups, as shown in Table 10.10. Because superalloys have low thermal conductivity, grinding fluid must be applied at the grinding area in plentiful amounts to prevent heat checking of the work surface. For fast removal of heat, highly sulfurized water-based soluble-oil emulsions are the best fluid for any wrought superalloy. Sulfurized oils are appropriate grinding fluids for all superalloys, but they remove heat less rapidly than the water-based soluble-oil emulsions.

Chlorinated oil, generally about 1% Cl, is particularly useful for the wet dressing of form-grinding wheels to a tolerance of 0.0002 in. (0.005 mm) or less. Chlorinated water-based soluble-oil emulsions can be used in dressing form-grinding wheels within tolerances wider than 0.0002 in. (0.005 mm). Synthetic solutions and water-based soluble-oil emulsions do not have this capability. The chlorinated straight oils and chlorinated soluble-oil emulsions are also applicable to other methods of grinding.

A disadvantage of chlorinated fluid for parts to be heat treated or put into service at high temperatures is that any residual or entrapped fluid can react with the alloy during high-temperature treatment or service of the work-

Table 10.10 Identification and classification of grinding fluids

Fluid	Remarks
Soluble-oil emulsions (regular)	
S1	Contains soap
S2	Contains soaps and fatty materials
S3	Emulsified kerosene
S4	Contains soap; a brand different from that in S1
Soluble-oil emulsions (heavy-duty)	
H1	Contains sulfur and chlorine
H2	Contains sulfurized fats; designed for stainless steel
H3	Contains sulfur and extreme-pressure additives, high percentage of fats
H4	Contains fatty materials, synthetic soaps; designed for stainless steel
H5	Contains lead additive but no sulfur or chlorine
Chemical (synthetic) solutions	
C1	Contains 35% potassium nitrite (KNO_2) before dilution for use
C2	Contains 40% sodium nitrite ($NaNO_2$) before dilution for use; no organic compounds
C3	Contains a moderate percentage of sodium nitrite
C4	Based on synthetic wax
C5	Synthetic lubricant and sulfurized fatty acid
C6	Same as C5 but without sulfur
C7	Contains fatty acid
C8	Same as C7, with ionic additive
Grinding oils	
G1	Transparent sulfochlorinated grinding oil containing fats, 4% S and 2% Cl (both active); viscosity, 230 SUS at 40 °C
G2	Dark sulfochlorinated grinding oil containing fats, 3% S and 0.5% Cl (both active); 190 SUS at 40 °C (100 °F)
G3	Inactive grinding oil containing fats, no added sulfur or chlorine; 300 SUS at 40 °C (100 °F)

Table 10.11 Effect of grinding fluid on the grinding ratio of four superalloys

	Grinding ratio obtained for:			
	U-500	J-1570	J-1570	HS-31
	Grinding wheel			
Grinding fluid(a)	A-60-H8-V		A-60-J8-V	
C1	3.5	2.8	...	...
C2	...	...	4.8	16
C3	...	...	3.9	15
H1	3.3	...	...	...
H2	1.5	...	...	...
C4	...	1.7	...	...
C5	...	1.4	...	...
H3	...	1.3	...	...
C7	...	1.3	...	...
S1	...	1.1	2.6	14
S2	...	...	2.5	12
S3	...	1.1	...	...
C8	...	1.1	...	...
H4	...	...	2.4	12
S4	...	...	2.3	13
Air(b)	...	0.9	2.1	12
Water	...	...	1.7	7

(a) 10% concentration. (b) Dry grinding

piece. Entrapment of fluid is especially likely in parts with small cavities, such as blind holes and other difficult-to-clean recesses. For this reason, some users of superalloy parts do not permit the use of chlorinated grinding fluids. In many applications, selection of the fluid is based on cost. Emulsions of soluble oil and water are the least expensive and grinding oils the most expensive grinding fluids.

Media and Speed Effects on Grindability. Table 10.11 shows the effects of 15 water-based fluid media on the *G*-ratio of selected heat-resistant alloys. A reminder—the *G*-ratio is the volume of metal removed per volume of wheel wear. The higher this index, the easier the metal is to grind. It should be noted that the concept of grindability does not involve grinding sensitivity, which is the susceptibility of the metal to cracking during or after grinding, nor does it involve the ease of obtaining a good surface.

In Table 10.11, a few data are included for the use of plain water or air. All the grinding fluids were at 10% concentration, which is higher than normal. The magnitude of improvement in *G*-ratio caused by grinding fluid increases with the concentration. Grinding dry proved less satisfactory than grinding with most of the water-based fluids, and grinding with plain water resulted in a very low *G*-ratio. The highest ratios (greatest ease of grinding) were obtained with synthetic fluids containing nitrite ions in considerable quantity.

In surface grinding of superalloys with straight wheels, the major differences among alloys or alloy groups lie in the wheel speeds and cross feeds permitted. Usually, an increase in wheel hardness causes an increase in the *G*-ratio and the grindability index. Decreasing the wheel speed is one way to reduce grinding heat and the probability of workpiece cracking.

Superalloys: A Technical Guide, Second Edition
Matthew J. Donachie, Stephen J. Donachie, p 203-210
DOI:10.1361/stgs2002p203
Copyright © 2002 ASM International®
All rights reserved.
www.asminternational.org

Chapter 11

Cleaning and Finishing

Introduction

Background. Cleaning is required to remove contaminants from the surfaces of parts made of superalloys. Shop soils such as oil, grease, and cutting fluids can be removed by conventional solvents or soaps. Metallic contaminants, tarnish, and scale resulting from hot working or heat treating operations must also be removed. Some contaminants such as lower-melting metals can cause severe surface attack and reduce a component to scrap.

Surface finishing may be necessary to improve component performance; however, many finishing operations commonly used for steel and other metals are not required for superalloys. This is due to:

- The inherent corrosion resistance of superalloys in a wide range of environments
- The fact that the end use of superalloy parts frequently does not require a polished finish

A frequent reason for surface finishing of superalloy components is to prepare them for a subsequent treatment, such as for the application of a coating. For strength reasons, a frequent surface treatment given to superalloys is shot (or bead) peening (note Example 4 at the end of this chapter). See also Chapter 12 for information on the role of surface condition on fatigue life of superalloys.

Metallic Contaminants. Parts made from heat-resistant alloys can accumulate traces of other metals on their surfaces after contacting cutting tools, forming dies, or machining and heat treating fixtures. Although metal contamination is not always harmful, its presence can be highly deleterious in certain cases. For example, Inconel X-750 may be unaffected by traces of zinc from drawing dies, but even the smallest particle of aluminum will readily alloy with the Inconel at elevated temperatures and degrade the corrosion resistance and mechanical integrity of the affected areas. Copper is another example of a metal that may affect some nickel-base alloys when they are subsequently exposed to high temperatures. Therefore, all surface contaminants should be removed from superalloys before they are heat treated or subjected to service at elevated temperatures.

The high-temperature strength and ductility of nickel-base precipitation-hardened superalloys are severely reduced by minute quantities of lead, bismuth, antimony, selenium, and arsenic. As noted previously, small amounts of aluminum, even though it is a normal alloy element addition, readily alloy with nickel-base superalloys at elevated temperatures and degrade the affected area. Also, copper and silver reduce the high-temperature strength of nickel-base superalloys. Use of low-melting metals that contain lead and bismuth was a common practice at one time in the fixturing of turbine airfoils for machining.

Tarnish. Tarnish is a thin oxide film that does not always have a harmful effect on the end use of parts made from superalloys. In fact, it can even be useful, such as when it functions as a bond for paint, a barrier to prevent diffusion from another alloy, or a retardant to further oxidation. However, other functional requirements can necessitate the removal of tarnish from parts. Tarnish should always be removed before welding or brazing.

Oxide and/or Scale. Oxide and scale are synonymous in some respects. The essence of superalloys is that they are not only strong at high temperatures but also are extremely oxidation resistant. The oxidation resistance is created by the formation of a layer of protective oxides of Cr_2O_3 and Al_2O_3. Oxides are sometimes called scales, even when they are relatively thin and protective in nature. However, scales are, perhaps, more often thought of as thicker layers of oxide rather than protective oxide films. In any event, oxide and/or scale removal is required in various aspects of superalloy manufacture and for efficient and consistent component operation.

Metallic Contamination Removal

Background. Many superalloys are extremely susceptible to what may appear to be minor changes in surface environment. For instance, residual stresses play an important role in the life of a component. Favorable residual stresses frequently are introduced by machining. An attempt to remove contaminants by mechanical or chemical means might result in a reduction in the favorable residual stresses. Alternately, production of unfavorable residual stresses might arise. As noted in Chapter 10, electrochemical machining of a nickel-base superalloy after conventional turning reduced the fatigue endurance stress capability by about 50%. Careful consideration needs to be given to the mechanical aspects of contamination removal.

Chemical removal means are no less of a concern, because some contaminants interact with cleaning chemicals to produce intergranular attack. This type of attack creates not only an undesirable surface appearance but also creates notches that will serve to dramatically lower fatigue and/or creep-rupture properties of affected superalloys. Intergranular attack is of great concern in the cleaning of investment castings.

Avoiding, Reducing, and Detecting Metallic Contamination. An obvious solution to metallic contamination is to avoid contact with the metallic elements that may attach themselves to the component surface. This is a reasonable solution in the case of low-melting metal fixturing situations but not possible when one considers the range of fixturing, tools, and so on in use in manufacturing processes. In operations such as cutting and forming, metal contamination can be avoided or sharply reduced by the use of lubricants. This is preferred practice, because lubricants can be removed easily and cheaply if they have not been baked or fired before the removal is attempted.

If contamination cannot be avoided, testing is recommended to determine the seriousness of the contamination. Physical appearance (stains, etc.), either as-machined, after heat treating operations, or after appropriate chemical solutions are applied, can indicate contamination. Heat treatment should be avoided unless it is clear that contamination is absent. Although metal contamination is not always harmful, all surface contaminants should be removed before superalloys are heat treated or subjected to service at elevated temperatures. Minor amounts (traces) of some elements can cause great damage.

An example of chemical processes to identify metallic contamination is the detection of lead. This element may be detected by the yellow precipitate that forms when the test solution shown in Table 11.1 is applied at 70 to 140 °F (21 to 60 °C) to the suspected surface.

In addition to physical appearance and the use of chemical testing, metallographic examination can be used to detect surface alloying. Also, mechanical tests such as bend tests (may indicate ductility loss owing to contamination) or hardness tests (could show high hardness and potential ductility loss) may be conducted to detect embrittlement caused by metallic contamination.

Mechanical Removal Methods. Dry or wet abrasive blasting with metal-free abrasives is an effective means of removing metal contamination, as are polishing with ceramic materials and wet tumbling. The shape of a component, the surface finish required, and the allowable loss of gage will determine the suitability of these mechanical methods.

Chemical Removal Methods. Chemical methods are used more often than mechanical

Table 11.1 Test solution to check for lead contamination

Chromic acid, 10 wt%
Sodium chlorate, 1.5 wt%
Water, 88.5 wt%
Apply at 70 to 140 °F (21 to 60 °C) to the suspected surface.
Yellow precipitate indicates presence of lead.

methods for removing metal contamination. A typical procedure for chemically removing iron, zinc, and thin films of lead is to first perform vapor degreasing or alkaline cleaning, and then immerse the parts in a 1 to 1 solution (by volume) of nitric acid (1.41 specific gravity, or sp gr) and water for 15 to 30 min at approximately 95 °F (35 °C). Water rinsing, followed by drying, completes the process.

Another procedure that has been successful in removing brass, lead, zinc, bismuth, and tin from nickel-base and cobalt-base alloys involves vapor degreasing or alkaline cleaning, followed by soaking at room temperature in a solution of nitric acid (7.22 oz/gal, or 54 g/L), acetic acid (20 to 50 oz/gal, or 150 to 375 g/L), and hydrogen peroxide (2.5 to 8.5 oz/gal, or 19 to 64 g/L).

Soaking time can vary from 20 min to 4 h, depending on the severity of the contamination, and is determined by visual observation of the reaction. After this treatment, parts must be rinsed thoroughly in water and dried. When possible, a test specimen should he immersed for the maximum time anticipated and examined for chemical attack before processing the first load of parts.

Nickel-base alloys should be acid etched to prepare for subsequent nondestructive inspection. The etching process removes smeared metal that may be present as a thin surface layer after machining and/or blast cleaning. The parts can be etched by immersing them in a bath containing hydrochloric acid (80%), hydrofluoric acid (13%), and nitric acid (7%) to remove the disturbed or smeared layer. This bath may leave smut that must be removed by a second bath containing iron chloride (22%), hydrochloric acid (75%), nitric acid (2%), and water. After being rinsed and dried, the parts can undergo visual and penetrant inspections. The extent of etching depends on the depth or thickness of the smeared layer. All of this layer should be removed. However, overetched parts will retain excessive amounts of penetrant.

Tarnish Removal

Background. The thin oxide (usually) film known as tarnish may not always be harmful to properties. It may even be useful for bonding or as a retardant to further oxidation. Nevertheless, tarnish generally should be removed from components for improved finishing-joining operations. For example, tarnish always should be removed before welding or brazing to ensure braze alloy spreading or intimate contact of the surfaces to be joined.

Mechanical Removal Methods. Abrasive cleaning methods such as those used for removing metallic contaminants also are used for removing tarnish. The applicability of these methods is determined by the configuration of the parts, the surface finish required, and the allowable loss of gage or dimension. However, abrasive cleaning can remove some metal and degrade surface finishes. Therefore, chemical means of removal may need to be used in such instances.

Chemical Removal Methods. Flash pickling is used more often than abrasive cleaning for tarnish removal. A typical flash pickling formula uses nitric acid (1.41 sp gr; 23 vol%), hydrofluoric acid (1.26 sp gr; 4 vol%), and water (73 vol%). Parts are immersed in this solution for 1 to 5 min at approximately 125 °F (52 °C). Warming the parts in hot water before flash pickling speeds tarnish removal. Water rinsing and drying must follow flash pickling.

Flash pickling solutions act rapidly, and care must be exercised to prevent overpickling and etching. The solutions are used at room temperature. If the bath is cold, it should be warmed slightly to prevent unduly slow action. Best results in flash pickling are obtained by first warming the parts by dipping them in hot water, placing them in the acid for a few seconds, and rinsing them again with hot water. Use a second dip in acid, if necessary. Badly tarnished metal may require a total of 3 min in acid, but the material should be withdrawn frequently from the bath and inspected to prevent overpickling.

Oxide and Scale Removal

Background. Oxide tarnish films can form on parts that are heated in reducing atmospheres, out of contact with air. Sometimes, these oxides can be removed by immersing the parts for 5 to 15 min in a tarnish-removing, flash pickling bath of the formulation given above. However, most superalloys form a tenacious oxide coating in the pres-

ence of air, carbon monoxide, or water because of their high content of oxide-forming metals, such as nickel, cobalt, aluminum, and chromium. The resulting oxides vary widely with alloy composition and furnace atmosphere. Usually, pickling is required for their removal. Scale conditioners are useful.

Scale develops on hot-forged, hot-formed, or heat treated parts that are processed in air. Oxidizing furnace atmospheres, high-sulfur-content fuels, and air leakage in furnaces cause heavy scale to form on nickel alloys. Usually, scale is tenacious and occurs in all gradations, including thick layers that result from heating in an oxidizing furnace using high-sulfur fuels. The scale that forms under such conditions has a dull, spongy appearance. Fine cracks may be present in the scale, and patches of scale, may break or spall from the surface. The underlying metal is rough, and the roughness cannot be corrected solely by pickling. In these extreme conditions, grinding or abrasive blasting to sound metal, followed by flash pickling, is recommended.

The most widely used methods for removing oxides or scale from heat-resistant alloys, in order of preference based on economic considerations, are: acid pickling, abrasive cleaning by tumbling or blasting, and descaling in molten salt. Alkaline scale conditioning is helpful in modifying the scale to facilitate its removal by these methods. When extremely-heavy oxide layers must be removed, grinding is an appropriate preliminary operation. Combinations of two or more methods are often used.

Mechanical Removal of Oxides and Scales. Abrasive blasting with dry aluminum oxide can be used to remove oxide and scale from all types of wrought and cast heat-resistant alloys. Silicon carbide is more expensive than aluminum oxide and is seldom used. Silica (silicon dioxide, or sand) has a limited application because of its lesser cutting ability. Grit sizes as coarse as No. 30 (0.023 in., or 0.59 mm) are recommended for cleaning forgings and castings. Finer grits, such as No. 90 and 100 (0.0065 and 0.0059 in., or 0.17 and 0.15 mm, respectively), are used for general blasting.

Metallic shot and grit should not be used to descale superalloys unless their use is followed by pickling to remove metal contamination. For parts that must be resistance or solid-state welded or brazed or that have highly tenacious scales produced by furnace atmospheres, pickling after dry abrasive cleaning is recommended, regardless of the abrasive used.

Wet abrasive blasting, known as vapor honing, also is used to clean heat-resistant alloys. This process uses No. 200 to 1250 silica abrasive particles (0.0029 to 0.0004 in., or 0.074 to 0.010 mm) mixed with water to produce a slurry that removes loose scale, discoloration, and soils. Metal loss is not excessive when normal pressures and exposure times are used. Surfaces that have been wet blasted are usually suitable for welding, brazing, electroplating, and final inspection; further cleaning is seldom necessary. Exceptions are the precipitation-hardened nickel-base superalloys with high combined titanium and aluminum contents, which require the special procedure previously discussed.

When spherical beads made of high-quality optical crown glass are used as the abrasive, stock loss is minimized. Bead sizes of 0.0015 to 0.0029 in. (0.038 to 0.74 mm) are generally used, and blasting pressures are kept below 60 psi (410 kPa) to prevent the beads from fracturing.

Surfaces that have been wet blasted are usually suitable for welding, brazing, electroplating, and final inspection processes; further cleaning is seldom necessary. Exceptions are alloys with a high titanium and aluminum content, which require the special procedure discussed in the section ‘‘Metal Removal by Acid Pickling.’’

Most of the general advantages and limitations associated with the abrasive cleaning of steel will also apply to superalloys. However, there is a risk of contamination from either metallic abrasives or abrasives that have been used to clean parts made from metals of widely different compositions. For example, superalloys should not be blasted with abrasive material that has been used to clean low-alloy steel, aluminum, copper, or magnesium. However, abrasives used to clean titanium and corrosion-resistant steels have been used to clean superalloys without serious contamination. The flash pickling of superalloys after abrasive cleaning provides additional assurance that no harmful surface contamination remains.

Wet tumbling by the barrel or vibratory method can be used to descale heat-resistant alloys, if the shapes and sizes of the com-

ponents are suitable. The removal of burrs and sharp edges is accomplished in the same operation. Shop soils are also removed, thus eliminating the need for preliminary degreasing. Parts are tumbled or vibrated in a mixture of acid descaling compound and metal-free abrasives and then subjected to a neutralizing cycle.

Precautions regarding metal contamination in wet tumbling are similar to those noted previously for abrasive blasting. Pickling is required after tumbling. It also is required before joining operations such as resistance fusion welding or solid-state bonding to remove residual smut, which can cause poor-quality weldments. There is less need for pickling prior to arc, electron beam, or other fusion welding, unless an inspection of the test weldments reveals porosity or inclusions that are a result of pickup from the tumbling process.

Mechanical removal of oxides or scales also may be accomplished by wire brushing, which is sometimes used to remove very light scale or surface discoloration. All brushes used on superalloys must have stainless steel bristles.

Scale conditioning is used to soften, modify, or reduce scale for easier and more uniform acid pickling, but is seldom required for removal of discoloration or interference coatings. A scale-conditioning bath consists of a highly alkaline aqueous solution, sometimes containing complexing and chelating compounds. The main purpose of these agents is to solubilize the scale as much as possible. The performance of a particular chelating agent depends on the affinity of the compound for the metal ions present, the pH of the scale-conditioning solution, and the physical and chemical composition of the scale. Typical multicycle descaling operations, including scale conditioning, are defined in Tables 11.2 and 11.3.

Minimal scale removal occurs during treatment in the alkaline scale-conditioning bath. Further treatment in highly alkaline solutions containing a strong oxidizing material, such as potassium permanganate, is often necessary. Scale on heat-resistant alloys sometimes contains carbon and incompletely burned and polymerized residues in addition to metallic oxides. These organic components react with the oxygen released by the alkaline oxidizing bath.

Metal Removal by Acid Pickling. After a scale is conditioned, it is subjected to acid pickling, during which most of the high-temperature scale either breaks away from or becomes so loosely attached to the parts that pressure rinsing with water completes the descaling. The acid pickle is usually a dilute nitric acid or a hydrofluoric-nitric acid solution. In addition to removing scale, pickling solutions that contain nitric acid will remove many surface contaminants through oxidation. However, because the acid solution attacks the base metal, it is necessary to limit the pickling time to prevent excessive metal loss or metal surface roughening.

Parts made from alloys that are high in aluminum and titanium, such as M-252 and Rene 41, must undergo a special procedure before welding or brazing. When parts are in the solution-treated condition and descaling is required, they are treated in a scale-con-

Table 11.2 Procedure for removing scale from superalloys

Operation	Time, min	Temperature, °C	Temperature, °F	Solution	Concentration
Precleaning cycle					
Vapor degreasing	5–10	87–88	185–190	Stabilized trichloroethylene	...
Emulsion cleaning	10–20	54–66	130–150	Emulsion cleaner	20 vol%
Scale-conditioning cycle					
Alkaline chelating	15–30	125–135	260–275	Caustic solution containing alkanol amines and aliphatic hydroxy acids	...
Alkaline oxidizing	60–120	95–105	205–220	Potassium permanganate	5 wt%
				Sodium hydroxide	20 wt%
				Water	bal
Pickling cycle					
Acid pickling	5–30	49–60	120–140	Hydrofluoric acid	4 wt%

Table 11.3 Procedure for removing scale from Inconel alloys, many of which may be classified as superalloys

Operation	Time	Temperature		Solution(a)	Concentration(a)
		°C	°F		
Alkaline conditioning	1–2 h	96–105	205–220	Sodium hydroxide	20 wt%
				Potassium permanganate	5 wt%
Rinse	15–30 s	Not heated	Not heated	Water quench and water spray	. . .
Acid pickling	5–10 min	60–71	140–160	Sulfuric acid (1.83 sp gr)	7.5 vol%
				Hydrochloric acid (1.16 sp gr)	12 vol%
Rinse	15–30 s	Not heated	Not heated	Water	. . .
Acid pickling	10–20 min	60–71	140–160	Nitric acid (1.41 sp gr)	20 vol%
Rinse	15–30 s	Not heated	Not heated	Water	. . .
Acid pickling	5–60 min(b)	49–54	120–130	Hydrofluoric acid (1.26 sp gr)	3.7 vol%
				Nitric acid (1.41 sp gr)	22 vol%
Rinse	15–30 s	Not heated	Not heated	Water	. . .

(a) Undefined remainder is water. (b) Type of oxide will determine immersion time required; until immersion time is established, inspect frequently to avoid overpickling.

ditioning solution, a procedure previously described, after which they are immersed in a solution of nitric acid (30 wt%) and hydrofluoric acid (3 wt%) for 5 to 10 min. Alloys in the aged condition are descaled anodically in an acid solution. A solution made for this procedure should contain sulfuric acid (75 wt%) and hydrofluoric acid (3 wt%). It should be operated using a current density of 20 to 40 A/ft^2 (215 to 430 A/mm^2) and graphite cathodes. The material should be immersed in the electrolytic cleaning bath for 3 to 12 min, and the operation will be complete when the amperage drops to nearly zero. Sodium sulfite (1.6 wt%) is used to reactivate the solution after a period of operation.

Superalloys containing less than about 12% Cr can undergo high metal loss or develop intergranular attack in pickling. When the susceptibility of a material to excessive metal loss or intergranular attack by acids is unknown, mechanical descaling is safer than acid pickling. In one instance, it was proved that acid descaling caused intergranular attack and subsequent loss of ductility in aged Rene 41, an alloy that contains 19% Cr.

Weld areas normally vary in composition and structure from the basis metal and do not react to the conditioning and pickling cycles in the same manner as the basis metal. Weld areas or the heat-affected zones often are susceptible to selective attack during pickling. Although inhibitors may eliminate or reduce selective attack, abrasive or other mechanical descaling methods, again, are preferable to acid pickling for removing scale from welded parts, unless a safe pickling procedure has been found for a given application.

Hydrogen embrittlement does not occur in superalloys as a result of aqueous descaling, although superalloys are not immune to it. Limited hydrogen embrittlement published data are available on superalloys.

Salt Bath Descaling. A salt bath is an effective first step in removing scale from heat-resistant alloys. The process is generally more expensive than acid pickling, particularly if production is intermittent, because of the cost of maintaining the bath during idle time. The electrolytic salt bath used to descale heat-resistant alloys contains fused caustic soda rather than sodium hydride. The parts and the tank are alternately negative and positive poles of a direct current circuit.

This fused caustic soda bath, which contains oxidizing salts such as sodium nitrate, is operated at 800 to 1000 °F (425 to 540 °C). It is slightly more effective than a sodium hydride bath on high-chromium alloys, such as type 310 stainless steel, and cobalt-base superalloys, such as L-605. Processing steps are similar for a hydride and a caustic bath. Parts are immersed in the oxidizing bath for 5 to 15 min, quenched in water, soaked in a solution of 5 to 10% sulfuric acid at 160 °F (70 °C) for 1 to 5 min, and then dipped in a solution of 15 to 20% nitric acid and 2 to 4% hydrofluoric acid at 130 to 140 °F (54 to 60 °C) for 2 to 15 min. A typical procedure for sodium hydride descaling and acid pickling of superalloys is given in Table 11.4.

Table 11.4 Procedure for sodium hydride descaling and acid pickling of heat-resistant alloys, including some superalloys

Operation	Time	Temperature		Solution(a)	Concentration(a), vol%
		°C	°F		
Sodium hydride descale	1–2 h	370–390	700–730	Sodium hydroxide	. . .
Quench	15–30 s	Not heated	Not heated	Water	. . .
Neutralizing rinse	1–3 min	RT to 60	RT to 140	Sulfuric acid	2–10
Brightening pickle	5–15 min	54–60	130–140	Hydrofluoric acid	2–4
				Nitric acid	15–20
Rinse	15–30 s	Not heated	Not heated	Water	. . .
High-pressure spray wash	(b)	Not heated	Not heated	Water(c)	. . .

RT, room temperature. (a) Governed by shape of part. (b) 1 min on parts with accessible surfaces. (c) Water pressure of 690 kPa (100 psi)

Finishing Processes

Background. As indicated earlier, many finishing operations that are commonly used for steel and other metals are not required for the superalloys for several reasons. In particular, these alloys are inherently corrosion resistant in a wide range of environments. Second, the applications of parts made from these alloys do not typically require a polished finish for either corrosion or cosmetic reasons.

Some typical finishing processes for superalloys could include:

- Electroplating
- Diffusion coating
- Overlay coating
- Ceramic coating
- Polishing
- Shot peening, including vapor honing

The oxide coating that develops during processing is of essential value to superalloys that are subjected to high temperatures in service. Consequently, the dense, tenacious oxide that develops on formed or machined-finished parts during final heat treatment is allowed to remain as protection against further oxidation. In fact, coatings are applied to enhance the surface corrosion resistance of superalloys. The coatings work by providing more aluminum and chromium than normally would be present in the base superalloy to ensure formation of a resistant oxide. The coatings provide the presence of an alloy element (chromium, aluminum) reserve to feed the regeneration of the surface oxide as time at temperature increases. Refer to Chapter 13 for more on coatings as finishing processes for superalloys.

Surface Finishes by Chemical (Electrochemical) Means. Chromium, copper, nickel, and silver are sometimes electroplated on superalloys in order to:

- Prepare for brazing
- Deposit brazing metal
- Provide antigalling characteristics
- Repair expensive parts or correct dimensional discrepancies

Although plating is not a normal finishing process for superalloys, conventional nickel plating processes are often used to assist in brazing. Deposits of nickel can vary in thickness from 0.1 to 1 mil (2.5 to 25 m). Superalloys, such as the precipitation-hardened nickel-base superalloys, that contain titanium or aluminum will require the thicker deposits. Silver and copper are the metals most often deposited as actual brazing materials. It should be noted, however, that silver and copper not consumed in a brazing process can pose surface degradation hazards for superalloys. Some brazing alloys are deposited as separate layers of their various constituent metals on a weight-percentage basis. Plate thickness depends on the amount of metal needed for brazing.

Surface Finishes by Mechanical Means. Polishing of superalloys is sometimes used to obtain a desired surface finish as well as to remove light scale or oxide from parts that are to be solid-state or resistance welded or brazed. Silicon carbide in various grit sizes is commonly used to prepare surfaces for brazing. Surfaces are usually prepared for welding by polishing with No. 90-grit aluminum oxide, set up with sodium silicate on a cloth wheel. Discoloration can be removed by polishing with No. 120-grit aluminum ox-

ide, used with a greaseless compound and a cloth wheel. Buffing is seldom required for the finishing of superalloys.

Shot peening currently is used to improve the mechanical properties of compressor blades, turbine-blade dovetails, and latter-stage turbine-blade airfoils by introducing favorable patterns of residual stress. Although all turbine-blade dovetails are peened with steel shot, glass beads are sometimes favored over metallic shot in other shot peening applications. Glass beads are not equivalent to metal shot for improving mechanical properties. However, the advantages of glass beads are that they:

- Pose no risk of metal contamination
- Remove virtually no metal
- Are available in smaller sizes than metallic shot and can therefore be used to peen areas that are difficult to reach when using metallic shot

Cleaning and Finishing Problems and Solutions

Comments. The complex oxides and scale that form on heat-resistant alloys often create production problems and require the use of special procedures to obtain the desired surfaces. A few examples follow to illustrate some aspects of cleaning and finishing of superalloys. All of the examples described subsequently are drawn from actual production experience. The examples identify cleaning and finishing problems and the procedures used to solve them.

Example 1. Turbine combustion chambers made from Hastelloy X Sheet. After heat treatment, the sheet exhibited irregular scale adherence, variations in surface finish, and loss of formability. An investigation disclosed that residual shop soils, such as lubricants, marking inks, and handprints, remained on the parts despite the solvent cleaning and vapor degreasing to which the parts were subjected before being heat treated. These soils were decomposing during heat treatment and causing carbon diffusion. The substitution of electrolytic alkaline cleaning for the methods previously used eliminated the difficulty.

In this procedure, parts were immersed for 5 min in a bath compounded to federal specification P-C-535 and operated at 180 to 200 °F (82 to 93 °C), using 6 to 8 V. Parts were anodic in the electrical circuit. The scale was easily removed by subjecting the heat treated parts to a 5 min immersion in a room-temperature acid pickling bath composed of 70% nitric acid (20 to 30 vol%), 60% hydrofluoric acid (10 to 15 vol%), and water (55 to 70 vol%).

Example 2. Removing annealing scale from superalloys. Conventional salt bath descaling and pickling failed to remove all annealing scale from stampings made from 19-9 DL iron-nickel-base superalloy, Hastelloy X and Inconel 600 solution-hardened nickel-base superalloys, and Inconel X-750, a lower-strength nickel-base precipitation-hardening superalloy. The sequence of operations performed on these stampings was either to form, degrease, remove metal contamination, anneal, and descale, or to immerse in molten salt and then pickle.

The difficulty in scale removal was traced to the open hearth, gas-fired annealing furnaces. It was found that the atmosphere was reducing while the burners were on, and that a thin, tight scale was produced. A satisfactory remedy was to adjust the burners to bring the oxygen content to 3%. The resulting scale was loose and easily removed by the usual descaling and pickling procedures.

Example 3. Welding 19-9 DL iron-nickel-base superalloy. Small cracks appeared in welded 19-9 DL iron-nickel-base superalloy tubing (0.050 in., or 1.3 mm wall) after annealing. The processing sequence was to form tubing from flat stock, degrease, perform an automatic seam weld, anneal, and descale. The tubing was formed on dies of zinc alloy but was not dezinced before being welded. Small amounts of zinc on the surface near the weld melted during welding. This initiated zinc diffusion, and the residual stresses around the weld were sufficient to crack the embrittled material. The problem was solved by pickling the tubing in 20% nitric acid to remove the zinc before welding.

Example 4. Insufficient fatigue strength. A single-crystal nickel-base superalloy was developed for gas turbine airfoil operations. The root attachment areas of blades made of the superalloy were deemed to be insufficient in low-cycle fatigue (LCF) strength. The solution was to shot peen the attachments of all blades, a process that brought LCF capability on a par with the former standard alloy.

Superalloys: A Technical Guide, Second Edition
Matthew J. Donachie, Stephen J. Donachie, p 211-286
DOI:10.1361/stgs2002p211
Copyright © 2002 ASM International®
All rights reserved.
www.asminternational.org

Chapter 12

Structure/Property Relationships

Introduction

Microstructure. Cobalt-base superalloys are solid-solution strengthened, although a few older alloys were γ′ hardened. Their strength was not sufficient to compete with nickel-base superalloys. Some nickel-base and iron-nickel-base superalloys also are solid-solution strengthened. However, the alloys used for highest-strength applications are the nickel- and iron-nickel-base superalloys that are hardened by γ′ or γ″ precipitation (in a face-centered cubic (fcc) matrix).

The γ′ in iron-nickel-base and first-generation nickel-base alloys generally is spheroidal, whereas the γ′ in later-generation nickel-base alloys generally is cuboidal. Under special circumstances, a rafted microstructure can be produced. Microstructure, particularly its γ′ characteristics, affects mechanical properties more than it affects physical properties. The volume fraction (V_f) of γ′ generally is about 0.2 or less in wrought iron-nickel-base superalloys but may exceed 0.6 in nickel-base superalloys. The γ″ phase is disk-shaped. There are insufficient alloy compositions to provide knowledge of a range for $V_f\gamma''$ in γ″-hardened alloys.

The microstructure for components of fixed chemistry is established by prior processing (casting, forging, etc., and heat treatment). In general, optimal properties are established at the end of the processing sequences; occasionally, property compromises are required, and one or more mechanical properties are not optimal. Alloys hardened by γ′ and γ″ are predominantly wrought, but those γ′-hardened alloys used at the highest temperatures normally are cast. Chemistries of some superalloys are provided in Chapter 1. General aspects of microstructure are given in Chapter 3.

Mechanical Properties. Both short-time properties and long-time properties are at issue for property-microstructure relationships. Short-time properties include the tensile (or compressive) strengths (yield and ultimate) produced by continuous fairly rapid application of loads to reach plastic deformation (proportional limit, 0.02% yield, 0.2% yield) or fracture. Elongation during and at the conclusion of a test is measured. Reduction in area at the conclusion of a test is recorded. Static modulus generally is not measured, at least in tests designed to produce strength data.

Creep-rupture properties are determined by longer-time, sometimes long-time, tests of metal under load, where the elongation generally is measured with time. Failure elongation is recorded. So-called minimum or secondary creep rates may be reported. Time to reach a fixed value of strain often is recorded. Extrapolation and interpolation of data are required to cover the desired range of design conditions. Frequently, only the failure time and elongation are recorded. Such tests are called stress-rupture tests. The word ''creep-rupture'' refers to tests where time to given creep values is recorded, but creep-rupture often is used interchangeably with stress rupture.

Cyclic (fatigue) tests also are run in the various fatigue regions. These tests generally are cyclic-rate dependent at high temperatures. Other cyclic tests include crack propagation tests, usually in fatigue but sometimes in creep.

Tensile properties usually are at issue up to the region of about 1400 °F (760 °C), while creep-rupture behavior is of more interest at higher temperatures. For a given alloy chemistry, creep and tensile strengths cannot be raised unilaterally or together; one property generally is optimized to the detriment of the other.

Solid-Solution Hardening. Some hardening is effected by placing solute atoms in the γ matrix (and the γ′ phase) of the superalloys. The exact nature of the hardening process need not be discussed here. However, the process is more complex than it at first may appear. Solute atoms in γ work in various ways to:

- Affect the local modulus in a grain
- Affect local atom arrangements in a grain
- Limit diffusion of atoms
- Change the stacking fault energy (SFE) of the matrix

With these effects, significant hardening can be achieved. Solutes that create asymmetric strain distortions are more effective than those that produce symmetrical distortions, at least for short-time properties. Generally, small interstitial atoms such as carbon produce asymmetrical distortions and thus are the more effective atoms (on a unit basis) at solid-solution hardening.

Atoms lowering the SFE tend to make it more difficult for dislocations (the dominant microstructural unit that effects deformation) to move in new directions. Thus, when moving dislocations in a lower-SFE matrix of an alloy encounter obstacles, they have more difficulty avoiding them by movement onto a new plane.

Role of Second-Phase Particles. In addition to atoms in solution, second-phase particles obstruct deformation. The most important second-phase particles are those of γ′ (and γ″). Those are discussed subsequently. The next most important particles are the carbides, which are ubiquitous in superalloys. The carbides act to impede deformation when they are in a grain. For high-temperature alloys, however, their most important role is to obstruct the movement of grain boundaries, which tend to slide when stressed above about 0.5 of the absolute melting point. Because of their importance, carbides are discussed further in appropriate sections on mechanical properties. Carbides must be suitably dispersed along the boundaries and must be reasonably stable when a component is put into elevated-temperature service.

Other particles are important. Borides can act similarly to carbides. Other particles, such as topologically close-packed (tcp) phases, generally are detrimental to mechanical properties. Inclusions, such as nitrides, sulfides, and so on, are detrimental. Inclusions are minimized with modern melting technology. Topologically close-packed phases, on the other hand, may not be present initially in the as-processed microstructure but appear after long-time exposure. Rules of thumb are available to minimize the likelihood of tcp phase formation. Elements such as boron and carbon often are not used in the highest-strength cast single-crystal nickel-base superalloys, so carbides and borides may be minimal in the microstructure.

Precipitation Hardening. As noted previously, γ′ precipitate particles can be found in spherical or cuboidal shapes in the grains of superalloys. In cast alloys, eutectic γ′ is possible. In early wrought γ′-hardened nickel-base superalloys, precipitate-free zones (PFZ) were evident after heat treatment of some alloys.

The shape of γ′ primarily is a function of alloy chemistry. However, heat treatment can effect some changes. Rafting of γ′ can be produced by appropriate heat treatment. (Rafts are long particles of the phase, with one dimension smaller than the rest.) Rafting may result from service exposure as well as from process heat treatment. Rafting, while physically possible in preservice heat treatment, usually involves prolonged heat treatment times. These times are incompatible with most production schedules and may actually be uneconomical to attain. Consequently, although rafted microstructures of single-crystal directionally solidified (SCDS) superalloys (the type that will best respond to rafting benefits) are possible, such rafted structures are not normally produced in actual components.

Although γ″ accounts for the bulk of the hardening in IN-718, the dominant (by amount produced) superalloy, there is less variety in the formation and distribution of γ″. The disk-shaped precipitates are distributed in the grains. Little is known about any aspects of γ″ in grain-boundary regions.

General Aspects of Precipitation Hardening in Superalloys

Summary of Effects. Strengthening by precipitate particles is related to many factors; the intrinsic strength and ductility of the precipitate are most important factors, but there are other important factors, such as:

- Coherency of γ' or γ'' precipitates with the γ matrix
- Antiphase boundary (APB) energy in the ordered γ' and γ'' phases; APB is the analog to the SFE energy mentioned previously. Because of ordering, dislocations in the ordered phase require large amounts of energy to disorder the precipitate as they pass through it.
- V_f of γ' or of γ''
- γ' particle size; not a lot is known about the effect of γ'' particle size. Also, γ'' has a disk morphology, not a globular morphology (cuboidal or spheroidal) as shown by γ'.

The correlation between strength and γ' size, although commonly made with model alloys in laboratories, sometimes may be difficult to prove out in commercial alloys over the range of particle sizes available. The γ' phase is precipitated over time, usually during the in-process aging heat treatment(s). Different sizes of γ' are possible, owing to different heat treatments.

The V_f of γ' is primarily a function of the alloy chemistry, although the temperatures of precipitation and the prior solution heat treatment may have a temporary effect on the V_f of γ' that is formed. When γ' is precipitated after a solution heat treatment that dissolves all (or most) of the γ' phase, it increases in both amount and size with time at temperature. Strength (associated with precipitate amount and size) usually increases, peaks, and eventually drops. Size is a function of time and temperature for any given alloy composition. The reasons for the peak in the strength curve with aging time (or precipitate size, distribution, etc.) are discussed subsequently.

Temperature Dependence of γ' Strength and Its Effect on Superalloys. One of the significant features of γ' is its unusual temperature dependence of the tensile properties. Customarily, pure metals and most alloys show a continuously decreasing short-time strength with increasing temperature. This is the case for solid-solution-strengthened superalloys such as Hastelloy X or L-605. The matrix γ phase in superalloys behaves in a normal fashion, with decreasing strength as temperatures increase.

The ordered γ' phase is different. The yield strengths of polycrystalline (PC) and SCDS cast specimens of unalloyed γ' show an increase of yield strength in the range between about −320 and 1470 °F (−196 and 799 °C). This strength increase with increasing temperature is dependent on solute content of the γ'. The combination of decreasing γ matrix strength with increasing γ' strength leads to a dip, then an upward swing in yield strength and, sometimes, in ultimate strength of γ'-hardened alloys between room temperature and about 1400 °F (760 °C). This behavior is not as strong with some γ'-hardened alloys as others.

Figure 12.1 shows the tensile yield strength of γ' as influenced by several solutes. Notice the peak in γ' strength between about 1200 and 1600 °F (649 and 871 °C). This γ' behavior results in an increase in superalloy strength as temperatures increase.

Concurrent with the upswing in superalloy yield strength is a corresponding drop in tensile ductility of γ'-hardened superalloys, with minima exhibited in the lower end of the same temperature range where short-time yield and ultimate strengths peak. Figure 12.2 shows the tensile strength curves for U-720 nickel-base superalloy with two different heat treatments. In one instance, the dip in strengths is visible; in the other instance, no strength dip is seen.

The reasons for absence of a clear definition of the peaking phenomena with temperature are:

- Lack of sufficient data
- Varying chemistry effects on the γ' phase
- Varying $V_f\gamma'$

In the authors' experience, when tested properly, single heats of most modern high-$V_f\gamma'$ superalloys show the traditional dip and upswing characteristic of the interaction of two different species, γ' and γ, which have different temperature responses to stress. Unfortunately, test data on short-time properties are often generated only at two temperatures,

usually room temperature and a single elevated temperature. Sometimes, only a single temperature is used. Meaningful data to spot trends and understand materials are not generated under those conditions. Moreover, when multiple heat data are used, it is the authors' experience that the typical data may follow the dip and upswing pattern described, but the design minima may not show much of a dip or peak. In some instances, design minima for γ'-hardened superalloys are shown as essentially flat from room temperature to the region of about 1100 °F (593 °C) or above, with decreasing strength capability at higher temperatures.

γ' Hardening of Superalloys. The γ' phase, dispersed in the γ matrix, provides the most significant strengthening of superalloy matrices, easily overpowering the solid-solution- (and carbide-) hardening effects. These effects are all additive, but the γ' precipitation effect is dominant.

Generally, in precipitation hardening, there is an increase in hardening brought about by increased amounts of a precipitate and changes in precipitate shape and size, as mentioned previously. Before the age-hardening peak is reached during precipitation, the operative strengthening mechanism involves cutting of γ' particles by dislocations and strength increases with increasing γ' size (Fig. 12.3) at a constant V_f of γ'. After the age-hardening peak is reached, strength decreases with continuing particle growth, because dislocations no longer cut γ' particles but bypass them. This effect can be demonstrated for tensile or hardness behavior in low-$V_f\gamma'$ superalloys (A-286, Incoloy 901, Waspaloy) but may not be as readily apparent in high-$V_f\gamma'$ alloys such as MAR-M-247, IN-100, and so on. For creep rupture, the effects are less well defined than for short-time properties such as tensile strength; uniform fine-to-moderate γ' sizes (0.25 to 0.5 μm) are preferred to coarse or hyperfine γ' for optimal properties.

Alloy strength in titanium- and aluminum-hardened alloys clearly depends on $V_f\gamma'$. The

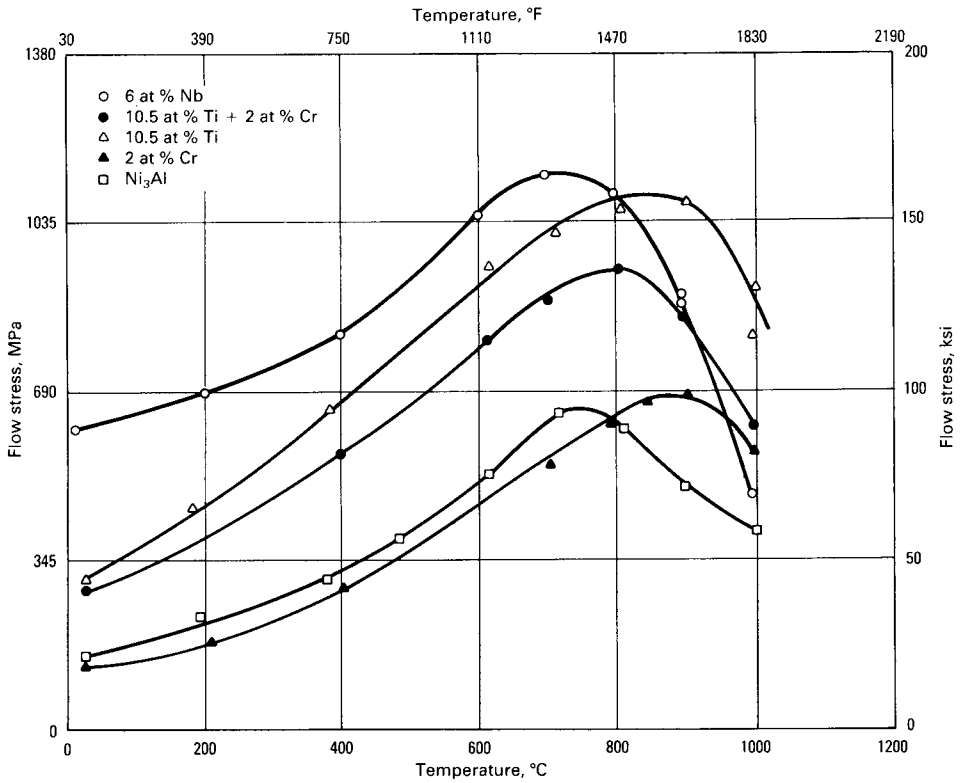


Fig. 12.1 Yield stress vs. temperature for γ' showing yield stress peak and the influence of solutes on Ni_3Al

$V_f\gamma'$, and thus strength, can be increased to a point by adding more hardener elements (aluminum and titanium—niobium as well, if a γ''-hardened alloy is desired). Alloy strengths increase as aluminum + titanium content increases (Fig. 12.4) and also as the aluminum-to-titanium ratio increases (Table 12.1). In wrought alloys, the γ' usually exists as a bimodal (duplex) distribution of fine γ', and all of the aluminum + titanium contributes effectively to the hardening process. In cast alloys, the character of the γ' precipitate de-

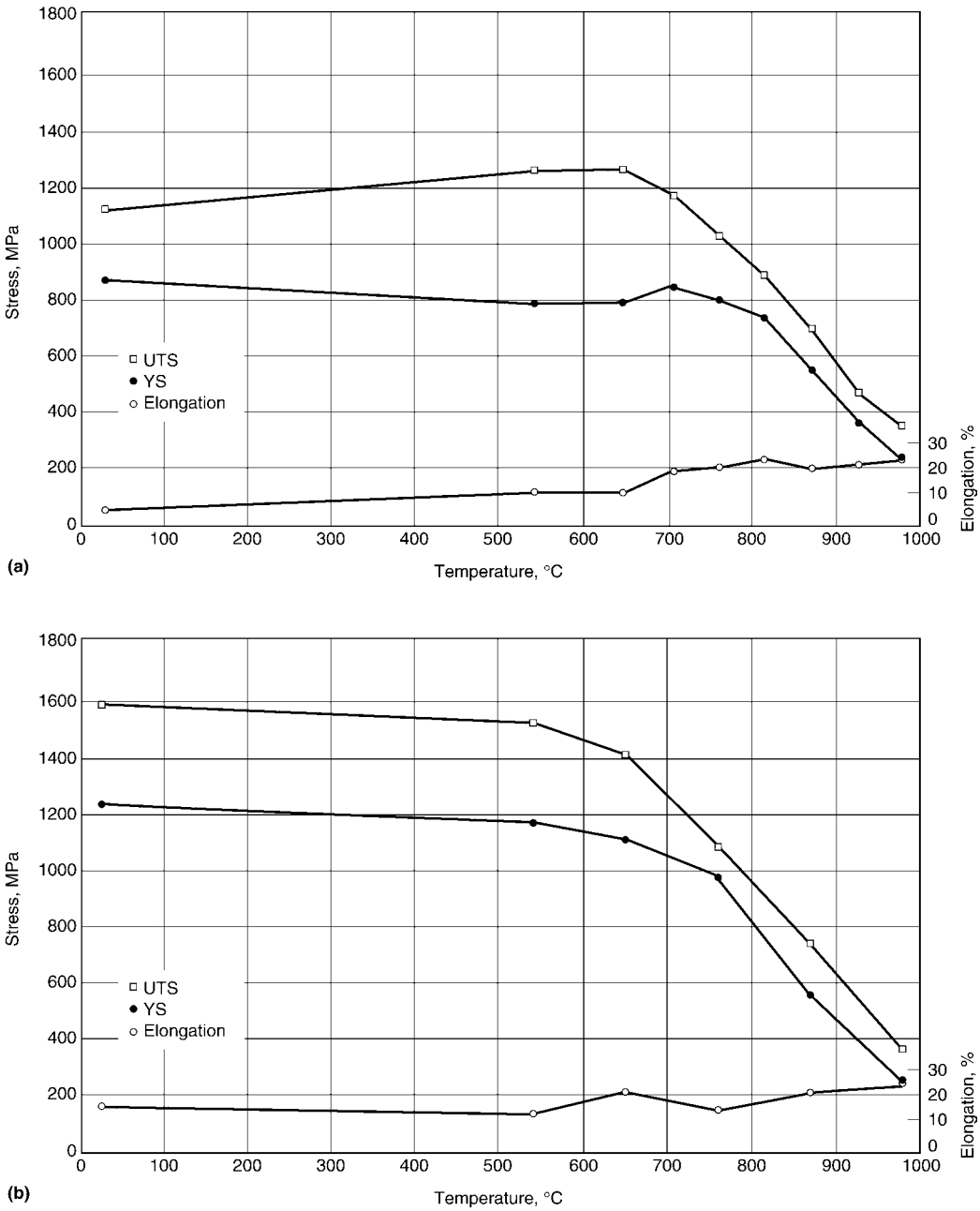


Fig. 12.2 Yield and ultimate strengths of U-720 nickel-base superalloy showing obvious peaking (a) and lack of peaking (b) for two different processing options

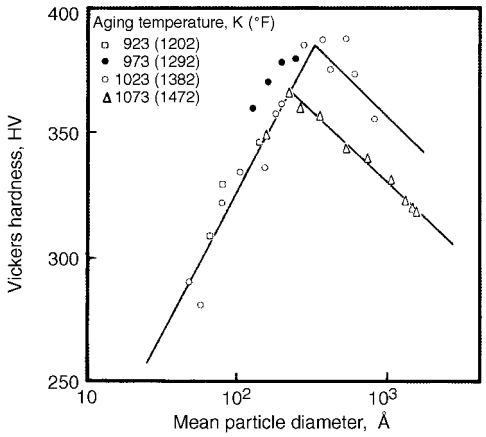


Fig. 12.3 Strength (hardness) vs. particle diameter in a nickel-base superalloy. Cutting occurs at low particle diameters, bypassing at high particle diameters. Note also that aging temperature affects strength in conjunction with particle size.

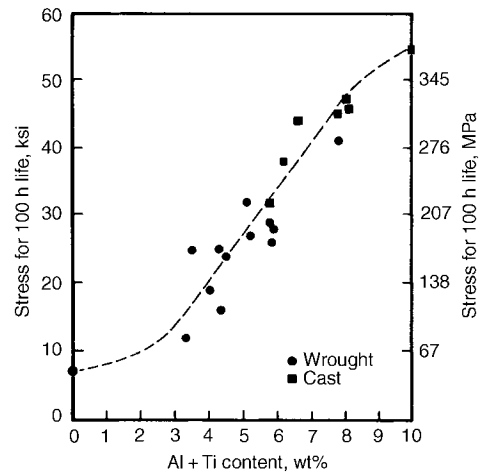


Fig. 12.4 Effect of aluminum + titanium content on the stress-rupture strength of wrought and cast nickel-base superalloys

Table 12.1 Useable Temperature versus Al/Ti ratio in PC cast nickel-base superalloys

Alloy	Al + Ti	Al/Ti	Useable temperature, °F (°C)
A-286	2.35	0.116	1200 (649)
Inconel W	3.15	0.280	1200 (649)
Waspaloy	4.25	0.420	1400 (760)
Rene 41	4.85	0.520	1400 (760)
U-500	6.00	1.00	1500 (816)
U-700	7.50	1.30	1800 (982)
MAR-M-200	7.00	2.50	2000 (1093)

veloped can be extremely variable because of the effects of casting segregation and component cooling rate. Large amounts of γ-γ′ eutectic and coarse γ′ may be developed during solidification. Subsequent heat treatment can modify these structures. Bimodal and trimodal γ′ distributions plus γ-γ′ eutectic can be found in cast alloys after heat treatment. Solution heat treatments at temperatures sufficiently high to homogenize the alloy and dissolve coarse γ′ and the eutectic γ-γ′ constituents can enable subsequent reprecipitation as a uniform fine γ′. Such heat treatments have improved creep-rupture capability. However, incipient melting temperatures limit the homogenization possible in many PC or columnar grain directionally solidified (CGDS) superalloys. For a CGDS nickel-base superalloy, MAR-M-200 + Hf, a direct correlation was shown to exist between creep-rupture life at 1800 °F (982 °C) and the V_f of fine γ′ (Fig. 12.5).

In general, to achieve the greatest precipitation-hardening effects in γ′-hardened alloys, it is necessary to solution heat treat the alloys above the γ′ solvus, although this procedure may cause excessive grain growth in wrought superalloys. One or more aging treatments are employed in order to optimize the γ′ distribution and to promote transitions in other phases, such as carbides. In some alloys, several intermediate and several lower-temperature aging treatments are used; in cast alloys used for airfoils, a coating cycle may precede the single aging treatment, or a coating cycle and a high-temperature aging treatment may precede an intermediate-tem-

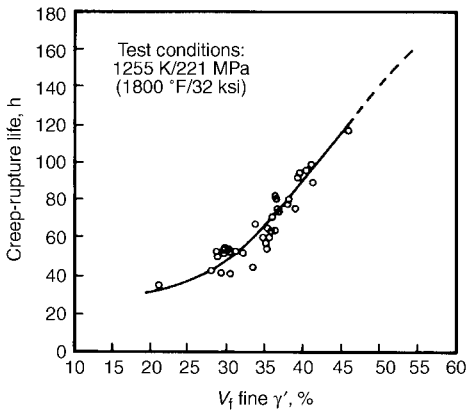


Fig. 12.5 Creep strength vs. V_f fine γ′ for CGDS MAR-M-200

perature aging cycle. In the very-high-$V_f\gamma'$ wrought alloys, multiple ''aging'' treatments frequently are used. Sometimes, multiple aging treatments consist of a sequence where dual cycles exist in a temperature range. For example, the first treatment may be at a somewhat lower temperature than the second; the third treatment will be at a much lower temperature and somewhat below the fourth aging treatment temperature. This type of treatment is called a yo-yo heat treatment and is not common but has been used for wrought powder metallurgy (P/M) IN-100 and related alloys.

When multiple aging treatments are used, a superalloy may show the bimodal or trimodal γ' distribution mentioned previously. As noted, bimodal γ' distribution is common in wrought nickel-base superalloys, while a bimodal or higher γ' distribution can occur with cast alloys, owing to casting segregation, coating treatments, and possible multiple age cycles.

An essential feature of γ' hardening in nickel-base superalloys is that a temperature fluctuation that dissolves some γ' does not necessarily produce permanent property damage, because subsequent cooling to normal operating conditions reprecipitates γ' in a useful form. Figure 12.6 provides a schematic of B-1900 PC cast nickel-base superalloy undergoing a sequence of exposures at various temperatures that might be encountered in component operation. When solutioning and coalescence of the γ' are not too severe and no melting has occurred, subsequent component operation in the aging temperature range or even subsequent removal and aging can produce a great deal of recovery of alloy properties. No significant recovery by aging or engine operation is possible if extensive coarsening, solutioning, or any incipient melting occurs.

In the final analysis, it is not possible to judge the performance of alloys by considering just the γ' phase. The existence of grains, their orientation relative to applied loads, their size, and the absence of grains (as in SCDS alloys) are all important considerations. For PC cast or wrought alloys, the strength of the γ'-hardened grains must be balanced by grain-boundary strength. If a γ'-hardened matrix becomes too strong relative to grain boundaries, then premature failure occurs at grain boundaries, because stress relaxation at the boundaries becomes difficult. If a γ'-hardened matrix is too weak, the alloy will fail through the grain at low levels of loading.

In γ'-hardened alloys, there are several other interactions with γ' during the deformation process. Loss of γ' strength by γ' coarsening has been noted. In some of the wrought superalloys with low-to-medium

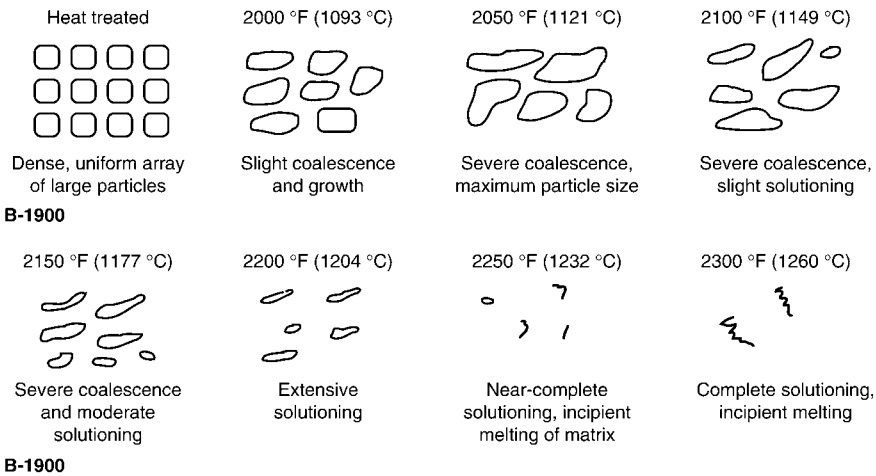


Fig. 12.6 Schematic of microstructure of B-1900 nickel-base superalloy as normally heat treated and after exposure of 2-10 h at successively higher temperatures. Irregular polygons represent γ' and black zig-zag marks are intended to represent areas of incipient melting.

$V_f\gamma'$, envelopes of γ' were observed to form in conjunction with and, in many instances, near the decomposing titanium-rich MC or in the vicinity of the developing $M_{23}C_6$. Sometimes, γ' was found to be depleted in the vicinity of a grain boundary. See the section ''Precipitate-Free Zones'' for more discussion.

γ'' Hardening of Superalloys. The γ'' phase relationship to properties has not been studied extensively, but γ'' hardening is restricted to a few wrought alloys and their cast versions and to temperatures below about 1300 °F (704 °C). Strength will be a function of V_f of γ''; however, any quantitative relationships established for γ'-hardened alloys will not hold for γ''-hardened alloys because of a difference in precipitate morphology (the γ'-hardened alloys use initial precipitates which are cuboids or spheres, while the γ'' precipitates are disks) and precipitate size. The nickel-chromium-aluminum-niobium alloys tend to have reversion conversion, or dissolution of the strengthening γ'' phase at relatively low temperatures. Bimodal γ'' distributions are not necessarily found, but γ'' coupled with γ' distributions form. Heat treatments for the nickel-chromium-aluminum-niobium alloys attempt to optimize the distribution of the γ'' phase as well as to control component grain size.

Although for many years a sequence of solution treatment followed by two-step aging was the preferred route to an appropriate γ'' distribution after an article was forged, this is no longer the case. This sequence has been replaced in many instances by a direct age process after cooling of the nickel-chromium-aluminum-niobium alloy article from the forging temperature. The forging temperature acts as a solution treatment, and sufficient niobium is retained in a desirable grain-sized matrix that uniform γ'' distributions with attendant γ' precipitate can be formed by direct aging.

The practical use of γ'' precipitation is restricted to nickel-base alloys with niobium additions in excess of 4 wt%. IN-718 is the outstanding example of an alloy in which γ'' formation has been commercially exploited. The V_f of γ'' in IN-718 is substantially in excess of that of γ'. Both γ'' and γ' may be found in alloys where γ'' is present, but γ'' will be the predominant strengthening agent. Although the strengthening behavior of γ'' phase has not been studied, similar considerations to γ' behavior as described previously probably pertain, that is, there will be an optimal γ'' size and V_f for strength. The most significant feature of γ'' is probably the ease with which it forms at moderate temperatures after prior solutioning by heat treatment or joining processes. Because of this behavior, a γ''-hardened alloy can be aged, after welding, to produce a fully strengthened structure with exceptional ductility.

The γ'' phase, not normally a stable phase, can convert to γ' and δ Ni_3Nb on long-time exposure. The strength of γ' is additive to that of γ'' phase. A lack of notch ductility in IN-718 has been associated with a γ'' PFZ; the γ'' PFZ can be eliminated and ductility restored by appropriate heat treatment. Alloys hardened with γ'' phase achieve high tensile strengths and very good creep-rupture properties at lower temperatures, but the conversion of γ'' to γ' and δ above about 1250 °F (675 °C) causes a sharp reduction in strength. Owing to this instability of γ'' above about 1250 °F (675 °C), it will be noted that IN-718 normally never is tested above that temperature. A fairly standard test temperature for virtually all types of elevated-temperature tests on IN-718 (and many other turbine disk alloys) is 1200 °F (649 °C).

Grain-Boundary Carbides in Nickel-Base Superalloys

Grain-Boundary Hardening. Carbides exert a profound influence on properties of wrought and cast alloys by their precipitation at grain boundaries. Carbon even plays a role in SCDS superalloys. In many superalloys, $M_{23}C_6$ forms at the grain boundaries after a postcasting or postsolution heat treatment thermal cycle such as aging. The actual role of carbides was undocumented until the 1950s, when the importance of chromium carbides such as $Cr_{23}C_6$ in optimizing creep-rupture properties of Nimonic 80A and Waspaloy was independently recognized.

Early studies of precipitation-hardened nickel-base superalloys relied on a single solution and a single age to generate properties. The single-aging temperatures most often were about 1300 to 1400 °F (704 to 760 °C) for these early wrought γ'-hardened superalloys.

The creep- and stress-rupture properties of Nimonic 80A, an early γ′-hardened superalloy, were optimal in tests at about 1300 °F (704 °C) when solution treatments were carried out at about 1975 °F (1080 °C) and were followed by a single age. Lower solution temperatures caused higher creep rates, and higher solution temperatures caused premature rupture failure at small creep strains. Figure 12.7 shows the results of varying solution treatment temperatures with and without a specific intermediate heat treatment (IHT) between solution and aging (see Fig. 12.8 for the effect of differing IHT on strength). When an intermediate-temperature heat treatment was introduced, higher solution temperatures gave better rupture life than previously possible (Figs. 12.7 and 12.8).

The microstructure of the stronger and weaker conditions was examined with the available techniques, and it was concluded and later confirmed that:

- No carbide particles or films were found when creep properties were poor.
- A chain of discrete particles, later identified as Cr_7C_3 or a similar chromium-rich carbide phase, existed at grain boundaries after an IHT.
- These particles played a major role in optimizing creep-rupture properties.

Subsequent to these investigations, more advanced metallographic techniques on the previously mentioned alloy and similar wrought superalloys detected that a discontinuous (zipper, cellular) carbide precipitation with γ′ occurred at the grain boundaries and led to reduced creep-rupture capability compared to alloys with globular discrete carbides in the boundary.

Basically, the effect produced by an IHT was for chains of discrete globular carbides (normally $Cr_{23}C_6$ in most wrought alloys) to prevent grain-boundary sliding in creep rupture while concurrently permitting sufficient ductility to be achieved in the surrounding grain that stress relaxation of the γ/γ′ could occur without premature failure. Based on this and similar work, an IHT was introduced to the process schedules for wrought alloys. Although this work was published for Nimonic 80A, an unpublished paper by Pratt & Whitney developed similar conclusions about maximizing creep-rupture life of Waspaloy nickel-base superalloy. Virtually all wrought alloys have been processed with dual aging schedules since the discovery of the beneficial effect of a discrete carbide grain-boundary distribution and the detrimental effects of discontinuous carbide/γ′ precipitation. The cycle temperatures varied (and still do) with alloy chemistry and local rules.

Although the preceding discussion centered on chromium-rich carbides such as $Cr_{23}C_6$, globular M_6C has been reported to

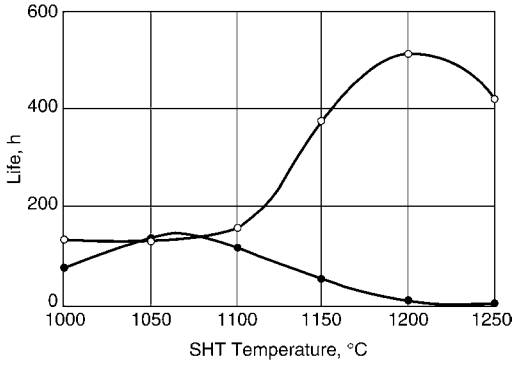


Fig. 12.7 Influence of solution heat treatment temperature on rupture life of Nimonic 80A nickel-base superalloy at 234 MPa (34 ksi) and 750 °C (1380 °F), showing effect of 1000 °C (1832 °F) intermediate heat treatment before aging. Open datapoints are SHT for 4 h. Cool to IHT and IHT for 16 h AC and age 16 h at 700 °C (1292 °F). Closed datapoints are SHT for 8 h AC and age 16 h at 700 °C (1292 °F).

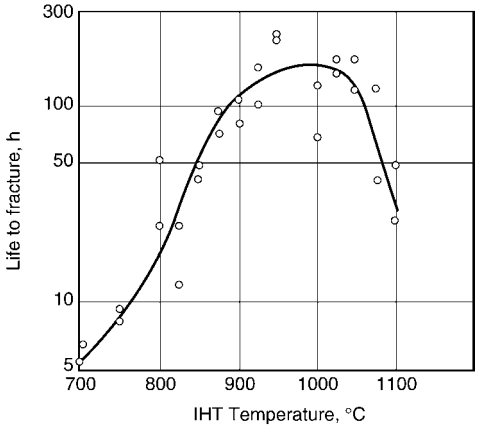


Fig. 12.8 Relationship between rupture life and intermediate heat treatment temperature for Nimonic 80A nickel-base superalloy at 234 MPa (34 ksi) and 750 °C (1380 °F). SHT for 3 h at 1250 °C (2282 °F). Transfer to IHT furnace and IHT for 24 h WQ and age 16 h at 700 °C (1292 °F).

provide similar benefits in retarding grain-boundary sliding.

The Reason for Discontinuous Cellular Carbides. When nickel-base superalloys are solution treated, some of the MC carbides present in the structure also are dissolved. The carbon from this dissolution process does not automatically dissipate. Rather, carbon atoms are available extensively in the solution-treated alloy. Upon rapid cooling of the heat treated article to room or ambient temperatures, the carbon is retained in supersaturation. On reheating to the normal temperature for a single age, the thermodynamic considerations of carbide precipitation favor formation of many chromium carbides at grain boundaries. The most efficient way that so much carbide can form is perpendicular to a grain boundary, and thus, so-called zipper or cellular discontinuous carbides precipitate (note Fig. 12.9). The extra boundary area produced by the carbide/γ' cellular precipitation is detrimental to stress-rupture life.

A Role of the IHT. The IHT, a treatment below the solution temperature but at a higher temperature than the original single-aging temperatures on which so many alloy properties were based, brings down the carbon supersaturation to a lower point by permitting carbides to form under less highly energetic conditions. The carbon supersaturation at the IHT temperature is more conducive to discrete particle growth. The result of the higher-temperature formation of the discrete carbides is that carbon energy potential is reduced and excessive amounts of carbides and extra interfaces for creep cracking will not be produced in the final age.

In the case of one Waspaloy specification, where the IHT is about 1550 °F (843 °C) for 24 h and final aging is at 1400 °F (760 °C) for 16 h, discrete $Cr_{23}C_6$ particles form and grow at the IHT. A significant amount of γ' is formed, but further γ' is created while the original γ' grows during the final aging treatment. Some additional $Cr_{23}C_6$ phase may be formed during the final age, but the distribution and interfaces between the $Cr_{23}C_6$ and the γ-γ' matrix have been established by the IHT, and the carbides remain discrete.

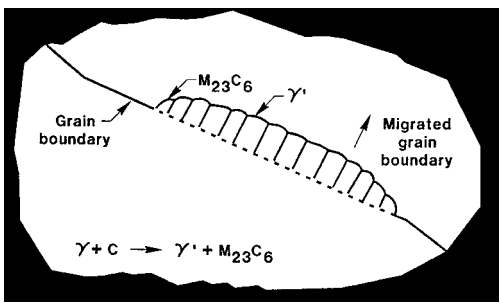


Fig. 12.9 Schematic representation of cellular carbide precipitation at a grain boundary in a nickel-base superalloy

Is an IHT Really Required? Acceptable mechanical properties do not always result from the initial solution and aging procedures developed for an alloy. To develop specified mechanical properties, changes of the following kind are often required:

- Adjust the solution temperature or time
- Adjust the single-aging temperature
- Add an IHT
- Add a second age or, if IHT is really acting as an age, add a third age
- Adjust the temperatures in the various IHT-age sequences
- Adjust (usually increase) age time

The IHT often is called an aging treatment, which it may be. Despite the beneficial aspects of the IHT on creep-rupture for some wrought superalloys, some applications require enhanced short-time strengths (yield and ultimate). Short-time strengths are increased with a greater amount of smaller γ' particles and a finer grain size. Intermediate heat treatments tend to promote somewhat coarser γ' particles. In the interest of greater yield and ultimate strengths, an additional age treatment might be added or the IHT might be eliminated. A lower solution temperature might be used to restrict grain growth and keep a finer grain size in a forged component. It is important to note that it is not only heat treatment that influences tensile properties; control of the thermomechanical processing sequence is important. Large grain-size reductions have been attained in superalloys by manipulation of the deformation processing going on in the forging operation. Better γ' distributions have been promoted by adding an age, deleting an age, and/or increasing aging time.

Another Role for the IHT. In an alloy hardened by a coherent γ' precipitate, as indicated earlier, dislocations may cut particles at small γ' particle sizes. One of the consequences of particle cutting is that subsequent

deformation may tend to be concentrated on the same deformation plane rather than dispersed in the matrix. This process leads to low ductility. On the other hand, smaller γ' sizes tend to lead to greater short-time strengths. Finer γ' sizes are associated with lower aging temperatures. The concentration of deformation produced by a fine γ' size arising from a single low-temperature age can promote notch sensitivity in short-time testing. An alloy can be strong as far as yield and ultimate strength are concerned, but fail prematurely if a notch is introduced.

The introduction of an IHT not only improved the resistance of a grain boundary to sliding and failure in creep rupture, but also promoted a dual size of γ' in an alloy. With more than one size of γ', it is possible to have small γ' that must be cut while having coarse γ' that must be bypassed. The result is an alloy with dispersed deformation and maximum ability to have good strength with sufficient ductility (caused by the dual γ' distribution) to resist notch failure. Thus, it is probable that the IHT serves a dual function by maximizing grain boundary ductility and resistance to high-temperature sliding while promoting improved lower-temperature ductility and notch failure resistance.

Acicular Carbide Formation. The ductilities of some nickel-base superalloys also have been impaired by a different mode of carbide precipitation, namely Widmanstätten (acicular) M_6C formation at grain and twin boundaries. While the effect is possible, it is not widely encountered. Widmanstätten precipitates do, in principle, appear to contribute to a lowering of the creep-rupture life, but practical illustrations with M_6C at grain boundaries are not easy to find. Examples of Widmanstätten precipitation usually are restricted to intragranular regions, although they may appear to nucleate at or near MC particles; however, acicular carbides sometimes may be found at grain boundaries.

Precipitate-Free Zones. Another effect produced by grain-boundary $M_{23}C_6$ carbide precipitation is the occasional formation, on either side of the boundary, of a zone depleted in γ' precipitate. These precipitate-free zones (PFZ) may have significant effects on rupture life of nickel- and iron-nickel-base superalloys. If such zones should become wide or much weaker than the matrix, deformation would concentrate there, resulting in early failure. Precipitate-free zones were widely noted in early γ'-hardened superalloys with low hardener content (and a titanium to aluminum ratio of 1.0 or higher). However, the more complex (higher $V_f\gamma'$) γ'-hardened superalloys do not show significant PFZ effects, probably because of their higher saturation with regard to γ'-forming elements. Cobalt additions were suggested to be beneficial for retarding the formation of denuded (depleted) γ' zones. Boron and zirconium were thought to be beneficial in this respect as well. See ''Beneficial ''Minor'' Elements Boron, Zirconium, and Hafnium'' and ''Some Observations on Cobalt in Nickel-Base Superalloys'' later for more discussion of the effects of cobalt and of minor elements such as boron.

An effect seen concurrently with PFZ and not often separated from it in the literature is the γ' envelope produced by breakdown of TiC and consequent formation of $M_{23}C_6$ or $M_6C + \gamma'$ (from the excess titanium). This process takes place primarily at grain boundaries but also around decomposing MC particles in the body of a grain. There is a general consensus that γ' envelopes, if formed, may be beneficial, owing to their ability to relax or absorb stresses in the vicinity of sliding boundaries. However, the precise role of the γ' envelope is not sufficiently established, and there is the remote possibility that the excess titanium-rich area is really either η or a metastable γ' that could transform to η in use. Envelopes of γ' are found in some high-$V_f\gamma'$ alloys

Carbide Films. If carbides precipitate as a continuous grain-boundary film, properties also can be severely degraded. $M_{23}C_6$ films were reported to reduce impact resistance of M252, and MC films were blamed for lowered rupture lives and ductility in forged Waspaloy. Figure 12.10 shows the presence of grain-boundary films in Waspaloy intentionally forged under conditions to cause grain-boundary films. Such conditions can consist of high-temperature soaking in a furnace preparatory to forging and then, for example, giving no or little reduction at a time of final forging. The result is an alloy with a great supersaturation of carbon, owing to solutioning of the MC. Upon post-forge solution treating of the Waspaloy at 1975 °F (1080 °C), MC carbides are favored by the extreme carbon potential, and without forg-

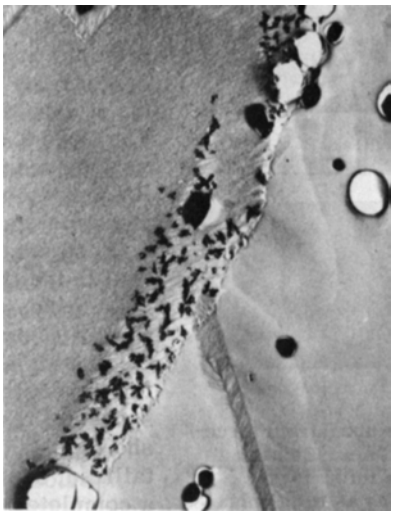


Fig. 12.10 Grain-boundary films of MC (black) in Waspaloy (extraction replica—black objects were standing vertically in grain boundary prior to extraction). Waspaloy was intentionally forged under poor conditions to cause grain-boundary films.

ing to break up any structures and create new precipitation sites, the carbon pops out at boundaries and forms films. The films are limited in ductility, and creep-rupture life is thus limited.

No Carbides at All. At the other extreme, when no grain-boundary carbide precipitate is present, premature failure also will occur, because grain-boundary movement essentially is unrestricted, leading to subsequent cracking at grain-boundary triple points.

Grain-Boundary Carbides in Other Superalloys

Iron-Nickel-Base Superalloys. The role of carbides at grain boundaries in iron-nickel-base superalloys is less well documented than for nickel-base alloys, although detrimental effects of carbide films have been reported.

Cobalt-Base Alloys. Studies of specific effects of grain-boundary carbides in cobalt-base alloys are even more sparse. The carbide distribution in cobalt-base alloys arises from the original casting or upon cooling after mill annealing for wrought cobalt-base alloys. The significantly greater carbon content of cobalt-base alloys leads to much more extensive grain-boundary carbide precipitation than in nickel- and iron-nickel-base alloys. Carbides at grain boundaries in cast cobalt-base alloys appear as eutectic aggregates of M_6C, $M_{23}C_6$, and fcc γ cobalt-base solid solution. No definitive study of the effects of varied carbide forms in grain boundaries on the mechanical behavior of cobalt-base superalloys has been reported.

The lamellar eutectic (carbides-γ cobalt) nature of carbides ($M_{23}C_6$-M_6C) in cast cobalt-base superalloys is interesting. A somewhat similar morphology of $M_{23}C_6$, occurring when it is precipitated in cellular form in nickel-base and iron-nickel-base alloys, leads to mechanical-property loss in such alloys, but lamellar eutectic does not seem to degrade cast cobalt-base alloy properties.

Carbide Precipitation—General Hardening

General Comments. Carbides affect the creep-rupture strengths of cobalt-base superalloys and some nickel- and iron-nickel base superalloys by formation within grains. These carbides are particularly evident in cast superalloys but also are present in wrought superalloys. The MC are predominant, because they are the first formed upon cooling from the molten state. Thus, cast alloys invariably have MCs located within the grains, although MC may be found at grain boundaries as well. Subsequent heat treatments, intentional or owing to service exposure, and/or wrought processing will modify the morphology, amounts, and types of carbides found in the grains of superalloys. Carbide formation is not uniform and regular, as is that of γ' precipitation. The carbides may be of different sizes and somewhat varying shapes, even for the same phase. Some secondary carbides within grains can be formed by precipitation on dislocations located near large primary carbides.

Carbides within grains act to impede basic dislocation movement, with an attendant increase in the strength of a superalloy. The strength increase obtained from a carbide dispersion in grains is less than that of the typical hardening caused by γ' precipitation but still may be significant.

Cobalt-Base Superalloys. In cobalt-base cast superalloys, script MC carbides are lib-

erally interspersed within grains, causing a form of dispersion hardening that is not of a large magnitude, owing to its relative coarseness. The distribution of carbides in cast alloys can be modified by heat treatment, but strength levels attained at all but the highest temperatures are substantially less than those of the γ'-hardened alloys. Consequently, cast cobalt-base alloys generally are not heat treated, except in a secondary sense through the coating diffusion heat treatment of 4 h at 1950 to 2050 °F (1065 to 1120 °C), which may be applied if a coating is required.

Wrought cobalt-base superalloys have carbide modifications produced during the fabrication sequence. Carbide distributions in wrought alloys result from the mill anneal after final working. Properties are largely a result of grain size, refractory-metal content, and carbon level, which indicates the V_f of carbides available for hardening.

True solutioning, in which all minor constituents are dissolved, is not possible in most cobalt-base superalloys, because melting often occurs before all the carbides are solutioned. Some enhancement of creep-rupture behavior has been achieved by heat treatment wherein some carbides are solutioned and then reprecipitated. Rupture time improvements can be gained by aging X-40 cobalt-base superalloy (Fig. 12.11). In view of the benefits of carbide precipitation, adjustments of the carbon content were considered as a possible beneficial approach to increases in the strength of cobalt-base superalloys. In fact, large increases were produced by increasing the carbon content of several cobalt-base superalloys, Vitallium and modified Vitallium (HA-21), as shown in Fig. 12.12. Rupture life was increased with carbon content in each alloy and peaked just below 1.2 wt%.

It is apparent that carbon content is one variable in strength of cobalt-base superalloys. Aging conditions are another. When aging temperatures were varied, aging of as-cast modified Vitallium alloy (Fig. 12.13) showed a peak in rupture life and minimum in ductility at an aging temperature slightly below 1400 °F (760 °C). As can be noted, the rupture-life improvement was very significant, almost a factor of 3.5 over the as-cast value. Response to aging can be assisted by cold work prior to aging. Studies of aged HA-25 alloys treated by cold work showed substantial strength improvements without much loss in ductility.

Although aging of a cobalt-base superalloy may lead to strength improvement, solution treating and aging is not suitable for producing stable cobalt-base superalloys for use above 1500 °F (815 °C) because of subsequent carbide dissolution or overaging during

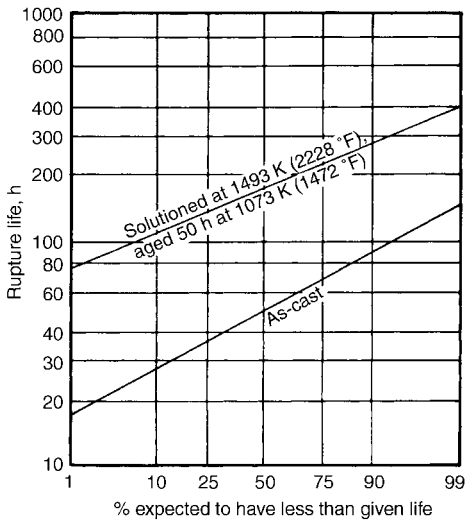


Fig. 12.11 Effect of solution heat treatment and aging on X-40 (HA-31) cobalt-base superalloy showing increase in strength resulting from carbide precipitation

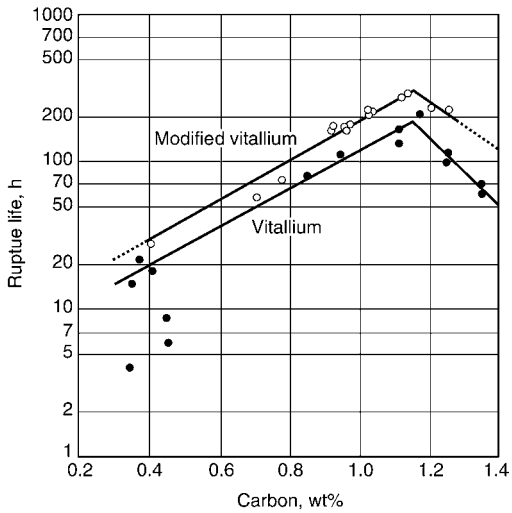


Fig. 12.12 Effect of carbon content on the stress-rupture life of Vitallium and modified Vitallium alloy at 816 °C (1500 °F)/207 MPa (30 ksi)

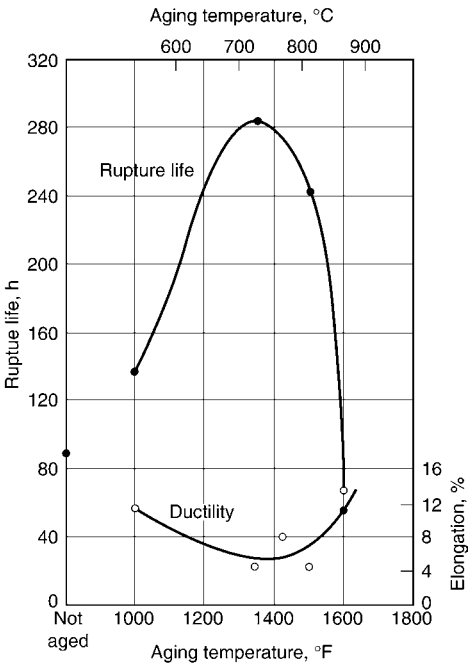


Fig. 12.13 Effect of aging on the rupture life and ductility of an as-cast modified Vitallium cobalt-base superalloy at 816 °C (1500 °F)/138 MPa (20 ksi)

service exposure. If the X-40 alloy shown in Fig. 12.11 had been aged or tested at a somewhat higher temperature, no improvement in stress-rupture strength would have been observed.

Nickel- and Iron-Nickel-Base Superalloys. Matrix carbides in nickel-base and iron-nickel-base superalloys also may be partially solutioned. MC will not totally dissolve, however, without incipient melting of the alloy. MC in such alloys tend to be unstable, decomposing to $M_{23}C_6$ at temperatures below about 1500 to 1600 °F (815 to 870 °C) or possibly converting to M_6C at temperatures of 1800 to 1900 °F (980 to 1040 °C) if the alloy has a sufficiently high molybdenum + tungsten content (Mo + $\frac{1}{2}$W $\geq$ 6 wt%). In some instances, the formation of M_6C is as intragranular Widmanstätten precipitates, in others as a blocky carbide particle. Matrix carbides generally contribute very small increments of strengthening to nickel- and iron-nickel-base superalloys. M_6C, despite its acicular form in some instances, did not appear to reduce properties of B-1900 nickel-base superalloy after exposure to produce the carbide.

An interesting microstructural trend has taken place with the advent of single crystals of nickel-base superalloys. Because no grain boundaries exist, there is little need for the normal grain-boundary strengtheners such as carbon. Consequently, very few matrix or subboundary carbides exist in first-generation SCDS alloys. Although the initial trend was to remove carbon completely from SCDS nickel-base superalloys, as time passed, the realization that sub-boundaries in single crystals could benefit from carbides has led to a relaxation of carbon restrictions, and low amounts of carbon are now permitted in many single-crystal alloys. (Hafnium, boron, and zirconium in limited amounts also may be permitted.) The trend in wrought P/M nickel-base superalloys continues to be toward reduced carbon and reduced carbide size as a means to limit fracture-mechanics-restricting defect sizes and numbers.

Perhaps the most common other role of matrix carbides (also shared by grain-boundary carbides) is a negative one: they may participate in the fatigue cracking process by premature cracking or by oxidizing at the surface of uncoated alloys to cause a notch effect. Oxidized carbides or precracked carbides from machining or thermal stresses can initiate fatigue cracks. Precracked carbides can be related to prior casting processes. Carbide size is important, and reduced carbide volumes and sizes in nickel-base alloys result in a reduction in precracked carbides.

The longer solidification times and lower gradients of early directional solidification (DS) processes often resulted in moderately large carbides that were more prone to cracking. However, improved gradients and the reduced carbon contents of SCDS alloys (few or no carbides) have resulted in substantial improvements in fatigue resistance, particularly over similarly oriented CGDS alloys with normal carbon levels. This effect is most noticeable in low-cycle fatigue (LCF) and thermal-mechanical fatigue (TMF).

Little evidence is available to determine if there is an effect of the absence of carbides on high-cycle fatigue (HCF), but beneficial effects might be anticipated if strength is not otherwise affected. Nevertheless, there is some evidence that a minimum carbide level

may be required for optimal fatigue resistance in certain superalloy-related systems. In an 18-8 austenitic stainless steel, the LCF and HCF life between 10^4 and 10^8 cycles at 1300 °F (704 °C) was higher with 0.05% C than without carbon.

Oxidized carbides can be minimized or prevented by several methods. Casting procedures and/or chemical composition may be modified to produce smaller primary carbides. Powder metallurgy processing may be used to produce the same result. Carbon content may be reduced if it is not specifically required to enable the alloy to attain the desired strength levels. Reduced carbon is the rule in SCDS and P/M superalloys. Of course, if operating temperature will be high, the alloy may be coated with an appropriate protective coating that leaves the carbides in a subsurface location.

It should be anticipated that there will be variability in the effects of intragranular carbon in nickel- and iron-nickel-base superalloys. Dependent on carbide size, distribution, type of carbide, cooling conditions, cracking owing to machining, oxidation or corrosion-induced notches, and the type of property being tested, carbides may be beneficial or detrimental to performance.

Effect of Noncarbide Formers on Carbide Formation. Although there is limited documentation, it frequently is assumed that noncarbide-forming elements do influence the formation of carbides. Cobalt, for example, has been claimed to modify the carbides in nickel-base alloys, and phosphorus has produced a more general, more finely dispersed and smaller carbide precipitation than carbon alone in a heat-resisting iron-nickel-base alloy. The modifying effect on carbides may be intragranular or intergranular, depending on the modifier and the base-alloy system.

IN-718 and the Role of δ Phase in Strengthening

Background. The heat treatment of IN-718 is similar in concept to that of the γ′-hardened superalloys, except that solution treatment and aging temperatures are lower. In this γ″-hardened alloy, both γ″ and δ phases are present in the microstructure. The δ phase is used for grain-structure (size) control in IN-718, just as the η phase can be used in A-286 (iron-nickel-base) and IN-901 (nickel-base) γ′-hardened superalloys. However, careful heat treatment is required to ensure proper precipitation of γ″ and δ phases. The latter phase is not coherent with the γ matrix and confers little or no strengthening of its own when present in large quantities. On the other hand, by ensuring the retention of a fine grain size, δ is responsible for considerable improvements in IN-718 strength. (See ''Heat Treatment of IN 718'' later about direct-age IN-718.)

IN-718 forms γ″ after solution treatment when aged in the range of about 1300 to 1650 °F (704 to 899 °C). The γ″ solvus is about 1670 °F (910 °C). The δ phase (depending on exposure time) precipitates in the vicinity of about 1600 °F (871 °C) and has a solvus temperature of about 1850 °F (1010 °C). IN-718 can be worked and heat treated above the δ solvus, or at a temperature between the δ solvus and the γ″ solvus for grain-size control, which is an important aspect of current high-strength IN-718 production. (See ''Heat Treatment of IN 718'' later for more discussion about IN-718 properties.)

IN-718 is customarily (standard heat treatment) solution heat treated at 1750 °F (954 °C) and then aged in a two-stage process at lower temperatures (see Chapter 8 for heat treating schedules). However, this temperature is not always sufficient to fully stress relieve or recrystallize the alloy, and formability is often inadequate. Higher-temperature solutioning at 1900 °F (1038 °C) has been found effective in enhancing formability but renders the alloy notch brittle in stress-rupture testing.

The Role of δ Phase in Preventing Stress-Rupture Embrittlement. Evaluation of the microstructure of high-temperature-solutioned IN-718 indicated a substantially decreased amount of δ compared to normal solution temperatures. The decrease in the amount of prior δ available to pin grain boundaries and provide notch ductility to IN-718 was a function of time at 1900 °F (1038 °C). Figure 12.14 shows micrographs of IN-718 given 20 min and 1 h, respectively, at 1900 °F (1038 °C). Prior δ can be seen in the specimen given 20 min, but the specimen given 1 h is devoid of δ. Tests on notch-sensitive IN-718 showed the longest time to rupture for any notch-sensitive specimen was 1.1

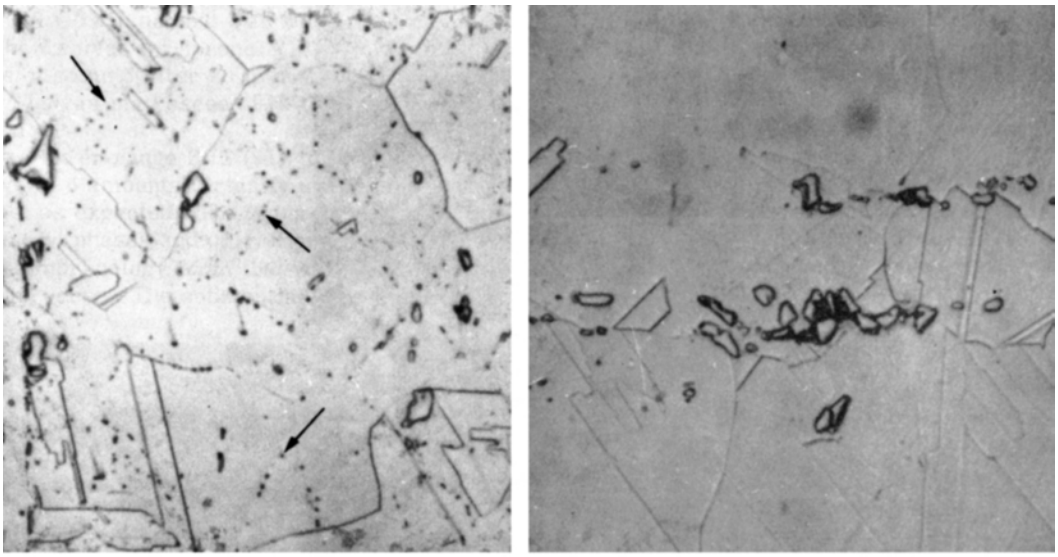


Fig. 12.14 Micrographs of IN-718 nickel-base superalloy after receiving a high solution treatment at 1038 °C (1900 °F) for differing times. (a) 20 min at 1038 °C, showing presence of prior δ-phase grain boundary precipitates (arrows). 550×. (b) 1 h showing absence of prior δ phase particles. 550×

h versus 153.5 h for the shortest time to rupture of any notch-ductile specimen.

Complete loss in notch ductility (resulting from the lack of prior δ to pin grain boundaries and provide notch ductility) in IN-718 was a function of time at 1900 °F (1038 °C) high-temperature solution treatment when compared to a conventional heat treatment at 1750 °F (954 °C). The preceding results suggest a likely behavior for γ″-hardened alloys. These alloys are dependent on an optimal amount and dispersion of δ for adequate creep-rupture properties. Without particles to pin the boundaries (or with continuous plates or films of particles), IN-718 and similar alloys can fail by intergranular cracking with limited ductility and will often be prone to notch failures.

By enhancing ductility through properly distributed grain-boundary particles of δ, notch properties should improve. The interposition of an IHT after excessively high-temperature solutioning and prior to aging was considered as a potential way to reprecipitate substantial amounts of δ phase in the grain boundaries and reduce or eliminate creep-rupture notch sensitivity.

Various IHTs were evaluated after a 20 min high-temperature solution at 1900 °F (1038 °C). At the customary solution temperature of 1750 °F (954 °C), results were not favorable. However, when a slightly lower IHT was used, notch ductility was restored. Unfortunately, no IHT successfully removed the notch sensitivity of IN-718 given a high-temperature solution treatment at 1900 °F (1038 °C) for 1 h (see Table 12.2). The γ″ phase clearly controls the basic strength of γ″-hardened superalloys such as IN-718 and IN-706. However, the δ size, distribution, and amount controlled the effective use of that strength in stress rupture and, as noted previously, in the production and retention of fine grain size for high tensile strength.

Cast and Wrought Superalloy Commentary

General Comments. Cast alloys generally behave differently from wrought alloys. This is particularly true of superalloys. Wrought alloys are more homogenous and finer-grain than cast alloys. The greater homogeneity enables more of the hardener elements to be taken into solution and thus to be effectively converted to γ′ or γ″ phases. Moreover, the

Table 12.2 Notch-rupture testing of IN-718 nickel-base superalloy after varying solution treatments and intermediate heat treatments. All tests of notch creep-rupture specimens at 690 MPa (100 ksi) and 649 °C (1200 °F)

Specimen No.	Solution heat treatment	Intermediate heat treatment	Time to rupture, h
1	1038 °C (20 min)	None	0.4
2	1038 °C (20 min)	None	0.3
3	1038 °C (20 min)	None	0.3
4	1038 °C (1 h)	None	0.1
5	1038 °C (1 h)	None	0.2
6	954 °C (1 h)	None	153.5
7	954 °C (1 h)	None	423.1(a)
8	917 °C (10 h)	None	424.1
9	917 °C (10 h)	None	143.2
10	1038 °C (20 min)	954 °C (3 h)	0.5
11	1038 °C (20 min)	954 °C (3 h)	0.4
12	1038 °C (20 min)	917 °C (10 h)	882.8(a)
13	1038 °C (20 min)	917 °C (10 h)	499.5(a)
14	1038 °C (20 min)	917 °C (10 h)	838.4(a)
15	1038 °C (20 min)	917 °C (10 h)	838.4(a)
16	1038 °C (1 h)	954 °C (3 h)	0.3
17	1038 °C (1 h)	954 °C (3 h)	0.6
18	1038 °C (1 h)	917 °C (10 h)	0.5
19	1038 °C (1 h)	917 °C (10 h)	0.8
20	1038 °C (1 h)	917 °C (10 h)	1.1

All specimens aged after solution or solution plus intermediate heat treatments. (a) Test discontinued

distribution of the γ' and/or γ'' should be more uniform and finer in size for wrought than for equivalent cast material. For a given amount of available γ', finer grain sizes should produce greater short-time strengths. Wrought precipitation-hardened alloys tend to have grain sizes that are finer than cast counterparts. The tensile strengths of wrought alloys, with comparable $V_f\gamma'$ to cast alloys (e.g., wrought IN-100 versus cast IN-100), are greater than those achieved in the cast alloys.

A typical wrought alloy might have had ASTM grain-size numbers of 0 to 6 prior to the introduction of current P/M processing and improved melting, ingot conversion, and forging practice. There was a major change in grain size of wrought products in the last quarter of the 20th century. Grain sizes of ASTM 8 to 12 are more common now (finer grain size is associated with greater ASTM grain-size numbers); some specifications may permit ASTM 14. Coarser grain size (lower ASTM numbers) would be desired for improved creep-rupture strength (see subsequent paragraphs for other comment).

By virtue of fine grain and a $V_f\gamma'$ now in the 50 to 60% range, tensile ultimate strengths (at room temperature) in the range of about 200 ksi (1379 MPa) are achieved with regularity. Ultimate tensile strength values as high as 235 ksi (1620 MPa) are produced in Rene 95 (see Table 2.1). Tensile strengths are limited by compromises with the amount of available γ' and the grain size. All available hardener cannot be taken into solution, or the grain size may no longer be restricted from growing.

Creep-rupture properties are increased by a greater $V_f\gamma'$, a greater V_f of fine γ', and a coarser grain size. Grain-size increases do not always lead to longer rupture lives. Most evidence points to a peak in rupture life (valley in creep rate) with increasing grain size (see Fig. 12.15 for Nimonic 80A wrought nickel-base superalloy).

At one time, wrought and cast versions of the same alloy were sometimes in use in contemporary applications. For example, Waspaloy and U-700 alloys were used in both wrought and cast form for turbine blades. Heat treatments for wrought applications differed from those for cast applications. Generally, wrought versus cast alloy comparisons are only academic, because cast alloys have carved out the niche of turbine airfoils and various cases in gas turbines, while disks and fabricated structures remain largely the province of wrought alloys. There are circumstances where cast alloys have found application in small gas turbine disks and where cast alloys (IN-718, IN-939) have replaced

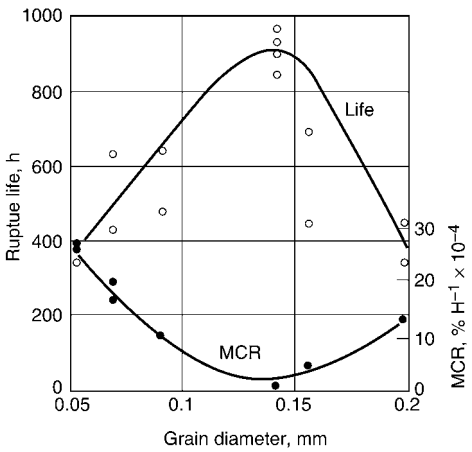


Fig. 12.15 Rupture life and minimum creep rate (MCR) of Nimonic 80A nickel-base superalloy at 750 °C (1380 °F)/234 MPa (34 ksi) vs. grain diameter of specimen tested

wrought fabricated construction in some large and small cases for gas turbines.

Heat Treating the Same Wrought Alloy for Different Property Applications. There was a period when the same wrought alloy might have been used for different purposes. For example, Waspaloy nickel-base superalloy was used in two wrought forms for turbine disk applications and one wrought form as turbine blades.

The different Waspaloy specifications arise from the fact that solution temperatures for any given heat of a material will have a significant impact on the degree of γ' solutioning and degree of recrystallization during heat treatment. Higher yield and ultimate strength are obtained in Waspaloy with finer grain sizes, which result when some γ' remains after cooling from forging and when solution treating is done at a temperature just below the γ' solvus. However, the best 1350 °F (730 °C) stress-rupture life is obtained with a coarse grain structure and a maximum amount of fine γ'. Consequently, for wrought Waspaloy when not only disks but blades were being made, at least two different specification conditions existed—a specification for disk (tensile strength limited) applications and another for turbine airfoil (stress-rupture limited) applications. Material was heat treated accordingly after forging. In a study done on Waspaloy, the following conditions were found to be optimal:

- 1850 °F (1010 °C), 4 h, oil quenched + 1500 °F (816 °C), 4 h, air cooled + 1400 °F (760 °C), 16, air cooled produced the best tensile strength for disk applications
- 1900 °F (1038 °C), 4 h, oil quenched + 1600 °F (871 °C) air cooled + 1400 °F (760 °C) air cooled produced the best 1350 °F (730 °C)/75 ksi (551 MPa) stress-rupture strength for airfoil applications

Because creep properties may tend to follow yield strength, and rupture tends to follow ultimate strength (rough approximation), it seems that heat treating an alloy for best creep properties might not be the equivalent of heat treating for best stress-rupture properties.

Figure 12.16 shows the influence of different heat treatments on the tensile and stress-rupture properties of Waspaloy. Generally, the turbine disk heat treatment favors the shorter-time or lower-temperature regime, while the turbine blade heat treatment produces better properties in the longer-time and higher-temperature regimes.

Heat Treating the Same Alloy for Different Forms. An analog to the preceding situation on heat treatment for various applications can be found in the heat treatment of some γ'-hardened nickel-base superalloys for various forms of the same basic alloy. Table 12.3 gives the thermal treatments for desired properties of IN-X-750 products, such as sheet, bar, and so on, and shows the range of precipitation-hardening conditions that may be used.

The Effect of Section Size on Creep-Rupture Properties. Although wrought superalloys have been used in thin sections or smaller diameters for many years, debits have not been reported for various section sizes, with a few exceptions. In the late 1960s, studies of section size of facts in thin sections were reported on some wrought superalloys. The influence of specimen diameter to mean grain diameter (size) was evaluated for rupture and minimum creep rate (MCR), and Fig. 12.17 shows the results. The smaller the ratio of specimen diameter to the grain diameter, the lower the creep-rupture property (lower life, higher MCR).

Specimen grain diameter (size) will affect the test specimen diameter (SD) to grain diameter (GS) ratio. Fine-grained superalloys such as the wrought alloys should have a greater SD/GS ratio than coarse-grained alloys for the same specimen size. Thus wrought alloys should show less debit with section size reductions than the coarser grained cast alloys. There are only a few data sets available on thin section size effects for either wrought or cast alloys.

Other than sheet, wrought alloys are used at thicknesses of fractions of an inch up to many inches. Many components will have several different section sizes over the volume of the component, for example, in a gas turbine disk, three distinct volumes can be identified. They are the bore (very thick), the web (fairly thin) and the rim (moderate thickness). Actual section size is dependent on component design (disk, airfoil, shaft, and so forth). Smaller aircraft gas turbine engines will have different section size problems than larger industrial gas turbines.

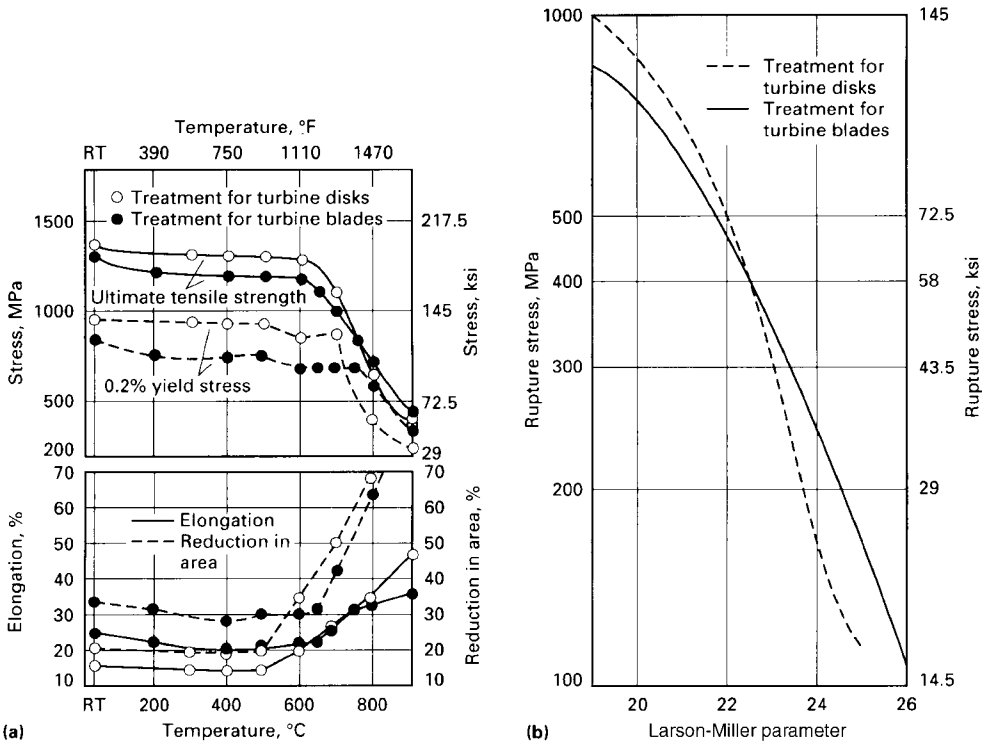


Fig. 12.16 Influence of different treatments on (a) the tensile properties vs. temperature and (b) rupture properties of Waspaloy nickel-base superalloy using Larson-Miller parameter (P_{LM}). Note: $P_{LM} = T(C + \log t)$ where C = Larson-Miller constant, T = absolute temperature, t = time in h. For this plot, C = 20, T = K

Table 12.3 Typical thermal treatments for precipitation hardening of IN-X-750 in various product forms

Form	Desired property	Thermal treatment
Rods, bars, and forgings	Strength and optimal ductility up to 595 °C (1100 °F)	Equalize: 885 °C (1625 °F), 24 h, air cool Precipitation: 705 °C (1300 °F), 20 h, air cool
	Optimal tensile strength up to 595 °C (1100 °F)	Solution: 980 °C (1800 °F), air cool Furnace-cool, precipitation: 730 °C (1350 °F), 8 h, furnace cool to 620 °C (1150 °F), hold 8 h, air cool
	Maximum creep strength above 595 °C (1100 °F)	Full solution: 1150 °C (2100 °F), 2–4 h, air cool Stabilize: 845 °C (1550 °F), 24 h, air cool Precipitation: 705 °C (1300 °F), 20 h, air cool
Sheet, strip, and plate	High strength at high temperatures	Annealed + Precipitation: 705 °C (1300 °F), 20 h, air cool
	High strength and higher tensile properties to 705 °C (1300 °F)	Annealed + Furnace-cool, precipitation: 730 °C (1350 °F), 8 h, furnace cool to 620 °C (1150 °F), hold 8 h, air cool(a)
Tubing	High strength at high temperatures	Annealed + Precipitation: 705 °C (1300 °F), 20 h, air cool
No. 1 temper wire	Service up to 540 °C (1000 °F)	Solution treated + cold drawn (15–20%) + 730 °C (1350 °F), 16 h, air cool
Spring temper wire	Service up to 370 °C (700 °F)	Solution treated + cold drawn (30–65%) + 650 °C (1200 °F), 4 h, air cool
	Service at 480–650 °C (900–1200 °F)	Cold drawn (30–65%) + 1150 °C (2100 °F), 2 h, air cool + 845 °C (1550 °F), 24 h, air cool + 705 °C (1300 °F), 20 h, air cool

(a) Equivalent properties in a shorter time can be developed by the following precipitation treatment: 760 °C (1400 °F) for 1 h, furnace cool to 620 °C (1150 °F), hold 3 h, air cool.

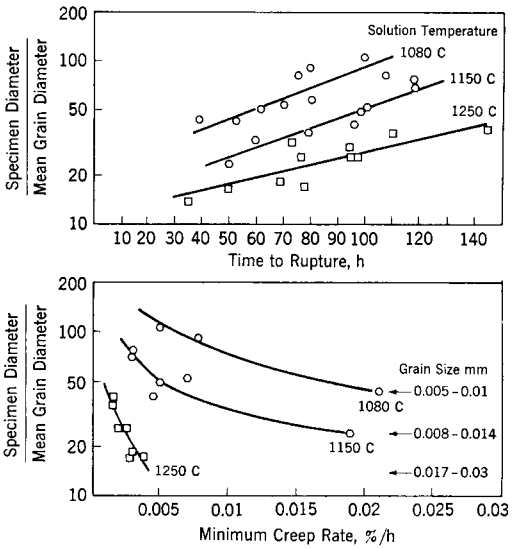


Fig. 12.17 Influence of specimen diameter/mean grain diameter ratio and solution temperature on the creep-rupture properties of a wrought nickel-base superalloy tested at 870 °C (1600 °F)/138 MPa (20 ksi). Note: Grain size was a function of solution temperature, as shown on MCR plot.

No debits have been reported for thin sections of wrought bulk superalloy components. Thinner sections in bulk components generally are still as much as an order of magnitude thicker than airfoil sections. As a rule, it actually is more realistic to think of bulk wrought superalloy products such as disks, cases, and so forth to be capable of suffering from a thick-section debit. This debit is produced by lack of adequate hot work and/or variations in cooling rate of thicker sections from the conditions in thinner sections of a component. (Note discussion about location of test specimens in the section ''The Effect of Location on Mechanical Properties.'')

Planar products such as sheet and plate may be ''naturally thin.'' Few, if any, data are available on section size effects in superalloy sheet and plate. However, effects of test specimen orientation have been studied. Working of alloys to produce sheet or plate can cause special oriented textures to appear. Thus, orientation of test specimens of wrought planar products relative to rolling direction in the plane of a sheet can show property variations. In-plane properties of superalloy bulk parts normally are determined but through-thickness data are not. Tensile and creep-rupture properties have been determined as a function of thickness and direction for some wrought and cast alloys where appropriate specimens can be taken. Fracture toughness data for superalloys have not been similarly investigated. Fracture behavior might be considerably different for thinner sections of an otherwise bulk superalloy component. Potential property variability, including debits, for thinner or for thicker section areas of a component, should be considered in the design process.

Cast superalloys, at least cast γ'-hardened nickel-base superalloy airfoils, suffer from section-size effects and from specimen manufacturing aspects (cooling rates, etc.). Limited studies have been done on PC, CGDS, and SCDS cast alloys, both with regard to section size and to the relative worth of cast-to-size (CTS) specimens versus specimens machined from components (MFC).

Generally, until the mid-1960s, mechanical property data used to set property standards for cast nickel-base superalloys were generated on cast test bars. Figure 12.18 shows the relative size of the early cast test bars used to generate turbine airfoil data. Experience began to show that separately cast test bars did not represent the cast airfoils. Consequently, test bars were taken from actual airfoils (Fig. 12.19). Table 12.4 shows the differences that were found for typical properties of B-1900 nickel-base superalloy when separately cast test bars were compared with specimens MFC (turbine blades). There are significant differences. Undoubtedly, the differences occurred because of cooling rate and other solidification variations in the superalloy casting processes.

Subsequent to the determination that MFC specimens gave generally lower results than CTS specimens, there began to be concern about the much thinner airfoils and airfoil wall thicknesses being generated for advanced cooling schemes. As blades (and some vanes) for aircraft gas turbines began to require cooling, they became complex devices with myriad cooling passages. Wall thicknesses under about 100 mils (2.5 mm) and in some instances as low as 20 mils (0.5 mm) were generated. Initial testing of thin section effects was on PC alloys such as cast U-700, IN-100, Rene 80, and B-1900 + Hf.

Tests could not hope to cover all stress ranges, temperatures, and component sizes (thicknesses), and so, limited test conditions were selected and data were generated on a few materials and at only a few material conditions. Data reported tended to be in terms of rupture life at a fixed test condition. Early literature data showed some severe drops in life with reductions in specimen thickness. Subsequent testing was on CGDS and then on SCDS cast superalloys. Data reported (but not on all alloys) were rupture life, time to 1% creep, and ductility at rupture. Typical results for such testing are shown in Fig. 12.20. It can be seen that there is a drop in life as section size decreases from the typical size of a solid blade part to about 20 mils (0.5 mm). Polycrystalline-cast superalloys

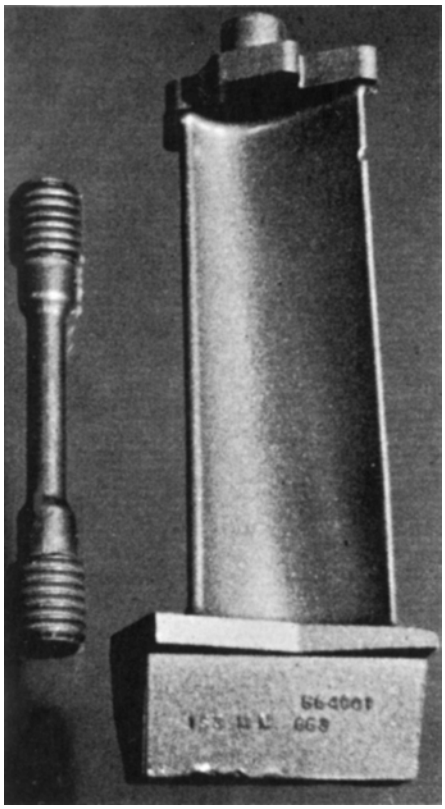


Fig. 12.18 Relative size of cast test bar and a typical solid first-stage turbine blade from a gas turbine engine

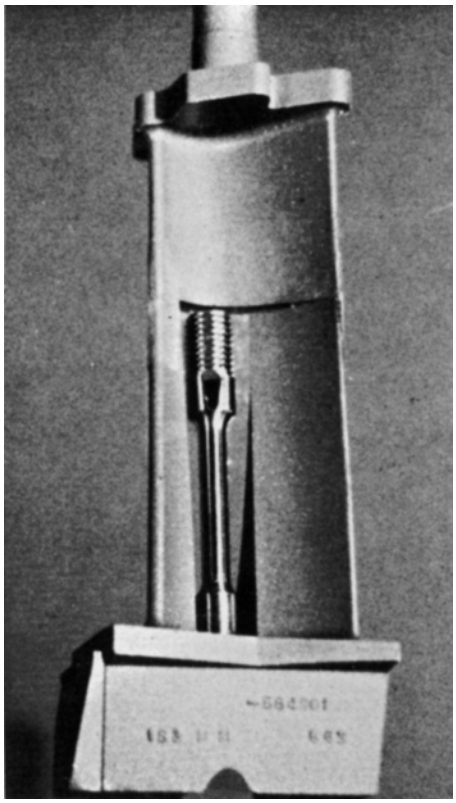


Fig. 12.19 Location and relative size of test bar from same first-stage turbine blade as in Fig. 12.18

Table 12.4 Variations in typical properties from test bars of B-1900 nickel-base superalloy machined from airfoil and cast to size

		0.250 in. (6.35 mm) diam Cast to size	0.178 in. (4.52 mm) diam From turbine blade
Room temperature	Tensile strength, psi (MPa)	135,000 (931)	115,000 (793)
	2% yield strength, psi (MPa)	108,000 (745)	100,000 (689)
	Elongation, %	7	3
Stress rupture 1800 °F/29,000 psi (982 °C/200 MPa)	Life, h	35	30
	Elongation, %	7	5
Creep rupture 1400 °F/94,000 psi (760 °C/648 MPa)	Life, h	75	25
	Prior creep(a), %	2.5	1.3

(a) Prior creep: % creep not more than 2 h prior to failure

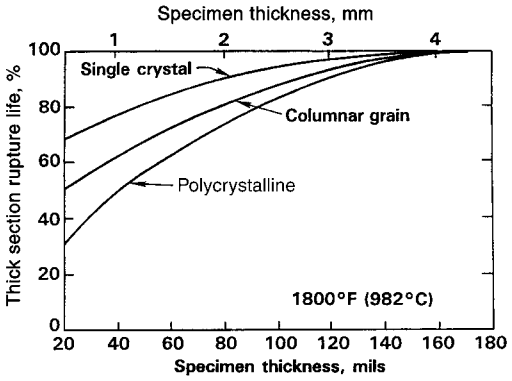


Fig. 12.20 Relative rupture life vs. thickness for PC, CGDS, and SCDS nickel-base superalloys life normalized to 3.8 mm (150 mil)

drop the most, while SCDS superalloys drop the least.

The Effect of Location on Mechanical Properties. Little documentation exists outside of proprietary files to substantiate the fact that test specimen location in or on a component can significantly influence the test results. Clearly, location must have an influence on wrought forged or P/M products, owing to cooling rates, deformation amounts, and so on. Cast airfoil properties should reflect cooling rates and local casting conditions. Support for actual test data to document or define location variations is always slim. Disk components can cost tens of thousands of dollars. Cast airfoils are quite expensive too, but their cost is minute compared to that of some of the turbine disks that are made. Even relatively inexpensive cast airfoils lack adequate component tracking data.

Over the years, the specimen requirements for specification acceptance testing of cast airfoils followed an evolutionary path such as:

- Cast-to-size (CTS) specimens required. Specimens were cast with each casting lot (for example, a given component and heat of alloy)
- Machined from component (MFC) specimens required. Specimens were taken from a solid airfoil made with each casting lot
- Either MFC or small-section CTS specimens permitted, but only one was required for each casting lot processed
- Either MFC or small-section CTS specimen permitted, but required on only one specimen for a given heat of an alloy

The effect of reduced requirements has made acceptance testing results tenuous descriptors of alloy properties, at best. The variability from CTS to MFC has already been demonstrated (Table 12.4). Persons trying to develop databases for cast superalloys should take note of the limited database likely to be available.

Turbine disk components also have experienced a similar reduction in data and relevance of data over the past several decades. The effect of test coupon location is just as significant for turbine disks as test location is for cast airfoils. Unfortunately, disk data are more proprietary than airfoil data. However, based on experience, it can be stated that ''best guess'' estimates are made of areas on a disk where a few test coupons can be located so as to represent the working/heat treatment conditions of a given disk. Test coupons (from which test specimens are machined) are, of necessity, placed on the exterior of a disk. Cooling rates have a very significant effect on properties. The amount of deformation is also important. There is no way that a test coupon in an external location can fully represent the microstructure and cooling rates that are found in the bore or even the center section of a rim of a large commercial turbine disk.

Table 12.5 shows room-temperature tensile properties for IN-901 nickel-base superalloy disk forgings at various locations for two heat treated conditions. Because the data do not indicate that these are average results, some of the variability noted may result from insufficient data. The point to note, however, is that specimen location can make a difference in results. Compare, in Table 12.5 the first (top condition) heat treatment results, the yield strengths for ''bore-axial-middle'' with ''rim-radial-bottom.'' There is nearly a 10 ksi (69 MPa) difference in these locations. Other locations did not show such a variance. Similarly, the maximum spread from low-to-high ultimate strength for the same (top condition) heat treatment in Table 12.5 is 21 ksi (145 MPa).

It is important, in the dissection and testing of the few disks devoted to data generation in a material or component development pro-

gram, that a correlation be made between test coupon results and the true results on specimens from the slowest cooling rate and/or least deformed sections of the disk component. For disks, tensile strength and burst margins are significant concerns. Past experience suggests that at the approximately 190 ksi (1310 MPa) tensile strength level, the average difference in ultimate strength from an approximately 2 in. (5.1 cm) thick disk section to a 5 in. (10.2 cm) thick section could be 10 ksi (69 MPa) or more.

While tensile properties are of more concern for disks, creep and stress rupture are the concerns for turbine airfoils. Figure 12.21 shows how the cooling rate (function of coolant, component shape, section size, etc.) can affect rupture lives on a PC cast nickel-base superalloy.

The Effects of Tramp Elements on Properties. The superalloys are susceptible to property degradation by interaction with a variety of elements known as tramp elements. These elements leave no visible microstructural change, but evidence from Auger electron spectroscopy confirms their concentrations at the grain boundaries. The elements lead, selenium, bismuth, thallium, tellurium, and so on along with sulfur and phosphorus are detrimental to creep-rupture properties, particularly of nickel-base superalloys. One might add to this element list the gases oxygen and nitrogen. Generally, these tramp elements are present in small quantities, perhaps up to about 500 parts per million (ppm). Most tramp elements are not removable except by vacuum induction remelting so, if contamination occurs, a heat must be scrapped.

The conclusion from research, principally on wrought superalloys, is that the harmful effects of tramp elements stem from the loss in ductility caused by their presence. Figure 12.22 shows the life of Nimonic 105 wrought nickel-base superalloy tested at 1500 °F (982 °C)/51 ksi (352 MPa). Notice that the stress-rupture lives all drop continuously. Notice

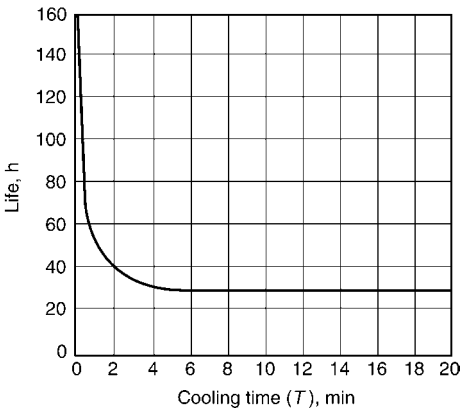


Fig. 12.21 Effect of cooling rate on stress-rupture life of a cast nickel-base superalloy at 982 °C (1800 °F)/200 MPa (29 ksi)

Table 12.5 Tensile properties at various locations in disk forgings of IN-901 in two heat treated conditions

Condition	Test location	Yield strength		Ultimate tensile strength		Elongation in 50 mm (2 in.), %	Reduction in area, %
		MPa	ksi	MPa	ksi		
1095 °C (2000 °F) for 2 h, water quench + 790 °C (1450 °F) for 2 h, water quench + 730 °C (1350 °F) for 24 h, air cool	Rim-radial-top	859	124.6	1178	170.8	15	16
	Rim-radial-bottom	907	131.6	1168	169.4	13	14
	Rim-radial-middle	880	127.6	1179	171.0	15	17
	Rim-axial-middle	858	124.4	1054	152.9	. . .	. . .
	Rim-tangent-middle	883	128.0	1175	170.4	13	17
	Bore-radial-top	874	126.8	1200	174.0	14	17
	Bore-radial-bottom	889	129.0	1131	164.0	. . .	. . .
	Bore-radial-middle	869	126.0	1172	170.0	16	20
	Bore-axial-middle	840	121.8	1154	167.4	. . .	. . .
	Bore-tangent-middle	859	124.6	1167	169.2	15	17
1010 °C (1850 °F) for 2 h, water quench + 730 °C (1350 °F) for 20 h, water quench + 650 °C (1200 °F) for 20 h, air cool	Rim-radial-top	924	134.0	1234	179.0	17	20
	Rim-radial-bottom	952	138.0	1240	179.8	17	21
	Rim-radial-middle	980	142.0	1258	182.4	19	29
	Rim-axial-middle	972	141.0	1255	182.0	21	31
	Rim-tangent-middle	986	143.0	1274	184.8	18	25
	Bore-radial-top	978	141.9	1248	181.0	18	24
	Bore-radial-bottom	976	141.6	1255	182.0	20	31
	Bore-radial-middle	968	140.4	1252	181.6	21	34
	Bore-axial-middle	940	136.4	1081	156.8	5	9
	Bore-tangent-middle	965	140.0	1253	181.8	20	31

also the drop in ductility (reduction of area) caused by the tramp elements.

The situation is much the same for cast alloys. Similar results to Fig. 12.22 are shown in Fig. 12.23 for the cast nickel-base superalloy MAR-M-002. It can be seen that impurity level tolerances are below 5 ppm for some elements. For bismuth, actual tolerance levels are less than 0.5 ppm.

The essence of the tramp element effect is that the minuscule amounts of tramp elements present congregate on the grain boundaries. With grain-boundary fracture favored by the high temperature, the tramp elements, which reduce the surface energy of the boundaries, will result in easier separation of the boundary and the grain. The result is low ductility fracture. Some elements (bismuth, lead, tellurium) of those tested are more prone to cause cracking than others. An alternate method of comparing data on tramp element effects (on cast alloys) is to plot the development of cracking (cavities) during creep. This process is shown for Nimonic 105 in Fig. 12.24.

As noted for thin section effects, the absence of boundaries or their positioning parallel to the loading axis have had beneficial effects on strength over and above that which occurs with PC cast alloys. Figure 12.25 shows that the DS benefits carry over to tramp element effects where cast MAR-M-002 alloy has been PC cast and produced also as a CGDS alloy. Note that the normalized rupture life for PC cast alloys shows a plunge in capability for a very small amount of bismuth. Columnar grain directionally solidified alloys fare somewhat better on being tested across the grain boundary, and CGDS alloys tested parallel to the grain boundaries showed virtually no degradation in strength because of tramp elements.

The beneficial effects of reduced nitrogen and oxygen have been noted. Table 12.6 shows more data on nitrogen and its effects on creep-rupture life and elongation of PC cast MAR-M-002. In addition, effects of silicon are shown.

For wrought superalloys, as noted previously, the tramp element effects are similar to those found for cast superalloys. However, the wrought alloys generally can tolerate a higher level of the tramp elements than can cast alloys. This effect may simply reflect the greater grain-boundary area of wrought products and the lower temperatures of creep-rupture testing of such products. Tensile behavior has been investigated along with creep-rupture behavior for wrought nickel-base superalloys. Figure 12.26 shows the effect of lead content on 1200 °F (649 °C) tensile properties of IN-718 nickel-base superalloy. Ultimate and yield strengths were unaffected, but ductility was reduced. Figure

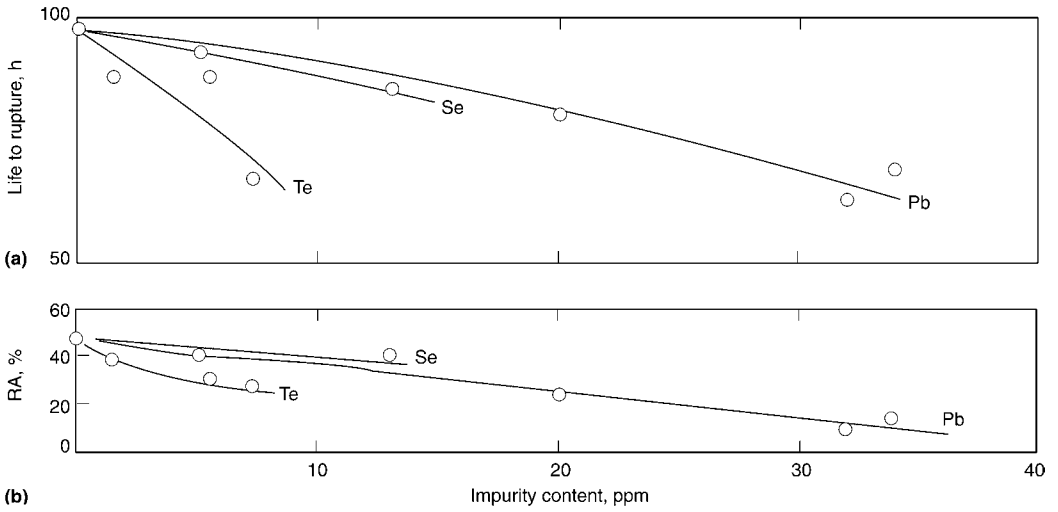


Fig. 12.22 Effect of lead, selenium, and tellurium on stress-rupture properties of Nimonic 105 wrought nickel-base superalloy at 815 °C (1500 °F)/350 MPa (50.8 ksi). (a) Life to rupture and (b) reduction of area (RA).

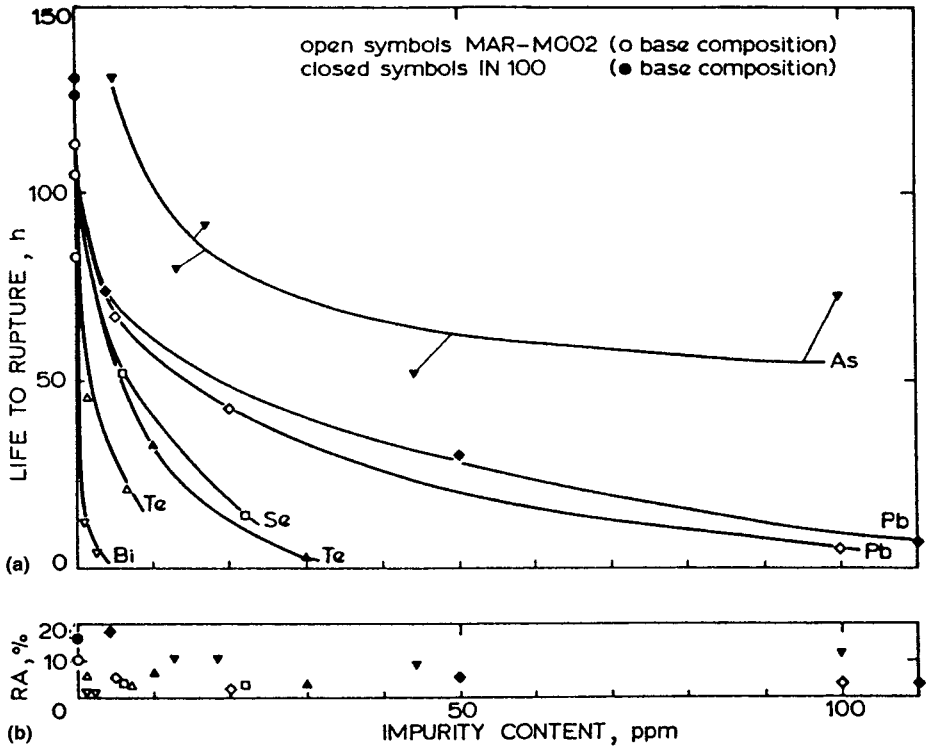


Fig. 12.23 Effect of arsenic, bismuth, lead, selenium, and tellurium on stress-rupture properties of cast nickel-base superalloy, MAR-M-002 (open symbols) tested at 850 °C (1562 °F)/465 MPa (67.5 ksi) and IN-100 (closed symbols) tested at 900 °C (1652 °F)/315 MPa (45.7 ksi). (a) Life to rupture and (b) reduction of area (RA)

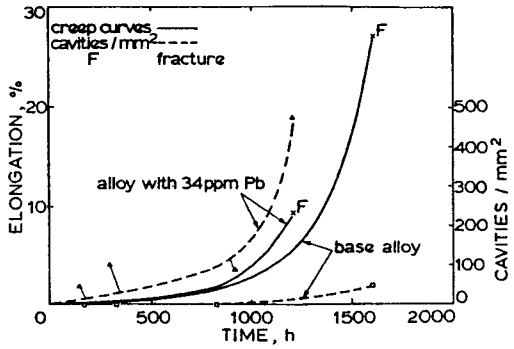


Fig. 12.24 Effect of lead on creep behavior and cavitation of Nimonic 105 wrought alloy at 815 °C (1500 °F)/232 MPa (33.7 ksi)

12.27 shows the effect of lead content on the 1200 °F (649 °C)/100 ksi (690 MPa) stress-rupture properties of the same alloy. Tramp elements are tightly controlled in nickel-base superalloys, as seen in Table 12.7.

Beneficial "Minor" Elements: Boron, Zirconium, and Hafnium. The grain boundaries are the weak link in high-temperature mechanical properties of superalloys. Failure generally is by intergranular cracking. Strengthening of grain boundaries and/or improvements in grain-boundary ductility help to enable full use of intrinsic grain (intragranular) strength. Within limits, significant improvements in mechanical properties can be achieved by additions of boron, zirconium, and hafnium to nickel-base superalloys. However, only limited microstructural correlations can be made. While nickel-base and, to some extent, iron-nickel-base superalloys may benefit from the addition of boron, zirconium, or hafnium, cobalt-base superalloy properties generally do not benefit much from such additions. MAR-M-509 is one current cobalt-base superalloy that contains zirconium, and MAR-M-302 and MAR-M-322 were alloys that contained 0.2 and 2.0% Zr. Zirconium additions require vac-

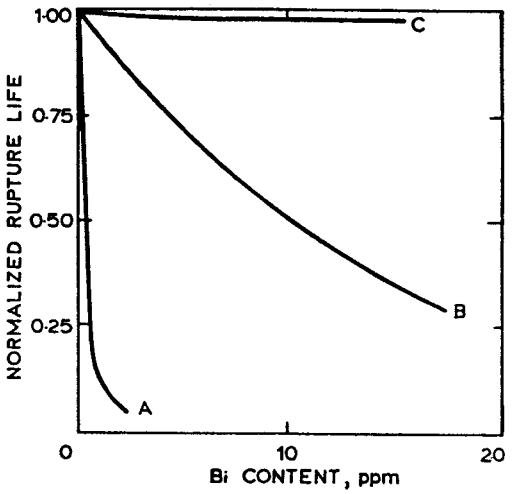


Fig. 12.25 Effect of bismuth content and microstructure on normalized rupture life for MAR-M-002 cast nickel-base superalloy in PC (A), CGDS transverse to boundaries (B), and CGDS parallel to boundaries (C) conditions

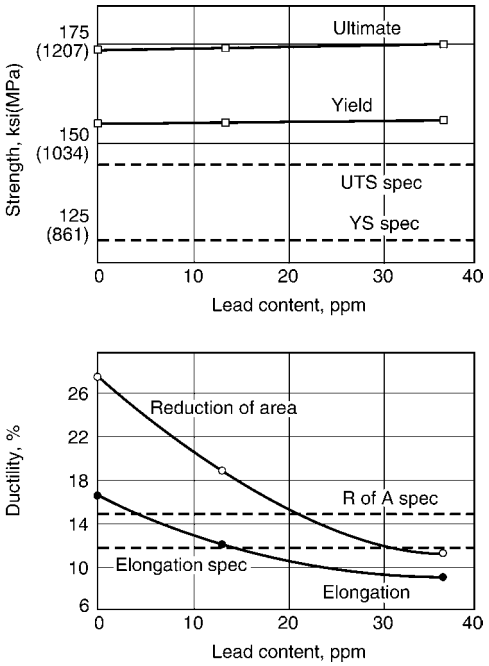


Fig. 12.26 Effect of lead content on 649 °C (1200 °F) tensile properties of IN-718 wrought nickel-base superalloy. UTS, ultimate tensile strength; YS, yield strength; R of A, reduction of area

uum melting to retain them; vacuum melting is not normally practiced for cobalt-base superalloys. Limited or no work has been reported on the effects of hafnium on cobalt-base superalloys. In general, the effects of minor elements have not been extensively studied for cobalt-base superalloys.

The mechanism for achieving creep-rupture ductility benefits with boron and zirconium additions in PC wrought and cast nickel-base (and iron-nickel-base) superalloys has been the subject of debate for many years. It was believed that boron and zirconium segregate to grain-boundary regions, owing to their misfits with the nickel matrix (γ phase). The presence of boron in nickel-base superalloys acts to modify the initial grain-boundary carbides and may help tie up deleterious elements such as sulfur and lead. Zirconium may act similarly. For an alloy such as Nimonic 80A, which relies on titanium (in addition to aluminum) for a significant contribution to γ' production, zirconium has been claimed to reduce residual sulfur that might otherwise bond to titanium and reduce the amount of titanium available for creation of γ'. Soviet superalloys were thought to have relied on such combinations of minor elements (bonding to tramp elements) for many years as a means to improve their superalloys, which (at that time) were not vacuum melted with the same effectiveness as those made in Europe and the United States.

Table 12.6 Stress-rupture results for base plus nitrogen or silicon-doped MAR-M-002 cast nickel-base superalloy

	σ = 695 MN m^{-2}, T = 760 °C		σ = 180 MN m^{-2}, T = 980 °C	
Cast	Life, h	Elongation, %	Life, h	Elongation, %
Base (0.0005% N)	98.2, 68.1, 76.5, 116.7, 118.3	1.8, 2.2, 1.4, 1.7, 1.2, 1.6	192.9(a), 103.8	. . ., 4.6
Base + 0.0024% N	34.6, 52.2, 61.0, 66.5, 49.2, 36.1	1.7, 1.2, 1.8, 1.2, 1.7, 1.4	114.2	3.8
Base + 0.0050% N	33.1, 64.7, 14.2, 15.4, 5.0	1.5, 1.5, 1.0, 1.6, 1.8	93.2, 94.4	. . ., 2.4
Base + 0.16% Si	77.9, 74.6, 98.5	1.8, 1.4, 1.5	102.8, 107.0	. . ., . . .

Note: σ, stress; T, temperature. (a) Did not rupture

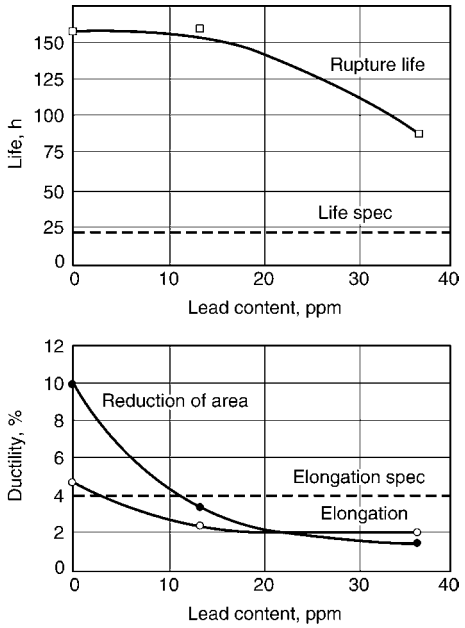


Fig. 12.27 Effect of lead content on 649 °C (1200 °F)/690 MPa (100 ksi) stress-rupture properties of IN-718 wrought nickel-base superalloy

Reduced grain-boundary diffusion rates may be obtained from beneficial minor elements, with consequent suppression of carbide agglomeration and of creep cracking. Borides formed in grain boundaries may act in a similar way to discrete carbides in promoting resistance to grain-boundary sliding while enhancing grain-boundary ductility.

Hafnium contributes to the formation of more γ-γ' eutectic in cast alloys; the eutectic at grain boundaries is thought (in modest quantities) to contribute to alloy ductility. Hafnium refines the MC in an alloy and favors formation of HfC over TiC. It is a strong oxygen, nitrogen, and sulfur scavenger. Hafnium also promotes grain-boundary γ' (probably enhances ductility) and better carbide grain-boundary distribution for pegging the boundaries. Owing to these effects, hafnium has found use for ductility improvement in PC and CGDS cast nickel-base superalloys. An early (1959) patent on hafnium use in wrought alloys failed to elicit any specific use. However, when certain PC cast alloys, such as B-1900, showed low ductility in 1400 °F (760 °C) creep-rupture testing, hafnium (about 0.5%) was added and promoted a consistently higher ductility. This higher ductility enabled designers to use the full potential of the alloy.

Hafnium also contributes strongly to improved ductility in transverse boundaries in CGDS alloys. When CGDS MAR-M-200 was developed, the intrinsic low ductility of the alloy at its grain boundaries (which were acted on by transverse airfoil stresses) did not disappear. Thus, while longitudinal properties were outstanding, the transverse grain bound-

Table 12.7 Allowable tramp element concentrations for selected nickel-base superalloys

	IN-718/MAR-M-247, typical alloy concentration					
	Commercial grade					
Element	Tooling applications	Other	Aerospace quality		Premium quality	
N, ppm	20+	60–100	60	5–15	10–25	1
O, ppm	5+	5–10	<5	<5	2	1
Si, wt%	0.05+	0.10–0.30 wt%	0.05–0.10	0.02–0.04	<0.02	0.008
Mn, wt%	0.01+	0.05+	<0.02	<0.002	<0.002	<0.002
S, ppm	15+	10–40	10–30	5–15	10	<5
Zr, wt%	. . .	<0.01	0.001	. . .	<10 ppm	. . .
Fe, wt%	0.10+	. . .	. . .	0.05–0.10	. . .	0.03
Cu, wt%	0.002+	0.08	0.01–0.05	0.002–0.005	<0.001	<0.001
P, wt%	0.002	0.005	0.005	<0.005	0.001–0.002	<0.001
Pb, ppm	<1	1–5	<1	<1	<1	<0.5
Ag, ppm	<0.5	<1	<1	<0.5	<0.5	<0.5
Bi, ppm	<0.3	<0.5	<0.5	<0.3	<0.2	<0.2
Se, ppm	<0.5	<1	<1	<0.5	<0.5	<0.5
Te, ppm	<0.3	<0.5	<0.5	<0.2	<0.2	<0.2
Tl, ppm	<0.3	<0.5	<0.5	<0.2	<0.2	<0.2
Sn, ppm	<5	15–40	<10	<5	<10	<5
Sb, ppm	<2	2+	<2	<1	<2	<1
As, ppm	<2	5	<2	<1	<2	<1
Zn, ppm	<2	2+	<2	<1	<2	<1

Note: + = or higher

aries still failed with very low ductilities in turbine airfoils. Designers were not able to use the initial CGDS MAR-M-200. However, addition of hafnium at a level of about 1.5% produced satisfactory ductility, and designers were able to use this alloy (PWA 1422) to its full capability.

While most minor elements are added in amounts much less than 0.1%, hafnium is found at levels from about 0.5% to nearly 2.0%. Customary levels might be 0.5% for PC cast nickel-base superalloys to 1.5% for CGDS cast nickel-base superalloys. Hafnium is not normally added for boundary improvement in SCDS superalloys but may be added for environmental-resistance reasons. Hafnium tends to form dross during melting and is added to nickel-base alloys at the minimum level needed to achieve desired properties.

The beneficial results of boron and zirconium can be seen in Tables 12.8 and 12.9. Rupture life is very greatly improved with a corresponding increase in rupture elongation (Table 12.8). Grain boundaries show far fewer cracks and denuded (missing fine γ') grain-boundary areas (Table 12.9). The reduction in cracking and minimization of loss of fine γ' explains the improved ductility noted. Additional studies have been done on the effects of minor elements on single crystals of superalloys. Results have shown that minor elements can cause changes in the basic deformation modes of single crystals. These results, while of great research value, are largely restricted to the intermediate-temperature range and have not found application in the highest temperatures, where SCDS alloys normally are employed.

The Role of Magnesium and Similar Elements. Magnesium is a beneficial element added to reduce sulfur in nickel-base superalloys (see Chapter 4). Elements such as calcium, magnesium, and cerium may be added to the melt as desulfurizers. Few published studies exist on magnesium effects. One study showed that residual magnesium, indicative of complete sulfur scavenging, improved the stress-rupture properties of IN-120 nickel-base superalloy (Table 12.10). Other studies on IN-718 and Waspaloy attribute the magnesium effect to changes in sulfur morphology from continuous grain boundary films to spherical sulfides.

Excess residual magnesium is likely to be less beneficial and, perhaps, detrimental. Residual concentrations of 30 ppm Mg improved the 1200 °F (649 °C) stress-rupture ductility of IN-718, and 350 ppm of Mg reportedly produced a five-fold improvement in the creep-rupture life of IN-102 at 1200 °F (649 °C). On the other hand, benefits at one temperature/stress condition have not been

Table 12.8 Effect of boron and zirconium on creep of U-500 nickel-base superalloy at 870 °C (1600 °F)/172 MPa (25 ksi)

Alloy	ε in primary creep	Life, h	Elongation, % in 4 D
Base	0.002	50	2
+0.19% Zr	0.002	140	6
+0.009% B	0.002	400	8
+0.009% B +0.01% Zr	0.002	647	14

Table 12.10 Effect of magnesium on stress-rupture behavior of IN-120

	Stress-rupture properties at 68.6 MPa (9.9 ksi) and 650 °C (1202 °F)		
Alloy	Life, h	Elongation, % in 4 D	Reduction of area, %
Base	122 to 188	10 to 17	11 to 30
+0.013% Mg	244	24	53
+0.016% Mg	278	31	60
+0.022% Mg	414	30	61
+0.027% Mg	467	29	63
+0.049% Mg	422	28	53

Table 12.9 Effect of boron and zirconium on the grain-boundary stability of U-500 at 870 °C (1600 °F)

	After ε = 0.012 in 200 h			After 200 h, no σ (a)
Alloy	Denuded grain boundaries(b)	Microcracks(b)	γ′- carbide nodules(b)	γ′- carbide nodules(b)
Base	264	314	418	230
+0.19% Zr	127	78	175	90
+0.009% B	60	30	63	60
+0.009% B +0.01% Zr	23	2	20	20

(a) No denuded grain boundaries or microcracks in any alloys without stress. (b) Number of features detected at 1000 D in 5 mm^2

matched by benefits at all conditions. Although the creep properties of MAR-M-002 were improved at 1562 °F (850 °C) by magnesium contents of up to 50 ppm, Fig. 12.28 shows that the 1922 °F (1050 °C) creep-rupture properties of the same alloy were degraded by magnesium. A $MgNi_2$ Laves phase is reported to form when excess magnesium is present in nickel-base superalloys.

A Few Observations on Yield Strengths of γ′-Hardened Superalloys. The yield strength of γ′-hardened superalloys has been discussed in connection with the temperature dependence of the yield strength of γ′. Some observations are in order with respect to yield strengths. Yield strengths are influenced by:

- Titanium-to-aluminum ratio
- Degree of solution heat treat
- Cooling rate from forging and from solution heat treat
- Aging sequence
- Presence of other hardeners in addition to aluminum and titanium
- Grain size
- $V_f\gamma'$

The titanium-to-aluminum ratio has a large effect. The higher the titanium-aluminum ratio, the higher the yield strength becomes. This occurs because coherency strains affect the yield strength, and such strains increase as the titanium level increases. In addition, the yield strength is affected by the titanium, because the APB energy increases with increasing titanium. As for the cooling rate effects, the faster cooling rate from solution treatment gives an opportunity for a greater amount of fine γ′ than normal. The rate needs to be about 35 °F (~22 °C) or faster for adequate cooling.

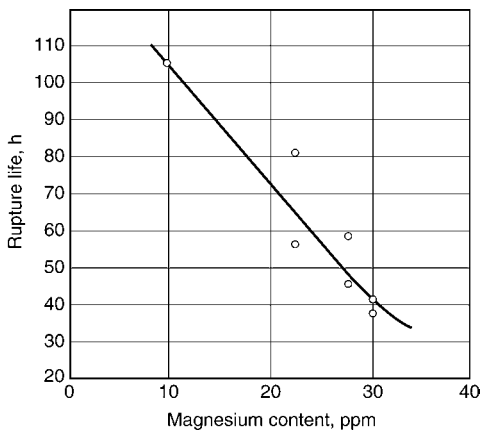


Fig. 12.28 Effect of magnesium content on stress-rupture properties of MAR-M-002 cast nickel-base superalloy at 850 °C (1562 °F)/108 MPa (15.7 ksi)

The yield strength of PC alloys is remarkably similar from one class of alloys to another. IN-792, IN-100, B-1900, and MAR-M-200 should have about the same typical temperature-dependence behavior for tensile strength. If enough data could be developed for each PC alloy, there would be subtle differences. However, recognizing the variability that exists from heat to heat and other test factors, a common shape of strength vs. temperature curves probably could be used for all the γ′-hardened nickel-base superalloys of a given $V_f\gamma'$. Columnar grain directionally solidified and SCDS cast materials will differ from PC cast superalloys. In particular, SCDS behavior will be decidedly orientation-dependent (see the section ''Columnar Grain Directionally Solidified and SCDS Cast Superalloys—Orientation and Other Effects'').

Some Observations on Cobalt in Nickel-Base Superalloys. About the start of the last quarter of the 20th century, a cobalt cost ''crisis'' developed, which focused attention on the use of cobalt in superalloys. The result was a brief flurry of effort to reduce cobalt in conventional nickel-base superalloys and to adapt existing low-cobalt or no-cobalt superalloys to expanded use.

Much of the original concepts behind cobalt additions to nickel-base superalloys must be inferred from studies of limited publications. It would appear that cobalt was not added to nickel-base superalloys until about 1945, when Nimonic 80A was converted to Nimonic 90 by the addition of cobalt. Scarcity had kept cobalt out of the nickel-base superalloys developed and used for World War II. After Nimonic 90 appeared, most subsequent alloys for the next 30 years had cobalt as a major alloy addition. U-700, a variant of Astroloy, reached a level of about 17%.

Some ''facts'' about cobalt can be found in the early literature. These are that:

- Cobalt additions decrease the aluminum and titanium solubility.
- Cobalt drives up the γ′ solvus.

- Cobalt thus helps stress-rupture life.
- Cobalt might help forgeability.
- Cobalt does not materially help other ''properties.''

The preceding facts were found repeated in the literature with little or no mechanical property substantiation. By reviewing the work published prior to 1979, it was possible to determine that the cobalt effect on γ' solvus is a function of the aluminum-to-titanium ratio. Modern alloys usually have aluminium-titanium ratios >1.0, but the alloys originally studied for cobalt effects had aluminium-titanium ratios <1.0. Figure 12.29 shows how cobalt was found to affect rupture life for one alloy. Similar results (peak in rupture life between 10 and 20% was shown) were obtained on another alloy in studies after 1979. Some studies concluded that 20% was an optimal amount of cobalt. The result of engineering studies was that cobalt in γ'-hardened nickel-base superalloys ranged between about 10 and 20% for nearly three decades up to about 1980.

Since 1980, some subsequent studies on cobalt in nickel-base superalloys showed that creep and stress-rupture capabilities of alloys heat treated for turbine airfoil applications were largely unaffected by a reduction in cobalt content in the range of cobalt studied. Alloys intended for disk applications had decreased creep and rupture properties if cobalt was decreased. The microstructural explanations for the cobalt effects are not clear-cut. Cobalt was found to influence γ'-γ'' interfaces and affect carbide distributions (differently in different alloys). Cobalt seems to affect γ' coarsening.

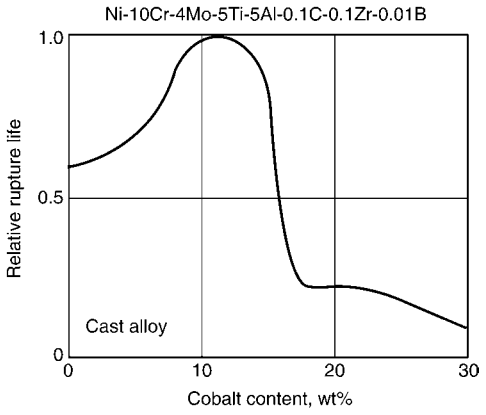


Fig. 12.29 Rupture strength at 1020 °C (1868 °F) of a nickel-base superalloy as a function of cobalt content, showing a peak at about 13% Co

From about 1980 on, less cobalt was used in new alloys at first, while alloys such as IN-718 and IN-713, which have no cobalt, gained greater use. However, cobalt continued to be used in alloys but with some alloys having as low as 5% or less cobalt (PWA 1480, SRR99, CMSX-2, CMSX-6—5%). More recent wrought and cast nickel-base superalloys have shown gradually increased cobalt levels again (Rene N4, Rene N5, Rene 95—8%; Rene 88—13%). Recent disk alloys such as IN-100 and MERL 76, which were adaptations of the cast IN-100 alloy, have retained the relatively high cobalt levels of their predecessors. IN-100 (15% Co) and MERL 76 (18.5%) were descended from IN-100; U-720 (14.5% Co) can claim descent from U-700 (17%) and Astroloy (15%). High cobalt levels can cause a propensity for tcp phase formation in long-time service. The extent to which the higher cobalt levels are balanced by adjustments in other elements and the actual service temperatures will determine the likelihood of tcp phase appearance.

Brief Comments on Refractory Metals. The refractory metals, vanadium, molybdenum, tungsten, niobium, tantalum, and rhenium, have been added to nickel-base superalloys. Tungsten and molybdenum were found to contribute strongly to solid-solution strengthening of γ at room temperature. Chromium, technically a refractory metal but best known for its effects on oxidation and hot corrosion resistance, also contributes strongly to room-temperature strength of γ. The effects of solid-solution strengthening persist to high temperatures and into the creep range (above about 0.5 of the absolute melting point).

In the high-temperature range, the effects of molybdenum and tungsten on diffusivity of some of the alloy species in γ seem to be one aspect of behavior. Reduced diffusivity of hardening elements such as titanium can contribute to improved creep strength by extending the times needed to coarsen γ' and dissociate or form certain carbides. Molybdenum and tungsten are found not only in γ but also in γ', affecting diffusivity in both. In the past several decades, rhenium has been added to CGDS and SCDS cast nickel-base superalloys, with substantial improvements

in creep-rupture properties. Rhenium probably works in a similar fashion to molybdenum and tungsten to reduce the coarsening rates of γ' at high temperatures. There are little published data on the specific strength improvements to be ascribed to molybdenum, tungsten, and rhenium, but microstructural studies have been made on their effects on γ' and carbide formation and behavior.

Tantalum, tungsten, and rhenium, with their higher melting points, have been found to be more effective strengthening additions for the creep range than vanadium, niobium, and molybdenum. Additions of refractory metals act also to change the APB energy or SFE in superalloys, dependent on whether or not a given element partitions to γ or γ'. It is not clear if the role of tantalum, tungsten, and rhenium relates to their solid-solution strengthening effects in γ, to a contribution of reduced γ' coarsening, or both. It has been reported that rhenium does not partition to γ', so its effects are thought mostly to lie in a strong reduction of γ' coarsening rate. Rhenium at amounts in the order of 6% has been found to participate in the formation of a high-rhenium-content sigma phase on long-time exposure in a nickel-base superalloy matrix.

The precious metals, such as platinum, also are effective creep strengtheners but are not cost-effective additions. Platinum is a strong γ' former and enhances alloy oxidation and hot corrosion resistance. Thin layers of platinum have been added to corrosion-resistant coatings to good effect. Chromium, titanium, niobium, hafnium, tantalum, molybdenum, and tungsten also affect the carbides formed in superalloys, as noted earlier.

Property Availability. For a discussion of the status of property data, refer to ''Overview, General Considerations'' in Chapter 2. As indicated there, superalloy property data are often minimal compared to expectations. Superalloys have a long history, but there are many superalloys that have been invented, and most have had extremely limited testing. Since the 1960s, many tests have been done by users rather than superalloy producers. Thus, such data are only disclosed in a limited way in the public domain. Data compilations actually found, whether plotted or tabular, may be concerned with older but still current alloys. The more recent alloys, including the P/M wrought, CGDS cast, and SCDS cast superalloys, may not be represented.

Wrought Superalloys—Physical, Tensile, and Creep-Rupture Properties

Properties: General. The compositions of some selected wrought superalloys were given in Table 1.1. Tensile and creep-rupture properties of selected wrought superalloys were given in Tables 2.1 and 2.2. Creep-rupture properties of selected superalloys also were given in Figs. 2.1 to 2.3. In addition, creep-rupture data are plotted specifically for wrought alloys in Fig. 12.30, where the 1000 h rupture strengths are given for selected nickel-base superalloys (including solid-solution-strengthened or γ'-hardened nickel-base, and oxide-dispersion-strengthened (ODS) superalloys). Figure 12.31 gives comparable information for the less-numerous wrought cobalt-base and iron-nickel-base superalloys.

The need to achieve the lowest rate of decrease in rupture properties with increased testing temperature or increased time favors more stable alloys over less stable ones in long-time applications, particularly power gas turbines. Long-term strengths (10000 h or longer) may show advantages for some alloys that are weaker in short-time (100 to 1000 h) applications. Figure 12.32 shows the 10,000 h rupture strengths of a small selection of largely solid-solution-strengthened nickel-base superalloys (compared with a few stainless steels and other heat-resistant alloys). Solid-solution- or carbide-strengthened superalloys often are used for high-temperature applications where stainless steels or heat-resistant alloys (such as Alloy 330) are not adequate.

Dynamic moduli and physical properties of selected wrought superalloys are given in Tables 12.11 and 12.12, respectively. A Larson-Miller parametric plot to describe stress-rupture characteristics over a wide range is given in Fig. 12.33. Several wrought cobalt-, iron-nickel-, and nickel-base superalloys are compared; however, data on wrought alloys Rene 95, IN-100, U-720, and Rene 88DT were not available. The cobalt alloys are provided for reference but are not likely to com-

pete with the other alloys, most of which would be available as forged components, particularly as gas turbine disks.

Wrought superalloys, except for those used in combustion devices, generally are used at the lower end of the high-temperature spectrum. In gas turbines, the range of applications consists of turbine and high-pressure compressor (HPC) disks and appropriate HPC airfoils (blades, vanes), where best-temperature capability is required. Tensile strengths (yield and ultimate) are dominant

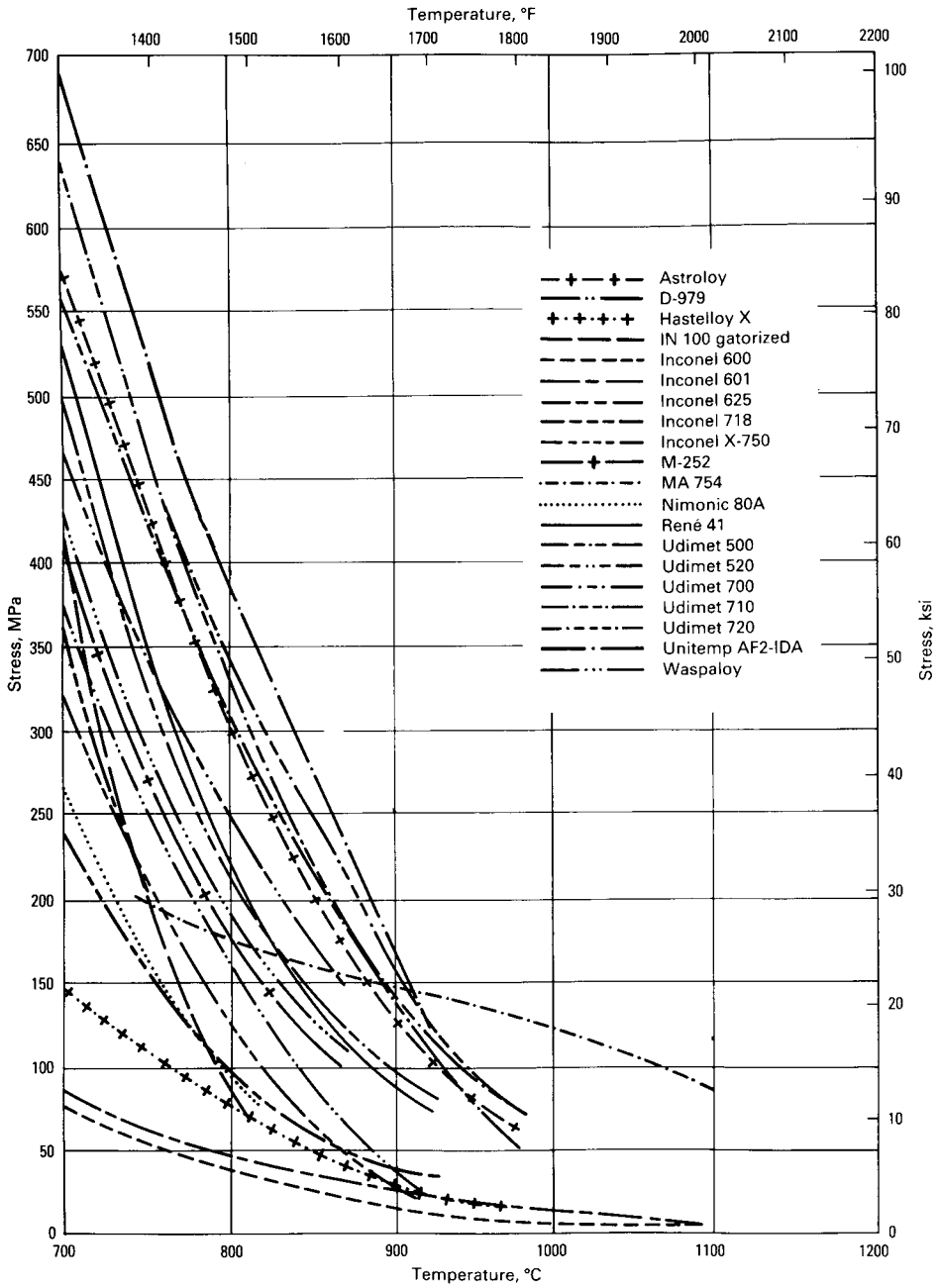


Fig. 12.30 1000 h rupture strength of selected wrought nickel-base superalloys vs. temperature

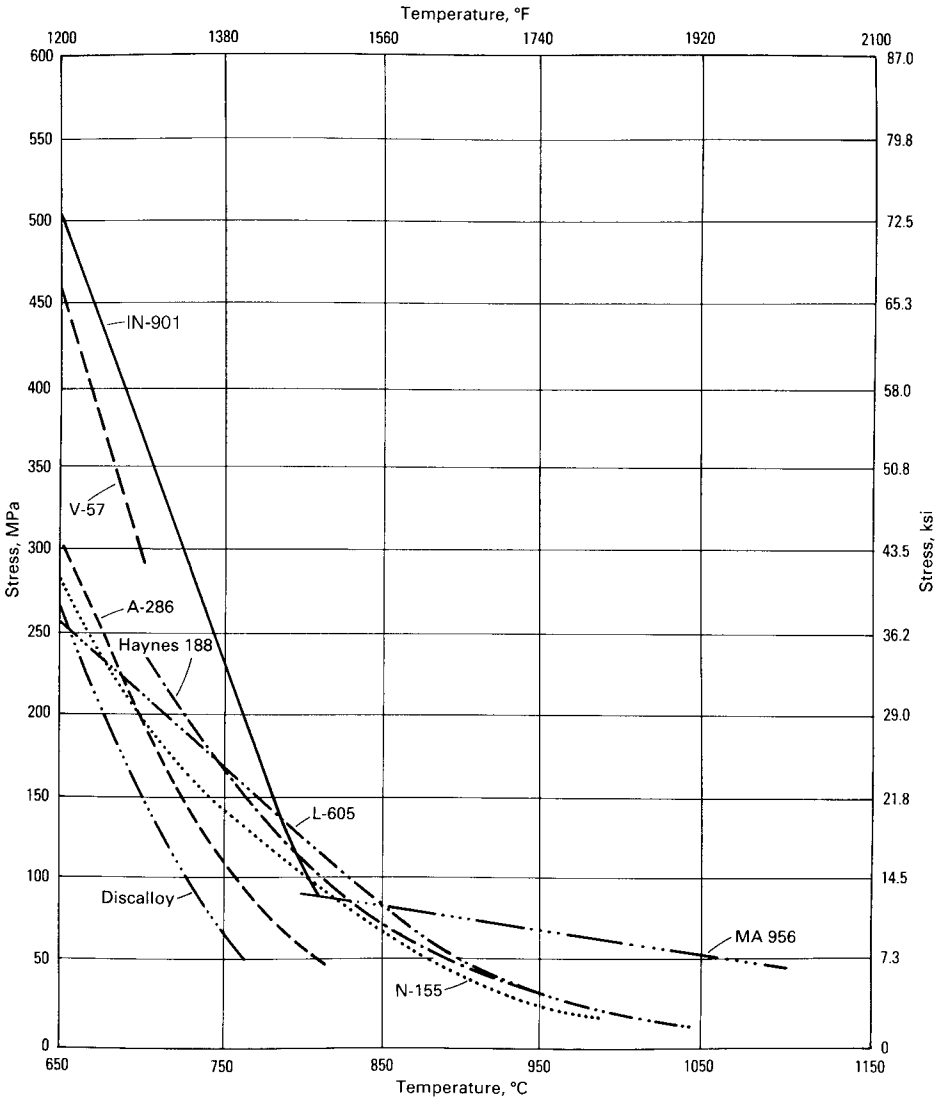


Fig. 12.31 1000 h rupture strength of selected wrought cobalt- and iron-nickel-base superalloys vs. temperature. Note the inclusion of iron-base ODS superalloy MA-956 for comparison.

concerns in wrought applications, but creep rupture (mostly creep) is important in the airfoil attachment areas of disks and also in some sheet applications. The need for strength at higher temperatures precludes the use of iron-nickel-base superalloys in most new applications, but wrought iron-nickel-base superalloys continue to have applications in existing products. Cost with adequate tensile strength makes iron-nickel-base (or high-iron nickel-base) superalloys attractive, particularly for industrial land-based gas turbines.

The need for high tensile strength led to the development of Rene 95 and to the conversion of IN-100 from a cast to a wrought superalloy. Other high-tensile strength wrought alloys have been investigated, and several have been produced. However, the additional fracture mechanics requirements for disks in the past 25 years have led to attempts to improve the crack propagation resistance. Consequently, tensile strengths have peaked and may, in fact, be somewhat lower for newer alloys or heat-treatment-modified older alloys.

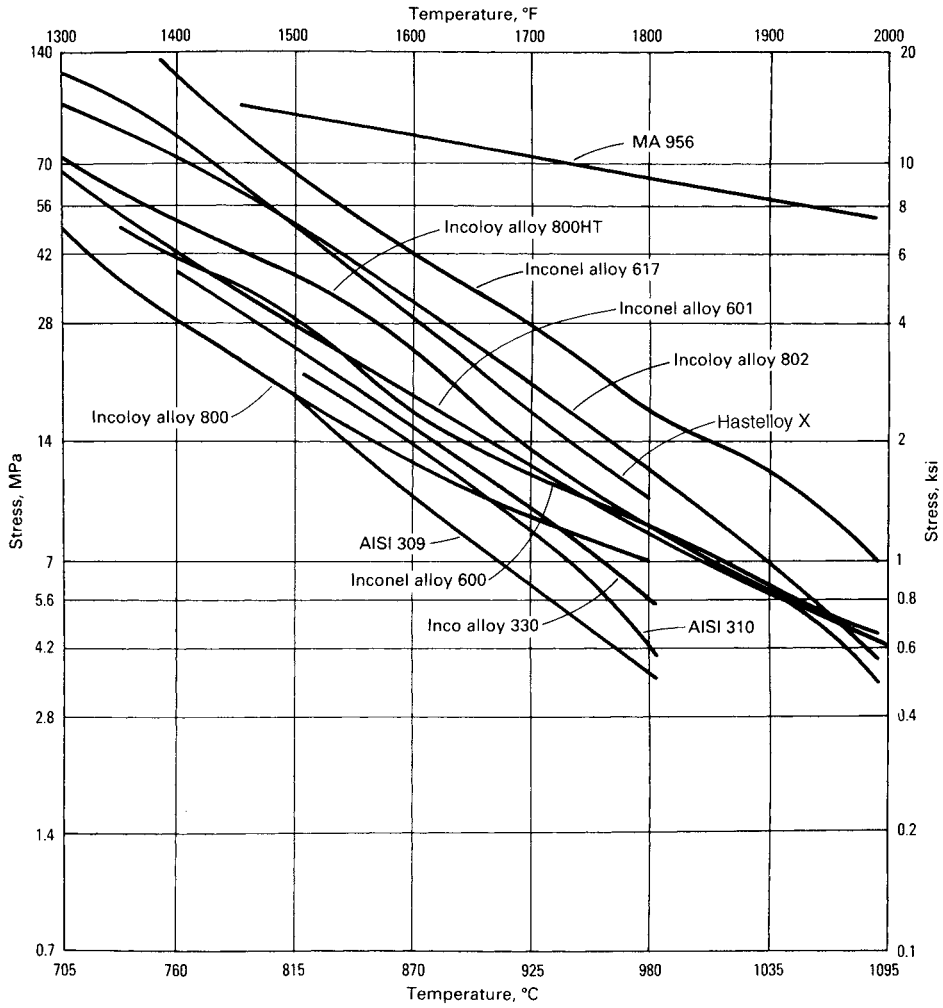


Fig. 12.32 10,000 h rupture strength of selected wrought solid-solution-strengthened nickel-base superalloys vs. temperature. Note the inclusion of several stainless steels and MA-956 ODS iron-base superalloy for comparison.

Rene 95 is a prominent high-tensile-strength nickel-base alloy for gas turbine disks. The alloy has been produced by:

- P/M—as-pressed (hot isostatic pressed, or HIP)
- P/M—extruded and forged
- Ingot metallurgy (cast, then wrought)

Table 12.13 gives a tabulation of the tensile properties of Rene 95 as a function of the processing and heat treatment mentioned above.

Powder metallurgy is the standard method for the production of very-high-strength nickel-base superalloys. Table 12.14 gives a summary of the tensile properties of P/M compacts of some of the current alloys. Note that IN-718 is included for comparison although IN-718 normally is not a P/M product.

Oxide-dispersion-strengthened superalloys invariably are wrought and, for the most part, are nickel-base alloys. MA-956 is the exception. One of the important advances in the past quarter-century was the maturing of the ODS process so that relatively simple shapes are available (see Chapters 7 and 15) ODS alloy applications are limited. However, in the interest of providing a balanced compilation of properties, Table 12.15 gives

Table 12.11 Dynamic moduli of selected wrought superalloys

		Dynamic modulus of elasticity									
		At 21 °C (70 °F)		At 540 °C (1000 °F)		At 650 °C (1200 °F)		At 760 °C (1400 °F)		At 870 °C (1600 °F)	
Alloy	Form	GPa	10^6 psi	GPa	10^6 psi	GPa	10^6 psi	GPa	10^6 psi	GPa	10^6 psi
Nickel base											
D-979	Bar	207	30.0	178	25.8	167	24.2	156	22.6	146	21.2
Hastelloy S	Bar	212	30.8	182	26.4	174	25.2	166	24.1	...	...
Hastelloy X	Sheet	197	28.6	161	23.4	154	22.3	146	21.1	137	19.9
Haynes 230	(a)	211	30.6	184	26.4	177	25.3	171	24.1	164	23.1
Inconel 587	Bar	222	32.1	...	...	...	...	...	...	...	...
Inconel 596	Bar	186	27.0	...	...	...	...	...	...	...	...
Inconel 600	Bar	214	31.1	184	26.7	176	25.5	168	24.3	157	22.8
Inconel 601(b)	Sheet	207	30.0	175	25.4	166	24.1	155	22.5	141	20.5
Inconel 617	Bar	210	30.4	176	25.6	168	24.4	160	23.2	150	21.8
Inconel 625	Bar	208	30.1	179	25.9	170	24.7	161	23.3	148	21.4
Inconel 706	Bar	210	30.4	179	25.9	170	24.7	...	...	...	...
Inconel 718	Bar	200	29.0	171	24.8	163	23.7	154	22.3	139	20.2
Inconel X750	Bar	214	31.0	184	26.7	176	25.5	166	24.0	153	22.1
M-252	Bar	206	29.8	177	25.7	168	24.4	156	22.6	145	21.0
Nimonic 75	Bar	221	32.0	186	27.0	176	25.5	170	24.6	156	22.6
Nimonic 80A	Bar	219	31.8	188	27.2	179	26.0	170	24.6	157	22.7
Nimonic 90	Bar	226	32.7	190	27.6	181	26.3	170	24.7	158	22.9
Nimonic 105	Bar	223	32.3	186	27.0	178	25.8	168	24.4	155	22.5
Nimonic 115	Bar	224	32.4	188	27.2	181	26.3	173	25.1	164	23.8
Nimonic 263	Sheet	222	32.1	190	27.5	181	26.2	171	24.8	158	22.9
Nimonic 942	Bar	196	28.4	166	24.1	158	22.9	150	21.8	138	20.0
Nimonic PE 11	Bar	198	28.7	166	24.0	157	22.8	...	...	...	...
Nimonic PE 16	Bar	199	28.8	165	23.9	157	22.7	147	21.3	137	19.9
Nimonic PK 33	Sheet	222	32.1	191	27.6	183	26.5	173	25.1	162	23.5
Pyromet 860	Bar	200	29.0	...	...	...	...	...	...	...	...
Rene 95	Bar	209	30.3	183	26.5	176	25.5	168	24.3	...	...
Udimet 500	Bar	222	32.1	191	27.7	183	26.5	173	25.1	161	23.4
Udimet 700	Bar	224	32.4	194	28.1	186	27.0	177	25.7	167	24.2
Udimet 710	Bar	222	32.1	...	...	...	...	...	...	...	...
Waspaloy	Bar	213	30.9	184	26.7	177	25.6	168	24.3	158	22.9
Iron base											
A-286	Bar	201	29.1	162	23.5	153	22.2	142	20.6	130	18.9
Alloy 901	Bar	206	29.9	167	24.2	153	22.1	...	...	...	...
Discaloy	Bar	196	28.4	154	22.3	145	21.0	...	...	...	...
Haynes 556	Sheet	203	29.5	165	23.9	156	22.6	146	21.1	137	19.9
Incoloy 800	Bar	196	28.4	161	23.4	154	22.3	146	21.1	138	20.0
Incoloy 801	Bar	208	30.1	170	24.7	162	23.5	154	22.3	144	20.9
Incoloy 802	Bar	205	29.7	169	24.5	161	23.4	156	22.6	152	22.0
Incoloy 807	Bar	184	26.6	155	22.4	146	21.2	137	19.9	128	18.5
Incoloy 903	Bar	147(c)	21.3	152(d)	22.1	...	...	...	...	...	...
Incoloy 907(d)	...	165(c)	23.9	165(d)	23.9	159(c)	23	...	...	...	...
N-155	Bar	202	29.3	167	24.2	159	23.0	149	21.6	138	20.0
V-57	Bar	199	28.8	163	23.6	153	22.2	144	20.8	130	18.9
19-9 DL	...	203	29.5	...	...	152	22.1	...	...	...	...
16-25-6	...	195	28.2	...	...	123	17.9	...	...	...	...
Cobalt base											
Haynes 188	Sheet	207	30	...	...	...	...	...	...	...	...
L-605	Sheet	216	31.4	...	...	185	26.8	...	...	166	24.0
MAR-M-918	Sheet	225	32.6	186	27.0	176	25.5	168	24.3	159	23.0
MP35N	Bar	231(c)	33.6	...	...	...	...	...	...	...	...
Haynes 150	...	217(c)	31.5	...	...	...	...	...	...	...	...

(a) Cold-rolled and solution-annealed sheet, 1.2 to 1.6 mm (0.048 to 0.063 in.) thick. (b) Data for bar, rather than sheet. (c) Annealed. (d) Precipitation hardened

mechanical and physical properties for two ODS superalloys.

Heat Treatment of IN-718. IN-718 is the dominant wrought superalloy in use today. It is less expensive than other nickel-base superalloys, more forgiving in fabrication practice, and capable of reaching excellent tensile-strength levels with good creep-rupture characteristics. A principal drawback is its limited temperature capability, which arises

Table 12.12 Physical properties of selected wrought superalloys

Designation	Form	Density, g/cm^3	Melting range		Specific heat capacity					
					At 21 °C (70 °F)		At 538 °C (1000 °F)		At 871 °C (1600 °F)	
			°C	°F	J/kg · K	Btu/lb · °F	J/kg · K	Btu/lb · °F	J/kg · K	Btu/lb · °F
Nickel base										
Astroloy	Bar	7.91	...	...	...	...	...	...	...	...
D-979	Bar	8.19	1200–1390	2225–2530	...	...	...	...	...	...
Hastelloy X	Sheet	8.21	1260–1355	2300–2470	485	0.116	...	...	700	0.167
Hastelloy S	Bar	8.76	1335–1380	2435–2515	405	0.097	495	0.118	595	0.142
Inconel 597	Bar	8.04	...	...	...	...	...	...	...	...
Inconel 600	Bar	8.41	1355–1415	2470–2575	445	0.106	555	0.132	625	0.149
Inconel 601	Bar	8.05	1300–1370	2375–2495	450	0.107	590	0.140	680	0.162
Inconel 617	Bar	8.36	1330–1375	2430–2510	420	0.100	550	0.131	630	0.150
Inconel 625	Bar	8.44	1290–1350	2350–2460	410	0.098	535	0.128	620	0.148
Inconel 690	Bar	8.14	1345–1375	2450–2510	...	...	...	...	...	...
Inconel 706	Bar	8.08	1335–1370	2435–2500	445	0.106	580	0.138	670	0.159
Inconel 718	Bar	8.22	1260–1335	2300–2435	430	0.102	560	0.133	645	0.153
Inconel X750	Bar	8.25	1395–1425	2540–2600	430	0.103	545	0.130	715	0.171
Haynes 230	...	8.8	1300–1370	2375–2500	397	0.095	473	0.112	595	0.145
M-252	Bar	8.25	1315–1370	2400–2500	...	...	...	...	...	...
Nimonic 75	Bar	8.37	...	...	460	0.11	...	...	...	...
Nimonic 80A	Bar	8.16	1360–1390	2480–2535	460	0.11	...	...	...	...
Nimonic 81	Bar	8.06	...	...	460	0.11	585	0.14	670	0.16
Nimonic 90	Bar	8.19	1335–1360	2435–2480	460	0.11	585	0.14	670	0.16
Nimonic 105	Bar	8.00	...	...	420	0.10	545	0.13	670	0.16
Nimonic 115	Bar	7.85	...	...	460	0.11	...	...	...	...
Nimonic 263	Sheet	8.36	...	...	460	0.11	...	...	...	...
Nimonic 942	Bar	8.19	1240–1300	2265–2370	420	0.10	...	...	...	...
Nimonic PE 11	Bar	8.02	1280–1350	2335–2460	420	0.10	585	0.14	...	...
Nimonic PE 16	Bar	8.02	...	...	545	0.13	...	...	...	...
Nimonic PK 33	Sheet	8.21	...	...	420	0.10	545	0.13	670	0.16
Pyromet 860	Bar	8.21	...	...	...	...	...	...	...	...
Rene 41	Bar	8.25	1315–1370	2400–2500	...	...	545	0.13	725	0.173
Rene 95	Bar	...	...	...	...	...	...	...	...	...
Udimet 500	Bar	8.02	1300–1395	2375–2540	...	...	...	...	...	...
Udimet 520	Bar	8.21	1260–1405	2300–2560	...	...	...	...	...	...
Udimet 700	Bar	7.91	1205–1400	2200–2550	...	...	575	0.137	590	0.141
Unitemp AF1-1DA	Bar	8.26	...	...	420	0.100	...	...	...	...
Waspaloy	Bar	8.19	1330–1355	2425–2475	...	...	...	...	...	...
Iron base										
Alloy 901	Bar	8.21	1230–1400	2250–2550	...	...	...	...	...	...
A-286	Bar	7.91	1370–1400	2500–2550	460	0.11	...	...	...	...
Discaloy	Bar	7.97	1380–1465	2515–2665	475	0.113	...	...	...	...
Haynes 556	Sheet	8.23	...	...	450	0.107	...	...	...	...
Incoloy 800	Bar	7.95	1355–1385	2475–2525	455	0.108	...	...	...	...
Incoloy 801	Bar	7.95	1355–1385	2475–2525	455	0.108	...	...	...	...
Incoloy 802	Bar	7.83	1345–1370	2450–2500	445	0.106	...	...	...	...
Incoloy 807	Bar	8.32	1275–1355	2325–2475	...	...	...	...	...	...
Incoloy 825(a)	...	8.14	1370–1400	2500–2550	440	0.105	...	...	...	...
Incoloy 903	Bar	8.14	1320–1395	2405–2540	435	0.104	...	...	...	...
Incoloy 904	Bar	8.12	...	...	460	0.11	...	...	...	...
Incoloy 907	...	8.33	1335–1400	2440–2550	431	0.103	...	...	...	...
Incoloy 909	...	8.30	1395–1430	2540–2610	427	0.102	...	...	...	...
N-155	Bar	8.19	1275–1355	2325–2475	430	0.103	...	...	...	...
19-9 DL	...	7.9	1425–1430	2600–2610	...	...	...	...	...	...
16-25-6	...	8.0	...	...	...	...	...	...	...	...
Cobalt base										
Haynes	Sheet	8.98	1300–1330	2375–2425	405	0.097	510	0.122	565	0.135
L-605	Sheet	9.13	1330–1410	2425–2570	385	0.092	...	...	...	...
Haynes 150	...	8.05	1395	2540	...	...	...	...	...	...
MP35N	...	8.41	1315–1425	2400–2600	...	...	...	...	...	...
Elgiloy	...	8.3	1495	2720	...	...	...	...	...	...

(continued)

(a) At 21 to 93 °C (70 to 200 °F). (b) At 25 to 427 °C (77 to 800 °F). (c) At 705 °C (1300 °F). (d) At 980 °C (1800 °F).

Table 12.12 (continued)

Designation	Form	Thermal conductivity: At 21 °C (70 °F) W/m · K	Thermal conductivity: At 21 °C (70 °F) Btu/ft² · in. · h · °F	Thermal conductivity: At 538 °C (1000 °F) W/m · K	Thermal conductivity: At 538 °C (1000 °F) Btu/ft² · in. · h · °F	Thermal conductivity: At 871 °C (1600 °F) W/m · K	Thermal conductivity: At 871 °C (1600 °F) Btu/ft² · in. · h · °F	Mean coefficient of thermal expansion, 10^{-6} K: At 538 °C (1000 °F)	Mean coefficient of thermal expansion, 10^{-6} K: At 871 °C (1600 °F)	Electrical resistivity, nΩ · m
Nickel base										
Astroloy	Bar	...	...	...	...	...	...	13.9	16.2	...
D-979	Bar	12.6	87	18.5	128	...	...	14.9	17.7	...
Hastelloy X	Sheet	9.1	63	19.6	136	26.0	180	15.1	16.2	1180
Hastelloy S	Bar	...	...	20.0	139	26.1	181	13.3	14.9	...
Inconel 597	Bar	...	...	18.2	126	...	...	...	...	...
Inconel 600	Bar	14.8	103	22.8	158	28.9	200	15.1	16.4	1030
Inconel 601	Bar	11.3	78	20.0	139	25.7	178	15.3	17.1	1190(a)
Inconel 617	Bar	13.6	94	21.5	149	26.7	185	13.9	15.7	1220(a)
Inconel 625	Bar	9.8	68	17.5	121	22.8	158	14.0	15.8	1290
Inconel 690	Bar	13.3	95	22.8	158	27.8	193	...	...	148
Inconel 706	Bar	12.6	87	21.2	147	...	...	15.7	...	...
Inconel 718	Bar	11.4	79	19.6	136	24.9	173	14.4	...	1250(a)
Inconel X750	Bar	12.0	83	18.9	131	23.6	164	14.6	16.8	1220(a)
Haynes 230	...	8.9	62	18.4	133	24.4	179	14.0	15.2	1250
M-252	Bar	11.8	82	...	...	...	...	13.0	15.3	...
Nimonic 75	Bar	...	...	...	...	...	...	14.7	17.0	1090(a)
Nimonic 80A	Bar	8.7	60	15.9	110	22.5	156	13.9	15.5	1240(a)
Nimonic 81	Bar	10.8	75	19.2	133	25.1	174	14.2	17.5	1270(a)
Nimonic 90	Bar	9.8	68	17.0	118	...	...	13.9	16.2	1180(a)
Nimonic 105	Bar	10.8	75	18.6	129	24.0	166	13.9	16.0	1310(a)
Nimonic 115	Bar	10.7	74	17.6	124	22.6	154	13.3	16.4	1390(a)
Nimonic 263	Sheet	11.7	81	20.4	141	26.2	182	13.7	16.2	1150(a)
Nimonic 942	Bar	...	...	...	...	...	...	14.7	16.5	...
Nimonic PE 11	Bar	...	...	...	...	...	...	15.2	...	...
Nimonic PE 16	Bar	11.7	81	20.2	140	26.4	183	15.3	18.5	1100(a)
Nimonic PK 33	Sheet	10.7	74	19.2	133	24.7	171	13.1	16.2	1260(a)
Pyromet 860	Bar	...	...	...	...	...	...	15.4	16.4	...
Rene 41	Bar	9.0	62	18.0	125	23.1	160	13.5	15.6	1308
Rene 95	Bar	8.7	60	17.4	120	...	...	...	...	...
Udimet 500	Bar	11.1	77	18.3	127	24.5	170	14.0	16.1	1203
Udimet 700	Bar	19.6	136	20.6	143	27.7	192	13.9	16.1	...
Unitemp AF1-1DA	Bar	10.8	75	16.5	114	19.5	135	12.4	14.1	...
Waspaloy	Bar	10.7	74	18.1	125	24.1	167	14.0	16.0	1240
Iron base										
Alloy 901	Bar	13.3	92	...	...	...	...	15.3	...	...
A-286	Bar	12.7	88	22.5	156	...	...	17.6	...	...
Discaloy	Bar	13.3	92	21.1	146	...	...	17.1	...	...
Haynes 556	Sheet	11.6	80	17.5	121	...	...	16.2	17.5	...
Incoloy 800	Bar	11.6	80	20.1	139	...	...	16.4	18.4	989
Incoloy 801	Bar	12.4	86	20.7	143	25.6	177	17.3	18.7	...
Incoloy 802	Bar	11.9	82	19.8	137	24.2	168	16.7	18.2	...
Incoloy 807	Bar	...	...	...	...	...	...	15.2	17.6	...
Incoloy 825	...	11.1	76.8	...	...	...	...	14.0(a)	...	1130
Incoloy 903	Bar	16.8	116	20.9	145	...	...	8.6	...	610
Incoloy 904	Bar	16.8	116	22.4	155	...	...	...	...	...
Incoloy 907	...	14.8	103	...	...	...	...	7.7(b)	...	697
Incoloy 909	...	14.8	103	...	...	...	...	7.7(b)	...	728
N-155	Bar	12.3	85	19.2	133	...	...	16.4	17.8	...
19-9 DL	...	...	...	...	...	...	...	17.8	...	...
16-25-6	...	...	...	15	104	...	...	16.9	...	...
Cobalt base										
Haynes 188	Sheet	...	...	19.9	138	25.1	174	14.8	17.0	922
L-605	Sheet	9.4	65	19.5	135	26.1	181	14.4	16.3	890
Stellite 6B	...	14.7	101	...	...	...	...	15.0	16.9	910
Haynes 150	...	...	...	0.75(c)	5.2	...	...	...	16.8(d)	810
MP35N	...	...	...	...	...	...	...	...	15.7(d)	1010
Elgiloy	...	1.0	7.2	1.4	10	...	...	...	15.8(d)	995

(a) At 21 to 93 °C (70 to 200 °F). (b) At 25 to 427 °C (77 to 800 °F). (c) At 705 °C (1300 °F). (d) At 980 °C (1800 °F).

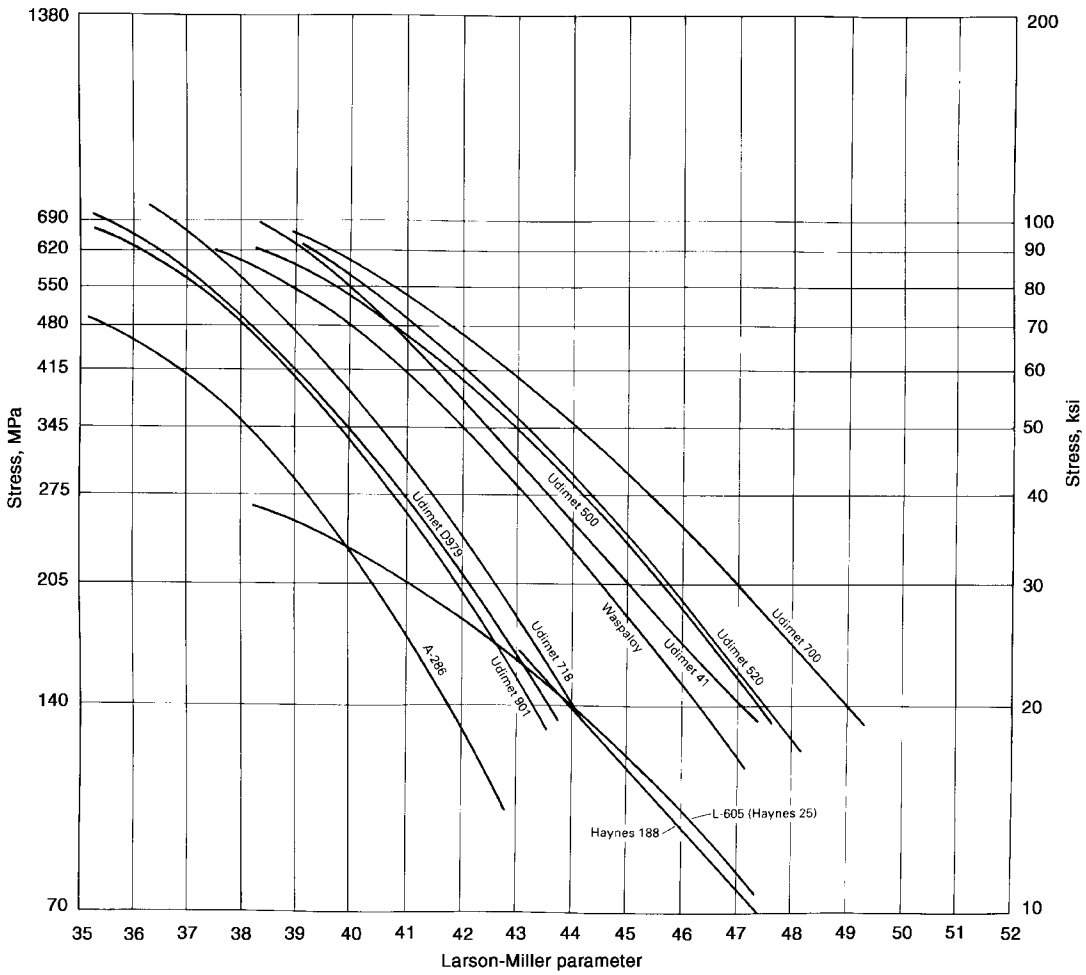


Fig. 12.33 Selected wrought superalloys compared using Larson-Miller parameter (P_{LM}). Note: $P_{LM} = T(C + \log t)$ where C = Larson-Miller constant, T = absolute temperature, t = time in h. For this plot, C = 20, T = °R

from the lower solvus temperature for this γ″-hardened alloy. As the dominant alloy, IN-718 deserves a separate discussion of strength capability, as given here.

Standard (STD) IN-718 normally is used in the solution treated and aged condition. The exact conditions have depended on the user, the application, and the property levels desired. Many aerospace applications, for example, gas turbine disks, require high tensile and fatigue properties. The standard IN-718 heat treatment for many years has been:

- Solution heat treat at 1700 to 1850 °F (927 to 1010 °C) for 1 to 2 h, air cool or faster
- Age at 1325 °F (719 °C) for 8 h, furnace cool to 1150 °F (621 °C)
- Hold at 1150 °F (621 °C) for a total aging time of 18 h, air cool

For highest strength levels, it was determined that forging below the δ solvus, quenching after forging, and performing the subsequent two-step age without a solution heat treatment resulted in substantial improvements in short-time properties. This direct aging (DA) process has become widely used but depends on the ability of the melting and conversion process at the alloy-producer stage to provide very high-quality, uniform billet material for component forging. Tight control of forging temperatures and processing is required. The DA heat treatment results

Table 12.13 Tensile properties of Rene 95 nickel-base superalloy, showing processing heat treatment conditions

Heat treatment/property	Extruded and forged(a)	Hot isostatic pressing(b)	Cast and wrought(c)
Heat treatment	1120 °C (2050 °F)/1 h AC + 760 °C (1400 °F)/ 8 h AC	1120 °C (2050 °F)/1 h AC + 760 °C (1400 °F)/ 8 h AC	1220 °C (2230 °F)/1 h AC + 1120 °C (2050 °F)/ 1 h AC + 760 °C (1400 °F)/8 h AC
Grain size, μm (mils)	5 (0.2) (ASTM No. 11)	8 (0.3) (ASTM No. 8)	150 (6) (ASTM No. 3–6)
40 °C (100 °F) tensile properties			
0.2% yield strength, MPa (ksi)	1140 (165.4)	1120 (162.4)	940 (136.4)
Ultimate tensile strength, MPa (ksi)	1560 (226.3)	1560 (226.3)	1210 (175.5)
Elongation, %	8.6	16.6	8.6
Reduction in area, %	19.6	19.1	14.3
650 °C (1200 °F) tensile properties			
0.2% yield strength, MPa (ksi)	1140 (165.4)	1100 (159.5)	930 (134.7)
Ultimate tensile strength, MPa (ksi)	1500 (217.6)	1500 (217.6)	1250 (181.3)
Elongation, %	12.4	13.8	9.0
Reduction in area, %	16.2	13.4	13.0

(a) AC, air cooled, Processing: −150-mesh powder, extruded at 1070 °C (1900 °F) to a reduction of 7 to 1 in area, isothermally forged at 1100 °C (2012 °F) to 80% height reduction. (b) Processing: −150-mesh powder, HIP processed at 1120 °C (2050 °F) at 100 MPa (15 ksi) for 3 h. (c) Processing: cross-rolled plate, heat treated at 1218 °C (2225 °F) for 1 h

in the highest tensile strengths for IN-718, although at a slight loss in stress-rupture capability. An intermediate level of high-strength (HS) IN-718 also is possible. Figure 12.34 shows typical properties of IN-718 as a function of processing. It is apparent in Fig. 12.34(a) that DA IN-718 possesses the highest ultimate tensile strengths among the three levels of IN-718 available. The stress-rupture capability, however, shows a crossover, and STD IN-718 is stronger in stress rupture at longer times.

A modified solution and age heat treatment is sometimes used for IN-718. This treatment uses a higher solution treat temperature, in the range of 1900 to 1950 °F (1038 to 1066 °C), and, as noted previously, will tend to produce notch brittleness in stress rupture.

Standard IN-718 has a grain size of ASTM 4 to 6 and is now relegated to less critical, difficult-to-make, or less highly stressed components. The HS IN-718 tends to a grain size of ASTM 6-8, while the DA IN-718 has grain sizes of about ASTM 8-10. The higher

Table 12.14 Properties of selected P/M processed nickel-base superalloys

Property	MERL 76	RSR 185	IN-100	LC Astroloy	Astroloy	Rene 95	IN-718
Condition	Gatorized	As-extruded	...	HIPed(a)	...	HIPed at 1121 °C (2050 °F)(a)	RS(b)
Grain size, μm	20	16–20	5	...	5	...	...
Properties at 25 °C (77 °F)							
0.2% yield strength, MPa (ksi)	1035 (150)	1380 (200)	940 (136)	932 (135)	936 (135)	1215 (176)	1240 (180)
Ultimate tensile strength, MPa (ksi)	1505 (218)	1860 (270)	1130 (164)	1380 (200)	1393 (202)	1636 (237)	1450 (210)
Elongation, %	38	8	8	26	...	...	18
Reduction in area, %	30	...	...	...	...	15	33.5
Properties at 649 °C (1200 °F)							
0.2% yield strength, MPa (ksi)	1050 (152)	...	1080 (157)	863 (125)	1025 (149)	1120 (162)	1035 (150)
Ultimate tensile strength, MPa (ksi)	1276 (185)	...	1290 (187)	1290 (187)	1300 (189)	1514 (220)	1173 (170)
Elongation, %	20	...	16	25	25	17	20
Reduction in area, %	20	...	...	...	...	...	32
Properties at 704 °C (1300 °F)							
0.2% yield strength, MPa (ksi)	1050 (152)	1104 (160)	1065 (154)	...	1030 (149)	...	...
Ultimate tensile strength, MPa (ksi)	1320 (191)	1310 (190)	1270 (184)	...	1160 (168)	...	...
Elongation, %	16	...	20	...	24	...	...
Reduction in area, %	23	...	...	...	...	...	...

(a) HIP, hot isostatic pressing. (b) RS, rapidly solidified

Table 12.15 Mechanical and physical properties of two oxide-dispersion-strengthened superalloys

Property	MA-754(a)	MA-956(b)
Mechanical		
Ultimate tensile strength, MPa (ksi)		
At 21 °C (70 °F), longitudinal	965 (140)	645 (94)
At 540 °C (1000 °F), longitudinal	760 (110)	370 (54)
At 1095 °C (2000 °F)		
Longitudinal	148 (21.5)	91 (13.2)
Transverse	131 (19)	90 (13.0)
Yield strength, 0.2% offset		
At 21 °C (70 °F), longitudinal	585 (85)	555 (80)
At 540 °C (1000 °F), longitudinal	515 (85)	285 (41)
At 1095 °C (2000 °F)		
Longitudinal	134 (19.5)	84.8 (12.3)
Transverse	121 (17.5)	82.7 (12.0)
Elongation, %		
At 21 °C (70 °F), longitudinal	21	10
At 540 °C (1000 °F), longitudinal	19	20
At 1095 °C (2000 °F)		
Longitudinal	12.5	3.5
Transverse	3.5	4.0
Reduction in area at 1095 °C (2000 °F), %		
Longitudinal	24	. . .
Transverse	1.5	. . .
1000 h rupture strength, MPa (ksi)		
At 650 °C (1200 °F)	255 (37)	110(c) (16)
At 980 °C (1800 °F)	130 (19)	65 (10)
Physical		
Melting range, °C (°F)	. . .	1480(d) (2700)
Specific heat capacity at 21 °C (70 °F), J/kg · K (Btu/lb · °F)	. . .	469 (0.112)
Thermal conductivity at 21 °C (70 °F), W/m · K (Btu/ft^2 · in. · h · °F)	. . .	10.9 (76)
Mean coefficient of thermal expansion at 538 °C (1000 °F), 10^{-6}/K	. . .	11.3
Electrical resistivity, nΩ · m	. . .	1310

(a) Data for bar form. Condition of test material was 1315 °C (2400 °F)/1 h/AC. (b) Data for sheet. Condition of test material was 1300 °C (2375 °F)/1 h/AC. (c) At 760 °C (1400 °F). (d) Approximate solidus temperatue

tensile and fatigue properties of DA IN-718 reflect the finer grain size of the DA product.

Directionality of Properties. Directionality of mechanical properties may occur in wrought superalloys. Intentional creation of directional mechanical properties is rare, although ODS alloys may be directionally recrystallized to improve longitudinal strength at the expense of strength in transverse directions. Plate and sheet of wrought alloys may show directionality of properties, owing to the method of working the materials. Published data on directional mechanical properties in wrought superalloys may be limited.

Wrought Superalloys—Fatigue and Fracture Properties

Fatigue and Fracture. Virtually all alloys are subject to fatigue in service applications. The fatigue is usually mechanically induced, but for some wrought alloys, may have a thermal component. Low-cycle fatigue occurs with gas turbine disks, cases, and other structures highly loaded in tension but not in creep-rupture conditions. Fatigue life is related to defects but also to the inherent noncyclic strength properties of an alloy. Low-cycle fatigue is related to yield strength, while HCF is related more to the ultimate strength of a superalloy. As temperatures increase, creep and rupture lives may play a more important role. In general, LCF receives more attention, because extended HCF exposure is usually likely only in the instance of design error, while LCF exposure occurs with each operation of a component.

Fracture data generally are found to be fracture mechanics data, but critical stress-intensity factors or other fracture data for superalloys are limited in the literature. Fracture mechanics data generally are discussed

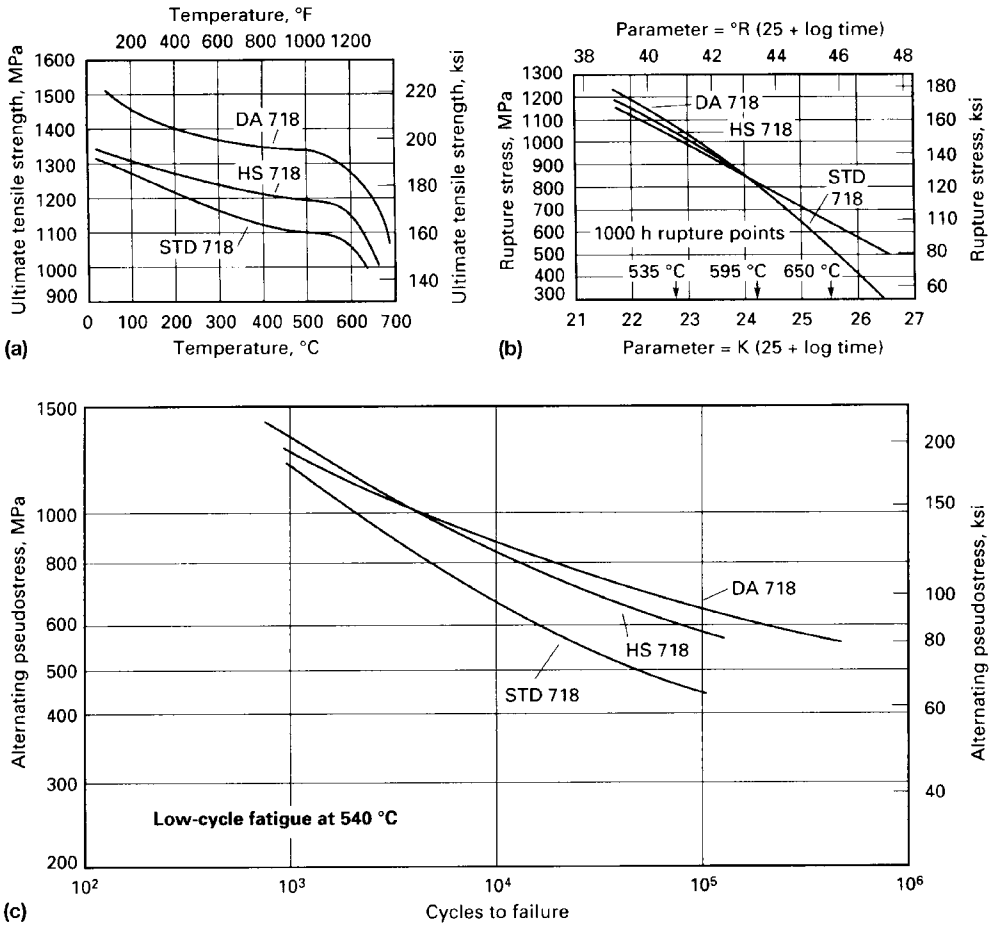


Fig. 12.34 Typical tensile and stress-rupture properties of IN-718 at three different processing conditions. DA, direct age; HS, high-strength processed; STD 718, standard heat treatment. (a) Ultimate tensile strength. (b) Rupture stress. (c) Fatigue at 540 °C (1000 °F)

in terms of crack propagation, usually for propagation in fatigue but also for creep-crack propagation.

Properties: LCF. The morphology and $V_f\gamma'$ (or γ'') affect crack growth behavior and LCF life. Low-cycle fatigue life is primarily controlled by defects in the alloy that result in the initiation of fatigue cracks by any mechanism that is not crystallographic in nature. The effects of defects on LCF depend on the size, shape, and location of the defects themselves. In wrought alloys, the defects are inclusions, carbide particles, or possible other microstructural abnormalities that provide for a low-ductility site where fracture may be initiated. The surface is a prime source of cracks, and cracking can initiate in a surface more readily if the customary surface residual stress has been removed. A defect of a given size is less detrimental if located internally rather than externally. IN-718 studies showed that finer precipitates result in longer LCF life, in many instances. Limited data are found on LCF (or HCF) life as a function of microstructural features such as grain size or the morphology and $V_f\gamma'$. Table 12.16 gives the LCF lives of IN-901 nickel-base superalloy in several grain sizes tested at 850 °F (454 °C). Note that, as expected from the strength effects of fine grain size on wrought products, the finer-grain material showed longer LCF lives.

Fatigue data do exist in the LCF range for superalloys produced by different methods and tested at a variety of conditions. Figure 12.35 provides a comparison of LCF behav-

Table 12.16 Effect of grain size on the LCF properties of IN-901 nickel-base superalloy at 454 °C (850 °F)

	Stress		Temperature		
Incoloy 901 grain size	MPa	ksi	°C	°F	Cycles to failure(a)
ASTM 2	205 ± 448	30 ± 65	455	850	9,000
ASTM 5	205 ± 448	30 ± 65	455	850	26,000
ASTM 12	205 ± 448	30 ± 65	455	850	200,000+
ASTM 2	205 ± 530	30 ± 77	455	850	5,000
ASTM 5	205 ± 530	30 ± 77	455	850	16,000
ASTM 12	205 ± 530	30 ± 77	455	850	137,000

(a) Average of eight tests at 454 °C (850 °F)

ior as a series of stress vs. number of cycles to failure (N_f) curves for Rene 95 nickel-base superalloy at several temperatures. Occasionally, strain-controlled LCF tests are run instead of the more common stress-controlled tests. Figure 12.36 compares the strain-controlled LCF properties of seven wrought nickel-base superalloys at 1200 °F (649 °C). It can be noted that there is crossover of property curves below about 10^3 cycles, and the curves are roughly parallel above that point.

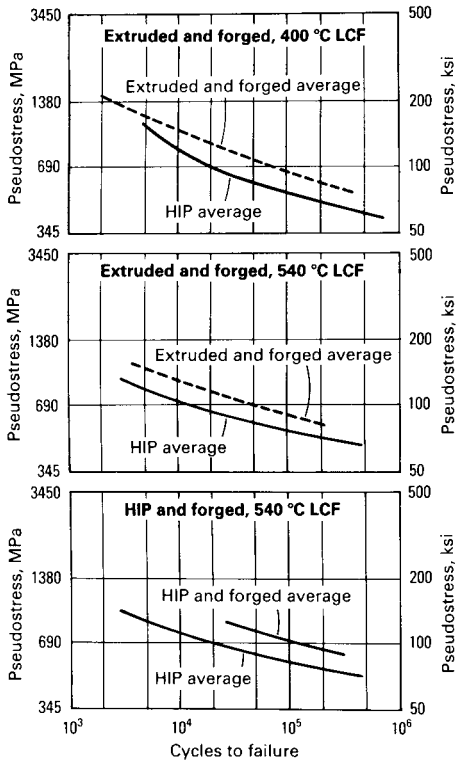


Fig. 12.35 Comparison of LCF lives of HIP vs. extruded + forged and HIP + forged Rene 95 nickel-base superalloy

At high strain amplitudes, weaker but more ductile alloys (e.g., Waspaloy, Astroloy) may be better in fatigue, owing to the dominance of ductility at that end of the cyclic curve. On the other hand, at 10^5 cycles (the customary reference for most LCF strength values) and up into the HCF range at 10^6 to 10^8 cycles, the stronger alloys, such as MERL 76 and Rene 95, dominate, because strength is the most important variable at low strain amplitudes. Strength is not a complete indicator of LCF capability, because the presence of more and/or larger defects in any given alloy can change the initiation and growth kinetics of a crack and promote earlier failure.

Thermomechanical processing of wrought superalloys can modify not only grain size, but also grain shape and orientation, dislocation substructure, and grain-boundary morphology of matrix and second phases. At one time, necklace structures (fine grains surrounding coarser grains) were produced in some alloys. All of these structural changes might result in improved LCF life if they slow the crack initiation process or the crack growth rate.

In Figure 12.35, it may be seen that the extruded + forged material showed longer life than the HIP or HIP + forged P/M material. Forging tends to disperse defects and, possibly, reduce their size, while the grain size usually is refined as a result of the deformation and annealing processes. Prior extrusion does a better job of consolidation than HIP if the product is a P/M one. Appropriate forging schedules may close unoxidized subsurface defects and may even eliminate the effects of prior particle boundary defects inherited in a P/M forging billet.

Low-cycle fatigue of superalloys is affected by secondary phase formation. It is reasonable to assume that tcp phases will af-

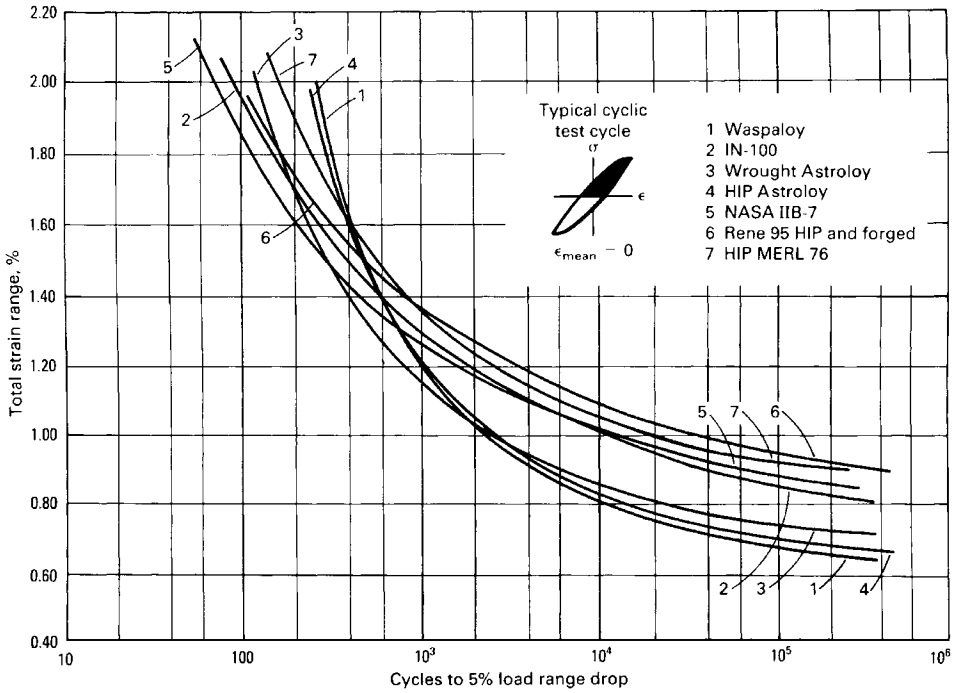


Fig. 12.36 Comparison of cyclic strain-controlled LCF properties of seven nickel-base superalloys at 649 °C (1200 °F)

fect property behavior, with results dependent on ductility changes and the changes in static and dynamic monotonic stress properties. An important factor controlling the properties of IN-706, a comparable alloy to IN-718, is the disposition of the η phase, which in this system is an Ni_3(Nb, Ti) precipitate. Correlations were shown between amount of η and LCF life. Figure 12.37 shows how the LCF life decreases as the percentage of intergranular η increases.

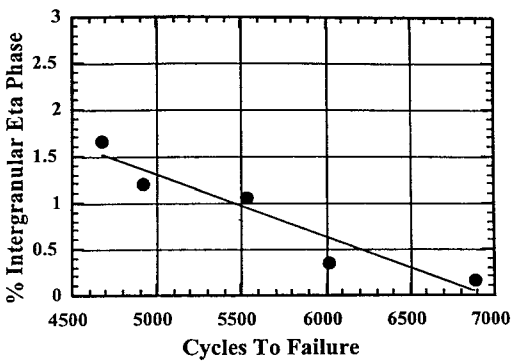


Fig. 12.37 Cycles to failure in LCF vs. amount of intergranular η in IN-706 nickel-base superalloy tested at 399 °C (750 °F)

Properties: Crack Growth. Not only is LCF behavior in superalloys determined, but also a related property, crack growth rate (*da*/*dN*), is measured and plotted versus ΔK (stress-intensity factor range, a fracture toughness parameter), as is shown in Fig. 12.38. Plots of *da*/*dN* are anticipated to have the form shown in the sketch of Fig. 12.39. The region of stable crack growth (power-law behavior—Paris' Law region—region 2) is the region in which *da*/*dN* can be expected to follow a straight line behavior. Region 2 is the region where the behavior of different alloys/microstructures is customarily compared. Region 1 represents slow crack growth or the threshold crack growth region, and crack movement in it is capable of being tracked for comparative purposes, although the extent of the region is limited. Crack growth rates in region 1 may be compared among alloys/microstructures. The ΔK value at the end of the threshold region can be compared with the values for other alloys/microstructures. Region 3, the unstable crack growth region, represents very rapid crack

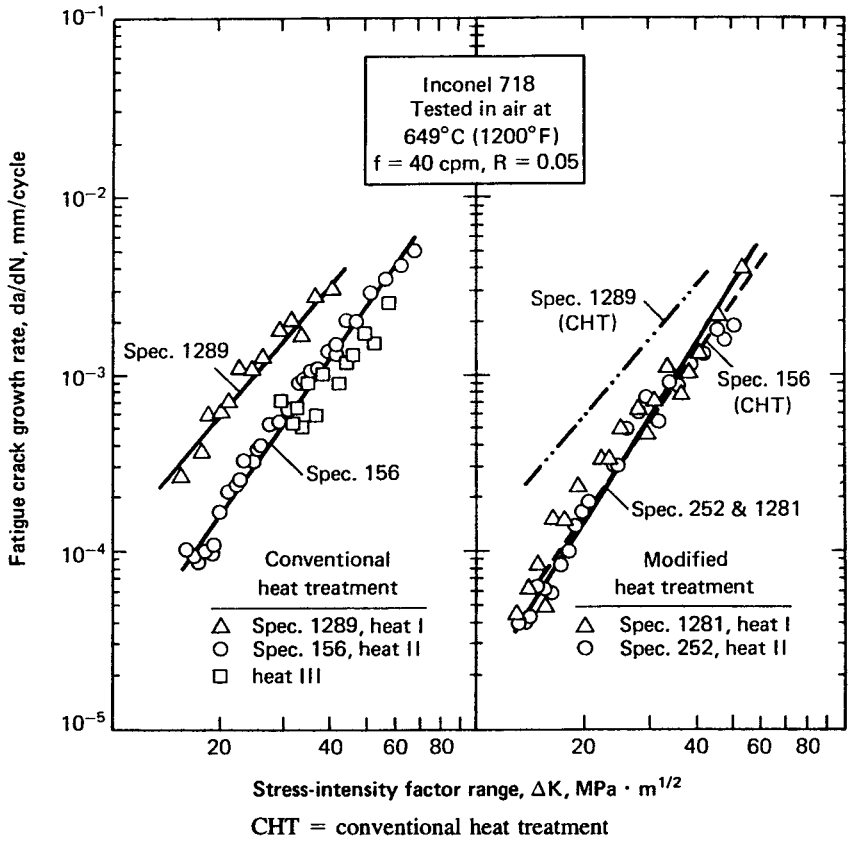


Fig. 12.38 Fatigue crack growth rate behavior of IN-718 nickel-base superalloy tested in air at 649 °C (1200 °F)

growth, and no comparisons of growth rates normally are possible in this region.

Microstructure plays an important role in the fatigue properties of nickel-base superalloys. Crack growth rate of wrought superalloys, usually nickel-base superalloys, is subject to the same constraints as found in the noncyclic properties. Grain size (resulting from forging and solution treatment) and γ' produced by aging affect crack growth rate. Crack growth rates for peak-aged γ' distributions were slower (better) than those for underaged specimens. Fine γ' causes somewhat slower growth rates than coarse or bimodal γ'. The influence of γ' on crack growth rate is seen for Waspaloy in Fig. 12.40. Grain size affects crack growth rate, with coarse-grained material being slower in growth rate than fine-grained superalloys. This behavior is illustrated for AP-1 nickel-base superalloy in Fig. 12.41 and for a related alloy, Astroloy, in Fig. 12.42. Figure 12.43 provides a comparison of the joint effects of γ' and grain size on the stable crack growth rates in Waspaloy nickel-base superalloy at room temperature. As expected, fine γ' and coarse grain size combine to provide the best crack growth resistance in this alloy.

Fatigue Properties: Effects Other Than Microstructure. In addition to the previously mentioned microstructural effects, LCF life and crack growth rates are affected by:

- Stress ratio
- Cyclic frequency of load/strain application
- Hold time and location during a cycle
- Environment
- Temperature

The near-threshold behavior of nickel-base superalloys has been shown to be affected by the stress ratio (R). When R is increased, the rates of crack propagation are significantly increased. The behavior of crack growth is capable of changing significantly with tem-

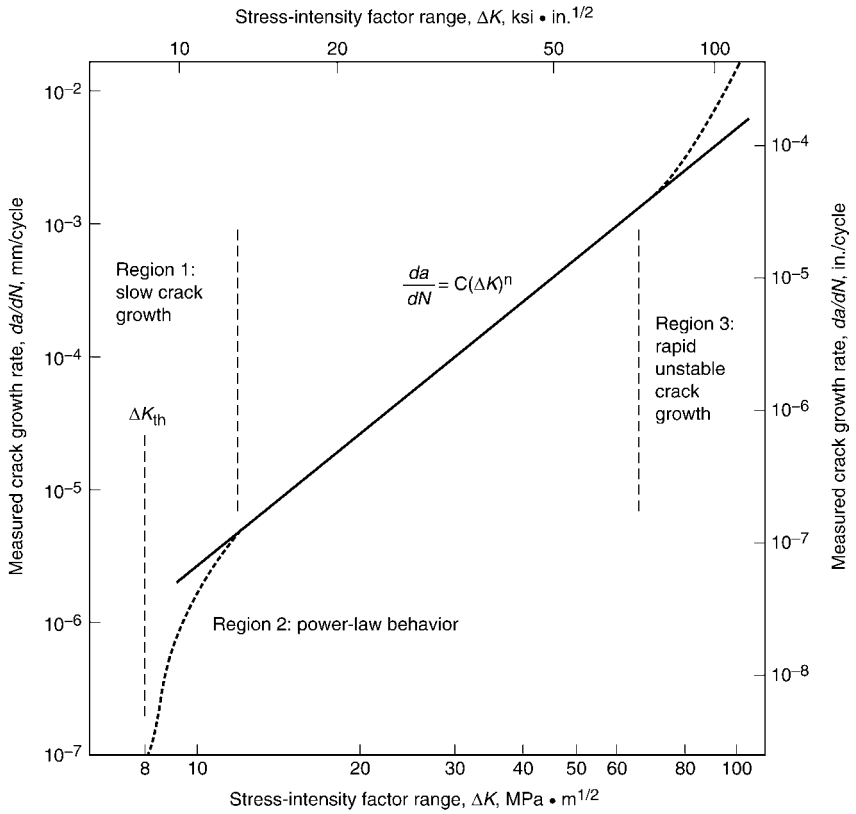


Fig. 12.39 Schematic of idealized fatigue crack growth curve. *R,* minimum stress divided by maximum stress in a fatigue cyce

perature for a given alloy. One of the continuing concerns is the interaction of LCF with creep-rupture at high temperatures. The introduction of hold periods (rather than just adjusting the continuous cyclic frequency of test) into strain-controlled fatigue tests was one approach to evaluating creep-fatigue interactions. Decreases in LCF capability of superalloys were detected when creep relaxation was permitted to occur during a fatigue cycle. A common interrupted LCF test uses hold periods at peak strain, although hold periods in compression, tension, or both have been studied. Figure 12.44 shows results of several hold periods on Rene 95 nickel-base superalloy at 1200 °F (649 °C) when compared to baseline ''no-hold'' testing. The influence of creep relaxation is evident.

Environment effects on crack growth are shown in Fig. 12.45 for IN-718 in air and helium at 1200 °F (649 °C). The crack growth rate is retarded by helium under these conditions. The addition of 5% H_2S or 5% SO_2 to the helium was found to result in crack growth rates higher than those in air. Fatigue crack growth in air frequently seems to be more rapid than in inert media (vacuum, helium), but that may not always be the case. Fatigue (and creep) crack growth may behave differently in air versus inert media, dependent on the cyclic rate of loading and loading temperature. Figure 12.46 shows the effect of hot corrosion media, air, and vacuum on the LCF behavior (cyclic plastic strain versus cycles to initiation) as a function of cycling rate. In vacuum, the cyclic rate effect was negligible, but in air and in hot corrosion media, it was significant. It should be noted that this was a test with failure defined as crack initiation, not specimen rupture; crack growth data were not reported.

Properties: HCF. High-cycle fatigue behavior of superalloys was the original fatigue property developed for engineering use; however, as it became obvious that LCF and, later, crack growth rate were more germane

to most gas turbine design problems, HCF testing became less prominent. Unfortunately, HCF data are now much less common than LCF, and crack propagation data and tabulations of older data are not readily found. Figure 12.47 shows the fatigue life in

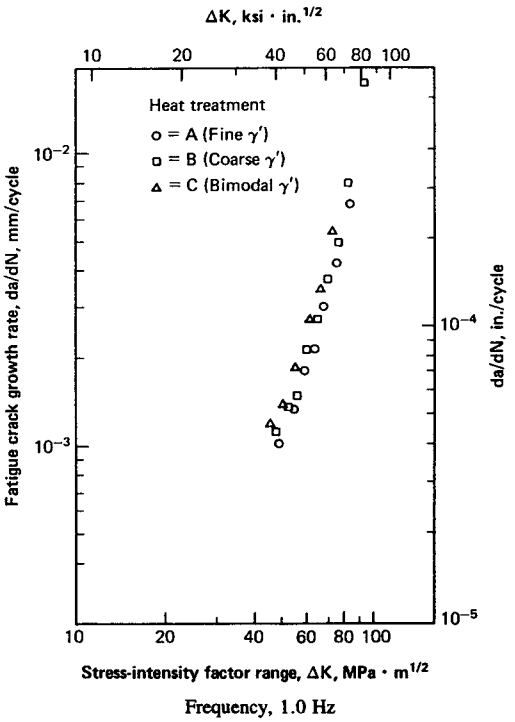


Fig. 12.40 Influence of γ′ size on cyclic crack growth rate of Waspaloy nickel-base superalloy at 649 °C (1200 °F)

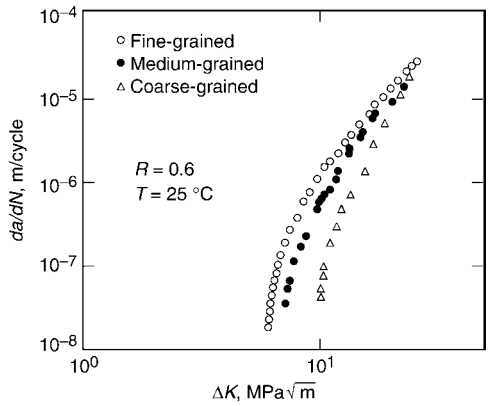


Fig. 12.41 Effect of grain size on fatigue crack growth rate of AP-1 nickel-base superalloy at room temperature

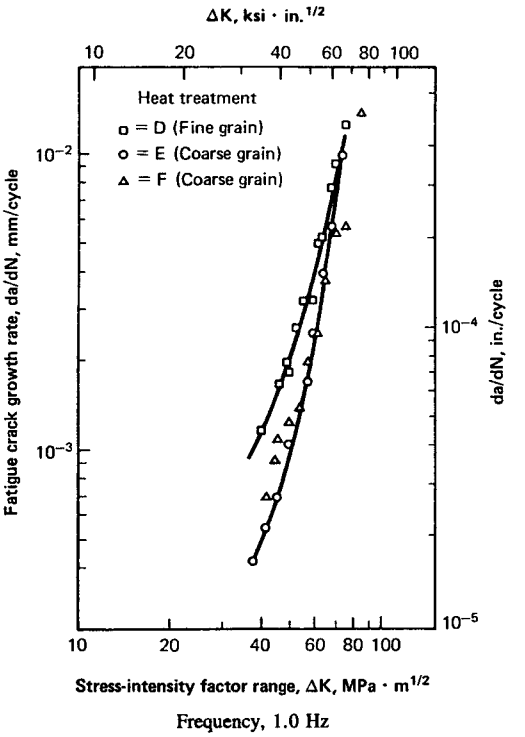


Fig. 12.42 Effect of grain size on fatigue crack growth rate of P/M Astroloy at 649 °C (1200 °F)

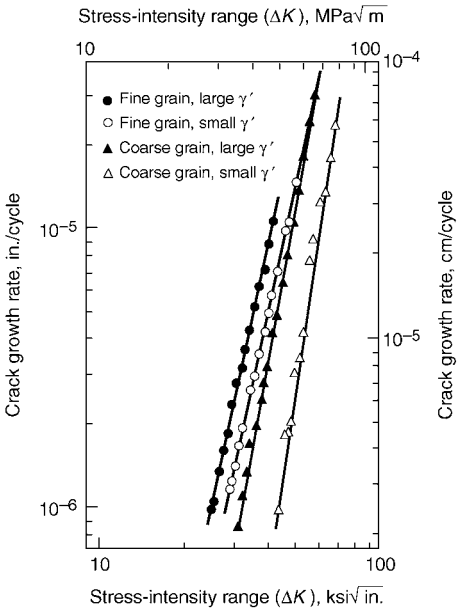


Fig. 12.43 Dependence of crack growth rate of Waspaloy nickel-base superalloy on γ′ size and grain size when tested at room temperature

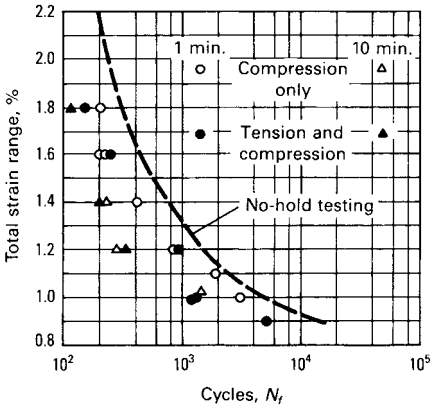


Fig. 12.44 Strain range vs. cycles to failure in LCF at 649 °C (1200 °F) for Rene 95 nickel-base superalloy, showing "no-hold" test results and data points for tests with different hold periods and locations

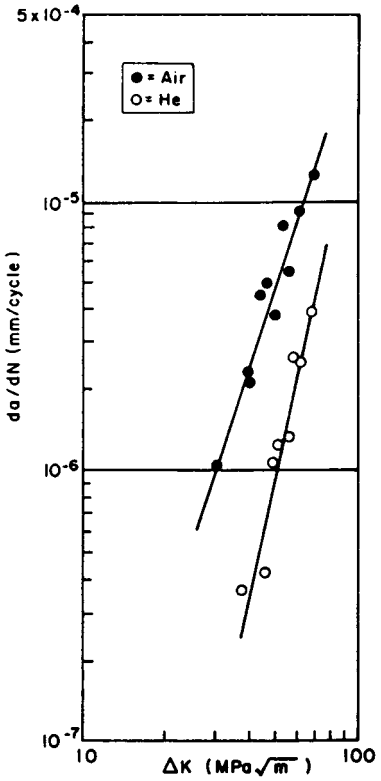


Fig. 12.45 Effect of air vs. helium on fatigue crack growth rate of IN-718 nickel-base superalloy at 649 °C (1200 °F)

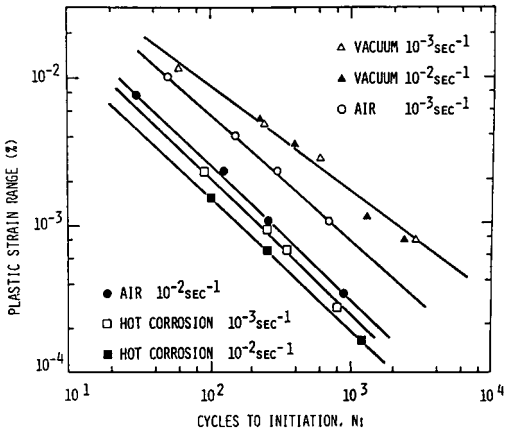


Fig. 12.46 Low-cycle fatigue behavior of IN 738 nickel-base superalloy in vacuum, air, and hot corrosion environments at 899 °C (1650 °F) and two cycling rates

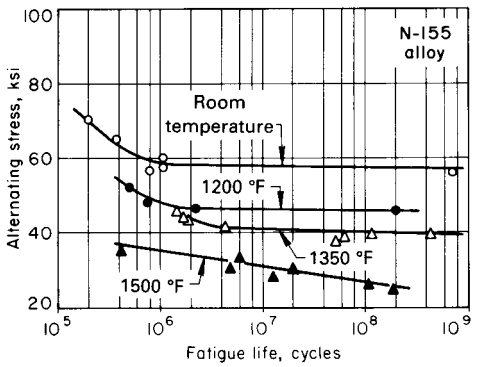


Fig. 12.47 Fatigue life of N-155 iron-nickel-base superalloy in the HCF range under reversed bending at various temperatures from room temperature to 816 °C (1500 °F)

the HCF region for N-155 iron-nickel-base superalloy as a function of temperature. Testing was in reversed bending. Testing in other modes and with varying stress ratios will affect results. Note that the HCF endurance limit decreases with increasing temperature, and a true endurance limit appears to be impossible to achieve when the temperature reaches 1500 °F (816 °C).

As noted earlier, there is an effect of reduced surface compressive residual stresses on fatigue life of a nickel-base superalloy. For IN-901, as shown in Table 12.17, the HCF endurance stress limit was drastically reduced when fatigue specimen surfaces were hand- or electropolished to remove residual

Table 12.17 Room-temperature HCF strengths of IN-901 nickel-base superalloy as affected by surface condition

Round specimens tested in reverse bending (10^8 cycles)		Flat specimens tested on air excitation rigs (10^7 cycles)	
Description	Fatigue strength, ksi (MPa)	Description	Fatigue strength, ksi (MPa)
Ground and machine polished (a)(b)	56 (386)(c)	Ground and hand polished(a)(d)	20–25 (138–172)
		Ground and hand polished(f)	30 (207)
Ground and machine polished (a)(e)	55 (379)	Ground and hand polished (g)	20 (138)
Ground and machine polished, glass bead blasted(b)	57 (393)	Ground and hand polished, glass bead blasted(f)	50 (345)
Ground and machine polished, electropolished 0.0004 in. (0.01 mm)/side(b)	25 (172)	Ground and hand polished, electropolished 0.0004 in. (0.01 mm)/side(g)	20 (138)
Ground and machine polished, 1200 °F (649 °C) (4 h) in vacuum(b)	42 (290)	Milled(f)	50–55 (345–379)
Ground and machine polished, completely reheat treated(b)	35 (241)		
Ground only(b)	30–35 (207–241)		

(a) Machine polishing consisted of circumferential polishing on centers with No. 1 and 2/0 polishing papers; the same abrasive papers were used in hand polishing all specimens except the MDL 3206 and MDL 2967 specimens, which were finished with 120-grit paper. (b) MDL 2331. (c) Fatigue strength at 10^7 cycles was 58–60 ksi (400–414 MPa). (d) MDL 2967 (width/thickness, 6:1). (e) MDL 2309. (f) MDL 3206 (width/thickness, 2:1). (g) SKP 3494 (width/thickness, 0.33:1)

Table 12.18 Effect of grain size on HCF of IN-901 nickel-base superalloy at 454 °C (850 °F)

Incoloy 901 grain size	455 °C (850 °F) Fatigue strength (10^7 cycles)		Fatigue ratio (FS/UTS)(a)
	MPa	ksi	
ASTM 2	315	46	0.32
ASTM 5	439	64	0.42
ASTM 12	624	91	0.55

(a) FS/UTS, fatigue strength to ultimate tensile strength

stress. Also, as might be expected, HCF life is a function of grain size, as shown in Table 12.18 for IN-901. The finer-grain-size materials show a higher ratio of endurance limit to ultimate tensile strength.

Cast Superalloys—Physical, Tensile, and Creep-Rupture Properties

Properties. The compositions of some selected cast superalloys were given in Table 1.2. Tensile and creep-rupture properties of selected wrought superalloys were given in Tables 2.3 and 2.4. Creep-rupture properties of selected superalloys also were given in Figs. 2.1 to 2.3. In addition, creep-rupture data are plotted for some cast cobalt- and nickel-base superalloys in Figs. 12.48 and 12.49. Some wrought alloys are included for comparison in Fig. 12.48. In Fig. 12.49, properties are shown for a few CGDS and SCDS nickel-base superalloys, with comparison to a PC cast nickel-base superalloy. Dynamic moduli and physical properties of selected cast superalloys are given in Tables 12.19 and 12.20, respectively.

For turbine airfoils, the primary application for cast superalloys, there are differing mechanical property requirements for two different regimes. For the attachment regions (the root) of turbine blades, temperatures are about 1400 °F (760 °C) or lower. Blade roots require sufficient high stress-rupture ductility, high tensile strength (actually tensile shear strength), and good LCF life for adequate root attachment durability. High creep resistance and excellent TMF resistance should be the hallmark of aircraft gas turbine blade airfoil sections, while the same is true for vanes but with creep resistance required in a lower stress regime. Airfoils for industrial gas turbines are expected to run for much longer time periods and see far fewer TMF cycles per operating hour. Consequently, for such airfoils, long-term creep resistance is a life-limiting factor, and temperatures are lower than those in aircraft gas turbines. When directionality of mechanical properties arises, as in the case of CGDS and SCDS cast superalloys, it can have a very marked effect on design and operation of components, not to mention its effect on the determination and designation of design properties for such alloys.

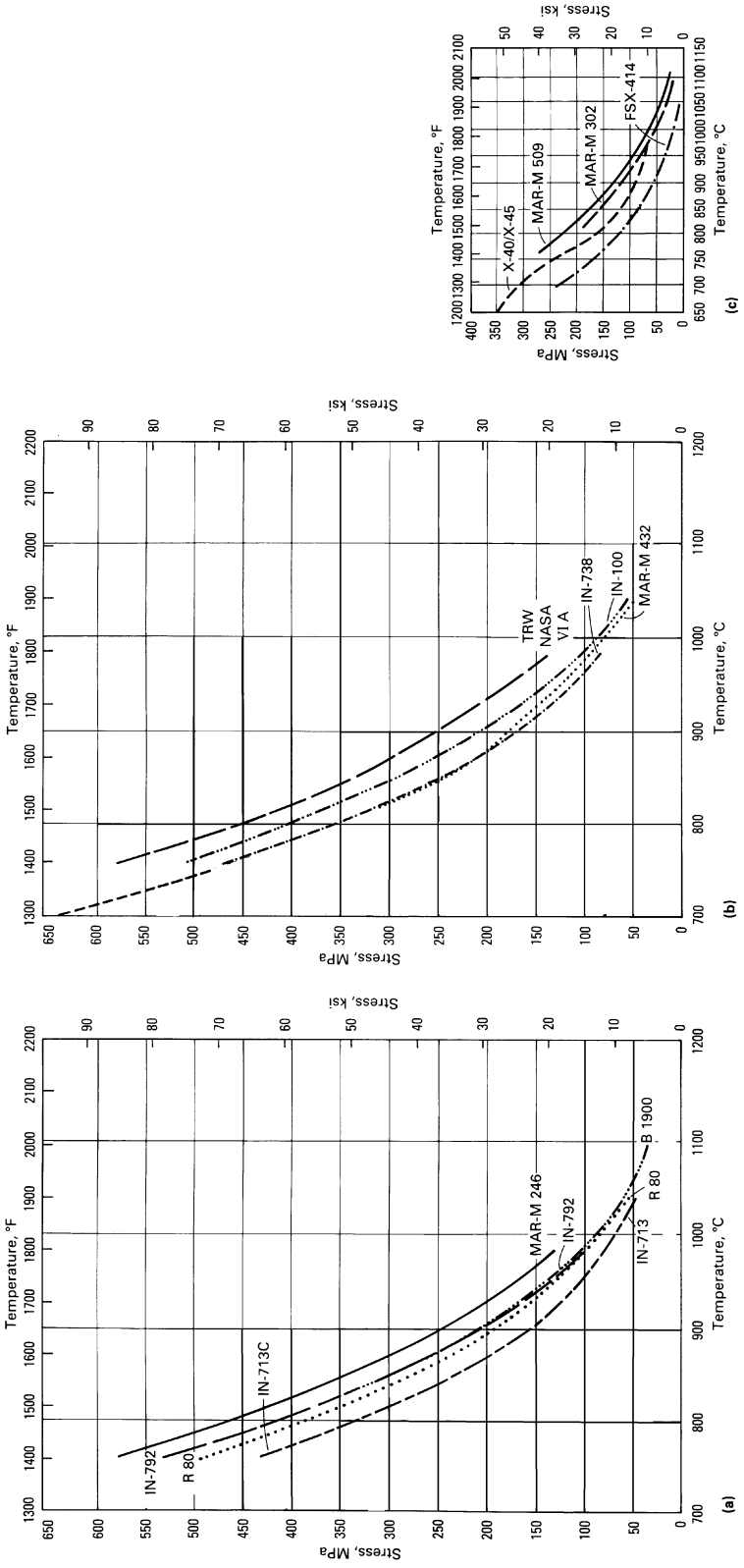


Fig. 12.48 Stress for 1000 h rupture life of selected PC cast superalloys of (a) and (b) nickel-base superalloys, (c) cobalt-base superalloys

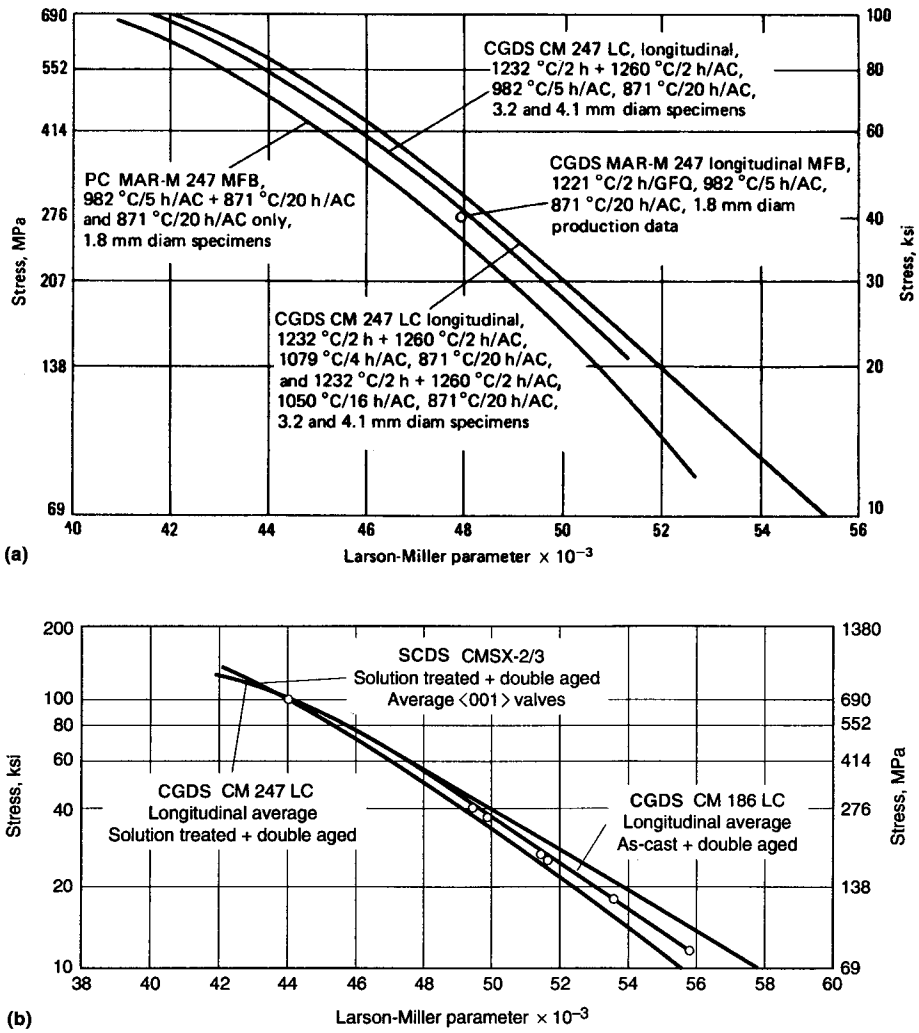


Fig. 12.49 Stress-rupture capability for (a) PC and CGDS and (b) CGDS and SCDS cast nickel-base superalloys using Larson-Miller parameter (P_{LM}). Note: $P_{LM} = T(C + \log t)$ where C = Larson-Miller constant, T = absolute temperature, t = time in h. For plot a, C = 20, T = K; for plot b, C = 20, T = °R

Polycrystalline Cast Superalloys: General. Polycrystalline cast iron-nickel-base superalloys have little or no application in the gas turbine industry, the primary user of superalloys. Polycrystalline cast cobalt-base superalloys have some application. Cast cobalt-base alloys were the earliest superalloys applied. Cobalt-base superalloys are designed around a cobalt-chromium matrix with additions of nickel (to stabilize the γ matrix), carbon (for carbides), and other elements, such as tungsten, molybdenum, tantalum, or niobium. Cobalt-base superalloys are usually melted and cast in air, with a few exceptions. The strength of cast cobalt-base superalloys comes from the grain-boundary and intragranular carbides as well as from solid-solution strengthening caused by other alloy elements. Most cobalt-base cast alloys are not heat treated, except for relatively low-temperature stress relief sometimes applied. All cobalt-base superalloys exhibit aging on exposure and become stronger (but less ductile) as a result of carbide reactions.

The strength of cobalt-base superalloys is determined by the alloy chemistry and the carbide distribution resulting from the casting process. Extensive studies of tensile and

Table 12.19 Dynamic modulus of elasticity for a few cast superalloys

	Dynamic modulus of elasticity					
	At 21 °C (70 °F)		At 538 °C (1000 °F)		At 1093 °C (2000 °F)	
Alloy	GPa	10^6 psi	GPa	10^6 psi	GPa	10^6 psi
Nickel base						
IN-713 C	206	29.9	179	26.2	...	...
IN-713 LC	197	28.6	172	25.0	...	...
B-1900	214	31.0	183	27.0	...	...
IN-100	215	31.2	187	27.1	...	...
IN-162	197	28.5	172	24.9	...	...
IN-738	201	29.2	175	25.4	...	...
MAR-M-200	218	31.6	184	26.7	...	...
MAR-M-246	205	29.8	178	25.8	145	21.1
MAR-M-247	...	...	...	...	...	...
MAR-M-421	203	29.4	...	...	141	20.4
Rene 80	208	30.2	...	...	...	...
Cobalt base						
Haynes 1002	210	30.4	173	25.1	...	...
MAR-M-509	225	32.7	...	...	...	...

creep-rupture properties have not been made. Data are available from manufacturers. Some cobalt-base superalloys have been produced in both cast and wrought forms. Figure 12.50 illustrates the benefits of a cast alloy over a wrought alloy of the same nominal composition. An illustration of the magnitude of the creep-rupture capability difference of cobalt-base and nickel-base superalloys can be seen in Fig. 12.51, where creep curves of PC cast nickel-base superalloys B-1900 and MAR-M-200 are compared with curves for PC cast WI-52 and MAR-M-302. The cobalt-base superalloys creep faster and fail sooner even though tested at a lower stress!

Cast cobalt-base superalloys are no longer being actively developed. However, cast cobalt-base superalloys continue to be employed as turbine vanes in aircraft gas turbines. Cobalt-base superalloys, despite short-time and lower-temperature disadvantages in tensile and creep-rupture properties, do generally have better longer-term, higher-strength creep-rupture capability than PC cast nickel-base superalloys. This behavior accounts for their use as turbine vanes. Furthermore, PC cast cobalt-base airfoils are capable of being weld repaired when cracked.

Polycrystalline cast nickel-base superalloys have increased in strength with time (look ahead to Fig. 15.2). Polycrystalline cast cobalt-base superalloys and then wrought nickel-base superalloys were employed as turbine blades until the early 1960s, with some introduction of PC cast nickel-base superalloys after about 1955. However, only a limited number of these superalloys were deployed before emphasis on development and application switched to the DS nickel-base superalloys. The PC cast alloys IN-713, U-700, IN-100, B-1900, and MAR-M-247 or variants thereof (e.g., IN-713 LC) were those employed in the aircraft gas turbine market in the United States. Subsequent to the realization of the need for hot corrosion resistance in turbine airfoils, the alloys IN-738, IN-792, Rene 80, and IN-939 were made available. IN-100, B-1900, and MAR-M-247 PC cast superalloys were introduced as high-pressure turbine blade materials for aircraft gas turbines. B-1900 was eventually phased out, owing to lack of hot corrosion resistance. Rene 80 was later introduced in aircraft gas turbine applications, while the IN-738/IN-792 family of alloys was primarily adapted to power gas turbine use. The higher-strength PC cast alloys were replaced by the DS materials, and some (e.g., IN-100) became low-pressure turbine airfoils, where higher creep-rupture strengths became necessary in advanced engines.

Data on the mechanical properties of PC cast nickel-base superalloys are moderate in amount. Extensive work was performed and published on IN-738. Data on all other alloys are substantially less, although IN-100 probably is one of the PC cast alloys most studied. Few compilations of data, have been made, but research and engineering studies continue on PC cast IN-100 and MAR-M-

Table 12.20 Physical properties of selected cast superalloys

Alloy	Density g/cm³	Melting range °C	Melting range °F	Specific heat At 21 °C (70 °F) J/kg · K	Specific heat At 21 °C (70 °F) Btu/lb · °F	Specific heat At 538 °C (1000 °F) J/kg · K	Specific heat At 538 °C (1000 °F) Btu/lb · °F	Specific heat At 1093 °C (2000 °F) J/kg · K	Specific heat At 1093 °C (2000 °F) Btu/lb · °F	Thermal conductivity At 93 °C (200 °F) W/m · K	Thermal conductivity At 93 °C (200 °F) Btu · in./h · ft² · °F	Thermal conductivity At 538 °C (1000 °F) W/m · K	Thermal conductivity At 538 °C (1000 °F) Btu · in./h · ft² · °F	Thermal conductivity At 1093 °C (2000 °F) W/m · K	Thermal conductivity At 1093 °C (2000 °F) Btu · in./h · ft² · °F	Mean coefficient of thermal expansion(a), 10^{-6} K At 93 °C (200 °F)	Mean coefficient of thermal expansion(a), 10^{-6} K At 538 °F (1000 °C)	Mean coefficient of thermal expansion(a), 10^{-6} K At 1093 °C (2000 °F)
Nickel base																		
IN-713 C	7.91	1260–1290	2300–2350	420	0.10	565	0.135	710	0.17	10.9	76	17.0	118	26.4	183	10.6	13.5	17.1
IN-713 LC	8.00	1290–1320	2350–2410	440	0.105	565	0.135	710	0.17	10.7	74	16.7	116	25.3	176	10.1	15.8	18.9
B-1900	8.22	1275–1300	2325–2375	...	...	...	...	...	...	(10.2)	(71)	16.3	113	...	...	11.7	13.3	16.2
Cast alloy 625	8.44	...	...	...	...	...	...	...	...	...	...	...	...	...	...	...	...	...
Cast alloy 718	8.22	1205–1345	2200–2450	...	...	...	...	...	...	...	...	...	...	...	...	...	...	...
IN-100	7.75	1265–1335	2305–2435	...	...	480	0.115	605	0.145	...	...	17.3	120	...	...	13.0	13.9	18.1
IN-162	8.08	1275–1305	2330–2380	...	...	...	...	...	...	...	...	...	...	...	...	12.2	14.1	...
IN-731	7.75	...	...	...	...	...	...	...	...	...	...	...	...	...	...	...	...	...
IN-738	8.11	1230–1315	2250–2400	420	0.10	565	0.135	710	0.17	...	...	17.7	123	27.2	189	11.6	14.0	...
IN-792	8.25	...	...	...	...	...	...	...	...	...	...	...	...	...	...	...	...	...
M-22	8.63	...	...	...	...	...	...	...	...	...	...	...	...	...	...	12.4	13.3	...
MAR-M-200	8.53	1315–1370	2400–2500	400	0.095	420	0.10	565	0.135	13.0	90	15.2	110	29.7	206	...	13.1	17.0
MAR-M-246	8.44	1315–1345	2400–2450	...	...	...	...	...	...	...	...	18.9	131	30.0	208	11.3	14.8	18.6
MAR-M-247	8.53	...	...	...	...	...	...	...	...	...	...	...	...	...	...	...	...	...
MAR-M-421	8.08	...	...	...	...	...	...	...	...	...	...	19.1	137	32.0	229	...	14.9	19.8
MAR-M-432	8.16	...	...	...	...	...	...	...	...	...	...	...	...	...	...	...	14.9	19.3
MC-102	8.84	...	...	...	...	...	...	...	...	...	...	...	...	...	...	12.8	14.9	...
Nimocast 75	8.44	1410(b)	2570(b)	...	...	...	...	...	...	...	...	...	...	...	...	12.8	14.9	...
Nimocast 80	8.17	1310–1380	2390–2515	...	...	...	...	...	...	...	...	...	...	...	...	12.8	14.9	...
Nimocast 90	8.18	1310–1380	2390–2515	...	...	...	...	...	...	...	...	...	...	...	...	12.3	14.8	...
Nimocast 242	8.40	1225–1340	2235–2445	...	...	...	...	...	...	...	...	...	...	...	...	12.5	14.4	...
Nimocast 263	8.36	1300–1355	2370–2470	...	...	...	...	...	...	...	...	...	...	...	...	11.0	13.6	...
Rene 77	7.91	...	...	...	...	...	...	...	...	...	...	...	...	...	...	...	...	...
Rene 80	8.16	...	...	...	...	...	...	...	...	...	...	...	...	...	...	...	...	...
Udimet 500	8.02	1300–1395	2375–2540	...	...	...	...	...	...	...	...	...	...	...	...	13.3	...	...
Udimet 710	8.08	...	...	...	...	...	...	...	...	12.1	84	18.1	126	...	...	...	...	...
Cobalt base																		
FSX-414	8.3	...	...	...	...	...	...	...	...	...	...	...	...	...	...	...	...	...
Haynes 1002	8.75	1305–1420	2380–2590	420	0.10	530	0.126	645	0.154	11.0	76	21.8	151	32.1	222	12.2	14.4	...
MAR-M-302	9.21	1315–1370	2400–2500	...	...	...	...	...	...	18.7	130	22.2	154	...	...	...	13.7	16.6
MAR-M-322	8.91	1315–1360	2400–2475	...	...	...	...	...	...	...	...	...	...	...	...	...	...	...
MAR-M-509	8.85	...	...	...	...	...	...	...	...	...	...	27.9	194	44.6	310	9.8	15.9	18.3
WI-52	8.88	1300–1355	2425–2475	420	0.10	...	...	...	...	24.8	172	27.4	190	40.3	280	...	14.4	17.5
X-40	8.60	...	...	...	...	...	...	...	...	11.8	82	21.6	150	...	...	...	15.1	...

(a) From room temperature to indicated temperature. (b) Liquidus temperature. Source: Nickel Development Institute

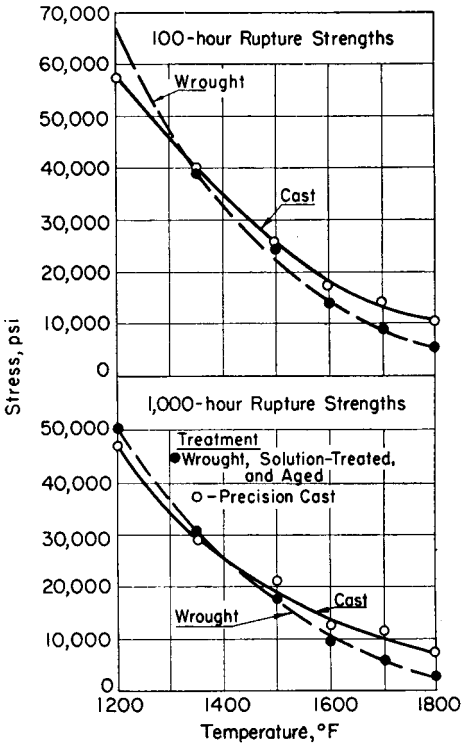


Fig. 12.50 Stress-rupture strengths at 100 and 1000 h for cast and wrought versions of the early cobalt-base superalloy S-816

247 as well as a few other alloys. IN-939 is a lower-strength but more hot-corrosion-resistant nickel-base superalloy may be used in industrial and marine gas turbines. Figure 12.52 shows 100 h rupture strength for selected cast nickel-base superalloys.

Polycrystalline Cast Superalloys: Ductility Effects. Tensile ductility for superalloys tends to drop to a valley in the region between about 1200 and 1600 °F (649 and 871 °C). Stress-rupture ductility for some higher-strength PC cast nickel-base superalloys also tends to show a minimum as well, in the 1400 °F (760 °C) region. Stress-rupture testing in this region was instituted to reflect superalloy capability under temperature/stress conditions that were thought to be representative of the attachment areas of turbine blades to disks. Generally, ductilities of early PC cast alloys were satisfactory. However, with high-strength PC cast alloys, ductilities at 1400 °F (760 °C) tended to be lower than previously experienced. One of the first alloys where this problem occurred was B-1900. The other was PC cast MAR-M-200. The latter alloy had so little ductility as to make it virtually unusable until the advent of DS processing, which was able to exploit the excellent creep-rupture strength properties of the alloy.

Not long after the introduction of B-1900, the rupture elongations of B-1900 specimens after testing at 1400 °F (760 °C) were found to be approaching values of less than 1.5% at rupture. Dependent on manufacturer and applications, turbine airfoil designers may use varying assumptions of percent creep extension that will be permitted in design. In the early period of adoption of high-strength PC cast superalloys, 1% creep was a design criterion, and stress to cause 1% creep in a given time was a commercial standard. With creep elongations decreasing to about 1.5% (minimum) for B-1900 and the need (for inspection and safety reasons) for a component to fail at no less than twice the expected design elongation, it was evident that a minimum B-1900 elongation value of about 1.5% would negate customary design procedures. Other alloys showed similar behavior, notable among them, MAR-M-200 (see preceding comment). Designers temporarily switched design criteria to use stress causing 0.75% creep (¾ of the then-current elongation design minimum), a standard compatible with a 1.5% creep-rupture elongation minimum.

In order to increase the 1400 °F (760 °C) elongation, several changes were suggested. Among them was improved foundry practice, which did show promise. However, the change actually adopted was the addition of hafnium to nickel-base superalloys, with an attendant improvement in ductility using the customary casting practice. Ductilities were improved sufficiently to allow the 1% (or higher) elongation minimum design requirement to be met. The limited number of new high-strength PC cast nickel-base superalloys developed since the 1960s have usually adopted hafnium additions for enhanced 1400 °F (760 °C) elongation.

The transverse properties of CGDS cast alloys such as MAR-M-200 were about the same as the properties of PC cast nickel-base superalloys. Consequently, it quickly became evident that improved ductility (in the transverse direction of testing) was a requirement for CGDS cast alloys as well as PC cast al-

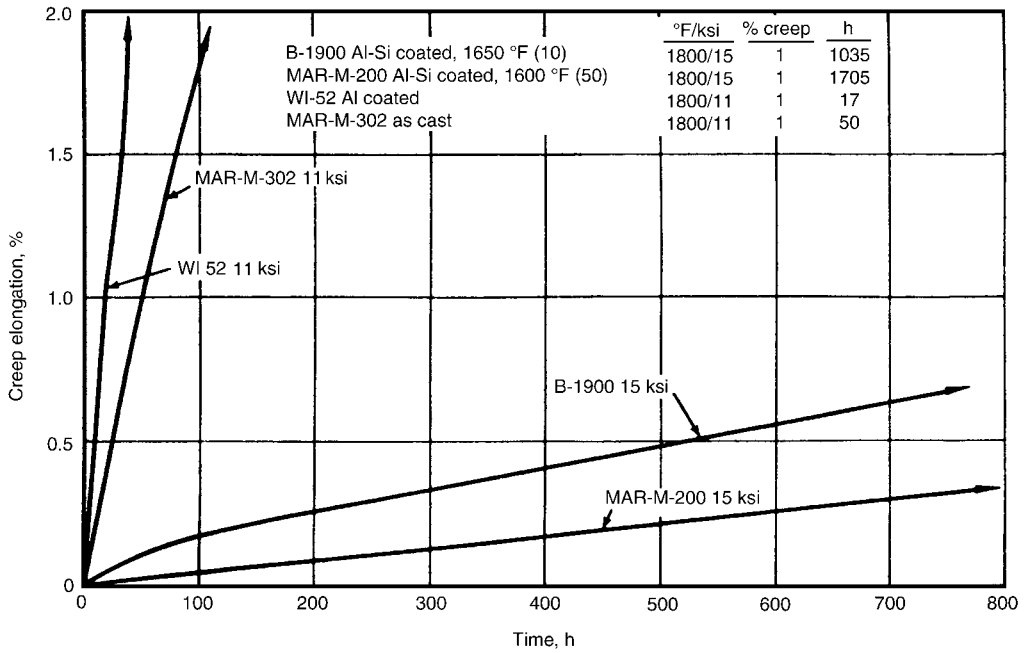


Fig. 12.51 Creep-rupture behavior of two cobalt-base (MAR-M-302 and WI-52) and two nickel-base (MAR-M-200 and B-1900) superalloys at 982 °C (1800 °F), showing the creep-rupture superiority of nickel-base to cobalt-base superalloys

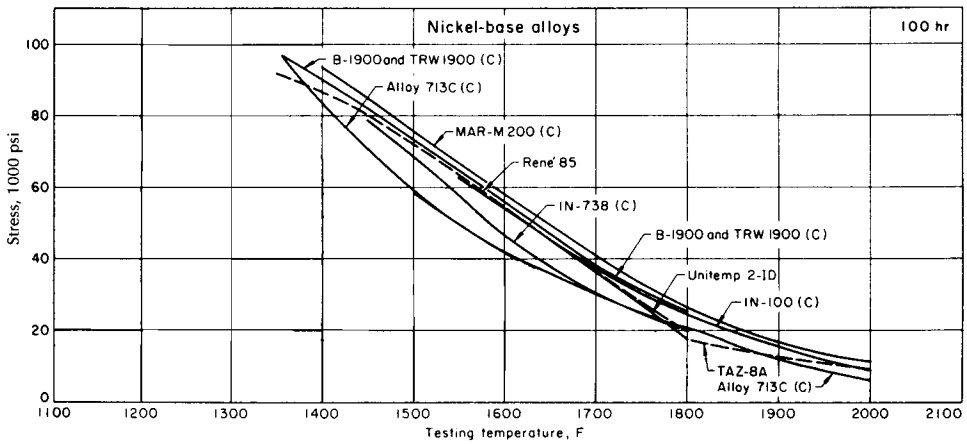


Fig. 12.52 100 h rupture strength of selected PC cast nickel-base superalloys vs. temperature

loys. Hafnium was found satisfactory (in higher percentages) for improving the ductility of these alloys. All cast high-strength nickel-base superalloys with grain boundaries (PC cast, CGDS cast) now employ hafnium additions to guarantee lower temperature—1400 °F (760 °C)—stress-rupture elongation.

Polycrystalline Cast Superalloys: Porosity and HIP. A related development in PC cast nickel-base superalloys was the realization that casting porosity, albeit small in volume—perhaps 1%—could result in reduced rupture life and rupture ductility. Hot isostatic pressing technology was introduced to the

nickel-base superalloy field, both in the production of wrought P/M superalloys and for the potential closing of porosity in airfoil castings. Hot isostatic pressing was applied to alloys such as B-1900 and MAR-M-247. Casting porosity was substantially removed, but property improvements were variable. One major benefit of HIP was the narrowing of the scatter band for some properties.

The Larson-Miller parametric plot of stress-rupture capability in Fig. 12.53 shows the narrowing of the scatterband for PC IN-738 when HIP processing is used.

Note the substantial decrease in scatter without a change in typical value. This behavior could permit a higher design minimum property to be reached. Design is based on minimum and typical properties and so improved properties in fatigue can result from HIP.

While minimum fatigue lives are improved by HIP, minimum rupture lives are not always improved. HIP is a heat treatment and will solution and change the primary γ' in the alloy. Subsequent solution heat treatment followed by aging is required to develop adequate properties. If the post-HIP solution treatment is not carried out at a temperature above the HIP temperature, the resulting γ' structure may be insufficient to produce optimal strength.

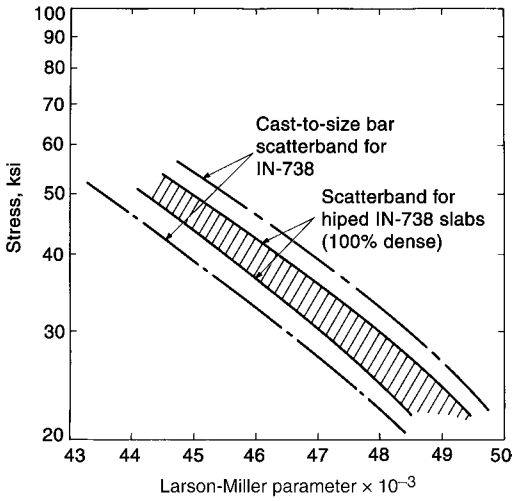


Fig. 12.53 Scatterbands for IN-738 PC cast nickel-base superalloy with and without HIP using Larson-Miller parameter (P_{LM}). Note: $P_{LM} = T(C + \log t)$ where C = Larson-Miller constant, T = absolute temperature, t = time in h. For this plot, C = 20, T = °R

It was claimed that rupture ductility also was improved by HIP, but experience indicates that alloys with adequate rupture ductility before HIP showed little or no improvement with HIP. Certain alloys such as Rene 80 that seemed more prone to casting porosity were regularly HIPed, but other alloys with less porosity, such as MAR-M-247, were not routinely HIPed.

A study on HIP (as well as coating) effects on MAR-M-247 and seven experimental alloys similar to MAR-M-247 showed varying results for tensile and creep-rupture properties. Table 12.21 gives a statistical picture of the effects of the HIP and coating processes. It is interesting to note that tensile properties are apparently improved, but rupture life may be reduced by HIP, although ductility indicators are increased. This is in accordance with prior results on B-1900 and MAR-M-247. Hot isostatic pressing of superalloys was found to improve fatigue life more consistently than it improved stress-rupture life. Fig. 12.54 shows the beneficial effect of HIP on HCF resistance of Rene 80. Although no statistical studies are available, it is generally considered that HIP is beneficial for both HCF and LCF life.

Columnar Grain Directionally Solidified and SCDS Cast Nickel-Base Superalloys: General. Cobalt-base superalloys are not DS processed nor are iron-nickel-base superalloys. All CGDS and SCDS cast superalloys are nickel-base. Unless otherwise noted, all alloys mentioned in discussions of CGDS and SCDS are nickel-base superalloys.

The basis for creating DS alloys is to align or eliminate grain boundaries. The process was particularly effective with alloys that possessed intrinsic grain strength but had grain boundaries with poor ductility. Their PC cast versions fractured in creep-rupture tests by intergranular failure at low elongations. The DS process for superalloys was demonstrated by General Electric but brought to commercial fruition by the efforts of Pratt & Whitney. The alloy chosen for CGDS, the first application of DS processing, was MAR-M-200, a very strong second-generation PC cast alloy that was difficult, if not impossible, to use in PC cast form.

An individual crystal is a single grain. Normally, PC cast structures consist of a random array of many roughly equiaxed grains, each of which is a single crystal. Columnar

Table 12.21 Statistical results of HIP and/or coating processing on the tensile and creep-rupture properties of MAR-M-247-type nickel-base superalloys

	Hipping	Coating	Hipping + coating(a)
Tensile properties			
0.2% yield stress	May go up	Always down	May go down
Ultimate tensile strength	(b)	Always down	May go down
Elongation	Normally up	May go up	May go up
Creep properties			
Life	May go down	Normally down	May go down
Elongation	Mostly up	May go down	(b)
Reduction in area	Always up	(b)	(b)

(a) This column is concerned with interaction only. (b) Effect not confirmed

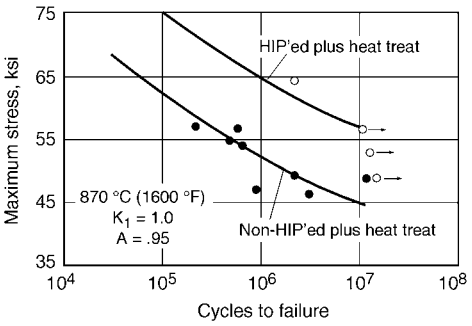


Fig. 12.54 Beneficial effect of HIP on high-cycle fatigue of PC cast Rene 80 nickel-base superalloy

grain directionally solidified processing makes an array of many grains, but each grain is elongated along the solidification axis. In the case of a single crystal, a single grain occupies the component space. For more information on DS processing, see Chapter 5.

As indicated in Chapter 3, the basic crystal structure of γ phase is cubic (fcc). Directions can be defined within the cube for purposes of reference between component and crystal and applied load and crystal. A particular direction can be referenced to a cube by use of a stereographic triangle, whereon the corners represent the three major directions in a cubic crystal. These directions are edge, face diagonal, and cube diagonal and are often referred to by the shorthand notation ⟨100⟩, ⟨110⟩, or ⟨111⟩. The ⟨100⟩ direction is the preferred natural growth direction and is the direction of the bundle of grains in a CGDS alloy. Similarly, SCDS alloys customarily have the ⟨001⟩ direction aligned along the component axis, although special techniques can align other crystallographic directions with the component axis. In general, the components are airfoils, and the longitudinal testing direction will correspond to the ⟨001⟩ natural growth direction either in a separately grown test specimen or a specimen machined from an airfoil.

Because of the alignment of grains, a CGDS alloy tested in the longitudinal (airfoil axis) direction develops longer rupture life than its PC cast counterpart. Single-crystal directionally solidified alloys last even longer. The life improvements are principally due to the lack of transverse boundaries in the loading direction.

Loads are transmitted both within a grain and across grain and subgrain boundaries. High temperature deformation causes failure in grain boundaries. CGDS alloys, despite the lack of longitudinal boundaries, eventually fail in creep-rupture, usually on transverse boundaries (or internal imperfections) where there are applied loads. There are imperfections (subgrain boundaries) that are created in the growth of single crystals. Thus, SCDS alloys contain subgrain boundaries and, eventually, fail in creep-rupture by cracking across those boundaries.

Figure 12.55 shows the creep curves for PC, CGDS, and SCDS versions of MAR-M-200 at 1800 °F (982 °C). Significant life improvements over PC cast alloys are possible with CGDS or SCDS processing. Table 12.22 gives more property information for the three casting types.

Early work on CGDS processing involved MAR-M-200 and other high-strength, high-$V_f\gamma'$ alloys previously processed by conventional casting techniques. Of these alloys, only MAR-M-200 showed promise. Other al-

loys, such as IN-100 or B-1900, did not seem to have a reasonable cost benefit for the strengths that were produced. Grain-boundary cracking in castings was a problem for MAR-M-200, as were the transverse-boundary cracking and low transverse strengths in creep-rupture testing. MAR-M-200 achieved acceptable properties after addition of hafnium, and CGDS component cracking during casting was reduced. The amount of hafnium (about 2%) to eliminate the grain-boundary cracking problems led to increased quality problems with the alloy, and final hafnium specifications represented a compromise between casting quality (inclusions, etc.), casting cracking, and transverse ductility in creep rupture. As wall thickness of airfoils was reduced, the castability of alloys such as MAR-M-247 was insufficient, even with hafnium added to enhance ductility, to make crack-free airfoils. CM-247LC was an alloy developed to eliminate such problems.

A variety of first- and second-generation CGDS alloys has been produced, and many have been used in gas turbines. Some alloys are:

- PWA 1422 (MAR-M-200 + Hf)
- Rene 125
- RR-2000
- MAR-M-247
- CM-247 (Rene 108)

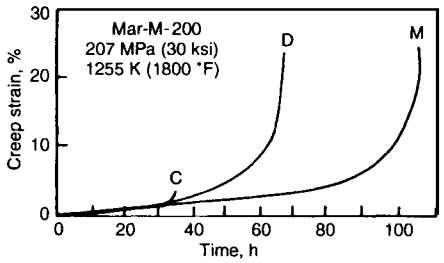


Fig. 12.55 Comparison of creep properties of MAR-M-200 nickel-base superalloy tested in three cast conditions at 982 °C (1800 °F)/207 MPa (30 ksi)

- MAR-M-002
- Rene 80H (Rene 80 + Hf)
- IN-792
- CM-186LC
- PWA 1426

In addition, several generations of SCDS alloys have been developed, although not all are in service. Some alloys are:

- PWA 1480
- Rene N4
- SRR 99
- RR-2000
- CMSX-2
- CMSX-6
- PWA 1484
- Rene N6
- CMSX-4
- CMSX-10

Among the accomplishments of DS processing has been the extension of the size of CGDS and SCDS parts that can be made. Columnar grain directionally solidified airfoils now can be made in lengths over 25 in. (63.5 cm), and comparable SCDS parts can be cast. Large SCDS components of IN-792 have been made for power gas turbines.

Single-crystal directionally solidified casting technology was pioneered by Pratt & Whitney, but initially there was limited interest in SCDS compared to CGDS versions of MAR-M-200 because of:

- Lack of creep strength improvement
- No significant improvement in TMF capability
- No change in the oxidation or hot corrosion resistance
- Higher potential cost

Only the ductility and transverse strength of the PWA 1422 (CGDS MAR-M-200 + Hf) composition were improved by SCDS processing. However, it was realized that there was potential for significant strength improvement as well if all of the γ' could be

Table 12.22 Creep-rupture properties of PC, CGDS, and SCDS MAR-M-200

	1400 °F/100 ksi			1600 °F/50 ksi			1800 °F/30 ksi		
	Rupture life, h	Elongation, %	Min creep rate, in./in./h	Rupture life, h	Elongation, %	Min creep rate, in./in./h	Rupture life, h	Elongation, %	Min creep rate, in./in./h
Polycrystalline	4.9	0.45	70.0×10^{-5}	245.9	2.2	3.4×10^{-5}	35.6	2.6	23.8×10^{-5}
Columnar grain	366.0	12.6	14.5×10^{-5}	280.0	35.8	7.7×10^{-5}	67.0	23.6	25.6×10^{-5}
Single crystal	1914.0	14.5	2.2×10^{-5}	848.0	18.1	1.4×10^{-5}	107.0	23.6	16.1×10^{-5}

dissolved and reprecipitated as fine γ′. The benefits of fine γ′ have been shown in Fig. 12.5. By complete solutioning of γ′, PWA 1422 was improved. The same type of improvement was deemed possible for SCDS alloys with less difficulty than had been encountered in full solutioning of PWA 1422. By removal of the minor elements, such as hafnium, carbon, boron, and so on, the incipient melting temperature of single crystals could be made many degrees higher. Full solutioning could be accomplished without worry about melting. Furthermore, it was clear that a SCDS alloy permitted more alloy modification to improve coated and uncoated turbine airfoil alloy corrosion resistance.

The first alloy developed to take commercial advantage of the previously mentioned concept (full solutioning) was PWA 1480, which offered a 45 to 90 °F (25 to 50 °C) improvement in strength (time to 1% creep) capability. PWA 1480 was uniquely suited to SCDS casting and has been used extensively since the 1980s. The remarkable property improvements outweighed any increased casting costs. Single-crystal directionally solidified alloys are in wide use in aircraft gas turbines at the present time and are expected to see significant use in industrial gas turbines. Not only was PWA 1480 successful, but its success (just as the success of CGDS alloy PWA 1422) inspired other organizations and companies to create comparable SCDS alloys.

Columnar Grain Directionally Solidified and SCDS Cast Superalloys: Tensile and Creep-Rupture Properties. Longitudinal tensile properties of CGDS MAR-M-200 are given in Fig. 12.56 and compared with the properties of PC cast MAR-M-200. These properties are consistent with previous discussion on tensile properties as influenced by γ′ behavior. The transverse tensile properties of a CGDS alloy should approximate the tensile properties of a PC cast version of the alloy. However, because the grain size of CGDS alloys generally is coarser than that of PC cast versions, the actual transverse yield strength of CGDS alloys may be as much as 10% below the PC cast values, at least up to about 1600 °F (871 °C).

An essential feature of CGDS processing of alloys is the ability to make maximum use of the intrinsic creep-rupture strength of an alloy composition. A comparison of creep-rupture properties of PC and longitudinal CGDS cast MAR-M-200 is given in Fig. 12.57. In Fig. 12.58, rupture life and time to 1% creep are plotted for longitudinal tests on CGDS MAR-M-200 + Hf (PWA 1422), a derivative of CGDS MAR-M-200. Figure 12.57

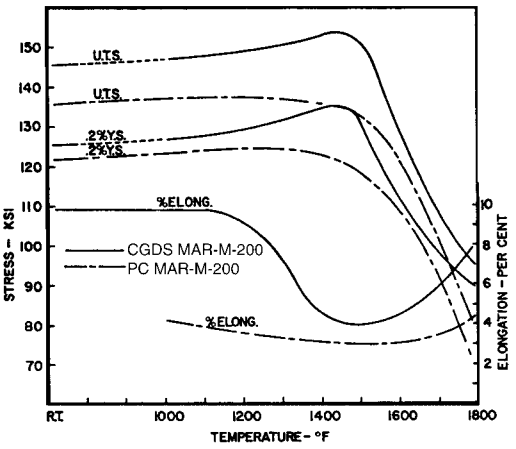


Fig. 12.56 Typical tensile properties of MAR-M-200 superalloy for PC cast and CGDS cast longitudinal direction. UTS, ultimate tensile strength; YS, yield strength; RT, room temperature

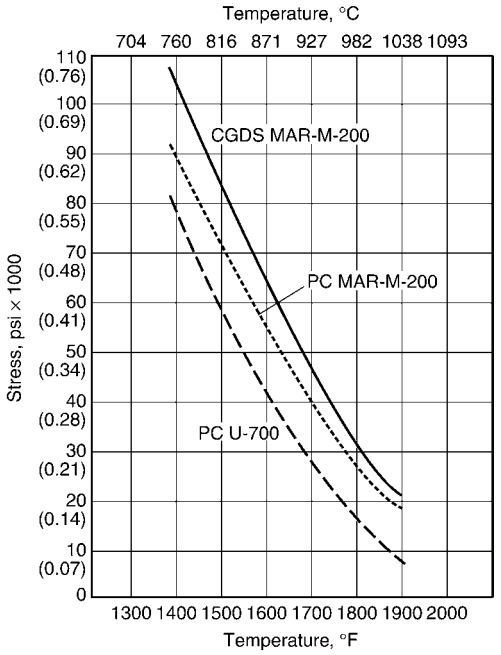


Fig. 12.57 Typical stress for 100 h rupture of MAR-M-200 superalloy CGDS longitudinal and PC cast alloys

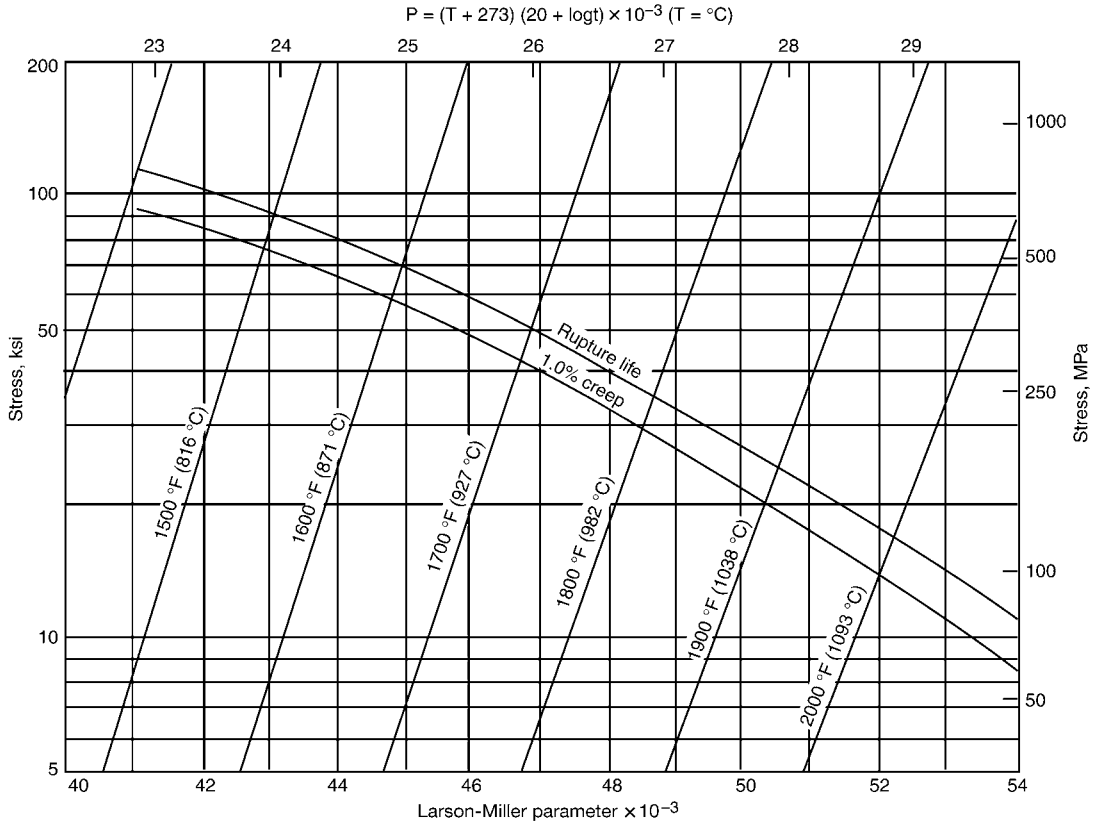


Fig. 12.58 Typical longitudinal stress-rupture and 1% creep properties for CGDS MAR-M-200 + Hf cast alloy using Larson-Miller parameter (P_{LM}). Note: $P_{LM} = T\,(C + \log t)$ where C = Larson-Miller constant, T = absolute temperature, t = time in h. For this plot, C = 20, T = °R (bottom) and °C (top)

clearly indicates the customary advantages of a CGDS structure over PC cast structures for stress-rupture capability.

Transverse creep strengths (at least for 1% creep) in a CGDS alloy are approximately the same as the values for the longitudinal direction. However, owing to differences in ductility, the transverse stress-rupture strengths may be lower. In some alloys, such as CGDS MAR-M-200, high creep strains (2.0%) were not attainable, particularly at intermediate temperatures where the limited ductility of the alloy prevented the achievement of creep strains much in excess of 1.0%. The addition of hafnium to CGDS MAR-M-200 was a factor in allowing maximum transverse stress-rupture lives to be attained through increased transverse ductility.

Not all PC cast alloys responded to CGDS processing with equal improvements at all test conditions. Some showed no improvements at all. Figure 12.59 shows the creep behavior at 1800 °F (982 °C) and 30 ksi (207 MPa) of three superalloys in PC and CGDS form. B-1900 and MAR-M-200 show significant improvements while IN-100 does not. Tests at a different condition (higher temperature, lower stress) indicated that IN-100 CGDS was improved over its PC cast version. The CGDS alloys initially used were all alloys developed for PC cast applications. Eventually, modifications in existing compositions and development of new compositions tailored for CGDS application were introduced.

Longitudinal moduli for CGDS and PC cast MAR-M-200 are shown in Fig. 12.60. Transverse modulus for CGDS alloys, also shown in Fig. 12.60, is discussed later. The longitudinal moduli of CGDS alloys are substantially lower than the moduli for PC cast alloys. Room-temperature values in the order

of about 18.2 ksi (~126 MPa) or about 60 to 63% of PC cast alloys are obtained for CGDS nickel-base superalloys. Single-crystal directionally solidified alloys, having the same ⟨100⟩ orientation as CGDS alloys, essentially have the same moduli in the longitudinal direction.

Physical properties for CGDS and SCDS cast alloys are not orientation-dependent. They essentially should be the same as for PC cast versions of an alloy. Many current CGDS and SCDS cast superalloys do not have PC cast counterparts. PWA 1422 can be approximated by PC cast MAR-M-200, although the hafnium addition to MAR-M-200 may have some moderate effect. Similarly, CGDS MAR-M-247 should be approximated by PC cast MAR-M-247, and CGDS Rene 80H by PC cast Rene 80. Values for some of the alloys are given in Table 12.20. The wide variation in the refractory metal content among other CGDS and SCDS alloys and the significant additions of rhenium can affect the physical properties in a measurable way. No simple correlation is available for estimating the physical properties of such alloys, and published data are often limited for them.

Single-crystal directionally solidified versions of existing alloys were a logical extension of CGDS processing, and the first SCDS superalloy was MAR-M-200. It saw no commercial application. In SCDS material, mechanical property determination is more complex than in CGDS products, because orientation of the test relative to the single-crystal axis is important. Figure 12.61 shows a stereographic triangle, the method for identifying location of loading or testing direction relative to the principal directions of a cubic crystal. Superimposed on the triangle are numbers representing specific test specimens. It can be seen that these specimens were located near the three principal crystallographic directions of an SCDS alloy. The test results also given in Fig. 12.61 show that crystallographic orientation is a significant factor in the creep curves obtained. Figure 12.62 shows the creep behavior resulting from

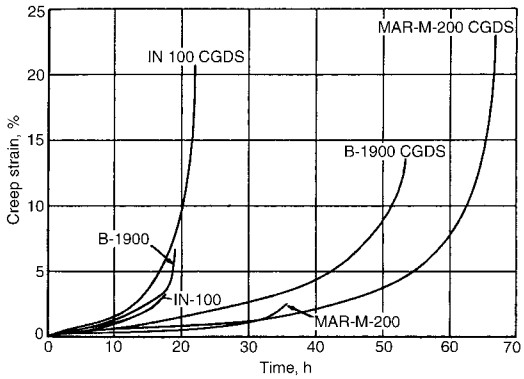


Fig. 12.59 Creep behavior of PC and CGDS cast alloys IN-100, B-1900, and MAR-M-200 at 982 °C (1800 °F)/207 MPa (30 ksi)

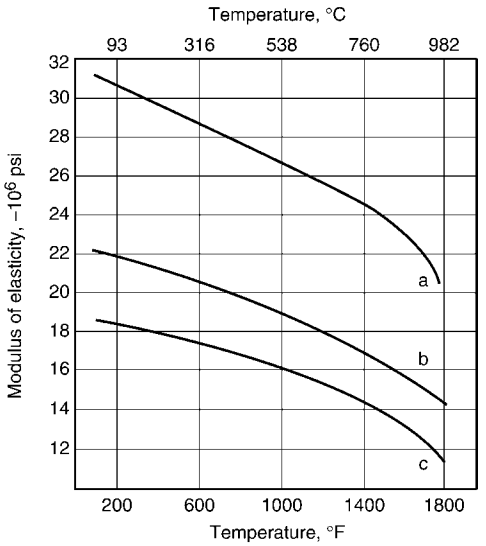


Fig. 12.60 Typical dynamic elastic moduli (Young's modulus) for MAR-M-200 superalloy, showing (a) PC cast, (b) transverse CGDS cast and (c) longitudinal CGDS properties

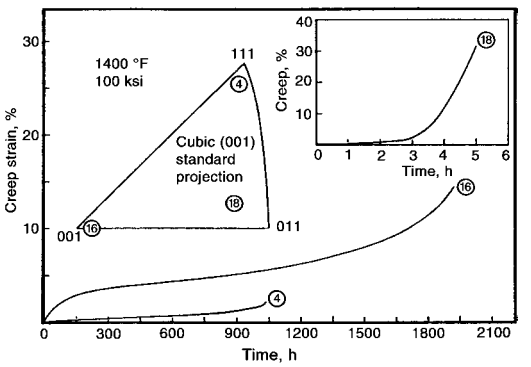


Fig. 12.61 Creep behavior of MAR-M-200 SCDS specimens with loading axes close to the [001], [111], and [011] directions, as shown in the stereographic triangle in the figure. Testing at 760 °C (1400 °F) and 689.5 MPa (100 ksi)

SCDS processing versus those for CGDS and PC cast versions of MAR-M-200. The ⟨001⟩ direction of growth, which is the favored natural growth direction, shows the best creep-rupture life in Fig. 12.61. It should not be inferred that the ⟨001⟩ direction will produce the maximum life at all $V_f\gamma'$, γ' size, test temperature, and stress conditions.

With no grain boundaries that would require strengthening, it was apparent that the boron, zirconium, and carbon (among others) added to enhance grain-boundary ductility were superfluous. By removing these elements, the melting point of an SCDS superalloy could be increased significantly. Better γ' solutioning could be expected, because higher solution temperatures could be employed. Also, with the elimination of boundaries and minor elements, significant changes in alloy chemistry were developed to create SCDS alloys designed solely for such an application. PWA 1480 was the first commercial SCDS alloy used in an aircraft gas turbine, but other first-generation SCDS alloys were introduced, as indicated previously. PWA 1480 offered about a 45 to 90 °F (~25 to 50 °C) improvement over PWA 1422 in terms of time to 1.0% creep, as seen in Fig. 12.63. The creep-property improvement, which increased with temperature, depended on the optimized chemistry of PWA 1480 and the ability to fully solution the coarse as-cast γ'. PWA 1480 proved to be a unique composition, because it also possessed some processing advantages over the SCDS versions of MAR-M-200 (without minor elements or cobalt).

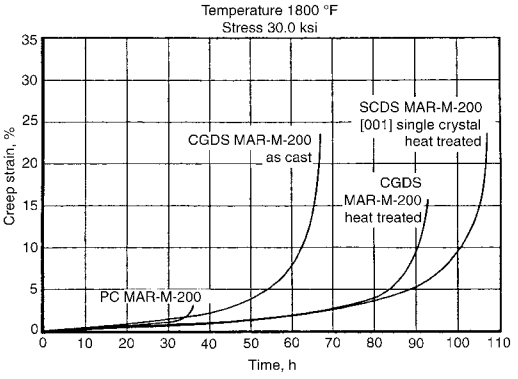


Fig. 12.62 Creep behavior at 982 °C (1800 °F) and 207 MPa (30 ksi) of PC cast with longitudinal SCDS and CGDS MAR-M-200 alloy

Although commercial SCDS alloys have no allowable high-angle boundaries (HAB), low-angle boundaries (LAB) are permitted within limits set by appropriate processing specifications. The LAB limit is usually about 6 to 10°. Owing to the gradual increase in limits for LAB (early SCDS applications set limits below 6°), there was concern for protecting against any deleterious effects of LAB on creep-rupture properties. The economics of keeping carbon low and concerns about LAB were factors in decisions to permit small amounts of carbon (and sometimes other elements) to be present in commercial SCDS alloys. The extent to which HAB can affect properties is shown in Fig. 12.64

Several available SCDS alloys from the CMSX series are compared with some CGDS alloys in Larson-Miller stress-rupture plots in

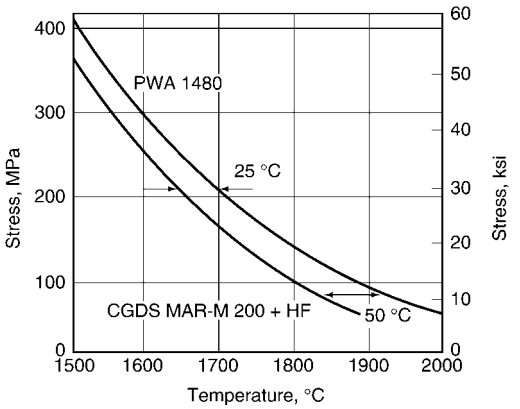


Fig. 12.63 Stress for 1% creep in 100 h vs. temperature for longitudinal direction in PWA 1480 SCDS and CGDS MAR-M-200 + Hf, showing benefits in operating temperature obtained from commercial SCDS alloy

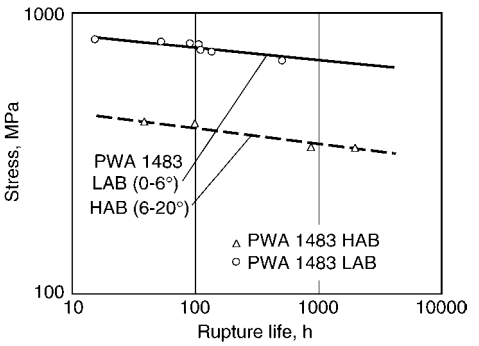


Fig. 12.64 Effect of HAB on 760 °C (1400 °F) life of SCDS IN-792-type alloy

Fig. 12.49. The increasing benefit of SCDS alloys over CGDS alloys as temperature increases is shown in Fig. 12.49(b) for CMSX-2/3 alloys compared with CM 247LC CGDS alloy. Some SCDS and CGDS superalloys are compared in a Larson-Miller 1.0% creep strength plot in Fig. 12.65. Figure 12.65 indicates not only the benefit for SCDS over CGDS but also indicates the effective temperature improvement that exists between a second-generation SCDS alloy (CMSX-4) and a third-generation SCDS alloy (CMSX-10). Another comparison (of a separate set of alloys) is shown in Fig. 12.66, where the stress-rupture curves for several CGDS and SCDS alloys are compared against PC cast IN-100. Again, the superiority of SCDS over CGDS alloys (and PC cast alloys) is apparent.

A fact not generally appreciated in the discussion of the strengths of CGDS and SCDS superalloys has been the role that alloy density will play in eventual alloy application. The use of ''heavy'' alloy elements (e.g., tantalum at amounts of 12.5% or rhenium at 6%) in alloys intended for turbine airfoil, particularly blade, applications has tended to increase the density of alloys. Table 12.23 gives densities of some selected SCDS alloys. Note that alloy density tends to increase as development progresses from first- to third-generation alloys. Increased strengths for alloys should be converted to specific (density-adjusted) strength when comparing newer alloys against older ones, at least for rotating component applications.

Columnar Grain Directionally Solidified and SCDS Cast Superalloys: Orientation and Other Effects. Columnar grain directionally solidified superalloys have moduli in the transverse directions that are greater than the longitudinal modulus (see Fig. 12.60). Single-crystal directionally solidified alloys have moduli that differ with direction of measurement in a single crystal. The transverse modulus of CGDS alloys can be considered to be constant in the transverse plane. The modulus in an SCDS alloy in the transverse plane to an airfoil will depend on the orientation of interest. Similarly, there is a Poisson ratio for PC cast alloys and for CGDS cast alloys (varies from transverse loading plane to longitudinal direction). However, the Poisson ratio in an SCDS cast alloy is a varying function of direction. It is possible to show for some directions of loading that the Poisson ratio becomes negative. Design of SCDS airfoils probably should be guided by appropriate elastic constants that would allow the determination of the orientation-dependent response of elastic properties.

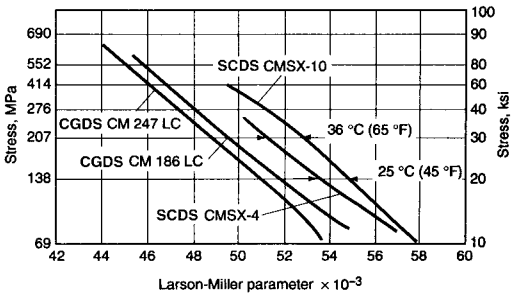


Fig. 12.65 Typical 1.0% creep strengths for CMSX-10 and CMSX-4 SCDS alloys and CM 186LC and CM 247LC CGDS alloys using Larson-Miller parameter (P_{LM}). Note: $P_{LM} = T\,(C + \log t)$ where C = Larson-Miller constant, T = absolute temperature, t = time in h. For this plot, C = 20, T = K

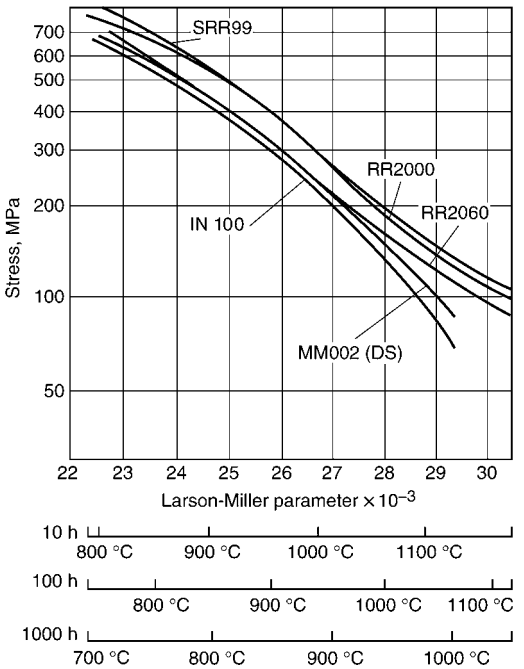


Fig. 12.66 Typical stress rupture strengths of several longitudinally oriented CGDS and SCDS alloys with a PC cast alloy, IN-100 using Larson-Miller parameter (P_{LM}). Note: $P_{LM} = T\,(C + \log t)$ where C = Larson-Miller constant, T = absolute temperature, t = time in h. For this plot, C = 20, T = K

Table 12.23 Density (and chemistry) of some SCDS casting alloys

Alloy	Density, g/cm³	Composition, wt%											
		Cr	Co	Mo	W	Ta	Re	V	Nb	Al	Ti	Hf	Ni
First generation													
PWA 1480	8.70	10	5	...	4	12	...	...	...	5.0	1.5	...	bal
PWA 1483	...	12.8	9	1.9	3.8	4	...	...	...	3.6	4.0	...	bal
Rene N4	8.56	9	8	2	6	4	...	...	0.5	3.7	4.2	...	bal
SRR 99	8.56	8	5	...	10	3	...	...	...	5.5	2.2	...	bal
RR 2000	7.87	10	15	3	...	...	...	1	...	5.5	4.0	...	bal
AM1	8.59	8	6	2	6	9	...	...	...	5.2	1.2	...	bal
AM3	8.25	8	6	2	5	4	...	...	...	6.0	2.0	...	bal
CMSX-2	8.56	8	5	0.6	8	6	...	...	...	5.6	1.0	...	bal
CMSX-3	8.56	8	5	0.6	8	6	...	...	...	5.6	1.0	0.1	bal
CMSX-6	7.98	10	5	3	...	2	...	...	...	4.8	4.7	0.1	bal
CMSX-11B	8.44	12.5	7	0.5	5	5	...	...	0.1	3.6	4.2	0.04	bal
CMSX-11C	8.36	14.9	3	0.4	4.5	5	...	...	0.1	3.4	4.2	0.04	bal
AF 56 (SX 792)	8.25	12	8	2	4	5	...	...	...	3.4	4.2	...	bal
SC 16	8.21	16	...	3	...	3.5	...	...	...	3.5	3.5	...	bal
Second generation													
CMSX-4	8.70	6.5	9	0.6	6	6.5	3	...	...	5.6	1.0	0.1	bal
PWA 1484	8.95	5	10	2	6	9	3	...	...	5.6	...	0.1	bal
SC 180	8.84	5	10	2	5	8.5	3	...	...	5.2	1.0	0.1	bal
MC2	8.63	8	5	2	8	6	...	...	...	5.0	1.5	...	bal
Rene N5	...	7	8	2	5	7	3	...	...	6.2	...	0.2	bal
Third generation													
CMSX-10	9.05	2	3	0.4	5	8	6	...	0.1	5.7	0.2	0.03	bal
Rene N6	8.98	4.2	12.5	1.4	6	7.2	5.4	...	...	5.75	...	0.15	bal

Figure 12.67 gives PWA 1480 compliance constants (from which stiffness constants can be calculated) as a function of temperature. It was reported that these values were identical to those for CMSX-2 SCDS alloy and was claimed that values in Fig. 12.67 should be very close to those for any SCDS nickel-base fcc-structured single-crystal alloy. Referring to the stereographic triangle (see Fig. 12.61), the variation of elastic modulus for PWA 1480 SCDS alloy as a function of orientation at room temperature can be plotted across the triangle, as shown in Fig. 12.68. Note that modulus values for SCDS alloys can vary from 18.2 to almost 45 Msi (126 to 310 GPa), dependent on loading axis in the single crystal.

Figure 12.61 indicated that creep-rupture results vary with orientation of an SCDS alloy relative to the loading axis. The amount

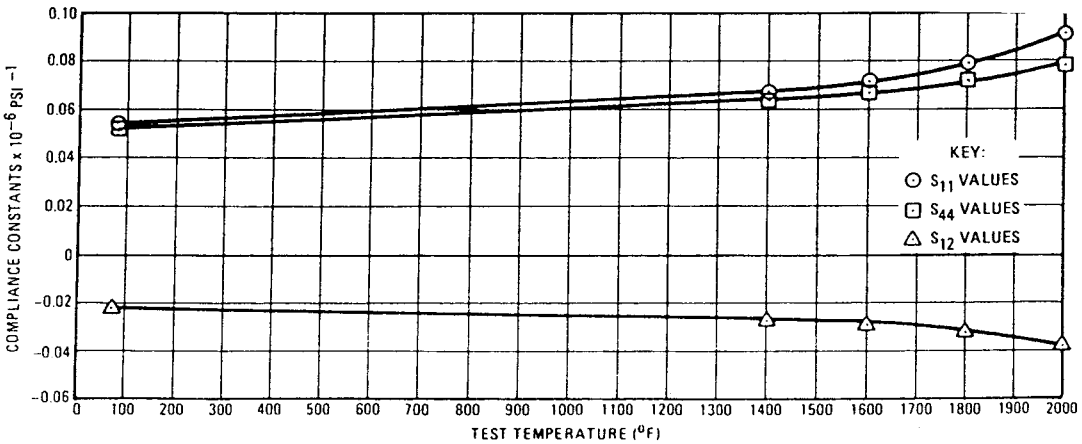


Fig. 12.67 PWA 1480 SCDS superalloy compliance constants vs. temperature

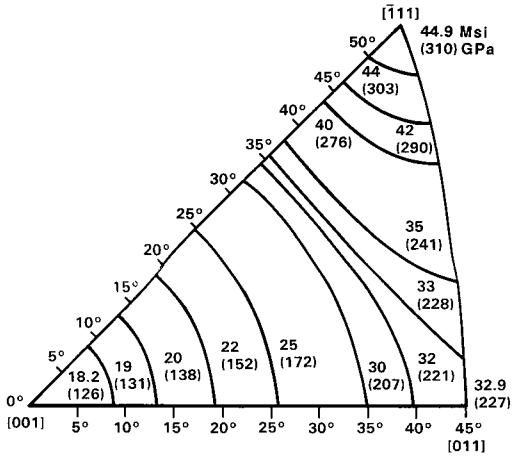


Fig. 12.68 PWA 1480 elastic modulus as a function of orientation at room temperature

of any orientation effect is a function of the temperature, stress, γ' particle size, and morphology plus $V_f\gamma'$. For the model SCDS alloy, MAR-M-200, Fig. 12.69 shows orientation effects on creep-rupture in tests at low-intermediate, intermediate, and high temperatures from 1400 to 1800 °F (760 to 982 °C). Creep curves are shown for specific orientations, and rupture lives are indicated for areas in the stereographic triangle. Figure 12.70 shows the effect of crystallographic orientation on stress rupture life of SCDS MAR-M-200 and MAR-M-247 in Larson-Miller parametric form. The best orientation for strength is ⟨111⟩ and the worst is ⟨011⟩. The naturally grown version ⟨001⟩ provides intermediate strength values but with other benefits as well.

There has been interest in tailoring the properties of SCDS alloys for maximum turbine airfoil strength in certain applications, but the costs of producing specially oriented airfoils compared to the natural ⟨001⟩ growth usually have prevented direct commercial application of special-oriented SCDS alloys. Another factor is that airfoils tailored for strength would likely have less than optimal moduli. This factor could impact TMF behavior and possible HCF interactions (see subsequent fatigue discussion).

A consideration not usually mentioned is that it is not possible to have SCDS alloys (or CGDS alloys for that matter) oriented so that the ⟨001⟩ growth direction is perfectly aligned with the airfoil component axis. The result is that there are deviations (usually designated by the symbol α) from a strict ⟨001⟩ orientation that are accepted by process specifications. When SCDS superalloys first were developed for commercial use, it was thought that α values of perhaps 5° or less from ⟨001⟩ would be reasonable. This value was soon found to be too restrictive from an economic point of view. Consequently, α values of $+/-10°$ are the norm. There are no published data to be found on the reduction in creep-rupture strengths from perfect alignment to that permitted commercially. Figure 12.71 (for PWA 1483 SCDS alloy) compares, on a Larson-Miller parametric basis, the creep-rupture life for customary ranges of $+/-10°$ to the life with an α of $+/-25°$. There is a significant life reduction produced by exceeding $+/-10°$ alignment.

Orientation also affects tensile properties in SCDS alloys. The yield strength is the property most studied in superalloys, although the work-hardening rates and resultant ultimate strengths are affected by orientation as well. Often, tensile studies for gas turbine blade applications have been made at temperatures from 1100 to 1200 °F (593 to 649 °C). This temperature often has been suggested as the appropriate temperature for studying blade root attachments, and some data to be presented have been determined in this range.

Studies of PWA 1480 have developed yield strength versus temperature data for the three principal orientations in both tension and compression, as shown in Fig. 12.72. There is a difference in orientation behavior between compression and tension tests. Tension-compression asymmetry in an SCDS superalloy is a function of orientation, as shown in Fig. 12.73. The asymmetry in the yield strength for SCDS alloys can be explained by detailed dislocation—γ' precipitate interactions, including changes in slip mode at higher temperatures. Such actions are not discussed in this book, but certain observations may be made for tensile yield strength behavior of SCDS alloys:

- Superalloy SCDS alloys (e.g., PWA 1480) with high $V_f\gamma'$ deform by standard octahedral slip when oriented near the ⟨001⟩ direction and by cube slip when oriented near the ⟨111⟩ direction.
- Shearing of the γ' particles is the principal strengthening mechanism.

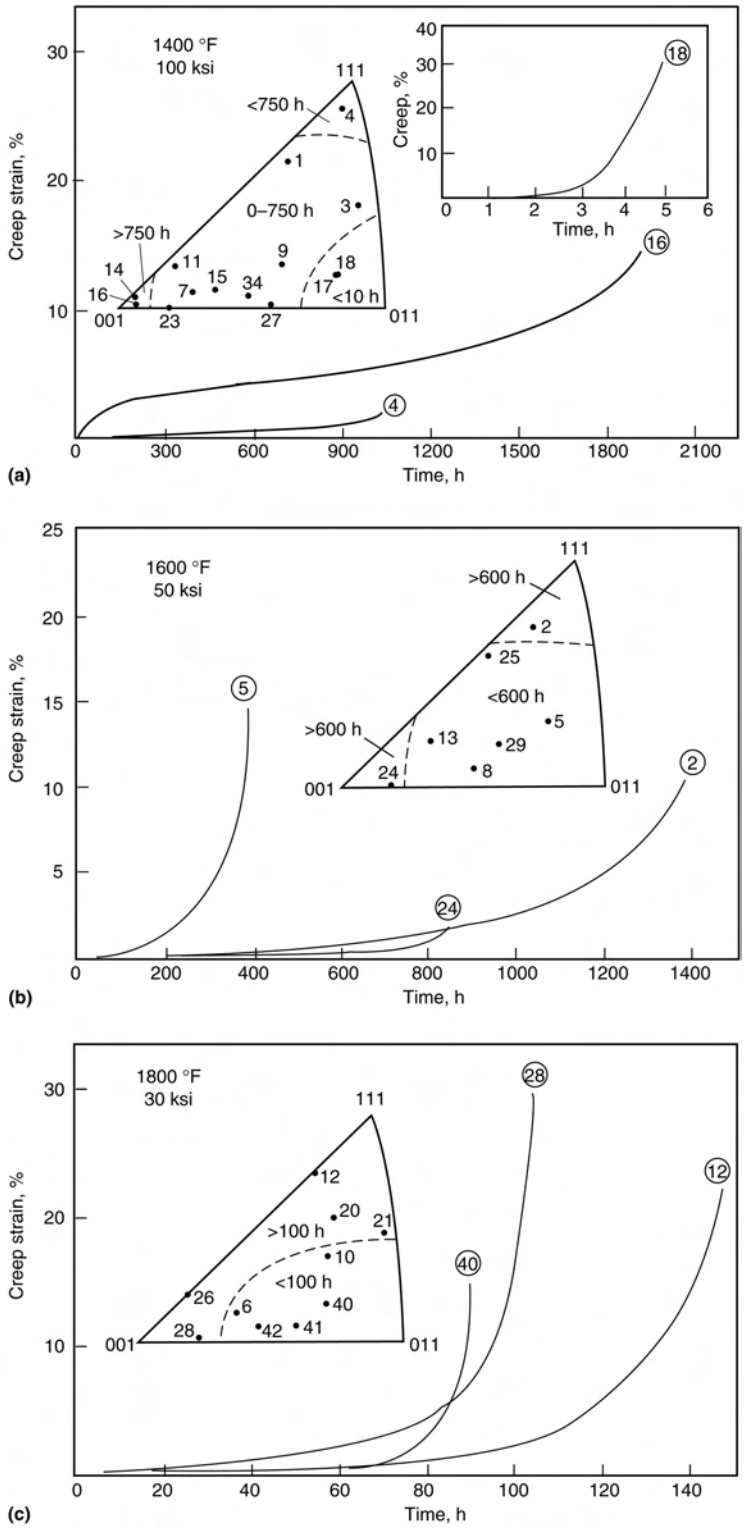


Fig. 12.69 Orientation dependence of creep behavior of SCDS MAR-M-200 at (a) 760 °C (1400 °F)/689.5 MPa (100 ksi), (b) 871 °C (1600 °F)/345 MPa (50 ksi), and (c) 962 °C (1800 °F)/207 MPa (30 ksi)

An important area that could be impacted by the orientation dependence of the yield strength is concerned with the shear criteria applied to turbine blade root attachments. The shear yield strength is used in some work to ensure designs that prevent yielding and detachment of root tangs in shear. Unfortunately, shear strengths are not normally determined. The yield strength usually is barely determined across the stereographic triangle at a single temperature. Designers have used adjustments to the minimum yield strength in a SCDS structure to set appropriate design limits. What is appropriate for a minimum? Figure 12.74 shows the typical yield strength

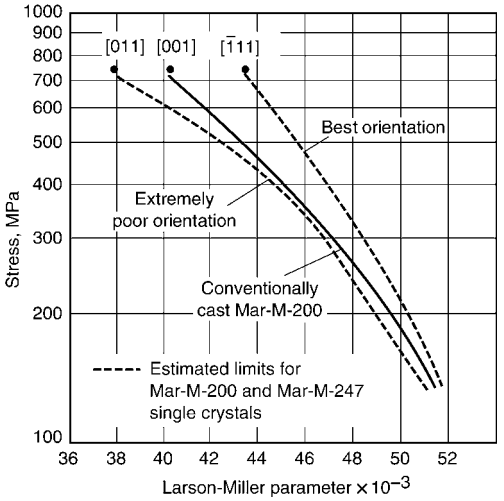


Fig. 12.70 Effect of crystallographic orientation on stress-rupture life for MAR-M-200 and Mar-M-247 using Larson-Miller parameter (P_{LM}) × 1.8. Note: $P_{LM} = T$ (C + log t) where C = Larson-Miller constant, T = absolute temperature, t = time in h. For this plot, C = 20, T = K

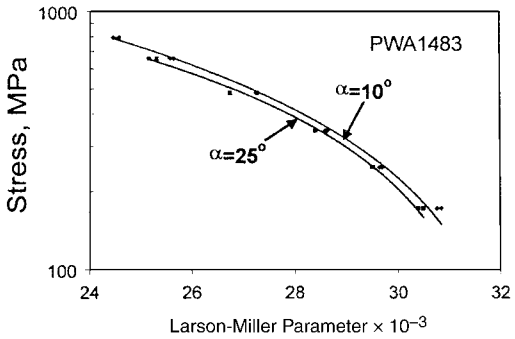


Fig. 12.71 Comparison of creep-rupture life of IN-792 type SCDS alloy with primary orientation deviations (α) of 10° and 25° using Larson-Miller parameter (P_{LM}). Note: $P_{LM} = T$ (C + log t) where C = Larson-Miller constant, T = absolute temperature, t = time in h. For this plot, C = 22, T = K

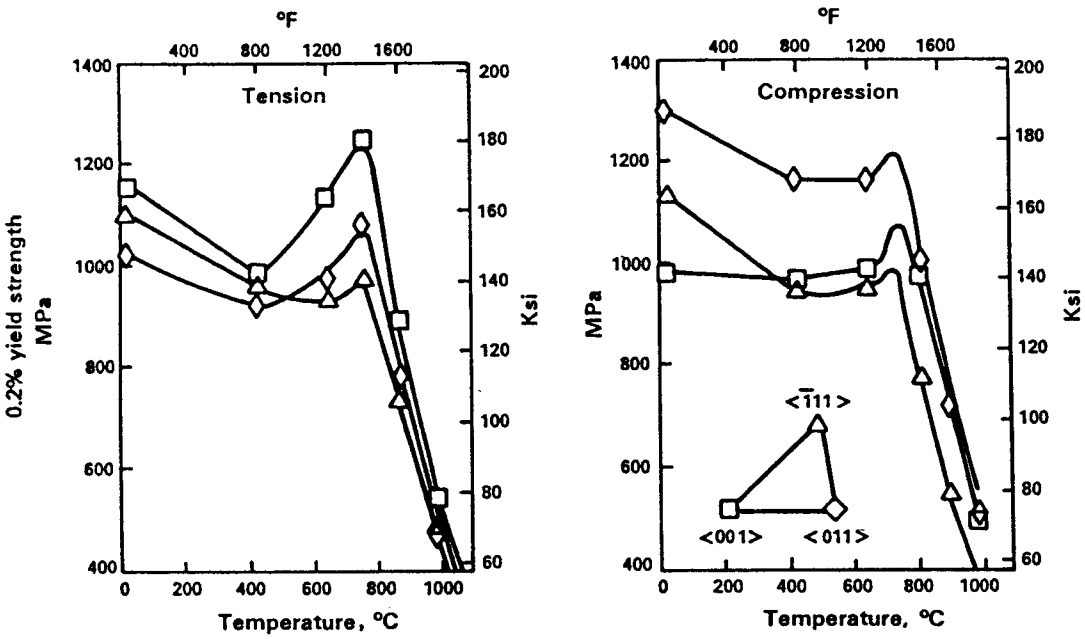


Fig. 12.72 Yield strength of SCDS PWA 1480 alloy as a function of temperature for the ⟨001⟩, ⟨011⟩, and ⟨111⟩ orientations in tension and compression

of PWA 1480 SCDS alloy versus orientation along the ⟨001⟩-⟨011⟩ boundary of the standard stereographic projection. Assuming that the SCDS alloy is properly aligned, then the applied shear stress ought to be acting in or across the plane defined by ⟨001⟩ and ⟨011⟩ directions. The lowest yield strength that should be reported for design purposes, therefore, should not be the minimum longitudinal yield stress but should be at least the lowest number for the yield strength along the ⟨001⟩-⟨011⟩ boundary. Data are rarely generated in sufficient amount to enable a true determination of the minimum yield strength to be applied in the case of shear criteria for SCDS blades. On the other hand, failures in shear have not been reported, leading many to the conclusion that lack of shear data (or ⟨001⟩-⟨011⟩ boundary data) is an academic, not commercial, problem.

Mention has been made of the effects of γ′ size on tensile yield strength. Figure 12.75

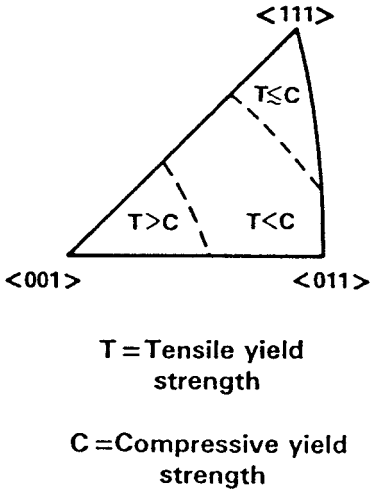


Fig. 12.73 Tension-compression asymmetry in SCDS superalloys is a function of orientation

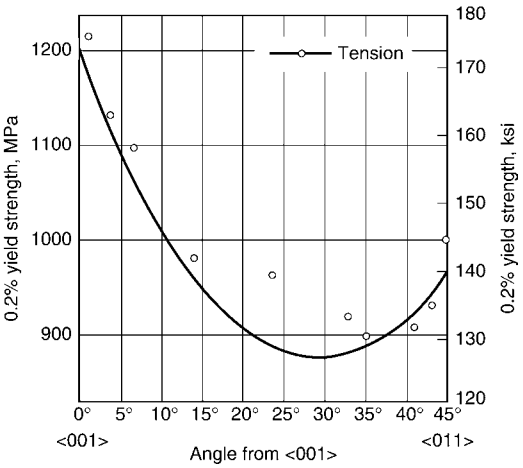


Fig. 12.74 Yield strength of PWA 1480 SCDS superalloy at 593 °C (1480 °F) vs. orientation along the ⟨001⟩-⟨011⟩ boundary of the standard stereographic projection

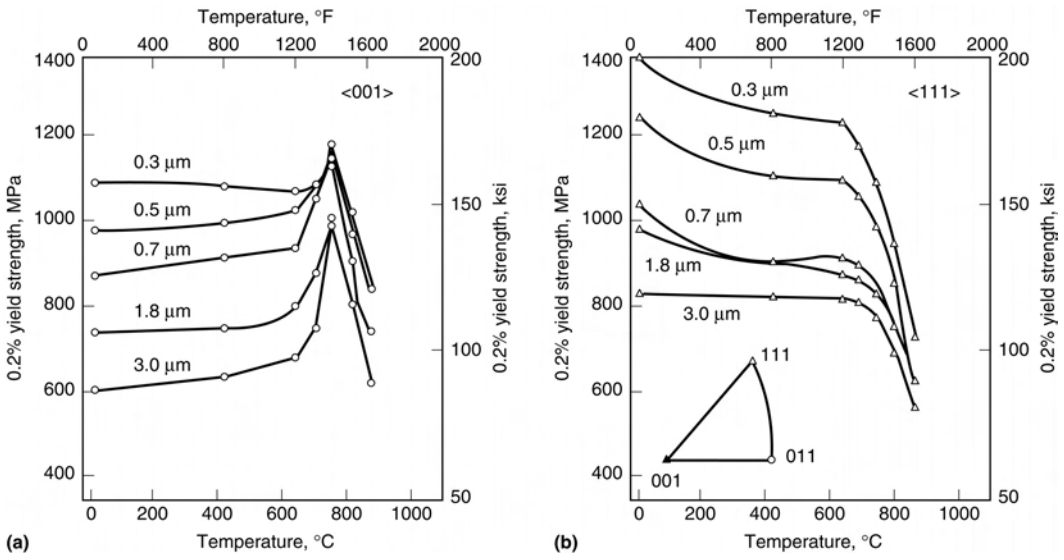


Fig. 12.75 Yield strength of PWA 1480 SCDS superalloy vs. temperature for various γ′ sizes (a) ⟨001⟩ orientation and (b) ⟨11⟩ orientation

shows the effect of γ' size on the yield strengths of PWA 1480 SCDS alloy in two orientations, ⟨001⟩ and ⟨111⟩. The finer γ' size is most effective in increasing the yield strength at lower temperatures, and effective but less so at intermediate and high temperatures for the standard longitudinal airfoil/specimen direction, ⟨001⟩. Some researchers claim that γ' size is not a factor at the peak yield strength condition, but the data in Fig. 12.75 do not seem to bear out that claim. In any event, the tensile yield strengths of SCDS alloys ought generally to exceed those of CGDS and PC cast alloys. Figure 12.76 compares the yield strengths of PC cast IN-100 versus longitudinal SCDS and CGDS cast alloys. At lower temperatures, the order of strength from stronger to weaker is SCDS, CGDS, PC cast. Interestingly, there are crossovers above about 1400 °F (760 °C). The actual behavior of any of these alloys is an intricate function of the parameters previously mentioned, namely $V_f\gamma'$, γ' size, temperature, and stress.

Columnar Grain Directionally Solidified and SCDS Cast Superalloys: Ductility/Elongation Considerations. An aspect of creep-rupture behavior not customarily addressed is the early (primary) creep region. Initial studies of a common alloy produced as CGDS or SCDS showed the customary large benefits in creep life (time to 1%, 2%, etc.) and in rupture life over PC cast versions of the alloy. However, in the very early regions of creep, perhaps up to 0.5% creep strain, the CGDS and SCDS alloy versions crept faster than the PC cast versions. Thus, if time to 0.5% creep were a design criterion, the PC cast alloys of lesser rupture life would have shown as the stronger of the three alloy forms. Supporting data have not been released or, when released, have not been recognizable, owing to the extremely small scale of the effect, the much larger scale of the overall plot, and the small dimensions of the graph.

The ductility of tensile specimens of SCDS superalloys also may be in question. The 1100 °F (593 °C) ductility of a SCDS alloy such as PWA 1480 may be extremely limited if the crystal is precisely oriented on ⟨001⟩. As deviations (permitted by specification) from ⟨001⟩ occur, ductility in tension at the intermediate temperatures increases. Because ductility is an indicator of resistance to notch failure, extraordinarily low tensile ductilities could affect component application. Data on this facet of SCDS alloys also are rarely published. Figure 12.77 shows the typical ductility for PC cast and longitudinal CGDS and SCDS cast alloys of the MAR-M-200 type. Single-crystal directionally solidified alloys typically have more ductility, although, as indicated, highly aligned alloys might show much lower ductilities, perhaps approaching 1%.

The ductility in creep-rupture usually is the ductility at issue for cast airfoil alloys. A large benefit in CGDS alloys during low-intermediate-temperature creep rupture was

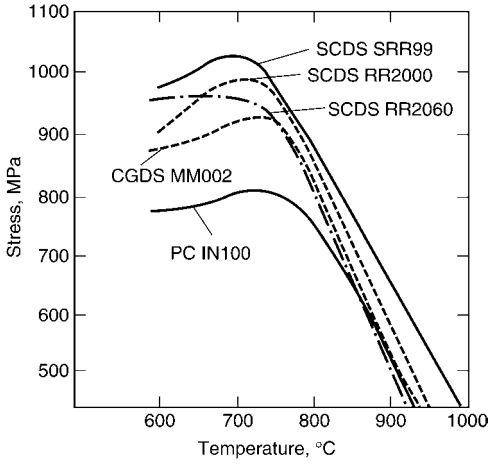


Fig. 12.76 Comparison of tensile yield strength (0.2% proof stress) for PC cast and longitudinal SCDS and CGDS cast alloys vs. temperature

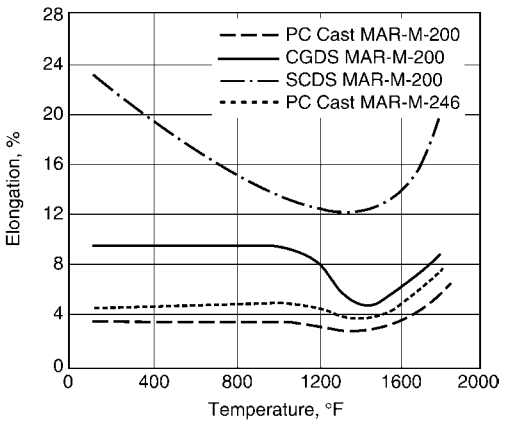


Fig. 12.77 Comparative longitudinal tensile elongation of MAR-M-200 and MAR-M-246 alloys as a function of temperature. Notice the superiority of typical SCDS elongation.

found in the substantial increase of the rupture ductility. Figure 12.78 shows the ductilities of PC cast and CGDS cast versions of several superalloys. Note the substantial increase in ductility for CGDS alloys when tested in the longitudinal direction. A slightly different presentation is made in Fig. 12.79, where the ductility of CGDS MAR-M-200 is contrasted with the rupture ductility of its predecessor, PC cast MAR-M-200, as a function of temperature. The minimum values of the CGDS version were greater than the average values for PC cast MAR-M-200.

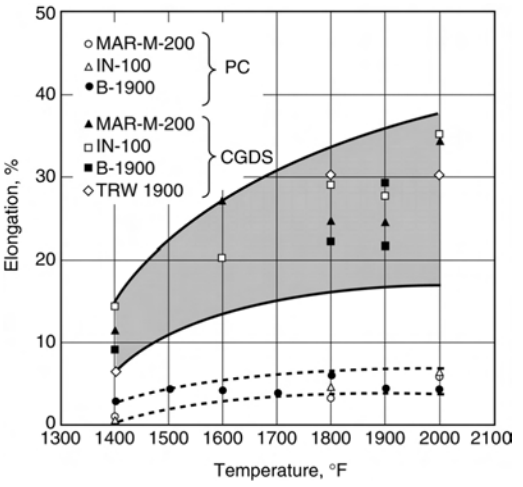


Fig. 12.78 Comparison of the rupture ductilities of several nickel-base superalloys in CGDS and PC cast conditions.

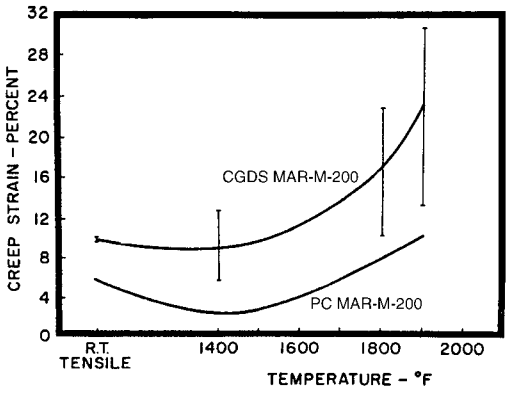


Fig. 12.79 Average rupture elongation of creep-rupture-tested longitudinal CGDS and PC cast MAR-M-200

Although not strictly a ductility/elongation issue, impact strength of cast superalloys occasionally becomes of interest. Published data are sparse. However, Fig. 12.80 gives a comparison of SCDS and PC cast superalloys with Nimonic 115 PC wrought nickel-base superalloy. Generally, cast impact strengths fall below those for wrought, but the SCDS alloy RR 2000 demonstrates superior resistance to Nimonic 115 above about 1400 °F (760 °C).

Columnar Grain Directionally Solidified and SCDS Cast Superalloys: Porosity and HIP. Even SCDS superalloys can exhibit casting porosity. Maximum creep and fatigue properties are developed if porosity is closed in SCDS and CGDS alloys. Figure 12.81

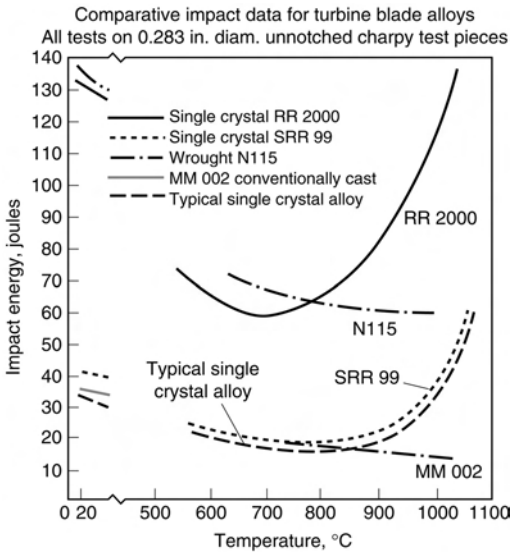


Fig. 12.80 Comparative impact data for turbine blade alloys as a function of temperature

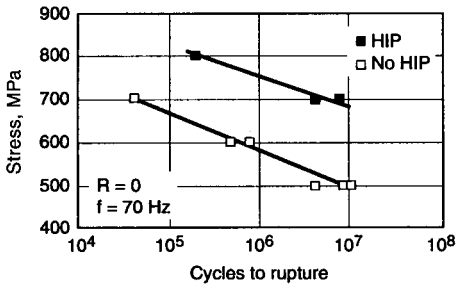


Fig. 12.81 Effect of HIP on the HCF behavior of longitudinal AM 3 SCDS cast alloy at 871 °C (1600 °F)

shows the beneficial effect of HIP processing on the HCF behavior of AM 3 ⟨001⟩ oriented single crystals at 1600 °F (871 °C). Most of HIP processing improvement favors fatigue properties, but it is believed that if HIP is used to close porosity, then creep-rupture properties also are increased. For some SCDS alloys, root concerns have prompted requirements for HIP to ensure maximum root ductility and LCF life, whereas previously HIP for airfoils has been aimed at rupture life improvements.

Low-Cycle Fatigue and Fracture of Cast Superalloys. The principal fatigue concerns for high-strength cast airfoil alloys are TMF and LCF. High-cycle fatigue is only a concern if a resonant condition should be created. Thermal-mechanical fatigue is an airfoil issue, while LCF is an attachment issue. The roots of blades may be LCF limited. Data on LCF are somewhat limited, while TMF data are more numerous. Thermal-mechanical fatigue testing frequently was not quantitatively useful, especially in the early applications of cast airfoils. Thermal fatigue (TF) tests were run with various schemes. Fluidized beds were employed to alternately heat and cool a bar, a tapered disk, or a simulated component. Sometimes, elaborate cyclic schedules were used. Results were somewhat useful in making comparisons about the TF capability of one alloy versus another, but hardly qualified as providing design numbers.

Thermal-mechanical fatigue is LCF failure produced by strains induced by thermal and mechanical means. Hence, the terminology, thermal-mechanical fatigue. Low-cycle fatigue concepts, when strain-controlled tests are run, can be used to understand (and predict) TMF behavior. The cyclic range at issue is from about 10^2 to 10^5 cycles. Classical strain-controlled LCF strain versus N_f plots are thought to result in straight-line relationships over most of the range. The number of cycles to failure may be defined in terms of cycles to first crack or to separation or to some predetermined load drop. Stress-controlled LCF tests are run as well. Figure 12.82 shows the differences between strain-controlled and stress-controlled testing. Specimens of differing orientations and processing conditions are used in this plot sequence, and it is not clear if meaningful design data could be retrieved from the tests. What is clear is that, for SCDS alloys, the higher the deviation from the ⟨001⟩ orientation, the shorter the fatigue life. From Fig. 12.82(a), it is clear that for a total strain range of 1.2%, the fatigue life was decreased by an order of magnitude when the crystal orientation moved away from only 6° off ⟨001⟩ to 22° from ⟨001⟩.

Owing to the relatively small level of plastic strain in the 1400 °F (760 °C) testing, one can plot the results as total stress versus N_f, as seen in Fig. 12.82(b). An examination of fracture surfaces showed that the cracks were initiated at microporosity, a fact that suggests that microporosity may play a principal role in SCDS fatigue life, at least for the alloy CMSX-2. Microporosity in commercial component single crystals can be as large as 50 to 80 μm, although it is never much above 10 μm in SCDS alloys made under laboratory conditions with very high temperature gradients. Single-crystal directionally solidified alloys exhibit load-controlled (stress-controlled) fatigue characteristics similar to those of PC cast alloys. Although the low SCDS modulus, at first glance, might be expected to result in very large strains in load-controlled fatigue with resulting poor fatigue life, no such degradation has been observed. It seems that in commercial SCDS applications, the fatigue life for most load-controlled situations turns out to be limited by stress concentrations that locally behave in a strain-controlled manner. The higher ductility and yield strength of SCDS alloys also are responsible, in part, for the good fatigue properties of SCDS alloys.

Microporosity is the principal fatigue crack initiation site in carbide-free SCDS superalloy airfoils. Elimination of microporosity in the root section by HIP (see the previous section on porosity and HIP) can enhance the fatigue life of SCDS alloys. If present, grain boundaries (LAB, HAB) or other defects, such as freckles or recrystallized grains, can initiate failure. As is the case for all cast alloys, fatigue is a more sensitive function of such defects than are tensile or creep strength.

It is desirable to observe how the three casting classes, PC, CGDS, and SCDS, compare in TMF. Figure 12.83 compares the average TMF lives of the classes using the applied TMF cycle seen in the inset of Fig. 12.83. There is a clear improvement of CGDS over PC cast alloys. This improve-

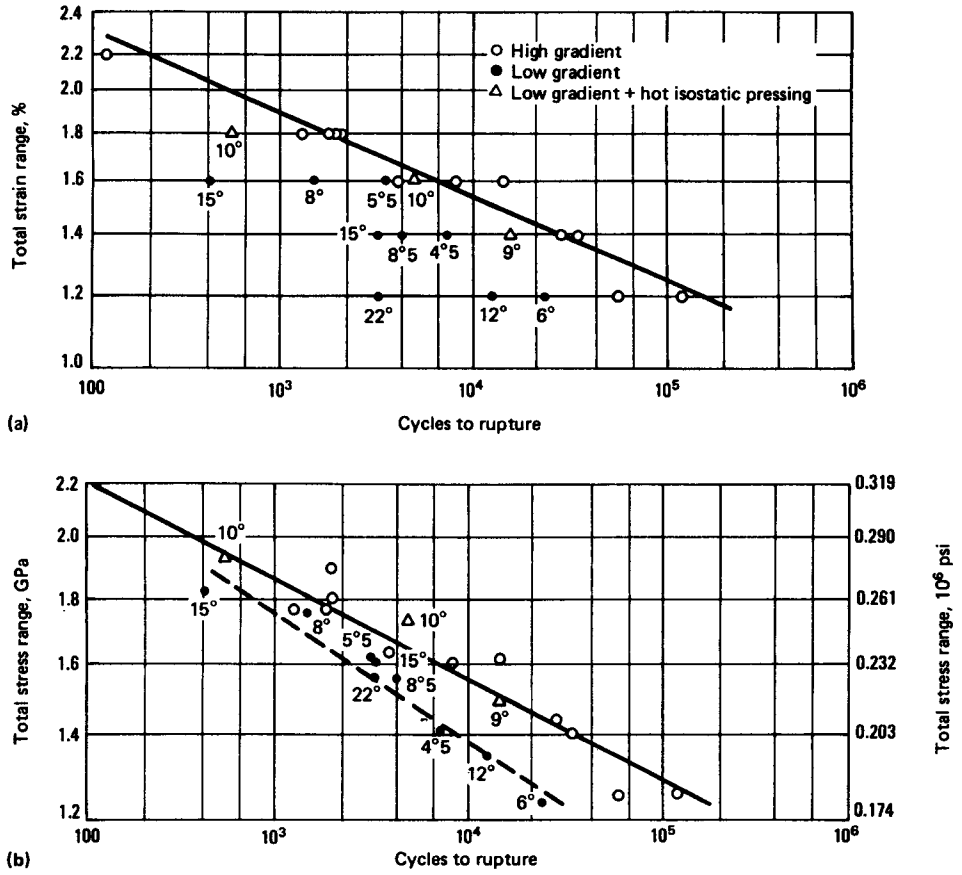


Fig. 12.82 Effect of thermal solidification gradient, orientation of specimen relative to ⟨001⟩ direction, and HIP on strain-controlled LCF behavior of CMSX-2 alloy at 760 °C (1400 °F). Test frequency = 0.33 Hz. (a) strain vs. N_f and (b) stress vs. N_f

ment arises from the fact that a significant amount of strain is thermally induced and is determined by the product of expansion coefficient × modulus × the temperature differential in the cycle. Because the method of strain inducement is the same for a given component regardless of structure, the only factor clearly changing from PC cast to CGDS is the modulus. The reduced modulus produces a dramatically lower strain; hence, a CGDS alloy lasts longer. The SCDS alloy is actually better than the CGDS alloy, yet has the same modulus. The explanation for this behavior lies in part in the absence of grain boundaries, which do contribute to cracking and failure.

Thermal-mechanical fatigue resistance generally is thought to be related to alloy creep strength, with stronger alloys exhibiting longer TMF life. Because SCDS alloys show higher creep strength than other cast forms, it is reasonable to expect better TMF lives from them. Specifically, creep during the higher-temperature compressive portion of the cycle I TMF test (shown by inset in Fig. 12.83) results in higher mean stress and reduced fatigue life. Thermal-mechanical fatigue is related to creep strength at the maximum cycle temperatures, and so SCDS alloys with their superior high-temperature creep strength have the potential for better TMF lives than CGDS alloys.

Another factor may enter into the fatigue situation, however, and that is the relatively low level of carbon and carbides plus absence of borides in SCDS alloys. Cracking of carbides has been shown to initiate fatigue failure. Figure 12.84 shows the fatigue prop-

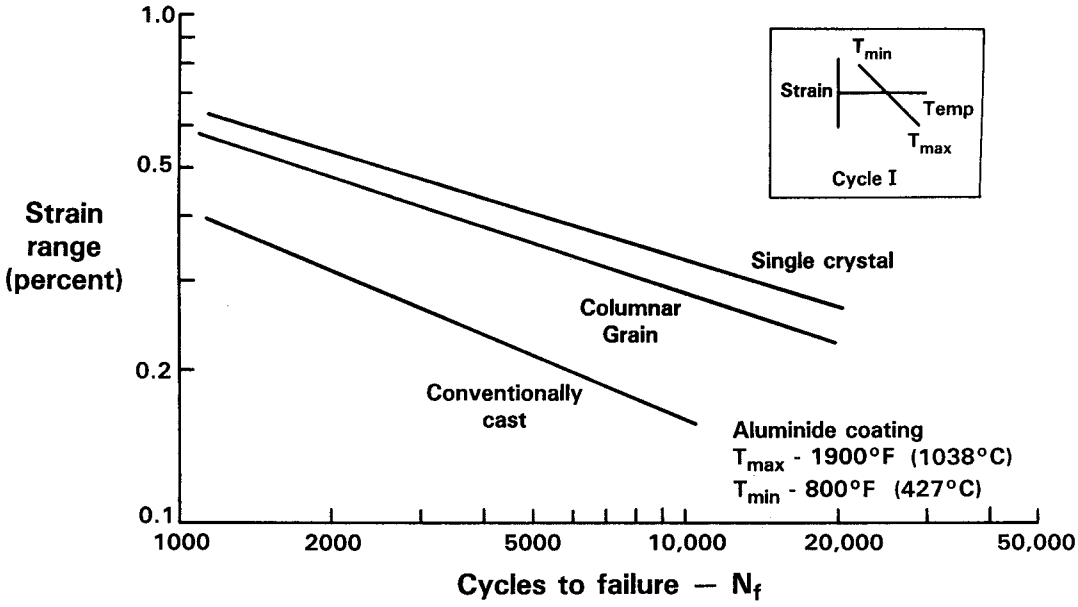


Fig. 12.83 Comparison of average TMF lives of PC, CGDS, and SCDS cast nickel-base superalloys

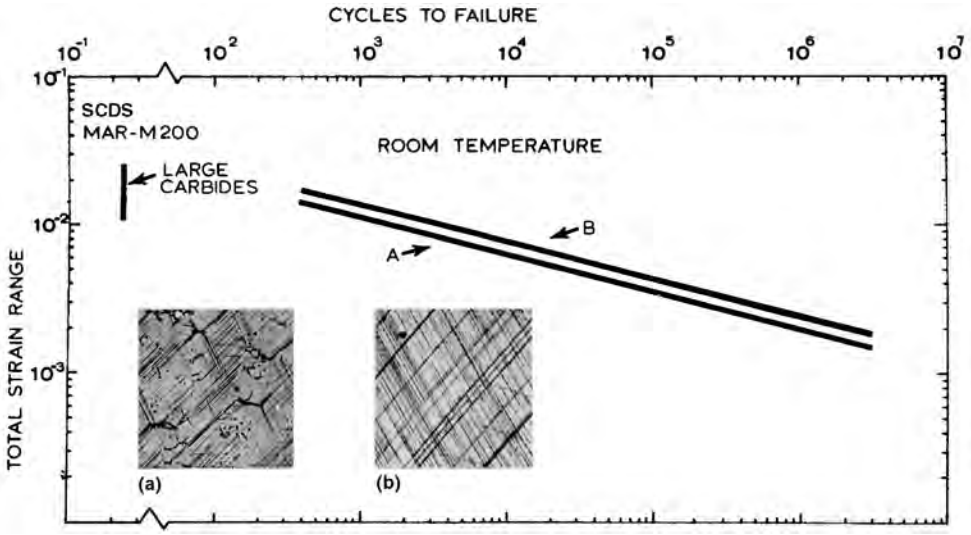


Fig. 12.84 Comparison of fatigue properties of SCDS MAR-M-200, with carbide sizes ranging from "large carbides" to "moderate" (a) to "carbide-free" (b)

erties of SCDS MAR-M-200 alloy, with carbide size ranging from ''large carbides'' to ''carbide-free.'' Carbide-free material performs better in fatigue, and low-carbon SCDS alloys should be better than CGDS alloys containing carbon.

Crack propagation in fatigue is an important alloy property, because much of total life often is spent in propagation, while initiation life may be relatively independent of alloy properties.

Effects of Coatings on Properties. It is a fact that most cast superalloys are coated for service operation. Coatings are discussed in Chapter 13. However, it should be noted that most alloys are tested with a coating applied.

The data in Fig. 12.83 is for specimens with an aluminide coating. A coating can have a significant effect on life by protecting against surface oxidation by protecting surface-connected borides, carbides, and other similar phases. Cracking initiates at the coating surface and propagates into the superalloy substrate, so alloy defects generally do not play as important a role in airfoil TMF, although defects are important in fatigue of uncoated sections.

One of the areas of concern for design data is the role of protective coatings on mechanical properties. Effects can be divided into static and dynamic effects. Mention of dynamic (cyclic) effects was made previously. Thermal-mechanical fatigue testing does employ appropriate coatings, but no extensive database exists even in that area.

Some facts about the static area are available. Limited creep-rupture data largely on PC and CGDS cast nickel-base superalloys indicate that:

- Coatings do not reduce the rupture life or creep strength of thick sections of superalloys, that is, sections > than 0.100 in. (0.254 cm) thick.
- Coatings do reduce the rupture life of thin sections of superalloys but only in proportion to the reduction of cross-sectional load area.
- Coating alloy lifetimes equal or exceed baseline rupture lives when stress is adjusted for the reduced cross-sectional area.
- Coating effects on thin-section rupture ductility are not clear (detrimental, neutral, and favorable effects can all be cited).

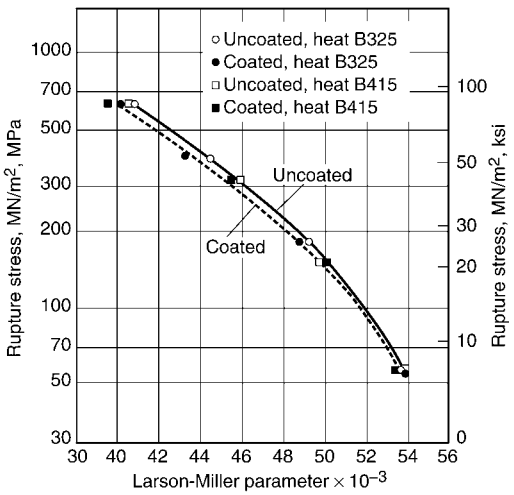


Fig. 12.85 Results of aluminide coated and uncoated stress rupture tests on Rene 120 nickel-base superalloy using Larson-Miller parameter (P_{LM}). Note: $P_{LM} = T(C + \log t)$ where C = Larson-Miller constant, T = absolute temperature, t = time in h. For this plot, C = undefined, probably 20, T = °R

There are no typical results to report on the effects of coatings on tensile behavior. There are limited data at low-intermediate temperatures, for example, 1400 °F (760 °C). At 1800 °F (982 °C), data suggested no effect of coatings on yield and ultimate strengths other than the effect of reduced cross section induced by the coating process. Most of the early published data were for aluminide coatings, which are less ductile but thinner than the overlay coatings. Data on coating effects have not been widely generated since the 1960s, and very little information is available relative to strength effects on more modern CGDS and SCDS alloys. A representative chart of the coating effect on stress rupture is given in Fig. 12.85 for Rene 120 and an aluminide coating. Exposure will affect the coating/base metal interaction, because all coatings will lose aluminum, and nickel from the base metal will diffuse into the coating. The extent to which this process degrades properties is not clear.

Cryogenic and Space Applications of Superalloys. Because the γ nickel-rich matrix of superalloys is ductile, and superalloys can be made very strong, these alloys were evaluated for subzero-to-true cryogenic applications. Most studies have been on wrought alloys of reasonably ductile nature. In particular, there has been great interest in IN-718 as a ductile, weldable, high-strength alloy. Most ductile wrought alloys proved to retain good ductility and toughness at low temperatures. Table 12.24 shows typical tensile properties of a few high-nickel precipitation-hardened superalloys used in cryogenic applications. IN-718 is one of these alloys. Other high-strength superalloys included the γ′-hardened alloy IN-X-750 and the γ″-hardened alloy IN-706. All of the alloys in Table 12.24 retain good ductility at their lowest testing temperatures. Notch tensile data indicate that they also retain good toughness at the lowest temperature of test. Ductility of heat treated weldments is low-

Table 12.24 Typical tensile properties of some nickel-base superalloys and weldments at room and subzero temperatures

Temperature		Tensile strength		Yield strength			Reduction
°C	°F	MPa	ksi	MPa	ksi	Elongation, %	in area, %
Hastelloy C sheet, cold rolled 20%, longitudinal orientation							
24	75	1140	165	1000	145	13	...
−196	−320	1520	220	1280	186	32	...
−253	−423	1740	252	1380	200	33	...
Inconel 600 bar, cold drawn, longitudinal orientation							
24	75	940	136	890	129	15	56
−78	−108	985	143	910	132	20	58
−196	−320	1160	168	1030	150	26	62
−253	−423	1250	181	1100	160	30	56
−257	−430	1280	186	1210	176	20	56
Inconel 706 forged billets(a)							
24	75	1260	183	1050	152	24	33
−196	−320	1570	228	1200	174	29	33
−269	−452	1680	243	1250	181	30	33
Inconel 718 sheet, longitudinal orientation(b)							
24	75	1330	193	1090	158	18	...
−78	−108	1490	216	1190	172	17	...
−196	−320	1730	251	1310	190	21	...
−253	−423	1740	252	1340	194	16	...
Inconel 718 bar, longitudinal orientation(c)							
24	75	1410	204	1170	170	15	18
−196	−320	1650	239	1340	197	21	20
−269	−452	1810	263	1410	204	21	20
Inconel 718 forgings, longitudinal orientation(c)							
24	75	1340	194	1150	167	24	35
−78	−108	1350	196	1190	172	29	45
−196	−320	1630	237	1300	188	26	34
−253	−423	1680	244	1320	192	28	42
−269	−452	1810	263	1410	204	21	20
GTA weld in Inconel 718 sheet, no filler metal(d)							
24	75	1320	191	1150	167	5	...
−196	−320	1560	226	1290	187	4	...
−253	−423	1730	251	1410	205	5	...
GTA weld in Inconel 718 forging, 718 filler metal(e)							
24	75	1260	183	2000	159	2	6
−196	−320	1430	208	1280	186	2	4
−269	−452	1650	239	1280	185	28	33
Inconel X-750 sheet, longitudinal orientation(f)							
24	75	1220	177	815	118	24	...
−78	−108	1320	192	875	127	28	...
−196	−320	1500	217	905	131	32	...
−253	−423	1590	230	940	136	32	...
Inconel X-750 bar, longitudinal orientation(f)							
24	75	1340	194	985	143	25	49
−196	−320	1570	228	1050	152	32	45
−253	−423	1700	246	1090	158	33	42
−257	−430	1720	249	1080	157	33	46
GTA weld in Inconel X-750 sheet, X-750 filler metal(g)							
24	75	1290	187	860	125	22	...
−78	−108	1340	195	915	133	24	...
−196	−320	1540	224	945	137	30	...
−253	−423	1660	241	1020	148	28	...
GTA weld in Inconel X-750 forged billet, F69 filler metal(e)							
24	75	1100	159	855	124	9	12
−196	−320	1110	161	930	135	6	9
−269	−452	1120	163	960	139	6	9

GTA, gas tungsten arc. (a) Aged 1 h at 980 °C (1800 °F), AC, 8 h at 730 °C (1350 °F), FC to 620 °C (1150 °F), held 8 h, AC. (b) Aged 1 h at 955 °C (1750 °F), AC, 8 h at 720 °C (1325 °F), FC to 620 °C (1150 °F), held 10 h, AC. (c) Aged ¾ h at 980 °C (1800 °F), AC, 8 h at 720 °C (1325 °F), FC to 620 °C (1150 °F), held 10 h, AC. (d) Weldment aged 8 h at 720 °C (1325 °F), FC to 620 °C (1150 °F), held 10 h, AC. (e) Weldment aged 1 h at 980 °C (1800 °F), AC, 8 h at 730 °C (1350 °F), FC to 620 °C (1150 °F), held 8 h, AC. (f) Annealed and aged 20 h at 700 °C (1300 °F). (g) Weldment aged 20 h at 700 °C (1300 °F), AC

Table 12.25 Fracture toughness of some nickel-base superalloys and weldments at room and subzero temperatures

Alloy and condition(a)	Form	Room-temperature yield strength		Specimen design	Orientation	Fracture toughness, K_{Ic} or $K_{Ic}(J)$, at:					
						24° C (75 °F)		−196 °C (−320 °F)		−269 °C (−452 °F)	
		MPa	ksi			MPa · $m^{1/2}$	ksi · $in.^{1/2}$	MPa · $m^{1/2}$	ksi · $in.^{1/2}$	MPa · $m^{1/2}$	ksi · $in.^{1/2}$
Inconel 706 (VIM-VAR) STDA	Forging	1065	154	CT	C-R	133(b)	121(b)	...	...	157(b)	143(b)
Inconel 706 (VIM-VAR) GTA weld, ST/W/STDA	Forging-weldment	1065	154	CT	...	...	...	...	...	58.2(b)(c)	53.0(b)(c)
Inconel 718 STDA	Bar	1170	170	CT	T-S	96.4	87.8	103	94.0	112	102
Inconel 718 (VIM-VAR) STDA	Forging	1165	169	CT	C-R	61.1(b)	55.6(b)	...	...	75.0(b)	68.2(b)
Inconel 718 (VIM-VAR) GTA weld, ST/W/STDA	Forging-weldment	1165	169	CT	...	...	...	51.1(b)(c) 66.2(b)(d)	46.5(b)(c) 60.2(b)(d)	51.7(b)(c) 60.9(b)(d)	47.1(b)(c) 55.4(b)(d)
Inconel X-750 (VIM-VAR) STDA	Forging	825	120	CT	C-R	...	...	...	...	76.1(b)(e)	69.2(b)(e)
Inconel X-750 (VIM) STDA	Forging	920	133	CT	C-R	...	...	...	...	145(b)	132(b)
Inconel X-750 (AAM-VAR) STDA	Forging	850	123	CT	C-R	...	...	...	...	237(b)	216(b)
Inconel X-750 (VIM-VAR) ST/W/STDA	Forging-weldment	825	120	CT	...	...	...	...	...	134(b)(c)(f) 176(b)(c)(g)	122(b)(c)(f) 160(b)(c)(g)

(a) VIM, vacuum induction melted; VAR, vacuum arc melted; AAM, air arc melted; ST, solution treated; W, welded. STDA for Inconel 706 and Inconel X-750: 980 °C (1800 °F) 1 h, AC, 730 °C (1350 °F) 8 h, FC to 620 °C (1150 °F), hold 8 h, AC. Solution treated direct age (STDA) for Inconel 718: 980 °C (1800 °F) 1 h, AC, 720 °C (1325 °F) 8 h, FC to 620 °C (1150 °F), hold 8 h, AC. Filler metals: F-718 for Inconel 706 and Inconel 718; Inco F69 for Inconel X-750. (b) $K_{Ic}(J)$. (c) Fusion zone. (d) Heat-affected zone. (e) This heat of Inconel X-750 had carbide precipitates at the grain boundaries, which caused abnormally low fracture toughness. (f) Gas tungsten arc weld. (g) Vacuum electron beam weld

ered but is not affected by extended exposure to subzero temperatures.

Table 12.25 gives fracture toughness data for some of the alloys in Table 12.24. These alloys normally retain a high degree of toughness at temperatures as low as −452 °F (−269 °C). Fracture toughness of fusion and heat-affected zones tends to be lower than that of the base metal.

For the alloys shown in the tables and for most wrought high-nickel matrix alloys, fatigue crack growth rates at subzero temperatures are either equal to or lower than the rates at room temperature for the same ΔK values. For design purposes, the use of room-temperature fatigue crack growth rate data for subzero applications has been deemed feasible. Results of fatigue tests at 10^6 cycles on axial and flexural specimens of several high-nickel matrix superalloys at room temperature and subzero temperatures indicate that, at 10^6 cycles, the fatigue strengths of ductile superalloys are higher at subzero temperatures than at room temperature.

One of the many applications for cast nickel-base superalloys is turbine blades for space vehicles and rocket engines. The most advanced SCDS alloys were evaluated for use in the U.S. space shuttle main engine. The subject is complex and not the basis for many published papers describing properties. As the blades would operate in contact with hydrogen and helium, studies were made of the effects of such elements on the properties of SCDS alloys such as PWA 1480, Rene N4, CMSX-2, and CMSX-4. Fracture behavior was studied relative to alloy chemistry and strength. PWA 1480 showed the best strength retention in hydrogen environments. The ⟨111⟩ orientation was found to be the most hydrogen-resistant orientation. Notched tensile testing showed results that varied with orientation and test temperature. Although not a low-temperature application, the hydrogen environment of the space shuttle main engine (SSME) main engine offers a challenging application, and the hydrogen initially is under storage at cryogenic conditions.

Superalloys: A Technical Guide, Second Edition
Matthew J. Donachie, Stephen J. Donachie, p 287-322
DOI:10.1361/stgs2002p287
Copyright © 2002 ASM International®
All rights reserved.
www.asminternational.org

Chapter 13

Corrosion and Protection of Superalloys

Overview

Introduction. Elevated-temperature corrosion resistance is to be a property associated with hot gas exposure and the wasting of metal by oxidation, mixed gas attack, and deposit-modified oxidation processes. Superalloys generally react with oxygen, and oxidation produces the prime environmental effect on superalloys. Combined attack of alloys simultaneously by two or more reactants is often called mixed gas attack. Gaseous-induced degradation of superalloys is the principal means of elevated-temperature corrosion attack, but deposits which significantly affect the gas-induced corrosion processes can be formed on superalloys. Deposit-modified high-temperature corrosion is usually called hot corrosion. It is an important means of superalloy degradation and, as noted later, may have names attached to specific forms of the deposit-modified corrosive attack.

Elevated-temperature oxidation is not the only surface degradation process in superalloy applications. It is important to recognize that certain superalloys of the cobalt family also find application at body temperature, where they are used as implants in a person and require resistance to body fluids for long times. This chapter is concerned primarily with the elevated-temperature wasting processes and mentions, only in passing, some aspects of corrosion resistance that may apply to the biomedical field.

In addition to volumetric removal of material, some superalloys interact with gases in ways that affect mechanical properties even when dimensions are not affected. Hydrogen, not only when introduced by contact with fluids at various temperatures after elevated-temperature exposure, but also by its presence as gaseous hydrogen in space-vehicle engines, can affect some superalloy mechanical behavior. Information about environmental degradation is found in Chapter 12, which deals with property-structure relationships.

Corrosion processes may be influenced greatly by the erosive effects of hot gases. The gas stream may include particles that erode the surface, destroying protective scales. The dynamic nature of the gas stream will affect the equilibria attainable at the surface. In short, it may not be possible to use information gathered by traditional laboratory testing of oxidation and corrosion processes under static conditions to reliably predict the behavior of superalloys in real-world applications.

The Oxidation Process Summarized. Oxidation, for the purposes expressed in this chapter, is the interaction of one or more metal atoms/ions with one or more oxygen atoms/ions to create an oxide. Some metals can form more than one oxide, and that is true for some of the elements in superalloys. There are three principal forms of oxidation:

- General or uniform oxidation (taking place at an exposed surface)
- Intergranular oxidation (occurring along grain boundaries)

- Internal oxidation (oxidation taking place below the external surface but not just at grain boundaries)

There is ample theoretical and practical understanding of the mechanisms of the oxidation process, and the thermodynamics and kinetics of the process are not covered in any detail in this chapter. For more extensive information, the reader is referred to the references in Appendix C.

The principal oxides that might form in a superalloy are those related to the basis metals and to chromium or aluminum, which are alloy elements added in considerable amounts for the purpose of effecting an improvement in the oxidation resistance (chromium) and strength (aluminum) of a superalloy. Oxides of particular interest are:

- Chromic oxide (Cr_2O_3)
- Aluminum oxide (Al_2O_3)
- Nickel oxide (NiO)
- Cobalt oxide (CoO)
- Spinel ($NiO \cdot Cr_2O_3$)

The protectivity of these oxides differs from one to another. By virtue of their slow growth rates, Al_2O_3 and Cr_2O_3 oxide scales are the most protective of all those that can be formed, but their growth requires adequate amounts of chromium and aluminum plus oxygen and oxide growth occurs more rapidly at higher temperatures. In general, Cr_2O_3 forms and is most protective below about 1600 °F (871 °C), while Al_2O_3 is protective at temperatures up to the melting points of the alloys. High temperatures are required to form adequate thicknesses of Al_2O_3 in a reasonable time. If the Al_2O_3 layer is eroded by hot gases or rubbed or scuffed accidentally, removing the Al_2O_3 layer, and operation is continued at temperatures where the protective layer will not reform very rapidly, catastrophic oxidation results.

The way in which nature promotes oxidation is by the selective oxidation of certain metal atom/ion species in the surface layer of superalloys. During the initial stages of oxidation, virtually all oxides that are stable thermodynamically will form. Although multiple oxides may form in the oxidation process, only one is likely to be dominant. While NiO (and the oxides of other alloy elements) may form initially at many surface locations when oxidation conditions are encountered, only one oxide spreads across the entire surface. That oxide is the dominant one; for current superalloys, the oxide is either Cr_2O_3 or Al_2O_3, depending on the chemistry of the alloy. (Refer to Fig. 13.1 and see also ''Gas Turbine Materials'' in the section ''Degradation by Gaseous Oxidation or Mixed Gases.'')

Mixed Gas Corrosion and Hot Corrosion Attack. Under certain conditions, the resistance of oxide layers to corrosion is drastically diminished. Mixed gases may promote

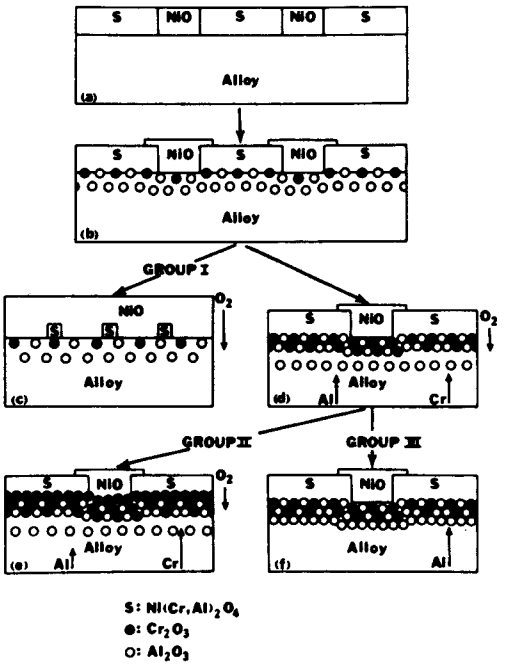


Fig. 13.1 Schematic diagram illustrating oxide scale development on nickel-chromium-aluminum alloys with time. (a) Conversion of a thin alloy surface layer to oxide by rapid uptake of oxygen. The oxide phases formed are determined by the composition of the alloy. (b) Diffusion within the alloy results in the formation of a Cr_2O_3 and Al_2O_3 subscale beneath the external scale. (c) For alloys with low chromium and aluminum concentrations, the subscale cannot become continuous, and NiO in the external scale predominates. This group of alloys could then be called NiO-formers. (d) For alloys with higher chromium and aluminum concentrations, the subscale becomes continuous, but aluminum is still oxidized internally. (e) For alloys with smaller aluminum concentrations, the continuous external scale becomes enriched in Cr_2O_3, but the aluminum is oxidized internally. This group of alloys could be called Cr_2O_3-formers. (f) For alloys with larger aluminum concentrations, the Al_2O_3 subscale zone becomes continuous beneath the duplex oxide. This group of alloys would be called Al_2O_3-formers.

increased attack. Certain elements from the atmosphere or within the alloy, separately or in conjunction, may act to significantly increase the rate of corrosion attack by producing deposits on the surface when the alloy is at high temperature. This latter corrosion has been called hot corrosion and is invariably associated with deposits on the surface of the component and the subsequent fluxing of the protective oxide layer, which is not only removed but prevented from being regenerated.

Some early deposit-modified corrosion processes were witnessed in the power turbine industry when the element vanadium in fuel was oxidized. V_2O_5 and vanadates, formed by reaction between salts and V_2O_5 condensed as liquids, were catastrophically corrosive. Other problems were encountered when superalloys in gas turbines intended for marine use interacted with sulfur and salt to produce unexpected degradation by a process called sulfidation. Green rot and other terminologies were used to describe various hot-corrosion-type degradation processes. As a result of hot corrosion failures and alloy studies, superalloys were created that were/are more resistant to hot corrosion than the initial high-strength cast airfoil superalloys such as IN-100 and B-1900 nickel-base superalloys.

Cobalt-base superalloys did not suffer as much from hot corrosion, owing to high chromium concentrations in such alloys; iron-nickel-base superalloys generally did not operate at temperatures sufficiently high as to encounter hot corrosion in normal short-to-moderate time exposure.

Protection Against Oxidation and Hot Corrosion. The oxides Cr_2O_3 and Al_2O_3 (plus SiO) protect against oxidation and hot corrosion, but not equally well. The ability of an alloy to be protected is limited by the chromium and/or aluminum content of the surface. Excessively high contents of either element are detrimental to mechanical properties and must be avoided. Furthermore, protection involves consumption of the element. That is, the protective aluminum or chromium are continuously removed by the environment and must be replenished by diffusion from the base metals.

The nature of protection for most superalloy applications at high temperatures is thus two-fold:

- The alloy is made as oxidation resistant as possible, consistent with mechanical-property goals.
- A suitable protective coating is placed on exposed surfaces.

The result of this two-pronged approach is that the structural alloy that is coated is left intact as the major load-carrying facet of the component. Meanwhile, the non-load-carrying coating can be tailored to have aluminum (or chromium) contents far in excess of that permitted by the normal chemistry restraints on base alloys. Thus, alloy development and coating development, while interrelated in the final analysis, can be carried on independently until the coating is to be married to the base superalloy.

Coatings have a very great advantage in their successful application to superalloys. When the coating is depleted, it ostensibly can be removed with little or, at least, acceptably small thinning of the original component. A new coating can be applied and the component reused. This concept has been in use with superalloys for nearly a half-century and works well for external surfaces that may easily be cleaned of a coating and, furthermore, easily inspected for complete coating removal and/or underlying alloy damage. Internal passages, such as the cooling passages in gas turbine engine airfoils, are a more challenging task. Removal processes have more constraints, and inspection is limited. Because the external surfaces take the brunt of the environmental attack, it may be sufficient to seal-off the internal passages and remove and refurbish the external surfaces only. See Chapter 14 for more on the subjects of refurbishment, repair, and recycling.

Oxidation/Corrosion Testing of Superalloys and Their Coatings

Background. Oxidation is not an easy property to measure. In unary and binary metal and alloy tests, much scientific study was done with the use of weight measurements. Simple tests, where exposure was made in a furnace and weight gain/loss measured after test, provided much of the early knowledge of superalloys and their constituent elements. More sophisticated tests in-

volved continuous recording thermal balances, wherein the weight changes were monitored as the oxidation process proceeded. In some instances, when hot corrosion testing was required, specimens were placed in a crucible with appropriate contaminants and exposed to high temperatures. This is not a satisfactory method for determination of the real-world behavior of a superalloy undergoing high-temperature oxidation.

In many applications of gas turbines, and in particular, in those used for aircraft propulsion, the gas temperature, and therefore the metal temperature, is cycled over quite wide ranges as the engine is operated, for example, at idle, takeoff, climb, cruise, and thrust-reverse power requirements. Such thermal cycling imposes a major effect on oxidation behavior of alloys and coatings, that of protective oxide spallation. This phenomenon is normally attributed to stresses arising from the different coefficients of thermal expansion of metal and protective oxide.

To deal with the complex combination of real-world factors, many laboratory tests were developed for screening and ranking of alloys and coatings. Because real-time evaluation of various coating/process/substrate/application permutations is not feasible in actual engines, these tests were attempts to create an approximation to the real-world situation. Some organizations have generated substantial databases for many coating/process/substrate combinations using these tests. These databases, in some form or other, have been used to select coatings for new and existing applications. Nevertheless, significant surprises in terms of actual versus predicted coating performance continue to occur in the field.

Dynamic Oxidation Effects. As suggested previously, one of the facts of oxide formation is that the oxide scales on superalloys are subject to spalling, owing to severe thermal stresses induced by the cyclic nature of most heat engine operations. Superalloys rarely operate at a single temperature but cycle between temperatures and, in the case of aircraft gas turbines, regularly cycle from ambient to extreme thrust temperatures. In continuous balance tests, superalloys that are protected by adequate layers of Cr_2O_3 or Al_2O_3 oxide scales generally show weight gains during test. No superalloy in real-world high-temperature conditions will show a weight gain. Superalloys lose weight as atoms are oxidized to scale and, eventually, depart the superalloy surface by spalling. The question that must be answered by testing is not ''Is there a weight loss?'' but rather ''How does the weight loss compare with other superalloys or coatings?'' Furthermore, it is important to understand how this comparison looks when the testing is done under simulated (or real) engine operating conditions.

Corrosion-Erosion Rig Testing. About 45 years ago, engineers began to look for ways to test the strength properties of candidate gas turbine airfoil materials under conditions more closely approximating those in an engine. One of the schemes included making simulated airfoils (actually little paddles) of appropriate alloys, welding a weight on the tip, and spinning a group of paddles in the exit gas stream of a fuel burner. Centrifugal force was expected to bend the paddles.

The strength results were not particularly valuable, but some engineers realized that spinning a paddle or other type of simulated airfoil in the hot gas stream might approximate the oxidation/corrosion conditions in a gas turbine. Thus burner rig testing was born. Simple rigs were replaced by more complex ones over the years, but the concept remains the same: burn the fuel of interest and impinge the exit gases onto a rotating spindle containing specimens of the alloys/coatings of interest. The rotation ensures that the gas temperature effects are averaged over all the specimens in a spindle. Special additives can be used to promote certain types of hot corrosion. Figure 13.2 shows an early burner rig used to evaluate superalloys and coatings for oxidation resistance. Not shown are the control panels that are used with such an apparatus.

Actually, the burner rigs are not just oxidation and hot corrosion test equipment, because the gas streams in turbine engines or rigs usually contain constituents that cause surface erosion. Thus, strictly speaking, burner rig testing is really corrosion-erosion rig testing. For convenience, differing organizations have shortened the name to burner rig or to erosion rig.

The results of such rig testing vary with the specimen design. Some specimens were really airfoil-shaped, some were round bars, others, as seen in Fig. 13.2, were something

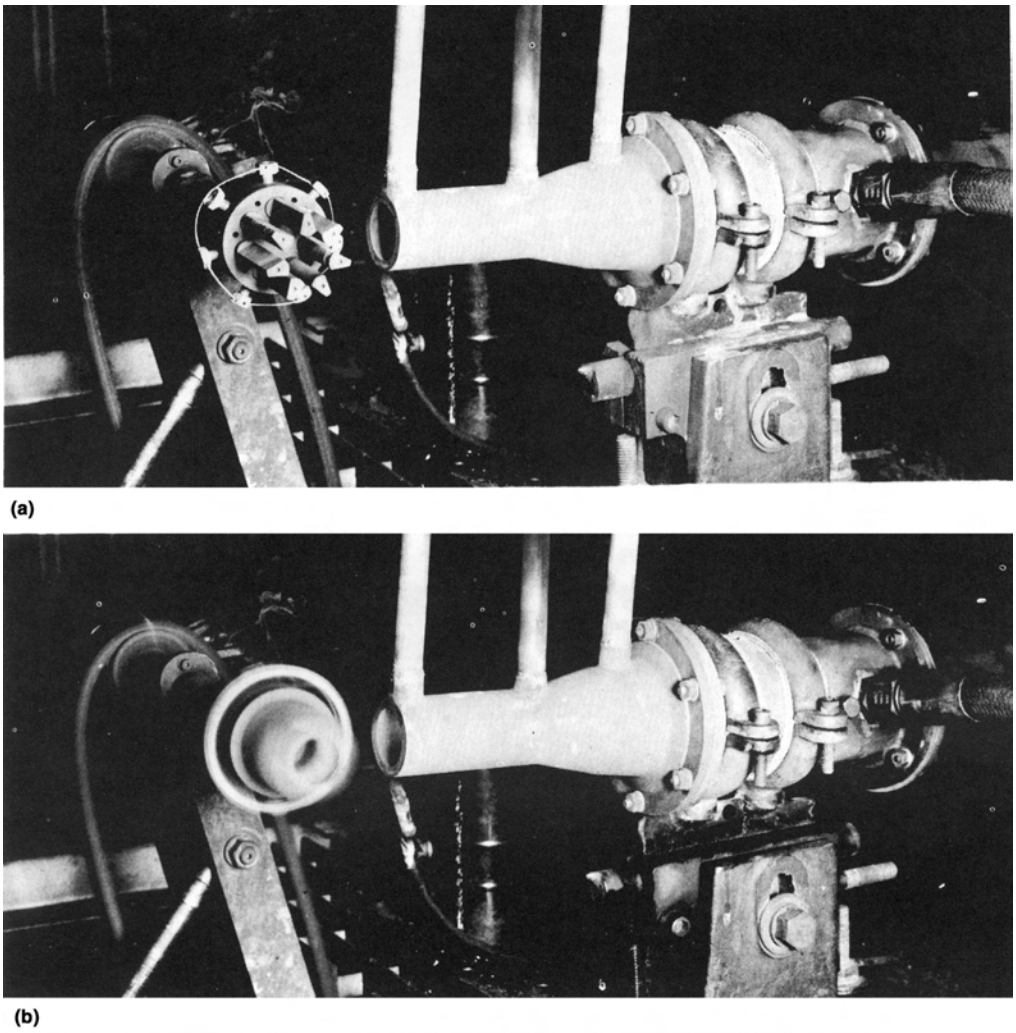


Fig. 13.2 Burner rig testing showing (a) specimens and test configuration and (b) operation

in between. Some specimens were in the order of 0.5 in. (12.7 mm) in diameter and others only ¼ that size. Some rigs were built to handle only a true airfoil without rotation. The results on an absolute basis thus vary considerably from one laboratory to another. The success of burner rig testing lies in the art of interpreting and presenting the results. Relative results from one rotating rig type to another probably are comparable. A typical set of burner rig test bars, in this case from a hot corrosion test, are shown in Fig. 13.3.

Measuring Oxidation and Presenting Data. Weight change was the first measurement made in rig testing. This property was mostly a weight loss, although during the very initial stages of testing (and for some alloys, a longer stage), some specimens may have shown weight gain. The reason for the occasional weight gain was that testing, for many years, was isothermal. Figure 13.4 shows isothermal weight change data plotted for several nickel-base superalloys as a function of exposure time. This test actually incorporated sulfur and salt to simulate hot corrosion effects, and shows the form of such plots.

Weight change measurements were made because it was not reasonable to cut up dozens to hundreds of samples continuously to

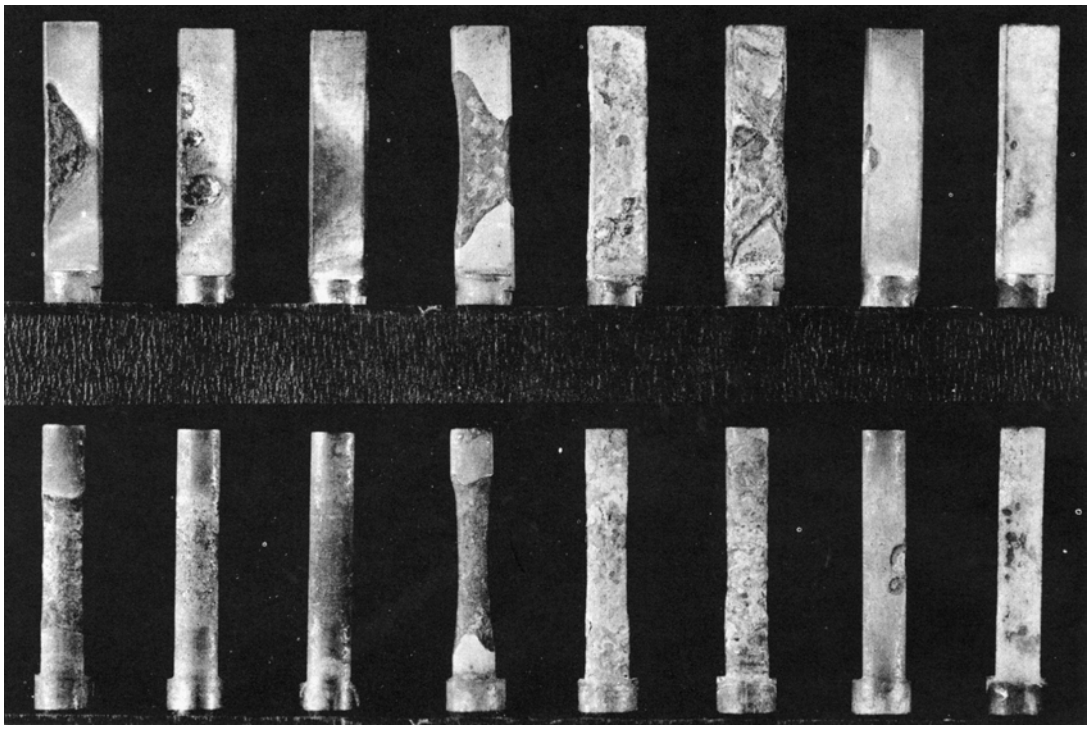


Fig. 13.3 Uncoated nickel-base superalloy erosion test bars after 899 °C (1650 °F) isothermal hot corrosion test. Left to right: cast Udimet 700, wrought Udimet 700, Waspaloy, IN-100, B-1900, MAR-M-246, INCO 728, and MC 102

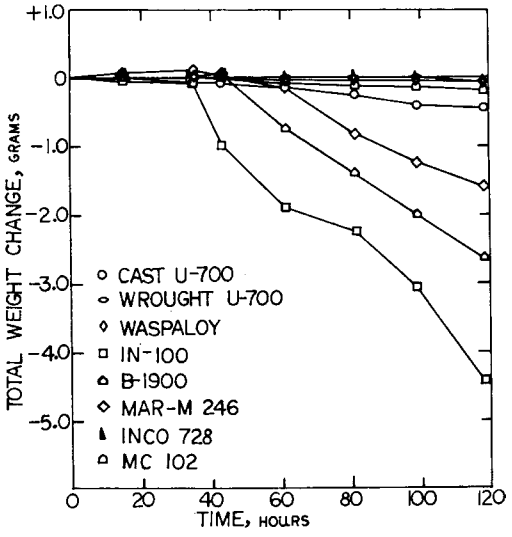


Fig. 13.4 Specimen weight change during 899 °C (1650 °F) isothermal hot corrosion test

get macrostructural and microstructural pictures of the progression of oxidation. With weight gain measurements, the same specimen could be used until the test was concluded, then cut for examination.

Thermal cycling took place only when a burner rig was shut down, usually after a day, several days, a week, and so on. The longer the time between shut downs, the less spalling of oxide scale caused by thermal stresses. In the mid-1960s, Pratt & Whitney introduced cyclic testing of specimens. A ''blade'' cycle and a ''vane'' cycle were introduced initially. Essentially, a rig was run isothermally at one temperature for a certain short time, then moved to a higher (or lower) temperature for another short time, then cooled to a low temperature using a blast of air. The cycle then was repeated many times to approximate gas turbine engine operating conditions.

Cyclic testing to the specifications of each interested laboratory has been the rule for the past 35 or so years. There is not necessarily a standard to which tests are run. Most

testing these days is probably run in support of coating development and evaluation. When hot corrosion is to be evaluated, appropriate contaminants are introduced to the gas path.

As emphasis switched to coating, rather than alloy, evaluation, weight gain/loss became an even more unreliable indicator of performance. Measuring standards were developed to evaluate such subjective quantities as amount of coating removed, depth of maximum attack, and so on. Behavior of a coating might be reported in such terms as ''time to 50% life of coating'' or similar quantities. In the instances of coating performance, as alloys and coatings got better, data had to be generated at higher and higher temperatures, because tests took longer and longer at lower (but not low!) temperatures. Tests that take hundreds of hours at temperatures around 2000 °F (1093 °C) may take tens of thousands of hours at 1750 °F (954 °C). These lower-temperature tests just are not run.

Because mechanical-property testing extrapolation with time and temperature has been reasonably successful, many engineers assume that a chemical property can be extrapolated as well. The assumption is made that the very high-temperature results can be extrapolated to the lower temperatures. Often, that may not be true, but no funds are available nor is time permitted to run a few tests, let alone the multiple tests needed to validate coating and alloy performance over a wide temperature range. This condition exists particularly in the gas turbine industry, not only in aircraft but also for industrial and marine gas turbines, where service times are expected to be much longer and operating temperatures are somewhat lower.

Designers are in need of hard data to predict life (coating life) versus time. No accepted industry practice exists for coating-life extrapolation versus temperature and time. Some organizations may plot data as observed life versus the reciprocal of absolute test temperature. This concept is at least in accord with rate theory. Other groups tend to plot life versus temperature. Neither of these routes is probably satisfactory. With the scarcity of data, it can be difficult to discriminate between approaches, especially over the small temperature range of testing. It is important to note that when order of magnitude extrapolations of data are being made, there is considerable likelihood of errors. Hopefully, these will not be on the optimistic side. Data from laboratory tests must be verified by engine testing.

Microscopic and macroscopic examination are important in revealing the extent of oxidation or hot corrosion damage. Visual appearance, enhanced by etching in some instances, is used to determine:

- Amount of coating lost (or remaining)
- Depth of metal loss
- Depth of internal oxidation (if any)
- Local oxidation down grain boundaries, and so on

In some laboratories, a ''calibrated eyeball'' is available to review every test. When the calibrated eyeball moves on, a new calibration will be needed to ensure consistency with prior test results!

Localized Corrosion Effects. Intergranular corrosion along grain boundaries or corrosion of phases in an alloy are not accounted for in the usual evaluation of alloy performance by weight change. Such attack can be devastating to superalloy strength and should be reported and highlighted in any evaluation of superalloy oxidation or hot corrosion. Because coatings generally are used on superalloys intended for the highest-temperature applications, where selective attack can occur more quickly, there may be no actual penetration of grain boundaries, oxidation of phases such as carbides, and so on, because they are covered by coatings. Nevertheless, any propensity for such attack ought to be a matter of record, in the event that it might occur in areas devoid of coating following elevated-temperature service.

Test Results for Coatings. While test results, if determined by consistent methods, including using the same data analyst, may be useful in setting limits or at least confirming relative corrosion resistance of basic superalloys, they may be somewhat misleading in the case of corrosion-protective coatings. As is seen later in the chapter, several important points are often overlooked in considering coating performance. These are:

- Coatings are influenced by diffusion of alloy elements from the base superalloy.
- Overlay coatings are thicker than diffusion coatings.

- Coating performance relative to other coatings is not likely to be a fixed percentage or absolute value over the entire service temperature-time range.

Overlay coatings may owe some of their performance superiority over diffusion coatings to the thickness differential. For a more accurate representation of capability, all coatings should have life data presented in normalized fashion, for example, as life per mil (μm) of coating versus temperature. Moreover, as is discussed subsequently, diffusion coatings and even overlay coatings are influenced by the alloy elements imported from the base superalloy. Favorable active element additions, such as hafnium, in the base superalloy can be incorporated in the coating and enhance performance. If that is the case, then the performance of a coating should never parallel that of the same coating on different alloy. However, there is usually not enough data to show the differences in performance of a coating on different alloy substrates. Many coating users and data providers assume similar performance of a given coating on a variety of alloys of similar (e.g., nickel) base metal.

Degradation by Gaseous Oxidation or Mixed Gases

Gas Turbine Materials. At intermediate temperatures—below about 1600 °F (870 °C)—general uniform oxidation is not a major problem. It has been known for many years that alloys of iron, nickel, or cobalt with chromium contents of the order of 20% have excellent oxidation resistance, and it is therefore not surprising that there has been a great deal of work on the oxidation behavior of these alloys.

Most interests initially centered on oxidation behavior of the basic nickel-chromium alloys. Three groupings of such binary nickel-chromium alloys were suggested as representative of the oxidation behavior of the nickel-chromium system. These groupings are:

- Those containing less than approximately 10% Cr
- Those containing between 10 and 25% Cr
- Those containing over 25% Cr

Commercial nickel- and cobalt-base superalloys are attacked by oxygen but not in the same way as binary alloys, because the presence of other elements affects the oxidation process. In commercial nickel-base superalloy development, efforts in composition development have long passed the ternary nickel-chromium-aluminum system. Quinary (5-element) or higher superalloy compositions are the rule, with major additions of cobalt and refractory metallic elements playing a dominant role. As noted previously, 12 to 14 elements may be controlled by specification in a nickel-chromium-aluminum superalloy. Furthermore, titanium is present as a hardener (in addition to aluminum), and carbon is also present. The complex interplay among alloy elements has been noted previously. It is not surprising then, that few complex superalloys have ever been studied in any detail to ascertain their oxidation resistance, kinetics, and mechanism of oxidation.

Some static (i.e., isothermal) oxidation data exist. Figure 13.5 shows the oxidation resistance of Nimonic alloys during continuous heating of foil for 100 h in air. It should be noted that Fig. 13.5 presents data on completely descaled alloys. All Nimonic alloys

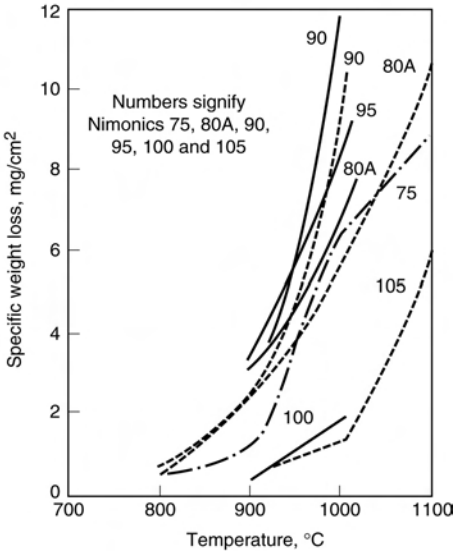


Fig. 13.5 Oxidation resistance of Nimonic nickel-base superalloys during continuous heating of foil for 100 h in air. Weight change determined after oxide descaling

have significant levels of chromium. The data in Fig. 13.5 show:

- The excellent resistance to oxidation of the nickel-base superalloys at temperatures below about 1650 °F (900 °C)
- The marked increase in oxidation resistance imparted by aluminum. (Nimonic Alloys 100 and 105 have about 5 wt% Al, whereas the other alloys have lower aluminum contents.)

For superalloys, the level of oxidation resistance at temperatures below about 1600 to 1800 °F (871 to 982 °C) is a function of chromium content (forms as a protective oxide); at temperatures above about 1800 °F (982 °C), aluminum content becomes more important in oxidation resistance (Al_2O_3 forms as a protective oxide). Chromium and aluminum can contribute in an interactive fashion to oxidation protection. The higher the chromium level, the less aluminum may be required to form a highly protective Al_2O_3 layer as noted previously. Figure 13.1 shows (schematically) the development of protective oxide scales on a nickel-chromium-aluminum superalloy.

As also noted previously, a comparison of the weight gain or weight loss in an alloy may not indicate the full extent of oxidation change. Superalloys are particularly susceptible to intergranular oxide penetration as well as to internal oxidation. Penetrations of the order of 2 mils (51 μm) or more below the plane front of ordinary oxidation are common. Information on oxide penetration is obviously of importance in the use of thin sheets for structural applications at high temperatures. Figure 13.6 shows the intergranular attack on several nickel-base alloys after 1 h static exposure, while Fig. 13.7 illustrates the effects of ten 1 h cyclic exposures on these same materials at the same temperatures. The solid-solution-hardened alloy Hastelloy X, with protection by Cr_2O_3 showed the least oxide penetration of the alloys tested.

The aluminum contents of many superalloys are insufficient to provide long-term Al_2O_3 protection, and so protective coatings are applied, as noted. These coatings also prevent selective attack that occurs along grain boundaries and at surface carbides (see Fig. 13.8) and inhibit internal oxidation or subsurface interaction of O_2/N_2 with γ' envelopes, a process believed to occur in nickel-base superalloys.

Some Comments on Oxide Scale Formation. During the initial stages of oxidation, virtually all possible oxides are formed. As oxidation continues, diffusion of atoms takes place, and changes in the scale development begin to occur. The important diffusing species in the binary alloys or complex superalloys are oxygen into the alloy and the outward diffusion of elements in the alloy. When oxygen diffusion is slow compared to that of elements in the alloy, then conditions become more favorable for lateral growth of oxides, and oxides spread over the surface of the alloy. The dominant oxide is the one that first

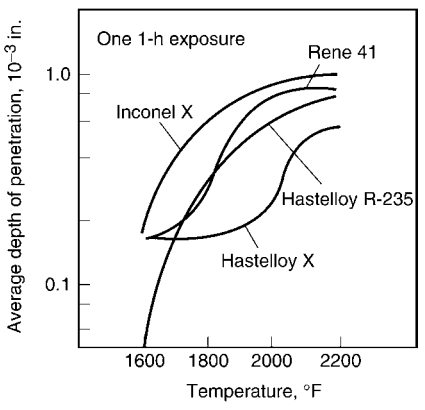


Fig. 13.6 Depth of attack as a function of temperature for various nickel-base superalloys after 1 h exposure

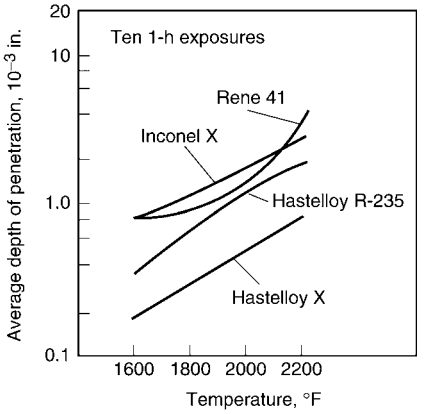


Fig. 13.7 Depth of attack as a function of temperature for various nickel-base superalloys after 10 cycles for 1 h exposures to the indicated temperatures

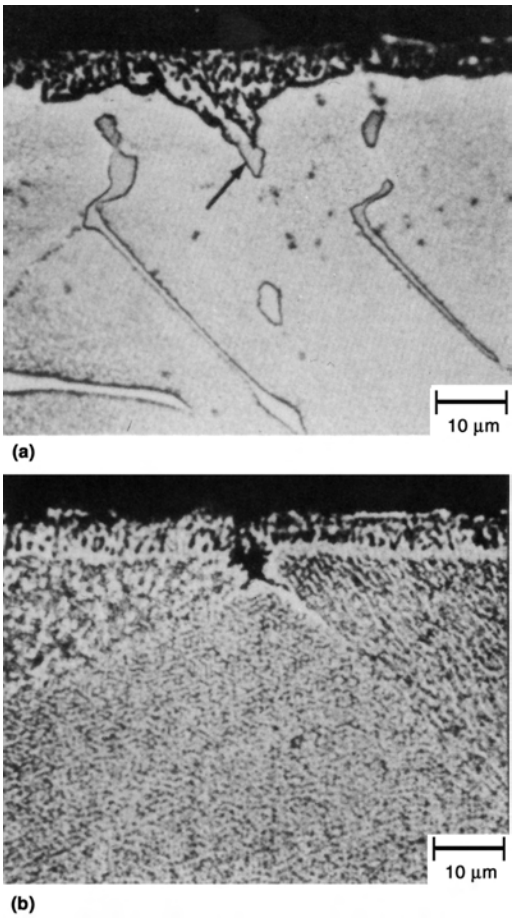


Fig. 13.8 Effects of nonuniform oxidation on superalloys. (a) Accelerated oxidation of MC carbide (arrow) at surface of MAR-M-200 nickel-base superalloy at 927 °C (1700 °F), and (b) accelerated oxidation of grain boundary in U-700 nickel-base superalloy at 760 °C (1400 °F)

achieves complete coverage of the surface. Secondary oxides remain, some as internal oxidation in the near-surface layer of the part.

The development of oxides on alloys thus can be described as a sequential process. Initially, there are many more oxides formed than can be supported kinetically or thermodynamically. Gradually, the thermodynamically more-stable oxides predominate. In order for one oxide in an alloy to have total dominance over the others, the oxide must be the most thermodynamically stable, and its formation and growth kinetics must be such that lateral growth is favored as opposed to formation of a discontinuous subscale.

Once complete, continuous oxide surface coverage occurs, further oxidation requires diffusion of oxygen through the oxide layer to the metal or diffusion of metal ions through the oxide toward the surface.

Binary Nickel- or Cobalt-Chromium Alloys. Small amounts of chromium in nickel, up to 5 to perhaps 8% Cr, actually increase the rate of oxidation of nickel. The oxide scale for binary alloys with less than 10% Cr consists of two layers, an outer compact layer of NiO and a porous inner layer composed of a mixture of NiO and $NiCr_2O_4$ (spinel structure). In addition, there is internal oxidation in the metal, with the formation of Cr_2O_3 particles.

In the intermediate range of chromium content (roughly 10 to 20% Cr), the overall oxidation rate decreases rapidly with increasing chromium. The oxide growth on the surface appears to be irregular; in some places a thin, apparently single-layered oxide forms; in other places one finds a thick oxide, apparently consisting of three distinct layers. The thin oxide and the layer adjacent to the metal in the thicker oxide are essentially Cr_2O_3. The next layer is a mixture of NiO and $NiCr_2O_4$, and the oxide furthest from the metal is NiO. Chromium is depleted from the metal beneath the scale, but there is no internal oxidation. After long times, the Cr_2O_3 layer is continuous over the specimen surface and is of fairly uniform thickness. At short times, the Cr_2O_3 layer is not continuous, and locally the chromium in the metal is internally oxidized, forming Cr_2O_3 particles in a chromium-depleted matrix. Apparently, the continuous layer of Cr_2O_3 develops in these regions only after a significant amount of the alloy has been oxidized.

In the more concentrated alloys, the external scale is predominantly Cr_2O_3, with a small amount of $NiCr_2O_4$. In general, there is no internal oxidation, but at long times, some internal oxide particles may appear.

The variation of oxidation rate of cobalt-chromium binary alloys with chromium content has the same general form as nickel-chromium binary alloys, but actual changes in oxidation behavior are displaced to higher chromium contents. In addition, the behavior seems to be much more sensitive to oxygen pressure. Above 15% Cr, the oxidation rate of binary cobalt-chromium alloys diminishes with increasing chromium content, but until

achieving 25% Cr, the structure of the scale produced is much the same. At 760 torr (101,324 Pa) of oxygen, a continuous Cr_2O_3 layer is not formed until the alloy contains over 30% Cr, while at 2 torr (267 Pa) of oxygen, a continuous Cr_2O_3 layer may develop with as little as 20% Cr.

Achieving the Right Oxide Protection in Real Alloys. In general, protective oxidation involves the diffusional transport of one or more of the reactants through the oxide layer, and it is plainly desirable that an oxide with a slow transport rate should be formed. In practice, therefore, it is common to aim for a continuous CrO_3 layer, and the slow rates of oxidation in the binaries correspond to the establishment of such a layer. However, Cr_2O_3 can be lost by the formation of the volatile oxide Cr_2O_3, and the rate of volatilization starts to become significant at about 2012 °F (1100 °C) in still air.

From both the transport and the volatilization points of view, it is more desirable to form an Al_2O_3 oxide. The transport of aluminum through Al_2O_3 is between 2 and 3 orders of magnitude slower than the transport of the metal ions in the spinel oxides, and oxidation/volatilization is negligible at normal temperatures. From studies of oxide maps for the ternary Ni-Cr-Al and Co-Cr-Al systems, it was found that alloys containing relatively low chromium and relatively high aluminum will form predominantly Al_2O_3 scales.

In agreement with this conclusion, the cast lower-chromium, high-aluminum superalloys IN-713C and B-1900, respectively, are found to form predominantly Al_2O_3 scales. Of course, Al_2O_3 scales are also formed on the high-aluminum coatings that are based on NiAl and CoAl and are used to protect superalloys from environmental attack.

Numerous compositional and microstructural aspects of superalloys may affect the oxidation process. Cast versus wrought is one aspect, fine grain versus coarse grain another. Certain elements can influence the selective oxidation of another element. As previously noted, chromium is beneficial to the oxidation of aluminum, permitting aluminum to be selectively oxidized at lower aluminum concentrations than would be possible if no chromium were present in an alloy. Silicon and elements such as yttrium or hafnium may produce similar effects on selective oxidation. Hafnium-containing versions of standard superalloys seem to be more oxidation resistant than the nonhafnium-containing versions. When elements such as hafnium are present in alloys, they can be transferred to a coating during the diffusion process and enhance the system life.

Scale adherence is also a matter of importance, because turbine airfoils (blades and vanes) are subjected not only to very high temperatures but also to large numbers of severe thermal shocks in operation. Unfortunately, Al_2O_3 scales have relatively poor thermal shock resistance, whereas Cr_2O_3 scales are quite good and are particularly adherent when the metal contains minor amounts of rare earths or oxide dispersions (see coating sections in this chapter). A number of techniques have been used to increase the adherence of superalloy scales. Active elements such as hafnium (mentioned previously), use of precious metals, and dispersions of oxide particles have been used, mostly with coatings, but active elements have been incorporated in some superalloys (e.g., lanthanum in HA-188).

As superalloys are used in service, the oxide that has been formed as a continuous layer over the alloy (or coating) becomes damaged (see preceding information), owing to thermal stresses that cause cracking and resultant spalling of oxide scales. Subsequent oxidation (assuming a sufficiently high temperature for the correct oxide to form) results in a regeneration of the favored protective oxide. This process takes longer now, because the protective alloy element must diffuse a longer distance than it did during the initial oxidation. Each time the oxide cracks and spalls, more of the protective alloy element is being depleted by selective oxidation, and each successive regeneration takes a longer time. Eventually, the alloy or coating becomes so depleted of protective alloy element that it will no longer be possible for the protective oxide to be formed as a continuous layer over the alloy surface. Now the next most thermodynamically stable oxide will become dominant. At this point, the alloy may become unsatisfactory for further use. If the surface being degraded is a coating, it is time for removal and recoating of the base superalloy.

Mixed Gas Attack. Mixed gas attack involves all the factors so far discussed relative

to oxidation. The difference now is that there is competition among the elements in the gas for elements in the alloy. Although this is a complex situation, because many more reaction possibilities exist, the end result is the same. The most thermodynamically and kinetically favored phase (oxide, nitride, or whatever) will attempt to form over the whole superalloy surface as a continuous layer. The end result will be either the single continuous layer or a scale that contains a mixture of reaction products. The most effective reaction product barriers are oxides, and the best resistance to mixed gas attack remains a continuous oxide scale. Even when continuous oxide barriers are developed on alloys exposed to mixed gases, the situation is more complicated than atmospheres where only oxygen is present or is the only reactive gas. Other reaction products can develop in the alloy beneath the external oxide barrier. Such corrosion microstructures develop, because the other phases are also thermodynamically stable but just not as stable as the oxide that formed the external continuous scale. Secondary scale products are shown in Fig. 13.9 for pure nickel and for pure chromium to illustrate the potential for multiple scale products in mixed gas attack.

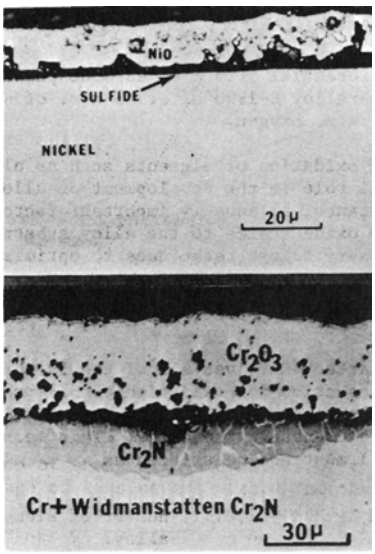


Fig. 13.9 Micrographs showing the formation of sulfide and nitride phases beneath the external oxide scales on nickel (top) and chromium (bottom) metals. Nickel exposed in flowing SO_2 for 8 h at 1000 °C (1832 °F). Chromium oxidized in air for 17 h at 1200 °C (2092 °F)

Hot Corrosion

Introduction. In many high-temperature applications of superalloys, the environment is much more corrosive than that involving oxygen in air. Under ideal conditions, degradation of alloy surfaces involves only reaction of the alloy surface with oxygen. This reaction forms a protective oxide film, which effectively limits the rate of alloy consumption to the extent that relatively long, useful lives are ensured. Most environments, however, involve some form of atmospheric or surface contamination, which can lead to accelerated corrosion and alloy consumption, often at catastrophic rates.

The operation of gas turbines creates the type of hostile environments, especially in the combustor and gas-generator sections, which can cause accelerated oxidation. This attack of alloy surfaces has been found to be caused by several types of contaminants, including gaseous contaminants that originate in the fuel and combustion air, as well as deposits in the form of solids or liquids that may condense from vapors also present in the combustion gas stream. But, as this discussion shows, this type of accelerated degradation is not limited to gas turbine applications but includes other applications such as boilers where superalloys will be exposed to combustion atmospheres and surface deposits.

In general, the defining characteristics of this high-temperature corrosion include the formation and deposition of salts such as sodium sulfate (Na_2SO_4), which may contain other constituents such as potassium, calcium, and magnesium, also as sulfates, and may contain chlorides (of the same elements). The hot gas stream may also contain vapors of the oxides of vanadium, lead, or other metals that may be naturally occurring (vanadium) in the fuel or present in the fuel from contamination (lead). Those kinds of contaminants tend to react with existing sulfate deposits to form a liquid or solid solution of sulfates or other species, such as vanadates. The essential defining characteristic of deposits formed on gas turbine blades and vanes is that of a sodium sulfate matrix usually containing other alkali metal or alkali

earth ingredients, sometimes traces of chlorides, and infrequently (in recent years), compounds of lead and vanadium.

The conditions in the combustion gas stream are thermodynamically and kinetically favorable for any alkali or alkali earth metals to be converted to sulfates by reaction of chlorides with sulfur dioxide and sulfur trioxide. An important consequence of this mix of sulfates, with or without the presence of other contaminants, is that the melting point may be depressed to the point that deposits may be liquid at temperatures as low as 1100 to 1200 °F (593 to 649 °C).

Terminology. Over the years, the accelerated corrosion caused by these deposits has been sometimes referred to as sulfidation (gas turbines) or fireside corrosion (coal-fired boilers), but in the gas turbine industry, the terminology ''hot corrosion'' has come to be universally used to define the form of elevated-temperature attack (e.g., >1200 °F (649 °C) caused by sulfate deposits. Under this umbrella, various mechanisms have been identified that have attempted to reconcile the metallurgical observations with the chemistry of corrosion processes. These mechanisms have attempted to explain the complex interactions between the gaseous environment, surface deposits, and alloy constituents that form the hot corrosion process. In addition, a substantial effort has been expended to understand the sources, the composition, and the mechanisms of the formation of the sulfate deposits.

Chemistry Leading to Hot Corrosion. The formation and deposition of sulfate deposits in gas turbines (or other machinery involving fossil-fuel combustion products) involves the reaction of impurities in the fuel and combustion air. The fuel is a source of sulfur and, to a lesser extent, may be a source of alkali metals, vanadium and lead, which are converted to sulfur oxides and sulfates. The combustion air is a major source of contaminants, such as sea salt, mineral dust, and others. Sea salt has as its major constituents sodium, magnesium, calcium and potassium chlorides, and sulfates; the proportions of chloride and sulfate are roughly 80 to 20 by weight. Minerals may enter the combustor as runway dust (calcium carbonates), sea sands, or iron-bearing particulates. Each of these can find its way into the surface deposits on hot alloy components.

In addition, transient combustion conditions may produce carbon deposits, which can increase the corrosivity of the deposit. Despite the complex chemistry of ingested contaminants, the composition of surface deposits has been carefully characterized by chemical analysis, and it has been found that they are principally sulfates; chlorides are rarely found except for machines operating at sea. Some fuelborne contaminants have been significantly reduced through improved refining (sulfur), selection of crude oils (vanadium), or from storage and transportation (lead). Control of airborne impurities has been more difficult; stationary turbines use air filtration methods.

Identifying Hot Corrosion. The first occurrences of hot corrosion on turbine hardware were seen as patches of extremely thick oxide scales, often green (then referred to as ''green-rot''), sometimes localized, and often so advanced that entire pieces of airfoils were consumed (Fig. 13.10). Microstructures of the remaining alloy exhibited severe alloy depletion and the presence of sulfides (hence ''sulfidation''), as indicated in Fig. 13.11. Laboratory studies eventually showed that the corrosion process could be modeled by sodium sulfate, or by contaminants selectively added to this sulfate, and by the manipulation of the gaseous environment over the sulfate deposit. These studies, in most cases, produced corrosion rates and morphologies indistinguishable from actual turbine corrosion.

It was determined that several types or mechanisms of corrosion attack could be identified, which depended on the quantity of salt present, the temperature, the gas composition, and the alloy composition. It was also found that cyclic thermal exposure tended to reduce the time needed for the hot corrosion to begin.

The period before the onset of severe attack is called the initiation stage, whereas the process of rapid, abnormal corrosion is called the propagation stage. In general, it is good to remember that the mechanisms—that is, both the metallurgical characteristics and the rates of attack—of both the initiation and propagation stages of attack will vary across a single superalloy component. These differences (for a single alloy or coating) result mainly from the nonisothermal environment and differences in the quantities of salt that are deposited on a component surface. It was

found, quite unexpectedly, for example, that corrosion rates for some materials at lower temperatures, for example, 1200 °F (649 °C), were significantly greater than rates at much higher temperatures, for example, 1800 °F (982 °C). Eventually, it was found that the mechanisms of corrosion in cooler regions of turbine blades and vanes are different from the hottest regions, and that alloys that were developed for high-temperature hot corrosion resistance did not always perform as well as expected at lower temperatures. Regardless of the differences in corrosion behavior corresponding to differing temperatures, all alloys exhibit an initiation and a propagation stage. Figure 13.12 provides a schematic diagram identifying factors that determine the transition from initiation to hot corrosion propagation.

Hot Corrosion as a Degradation Process. Hot corrosion is an accelerated oxidation process that occurs when a normally protective oxide scale is degraded or destroyed by a salt deposit and is unable to reform. Instead, the oxide scales that form tend to be porous and nonprotective of the alloy surface; consequently, rapid, often catastrophic, oxidation rates result. The degradation or disruption of the normally protective oxide scales such as Al_2O_3 and Cr_2O_3 can occur by several mechanisms, including penetration and/or stripping of the scale by chemical reaction of the salt with the oxide scale. Such ''fluxing'' reactions involve dissolution of the scales to form products such as aluminates and chromates, which are in solution in the salt. A requisite condition for fluxing to occur is that the salt be liquid or that a liquid be formed as a result of a solid-solid reaction. A second requisite condition for fluxing to occur is that the acidity (or basicity) of the molten salt be such that the oxide scale is thermodynamically unstable, therefore favoring the forma-

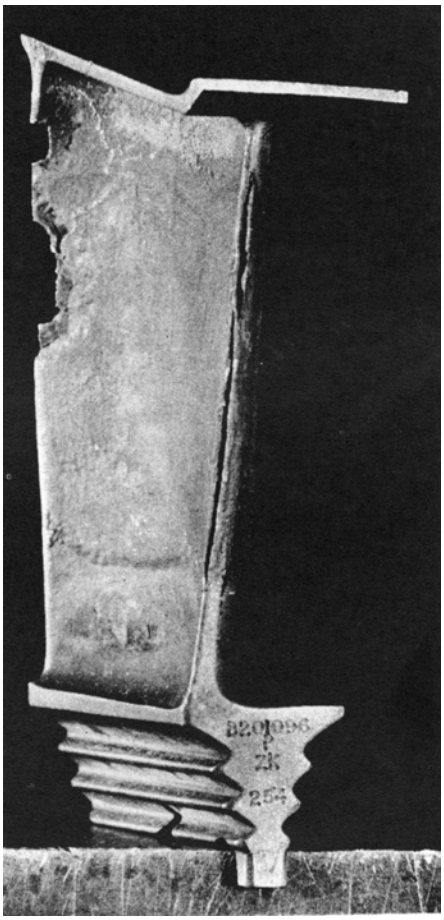


Fig. 13.10 Nimonic 100 nickel-base superalloy first-stage turbine blade from turboprop engine showing deterioration from sulphidation-type hot corrosion

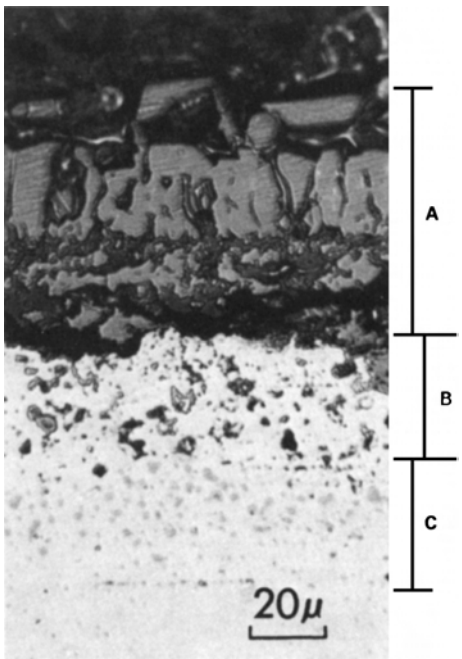


Fig. 13.11 Type 1 hot corrosion attack on a Ni-20Cr-2ThO_2 oxide-dispersion-strengthened superalloy. Specimen was coated with Na_2SO_4 and oxidized in air at 1000 °C (1832 °F). (a) Nickel-rich scale, (b) CrO_3 subscale, and (c) chromium sulfides

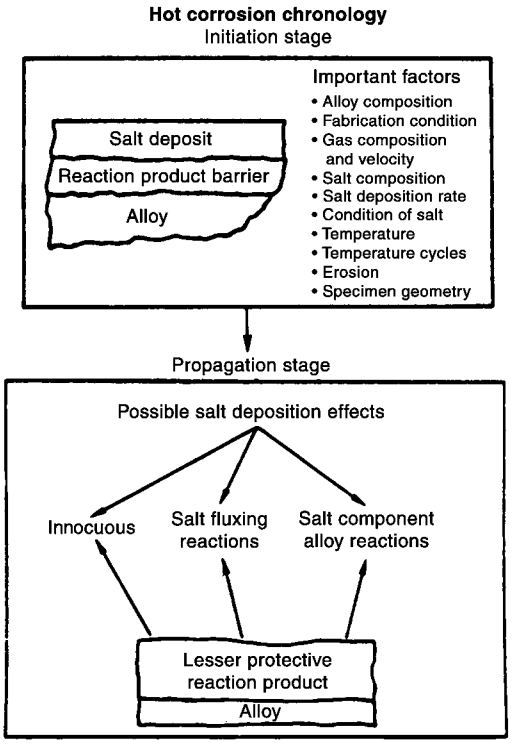


Fig. 13.12 Schematic diagram identifying factors that determine the transition from initiation to hot corrosion propagation

tion of a nonprotective (soluble) reaction product.

The liquid sulfate medium is important, because transport of reactants, such as oxygen and sulfur, and products such as aluminates is much more rapid in a liquid than for solid-state reactions; this rapid transport is a key aspect of corrosion rates that can be catastrophic. Even if the salt deposit freezes on the component surface, reactions with existing oxide scales may reduce the melting point of the deposit by hundreds of degrees so a liquid can be produced. Reaction of sodium sulfate with CoO is an example of this. Vanadium oxide can also react with sodium sulfate to lower the melting point of the deposit. Lower melting temperatures, of course, can set the stage for corrosion at lower component temperatures.

The acid-base character of the sulfate deposit is affected by many factors, including the partial pressure of sulfur trioxide in the gas stream; reactions with the alloy, which may deplete the melt of oxygen and sulfur; as well as by reactions with certain transition metal oxides. In describing acid-base molten salt reactions, it is useful to consider that these salts are ionic in nature, and that the melt is made up of sodium (+) ions as well as sulfate (=) and oxide (=) ions. It is the thermodynamic activity of oxide ions in equilibrium with sulfur trioxide that establishes the basicity of the melt; the sulfur trioxide activity (partial pressure) fixes the acidity.

The chemistry behavior of the deposits is analogous to aqueous corrosion in acid-base solutions, where the critical ionic species defining the basic side is the hydroxide ion or, for the acid side, the hydrogen ion. Reactions with alloys that consume oxide ions shift the chemistry of the molten salt to the acid side; conversely consumption of sulfur trioxide makes the deposits more basic. Oxides of superalloys and coatings can be unstable (be fluxed) in sulfate melts on either the basic side (basic fluxing) or on the acid side (acidic fluxing). These ''mechanisms'' of acid fluxing or basic fluxing can, of course, occur over a wide temperature range and are the principal causes of the hot corrosion of superalloys and coatings. It is useful to note that fluxing corrosion is not unique to superalloys or gas turbine engines but was recognized as the cause of corrosion of ferrous alloys used in coal-fired boilers. That corrosion involved acid fluxing by sulfate deposits where the acidity was established by high partial pressures of sulfur trioxide in the combustion gas.

Figure 13.13 provides a diagram identifying possible alloy systems susceptible to attack via the principal hot corrosion propagation modes. Subsequent sections discuss in somewhat greater detail the ways in which reactions between molten salt deposits and alloys can change the acid-base chemistry of the deposit to make it corrosive.

High-Temperature Hot Corrosion. While no exact temperature limits can be stated for the higher temperature regime of hot corrosion, there has been general agreement that high-temperature hot corrosion occurs in the approximate temperature range of 1600 to perhaps as high as 2000 °F (871 to 1093 °C). Historically, this was the range of temperatures used in laboratory tests, and the morphology of test specimens replicated to a high degree most of the corrosion features of turbine blades. Practically, the range of high-temperature hot corrosion is often set at 1600

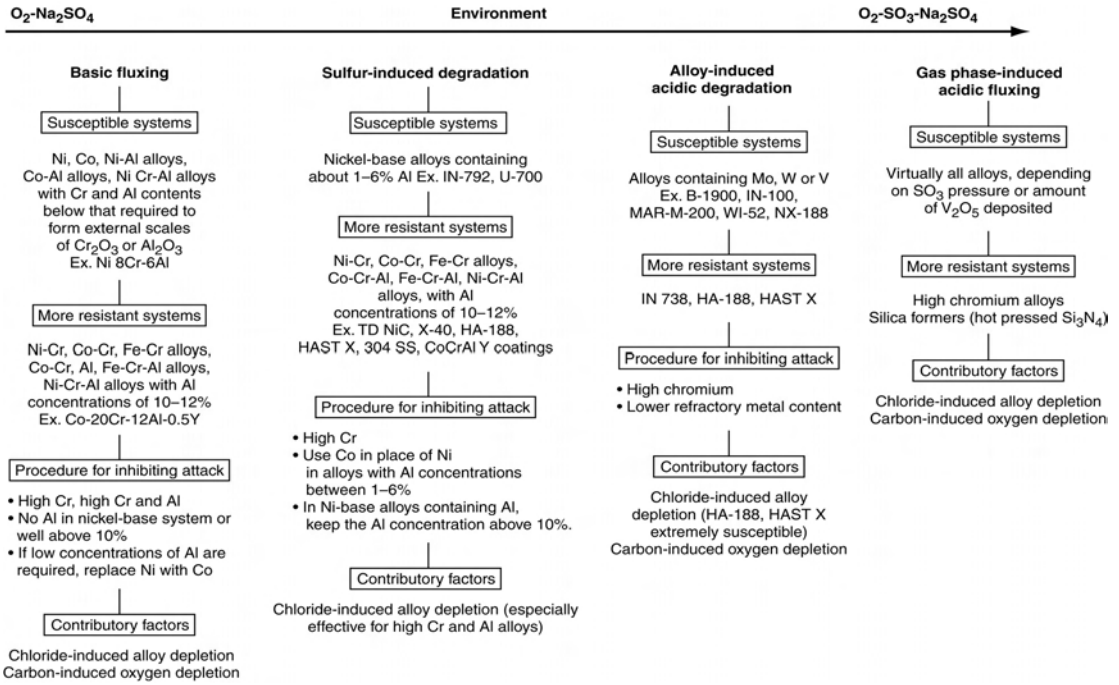


Fig. 13.13 Diagram identifying possible alloy systems susceptible to attack via the principal hot corrosion propagation modes

to 1850 °F (871 to 1010 °C). High-temperature hot corrosion, often referred to as type 1 hot corrosion, has usually been seen in aircraft turbines in the hotter regions of blades and vanes. Hot corrosion at high temperatures can occur by several mechanisms, depending on alloy composition.

Initiation of Type 1 Hot Corrosion—Model Systems. The hot corrosion of unalloyed cobalt and nickel as well as binary alloys with chromium, binary alloys with aluminum, and ternary alloys with chromium and aluminum all undergo basic fluxing during the initiation stage of attack. An understanding of these simple systems is useful, because they form the basis not only for superalloys themselves, but for coating systems as well.

Initiation begins with consumption of oxygen in the sulfate melt; oxygen depletion leads to increases in the thermodynamic activity of sulfur. The net result of both changes is an increase in the basicity (an increase in the oxide ion activity) in the molten deposit, which can flux the oxide scales (NiO, CoO, on nickel and cobalt; Al_2O_3 and Cr_2O_3 on the binary and ternary alloys). During this initiation stage, sulfur diffuses through the oxide scales to form sulfides in the metal or alloy beneath the scales. The composition or type of sulfides formed depends on the composition of the material, but they may be sulfides of nickel, cobalt, aluminum, or chromium. Depending on temperature, quantity of salt, and the type of oxide scale, the duration of the initiation period may be only a few seconds. Disruption of the oxide scales signals the transition to the propagation stage of attack.

For alloys that form Cr_2O_3, the initiation stage may be on the order of many hours, because, while Cr_2O_3 reacts somewhat with the basic melt, stripping of the scale does not occur. For these alloys, sulfur continues to migrate through the protective oxide scales to form sulfides of chromium and eventually of nickel. The formation of sulfides eventually causes disruption of the scales and the propagation process is initiated.

Similarly, Ni-Cr-Al and Co-Cr-Al alloys, which form Al_2O_3 during oxidation, may have extended initiation stages. For these systems, stripping of an initially-formed oxide film may be followed by the formation of

Cr_2O_3, which is more resistant to basic fluxing; initiation is thus extended. Eventually, however, sulfide formation leads to scale disruption and the propagation stage. Alumina-forming binary and ternary alloys with very high aluminum concentrations (i.e., >20 wt%) are able to maintain stable oxide films for longer periods; eventually, the formation of sulfides causes disruption of the scale and propagation ensues.

Ternary alloys of Ni-Cr-Al or Co-Cr-Al modified by additions of tungsten or molybdenum essentially behave as the ternary bases during the initiation stage of attack. Sulfides of chromium are formed, and salt deposits become basic to the point of destroying Al_2O_3 scales. The onset of propagation for these quaternary alloys may correspond with formation of sulfides, or the reaction of oxides of tungsten or molybdenum with the salt. Alloys that are capable of forming Cr_2O_3 after formation of Al_2O_3 has ceased have longer initiation stages; initiation ends as described previously.

Propagation of Type 1 Hot Corrosion—Model Systems. For cobalt and nickel, propagation is by basic fluxing; the molten salt deposits remain basic due to rapid oxygen uptake and sulfide formation; porous oxides form in the molten salt by precipitation. Corrosion continues as long as sulfate deposition continues.

Alloys with chromium or aluminum, or aluminum plus chromium, suffer propagation attack partly by oxidation of sulfides in the alloy zone beneath the oxide scale. This sulfur-induced mode of attack is sometimes referred to as sulfidation. Disruption of the oxide scales occurs by preferential oxidation of sulfides, which results in formation of SO_2 gas of sufficient pressure to rupture the scale. In high-aluminum alloys, the aluminum sulfide particles are oxidized; in binary nickel alloys with chromium and ternaries with aluminum plus chromium, oxidation of chromium and nickel sulfides occurs. In this case, the requisite condition is the presence of nickel sulfide phase as a liquid. While sulfidation attack is a part of the propagation mode, continued deposition of sulfate leads to conditions of basic fluxing in the outer portions of the scale and to oxidation of sulfides in the outer zone of the alloy itself. Cobalt binary and ternary alloys are not susceptible to this mode of attack.

Propagation corrosion of alloys containing molybdenum or tungsten occurs by acidic fluxing. Oxides of these elements react with the sulfate to produce strongly acidic conditions. This occurs when protective oxides are no longer formed on the alloys. The corrosion process is self-sustaining, in that decomposition of the salt is not required; the molten salt becomes a solvent for the dissolution and precipitation of oxides of all of the elements in the alloy. Protective scales cannot be formed, and a relatively uniform corrosion front moves inward to consume the alloy rapidly. There is very little alloy depletion and sulfide formation ahead of the corrosion front, owing to the speed of the corrosion process.

Type 1 Hot Corrosion—Superalloys and Coatings. Much of the high-temperature corrosion of superalloys and coatings can be explained on the basis of the behavior of the model alloys described previously. The initiation stages of all alloys occur as described previously. Depending on alloy or coating composition, the propagation stages may involve basic fluxing, basic fluxing/sulfidation, or acidic fluxing modes of attack. Some generalizations can be made for alloys and coatings alike: higher aluminum and chromium contents tend to promote longer initiation periods; certain strengthening elements such as molybdenum (B-1900), tungsten (MAR-M-200), or vanadium (IN-100), which can form acidic melts, tend to produce acidic fluxing and accelerate attack; tantalum, however, tends to be innocuous, from a hot corrosion standpoint.

Practical superalloy experience has demonstrated that high chromium contents are required for good corrosion resistance, as shown in Table 13.1. The trend in the 1960s to lower chromium while increasing alloy strength through the addition of other elements rendered most high-temperature alloys, particularly the high-strength casting alloys, very susceptible to hot corrosion. In the intervening years since hot corrosion problems were encountered with high strength alloys, chromium levels have been adjusted for alloys needing good corrosion resistance. For other alloys (e.g., PWA 1480 single-crystal nickel-base alloy), levels of chromium have been reduced to as little as 5% for use as airfoils that operate at temperatures above the high-temperature hot corrosion range.

Table 13.1 Effect of chromium content on the hot corrosion resistance of nickel- and cobalt-base superalloys

Alloy	Chromium content in alloy, %	Loss in sample diameter (a), mm (mils)			
		870 °C (1600 °F) 500 h	950 °C (1750 °F) 1000 h	980 °C (1800 °F) 1000 h	1040 °C (1900 °F) 1000 h
MAR-M-200	9.0	1.6 (64.4)	3.3+ (130+)	...	...
IN-100	10.0	3.3+ (130+)	3.3+ (130+)	...	...
SEL-15	11.0	3.3+ (130+)	3.3+ (130+)	...	...
IN-713	13.0	3.3+ (130+)	2.0+ (77+)	...	...
U-700	14.8	1.7+ (66+)	1.6 (63.9)	...	...
SEL	15.0	1.2 (45.8)	1.3 (51.8)	0.3 (11.4)	...
U-500	18.5	0.2 (7.6)	0.8 (31.7)	0.7 (29.3)	...
Rene 41	19.0	0.3 (10.3)	...	0.8 (30.8)	...
Hastelloy X	22.0	...	0.3 (12.0)	0.4 (15.2)	...
L-605 (alloy 25)	20.0	...	0.4 (15.3)	0.3 (11.3)	1.1 (41.9)
WI-52	21.0	0.5 (21.4)	0.5 (18.2)	...	1.9 (73.9)
MAR-M-509	21.5	...	0.3 (10.9)	...	0.8 (31.8)
MAR-M-302	21.5	0.14 (5.4)	0.3 (10.0)	...	0.6 (23.1)
X-40	25.0	0.11 (4.2)	0.3 (11.6)	...	0.5 (18.5)

(a) Results of burner rig tests with 5 ppm sea salt injection

In addition, practical superalloy experience is in general agreement with that derived from model alloys regarding the effects of molybdenum, tungsten, and vanadium. Examples of alloys found to be susceptible due to such elements include not only B-1900, MAR-M-200, and IN-100 mentioned previously but also such alloys as NX-188 and WI-52. Some earlier alloys such as U-700 and Waspaloy, while containing substantial levels of molybdenum, derive improved corrosion resistance from higher chromium levels than those in the high-strength casting alloys mentioned.

More recently, moderate-strength cast alloys such as IN-738 and higher-strength cast alloys such as IN-792 have achieved greatly improved corrosion resistance with significantly reduced levels of molybdenum, low levels of tungsten, and beneficial levels of chromium (12 to 15%). Another characteristic of IN-738 and IN-792 is the replacement of some aluminum with titanium. Some claims have been made that the additions of titanium have been at least partly responsible for the improved corrosion resistance of these alloys. On the other hand, beneficial effects of titanium have not been substantiated in laboratory tests. Rather, it seems more probable that the fact that these alloys (IN-738, IN-792) tend to form Cr_2O_3, rather than Al_2O_3, is the reason for the improved corrosion resistance.

In summary, alloy compositions with the higher-chromium, much-reduced molybdenum, substitution of tungsten and tantalum for molybdenum have virtually eliminated the propensity for acidic propagation corrosion.

Coatings such as the diffusion aluminides (see later sections in this chapter) represent surface modifications of the superalloys themselves. Most diffusion coatings contain all of the elements present in the superalloy, but these are diluted by the large quantity of aluminum. Depletion of aluminum and chromium can occur during type 1 hot corrosion initiation, after which propagation degradation can occur via preferential oxidation of sulfides, or partially by the acidic fluxing under the influence of certain refractory metals originating in the base alloy. The corrosion resistance of aluminides to high-temperature degradation has been increased by surface modifications using platinum (and some other noble metals) and by the incorporation of silicon (a characteristic of some slurry aluminides). These elements appear to prolong the initiation period by improving the integrity and adherence of the Al_2O_3 scales. However, the propagation modes appear to be the same as for normal aluminide coatings. Figure 13.14 shows the effect of a nickel-aluminide-type coating on improving the hot corrosion resistance of an IN-713 nickel-base superalloy turbine blade compared with an uncoated blade.

MCrAlY-type overlay coatings are discussed later in this chapter. The hot corrosion of such coatings occurs essentially as described previously for model alloys based on M-Cr-Al. The effect of yttrium introduced

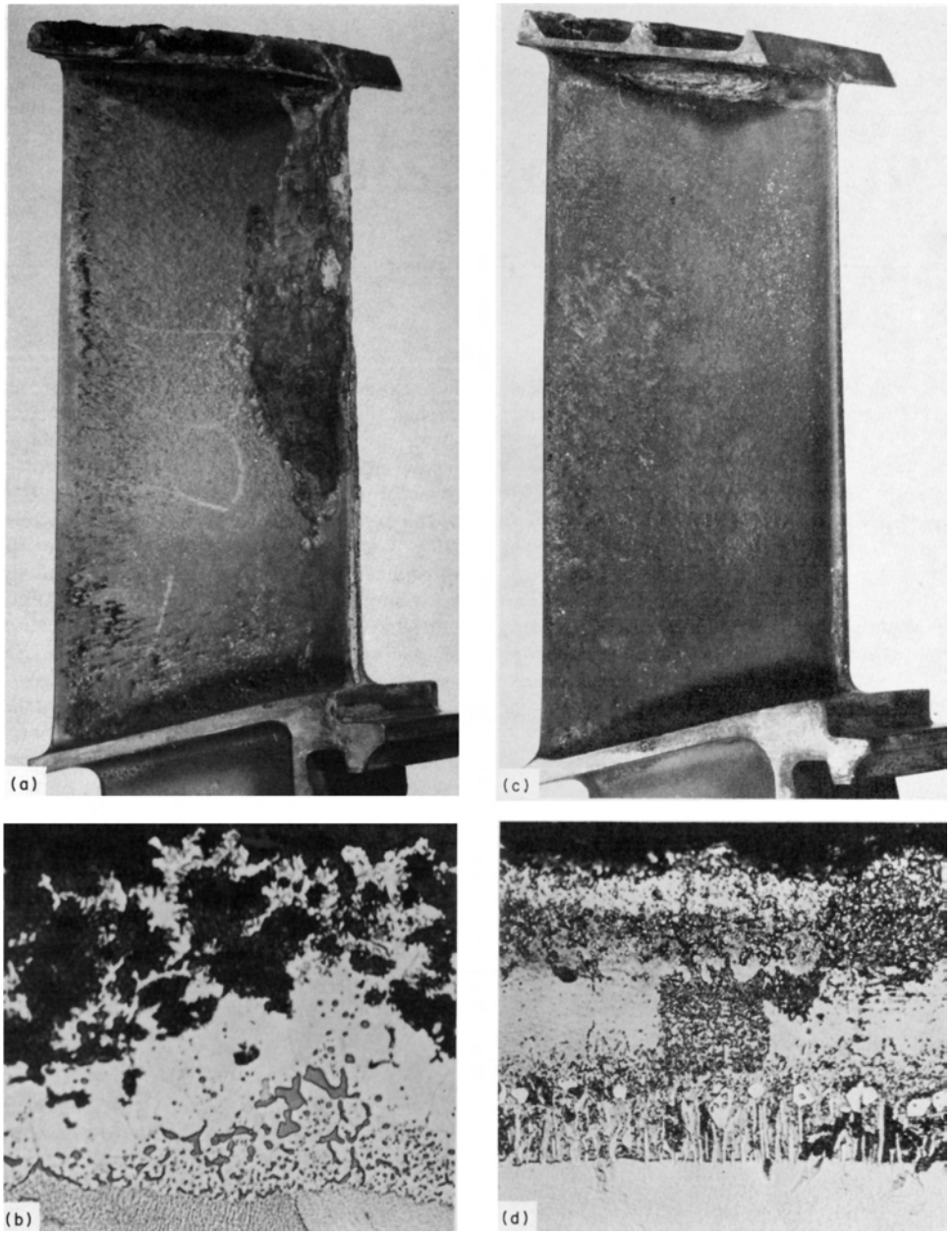


Fig. 13.14 Effect of a nickel-aluminide-type coating on the hot corrosion resistance of an IN-713 nickel-base superalloy turbine blade compared with an uncoated blade. (a) Uncoated blade after 118 test cycles, (b) micrograph showing severe degradation of IN-713 by hot corrosion, (c) aluminide-coated blade after accelerated hot corrosion testing in an engine, and (d) micrograph showing only slight degradation of coating

into the ternary M-Cr-Al is to improve the integrity and adherence of the Al_2O_3 scales, thereby prolonging the initiation stage. In addition, it is possible to further delay the onset of propagation through the control of the aluminum and chromium concentration, higher levels of each element being ''better'' in every case, depending on mechanical-property limitations.

In general, the group of MCrAlY coatings,

in which M = Ni or Ni + Co, has superior corrosion resistance versus those based on nickel alone. NiCrAlY coatings can provide improved protection of superalloys that have poor resistance, mainly by eliminating the interaction of the refractory metal constituents of the alloy with the environment and by extending the initiation stage. On the other hand, the propagation mode—preferential oxidation of sulfides (sulfidation)—is very rapid, leading to short coating lives in even moderate hot corrosion environments. However, additions of cobalt to NiCrAlY coatings greatly improves corrosion resistance. CoCrAlY coatings have the best resistance to attack at high temperatures for given levels of aluminum and chromium. This is due to the inherent resistance of cobalt-base alloys to the sulfidation propagation mode. The ability to tailor the chromium content of MCrAlY coatings to the airfoil environment has led to a series of coating compositions that target a range of hot corrosion conditions from mild (12 to 15% Cr) to severe (22 to 35% Cr).

Low-Temperature Hot Corrosion. The earliest studies of hot corrosion indicated that all attack was occurring at high temperatures, for example, >1650 °F (899 °C). In the early 1970s, however, modes of attack were observed—especially in marine and industrial turbines—that did not appear to be the same as seen previously. First of all, the temperature of the hardware was known to be lower; in particular, ''low-power'' operation of marine engines intended to improve airfoil life had the exact opposite effect. Some airfoils (even those with CoCrAlY coatings) had lives of only a few hundred hours. Based on laboratory studies, it was determined that the mode of hot corrosion attack was indeed different from those seen at higher temperatures. Because this was the second type of attack seen (historically), it is often referred to as ''type 2'' hot corrosion, or sometimes simply ''low temperature'' attack. Figure 13.15 provides a sketch of anticipated (A) oxidation attack rate and actual (B) test rig and engine hot corrosion rates for a nickel-base superalloy turbine airfoil. Low-temperature attack rates based on extrapolated rates from high-temperature oxidation tests or from intermediate-to-high-temperature hot corrosion rates underestimated the degree of attack.

Laboratory studies have shown conclusively that type 2 hot corrosion is due to acidic fluxing and occurs in the very approximate range of 1200 to 1500 °F (649 to 816 °C). This acidic fluxing arises from the inherent acidity of the as-deposited sulfates,

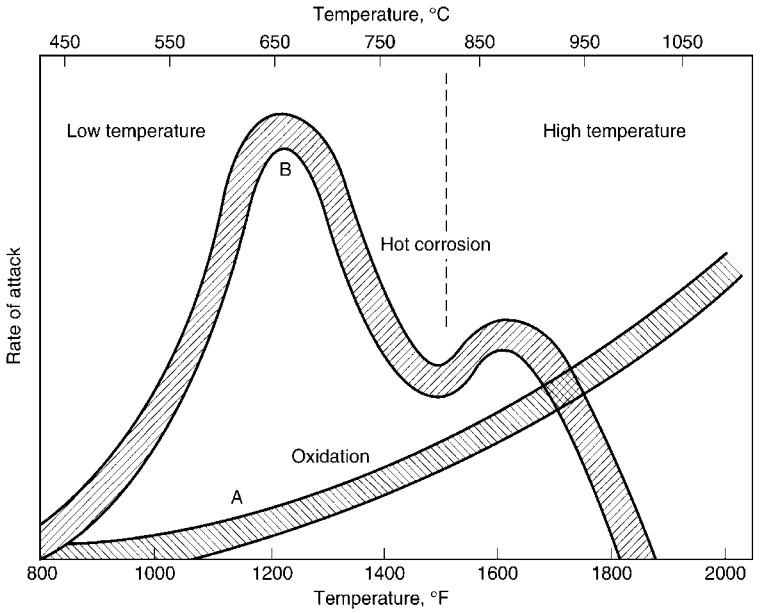


Fig. 13.15 Sketch of anticipated low-temperature attack rate (A) vs. actual (B) test rig and engine hot corrosion rates for a nickel-base superalloy turbine airfoil

whose acidity is caused by the partial pressure of sulfur trioxide in the combustion gas stream. The nature and mechanism of this corrosion is essentially identical with that which has been identified as the cause of fireside corrosion in coal-fired boilers. Figure 13.16 provides a more inclusive three-dimensional schematic illustration of the temperature and gas compositions over which hot corrosion propagation is important, showing the hot corrosion attack ''spiking'' in certain areas of the low-temperature hot corrosion regime. Figures 13.15 and 13.16 offer visual depictions of the hot corrosion regimes. Although both figures show the low-temperature peak in attack rate, the creators of Fig. 13.16 did not offer any indication of a high-temperature peak, such as seen in Fig. 13.15. Many investigators believe that there are two peaks in hot corrosion attack. It should be noted that actual temperatures and relative rates may differ from one investigation to another, so that differences may exist among laboratories and will exist for different components in service. A single turbine blade might exhibit a wide range of hot corrosion structures resulting from a variety of hot corrosion conditions.

Corrosion of superheater or reheater surfaces was found to have been caused by molten sulfate deposits at metal temperatures as low as 750 to 900 °F (399 to 482 °C). The corrosion reaction was driven by the acidity of molten sulfates, which dissolved iron oxide scales to form iron sulfates. The common factor in type 2 hot corrosion is the combustion of fossil fuels containing sulfur, which is oxidized to sulfur dioxide and sulfur trioxide in the combustion process. Higher sulfur concentrations in the fuel yield higher sulfur trioxide partial pressures. Thermodynamically, the presence of these sulfur-oxide gases causes the equilibrium between the sulfur oxides to shift to higher sulfur trioxide pressures at lower temperatures. This process increases the tendency for gas-phase acidic fluxing at lower temperatures. Cleaner aircraft jet fuels (not used for industrial turbines) tend to produce much less severe environmental conditions than do marine diesel oils (or coals) which are the typical fuels for marine and industrial gas turbine applications.

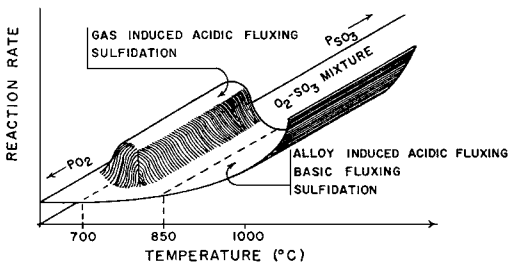


Fig. 13.16 Schematic illustration of the temperature and gas compositions over which hot corrosion propagation is important. Note the high rate shown at low temperatures by the gas-induced acidic fluxing

Type 2 Hot Corrosion—Superalloys and Coatings. Initiation and propagation attack of uncoated superalloys occurs by acidic fluxing. The initiation phase may involve reaction with oxides on the alloy surface with solid sulfate deposits to form liquid sulfate solutions containing aluminum, nickel, cobalt, or refractory metal ions. Chromium-oxide scales appear to be much more resistant to this type of attack. Often, the initiation is localized and is characterized by pitting attack associated with refractory metal carbides that intersect the surface. Pitting corrosion observed on turbine blade roots, and occasionally turbine discs, is caused by this type of attack.

Superalloy coatings exposed at low temperatures also degrade by acidic fluxing—both initiation and propagation stages. In general, the aluminide coatings, even platinum-modified coatings, which have good resistance at higher temperatures have poor resistance to this type of attack. Similarly, the performance of many overlay coatings, especially CoCrAlY coatings, has been poor in low-temperature applications. Laboratory studies have shown that this results from reaction of CoO with solid (or semisolid) sulfates to form liquids at temperatures as low as 1200 °F (649 °C). Once formed, the liquid is sufficiently acid to strip the normal Al_2O_3 scale; also, at lower chromium levels (e.g., <15 to 20%) in the coating, protective Cr_2O_3 cannot be formed, and corrosion rates are very rapid.

The benefit of increased chromium content in superalloys and MCrAlY coatings has been conclusively demonstrated. The development of IN-939 represents a major improvement in superalloy hot corrosion resistance over IN-738; this improvement in

corrosion resistance is attributable to the higher chromium levels (22% Cr), the low (2%) tungsten level, and the absence of molybdenum. Similarly, CoCrAlY overlay coatings with chromium levels in the range of 27 to 35% have significantly improved corrosion lives, particularly in marine and industrial turbine applications. It also has been determined in laboratory tests that CoCrAlY coatings modified with outer layers enriched by silicon were much more resistant to type 2 attack when compared with conventional coatings.

Effects Produced by Chlorides and Carbon. For many years, chlorides (such as those in sea salt) were suspected as playing a significant role in the hot corrosion process. This was particularly true for marine turbines and some industrial turbines operating in coastal installations. In some cases, analysis of salt deposits indicated that chlorides comprised several percent by weight of the sulfate matrix. Laboratory tests with mixtures of Na_2SO_4 and NaCl applied to the surfaces of superalloys and coatings clearly demonstrated that chloride can accelerate the hot corrosion of some alloys. On the other hand, detailed examination of test materials showed that the morphology of attack (i.e., the microstructures) was significantly different from those seen in corroded turbine blades. On this basis, it was concluded that although chlorides can make sulfate deposits more corrosive, the features caused by chloride-induced attack did not resemble hot corrosion of turbine hardware.

The occasional presence of carbon deposits on turbine airfoils, particularly during engine start-up, shutdown, or from fuel ''streaking'' caused by defective or clogged fuel nozzles, has also been suspect as an accelerating agent for hot corrosion. While the effects of carbon have not been as thoroughly studied as other contaminants, the potential role of carbon can easily be described—at least theoretically. The strong reducing potential of carbon is such that if it coexists with a sulfate deposit, the oxidizing potential (oxygen activity) of the sulfate will be reduced, and consequently, the sulfur activity will be increased. If sulfur diffuses through the alloy-oxide scale, thereby being removed from the melt, the melt will become more basic; basic fluxing of the alloy can potentially occur. The mechanism would be exactly like that which occurs during the corrosion of nickel, except in that case, the oxygen is removed from the melt by nickel. So, if present on the surface of an alloy or coating, carbon can be expected to make the sulfate deposits more basic, raising the possibility of accelerating the hot corrosion process.

Ranking Superalloy Hot Corrosion Performance. Although various attempts have been made to develop figures of merit to compare superalloys, these have not been universally accepted. Certain alloys have become what might be described as standards of nonexcellence. IN-100 (contains vanadium) and B-1900 (contains significant levels of molybdenum) rank as a 1.0 (at the bottom) on a relative scale of increasing corrosion resistance. Alloys such as MAR-M-200 rank higher, but not much better, at around 1.5 or so. The truly hot-corrosion-resistant alloys (but not of maximum high-temperature strength) such as IN-738 rank about 3.0 on a relative scale. The near standardization of such alloys as IN-738 and IN-939 for first-stage blades/buckets, and FSX-414 for first-stage vanes/nozzles in industrial gas turbines implies that these are the accepted best compromises between high-temperature strength and hot corrosion resistance, because such gas turbines must operate for longer times between inspections than aircraft gas turbines and at lower temperatures, which promote gas-induced acidic fluxing hot corrosion.

For maximum uncoated hot corrosion resistance, chromium contents in excess of 20% appear to be required. A typical alloy of this type is IN-939. However, such alloys are not capable of achieving the strengths of the high-volume fraction $(V_f)\gamma'$ alloys, such as MAR-M-247. Cobalt-base superalloys and many iron-nickel-base alloys have chromium levels in the >20% range, most nickel-base superalloys—especially those with high creep-rupture strengths—do not have high chromium levels because a high chromium content is not compatible with the high $V_f\gamma'$ required for maximum strength. Alloys with increased titanium contents (higher titanium-aluminum ratios), in combination with slightly increased chromium contents (12 to 14%), seem to have improved resistance. Thus, alloys with adequate strength together with improved resistance to hot corrosion have been produced (IN-738, IN-792, Rene 80). Higher titanium-aluminum ratios also

are not particularly compatible with maximum $V_f\gamma'$ and highest strengths. Some of the above alloys represent the compromises in strength that have had to be made for the sake of hot corrosion resistance. In order to have increased hot corrosion resistance and better strengths for industrial and marine power turbines, hot-corrosion-resistant superalloys such as IN-792 now are being investigated as single-crystal directionally solidified airfoil components.

Surface Protection Against Hot Corrosion. For applications requiring the highest strengths, coatings are required for moderate, but not exceedingly long, operating times between overhaul or inspection. Overlay coatings have the potential to provide the best surface protection, because wide flexibility is possible regarding composition variations to achieve maximum protection for a given application. For high-temperature applications, CoCrAlY coatings with 17 to 22% Cr and 10 to 12% Al have been found to provide excellent protection for all but the most severe salt environments. Alternatively, NiCoCrAlY coatings have demonstrated very good corrosion resistance and improved mechanical properties over CoCrAlY. For severe environments, chromium levels may be increased further.

Some modified diffusion aluminide coatings have shown excellent resistance to high-temperature attack. These include coatings with platinum or silicon surface enrichments.

For lower-temperature surface protection, CoCrAlY overlay coatings with very high chromium levels (25 to 35%) are required for maximum protection. Aluminide coatings have proved to be unsatisfactory for lower-temperature turbine airfoil service.

Some Alternatives for Stationary Turbines. Stationary turbines, such as those used in marine applications and for power generation, offer opportunities for control of environmental factors not practical for aircraft engines. Inlet air filtration is now widely used to reduce the levels of salt ingested. This has dramatically reduced the severity of hot corrosion. For engines required to use lower-grade fuels containing higher sulfur contents, or fuels containing vanadium, fuel additives may be used to mitigate acidic corrosion, especially at lower temperature. Oxides or other forms of magnesium and calcium have been used to neutralize the acidity of deposits. This approach has potential drawbacks, the foremost being the fouling of blade and vane surfaces with heavy deposits, which results in degraded aerodynamic conditions and reduced efficiency.

Lastly, it has been demonstrated that periodic washing of the entire engine (compressor, combustor, and turbine) with fresh water will effectively remove corrosive sulfate deposits.

Coatings for Superalloy Protection

Background. In the gas turbine and other similar applications, temperatures are high, and superalloy surfaces are degraded by oxidation and hot corrosion. Owing to the cyclic temperature fluctuations, surface cracking and spalling of oxide scales can occur during oxidation or during the initial stage of hot corrosion. Protection of superalloy surfaces is required to minimize the effects of oxidation, spalling, and hot corrosion. The available amounts of those critical elements, such as chromium and aluminum, which are selectively oxidized to form protective oxides on superalloys, are limited by mechanical-property considerations. The cyclic oxidation and hot corrosion properties of many superalloys are inadequate for desired applications. This is particularly true for those applications which require metal temperatures above approximately 1500 °F (816 °C). Moreover, as indicated previously, the lower-temperature limit for salt-induced hot corrosion may be as low as 1200 °F (649 °C). Thus, external protection is applied to superalloys in the form of coatings to protect against not only the high temperature but also the lower-temperature regions of hot corrosion and oxidation.

Early coating technology was based on simply increasing the surface concentration to a depth of a few mils (μm) of, for example, chromium or aluminum to form the corresponding protective oxides for a longer time under cyclic conditions. Contemporary coating technology now recognizes the desirability of improved oxide adherence to further prolong the effective use of these elements, particularly aluminum. Thus, the definition of enhanced oxidation resistance as a major requirement of protective coatings can be refined to include requirements for an

increased reservoir of those elements that form protective oxides, and enhanced adherence of those oxides under thermal cycling conditions.

Coating Types. Development of increased strength (increased $V_f\gamma'$) in nickel-base superalloys led to reductions in chromium content as noted previously. Although some alloys displayed an improved resistance to oxidation, owing to greater aluminum contents, not all were satisfactory in oxidation, and most were susceptible to hot corrosion. Intergranular and carbide attack also worsened as operating temperatures escalated.

Furthermore, some of the more oxidation-resistant alloys were found not only to be susceptible to hot corrosion, but to be very poor in resistance to it. Thus, as indicated previously, to protect against local oxidation and later, against hot corrosion and similar fluxing reactions, corrosion-protective coatings were applied to superalloys. In the 1980s and 1990s, ceramic thermal barrier coatings (TBC) were developed to reduce superalloy exposure temperatures. The TBCs are intended to let superalloys operate in a less demanding mechanical-property regime as well as to achieve benefits of reduced corrosion rates associated with lower temperatures. Substantial decreases in temperatures on component surfaces have been achieved through use of TBCs. Thermal barrier coatings commonly are used in conjunction with corrosion-protective overlay coatings that serve as a base-coat to bond the ceramic TBC outer coating to the superalloy.

Corrosion-protective coatings are of two types: aluminide or chromium (diffusion) coatings and overlay coatings. Use of coatings is a preferred method of protecting superalloy surfaces from environmental attack, because:

- Coatings (at least overlay coatings) can be tailored to the hostile environment anticipated.
- Development of base alloys for strength is less inhibited, because significant protection (but not all of the protection) is provided by the coating.
- Coatings provide an opportunity to refurbish worn surfaces after exposure and environmental attack without causing significant degradation of the base metal.

Considering a specific coating-base superalloy system, the major conditions that may affect surface behavior in a gas turbine are:

- Gas and metal temperature
- Gas composition, including extraneous contaminants
- Gas and metal temperature cycling
- Gas pressure and velocity

The coating–base alloy system is a concept that is important to grasp. As indicated previously, beneficial elements in the underlying superalloy can influence coating behavior in a favorable way. Conversely, detrimental elements can degrade coating performance. There are certain requirements for corrosion-resistant coatings to be used on superalloys for gas turbine use. They may be stated as follows:

- They must be resistant in the thermal stress environment.
- They must be metallurgically bonded to the substrate.
- They must be thin and uniform.
- They must have self-healing characteristics.
- They must be ductile enough to withstand substrate deformation without cracking.
- They must not degrade the mechanical properties of the substrate.
- They must have diffusional stability.

Aluminide (Diffusion) Coatings. The most common type of coating for environmental protection of superalloys is the aluminide diffusion coating, which develops an aluminide (CoAl or NiAl) outer layer with enhanced oxidation resistance. This outer layer is developed by the reaction of aluminum with the nickel or cobalt in the base metal.

Some use has been made of aluminides containing chromium or silicon, and, in recent years, extremely thin layers of noble metals such as platinum have been used to enhance the oxidation resistance of aluminides. The oxidation resistance of aluminide coatings is derived from formation of protective Al_2O_3 scales. Aluminide diffusion coatings generally are thin, about 2 to 3 mils (50 to 75 μm). They consume some base metal in their formation and, although deposited at intermediate temperatures, are invariably diffused at temperatures of about 1900 to 2050 °F (1040 to 1120 °C) prior to being placed in service. As an illustration of the benefits of

coatings in severe-duty environments, Fig. 13.14 shows the effects of an aluminide-type coating on the hot corrosion resistance of an IN-713 nickel-base superalloy turbine blade. Coatings properly selected and tailored for an application are very effective in preserving the underlying superalloy surfaces.

Overlay Coatings. These coatings generally are referred to as MCrAl or MCrAlY coatings and are derived directly from the vapor deposition process. They do not require diffusion for their formation. The constituent denoted by ''M'' in these designations has at various times been iron, cobalt, nickel, or combinations of nickel and cobalt. A high-temperature heat treatment at 1900 to 2050 °F (1040 to 1120 °C) is performed to homogenize the coating and to ensure its adherence to the substrate.

MCrAlY coatings are approximately twice as thick as aluminide coatings, and, through incorporation of yttrium to improve oxide scale adherence, overlay coatings can be made to have improved corrosion resistance. An advantage of MCrAlY coatings is that their compositions can be tailored to produce greater or lesser amounts of chromium or aluminum within the coating, and thus the protectivity and mechanical properties of the coating can be balanced for optimal performance.

Thermal Barrier Coatings. Thermal barrier coatings have provided enough insulation for superalloys to operate in temperature environments as much as 300 °F (149 °C) above their customary operating range. The TBCs are ceramics, most notably, plasma-sprayed (PS) partially stabilized zirconia. These ceramic coatings use an underlay of a corrosion-protective layer, which is typically a coating such as an MCrAlY that provides for oxidation resistance and the necessary roughness for topcoat adherence.

Thermal barrier coatings may not provide as much oxidation protection (arising from aluminum and chromium) as straight overlay coatings. However, the reduced temperatures on the MCrAlY layer in the TBC system and at the superalloy surface result in lower oxidation potential.

Diffused Aluminide Coatings

Background. Blades and vanes made from nickel- and cobalt-base superalloys that are used in the hot sections of all gas turbine engines are coated to enhance resistance to hot corrosion. The most widely used coatings are those based on the intermetallic compounds NiAl and CoAl, which are formed by the diffusion interaction of aluminum with surfaces of the nickel- and cobalt-base superalloys, respectively. Diffusion chromium coatings are also used to protect against certain forms of molten-salt hot corrosion. The majority of these diffusion coatings are manufactured by pack diffusion (''cementation'') and related ''gas phase,'' or out-of-contact, processes.

The first coatings widely used for the protection of superalloy gas turbine airfoils were based on surface enrichment of, for example, cobalt-based alloys. In particular, the alloy WI-52 which had limited oxidation resistance, experienced substantial life increases when protected with aluminum. Shortly after the application of aluminide coatings to cobalt-base superalloys, similar coatings were applied to nickel-base superalloys. Iron-nickel-base superalloys did not operate in regimes where coating was necessary. One of the earlier coatings widely applied was produced by diffusion of a slurry of an aluminum-rich alloy powder. The slurry was diffused at 1975 °F (1080 °C), and the alloy was then given its precipitation heat treatment. Later developments incorporated a more conventional pack cementation process.

Diffused Aluminides. Evaluation of the diffusion coating processes for aluminizing nickel- and cobalt-base superalloys revealed what were called two archetypal structural types, illustrated in Fig. 13.17. The structural types of diffusion coatings obtained are dependent on the aluminum (thermodynamic) activity in the particular fabrication process involved. This activity determines the nickel-aluminum intermetallic phase, Ni_2Al_3 or NiAl, formed on the alloy surface by reaction with aluminum species in the gas phase. Coating structures, such as shown in Fig. 13.17, are commonly referred to as ''inward'' and ''outward'' diffusion types.

Although slurry coatings worked reasonably well, better control of coating thickness was achieved in pack processes. Consequently, slurry coatings are no longer in general use. Diffusion coatings are usually applied by ''pack diffusion'' processes, which are a form of chemical vapor deposition

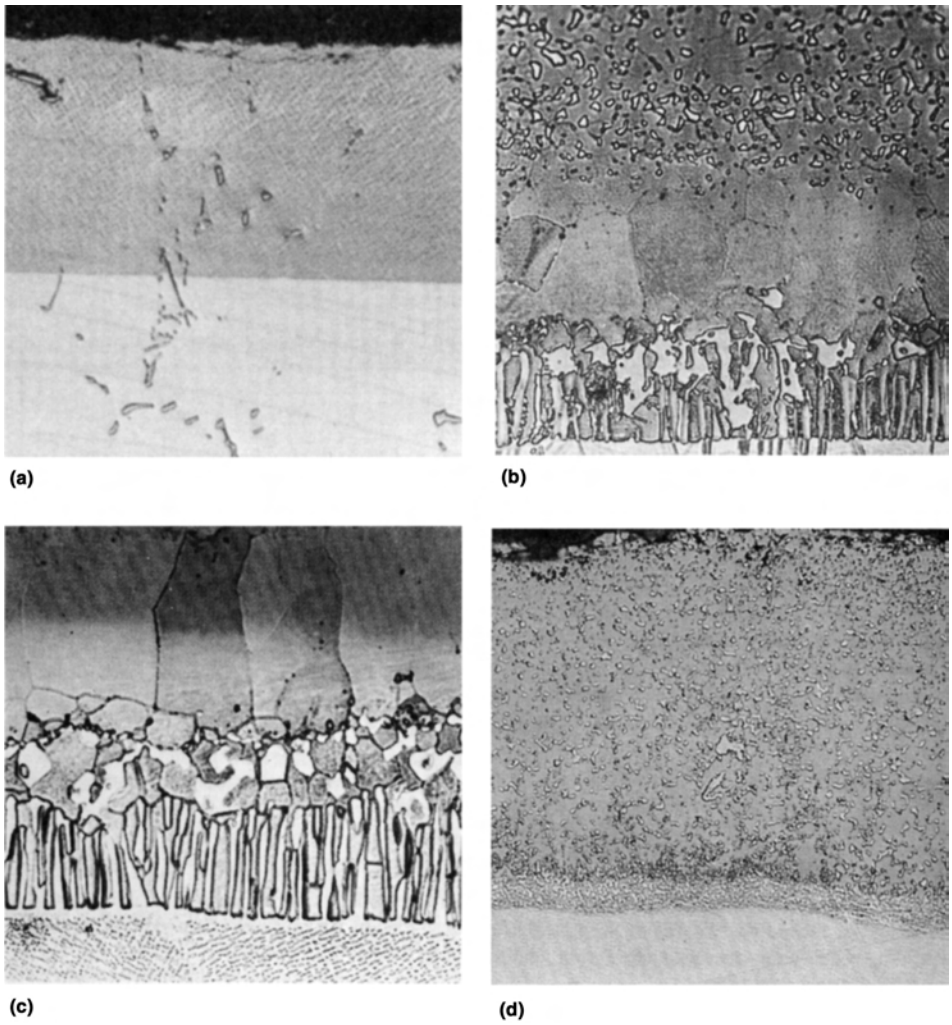


Fig. 13.17 Archetypical microstructures of aluminide coatings formed on a typical nickel-base superalloy. (a) Inward diffusion based on Ni_2Al_3, (b) same as (a) but heat treated at 1080 °C (1975 °F), (c) outward diffusion of nickel in nickel-rich NiAl, and (d) inward diffusion of aluminum in aluminum-rich NiAl

(CVD). The pack produces aluminum and other elements as gaseous metal halides, and these ''gaseous metals'' are transported through the pack to encounter the component to be coated and deposit on it, diffusing partly into the surface. Pack coatings are carried out at intermediate temperatures dependent on the chemistry of the pack and, to some extent, on the experience of the producer. In this respect, a pack process represents a heat treatment. Chemical vapor deposition, in the strictest sense, is the introduction of a vapor of predetermined composition into a coating chamber, where it reacts with accessible surfaces of a component. The resultant coating has greater throwing power than pack coatings when it comes to penetrating the cooling passage labyrinths of modern air-cooled turbine airfoils. Another aspect of CVD is its reported better control of vapor chemistry, which should have a beneficial effect on the coating chemistry produced.

Pack diffusion coating may be considered as a CVD process carried out with the aid of a powder mixture (pack) in or near which the part to be coated (substrate) is immersed or suspended and containing the element or el-

ements to be deposited (source), a halide salt (activator), and an inert diluent such as Al_2O_3 (filler). When the mixture is heated, the activator reacts to produce an atmosphere of source element(s) halides that diffuse in the pack and transfer the source element(s) to the substrate on which the coating is formed. The aluminide coatings continue to find use on airfoils in today's gas turbines. They provide only limited protection in gas turbine applications involving very high surface temperatures, for example, 2000 °F (1093 °C), or severe hot corrosion environments. However, they are still in very wide use in less demanding applications. Moreover, pack coatings are not line of sight (in contrast to overlay coatings) and can be used to coat internal cooling passages when a coating is desired. Oxidation and hot corrosion resistance of these coatings, as might be expected, are, in part, dependent on the base alloy composition. Modest improvements in oxidation and/or hot corrosion resistance have been achieved by modifying the superalloy surface with elements such as chromium or noble metals such as gold, palladium, or platinum prior to aluminizing.

Owing to the chemistry variations of superalloys, a given set of processing conditions for pack or CVD coating deposition will result in different coating chemistries and thicknesses on different alloys. All things being equal, a coating on a cobalt-base superalloy will probably be thinner than one on a nickel-base superalloy. The nature of the interdiffusion zone that forms where the coating and base alloy join can vary significantly, dependent on absence or presence of grain boundaries, presence of minor elements, and so on. As indicated previously, the presence of certain elements such as hafnium in the superalloy may have beneficial effects on the oxidation resistance of the coating/superalloy system.

Mechanical properties of aluminide coatings, typified by ductility and the related thermal fatigue resistance, are not amenable to significant improvement because of the inherent lack of low-temperature ductility of the intermetallic compound NiAl, which is the matrix of all such coatings.

Diffusion coatings based on surface enrichment with chromium received some attention in the early years of diffusion coating development. Chromizing became of interest and was applied in various forms to some of the first- and second-generation cast alloys, with limited success. Combinations of light chromium coating coupled with diffused aluminide coatings found some applications. Owing to the concerns about hot corrosion, there have been some limited applications of chromium diffusion coatings for protection of utility gas turbine airfoils, which do not operate at such high temperatures as diffusion aluminide coatings. Temperature capabilities of such chromium coatings are ultimately limited by the volatility of CrO_3, formed by reaction of Cr_2O_3 protective scales with oxygen. Surface enrichment of nickel-base superalloy coatings with silicon, chromium, and/or platinum has also been studied for protection against hot corrosion.

Coating Formation Mechanisms. Diffusion aluminide coatings on superalloys are classified by microstructure as being of the ''inward diffusion'' or ''outward diffusion'' type. The classification was derived from studies of aluminide coating formation on a typical nickel superalloy, U-700. It was observed that for pack mixes containing pure aluminum (unit or ''high'' activity), coatings formed by predominant inward diffusion of aluminum through Ni_2Al_3 and, deeper in the coating, through aluminum-rich NiAl (for pure nickel, by inward diffusion through Ni_2Al_3 only). The diffusion rates are high—practical coating thicknesses can be achieved in a few hours at 1400 °F (760 °C). A typical as-coated microstructure is shown in Fig. 13.17(a). Upon further heat treatment at, for example, 1975 °F (1080 °C) for 4 h, the microstructure shown in Fig. 13.17(b) is formed —the coating matrix is now NiAl. The single-phase region in the center of the coating is nickel-rich NiAl, grown by predominant outward diffusion of nickel from the substrate alloy to react with aluminum from the top layer. The inner layer, or so-called interdiffusion zone, consists of refractory metal (tungsten, molybdenum, tantalum, etc.) carbides and/or complex intermetallic phases in a NiAl and/or Ni_3Al matrix, formed by the removal of nickel from the underlying alloy, thereby converting its Ni-Ni_3Al structure to those phases.

If the activity of aluminum in the aluminum source is reduced (by alloying with, for example, nickel or chromium) to a level where nickel-rich NiAl is formed at the sur-

face, the coating, shown in Fig. 13.17(c), grows by predominant outward diffusion of nickel from the substrate to form NiAl by reaction with aluminum from the source. The lower layer of this coating is formed as previously described. Diffusion rates are relatively low, so the coating process must be carried out at higher temperatures—usually greater than 1832 °F (1000 °C). A coating with a matrix of NiAl formed by this diffusion mechanism is shown in Fig. 13.17(d). Upon further heat treatment, this coating will stabilize with a structure similar to that shown in Fig. 13.17(b).

The preceding mechanisms apply equally to those coatings formed by out-of-contact or CVD processes, from slurry ''slip packs,'' and from aluminum alloy powders deposited on superalloys by slurry spraying or by slurry electrophoresis. Coatings applied by spraying (or electrophoretically depositing) aluminum on the component and then heat treating, form a coating by causing dissolution of the superalloy into the melt until the melt solidifies. This step is followed by diffusion of aluminum, similar to that described previously.

All known aluminide-based coatings on nickel superalloys, including those modified by chromium, platinum, and silicon, have one of the archetypal microstructures described previously. It is anticipated that similar mechanisms apply to the coating of cobalt superalloys. The absence of aluminum in many of these alloys precludes the formation of the interdiffusion zone common to most nickel superalloys. Rather, a refractory metal (tungsten, chromium) carbide forms at the juncture to the base alloy. As described for similar nickel-base alloys, this refractory metal carbide and Al_2O_3 formed from oxygen in the aluminum-free alloys can also compromise the adherence of the coatings. Special processing conditions, involving slow coating growth at high temperatures (up to 2000 °F, or 1095 °C) from relatively low-aluminum activity sources, can sometimes be used to achieve satisfactory coating adherence. Minor additions of aluminum (1 to 2%) to cobalt superalloys completely obviate these problems—stable interdiffusion zones then form analogous to those on most nickel superalloys.

Coating Protection and Degradation. Simple aluminide coatings resist high-temperature oxidation by the formation of protective layers of Al_2O_3 and can be used up to about 2100 °F (1149 °C). The coatings degrade by loss of aluminum due to spalling of oxides under thermal cycling conditions. Certain reactive elements, such as hafnium in a base superalloy, may be introduced into a coating during aluminizing by an inward coating process. If this happens, the reactive element may significantly improve adherence of the protective Al_2O_3 scales and therefore extend coating life. Unfortunately, although oxidation resistance of certain superalloys (e.g., PWA 1487, HA-188) is markedly increased by better scale retention promoted by reactive element additions (as is the oxide scale on overlay coatings), it is rare for such reactive elements in the base superalloy to be transferred to a diffused aluminide coating.

At temperatures above about 1832 °F (1000 °C), interdiffusion of the coatings with substrates contributes significantly to degradation. Practical coating service lives are limited to operating temperatures of 1600 to 1800 °F (870 to 980 °C), with only short excursions at the highest temperatures.

Chromium modifications, made by diffusion chromizing prior to aluminizing or by codeposition of aluminum and chromium, have enhanced resistance to various forms of molten-salt hot corrosion. Electroplating with a thin layer of platinum (or, possibly, gold, palladium, or rhodium) followed by aluminizing forms a coating with substantially improved resistance to both oxidation and high-temperature (type I) hot corrosion. Additions of up to about 5% Si improve both oxidation and hot corrosion resistance. Silicon can be codeposited with aluminum by pack cementation and related out-of-contact processes. So-called slurry processes, wherein a liquid suspension of aluminum and silicon powders is applied to the alloy surface, then dried and fired at elevated temperatures, can also be used to incorporate silicon.

The oxidation and hot corrosion resistance of these coatings are more or less influenced by the composition of substrate alloys, as mentioned previously. Tantalum and hafnium in the base alloy improve cyclic oxidation and hot corrosion resistance of inward-type coatings, the latter element by improving the adherence of the protective layer of Al_2O_3. Molybdenum, vanadium, and tungsten, when present in the base alloy and incorporated

into an inward diffusion coating, compromise hot corrosion resistance.

Technology of Diffusion Coatings. A flow path for a typical production-scale pack cementation process is shown in Fig. 13.18. The process of creating a coating includes not only the coating process but other details as well. Some routine facets of coating application may include:

- Precoating inspection
- Surface preparation
- Masking

Visual and flow inspection of cooled airfoils before coating affords a last opportunity to determine if all surfaces are suitable for the intended use. Oxidized surfaces and the remains of investment casting core and shell materials can interfere with coating deposition and compromise useful service lives.

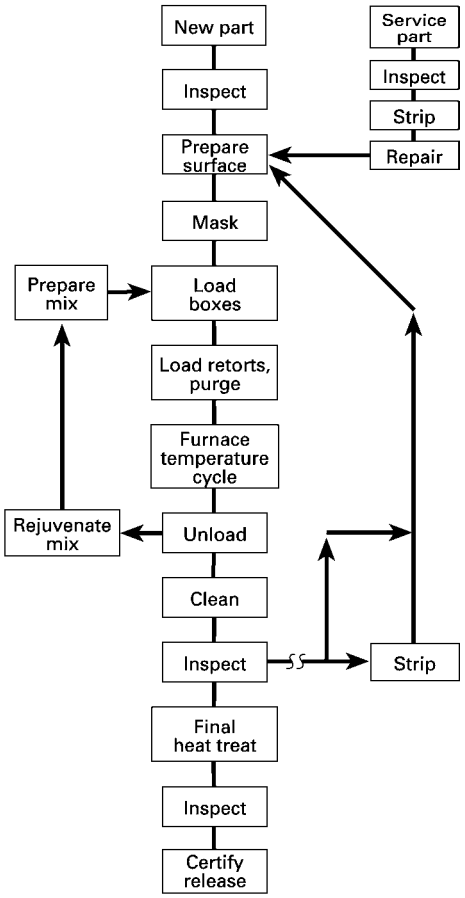


Fig. 13.18 Flow diagram for typical pack diffusion coating process

Surface preparation to remove superficial oxides may be accomplished on PC cast superalloys by grit blasting with intermediate-sized alumina grit. Silicon carbide grit is not used. Entrapped carbide can form low-melting eutectic phases with superalloys on subsequent heat treatment. Directionally solidified nickel-base superalloys may not permit grit blasting out of concern about development of recrystallized surface grains which, if formed, would degrade mechanical properties. Vibratory finishing may be used where a surface finish is specified to achieve a design intent. Removal of oily machining residues from surfaces by vapor degreasing or low-temperature burnout may be required before coating.

Masking may be required to prevent coating on critical mechanical contact surfaces. This can be accomplished with mechanical, oxide barrier, or chemically reactive masks. Complete exclusion of coating by mechanical masks is difficult for processes with high throwing power, a property common to dissusion coating processes run at higher temperatures, for example, >1600 °F (871 °C). Coating before machining, to obviate expensive masking requirements, is recommended.

Furnaces with specified temperature capability and uniformity and associated inert gas delivery systems are required and are the most costly components of coating plants. For most processes, coating boxes are loaded into retorts constructed of high-temperature alloys and are capable of being sealed (sand, glass, or water-cooled seals) to exclude air. A supply of inert gas, argon, or hydrogen is required to purge retorts free of air and moisture and to maintain an inert environment during the coating cycle.

A coating cycle includes bringing the retort and contents to temperature, holding at temperature for several hours, and then cooling to ambient temperature while maintaining the inert gas environment. Coating temperatures range from 1200 °F (649 °C) for low-temperature inward diffusion aluminizing to as high as 2100 °F (1149 °C) for outward diffusion aluminizing of nickel superalloys. Processing times range from 4 to 24 h, respectively. Some examples of time-temperature cycles are given in Table 13.2.

Unloading the retorts and boxes, separating the parts from powders and masking devices, and cleaning the parts, including thorough

Table 13.2 Information on pack diffusion coating process parameters

Coating type	Source composition	Processing parameters
Pack aluminizing, inward diffusion in Ni_2Al_3 in nickel alloys(a)	5–20% Al (Al-10Si), 0.5–3% NH_4Cl, balance Al_2O_3 powder	1 to 4 h at 650 to 680 °C (1200 to 1255 °F) in air, argon, H_2; heat treat 4 to 6 h at 1095 °C (2000 °F) in argon
Pack aluminizing, inward diffusion in NiAl in nickel alloys(b)	44% Al, 56% Cr NH_4Cl, balance Al_2O_3 powder	5 to 10 h at 1040 °C (1900 °F) in vacuum (argon, H_2)
Pack aluminizing, outward diffusion in NiAl in nickel alloys(c)	2–3% Al, 20% Cr, 0.25% NH_4HF_2, balance Al_2O_3 powder	25 h at 1040 °C (1900 °F) in argon
Pack aluminizing of cobalt alloys(d)	8% Al, 22% Cr, 1% NH_4F, balance Al_2O_3 powder	4 to 20 h at 980 to 1150 °C (1800 to 2100 °F) in argon
Gas-phase aluminizing, outward diffusion in NiAl in nickel alloys(e)	10% CO_2Al_5, 2.5% NaCl, 2.5% $AlCl_3$, balance Al_2O_3 powder	3 h at 1095 °C (2000 °F) in argon
Gas-phase aluminizing, outward diffusion in NiAl in nickel alloys	30% Al–70% Cr alloy granules, NH_4F	4 h at 1150 °C (2100 °F) in argon
Pack or gas-phase chromizing of nickel alloys(f)	15% Cr, 4% Ni, 1% Al, 10.25% NH_4Br or NH_4Cl, balance Al_2O_3 powder	3 h at 1040 °C (1900 °F) in argon

(a) U.S. Patent 3,544,348. (b) U.S. Patent 3,625,750. (c) U.S. Patent 3,716,398. (d) U.S. Patent 3,257,230. (e) U.S. Patent 4,132,816. (f) U.S. Patent 3,801,353

water washing, are currently labor intensive. Blades and vanes usually require further heat treatment to cause proper development of the coating and/or to obtain optimal mechanical properties of the substrate alloy. Such treatments require inert or vacuum environments with the same rigid temperature controls as the coating thermal cycle (see Chapter 8).

Overlay Coatings

Background. When gas path temperatures began to rise significantly for airfoils in aircraft gas turbines, it was surmised that a higher-aluminum content coating would be beneficial to long-time oxidation resistance of superalloys. Aluminum (and especially chromium) content of coatings applied by pack or CVD is limited by thermodynamic conditions. An overlay of a corrosion-resistant material not applied by diffusion processes might provide a greater aluminum reservoir, by virtue of a thicker coating. At the time (mid-1960s) when such thoughts surfaced, the electron beam furnace and similar devices became available, at least on a contractual basis. It was thought that the evaporation of a suitable coating material could be accomplished by impingement of an electron beam, and that the resultant vapor produced could be deposited (by line of sight) on a suitable component. Thus, electron beam physical vapor deposition (EBPVD) became a superalloy coating method. Probably the first material used for EBPVD of such a coating was a variant of Kanthal (Kanthal Corp.), a heating element material. This was the origin of FeCrAl coatings and the overlay coating process. Subsequently, CoCrAl and NiCrAl materials and combinations (NiCoCrAl) thereof were deposited and tested. The concept of an active element addition was introduced, and the MCrAlYs were born.

Overlay coatings differ from diffusion coatings in that interdiffusion of the coating with the substrate is not required to generate the desired coating structure/composition. Overlay coatings do not rely on reaction with the substrate for their formation. Instead, a prealloyed material applied over the substrate determines the coating composition and microstructure. However, adhesion of the coating to the substrate is effected by some elemental interdiffusion.

MCrAlY Coatings—General. Overlay coatings, typified by the so-called MCrAlY series (where M = iron, cobalt, nickel or combinations thereof), allow increased flexibility of design of compositions tailored to a wider variety of applications. A structure typical of contemporary overlay coatings is shown in Fig. 13.19. With MCrAlY coatings, oxidation resistance, hot corrosion properties, and ductility can be varied over wide ranges to meet requirements for aircraft, utility, and marine propulsion applications. MCrAlY coatings are widely applied on a production scale. Although originally produced by

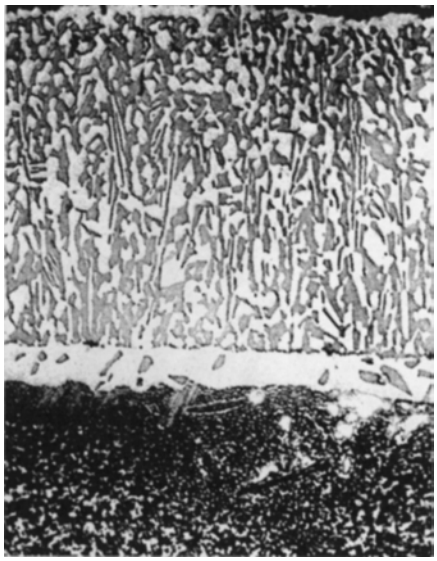


Fig. 13.19 Typical MCrAlY overlay coating. Gray phase is CoAl or NiAl dispersed in white nickel or cobalt solid solution

EBPVD, various other processes for coating fabrication, such as plasma spray (PS), sputtering, and foil cladding, were evaluated.

These coatings essentially comprise a monoaluminide (MAl) component contained in a more ductile matrix of solid solution (γ), in the case of CoCrAlY coatings, or a mixture of γ and γ' Ni_3Al phase, in the case of NiCrAlY coatings. NiCoCrAlY and FeCrAlY modifications also are available. The matrix is nickel- or cobalt-base and contains a rather large amount of chromium and an intermediate amount of aluminum. Aluminum provides the primary protection against oxidation through the formation of a slow-growing (Al_2O_3) scale. The supply of aluminum for formation of protective (Al_2O_3) scales comes largely from the dispersed MAl phase during the useful life of such coatings. The contained chromium is important in combating hot corrosion and also increases the effective aluminum chemical activity.

Not only is the life of an overlay enhanced over standard diffusion coatings, but also the solid-solution matrix of the overlay provides a ductility level in this coating class that is generally not possible with diffusion coatings. Figure 13.20 shows the ductility differences between CoCrAlY overlays and the nickel-aluminides that make up standard diffusion aluminide coatings. The enhanced ductility imparts much improved resistance to thermal fatigue cracking (refer to Chapter 12). A small amount of yttrium usually is included in overlay coatings to improve the adherence of the oxidation product.

MCrAlY Coatings Specifics. In the MCrAlY family, CoCrAlY coatings are recognized as being superior in hot corrosion resistance, whereas NiCrAlY coatings possess the better oxidation resistance. The range of NiCoCrAlY coatings may be tailored for a desired compromise between oxidation and hot corrosion resistance. MCrAlY coatings may contain 15 to 25% Cr, 10 to 15% Al, and 0.2 to 0.5% Y in addition to the basis nickel, cobalt, or nickel plus cobalt matrix constituents. Iron is not normally used for MCrAlY coatings at this time.

The general features of MCrAlY coatings are:

- An oxide scale on the outer surface
- Immediately beneath the scale, material that has a modified composition depleted in aluminum
- A layer of the coating alloy
- An interdiffusion zone in contact with the substrate

The composition and microstructure of the coating alloy depend on postdeposition treatment and service exposure. The interdiffusion zone functions as a bonding layer between coating and underlying alloy substrate. The composition of overlay coatings, as well as that of the substrate, affects the extent of coating-substrate interdiffusion during service. Coating composition may be adjusted to achieve a good thermal expansion fit with a given superalloy substrate.

Technology of Overlay Coatings. Overlay coating processes of primary importance today are EBPVD and PS. The EBPVD technique generally produces higher-quality coatings, while PS has an equipment-cost advantage.

Electron beam physical vapor deposition emerged in the 1960s as the primary overlay coating production method. The process allows the deposition of metals via vapor transport in a vacuum without the need for a chemical reaction. The vapor source can be produced by several methods, but electron beam (EB) evaporation is the most commonly used technique for coating turbine

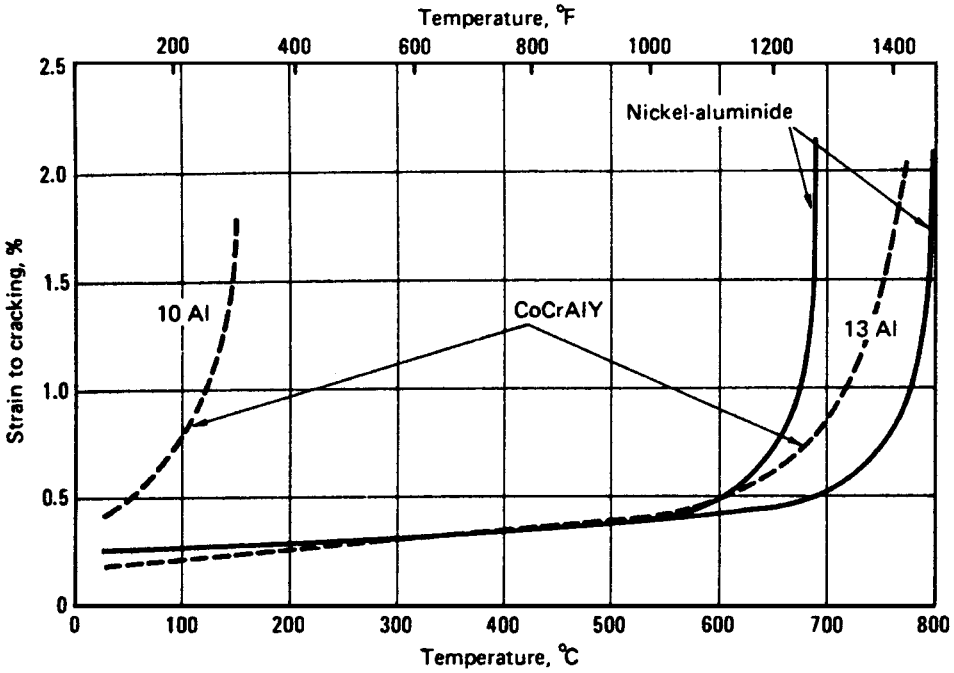


Fig. 13.20 Ductility of CoCrAlY overlay and standard diffused aluminide coatings showing ductility improvements possible with appropriate overlay compositions

components. A cloud of metal atoms impinges on the preheated part surface and condenses out into equilibrium or metastable phases. Carrying out the process at elevated temperatures promotes the formation of a dense coating and coating adhesion.

The chemistry of the deposited coating (before heat treatment) is not the same as the chemistry of the ingot that is vaporized to produce the coating. Owing to differences in the vapor pressures of the constituent elements, the evaporation rate and consequent transport of metal atoms produce a changed chemistry.

The EBPVD process results in an as-deposited coating structure that is typically oriented perpendicular to the substrate surface (columnar structure). This is caused by fast-growing grains of the coating alloy that propagate through the coating thickness. Separations between adjacent grains of the deposited coating, known as leader defects, or columnar voids, often are present, especially on convex surfaces. Shot peening and laser glazing can be used to close these defects to prevent premature corrosive attack and thermal fatigue cracking. The microstructure of an EBPVD coating also can be altered by varying the substrate temperature and by bombarding the substrate with energetic particles, such as plasma or ion beam, that can break up the columnar structure and improve coating density.

Plasma-sprayed coatings are produced by injecting a prealloyed powder into a high-temperature plasma gas stream (via a PS gun) and depositing the melted particles on the substrate surface. The molten particles solidify on contact, forming the coating. The process generally is carried out in a low-pressure vacuum chamber (hence the term low-pressure plasma spraying, or LPPS), which minimizes the formation of oxide defects within the as-deposited coating. Alloy chemistry of the ingot to be melted and sprayed will differ from that of the EBPVD process, because the complete ingot is melted, not selectively vaporized, and the chemistry on impact at the component should be the same as that melted into the plasma gas stream.

The high velocity at which the molten metal particles are directed at the substrate

causes the molten droplets to ''splat'' against the substrate and spread out in a direction parallel to the surface. A typical as-coated microstructure contains splat interfaces parallel to the surface. A diffusion heat treatment eliminates the individual splat layers, and the resulting structure assumes a two-phase nature similar to that of an EBPVD coating. The surface finish of a PS coating generally is rougher than that of an EBPVD coating. A finishing operation, such as abrasive slurry or controlled vapor blasting, can be used to achieve the required smooth surface.

In the same manner as for diffusion coatings, it is important to note that the task of creating a coating includes not only the coating process but other details as well. For overlays, some routine facets of coating application also may include:

- Precoating inspection
- Surface preparation
- Masking

Cleanliness and attention to detail is always important in the technology of superalloys, and never more so than in the preparation for coating and actual coating of components.

MCrAlY Protection and Degradation. The composition and microstructure of the deposited film are the two major factors that determine overlay coating corrosion resistance. The typical composition of a MCrAlY film is 20% Cr, 10% Al, and 0.3% Y, with the balance (M) being iron, cobalt, nickel, or nickel-cobalt. Acceptable composition tolerances depend on the specified nominal composition. The compositions of films obtained in practice usually fall within acceptable tolerance ranges. For example, if the chromium range specified for a NiCoCrAlY deposit is 16 to 22%, the range for a production coating will be approximately 16.5 to 21.5%.

The oxidation pattern of MCrAlY overlay coatings is similar to that of diffusion aluminide coatings. Elements such as yttrium improve the resistance of the Al_2O_3 scale to spalling. The most widely used overlay coating for oxidation resistance is the NiCoCrAlY type. The addition of cobalt also improves coating ductility.

In the oxidation process, grains of aluminum-rich β phase convert to islands of γ', eventually leaving only the less oxidation-resistant γ matrix phase. Substrate composition can influence oxidation resistance. Similarly, the addition of elements such as silicon, tantalum, and hafnium to the overlay can improve oxidation resistance, although at the expense of some ductility. Compositional flexibility offers the opportunity to tailor overlay coatings for optimal performance.

The resistance of MCrAlY coatings where hot corrosion is severe has been improved in direct proportion to increases in the chromium content. For maximum airfoil life, especially in marine and industrial engines, levels of 25 to 35% have been used. In addition, CoCrAlY coatings are more resistant to the effect of sulfur-induced attack and are therefore more effective than MCrAlY coatings containing Ni or Ni + Co. This increase in performance is achieved at some expense to ductility.

One interesting aspect of overlay coatings is that MCrAlY overlay coatings have a higher melting point than diffusion coatings. This means that when temperatures get too high, melting does not occur in the interdiffusion zone at temperatures lower than the melting point of the bulk coating. Overlay coatings have survived exposure temperatures as high as 2350 °F (1288 °C) without melting.

Thermal Barrier Coatings

Background. The hot corrosion (and oxidation) resistance of coated turbine blades can be further improved by applying a layer of thermal insulation to reduce actual metal temperatures in components. This TBC must be sufficiently thick, have a low thermal conductivity and high thermal-shock resistance, and have a high concentration of internal voids to further reduce thermal conductivity to a value well below that of the bulk material. The temperature difference between the outer surface of a TBC and the outer surface of the underlying corrosion-resistant film can be as high as 270 °F (150 °C), and the delta of temperature is sometimes quoted as being up to 300 °F (188 °C). In addition to reducing the temperature at the surface of the superalloy, these coatings also reduce thermal-shock loads on the blades; rapid changes in ambient temperature are moderated and attenuated before they reach the substrate.

Ceramic TBCs, typified by the structure and composition illustrated in Fig. 13.21, have been used for over 40 years for extending the oxidation and thermal fatigue durability of sheet metal components in aircraft gas turbine engines.

Thermal Barrier Coating Systems. A TBC system consists of an insulating ceramic outer layer (top coat) and a metallic inner layer (bond coat) between the ceramic and the substrate. Both the top coat and bond coat can be applied by PS (in air or as LPPS) or EBPVD. A schematic of a typical TBC system is shown in Fig. 13.22. Current TBCs are yttria-stabilized zirconia, that is, zirconium oxide (ZrO_2-zirconia), with 6 to 8% (by weight) of yttrium oxide (Y_2O_3-yttria) to partially stabilize the tetragonal phase of ZrO_2 for good strength, fracture toughness, and resistance to thermal cycling. The coatings are relatively inert, have a high melting point, and have low thermal conductivity. Thus, they are able to reduce the effective gas temperature by significant amounts on airfoil components of gas turbines.

All such coatings in practical use today are applied by PS. Model experiments at National Aeronautics and Space Administration laboratories emphasized the potential of such coatings for increasing longevity or decreasing cooling air requirements (equal to decreasing fuel consumption) by their use as insulating layers on hot-section airfoils in all types of gas turbine engines.

Technology of TBCs. Air-plasma sprayed coatings contain porosity and microcracks that help to redistribute thermal stresses but also provide corrosion paths through the coating. Low-pressure plasma spray coatings provide high coating purity and essentially eliminate oxides and porosity. Electron beam physical vapor deposition coatings have a columnar grain morphology (Fig. 13.23) in which individual grains are strongly bonded at their base but have a weak bond between grains. The major advantage of this columnar outer structure lies in the fact that it reduces stress buildup within the body of the coating. Strain within the coating is accommodated by free expansion (or contraction) of the columns into the gaps, which results in negligible stress buildup. The columnar structure of EBPVD zirconia TBCs has the disadvantage, however, of increasing heat conductiv-

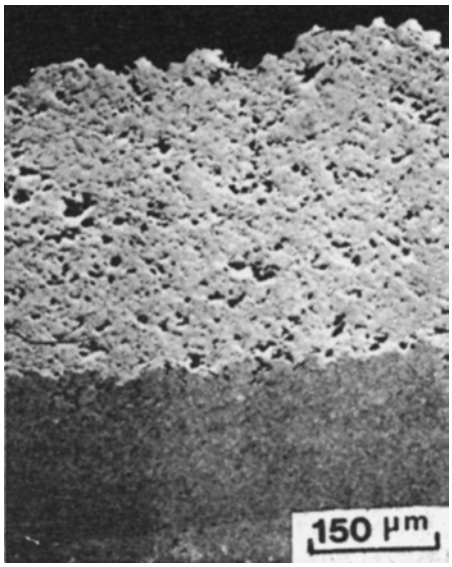


Fig. 13.21 Typical thermal barrier coating produced by plasma spraying zirconia on MCrAlY underlayer

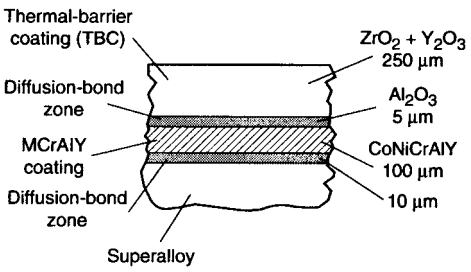


Fig. 13.22 Schematic of a multilayer thermal barrier coating system produced using a combination of EBPVD and PS techniques. Left, generic description; right, a specific TBC system

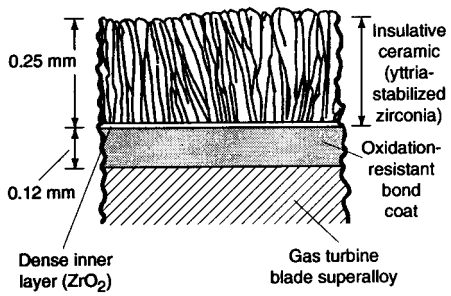


Fig. 13.23 Cross-section sketch illustrating the strain-tolerant columnar grain ZrO_2 microstructure of EBPVD zirconia thermal barrier coatings

ity by a factor of about 2 as compared to plasma-sprayed TBCs.

Figure 13.23 also shows that a thin, dense ZrO2 layer occurs between the bond coat surface and the upper columnar zirconia structure. This phase grows under oxygen-deficient conditions just at the beginning of zirconia deposition, and its thickness is controlled by how quickly the oxygen bleed is activated in the vacuum chamber of the EBPVD apparatus after zirconia coating commences. This dense, interfacial ZrO_2 film is critical to the life of the EBPVD coating in that it provides for chemical bonding between the columnar zirconia and the oxidation-resistant bond coat. If, however, this interfacial film becomes too thick (>2 μm), it may sustain and transmit compressive stresses sufficient to cause cracking within the outer zirconia coating.

The metallic (MCrAlY) bond coat aids in the adhesion of the ceramic topcoat, protects the substrate from hot corrosion and oxidation, and helps in handling expansion mismatch between the ceramic and superalloy. For best adhesion of EBPVD thermal barrier coatings, the bond coat surface should be smooth or, preferably, polished, in contrast to plasma-sprayed TBCs, which require a rough bond coat.

Thermal Barrier Coating Performance. As discussed previously, TBCs generally consist of a metallic bond coating (typically MCrAlY applied by LPPS or EBPVD) and a thick ceramic top coat (typically stabilized ZrO_2 deposited by LPPS or EBPVD). The microstructure of EBPVD ceramic is fundamentally different from that of PS ceramic. The EBPVD ceramic grows in a columnar microstructure when processed under the appropriate manufacturing conditions.

Despite their columnar microstructure, thin EBPVD coatings can be dense and serve as a diffusion gas barrier at high temperatures. Moreover, as noted, the columnar structure guarantees an improved strain and stress tolerance, because the individual columnar grains are not bonded to each other. However, each columnar grain is tightly bonded to the substrate (MCrAlY bond coat). Thermal stress within the coatings occurs due to a mismatch between the thermal expansion coefficients of the metallic substrate and the coating, and due to transient thermal gradients during rapid thermal cycling. Depending on deposition conditions, the EBPVD technique also may induce some stress within the coating. This intrinsic compressive stress may act as a ''prestress'' that diminishes coating failure due to tensile thermal stresses at elevated temperatures.

The LPPS process also induces some residual stress, due to substrate heating and deposition of a stress-free coating at the deposition temperature. Thermal residual stress develops during cooling to room temperature. Failure of TBCs in service generally is attributed to stress that develops during cooling after high-temperature exposure, and to transient thermal stress that develops during rapid thermal cycling. Failure occurs primarily due to thermal expansion mismatch between the ceramic and metallic layers and environmental attack of the bond coat. The use of Y_2O_3 to stabilize the ceramic coat, together with an MCrAlY-type bond coat, provides the maximum thermal fatigue resistance of TBCs.

Thermal barrier coatings have been tested on sheet metal, where they have performed well for many years. They have been tested on stationary airfoil (vane) platforms, where they demonstrated outstanding durability, as shown in Fig. 13.24. Rotating airfoil gas path surface TBCs have been evaluated for durability, with success as well. A concern for rotating structures is the density of TBCs, which adds to the centrifugal pull on a blade as it rotates in a gas turbine.

Coating Comparisons

Ductility. Coatings must be capable of tolerating strain due to thermal expansion mismatch and mechanical loads, in order to retain coating-substrate integrity. The ductile-to-brittle transition temperature (DBTT) concept—the temperature at which coating ductility begins to change—is used to describe the ability of a coating to tolerate strain. Above the DBTT, a coating behaves in a ductile manner; below the DBTT, the coating is brittle. The DBTT is affected by several factors, including coating composition, coating application process, coating thickness, surface finish, and strain rate. The DBTT should be as low as possible so that cracking in the coating does not occur in service, because the cracks may then propagate into the substrate.

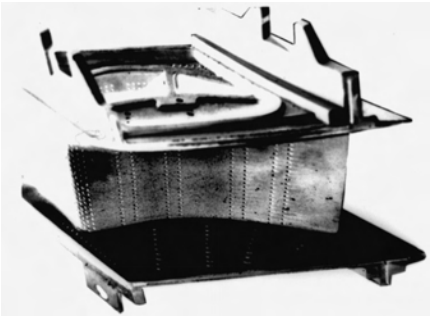


Fig. 13.24 A TBC coated first-stage vane from a Pratt & Whitney large commercial engine after 9300 h of flight service. Note excellent condition of vane

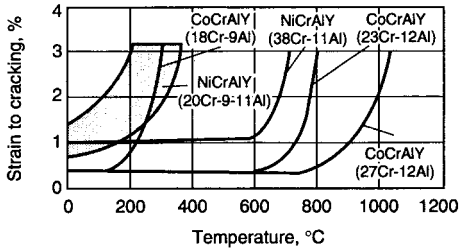


Fig. 13.25 Ductility of several MCrAlY overlay coating compositions showing role of cobalt and chromium on ductility. Also, the figure shows the relative ductility of NiCrAlY and CoCrAlY coatings.

MCrAlY overlay coatings generally have a lower DBTT than diffusion coatings (refer back to Fig. 13.20), because their chemical composition can be controlled to adjust the DBTT. The DBTT of aluminide diffusion coatings is a function of aluminum content, increasing with increasing aluminum. Platinum additions (and probably other noble metals) are claimed to raise the DBTT of aluminide coatings.

For overlay coatings, NiCrAlY coatings have a higher DBTT than CoCrAlY coatings. The DBTT of both coatings is increased with increasing chromium and/or aluminum content (Fig. 13.25). NiCoCrAlY coatings containing 20 to 26% Co are significantly more ductile than either NiCrAlY or CoCrAlY coatings. Ductility of aluminide diffusion coatings can sometimes be enhanced by laser remelting of the coating. A thin surface layer of the coating is melted and rapidly quenched by the cold bulk solid substrate, thus refining the grain size of the coating. Smaller grain sizes usually equate to better ductility in metals.

Protective Coating Pros and Cons. The ability of a coating to provide satisfactory performance in high-temperature applications is measured by whether it can remain intact, resist oxidation and corrosion, and avoid cracking. Generally, diffusion aluminide coatings are limited by their oxidation behavior; overlay coatings are limited by their susceptibility to thermal-fatigue cracking in cyclic conditions as well as by their line-of-sight deposition process; and TBCs are limited by the thermal-expansion mismatch between the ceramic and metallic layers and by environmental attack of the bond coat.

Superalloys: A Technical Guide, Second Edition
Matthew J. Donachie, Stephen J. Donachie, p 323-337
DOI:10.1361/stgs2002p323
Copyright © 2002 ASM International®
All rights reserved.
www.asminternational.org

Chapter 14

Failure and Refurbishment

Overview

The Basics. Resistance to microstructural change or to mechanical deformation is a sensitive function of time, temperature, stress, and environment. At lower temperatures, in nonvibratory service (below the yield strength), operational loads on components can be carried indefinitely in the absence of any corrosive phenomena. At higher temperatures, about 0.5 of the absolute melting temperature, finite lifetimes exist. The reasons for finite lives at higher temperature vary but can be explained in simple terms as an extension of natural laws that seek equilibrium.

Microstructures want to reach equilibrium; new phases form, old ones are dissolved or agglomerate. Oxidation or hot corrosion wants to consume metal atoms and thus reduces component dimensions and/or introduces notches. It may even introduce undesirable gaseous elements, but all this is dependent on time and the provision of energy by high temperatures.

At ordinary temperatures, the strengths of most metals are measured in terms of short-time static properties such as yield strength or ultimate strength, but at high temperatures, creep extension occurs and will lead to rupture if sufficient time elapses under the environment and mechanical loading. Similarly, the fatigue (cyclic) capability will be reduced. There may be an interaction of creep and fatigue, owing to the temperature, stress, and time conditions.

When times or temperatures exceed normal test or operating levels, alloys are exposed to substantially different operating environments from those ordinarily experienced and may behave in a manner that could not have been predicted from normal test data.

What Is Failure? Failure may be separation or it may just be inability of a component to perform its mission. Not all failures are caused by cracking or fracture. If a coating is degraded, a component may be susceptible to surface attack and failure has occurred. Similarly, if a part creeps during operation so that the part begins to impinge on another part, failure has occurred.

In the general sense, elevated-temperature failure modes may be classified as creep rupture, fatigue (low or high cycle—LCF or HCF), thermal-mechanical fatigue (TMF), tensile overload modified by environmental interactions, crack growth (from a new crack or an existing imperfection), or combinations thereof. By examination of fracture surfaces and comparison of component operating conditions with available creep, tensile, fatigue, and thermal fatigue data, the failure mode may be established. This type of analysis may be sufficient for most failure investigations; however, for much engineering application and all development and research work, the metallurgical subtleties of failure must be evaluated. Stress, time, temperature, and environment may act to change the metallurgical structure during test so as to induce failure by a reduction in strength. (In some cases, the changes may enhance strength.) The structural changes may be termed ‘‘metallurgical instabilities,’’ and, while they influence all modes of failure, these instabilities are sometimes conveniently described in terms of their influence on steady load-creep properties.

Overheating and Microstructural Stability

General. Superalloys normally respond to heat treatment, and thus, exposure of these alloys to elevated temperatures, with or without stress, can cause microstructural changes and resultant changes in properties, as indicated previously. Generally, the higher the exposure temperature, the more rapid the structural change. At the highest exposure temperatures, an alloy may be subject to incipient melting. As exposure temperature decreases, the type of microstructural degradation may change. In addition, oxidation and surface corrosion may take place at all temperatures for which these alloys are normally specified.

This section deals principally with the effects of microstructural changes, melting and corrosion on nickel-base and cobalt-base superalloys for temperatures at or above about 1400 °F (760 °C) and mostly above 1500 °F (816 °C). It also touches briefly on microstructural changes affecting nickel-base and iron-nickel-base superalloys at temperatures below 1500 °F (816 °C). Accelerated oxidation (hot corrosion) induced by salts in marine and industrial environments at temperatures below 1500 °F (816 °C) down to about 1300 °F (704 °C) or lower is not considered. (See Chapter 13 for some discussion about hot corrosion at lower temperatures.)

Overheating and Incipient Melting. Overheating, in the broad sense, consists of exposing a metal to excessively high temperatures for short periods of time. ''Excessive'' is a relative word. For some alloys, exceeding 1200 °F (649 °C) can be considered excessive temperature. Allowable metal temperatures for wrought superalloys in structural applications generally do not exceed about 1400 °F (760 °C) for gas turbine disks but may be higher for less heavily loaded sheet alloy applications. In applications where the component does not bear a significant load, allowable temperatures may exceed 2200 °F (1204 °C), assuming that incipient melting is not a problem.

In general, any temperature can be considered to be in the overheating range when it:

- Causes melting
- Causes strengthening phases to dissolve in the matrix, or
- Causes extensive oxidation or corrosion.

Results of overheating depend on the maximum temperature reached by the metal and time at temperature.

Nickel-base and cobalt-base superalloys generally have incipient melting temperatures above about 2150 °F (1175 °C). Table 14.1 gives some melting and γ' solvus temperatures for a few wrought superalloys. Table 14.2 gives similar limited information on cast superalloys. Figure 14.1 shows the microstructures of two typical wrought superalloys before and after incipient melting.

Incipient melting reduces grain-boundary strength and ductility. It thus reduces alloy rupture capabilities. Once a component has exceeded its incipient melting point, normal properties cannot be fully restored by any customary heat treatment. In cast alloys, incipient melting may occur at temperatures substantially below the temperatures predicted from alloy composition. This behavior results from alloy segregation to grain boundaries and interdendritic areas during solidification. In wrought alloys, incipient melting, if it occurs, takes place at a temperature much closer to the general alloy melting temperature (solidus), and overheating actually may cause significant portions of the structure to melt.

Table 14.1 Melting and γ' solvus temperatures for wrought superalloys(a)

Alloy	Incipient melting temperature, °F (°C)	γ' solvus, °F (°C)
A-286	. . .	1570 (855)
Astroloy LC	. . .	2050 (1120)
Rene 95	. . .	2050–2135 (1120–1160)
IN-901	. . .	1725 (940)
U-700	2220 (1215)	2070–2100 (1130–1150)
Hastelloy X	2280 (1250)	. . .
HA-25 (L-605)	2425 (1330)	. . .
HA-188	2375 (1300)	. . .
IN-617	2430 (1330)	. . .
IN-625	2350 (1290)	. . .
IN-X-750	2540 (1395)	. . .
Nimonic 80A	2480 (1360)	1760–1795 (960–980)
Nimonic 90	2390 (1310)	1795–1830 (980–1000)
Nimonic 105	2355 (1290)	1870–1940 (1020–1060)
Nimonic 115	. . .	2085–2120 (1140–1160)
Nimonic 263	. . .	1670–1695 (910–925)
Rene 41	2250 (1230)	1925–1960 (1050–1070)
U-500	2300 (1260)	1920–2010 (1050–1100)
Waspaloy	2425 (1330)	1875–1900 (1025–1040)
M-252	. . .	1850 (1010)
IN-100	. . .	2155–2190 (1180–1200)

(a) Intended to indicate general trends in alloys. See Table 1.1 for chemistries. Temperatures from many sources. Max-min data range used; alloys may not display this much variation. Sometimes only one source/temperature available. Approximations only, rounded to 5°

Table 14.2 Melting and γ′ solvus temperatures for cast superalloys(a)

Alloy	Incipient melting temperature, °F (°C)	γ′ solvus, °F (°C)
IN-713LC	...	2155–2195 (1180–1200)
IN-713C	...	2160–2195 (1180–1200)
Rene 80	2240–2250 (1225–1230)	2100 (1150)
Rene 120	2200 (1200)	...
CG MAR-M-200 + Hf	2150–2230 (1175–1220)	...
PWA 1480	2400–2425 (1315–1330)	...
MAR-M-509	2350 (1290)	...
IN-MA-754	2475 (1355)	...
IN-738LC	...	2120–2145 (1160–1175)
IN-100	2150–2200 (1175–1200)	2160 (1180)
MAR-M-200	2300 (1260)	2160–2195 (1180–1200)
B-1900	2300 (1260)	2100 (1150)
B-1900 + Hf	2225 (1220)	...
IN-792	...	2010–2100 (1100–1150)
Rene 77 (U-700)	...	2085 (1140)
MAR-M-246 + Hf	...	2160–2195 (1180–1200)
CMSX-3	2400 (1315)	...
CGDS MAR-M-247 + Hf	2270 (1245)	...

(a) Intended to indicate general trends in alloys. See Table 1.2 for chemistries. Temperatures from many sources. Max-min data range used; alloys may not display this much variation. Sometimes only one source/temperature available. Approximations only, rounded to 5°

Corrosion, Alloy Depletion, and Coatings. Overheating may deplete alloying elements that provide oxidation resistance. Oxidation processes are thus accelerated on return of the alloy to normal operating temperatures. Even if prolonged exposure to overtemperature does not result in mechanical failure, it frequently will cause excessive surface corrosion. This, in turn, can reduce the strength of the alloy. Even if an alloy is coated for oxidation resistance, the coating will be degraded by surface attack, and eventually, mechanical properties of the alloy will be affected. The alloy under a coating may also degrade rapidly because of excessive interdiffusion of alloying elements, if temperatures exceed the normal operating range.

As a rule of thumb, alloys used in structural applications should not be exposed at temperatures within about 225 °F (140 °C) of their incipient melting temperatures. The strength and oxidation resistance of the alloy and the operating environment will determine how close actual metal temperatures may approach the suggested upper limit.

An important factor to consider when dealing with coated superalloys is the reduction in incipient melting temperature of the system (coating/base metal) that may result from the change in composition brought about by diffusion. For example, for aluminide coatings on an alloy such as U-700, which has an incipient melting temperature of about 2220 °F (1215 °C), incipient melting may occur in the inner diffusion zone at temperatures between 2150 and 2175 °F (1175 and 1190 °C). Incipient melting in coated systems often leads to accelerated degradation of the coating.

Dissolving γ′ Hardening Phases. At temperatures that cause neither incipient melting nor surface degradation, alloy strength still may be reduced, because strengthening phases are taken into solution. Wrought nickel-base alloys frequently are strengthened by a dispersion of the phase γ′, Ni_3 (Al, Ti). In wrought alloys, the γ′ phase can be taken into solution at temperatures of about 2150 °F (1175 °C) or less (see Table 14.1). For cast alloys, the temperature will be higher (see Table 14.2). Service exposure at or near the solution temperature will reduce the amount of γ′ phase and thereby reduce alloy strength.

Prolonged operation at temperatures within the solution range is inadvisable, although occasional excursions into this range may be tolerated. If γ′ phase is dissolved, it can be reprecipitated as fine particles by subsequent aging; original property levels can be reasonably recovered, assuming there was no other damage due to stress or oxidation. However, properties will not be recovered if slow cooling is used after extensive solution has oc-

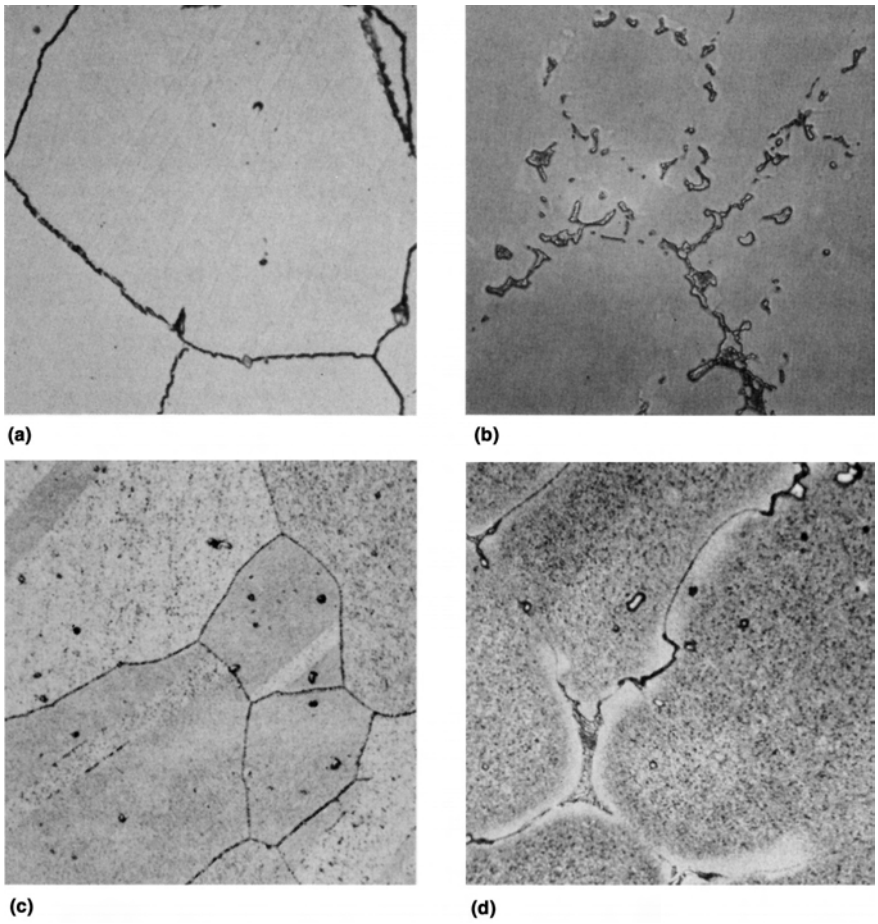


Fig. 14.1 Effect of incipient melting on microstructure of two nickel-base superalloys, IN-617 and U-700. (a) Inconel 617: No melting (500×, unetched). (b) Inconel 617: Incipient melting (500×, unetched). (c) Udimet 700: No melting (500×, lactic acid + HCl + HNO_3 etch). (d) Udimet 700: Incipient melting (500×, lactic acid + HCl + HNO_3 etch)

curred or if the material is held at a high temperature so that coarse γ' forms while fine γ' dissolves.

Figure 14.2 compares the life of a nickel-base alloy in two conditions: solution treated only (no precipitation heat treat) versus the same alloy fully heat treated. This figure illustrates significant reduction in strength that occurs if a γ'-hardened alloy has been exposed to a solution treatment temperature and not re-aged. During very long-time low-stress applications within the aging-temperature range, after solution treatment, a lesser reduction of strength occurs.

In actual applications, service exposures do not fully solution an alloy. Furthermore, the dissolved γ' can/will reprecipitate on the existing γ' or form new γ' during lower- (but still high) temperature service operation.

Dissolving and Modifying Carbides. Carbide phases in superalloys behave somewhat like γ', but subsequent reprecipitation is not easily controlled. Carbides are taken into solution or agglomerated during over-temperature exposure, and there can be substantial variations in the amount, form, and distribution of the resulting carbide structure. In Hastelloy X, a solid-solution-hardened nickel-base superalloy, there are large differences in the volume fraction (V_f) and structure of carbides between normal temperature and over-temperature exposures. During overtemperature exposure, carbide form and distribution are considerably changed, due to agglomer-

ation and rounding of particles. As a result, for example, mechanical properties of Hastelloy X are reduced, as shown in Fig. 14.3 for room-temperature strength after exposure at 1900 °F (1038 °C) in air. Similar results were obtained from a series of exposures at about 2100 °F (1149 °C).

Extensive carbide precipitation frequently can occur in alloys when there is a change in carbide type from that present in the mill-annealed condition. Figure 14.4 shows Haynes 188, a cobalt-base wrought alloy, before and after exposure for 6000 h at 1600 °F (871 °C). During exposure, M_6C carbides dissolved and were replaced predominantly by $M_{23}C_6$ carbides and, to a lesser extent, by Laves phase. Significant losses in ductility resulted from the precipitation shown in Fig. 14.4. Similar results have been shown for other cobalt-base alloys.

In solid solution/carbide hardened superalloys where extensive carbide precipitation or agglomeration occurs, it is frequently possible to recover the original carbide distribution and a major portion of alloy properties by solution heat treatment. For example, it is claimed that Haynes 188 can recover original room-temperature ductility by heat treatment at 2150 °F (1175 °C) for 15 min.

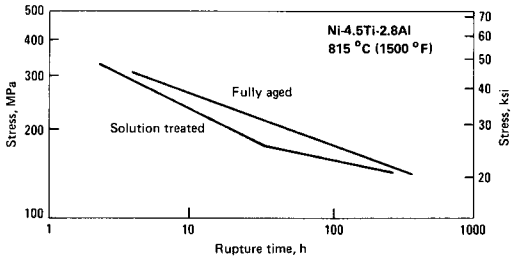


Fig. 14.2 Log-log plot of stress vs. rupture life for a nickel-aluminum-titanium γ′-hardened alloy

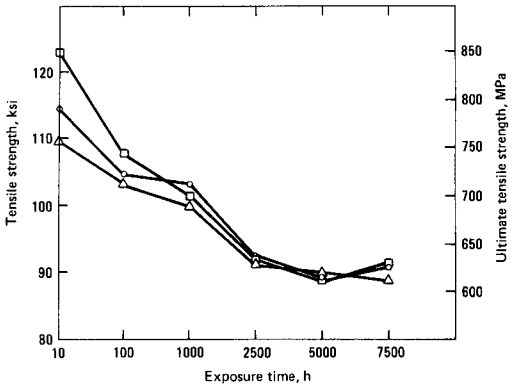


Fig. 14.3 Room-temperature tensile strength vs. exposure times at 1038 °C (1900 °F) in air for Hastelloy X nickel-base solid-solution and carbide-strengthened superalloy

Microstructural Degradation

Normal Operation Above 1400 °F (760 °C). Some alloys are exposed to extremely high temperatures in furnace and petrochemical applications, but the loads are not high. Alloys for gas turbine applications generally are exposed to the most demanding combinations of high temperature and stress.

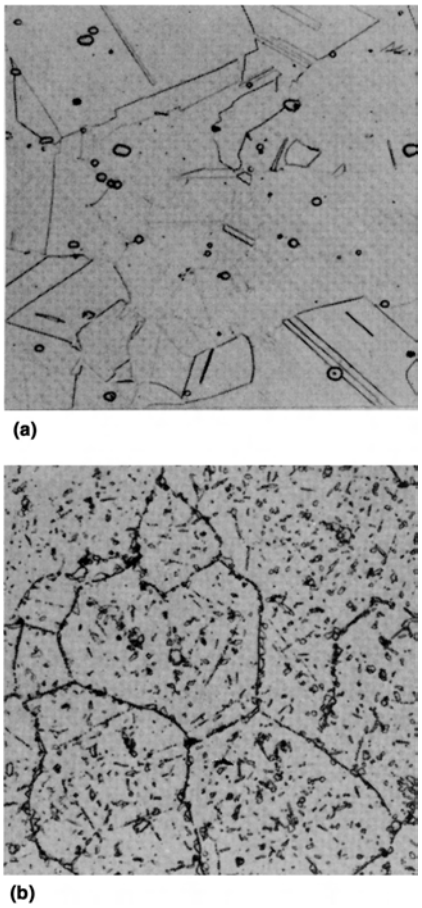


Fig. 14.4 Microstructure of solution treated Haynes 188 wrought cobalt-base superalloy before and after exposure at 871 °C (1600 °F). (a) Before. (b) After 6244 h exposure. Etched in HCl + H_2O_2, 500×

Wrought alloys have been used in the past for turbine blades and vanes in aircraft gas turbines. The approximate metal temperature range for airfoils of such alloys, when used, was about 1340 to about 1500 °F (about 727 to about 816°C). In contrast, the metal temperature may range as high as 2000 °F (1093 °C), perhaps higher, for airfoils of some cast superalloys.

Within the range of about 1340 to 2000 °F (727 to 1093 °C), microstructural changes readily occur with time at temperature. Furthermore, when stress is applied, the changes may be accelerated. The principal changes are:

- Breakdown of primary carbides and formation of secondary carbides
- Agglomeration of primary geometrically close-packed strengthening phases such as γ'
- Formation of topologically close-packed (tcp) phases such as sigma, Laves, and mu

The first two processes described are an extension of the normal strengthening process. These reactions are recognized during the design of components, and allowances are made for their effects on alloy strength at moderate times.

Carbide transition and γ' agglomeration do reduce strength with time but generally are not as detrimental to ductility and creep-rupture life as formation of tcp phases. Figure 14.5 shows the microstructure of U-700 nickel-base alloy before and after exposure at 1600 °F (871 °C). During exposure, the γ' became agglomerated, and $M_{23}C_6$ carbides formed.

Generally, design parameters take into account γ' agglomeration if it is experienced in the moderate times used to test alloys (most often, 20 to 1000 h). However, for significantly longer times at normal temperatures, γ' agglomeration may reduce alloy strength below predicted values. An indication of the manner in which γ' coarsening can change the initial behavior of an alloy can be seen in Fig. 14.6. This figure shows that, for B-1900 nickel-base superalloy behaving in a normal way (and fully characterized with this behavior), the expected coarsening agglomeration of the hardening γ' phase reduces alloy strength. It should be obvious that unexpectedly high coarsening rates, such as might be produced by overtemperature,

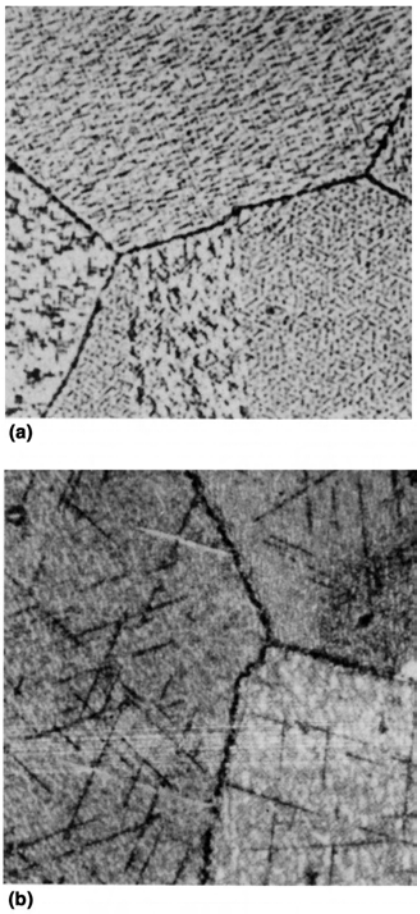


Fig. 14.5 Microstructure of solution treated and aged U-700 nickel-base superalloy before and after exposure at 871 °C (1600 °F). (a) Before. (b) After 500 h exposure. Etched in Kalling's reagent, 100×

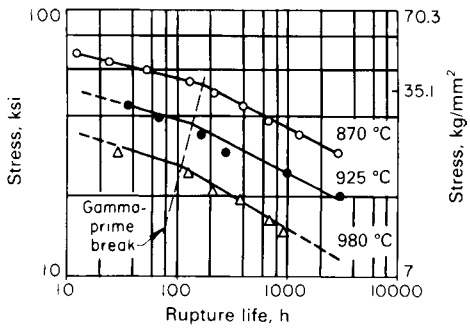


Fig. 14.6 Log-log plot of stress vs. rupture life for nickel-base superalloy B-1900 showing property drop-off attributed to γ' coarsening

would aggravate the situation and lead to more rapid drops in alloy strength.

Changes in carbide phases also adversely affect strength, although initially there may be increases in strength as additional carbides precipitate. In the wrought cobalt-base solid-solution alloy HA-25 (L-605), carbide precipitation at 1500 °F (816 °C) is responsible for alloy hardening in both early and late stages of exposure. In the late stages, $M_{23}C_6$, M_6C, and Laves phase participate in strengthening. In Hastelloy X, extensive precipitation occurs at 1300 to 1450 °F (704 to 788 °C). As a result, sigma, mu and a dense intragranular secondary M_6C carbide can occupy as much as 27 vol% of the structure. As primary M_6C carbides coalesce, there is a continual reduction in strength; formation of small secondary carbides and tcp phases enhances strength but also reduces ductility.

Figure 14.7 compares the strength of U-700 with and without sigma formation. As sigma forms, creep-rupture strength of the alloy is reduced. Furthermore, room-temperature ductility is greatly reduced, and ductility at temperature may be reduced.

Alloy design procedures are now available to assist in minimizing detrimental tcp phase formation in nickel-base and cobalt-base superalloys. Every element is assigned an electron vacancy number, N_v. The matrix composition after normal precipitation is then determined. The N_v for the alloy (matrix) is computed by summing the products of elemental N_v times atomic fraction for each element present. For nickel-base superalloys, if the N_v of the alloy exceeds about 2.4, tcp phase formation is likely. For cobalt-base superalloys, the corresponding N_v is about 2.6. By proper adjustment of alloy composition, it is often possible to maintain base-alloy strength while reducing susceptibility to tcp phase formation. Application of the N_v concept has helped to improve long-time creep-rupture behavior of alloys by reducing microstructural degradation at normal operating temperatures.

Formation of tcp phases is not restricted to γ'-hardened nickel-base and cobalt-base carbide-hardened superalloys. Solid-solution superalloys such as Hastelloy X also may show a tendency to tcp phase formation above 1340 °F (727 °C). A Ni-Cr-Mo sigma phase was identified in Hastelloy X exposed for more than 2500 h at 1300 and 1450 °F (704 and 788 °C). Mu phase was also identified in specimens aged at temperatures between 1300 and 1750 °F (704 and 954 °C). However, mu was most prominent in specimens aged at 1600 and 1750 °F (871 and 954 °C). Figure 14.8 shows the microstructure of Hastelloy X after a 2232 h creep test at 1400 °F (760 °C). Note the large number of particles in the structure.

Normal Operation Below 1400 °F (760 °C). For alloys normally used at temperatures of 800 to 1400 °F (425 to 760 °C), melting by overtemperature is not a problem; microstructural changes are important. Hot corrosion and other accelerated oxidation is important for some alloys. The alloys that have been used at these low temperatures are certain iron-nickel-base and nickel-base precipitation-hardening superalloys such as A-286, Incoloy 901, V-57, Waspaloy, Astroloy, IN-718, Rene 95, and IN-100 (MERL 76), for

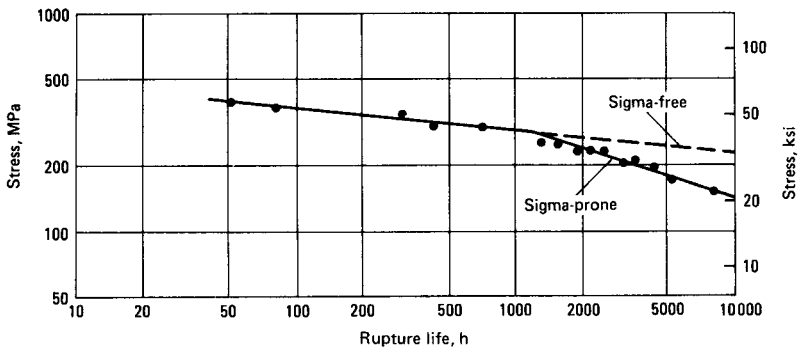


Fig. 14.7 Log-log plot of stress vs. rupture life for nickel-base superalloy U-700 at 815 °C (1500 °F) showing property drop-off attributed to σ phase formation

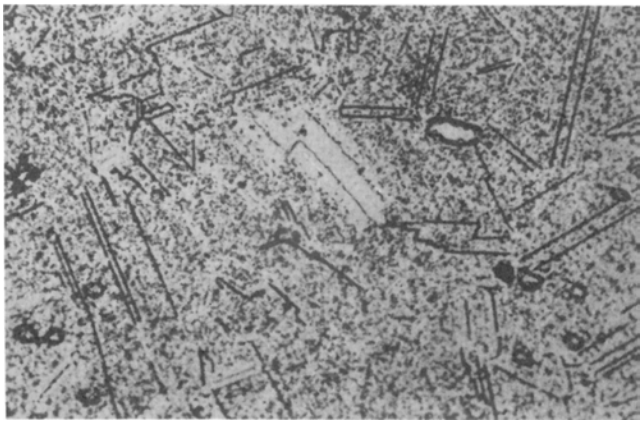


Fig. 14.8 Microstructure of Hastelloy X nickel-base superalloy after creep exposure for 2232 h at 760 °C (1400 °F). Etched in 10% chromic acid, 500×

instance. These alloys generally are considered microstructurally stable at the temperatures for which they are employed as disks.

If nickel-base alloys such as Waspaloy, Astroloy, and Rene 95 are exposed for prolonged times at metal temperatures that exceed about 1200 °F (649 °C), the strengthening phase may coarsen slightly. The same effect may occur above 1100 °F (593 °C) for other iron-base or iron-nickel austenitic alloys. IN-718 is subject to sharp reduction in properties when used above about 1200 °F (649 °C).

Unless the wrought disk alloys are operated at temperatures well into or above their aging-temperature ranges, no significant microstructural effects will be noted. Carbide precipitation at dislocations may be significant when operating times at 900 to 1200 °F (480 to 649 °C) exceed 10,000 h. However, there are little published data to support the existence of significant effects of thermal exposure on creep-rupture behavior, although notch behavior may become important. At these temperatures, surface oxidation is not generally a problem, although long-term exposure to certain highly corrosive environments may produce surface attack, such as hot corrosion (see Chapter 13).

IN-718 deserves some mention, because it often is used at temperatures above its final aging temperature of 1150 °F (621 °C). Although some minor coarsening of the γ″ phase may take place, no detrimental effects normally occur at temperatures up to 1200 °F (649 °C). If overheating to above 1300 °F (704 °C) should occur, the strengthening γ″ phase is degraded; significant sigma phase or alpha chromium precipitation can occur, with resultant losses in strength.

Failures of Superalloy Components

Introduction. Chapter 13 and the preceding sections of this chapter have suggested some of the difficulties that may arise in the application of superalloys. Under prolonged application at elevated temperatures, even the most well-designed component eventually will exceed its service life. If the life is exceeded prematurely, then failure has occurred. This section presents a few examples of failures arising from high-temperature applications of superalloys.

Example 1: Gas Turbine Combustion Chamber. Gas turbines require a combustion chamber in which to burn the fuel to produce the hot gases that drive the turbine. In some engines, the combustors are very large (annular combustors), and in others are individual cans, as seen in Fig. 14.9. This figure shows wear and stain marks, which result from excessive oxidation. While this sort of problem may be prevented or minimized by use of a protective oxidation-resistant coating or a thermal-barrier coating, there are other mechanical problems that can occur. A magnified view of a section of the combustion chamber is shown in Fig. 14.10. Note the TMF cracking that has occurred.

Example 2: Bowing of a Turbine Vane. Generally, superalloy characteristics are well documented before engine evaluation. Sometimes, materials showing promise have been evaluated before a complete characterization. Sometimes, of course, engine operating conditions are not what designers have intended. In any event, Fig. 14.11 shows a cobalt-base superalloy turbine vane that was overheated and so was insufficiently strong in creep at the temperatures/stresses achieved in the midspan region of the component. The result was a creep process that produced the bowing of the vane. The solution to this sort of a problem is to change the alloy or improve its strength.



Fig. 14.9 Engine-operated aircraft gas turbine combustion chamber showing metal loss and degradation, owing to oxidation

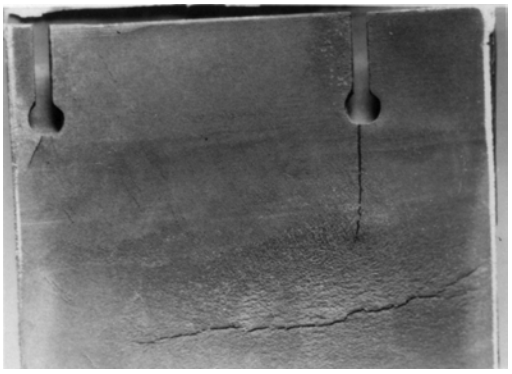


Fig. 14.10 Enlarged view of area of combustion chamber showing examples of thermal-mechanical fatigue cracking

Example 3: TMF Cracking of a Turbine Airfoil. Figure 14.12 shows two first-stage wrought turbine blades with leading-edge cracks found after engine operation. Figure 14.13 shows the appearance of the leading



Fig. 14.11 Engine-operated turbine vane showing bowing caused by creep of the component

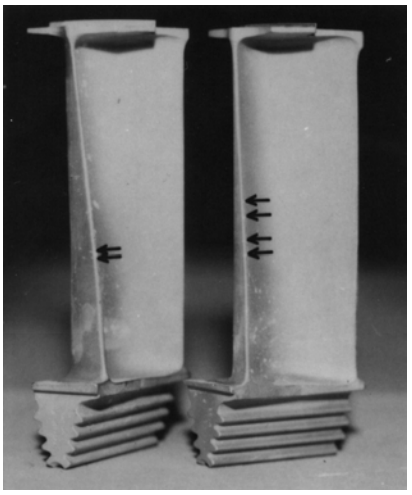


Fig. 14.12 First-stage turbine blades of a wrought nickel-base superalloy showing cracks (arrows) caused in the leading edge by TMF

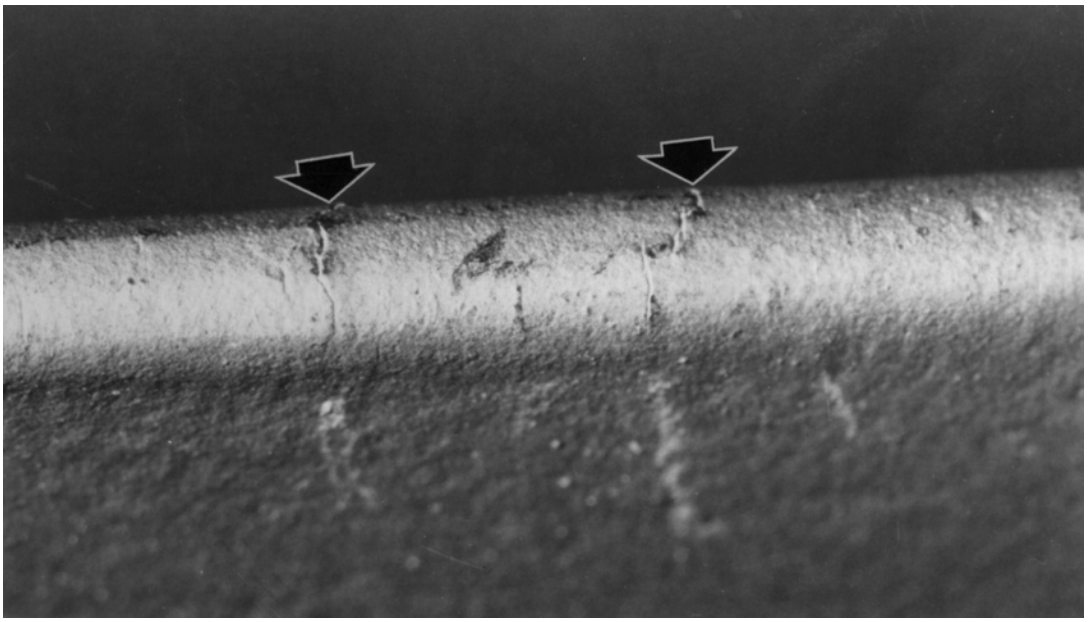


Fig. 14.13 Thermal fatigue cracking in turbine blade

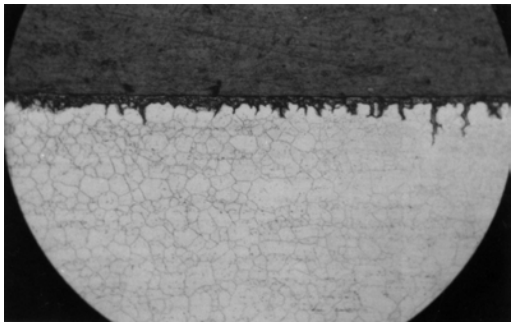


Fig. 14.14 Leading edge of a Waspaloy nickel-base superalloy turbine blade showing intergranular oxidation attack

edge of a cracked airfoil, clearly indicating the TMF cracking. Thermal-mechanical fatigue cracking normally occurs on the leading or trailing edges of turbine airfoils, as indicated. The cracking results from the repeated application of the thermal stresses developed due to nonuniform heating and cooling during engine acceleration and deceleration. The substitution of a stronger polycrystalline (PC) cast nickel-base superalloy (B-1900) for the wrought alloy (U-700) resulted in a four-fold increase in the number of engine cycles required to produce such cracks. Subsequent introduction of columnar grain directionally solidified (CGDS) nickel-base superalloys resulted in even greater improvement, owing mostly to the substantial reduction (about 40%) in the elastic modulus along the blade axis. Lower modulus meant reduced strains and so, longer life. Columnar grain directional solidification also permitted the development of somewhat stronger alloys, which added to the TMF capability improvement. Single-crystal directionally solidified nickel-base superalloys have extended the TMF improvement.

Example 4: Surface Attack by Oxidation. Figure 14.14 shows the leading edge of a wrought Waspaloy turbine blade after engine operation. Intergranular attack produced surface roughness and oxidation to a depth of 0.009 in. (0.23 mm). This type of attack prompted the use of coatings to protect superalloy airfoils. Figure 14.15 gives a comparison of oxidation attack on WI-52 cobalt-base superalloy, showing the effectiveness of coatings. Hot corrosion attack also can occur (refer to Chapter 13; in particular, see Figs. 13.14–13.16).

Example 5: Fracture in Creep Owing to Low Ductility. Figure 14.16 shows the attachment section of a turbine blade that failed, owing to insufficient rupture ductility during creep. The root attachment areas of turbine

blades are highly stressed, compared to airfoils, and have intrinsic notches, owing to the serrations of the attachments. One of the original high-strength cast nickel-base superalloys had exceptional strength properties, but rupture ductilities amounted to only about 0.25% at minimum. Because blade lives tend to be designed on the basis of 1% or more creep in the airfoil and the assumption of similar amounts of available creep elongation in the root attachments, such low ductilities were an invitation to failure.

In the instance shown, the top of the blade (platform and airfoil) parted company from the root area. The eventual solution to this particular problem with the given alloy, MAR-M-200 nickel-base superalloy in PC cast form, was to produce the component in CGDS cast form. With the addition of some hafnium (about 1.5%), the alloy shown went on to become a very successful turbine blade material, with hundreds of thousands of useful operating hours accumulated.

Example 6: Improper Heat Treatment Leads to Blade Stretch. Figure 14.17 shows extensive creep damage to a turbine blade that was improperly heat treated and then run in an experimental engine. The improper heat treatment left the blade insufficiently strong in creep for the application intended. The stretching and necking due to creep are readily apparent, and the shroud at the blade tip has been worn off.

Example 7: TMF Cracking in Other Combustor Components. Components of the combustor section of gas turbines are susceptible to TMF, which, much as normal fatigue cracking, produces cracks that are difficult to distinguish from cracking produced by creep or creep rupture. Experience and extensive knowledge of application conditions may be required to validate the causes of cracks such as the ones shown in Fig. 14.18. These cracks were produced by thermal stresses in a for-

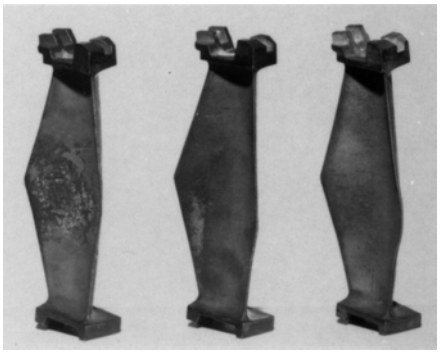


Fig. 14.15 Comparison of coated and uncoated WI-52 cobalt-base superalloy turbine vanes after engine test. Left, uncoated vane (note severe midspan attack on pressure surface); center, dip-coated airfoil with slight attack; right, vapor-deposit coated vane showing no attack

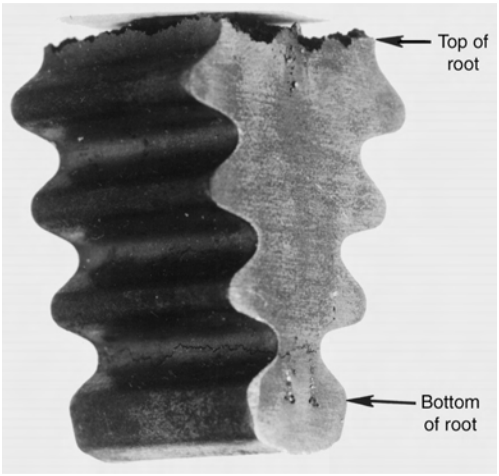


Fig. 14.16 Blade root failure, owing to low ductility of polycrystalline cast MAR-M-200 nickel-base superalloy

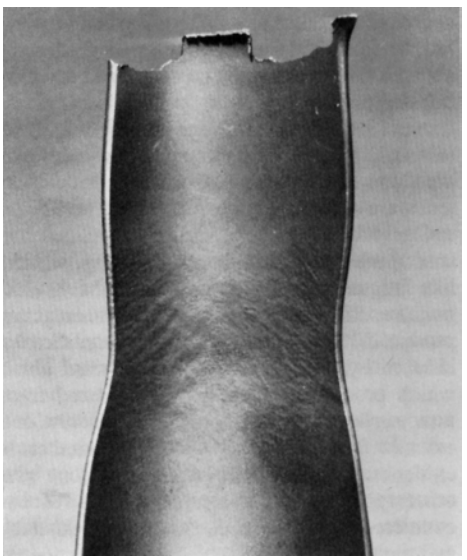


Fig. 14.17 Stretching and necking, owing to excessive creep in improperly heat treated nickel-base superalloy turbine blade. Note pinching of upper midspan region and extreme wear at blade tip

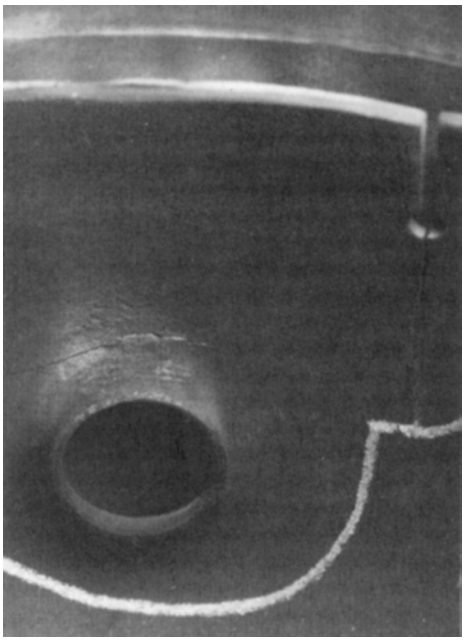


Fig. 14.18 Thermal-mechanical fatigue cracking on internal surface of a nickel-base superalloy forward liner of a gas turbine combustor. Note: One crack extends from a keyhole slot (right), while another can be seen in the area adjacent to an airhole (left). 1.5×

ward liner of a can-type combustor. One extends from a keyhole slot, and another is evident adjacent to an airhole. Among the other types of combustor failures found are distortion, extreme oxidation, and melting.

Example 8: Fatigue Cracking in Turbine Disk. At lower temperatures, less than about 1400 °F (760 °C), there may be failure of components as well. Barring gross errors in design, the failures at these temperatures are likely to be from fatigue. Wherever stress concentrations are high, fatigue is the most common mechanism of failure. Figure 14.19 shows cracking that was introduced in the rivet slot of a nickel-base superalloy disk. The cracking was induced by low-cycle applications of relatively high loads and so, is an LCF crack. In disks, LCF stems from stresses imposed by the combined effects of centrifugal loading by blades, the body load of the disk, and the thermally induced load between disk rim and bore. Discontinuities such as rim slots and boltholes are typically the sites for initiation of LCF cracks.

Damage Recovery, Refurbishment, and Repair

Recovery of Creep Damage. An aspect of microstructural and creep degradation that has received some attention, with limited commercial application, is the reported ability to heat treat creep-exposed alloys to recover creep-rupture strength. During creep exposure, alloys gradually form cavities (holes) along grain boundaries, and these cavities lead to the intergranular fracture which is characteristic of elevated temperature failures. In addition, there is carbide breakdown and γ' phase coarsening, such as that discussed previously.

When these processes have not proceeded for an excessively long time, it is claimed that complete recovery of strength is possible by using a solution heat treatment. However, ductility at rupture is reduced. Figure 14.20 illustrates the effect of one such treatment on the creep behavior of Nimonic 105 at 1600 °F (871 °C). The concept was investigated for Nimonic 115 wrought alloy and some for cast alloys as well, with variable results.

It has been determined that hot isostatic pressing (HIP) may significantly accelerate

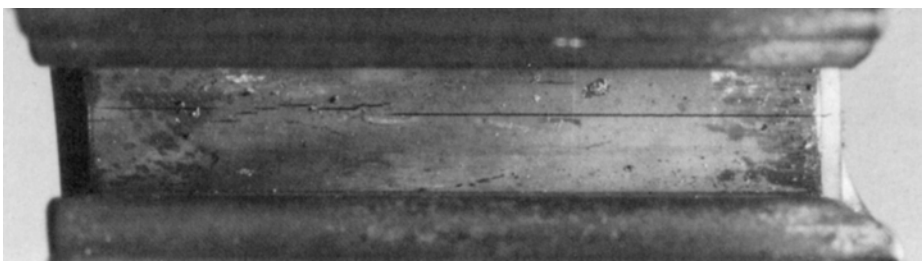


Fig. 14.19 Low-cycle fatigue cracking induced by thermal strains in the rivet slot of a nickel-base superalloy disk

the healing process, at least for creep cavities that do not extend to a free surface (see, for example, Fig. 14.21). Hot isostatic pressing has merit, but any process designed to produce recovery of mechanical properties, not just restoration of a surface, relies on faith that the current condition of the component relative to its mechanical life is known. The essence of the recovery process is that components must be tracked and somehow recorded as to their service environment, including stresses, times, and so on of exposure.

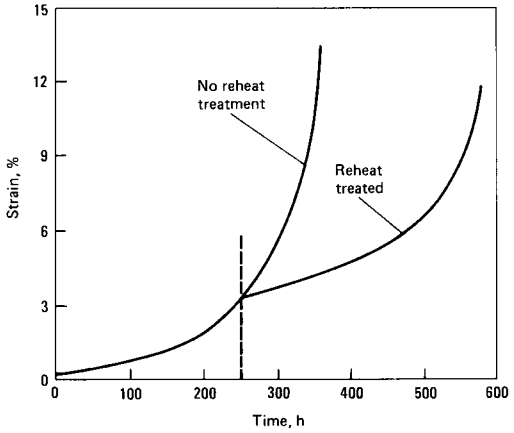


Fig. 14.20 Effect of a single reheat treatment on creep of Nimonic 105 at 871 °C (1600 °F). Curve at right is for specimen reheat treated after 250 h creep exposure, then continued in test

Presumably, a time can be picked when a given component (or set of components, as in the case of turbine airfoils) can be removed from an engine for recovery treatment. The logistics of monitoring components and the costs of recovery have limited the application of creep-strength recovery techniques. Another factor has been the limited-to-nonexistent recovery of creep-rupture ductility. Test results on complicated nickel-base superalloys showed that life, but not ductility, could be recovered. As most designs use (hopefully) safe design criteria, (where human safety is concerned, as in aircraft turbines) the possibility that a part might be put into service with substandard creep-rupture ductility is not one calculated to warm a designer's heart.

One area where tracking is more convenient appears to be that of land-based gas turbines. Although the creep-recovery process has been known since the 1960s and was claimed to be in use for some European military applications in the mid-1970s, the process has not generated much enthusiasm outside of the land-based gas turbine area.

Refurbishment and Repair of Gas Turbine Components. The turbine and combustor sections and some compressor components are the principal areas where superalloys find use in gas turbines. Lesser-strength superal-

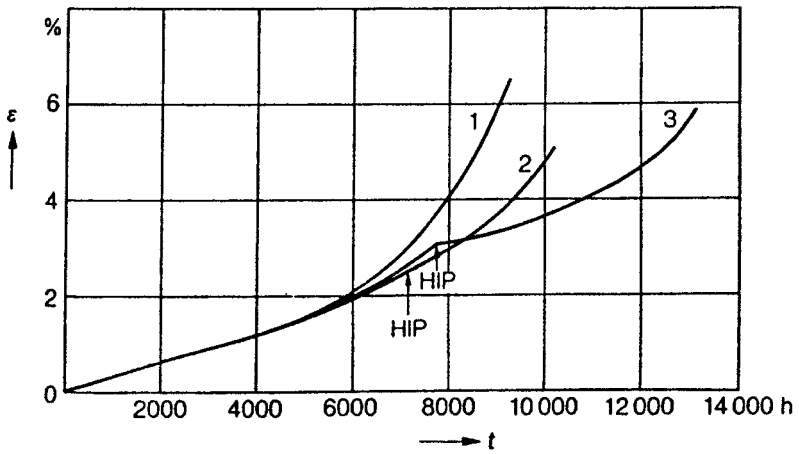


Fig. 14.21 Effect of hot isostatic pressing on creep behavior of IN-738LC nickel-base superalloy at 850 °C (1562 °F). 1, Test to fracture without interruption. 2, Retest after HIPing without surface machining. 3, Retest after HIPing with 0.5 mm surface skim. t, Time. ε, Strain

loys, particularly those with exceptional corrosion resistance to certain environments, do find use outside the gas turbine field. For aircraft gas turbines, the cost of the turbine-assembly components has been reckoned at times to be about 25 to 30% of the cost of an engine. This is a considerable sum for a region of the engine that is largely superalloy in composition. The desire to fully use the existing components is understandable. Thus, not only has there been pressure on designers to maximize design concepts for optimal performance with existing materials, but also there has been pressure on metallurgists to create better materials. Superalloy metallurgists have responded admirably to the challenge, but challenges exist to reuse components which have been declared by inspection or by design rule to be no longer serviceworthy in a given engine.

Refurbishment and repair represent a way to increase effective component life and cut costs. Although refurbishment should include refreshing the mechanical-strength life of a component, this area is fraught with problems and concerns and was, therefore, covered in the preceding section of this chapter.

Refurbishment and repair in the present context means:

- Straightening (removal of prior deformation)
- Recoating or coating specific surfaces that have been degraded by the environment
- Using joining techniques to close a crack
- Machining to blend impact damage or remove certain corrosion attack
- Attaching missing parts, such as wear-resistant blade tips

Not all of these actions are performed on a given unit, but variants of all are performed at some time on gas turbines. Non-rotating components, such as sheet metal structures and stationary airfoils (vanes) for gas turbines, have seen extensive application of some techniques for repair and/or refurbishment. Coatings are routinely removed and airfoils recoated; even coatings on rotating airfoils such as turbine blades are restored. Vanes that bowed too much have been recambered to restore original airfoil profiles. Cracked PC cast vanes, primarily cobalt-base superalloys, are welded, recoated, and returned to service. For low-pressure turbine blades that have hardfacing to provide wear resistance at rubbing tips, new hard face has been welded in place.

Some concerns about refurbishment and repair should be noted:

For coatings:

- It is imperative for successful recoating that all the old coatings be removed.
- Masking may be required to prevent coating removal from certain areas, such as cooling passages.
- The recoating process can only be used a finite number of times, because the stripping process removes some metal each time. Continued recoating can result in undesired reduction in wall thickness on cooled airfoils.
- Quality control is essential to ensure that no cracks are created or ignored during the process. There is evidence that hydrogen cracking can be induced in single-crystal alloys by the coating-stripping process.

For straightening:

- Extreme care must be taken to avoid cracking.
- The process is most effective for wrought components.
- Although some claim otherwise, PC cast vane airfoils (cobalt-base superalloys) for aircraft gas turbines can be straightened.
- The process is probably best done hot, but there is the need to avoid overaging.
- The process is not particularly widely used.

For joining:

- Brazing may be used to fill cracks, provided the component being brazed is not TMF life-limited. TMF life of brazed parts is unacceptable.
- Gas tungsten arc welding or electron beam welding can be used to repair weld cobalt-base and solution-hardened nickel-base superalloys for nonrotating components. IN-738LC precipitation-hardened nickel-base superalloy has been welded successfully for land-based gas turbine applications but requires postweld heat treatment to recover properties. Welding of high-strength PC cast nickel-base superalloys such as B-1900 was not found satisfactory to pro-

duce parts that would be desirable to return to service.
- Inserts have been welded in place on nonrotating parts. The manufacture of such inserts and the machining and positioning of them for machining is expensive.
- Electron beam, laser, or plasma arc welding are costly.

To provide reliable service after rejuvenation and repair, regions recoated, welded, or whatever should be limited to the lower-stressed regions of components and be done on nonmission- (nonsafety-) limiting components in a gas turbine or other device. The objective of rejuvenation/repair is to extend the total life of parts at a price that gives the greatest benefit in cost of ownership to a gas turbine operator. There are many constraints, as indicated previously. Time to rejuvenate/repair a component can exercise a considerable effect on the usefulness of a rejuvenation or repair. Processes are available to provide reasonable extensions of the lives of components in gas turbines. However, it would appear that rejuvenation by recoating a component for a limited number of times is the process routinely found most cost-effective.

Despite the increasing costs of bringing new alloys and/or processes on-board, it seems more economic and agreeable from a safety standpoint to increase engine durability and reduce costs by alloy and process development for new production, not reworking already engine-exposed materials and components.

Superalloys: A Technical Guide, Second Edition
Matthew J. Donachie, Stephen J. Donachie, p 339-351
DOI:10.1361/stgs2002p339
Copyright © 2002 ASM International®
All rights reserved.
www.asminternational.org

Chapter 15

Superalloys—Retrospect and Future Prospects

The 20th Century

Progress to the 1960s. By grouping the last century in approximate 20 year periods, a compact impression of the development of superalloys can be formed. The 20th century saw the understanding and adaptation of chromium as an additive to the transition metals iron, nickel, and cobalt, with marvelous beneficial effects on the corrosion resistance, both aqueous and gaseous. From nickel-base resistance wires and cobalt-base wear- and temperature-resistant alloys, it was a short jump in time to the stainless steels. From the start of the 20th century, about the time that Nichrome and Stellite (Deloro Stellite Inc.) products became available, it was a scant 15 to 20 years until the rustless irons (stainless steels) were in production during the 1920s.

By the end of another 20 years, approaching the start of World War II, the basis for current superalloys was laid with the development of a broad range of austenitic stainless steels, introduction of the cobalt-base alloy Vitallium, and the adaptation of the various strains of stronger Nichrome materials by the International Nickel Co., who introduced them to commercial use as Nimonic (Special Metals Corp.) and Inconel (Special Metals Corp.) products.

Carbide hardening was used to create the cobalt-base alloys, and, although the fundamentals of precipitation hardening were still being discovered, precipitation hardening nickel-base alloys were developed. At that time, the word ''superalloys'' had not yet been coined. The cobalt-base alloy Vitallium was relatively strong, but the nickel-base and iron-nickel-base products were wrought and relatively weak in creep rupture by today's standards. Nevertheless, many of the alloys of the 1940s time frame (Vitallium, Inconel X) still have use today.

From the 1940s to the 1960s, major advances occurred. The need for high-strength, high-temperature-resistant superalloys soared with the introduction of the gas turbine engine for aircraft applications. Iron-nickel-base superalloys were developed further as wrought materials, new cobalt-base superalloys were invented and brought to market, while both wrought and cast nickel-base superalloys became the predominant alloys of choice for the most strength-critical applications.

The development of vacuum melting technology for superalloys provided for a quantum leap in capability. Oxygen (and nitrogen) reduction enhanced strength and improved the efficiency of hardener additions, such as titanium and aluminum. Consequently, existing superalloys, for example, Waspaloy, gained significant amounts of strength by application of the vacuum melting process. Concurrently, the availability of vacuum melting made a new generation of cast, age-hardenable nickel-base superalloys, such as IN-713, more feasible. The quest for higher-temperature capability was paying dividends. At the same time, particularly in the mid-1950s, research on the nickel-base superalloys became very intense.

Charting Strength/Temperature Progress. Most historical charts of superalloy progress start with temperature capability of alloys about 1940. Some do not even start until 1950. The charts in Fig. 15.1 give a general overview of the increase in temperature capability from the mid-1940s to about 1970. In Fig. 15.1, alloys are treated separately by application, a realistic method of evaluating alloy capability. Fig. 15.2, however, groups all superalloys considered into a single chart.

Charts such as in Figs. 15.1 and 15.2 are the consequence of a need to put perceptions and thoughts on one or a few pieces of paper. Business practices are geared to the concept of the visual and instant presentation of a result, no matter how complex the concept leading to the result may be! It should be apparent by comparing the charts of Figs. 15.1 and 15.2 that the depiction of the capability of a complex superalloy by a single dot on a simple graph is a gross oversimplification. Nevertheless, we use such graphs,

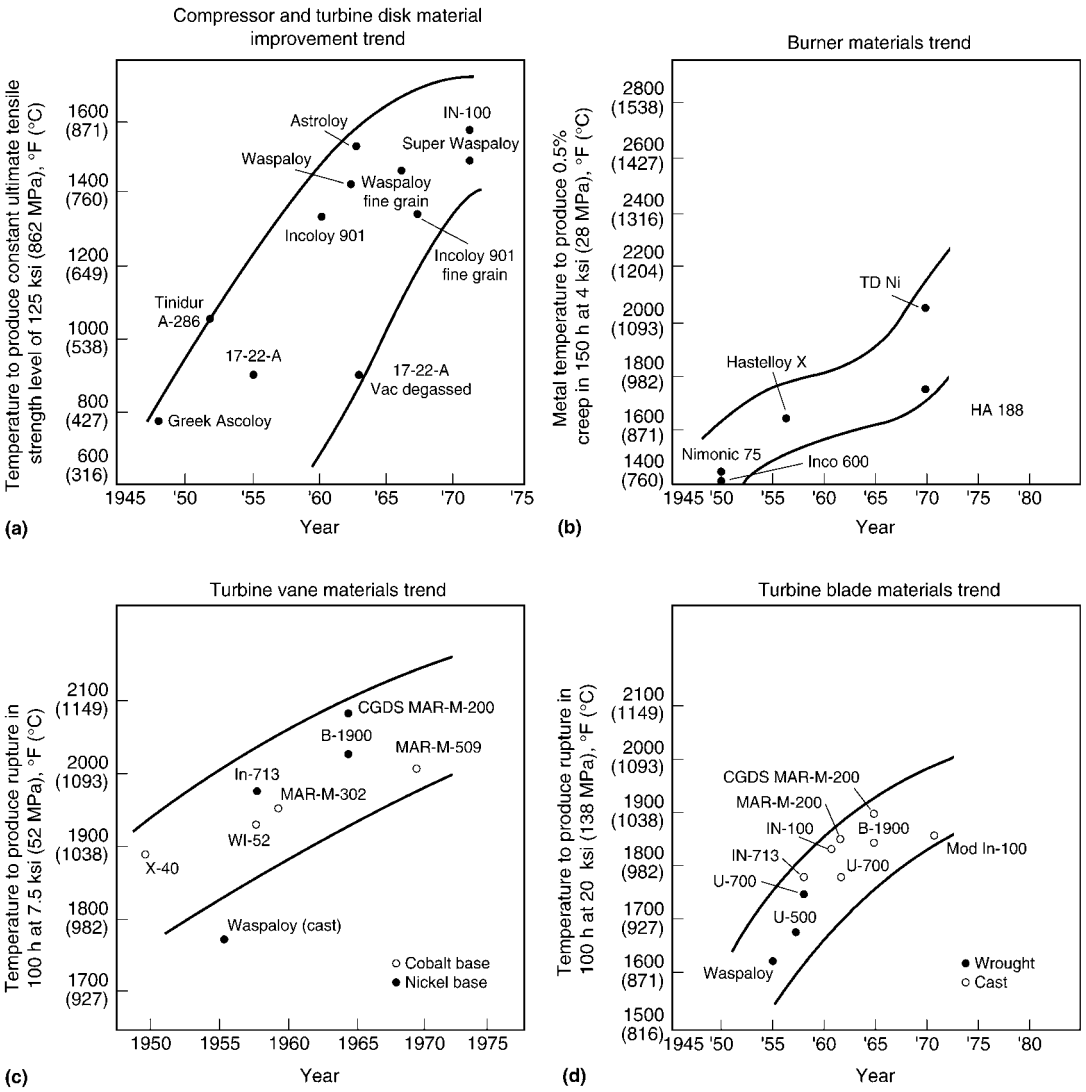


Fig. 15.1 Temperature-strength capability of selected superalloys as a function of year of availability (about 1945–1970). (a) Compressor and turbine disks, (b) burner cans and combustors, (c) turbine vanes, and (d) turbine blades

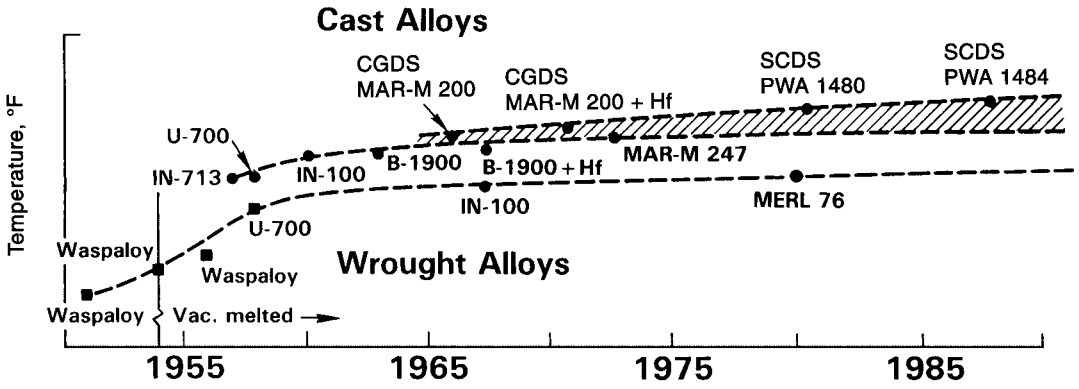


Fig. 15.2 Temperature-strength capability of selected nickel-base superalloys as a function of year of availability (about 1950–1990)

because they help to illustrate the many advances of the past half-century. Each researcher or presenter of a superalloy time line no doubt would have a bit different way of presenting such information.

Creep-rupture strength is not the only factor in the successful application of a superalloy. Figures 15.1(c) and (d) use rupture life; Fig. 15.1(b) uses creep life, and Fig. 15.1(a) uses ultimate tensile strength as a criterion. Thermal-mechanical fatigue resistance can be very significant, as can coated corrosion resistance. Tensile and low-cycle fatigue (LCF) properties play important roles in larger components such as gas turbine disks and might well form the basis for a different comparison of alloys.

Figures 15.1 and 15.2 use the concept of temperature capability to illustrate points. Temperature capability is a function of the location in strength-temperature-environment-time space where it is determined. Figure 1.1 used the 100 h rupture strength as a criterion. A related criteria is used in Fig. 15.1(d), where the criterion is the temperature that would be allowed if a superalloy were to fail in 100 h at a specific stress, in this instance, 20 ksi (138 MPa). Note that the alloys depicted in Figs. 15.1(a) and (d) are all nickel-base superalloys (with the exception of some steels in Fig. 15.1(a).

In the 1950s, the cobalt-base superalloys were still in wide use as cast turbine airfoils, and cobalt-base sheet superalloys were becoming available. However, by the early 1950s, it was clear that the nickel-base superalloys would exceed cobalt-base superalloys in creep-rupture strength. Moreover, the science of γ'-hardened nickel-base superalloys was building an information base that would enable even more substantial advances in strength than evident at that time.

The alloys depicted in the figures are but a few of those that were available by the mid-1960s. Starting with Nimonic 80A or Inconel X as a baseline, moderate progress was made with wrought alloys until about 1953. At that point in time, Waspaloy represented the strongest of the available wrought nickel-base superalloys. With vacuum melting replacing air melting, identical compositions of superalloys such as Waspaloy or similar alloys showed immediate, significant, strength improvements. Moreover, with vacuum melting in place, it was possible to add more hardeners than previously, and thus, still further improvements were possible with nominally the same alloy. This behavior is shown, also for Waspaloy, in Fig. 15.2. By about 1955 to 1957, the conventional wrought nickel-base superalloys such as U-700 (Astroloy variant) had reached their peak of progress, and the growth curve for temperature capability had leveled off.

About the same time, cast alloys such as IN-713 and U-700 provided another discrete jump in capability, and, by the mid-1960s, cast nickel-base superalloys were established as the materials for airfoils in the most demanding (strength/temperature) gas turbine applications, such as the high-pressure turbine (HPT) airfoils. Directional solidification (DS) had just been demonstrated for real air-

foils, and efforts began to develop DS technology for future airfoil use.

The Last Four Decades. While cast high-strength/high-temperature-capability nickel-base superalloys such as IN-100 and MAR-M-200 were available by about 1961, it was several more years before cast nickel-base superalloys became routinely used for HPT airfoils in aircraft gas turbines. Concurrent with this commercial evolvement, DS technology began to be used to produce columnar grain (CGDS) materials for future military engines. In addition, more advanced high-property-capability polycrystalline (PC) cast superalloys became available. It was a golden age for superalloy developers. Hundreds of alloy compositions were tried and many brought to the market place. Commercial alloy development was being supported by the United States government through its military branches, the space agency, and others; it also was being conducted by the major gas turbine manufacturers. Alloy producers, as well, worked on company funds or government contracts to raise the bar that superalloys could jump!

By the end of the 20 year period from about 1960 into the early 1980s, not only were columnar grain directionally solidified materials available and operating in gas turbines, but also single-crystal directionally solidified (SCDS) casting alloys had been produced. Figure 15.2 illustrates the extended range of temperature capability represented by this new technology (CGDS and SCDS). It is worth noting that available published data began to become more and more generic as time passed; for example, temperature was still plotted versus year in Fig. 15.2, but the criterion for defining the precise temperature values disappeared!

Figure 15.2 shows that CGDS alloys such as MAR-M-200 had been modified with hafnium by the 1980s, while second-generation CGDS alloys and first-generation SCDS alloys had emerged by 1990. Even PC cast alloys were advanced by the invention of MAR-M-247. An essential point to note from Fig. 15.2 is that the growth line for cast alloys also became much less steep than it was initially projected. In fact, the growth line for castings was not too dissimilar to that for wrought alloys, with a substantial but fairly constant increment in capability between them.

Another characteristic of the period from 1960 to about 1980 was the trend to convert strong cast nickel-base superalloys to wrought products. IN-100, initially a cast alloy, was successfully adapted to a wrought form using powder metallurgy (P/M) processing to produce HPT turbine disks. Other variations of IN-100 (e.g., MERL 76) subsequently were developed solely for use in wrought form. Variations of the cast alloy B-1900 were roll forged in the early 1960s to produce turbine blades, but, because wrought blades were being replaced by cast ones, further efforts were abandoned.

As the last 20 year period of the century commenced, second-generation SCDS nickel-base superalloys such as PWA 1484 soon became available to challenge the first-generation SC superalloys such as PWA 1480. By the 1990s, second-generation SCDS superalloys were standard in many aircraft gas turbine applications. So-called third-generation SCDS alloys are claimed. The description of these latter SCDS alloys as third generation is somewhat tenuous, because the alloy behavior is mostly modified by a sharp increase in the rhenium content of the alloys. Rhenium additions went from 0% in first-generation alloys to about 3% in second, and in the realm of 6% in third-generation SCDS nickel-base superalloys. The newer alloys have merit, but temperature capability is not likely to be much greater, nor is the TMF capability likely to be increased more than a fraction over that of the first- and second-generation nickel-base superalloys.

Contemporary with the development of alloys, from 1960 to the present, was the realization that coatings would be needed to protect component surfaces from degradation owing to gaseous and deposit-modified corrosion. Aluminide diffusion coatings were applied with increasing frequency, and MCrAlY-type (where M = metal such as Fe, Ni, Co or combinations thereof) overlay coatings were developed for commercial use. Substantial increases in life at engine operating temperatures and the minimization of hot corrosion attack in many applications resulted from such coatings. Unfortunately, it is difficult to chart coating performance, because it is so highly dependent on the substrate alloy, coating application process, and the actual operating environment. No satis-

factory chart comparable to Fig. 15.2 exists for coatings.

Other Charting Processes for Superalloys. Temperature is not the only variable which has been used to describe the advancing capability of superalloys with time. Other charting methods have been employed. Figure 15.3, for example, shows advances in (wrought) turbine disk materials from 1940. The chart is over 20 years old and assumed advances that were not made. The alloys depicted appear to show several distinct stages of yield-strength-capability growth. However, when the P/M growth spurt is examined, it turned out to be an expected but unrealized (commercially) property level. The dotted lines in Fig. 15.3 indicate the real track of disk superalloy improvement in the past 20 years. Most of the actual disk alloys developed or adapted to P/M production lie on a rather flat extension of the vacuum melting region following Rene 95 in Fig. 15.3. In other words, a short-time strength chart for P/M superalloys also shows a leveling off of strength capability for wrought disk alloys in a manner comparable to that for cast nickel-base turbine airfoil or conventional wrought turbine disk superalloys.

A plot similar to Figs. 15.1 and 15.2 has been made (Fig. 15.4) for the temperature capability of turbine blade alloys used in the United Kingdom. With a specific criterion of 1000 h creep-rupture failure at 21.8 ksi (150 MPa), wrought and cast alloys (with PC, CGDS, and SCDS indicated) are compared. In general, this plot conforms to Fig. 15.2 and 15.3.

During the last 20 years of the 20th century, efforts on second-generation SCDS superalloys culminated in the introduction of such alloys in aircraft gas turbines, as noted previously. Concurrently, aircraft investment-casting technology was adapted to casting of the more hot-corrosion-resistant turbine airfoil alloys used in land-based gas turbine power-generation applications.

Land-based gas turbines use markedly larger blades and disks than do aircraft gas turbines. The size of components thus poses major production challenges that cannot be represented easily by charts. Taking 1980 as a starting point and IN-738 as the base alloy, advances for land-based gas turbine airfoils were made by taking highly hot-corrosion-resistant and strong nickel-base superalloys and processing them by DS methods. For example, CGDS IN-792 was produced, and, eventually, SCDS IN-792 was made in the very large sizes needed for land-based turbines. Various other alloys have been investigated as CGDS and SCDS products. Figure 15.5 shows a representation of the temperature-capability increases in land-based gas turbine airfoils since 1970.

It was desired to utilize wrought superalloys for disk and rotor applications. At one time, IN-718 (the most frequently used superalloy for aircraft gas turbines) could only be produced at maximum sizes of 20 in. diameter. Thus, truly large industrial gas turbines for land-base power generation continued to use steel rotors or, in some cases, superalloys such as IN-706. (IN-706 is less segregation-prone than IN-718 and can more easily be produced in larger diameters.) At the turn of this century, improved vacuum arc

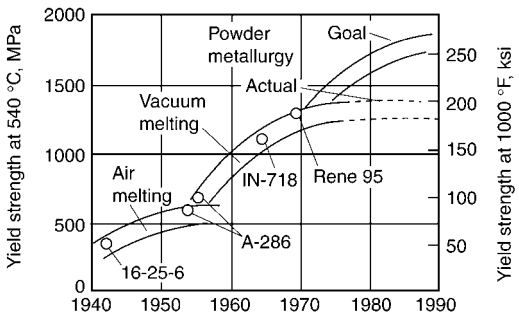


Fig. 15.3 Advances in disk superalloy yield strength as a function of year of availability (about 1940–1990) showing projected goals for powder metallurgy alloys and actual results (dotted line)

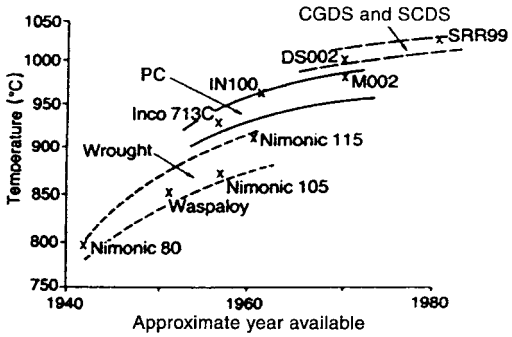


Fig. 15.4 Temperature-strength capability of selected nickel-base superalloys as a function of year of availability (about 1942–1980). Temperature determined for 1000 h life at 150 MPa (21.8 ksi). Note: This figure is not from same data sources as Fig. 15.1–15.3.

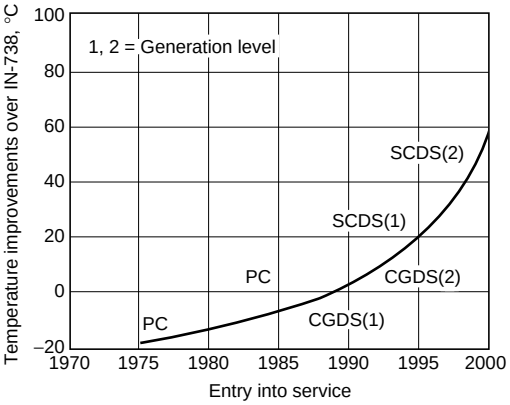


Fig. 15.5 Increases in temperature-strength capability of cast nickel-base superalloys for airfoils of large utility gas turbines as a function of year of availability (about 1950–1990). Results referenced to IN-738, showing advances for polycrystalline (PC), columnar grain (CG), and single-crystal (SC) directionally solidified (DS) alloys

remelting (VAR) techniques and ultra-tight composition control have expanded the size capability of IN-718 to 30 in. ingot, resulting in the ability to process IN-718 to the large disk sizes needed in modern industrial gas turbines.

Advanced wrought alloys for land-based gas turbine disks were sought as well during this time. Materials such as IN-100 were much too low in chromium content to be considered for these applications, but alloys of that strength level were desired. U-720, a nickel-base superalloy for cast and wrought turbine blades, evolved as a turbine disk material. Reductions in chromium content (to avoid sigma phase formation) and in minor elements (carbon and boron, to reduce stringers and clusters of carbides, borides, or carbonitrides) created an alloy known as U-720LI. This alloy and U-720 have been of considerable interest for land-based gas turbines and, in fact, have been incorporated in some aircraft gas turbines.

Evaluating Progress. What did these advances bring to component design and the designer?

- Nickel-base superalloys that can be used to a higher fraction of their absolute melting points than alloys in any other metal systems
- Temperature-(strength) capability increases (based on creep rupture) of over 400 °F (250 °C) since the 1940s
- Temperature-(strength) capability advances of about 25 to 50 °F (15 to 30 °C) per new alloy over each prior alloy placed in service during the past 40 years
- Enhanced resistance to TMF
- Increased use of many critical (and often costly) materials, such as tantalum and rhenium
- Reduced forgeability/formability of superalloys
- Increased oxidation capability of superalloys
- Reduced hot corrosion capability of superalloys
- Increased reliance on coatings for surface protection against corrosion
- Partial reliance on thermal barrier coatings for protection against high temperatures
- Increased manufacturing complexity (in part, owing to design complexities)
- Increased costs
- Superb vacuum melting technology, greatly enhanced investment-casting technology, electron beam and plasma coating deposition technology, and P/M fabrication technology

Most of the preceding represents goodness to the designer, but some factors, especially increased costs and manufacturing complexity, are undesired but expected outcomes of the advances in superalloy capability.

Past Projections Revisited. In 1986, the American Society for Metals published, via an article by Ross, et al., (Superalloys in 2001, *Advanced High Temperature Alloys*, ASM), a projection about Superalloys in 2001. A current projection of the future might well benefit from a review of the past projection. Some of the conclusions of 15 years ago were:

- Quality will be higher, costs lower.
- The superalloy application regime will be about the same as today, but there will be new, advanced alloys in some of the applications.
- Revolutionary changes in processing and quality-assurance methods are expected.
- The superalloy producers in the year 2001 may not all be the same ones we have today.

These were very conservative predictions; some came true. Costs are, unfortunately, not significantly lower, but quality is higher today (21st century) than ever before. Process improvements have been steady but hardly revolutionary. The business climate of the late 20th century led to the vindication of the last prediction mentioned above, the superalloy manufacturing business has undergone a revolutionary change with the agglomeration of activities in large business entities. For example, Special Metals Corp., one of the premier superalloy melting houses, is comprised of its original melt shop plus the former United States and United Kingdom facilities of the International Nickel company. Cytemp, a one-time major melt shop is no longer in operation. Forging houses have merged and, in turn, been acquired by organizations with no previous forging experience or facilities. In short, while continued steady and evolutionary progress has been made in the introduction of improved products, the revolutionary changes have occurred among the organizations providing the products.

Quality and costs were uppermost concerns in 1985; they remain so today!

The 21st Century

Alternate materials may be possible in coming years, but, based on past projections and results, there is little likelihood of chemical changes to, for example, intermetallics or refractory metals as viable alternates. This book is concerned with the superalloys and does not discuss alternates outside the normal superalloy regime.

Kinds of superalloys other than ordinary cast and wrought-P/M materials have been explored over the years, with limited to zero success. For a number of years, fiber-reinforced superalloys were touted as a great leap forward but were not successful in achieving commercial development. Oxide-dispersion-strengthened (ODS) superalloys, on the other hand, have achieved a very limited use in aircraft gas turbines.

A problem for the ODS superalloys is manufacturing complexities and the development of adequate strength in the root attachment area of ODS superalloys designated for turbine blades. Short-time strength of ODS superalloys generally is inadequate for turbine blade application. Oxide-dispersion-strengthened alloys can have very high melting points, excellent high-temperature creep-rupture strength, and superb oxidation resistance. Thus, ODS alloys find application in turbine vanes for some military aircraft gas turbines, an application where short-time strength properties are not of concern. However, ODS superalloys, while often considered for commercial aircraft gas turbines and for land-based turbines, have not made much progress in several decades. High costs, anisotropy introduced by processing, and quality concerns combine to minimize opportunities for ODS introduction. Higher costs for property balances, which are not as good as those in cast superalloys, plus inability to accept creation of the complex and convoluted cooling passages used to reduce component temperature, make widespread adoption of ODS superalloys unlikely.

Rapid solidification rate (RSR) processing has been used with little success. The (usually) nonequilibrium ultrafine grain size or noncrystalline powders, ribbons, and so on produced by RSR have not been amenable to the creation of a product with increased temperature-strength capabilities. Nanocrystalline technology, which may use RSR to produce products, has been claimed to offer great promise for materials but is unlikely to be of much advantage to the superalloys themselves, although improved thermal barrier coatings (TBCs) are not out of the question.

Process Modeling. One of the more significant developments of the last decade of the 20th century is one that will continue to become more important in the 21st century. From treatment of solidification of large ingots several feet (⅔ of a meter) in diameter to studies of aircraft gas turbine HPT airfoils, from cogging and forging to die filling and consolidation in P/M superalloys, process modeling has become an accepted tool.

At this time, each modeling event is unique. Corporations and individuals have studied the manufacturing processes of interest and set out to model them, using appropriate algorithms and computer facilities. Modeling of the solidification and deformation of IN-718 remelt ingots has been conducted. Process parameters and appropriate

parameters of materials are claimed to be capable of defining the following in IN-718:

- Grain structure
- Grain size
- Interphase spacing
- Structural transitions
- Microsegregation defects
- Secondary phases (Laves, δ)

It also has been claimed that the modeling process is sufficiently mature to be used for remelting process development and optimization (see Chapter 4). Single-crystal nickel-base superalloy investment casting has been modeled with interesting results, but much remains to be done before predictions of the type claimed previously are possible for these many-orders-of-magnitude-smaller parts. Related developments have seen the creation of finite-element modeling methods to predict the grain size variations in the cogging process for ingots.

Many programs have been investigated and developed for predicting such alloy characteristics as the liquidus and solidus temperatures of γ′-hardened nickel-base superalloys. Casting simulation software such as ProCAST and other programs such as MTDATA have been used to create the desired results. The ability to determine, to a high degree of accuracy, the window of temperature in which a high-$V_f\gamma'$ alloy can be heat treated is an important part of maximum utilization of the strength capability of a SC superalloy. Modeling may help.

Knowledge of the propensity of an alloy to topologically close-packed (tcp) phase formation is another important aspect of alloy design and subsequent manufacturing processing. Various programs purporting to assist or complete alloy design in nickel-base superalloy systems have been around for years. In general, in the authors' opinion, all such programs may provide guidelines, but are insufficient methods on which to base alloy development. Some 50 years ago, Zener predicted that alloy development/design would be conducted with algorithms using basic thermodynamic and physical property data. The authors do not perceive that such a result is possible at this stage for nickel-base superalloys.

Modeling of solidification kinetics and microstructural response to mechanical and thermal influences may be feasible. However, the essence of all modeling of such processes is the need for materials property parameters that often are not well determined. In the authors' experience, the following properties are rarely determined with great accuracy for any given alloy:

- Dynamic elastic modulus variation with temperature
- Thermal expansion coefficient variation with temperature
- Thermal conductivity variation with temperature
- Density

These properties are often not determined at all or are determined only by a single measurement or two. They are rarely published in the technical literature and frequently represent only a single heat (cast) of material. Estimates of properties are frequently made using comparable materials. In one instance of which the authors are aware, initial measurements of the physical properties and modulus of an alloy were done with three test runs. Some five years later, another heat of material was measured at the original test laboratory, with dramatically different results for the physical properties (no modulus measurements were made). No change in alloy chemistry had occurred.

Inquiries with the external test source failed to elicit any comments other than a statement that the original test engineer had left. The organization had no records of the initial test and did not know (nor care) why there was a difference. With data such as this, meaningful predictions are going to be more difficult to make. In the authors' experience, variations of $+/-10\%$ are possible in reported values of dynamic modulus, with similar variations possible on physical properties. Even density has been revised for alloys over the years, despite the fact that no change in chemistry has been reported.

Modeling in all its broad forms is a significant step in the direction of reduction of manufacturing costs. The authors suggest that it will not be a totally effective tool without better physical and mechanical property data on a wide range of superalloys. Modeling will not be accurate and may not be widely used without many confirmation tests on ingots or components, a process that may be quite costly. A large ingot of IN-718 may represent a metal cost of several hundred-thou-

sand dollars, essentially only partly recoverable by recycling the scrap. A turbine disk forged from an increment of a billet produced from such an ingot may represent a cost of tens of thousands of dollars after it is fabricated and then cut up for testing. The fabrication cost of the disk is not recoverable!

There is a need to develop improved models. However, the will also is needed to spend the money necessary to generate data for basic materials, especially to cut up ingots and components for thorough examination and, as modeling development proceeds, to make the resultant commitment to downgrade costly alloy as scrap. These requirements may be a powerful deterrent to rapid expansion of process and alloy modeling.

In the long run, modeling programs such as those directed at large ingot solidification or the cogging and forging of alloys should pay off in decidedly reduced costs of manufacturing process development. Whether that payoff is soon or distant is uncertain. The developers of a program for predicting IN-718 grain size arising from cogging operations suggest that modeling may enable future development of a reliable process for producing the long-desired dual-property turbine disk with optimal mechanical properties.

Projections for the Near Future. Newer manufacturing processes have been tried or suggested for improving the existing superalloys. The concept of processing, not alloy development, as the best route to alloy improvement was suggested by one of the authors about 30 years ago. It is obvious that process development is essential to superalloy growth. A review of the success of the forging and the investment-casting industries and the growth in HPT airfoil capability indicates great progress has occurred, virtually all of it achieved by process developments.

While it is true that many alloys were invented during the last 40-year period, the ability to develop maximum-strength alloys was the result of the application of improved processing. Metallurgists learned how to conventionally forge an existing wrought/cast superalloy, Astroloy. They learned, as well, how to adapt superplastic-type forging processes to better forge such materials, both those from ingot metallurgy and those from P/M processing. In the cast alloy area, the DS process permitted the application of previously unusable alloys (MAR-M-200, initially a low-ductility PC alloy, now made by CGDS processing). The DS process allowed the chemistry changes needed to further increase alloy strength through more usable γ' hardener and melting temperature increases (PWA 1480 made by SCDS processing). Step heat treatments were devised to increase the V_f of fine γ', thus increasing alloy strength capabilities of many cast alloys.

Temperature-strength limits have been nearly reached for cast superalloys, and the likelihood of a development spurt that will add another 25 to 50 °F (15 to 30 °C) to the current third-generation SC superalloy capability is minimal. Better TBCs may reduce metal temperatures and allow higher operating regimes, but the superalloys are unlikely to get much better for aircraft gas turbines. On the other hand, where temperature per se is not the problem, but where crack growth, LCF life, and tensile properties are of concern (as in turbine disks), advancements still can be made. A more crack-growth-resistant nickel-base disk alloy is all but certain; perhaps it is here now, dependent on how you read industry reports.

Additions of rhenium have reached 6% in third-generation superalloys, and ruthenium is now being added as well. Significant understanding of the roles of precipitate mismatch has been achieved. Modifications of rhenium-containing alloys with and without ruthenium purportedly show further strength improvements over the 3% Re superalloys previously developed. The development of the new alloys has produced higher densities. Thus, the specific strength of new alloys containing larger amounts of rhenium and/or ruthenium may not be much superior to existing SCDS superalloys. When one considers the cost benefit situation for alloys containing elements such as rhenium, ruthenium, and even platinum or iridium, it is hard to perceive that the marketplace will accept many of these new SCDS alloys. Improved processing may continue to offer more cost/performance benefits than new alloys with ''exotic'' elemental additions.

Third-generation SCDS superalloys will find application in the aircraft gas turbine industry. Growth of alloy compositions is likely to stagnate, but work on investment-cast processing will continue to increase quality, speed of delivery, and product quality. Investment-casting costs will be benefited by

more use of rapid prototyping. Increased attention will be devoted to the casting of ultrathin (10–20 mils, or 0.025–0.050 mm) sections with high-detail features (e.g., small cast-in pins on a thin panel). At the end of the 20th century, more modest-size parts, formerly fabricated from multiple wrought and cast components, may be cast as single units at cost savings of as much as 50–80% over costs.

There also is the possibility of commercial acceptance of the concept of rafted γ' structures. In SCDS cast alloys, the stress alignment of γ' that has long been known to take place in grains of nickel-base superalloys can be used to advantage, owing to the presence of just a single grain. Under an applied stress at elevated temperatures, the discrete γ' cuboids (or spheres) tend to link up to form somewhat plate or raftlike structures. These structures are called γ' rafts. Dependent on the crystallographic orientation, the mismatch of the lattice parameters and elastic moduli, and the sign (tension or compression), various rodlike or platelike γ' morphologies can develop during creep deformation. Most SCDS cast alloys have an <001> orientation. The result of this orientation is that γ' plates (rafts) form perpendicular to a tensile stress axis or parallel to a compressive stress axis at high temperatures where creep can occur. The rafts thus are the product of a directional coarsening process and, when formed, seem to be stable throughout most of a creep-rupture test, because the rafts and their γ-γ' interfaces resist creep deformation by making it more difficult for dislocation bypassing to occur. It has been shown for some alloys (commercial and model) that effective creep-rupture strengthening is achieved by rafting. The difficulty in applying the technique lies in the geometry of the components and the long times or pretreatments often needed to effect satisfactory rafting. Unless a cost benefit can be shown for the rafting process after a commercial heat treating (under load) methodology is developed, it is not likely that many, if any, rafted γ'-hardened alloys will be used.

The melting industries will make even larger ingots available for conventional ingot-metallurgy forged disks of the existing alloys, such as IN-718 and U-720, used in gas turbines. Quality will continue to improve for ingots. Significant effort no doubt will occur on production of larger disks for the land-based gas turbines, again, mostly with current superalloys.

Table 15.1 Turbine airfoil alloy application metal temperature vs. melting point or range

Classes of superalloys	Max useful temperature, °F (°C)	Incipient melting point, °F (°C)
Conventionally cast	2050 (1121)	2200–2250 (1204–1232)
CGDS	2050 (1121)	2200–2250 (1204–1232)
SCDS	2250 (1232)	2330–2400 (1277–1316)
ODS	2450 (1343)	2550 (1399)

Useful operating metal temperatures for cast superalloys will not be greatly different from those achieved in the 1980s, when SCDS superalloys had been operating successfully in aircraft gas turbines for many years. Table 15.1 lists suggested useful temperatures and corresponding melting temperatures for classes of superalloys existing at about the end of the 1980s. Since then, some SCDS alloys have moderately advanced the upper limit of useful temperature, but PC and CGDS superalloys have temperature capabilities about the same today as at the end of the 1980s. Useful operating temperatures for disks will not change much in the future either, but effective mechanical-property capability will go up as defects are made less common and smaller in wrought products and damage-tolerant microstructures are created.

Dual-property wrought disks will continue to be developed but may not meet necessary design criteria (crack/defect size, strength, etc.) very soon. Cast integral disk/blade concepts still will not be applied to large aircraft gas turbines, though they will remain an option for smaller gas turbines. Large structural-casting use will continue to expand, but it is unlikely that additional alloys will be used. IN-718 will continue to be the most-used wrought superalloy and the alloy of choice for large structural castings. Land-based gas turbines will expand use considerably, with attendant need for more superalloys. IN-939 is being cast in ''case-type'' components as much as 1 ft (0.3 m) in diameter and 6 in (~18 cm) in height. Larger castings may be required for utility gas turbines.

Modeling will be extended across the board from forging to casting, coating to primary melting, and, judiciously applied, mod-

eling efforts should lead to reduced process development costs.

Newer alloys, especially cast nickel-base superalloys for turbine airfoils, will continue to be evaluated for the land-based gas turbines. However, the cost of evaluating an alloy and bringing it to production application as a turbine component, whether for an aircraft turbine or a land-based turbine, will continue to be many millions of dollars per alloy, and it may not be cost-effective to adopt new alloys, owing to the high cost of alloy invention and process development for the alloy. As an example, the number of alloys actually used for turbine blades and vanes by any given aircraft gas turbine company since 1950 can probably be counted on the digits of both hands. It takes an exceptionally good projected improvement in properties, a major application crisis, or both to force the hand of designers and project engineers to spend the money needed to upgrade a gas turbine or fix a problem. Hundreds of potentially good alloys were created in United States during the 1960s and 1970s. Perhaps a dozen reached manufacturing maturity.

Cast turbine airfoil surface degradation will continue to be a problem in certain applications. A large potential still exists for the improvement of coatings to protect against degradation. Improvements in existing coating deposition processes are possible to lower costs and/or improve properties. While no specific new processes have been reported, cost reductions should occur, and overlay chemistries may change. Tailored coatings for specific substrate alloys are a possibility, as opposed to the generic use of overlay coatings today.

More aggressive recycling efforts will be made to increase the percent of same-alloy scrap available to melters for wrought or cast alloy applications. The recurring national and international energy concerns will mandate this approach. Increased use of scrap may put pressure on manufacturers who will be trying to increase or at least to hold the line on quality.

Some Current Improved Alloys. Columnar grain directionally solidified cast alloys for aircraft gas turbines have been claimed to be improved by using rhenium (originally used for SCDS alloys). CM-186LC is a cast superalloy with 3% Re and a $V_f\gamma'$ of 70%. The alloy contains hafnium (for transverse grain-boundary ductility) and reportedly has improved resistance to property degradation caused by grain-boundary misorientations up to 25°. That property means more castings can be accepted, and component casting yield is improved. The result is an improved CGDS alloy that, although not as strong as an SCDS superalloy, has excellent properties and a component cost as much as 50% less than that of a conventional nickel-base SCDS superalloy.

Improved SCDS alloys have been developed by gas turbine companies, but little detail has been provided. CMSX-10 (Cannon-Muskegon Corp.) alloy has been introduced as a third-generation SCDS superalloy. The use of 6% Re in the alloy is claimed to produce about a 50 °F (30 °C) improvement over second-generation alloys such as CMSX-4 (Cannon-Muskegon Corp.) PWA 1484, and Rene N5. One drawback to CMSX-10, stemming from its low diffusion rates, is an extremely long (30–35 h) solution heat treatment time. The long solution times for some SCDS superalloys and the use of costly alloy elements (such as rhenium) are significant factors in keeping costs of components high. High-rhenium alloys may be prone to tcp phase formation with long-time exposure and a resultant degradation in creep-rupture strength.

As noted, wrought U-720 and U-720LI are being applied and/or evaluated for industrial gas turbine use as disks. U-720LI has been produced by P/M processes and standard ingot metallurgy is the preferred practice at this time.

Figure 15.6 summarizes, in yet another temperature-capability chart, some of the many superalloys mentioned in this book. Slight modifications have been made from its original form to make the chart more applicable to current practice. The reader should keep in mind that even this presentation omits many worthy alloys, quite a few of which are or were widely used. The figure also projects ODS γ'-hardened alloys to levels not achieved in applications.

Longer-Term Projections. Long-term projections of the demise of superalloys have been standard for a quarter century. Competitor materials continue to flounder and will do so for aircraft gas turbines in the long term as well. It is possible that spray-formed-to-shape

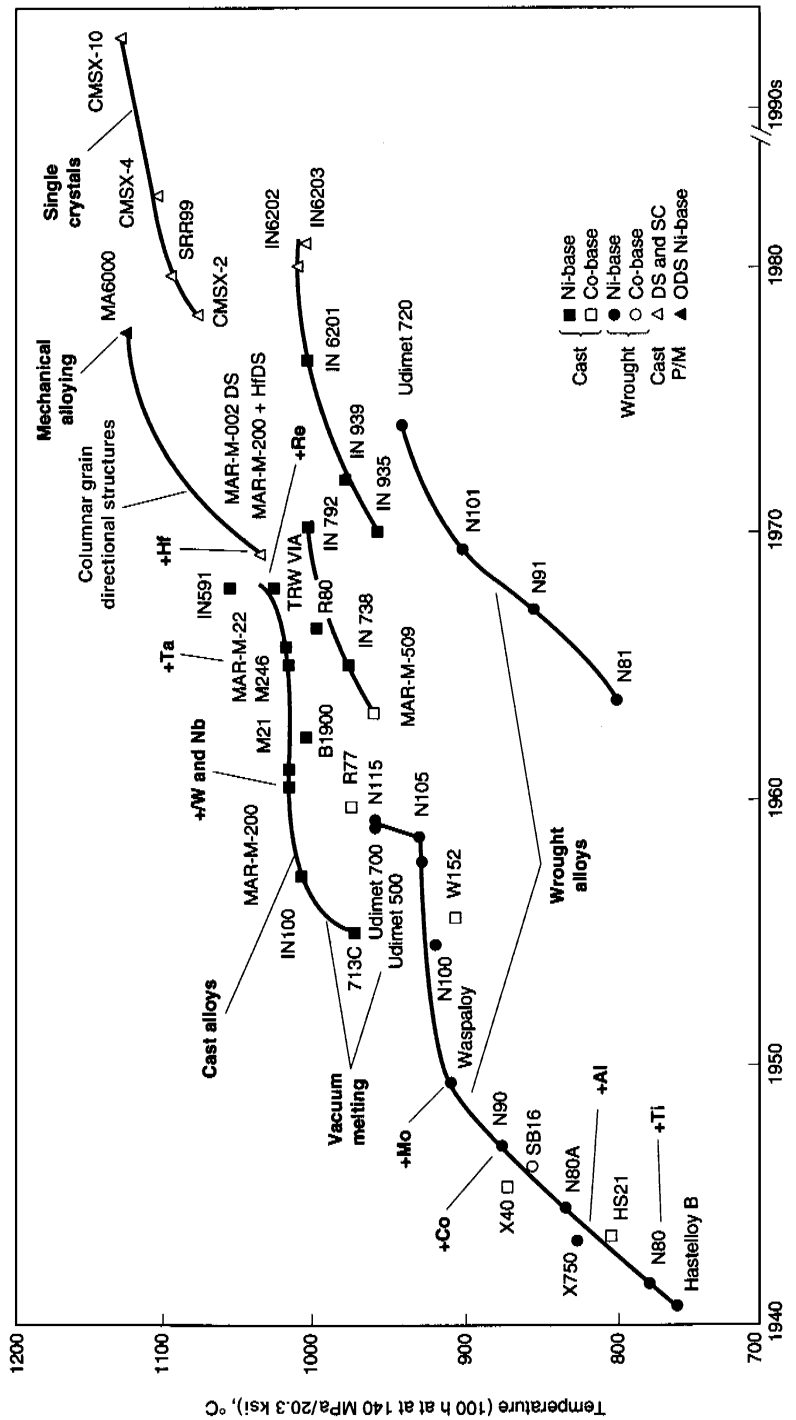


Fig. 15.6 Increases in temperature-strength capability of superalloys as a function of year of availability (about 1942–mid-1990s)

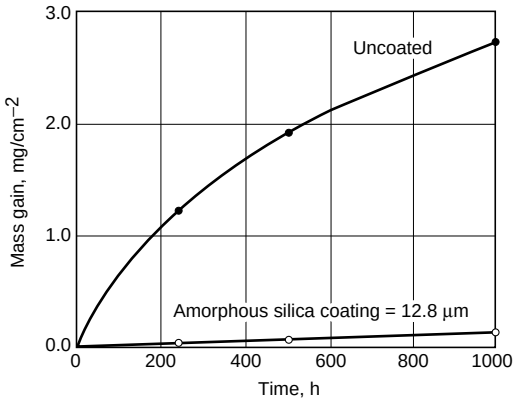


Fig. 15.7 Effect of amorphous silica in protecting IN-939 nickel-base superalloy during oxidation at 899 °C (1650 °F) for 1000 h

powder components may be of value, but lack of plastic deformation of the product is likely to lead to unacceptable risks in application. Improved TBCs, for example, using laser fusion to seal the surface, may have merit.

Silica (amorphous) may turn out to be a method of protecting the surface of airfoils in land-based gas turbines. Figure 15.7 illustrates the beneficial effects of such a coating in protecting a very hot-corrosion-resistant nickel-base superalloy, IN-939, against corrosion. These tests, at 1650 °F (899 °C), a temperature in the hot corrosion region, were oxidation tests, not hot corrosion tests. The oxidation-resistance potential is significant. It is not clear if this was a cyclic oxidation test or what the results would have been if contaminants had been introduced to cause hot corrosion.

As for other projections, the authors have none, except to state that future use of superalloys should continue at the present at a slightly increased rate. A large number of new chemistries may not be forthcoming, but only the superalloys are capable of reliably satisfying the demands of the gas turbine industries and other areas such as energy exploration and delivery. There are no demonstrable replacements with the strength, ductility, and corrosion-resistance balance of such alloys. The coating/alloy combinations will continue to improve, if only slightly, and manufacturing capability will ensure that larger disks, larger structural castings, and larger investment castings will be available to meet customer requirements. Quality will continue to improve.

Superalloys: A Technical Guide, Second Edition
Matthew J. Donachie, Stephen J. Donachie, p 353-355
DOI:10.1361/stgs2002p353
Copyright © 2002 ASM International®
All rights reserved.
www.asminternational.org

Appendix A

Source Information

Some Superalloy Information/Product Sources

This is only a partial list. Not all companies or institutions active in superalloys are represented. No recommendation is made or implied by this list. Moreover, the changing industry mix may make some parts of this list obsolete. All information compiled April 2001.

Product	Possible source
General information	ASM International, Materials Park, OH; www.asminternational.org Nickel Development Institute, Toronto, ON, Canada; www.nidi.org Cobalt Development Institute, Guildford, Surrey, U.K.; www.cobaltdevinstitute.com International Chromium Development Institute, Paris, France; www.chromium-assoc.com Specialty Steel Industry of North America, Washington, D.C.; www.ssina.com The Minerals, Metals and Materials Society/American Institute of Mining, Metallurgical and Petroleum Engineers, New York, NY; www.tms.org
Melting/ingot production, forming and/or mill products	Special Metals Corporation, with locations at New Hartford, NY; Huntington, WV; and Hereford, U.K.; www.specialmetals.com Carpenter Technology Corporation, Wyomissing, PA; www.cartech.com Haynes International, Kokomo, IN; www.haynesintl.com Teledyne Allvac, an Allegheny Technologies Co., Monroe, NC; www.allvac.com Cannon-Muskegon Corp., Subsidiary of SPS Technologies, Muskegon, MI; www.greenvillemetals.com/cmgroup.htm Howmet, with locations world wide, including Dover, NJ and Devon, U.K.; www.howmet.com Doncasters PLC, with locations including Sheffield, U.K.; www.doncasters.com Precision Rolled Products, Florham Park, NJ; no Web site
Investment castings	Howmet Corp., with locations including Hampton, VA; Whitehall, MI; LaPorte, IN; Wichita Falls, TX; Devon, England; Gennevilliers, France; Dives, France; and Terai, Japan; www.howmet.com Precision Cast Parts, with locations including Minerva, OH; Cleveland, OH; Mentor, OH; and Douglas, CA; www.precast.com Doncasters Precision Castings, with locations including Droitwich, Worcs, U.K.; Bochum, Germany; Groton, CT; www.doncasters.com Hitchiner Manufacturing Co., Inc. Gas Turbine Div., Milford, NH; www.hitchiner.com
Forgings	Wyman Gordon Co., with locations including N. Grafton, MA; Livingston, Scotland; and Houston, TX; www.wyman-gordon.com Schlosser Forge, Cucamonga, CA; www.aerospace-engine-parts.com Ladish Co, Inc., Cudahy, WI; www.ladish.com Carlton Forge Works, Paramount, CA; no Web site Carmel Forge, Tirat Carmel, Israel; Web site unknown Doncasters PLC, with locations including Monk Bridge, U.K.; Blaenavon, U.K.; Leeds, U.K.; www.doncasters.com Thyssen Umformtechnik, Remscheid, Germany; www.tut-gmbh.com Fortech, Clermont-Ferrand, France; Web site unknown Firth Rixson, with locations including Monroe, NY and Verdi, NV; www.firthrixson.com Forged Metals, Fontana, CA; www.forgeman.com

(continued)

Some superalloy information/product sources (continued)

Product	Possible source
Coating and/or refurbishment/repair	Chromalloy Gas Turbine Corp., with locations including Carson City, NV; Gardena, CA; Orangeburg, NY; Harrisburg, PA; Middletown, NY; Columbus, IN; Manchester, CT; and Phoenix, AZ; Web sites including www.chromalloy-cnv.com, www.chromalloy-cla.com, and www.chromalloyhit.com
	Sermatech International Inc., with locations including Limerick, PA; Muncie, IN; Houston, TX; and Manchester, CT; www.sermatech.com

Sources for Collected Property Data on Superalloys

Sources of collected property data on superalloys are not all that plentiful. Collection does not necessarily imply tabulation or explanation. Some collections previously updated at regular intervals may no longer be kept current. Publishers have made efforts to collect data, and it is common at this time to find databases about general materials on CD-ROM more often than in printed documents.

Data often represent available collected, not analyzed, test results. Limited data sources, heats of metal, and testing make typical data the norm for data collections, although some collections provide validated statistical information and could be used to produce design minima. Number of heats (casts) of metal, number of tests, number of component shapes, relationship of the test specimen location to the component location to be represented (integral test specimen versus specimens that are cut up from actual components), accuracy of heat treatment, and so on all play a role in the value determined for a given mechanical property. Mechanical-property data are more prone to variation according to the preceding variables than are physical property data. On the other hand, physical property data are infrequently generated.

Potential sources of superalloy data

Name	Owner or provider	Comments
Aerospace Materials Handbook	CINDAS/USAF-CRDA, Handbook Operations, Purdue University	. . .
Mil-Hdbk-5H	Coordinator, Handbook Actitivies Wright Patterson AFB Dayton, OH	This activity may be changed, owing to funding constraints.
Damage-Tolerant Handbook	Materials and Ceramics Info. Ctr. Battelle Memorial Inst. Columbus, OH	Old item that is not current
Atlas of Stress-Strain Curves	ASM International Materials Park, OH	. . .
Atlas of Creep and Stress-Rupture Curves	ASM International Materials Park, OH	. . .
Atlas of Fatigue Curves	ASM International Materials Park, OH	. . .
Atlas of Stress-Corrosion and Corrosion Fatigue Curves	ASM International Materials Park, OH	. . .
ASM Handbook, Vol 1–20	ASM International Materials Park, OH	Also available on CD-ROM. Not all volumes contain property data.
Materials property data on CD-ROM	ASM International Materials Park, OH	. . .
Pure Materials Properties: A Scientific and Technical Handbook	ASM International Materials Park, OH	. . .
Alloy Digest	ASM International Materials Park, OH	Also available on CD-ROM

(continued)

Potential sources of superalloy data (continued)

Name	Owner or provider	Comments
ASM Specialty Handbooks: *Nickel, Cobalt, and Their Alloys* and *Heat-Resistant Materials*	ASM International Materials Park, OH	. . .
Handbook of Corrosion Data, 2nd ed.	ASM International Materials Park, OH	. . .
Heat Treater's Guide: Practices and Procedures for Nonferrous Alloys	ASM International Materials Park, OH	Property and microstructure data sheets included
Supplier literature	Various	Subject to the comments in paragraph 2 at the beginning of this section

Superalloys: A Technical Guide, Second Edition
Matthew J. Donachie, Stephen J. Donachie, p 357-363
DOI:10.1361/stgs2002p357
Copyright © 2002 ASM International®
All rights reserved.
www.asminternational.org

Appendix B

Some Additional Microstructural Information

Introduction

An expansion of the microstructural information on superalloys is provided in this appendix. The use of electron vacancy calculations (electron vacancy number, N_v) to estimate the resistance of superalloys to the formation of topologically close-packed (tcp) phases is discussed, and a procedure for N_v calculation is given in tabular form. A further brief discussion and table is provided on carbide formation. In addition, more micrographs are presented to provide a better visual image of certain metallographic features mentioned in the text but not illustrated there.

Topologically Close-Packed Phase Formation

General. Topologically close-packed phases are those such as σ, μ, and Laves (among others) that generally are brittle and detrimental to the mechanical properties of superalloys, particularly nickel-base superalloys. These phases can form in iron-nickel- and cobalt-base superalloys as well. Based on early studies on stainless steels, these phases, and particularly σ phase, can be controlled by adjustments in alloy chemistry. Moreover, these phases are not always detrimental. Much evidence exists to show that very small amounts of σ may be beneficial to creep-rupture strength. There were attempts, at times, even to design alloys based on σ as a strengthening phase.

The detrimental effects of tcp phases depend to a large extent not only on tcp phase ductility shortcomings but also on:

- Phase morphology
- Volume fraction of tcp phase
- The extent to which the tcp phase may deplete the γ matrix of alloy elements required for γ or γ′ strengthening

In early studies of cast and wrought nickel-base superalloys, some heats of IN-713C (cast) and Rene 41 (wrought) contained σ, yet showed no strength loss. Tensile strength is not generally affected by tcp phase formation, but ductility and notch strength might be lowered. Creep strength may actually be increased in the early stages of tcp phase formation, but stress-rupture strength is soon degraded if significant tcp phase is formed.

Topologically close-packed phases normally may not be constituents found in a given superalloy, but minor composition changes may initiate tcp formation. Other phases may be nucleated as well. A cast nickel-base superalloy containing over 10% W and normal carbon contents displayed no μ or α-tungsten. When the carbon content was lowered without testing or microstructural investigation, property values in production heats began to decline, and excess creep strain was noticed in service applications. The lower carbon had made more tungsten available, and it had caused the formation of μ-phase. Restoration of the carbon content eliminated the problem.

Predicting TCP Phase Formation. Although σ was well known in the stainless steel field, experience with its formation at high temperatures in nickel-base superalloys was little known or recognized until the early to mid-1960s. At that time, Special Metals Corp. (Boesch and Slaney) reported σ formation in aircraft gas turbine blades of U-700 alloy, a fact confirmed by Pratt & Whitney (Johnson and Donachie). Electron vacancy theory studies had been made in preceding decades and seemed to be applicable to the base superalloy elements (iron, cobalt, nickel), which are transition metals in the periodic table and have unfilled 3*d* electron shells. Using the theory, Boesch and Slaney (B & S) developed the first quantitative system to calculate N_v number and identify the tendency of a given alloy to formation of tcp phases.

Shortly after the B & S efforts were published, a graduate student, Woodyatt, in conjunction with Sims and Beatty (WS & B) at General Electric made a more elaborate presentation of the process. Woodyatt, Sims, and Beatty adopted the acronym PHACOMP (for phase computation) for their process and proceeded to advance its use as a valuable tool for understanding and predicting tcp formation.

In the time frame of the mid-to-late 1960s, with the publication of papers such as those showing σ formation (see Figs. B.1 and B.2 based on graduate studies by Johnson during 1964–1965), a great deal of interest arose in phase stability of superalloys. Many companies and government agencies set out to learn the intricacies of N_v calculation and its value in tcp phase prediction. Contractual studies were done using various proposed N_v calculation schemes, all of which, at that time, were empirical. Regardless of the method, the acronym PHACOMP stuck and became a generic statement of process, regardless of actual technique employed.

The essence of PHACOMP processes is that elemental N_v are assigned to the major alloy elements in a superalloy, almost exclusively nickel-base superalloys. By summing up the fractional numbers (see Table B.1), an average N_v can be determined. It was demonstrated for a wide variety of complex alloys that the tendency for σ formation (and, by inference, for other tcp phases) increases with increase in the average electron vacancy number, N_v^{avg}, for the matrix.

There was clearly a need in this type of calculation system to incorporate the effects of carbides, borides, and γ′ formation on the γ matrix composition from which the tcp is presumed to form. A plethora of PHACOMP systems existed by 1968 when the first Seven Springs Symposium was held. This initial meeting of the now world-renowned event was known as the International Symposium on Structural Stability (in superalloys). The organizing committee, consisting (alphabetical order) of Boesch, Donachie, Grant, Lherbier, Richmond, and Sims, decreed that a specific N_v procedure would be used to compare stability values. The details of the procedure (known at the time as N_v ref) are given in Table B.2.

The outcome of the calculations must, of necessity, be applied as some practical indicator of tcp formation tendency. The original B&S plus WS&B work suggested that, if N_v^{avg} exceeded or equaled 2.50, sigma would appear. However, there were discrepancies in actual alloys. It became necessary to set limits based on a consistent long-time exposure scheme. It became common to use 5000 h at 1500 °F (816 °C) as an exposure condition. Many other adjustments were made, often unique to a given research or engineering group. Suffice to say, when N_v^{avg} is determined for an alloy system, values in excess of about 2.43 are considered to portend sigma formation. Values of critical N_v^{avg} may vary for different alloy bases and for different tcp phases. However, the concept has proven quite valuable in alloy development over the years, and improved schemes beyond those used in the 1960s and 1970s have been claimed. On the other hand, many superalloy

Table B.1 The determination of the average electron vacancy number, N_v^{avg}

For a wide variety of complex alloys, the tendency for σ-phase formation increases with increase in N_v^{avg} for the matrix, given by the following equation:

$$N_v^{avg} = \sum_{i=1}^{n} M_i(N_v)_i$$

where N_v^{avg} = average electron vacancy number
M_i = the atom fraction of particular element
N_v = individual electron vacancy number of particular element
n = number of elements in the matrix

Table B.2 Reference method for calculation of electron vacancy number (N_v ref), as required in 1968 and still frequently used

1. Convert the composition from weight percent to atomic percent.
2. After long-time exposure in the sigma-forming temperature range, the MC carbides tend to transform to $M_{23}C_6$.
   a. Assume one-half of the carbon forms MC in the following preferential order: TaC, NbC, TiC.
   b. Assume the remaining carbon forms $M_{23}C_6$ of the following composition: Cr_{21} (Mo, W)$_2C_6$ or $Cr_{23}C_6$ in the absence of molybdenum or tungsten.
3. Assume boron forms M_3B_2 of the following composition: $(Mo_{0.5}Ti_{0.15}Cr_{0.25}Ni_{0.10})_3B_2$.
4. Assume γ' to be of the following composition: Ni_3(Al, Ti,Ta,Nb,Zr,0.03Cr(a)).
5. The residual matrix will consist of the atomic percent minus those atoms tied up in the carbide reaction, boride reaction, and the γ' reaction. The total of these remaining atomic percentages gives the atomic concentration in the matrix. Conversion of this on the 100% basis gives the atomic percent of each element remaining in the matrix. It is this percentage that is used in order to calculate the electron vacancy number.
6. The formula for calculation of the electron vacany number is as follows:

$$(N^{avg}\ \text{ref}) = 0.66\ \text{Ni} + 1.71\ \text{Co} + 2.66\ \text{Fe} + 3.66\ \text{Mn} + 4.66\ (\text{Cr} + \text{Mo} + \text{W}) + 5.66\ \text{V} + 6.66\ \text{Si}$$

(a) 0.03% of the original atomic percent

Table B.3 Carbide reactions in nickel-base superalloys. Reactions vary with alloy composition.

The principal carbide reaction in many alloys is believed to be the formation of $M_{23}C_6$:

$$MC + \gamma \rightarrow M_{23}C_6 + \gamma' \text{ or}$$

$$(Ti,Mo)C + (Ni,Cr,Al,Ti) \rightarrow Cr_{21}Mo_2C_6 + Ni_3(Al,Ti)$$

The carbide M_6C can form in a similar manner.

Also, M_6C and $M_{23}C_6$ interact, forming one from the other, depending on the alloy:

$$M_6C + M' \rightarrow M_{23}C_6 + M''$$

or

$$Mo_3(Ni,Co)_3C + Cr \leftrightharpoons Cr_{21}Mo_2C_6 + (Ni,Co,Mo)$$

For example, Rene 41 and M-252 can be heat treated to generate MC and M_6C initially, with long-time exposure causing the conversion of M_6C to $M_{23}C_6$.

customers continue to use the older methods. Manufacturers calculate N_v^{avg} based on customer requirements.

Carbide Reactions. As noted in the text, the common classes of carbides are MC, $M_{23}C_6$, M_6C, and M_7C_3. The carbide morphology has been indicated, but not much was indicated regarding the actual carbide reactions. MC carbides are believed to be the principal source of carbon in most nickel-base superalloys below 1800 °F (982 °C), and the carbon available during heat treatment usually comes from breakdown of MC. MC decomposes slowly during heat treatment and service, releasing carbon for several important reactions, which are shown in Table B.3. The carbide reactions lead to carbide precipitation in various locations but typically in grain boundaries, as noted in the text.

Microstructures. Figures B.1 through B.14 provide some microstructural detail not presented in the text. The presence of constituents such as γ-γ' eutectic and phases such as σ, γ'', δ, η, plus microstructures showing γ' coarsening and γ' envelopes may be of interest. The concept that carbides might precipitate on dislocations nucleated from excess deformation around another carbide may be of interest as well. Not all possible superalloy microstructures are intended to be shown, nor all variants of some microstructural conditions. Microstructures vary with chemistry, heat treatment, coatings, exposure, and so on. The microstructures shown in this appendix are intended to supplement those previously presented in the text. However, for specific alloys and conditions, actual metallographic work or more literature research will need to be done to provide definitive knowledge of the phases and their distribution in any given alloy.

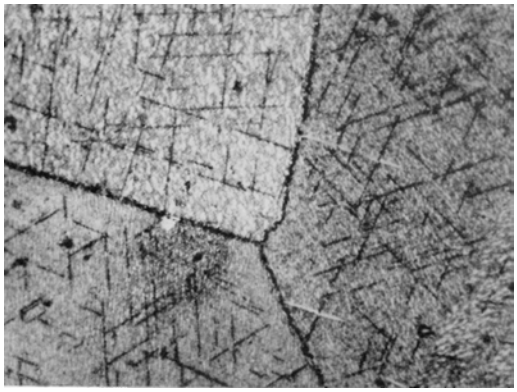


Fig. B.1 Sigma Phase (platelets) in fully heat treated wrought U-700 nickel-base superalloy after 3000 h. Several exposure temperatures used; probably exposed at 816 °C (1500 °F). Kalling's reagent; 400×

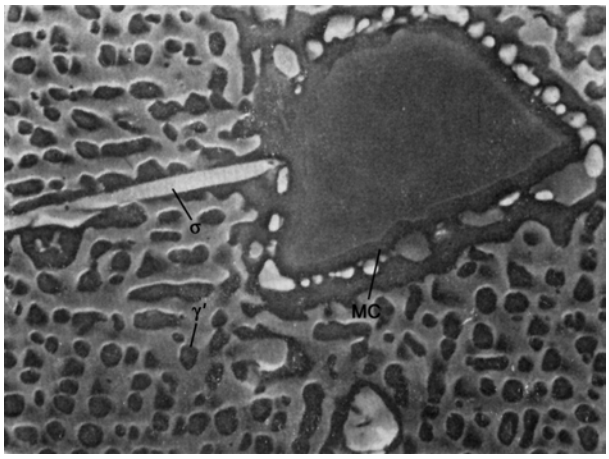


Fig. B.2 Wrought U-700 nickel-base superalloy after 816 °C (1500 °F) for 3000 h, showing acicular sigma phase growing from blocky MC carbide. Coarsened γ′ also visible. 4000x

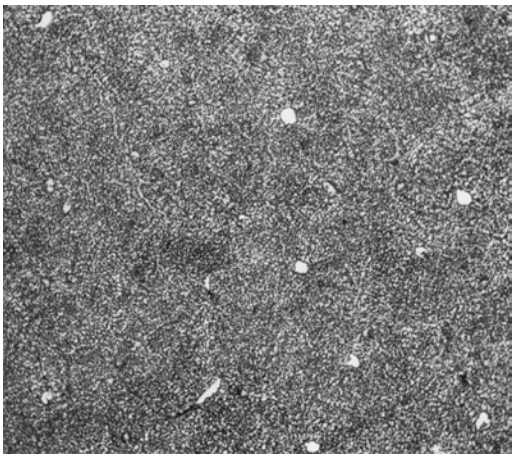


Fig. B.3 As-cast IN-100 nickel-base superalloy microstructure showing white islands of γ-γ′ eutectic. 100×

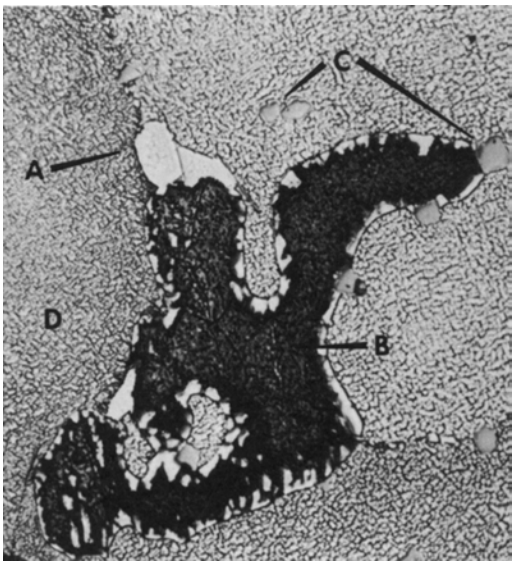


Fig. B.4 As-cast IN-100 nickel-base superalloy microstructure showing (A) γ-γ′ eutectic, (B) probable γ precipitate in eutectic, (C) γ matrix, and (D) γ′ precipitate in γ. Marble's reagent; 500×



Fig. B.5 Wrought U-500 nickel-base superalloy after 871 °C (1600 °F) for 1000 h showing overaged γ' in γ and γ' envelopes surrounding $M_{23}C_6$ in grain boundary. 10,000×

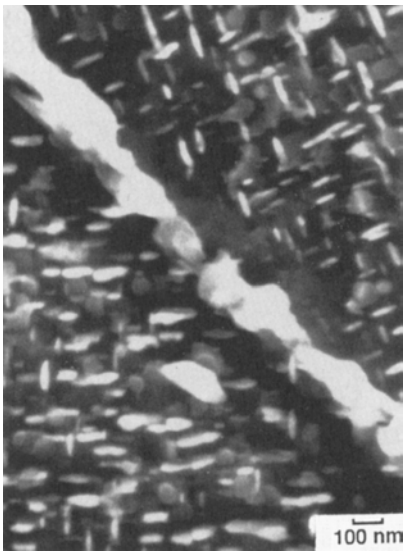


Fig. B.6 Wrought IN-718 nickel-base superalloy after 871 °C (1600 °F) for 7300 h at 469 MPa (68 ksi) showing δ at grain boundary, γ' (cuboids) and γ'' (disks) in grains. The specimen was electropolished and etched with methanolic 10% HCl.

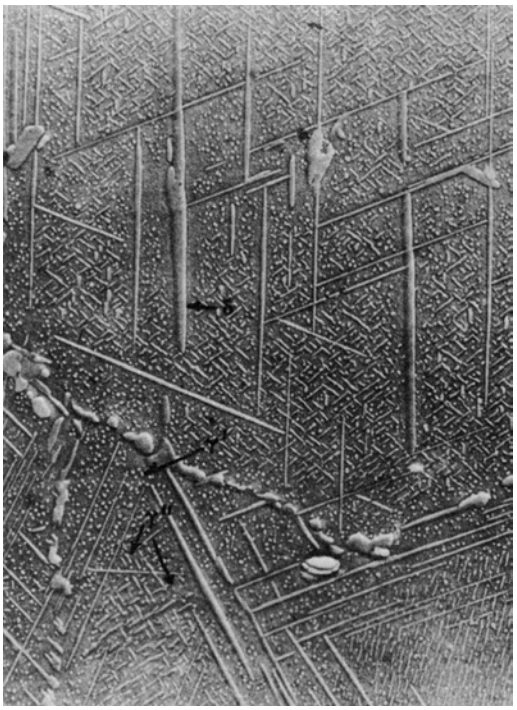


Fig. B.7 Wrought IN-718 nickel-base superalloy after 704 °C (1300 °F) for 6048 h at 255 MPa (37 ksi) showing δ platelets, spheroidal γ', and small disks of γ''. Note precipitate depletion around δ plate. 5000×



Fig. B.8 Cast Rene 220 nickel-base superalloy using dark-field electron microscopy. Showing γ″ disks with finer, less extensive γ′ in background. The specimen was electropolished and etched with methanolic 10% HCl.

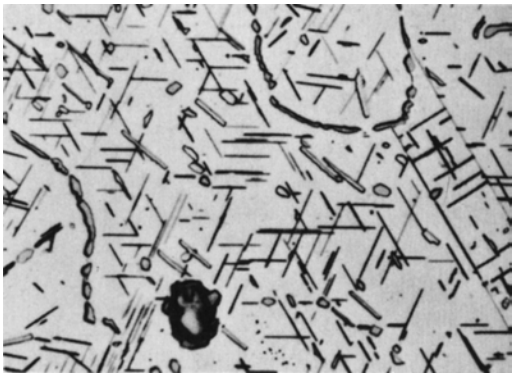


Fig. B.9 Precipitation of η phase (needlelike) in A-286 wrought iron-nickel-base superalloy after 816 °C (1500 °F) for 546 h. 15 mL HCl, 10 mL HNO_3, and 10 mL acetic acid. 1000×

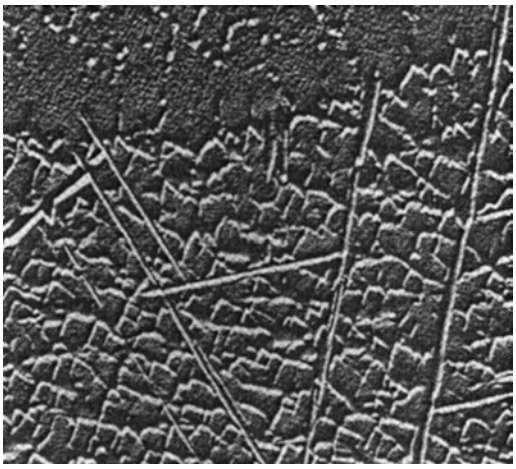


Fig. B.10 Cast IN-100 nickel-base superalloy microstructure after exposure at 760 °C (1400 °F) for 5000 h, showing Widmanstätten platelets of tcp sigma phase. HCl, ethanol, H_2O_2. 500×

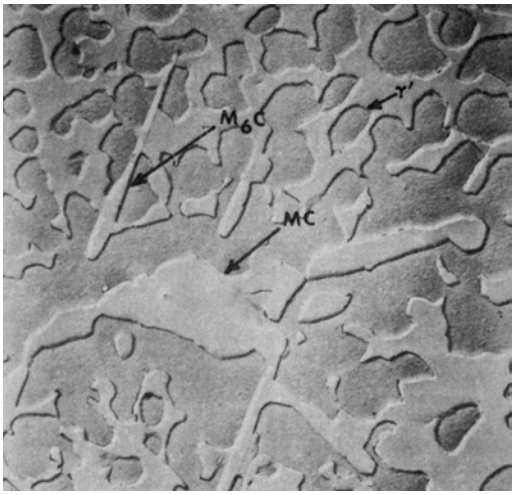


Fig. B.11 Cast B-1900 nickel-base superalloy after 928 °C (1800 °F) for 400 h showing acicular M_6C, blocky MC, and coarsened γ′ cuboids

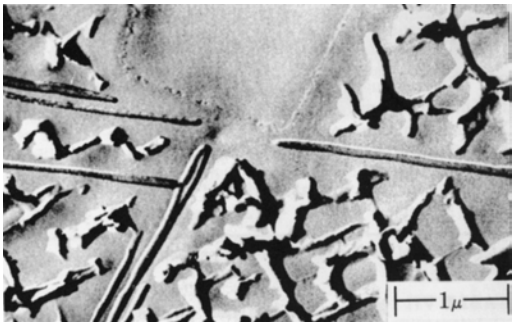


Fig. B.12 Cast IN-100 nickel-base superalloy after 816 °C (1500 °F) for 1006 h showing coarsened γ′ cuboids, sigma platelet surrounded by γ′ envelope, and cubic (blocky) MC at top center

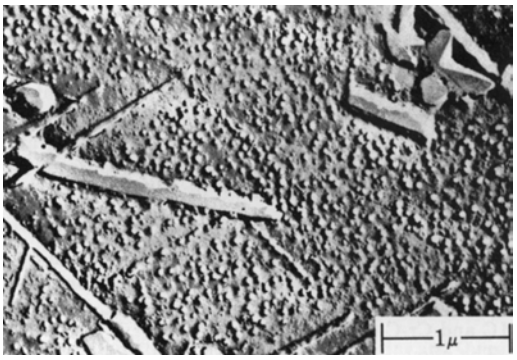


Fig. B.13 Wrought IN-901 nickel-base superalloy showing blocky Laves, spheroidal γ′, and thin plates of η

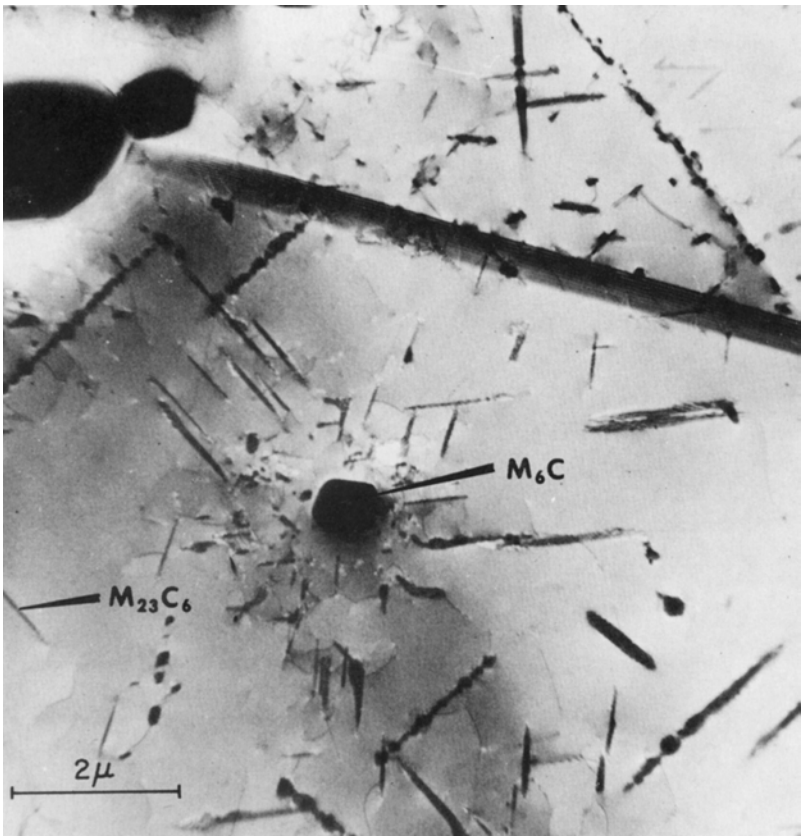


Fig. B.14 Wrought Hastelloy X solid-solution-hardened nickel-base superalloy microstructure; carbide precipitation has been influenced by deformation. Dislocations have formed around a primary M_6C, and $M_{23}C_6$ have precipitated on some of them. Thin-foil specimen. Original magnification: 11,000×

© 2002 ASM International. All Rights Reserved.
Superalloys: A Technical Guide (#06128G)

Subject Index

A

Abrasive blasting 206
dry 206
for scale removal 206
wet 206
wet or dry, for removing metal contamination 204
Abrasive cleaning 205, 206
Abrasive grinding 179
Abrasive tumbling 206
Acid cleaning 179
Acid etching 205
Acidic fluxing ..... 301, 302(F), 303, 304, 306–307
alloy induced ..... 307(F)
gas-induced ..... 307(F)
Acid pickling ..... 179, 206, 207, 208, 209(T)
procedure for removing scale superalloys 207(T)
Advanced nickel-base single-crystal superalloys, incipient melting temperatures 3, 8
Aerodynamically heated skins, as application of superalloy ..... 9(T)
Aerospace applications ..... 283–286(T)
See also Aircraft applications; Applications; Turbine engines.
bellows joint of rocket, welded ..... 186(F), 187
cobalt-base P/M superalloys 134
gas turbine disks ..... 23–24(F)
mechanically alloyed ODS alloys 133
nickel-base superalloys, welded ..... 186–187(F)
rotor assembly, of P/M superalloys 134
of standard IN-718 248
Afterburners, as application of superalloy ..... 9(T)
Aging ..... 139, 140(T), 141(T), 145
of cast superalloys, to develop properties 265
double-aging sequence 141, 142
during brazing 150
factors influencing selection or number of steps 140
of filler metals 167
of forged structure to retain grain structure 105
furnace availability consideration 146
gamma prime precipitation 213
hydrogen/carbon monoxide gas, explosion hazard 144
after joining 150
of precipitation-hardenable alloys 165
of precipitation-hardenable nickel-base alloy after welding 166
precipitation-hardened superalloys 161
with precipitation hardening 216–217
procedures 139–142
protective atmospheres for 145
quadruple-aging treatments 141
salt bath use 145
of weld 154
yo-yo treatments 141–142
Air atmosphere, effect on welding 150
Air blasting 179
Aircraft applications. *See also* Aerospace applications; Turbine engines.
AGT disk forging, deformation and metal removal ..... 96–97, 98(F)
aircraft gas turbine (AGT) disks, forging of ..... 96–97(F), 98(F)
airfoils ..... 23–24(F), 89
airfoils, cobalt-base superalloys for 91
airfoils, columnar grain directionally solidified ..... 85, 88(F), 89(F)
airfoils, incipient melting 139
airfoils, of ODS alloys 117
airfoils, P/M superalloys not widely used 129
airfoils, single crystal directionally solidified ..... 85, 88(F), 89(F)
airfoils, wrought superalloys 91
blade and vane, grain size of P/M products 127
blades, forged 91
broaching of gas turbine components 196
combustor/augmentor assemblies, of mechanically alloyed ODS alloys 132
combustor nozzles, P/M processed 118
complex turbine blades, polycrystalline investment-cast ..... 84, 87(F)
compressor disks, powder metallurgy processed, weight reductions ..... 117, 118(F)
disk, flat ..... 114(F)
disks, forged ..... 91, 95, 96, 97(F)
exhaust mixer nozzle component ..... 114(F)
forged parts, weights ..... 96, 97(F)
forged preforms 95
gas turbine disks ..... 23–24(F)
high-pressure turbine airfoils 341, 342

© 2002 ASM International. All Rights Reserved.
Superalloys: A Technical Guide (#06128G)
www.asminternational.org

Aircraft applications (continued)
hollow blades, investment-cast polycrystalline ..... 84, 87(F)
integral disk-shaft, forged ..... 96, 97(F)
integral nozzles, investment-cast polycrystalline ..... 84, 88(F)
integral rotors, investment-cast polycrystalline ..... 84, 88(F)
investment cast products..... 79, 80, 83, 84(F)
mechanically alloyed ODS alloys.....132–133
melting temperature vs. metal temperature ..... 348(T)
noise suppressor assembly ..... 114(F)
nozzles, of mechanically alloyed ODS alloys..... 132
ODS superalloys 345
platforms, of mechanically alloyed ODS alloys..... 132
precipitation-hardened superalloys 91
precision investment castings 89
shaft/disk combinations 96
shafts.....96
shot peening of components 210
solid-state welding processes 173, 174, 175
static airfoils (forged vanes), mechanically alloyed 131
temperature-strength capability of superalloys as function of year of availability..... 340(F)
thermal barrier coatings..... 321, 322(F)
turbine airfoils, cobalt addition effects..... 240
turbine blades..... 228
turbine blades, final machined.....99, 100(F)
turbine blades, forging .....99, 100(F)
turbine blades, oversize.....99, 100(F)
turbine blades, precision-forged .....99, 100(F)
turbine disks 228
turbine disks, P/M processed ..... 119, 125, 127–128(F)
turbine engines, as HIP-Astroloy..... 119
turbine engine shroud, welded...185(F), 186–187
turbine guide vanes and segments, polycrystalline cast cobalt-base..... 84, 86(F)
turbine shaft, forging.....99(F)
turbine vane castings, transient-liquid-phase-bonded..... 185(F), 186
turbine vanes, of cast cobalt-base superalloys 261
vane airfoils, of mechanically alloyed ODS alloys..... 132
vanes, broaching of..... 197(T)
vanes, friction welding of 175
vanes, of mechanically alloyed ODS alloys... 133
Aircraft engines, as application of superalloys 1
Aircraft gas turbine components 23
as application of superalloys..... 9(T)
weight (%) composed of superalloys..... 8
Air filtration methods, to control airborne impurities causing hot corrosion 299
Airfoils. *See* Aircraft applications; Turbine engines, airfoils.
Alkaline chelating, procedure for removing scale superalloys ..... 207(T)
Alkaline cleaning 205
Alkaline oxidizing, procedure for removing scale superalloys ..... 207(T)
Allied Signal dual-alloy turbine wheel concept..... 119
Allied Signal engines, using as-HIP powder metallurgy superalloys ..... 121(T)
Alligatoring 107
All-molten temperature, superheat required and temperature control 55
Alloy depletion 142
Alloy-induced acidic degradation..... 302(F)
Alloying, mechanical. *See* Mechanical alloying.
Alloying elements
of borides 26
as brittle phase formation cause.....30
of carbides 25, 26
enhancing coating life.....30
for grain boundary control 30
in nickel-base superalloys ..... 30, 31(F)
for oxidation resistance 30
of superalloys..... 29–30(T)
for tramp-element control 30
Alloy-lean vacuum arc remelted (VAR) ingot edge.....64
Alloy segregation. *See* Segregation.
Alloy systems, susceptible to hot corrosion propagation modes..... 301, 302(F)
Aluminates 300, 301
Aluminide (diffusion) coatings. *See also* Aluminum; Coatings ..... 304–306(F), 310–316(F,T)
10 Al, ductility ..... 318(F)
13 Al, ductility ..... 318(F)
for cast superalloys..... 282–283(F)
CoCrAlY, ductility..... 318(F)
development 342
hot corrosion resistance..... 304, 305(F)
inward diffusion type .....311, 312(F), 313, 315, 316(T)
modified for protection against hot corrosion 309
noble metal addition effect on ductile-brittle transition temperature 322
not for lower-temperature turbine airfoil service 309
outward diffusion type.....311, 312(F), 313–314, 315, 316(T)
Aluminizing.....311–316(F,T)
Aluminum
addition during EAF/AOD process 45
addition during vacuum induction melting 55
as alloying element.....20, 29(T), 30, 106
composition of freckle vs. matrix.....41(F)
composition ranges as superalloy alloying additions.....29(T)
content effect on forgeability of nickel-base superalloys ..... 103(T)
content effect on hot cracking susceptibility.. 151
content effect on oxidation resistance..... 295
content effect on weldability..... 149

© 2002 ASM International. All Rights Reserved.
Superalloys: A Technical Guide (#06128G)
www.asminternational.org

content in ESR electrode 58
effect on density as alloying addition 3
effects, nickel-base precipitation-strengthened superalloys 31
forming hardening precipitates 30
as gamma prime strengthener.....154
hardener content effect on welding problems.....154, 155(F)
intergranular attack 142–143
as metallic contaminant.....203
in nickel-base superalloys 30
for oxidation resistance 30
as precipitate former in nickel-base superalloys .....31(F)
precipitate-forming element for P/M disk alloys.....128
retained in solution by quenching 139
as stable-oxide former 144
for surface protection in nickel-base superalloys .....31(F)
Aluminum oxide 30, 179, 180, 204, 288, 302, 303
formation and hot corrosion resistance.....304
removal from part to be brazed 182
scale formation in ternary Ni-Cr-Al and Co-Cr-Al systems.....297
Aluminum oxide-formers ..... 288(F)
Aluminum reduction, increasing temperature of melt 45
American Society for Testing and Materials (ASTM) specifications, F 799, cobalt-base superalloy orthopedic implants 133
Anisotropy, of ODS superalloys.....345
Annealing. *See also* Bright annealing; Full annealing; In-process annealing; Mill annealing; Solution annealing 108, 110, 144–145
with forging.....102
lubricant removal before..... 111
mechanically alloyed ODS alloys.....132
prior to brazing.....182
protective atmospheres for 143–144
softening precipitation-hardenable nickel-base superalloys 112
wrought heat-resisting alloys ..... 137(T)
Annulus.....57, 63(F)
effect on frequency of formation of solidification white spots 66
of electroslag remelting.....68
of vacuum arc remelting.....59
Anodic electrolytic cleaning..... 178
Antimony
as detrimental tramp element in nickel-base superalloys .....31(F)
as metallic contaminant.....203
as tramp element.....235, 237(T)
Antiphase domain boundary (APB).....32–34
energies.....34, 213, 239, 241
AOD. *See* Electric arc furnace/argon oxygen decarburization process.
APB. *See* Antiphase domain boundary.
Applications.....8–9(T)
elevated-temperature.....22–23
APU. *See* Auxiliary power unit.
Arc gap .....57, 60(F), 62–63(F)
definition 60
melt voltage changes across ..... 60(F), 61(F)
Arc welding. *See* Gas metal arc welding (GMAW); Gas tungsten arc welding (GTAW); Shielded metal arc welding (SMAW); Submerged arc welding (SAW).
Argon. *See also* Atmospheres; Shielding gases.
addition during vacuum induction melting to control vaporization 55
as detrimental tramp element in nickel-base superalloys .....31(F)
Argon atomization 121
Argon oxygen decarburizing vessel ..... 45–46, 48–49(F)
refractory lining.....48
schematic of .....48(F)
temperature raised by exothermic reactions 49
Arsenic
as detrimental tramp element in nickel-base superalloys .....31(F)
as metallic contaminant.....203
as tramp element..... 234, 235(F)
ASTM. *See* American society for Testing and Materials.
Atmospheres
for brazing 175, 180–181
and descaling 210
dry argon.....143, 144
dry hydrogen 143, 144
effects on low-cycle fatigue behavior ..... 255, 257(F)
endothermic..... 143(F), 144
exothermic 143–144
for precipitation treatment..... 144
protective.....143–144
vacuum 143, 144
Atomization.....118, 119, 121
Attritor ball milling..... 130, 131(F)
Auger spectroscopic analysis, tramp element presence determined by.....30
Augmentor (afterburner) rear liner, application reason for Haynes 188.....76(T)
Austenitic stainless steels. *See* Stainless steels.
Autoclave, component size limits for insertion 125
Autoclave leaching, modification of processes ...86
Auxiliary power unit (APU) engines, P/M turbine disks for..... 119
Average electron vacancy number, determination of.....358(T), 359

B

Backing bars.....164
Backing rings..... 166, 170(F)
Backing strip ..... 166, 170(F)
Backing welds ..... 170(F)
Barrel tumbling, wet.....206–207

© 2002 ASM International. All Rights Reserved.
Superalloys: A Technical Guide (#06128G)
www.asminternational.org

Basic fluxing ..... 301, 302–303(F), 307(F)
and carbon deposits reaction with sulfate deposits 308
Basic fluxing/sulfidation 303
Batch heating 144–145
bcc. *See* Body-centered cubic crystal structure.
bct. *See* Body-centered tetragonal crystal structure.
Bead peening 203
Belt conveyor furnaces 144
Bending 108
Billet cogging 75
Billets
consolidation techniques 124–125
extrusion 125
fine-grained, powder metallurgy processed 117, 119
forged precompacted powder 126
grain size of HIPed vs. extruded 126
hot compaction by extrusion 126
Bimodal gamma prime distribution 217
Binders, for brazing filler metals 178
Biomedical applications. *See* Medical applications.
Biscuit 61, 69
Bismuth
alloyed with fixturing metals for VIM 51–52
as detrimental tramp element in nickel-base superalloys ..... 31(F)
as metallic contaminant 203
removal through vacuum arc remelting 57
as tramp element ..... 30, 233–237(F,T)
Blades, turbine. *See* Turbine engines, blades.
Bleedout ..... 71(F)
Blooming 74
Body-centered cubic (bcc) crystal structure ..... 25, 26(F)
Body-centered tetragonal (bct) crystal structure ..... 25, 27(T)
of gamma double-prime precipitate 31
Bolts, as application of superalloy ..... 9(T)
Bonding 150
Borazon, for grinding superalloys 193
Borides 26, 31–32, 37, 212
See also Matrix borides
and minor element additions 237
in SCDS superalloys 281
Boring 195
Boron
addition to improve creep-rupture resistance 37
as alloying element ..... 26, 29(T), 30, 31(F), 106, 224
for grain-boundary phases in nickel-base superalloys ..... 31(F)
intergranular attack along grain boundaries 143
mechanical properties improved by addition of ..... 235–238(T)
as melting-point depressant for brazing ..... 176, 177(T), 181
to retard formation of denuded (depleted) gamma prime zones 221
as source of liquation cracking 159
Boron hydrides 144
Boron oxidation 142
Box furnaces 144, 145
Brass, cracking contributor 159
Brazeability 2
Brazing ..... 135, 149, 150, 152, 175–183(F,T), 336
aspects of 175–176
atmospheres for 175, 180–181
cleaning methods 178–179
cleanliness for 181–182
cobalt-base superalloys ..... 183, 184(T)
contaminants of brazing area 178
definition 175
filler melting temperature 150
filler metals ..... 150, 176–178(T)
filler metals, compositions for elevated-temperature service ..... 177(T)
filler metals, product forms 178
fixturing, hot and cold 180
fixturing materials 180
melting-point depressants 176, 181
nickel-base superalloys 181–183
ODS alloys 183
with solution treating 147
specifications 161
surface cleaning and preparation 178–179
surface preparation 209
techniques 175, 180–181
thermal cycles for nickel-base superalloys 182–183
Bridging cracks 163
Bright annealing 144
Brittle phase formation, alloying elements causing 30
Broaching 196
cleaning of workpieces 197
cutting fluids for 197
tool modifications ..... 196–197(F,T)
Buffing 210
Bulge forming, speeds for ..... 110(T)
Bulk charger ..... 52, 53(F), 54
Burner hardware, of mechanically alloyed ODS alloys 133
Burner rig testing ..... 290–292(F)
Burnishing 179, 200
Burnout, to remove pattern in investment casting 83
Butt joints ..... 170–171(F), 172(F)

C

CAD. *See* Computer-aided design.
Calcium
as addition during vacuum induction melting 55
as beneficial minor alloying element in nickel-base superalloys ..... 31(F)
as desulfurizer 238
Calcium fluoride, as constituent in electroslag remelting slags 70
Calcium fluoride + oxide, slag composition for electroslag remelting 57
Calcium sulfide 55
formation during EAF/AOD process 49

© 2002 ASM International. All Rights Reserved.
Superalloys: A Technical Guide (#06128G)
www.asminternational.org

CAP process. *See* Consolidation by atmospheric pressure.
Carbide attack, showing need for coatings 310
Carbide films 128, 221–222
in double-aged Udimet 500 142
Carbide formers ..... 119, 128(T)
Carbide-hardened alloys 139
Carbide-hardened cast cobalt-base superalloys, welding 151
Carbide-hardened superalloys, heat treatment 146
Carbide-hardened wrought cobalt-base superalloys, welding 151
Carbide phases 153
Carbide-phase-strengthened superalloys, stress-rupture strength ..... 3(F)
Carbide phase strengthening. *See* Carbide precipitation.
Carbide precipitation ..... 222–225(F), 327–330(F)
cobalt-base superalloys ..... 222–224(F)
iron-nickel superalloys ..... 224–225(F)
nickel-base superalloys ..... 224–225(F), 361(F), 362(F), 363(F)
noncarbide formers effect 225
of solid-solution-strengthened nickel-base superalloys 28
Carbides. *See also* Carbide precipitation ..... 19, 35–37(F), 212
acicular 221
additions for prevention of formation 37
alloying elements for 31–32
as constituent 35
discontinuous cellular 220
dissolution with gamma prime phases 147
formation 35
formation during aging 141
functions of 31–32, 35–37
grain-boundary ..... 33(F)
grain-boundary, in nickel-base superalloys ..... 218–222(F)
in iron-nickel superalloys 222
lamellar eutectic nature 222
no presence, and premature failure 222
overheating and dissolution and modification of 326
oxidized 224, 225
oxidized, in precipitation-hardened nickel-base alloy ..... 142, 143(F)
partial dissolution due to long solution heating exposure 146
phases 25
prior particle boundaries (PPB) 119
reactions in nickel-base superalloys ..... 359(T)
refractory metal addition effects on formation of 241
in SCDS superalloys 281
script ..... 33(F)
and solidification 41
as strengthening mechanism 25
types ..... 31, 35–37(F)
zipper discontinuous carbides ..... 220(F)
Carbide tools ..... 191, 192(T)
Carbon
as alloying element ..... 29(T), 30, 31(F), 106
content, and carbide formation, MC carbides 37
content, and tcp phase formation 357
content effect in nickel-chromium alloys 294
for grain-boundary phases in nickel-base superalloys ..... 31(F)
Carbonitride agglomerates 129
Carbon pickup 142, 143
Carburizing potential
of dry hydrogen atmospheres 144
of endothermic atmospheres 144
Cases, as application of superalloy ..... 9(T)
Cast carbide-hardened cobalt-base superalloys, welding 151
Cast cobalt-base superalloys
creep-rupture strength ..... 261, 264(F)
microstructure ..... 33(F)
stress-rupture strength ..... 261, 263(F)
Casting dies, as application of superalloy ..... 9(T)
Castings. *See also* Cast cobalt-base superalloys; Cast nickel-base superalloys; Cast superalloys 89–90
compositions ..... 6–7(T)
Cast nickel-base superalloys. *See also* Columnar grain directionally-solidified superalloys; Single-crystal directionally-solidified superalloys.
CGDS superalloys, crystal structure 265–266
CGDS superalloys, stress-rupture strength ..... 258, 260(F)
creep-rupture strength ..... 261, 264(F)
microstructure ..... 33(F)
Castor oil 111
Cast precipitation-hardened superalloys, heat treatment 146
Cast superalloys. *See also* Alloy Index; Cast cobalt-base superalloys; Castings; Cast nickel-base superalloys; Columnar grain directionally-solidified superalloys; Single-crystal directionally-solidified superalloys; Superalloys.
applications 15
compositions ..... 6–7(T)
density ..... 258, 262(T)
directionally solidified (DS) 15, 18
ductility 15
dynamic modulus of elasticity ..... 258, 261(T)
fabricability and ductility 91
gamma prime solvus temperature ..... 325(T)
grain size effect on strength 18
grain sizes 29
heating/cooling rates 147
hot corrosion resistance 261
incipient melting temperature ..... 325(T)
mean coefficient of thermal expansion ..... 258, 262(T)
melting range ..... 258, 262(T)
physical, tensile and creep-rupture properties ..... 258–286(F,T)

© 2002 ASM International. All Rights Reserved.
Superalloys: A Technical Guide (#06128G)

Cast superalloys (continued)
polycrystalline, ductility effects 263–264
polycrystalline equiaxed 15
section-size effect on creep-rupture strength .. 230
service temperature 15
specific heat.....258, 262(T)
stress-rupture strength.....258, 259(F)
test coupon location effect on mechanical property data.....231(T), 232–233(F,T)
thermal conductivity.....258, 262(T)
wrought superalloys compared, strengthening mechanisms .....226–241(F,T)
Cast-to-size (CTS) specimens 230, 232
Cathodic electrolytic cleaning 178
Cavitation, lead contribution as tramp element, wrought alloy..... 234, 235(F)
Cementation process..... 311
Centrifugal atomization..... 121
process description ..... 122–123(F)
Centrifugal atomization with forced convective cooling (RSR), process steps in powder production..... 121(T)
Ceramic castings, and support fixturing 145
Ceramic coating 209
Ceramic inclusions, minimization methods for defects ..... 128(T)
Ceramic knock-off, causing plastic deformation from investment casting 87
Ceramics
of investment-cast mold 81
as turning tools for superalloys..... 194
Ceramic shell process, for investment casting....80
Ceramic shells, built through computer-aided design 89
Cerium
as alloying element..... 29(T), 31(F)
as desulfurizer..... 238
CFM International engines, using as-HIP powder metallurgy superalloys ..... 121(T)
CGDS. *See* Columnar grain directionally-solidified (CGDS) casting superalloys.
Chemical cleaning. *See also* Cleaning 178–179
Chemical grain etch, for investment-cast products 82
Chemical industry applications. *See also* Petrochemical industry..... 9(T)
Chemical removal methods
for metallic contaminants.....204–205
for tarnish 205
Chemical vapor deposition (CVD) 316
of aluminide coatings 311–312, 314
Chill
application with investment casting 83
die 97
Chill bars..... 164
Chips, of superalloys in VIM 51–52
Chlorides, and hot corrosion 299, 308
Chlorinated oils..... 111
Chromates..... 300
Chromic oxide.....288, 296, 297, 302–303
formation and hot corrosion resistance..... 304
Chromic oxide-formers (Cr_2O_3) ..... 288(F)
Chromium
addition for corrosion resistance 339
as addition to nickel-base superalloys....240–241
alloying effect on corrosion resistance 8
as alloying element..... 29(T), 30
in brazing filler metals.....176, 177(T), 181
as brittle phase formation cause.....30
in cobalt-base superalloys 30
composition of freckle vs. matrix.....41(F)
composition ranges as superalloy alloying additions.....29(T)
content effect on forgeability of nickel-base superalloys ..... 103(T)
content effect on hot corrosion resistance of superalloys ..... 303, 304(T)
content effect on oxidation resistance 295
cost..... 8, 46
effect on density as alloying addition 3
effects, nickel-base precipitation-strengthened superalloys 31
in iron-nickel superalloys.....30
in matrix of mechanically alloyed superalloys 129
in nickel-base superalloys 30
for oxidation resistance 30
preferential oxidation.....142–143
refining of.....46
as solid-solution element of nickel-base superalloys 31
for surface protection in nickel-base superalloys .....31(F)
Chromium alloys, straight. *See* Iron-chromium alloys.
Chromium boride, crystal structure and phases observed.....28(T)
Chromium carbides..... 218, 219–220
formation.....37
phases observed, crystal structure.....27(T)
Chromium-cobalt alloys, crystal structure and phases observed.....28(T)
Chromium-iron-molybdenum-nickel alloys, crystal structure and phases observed .....28(T)
Chromium-nickel-molybdenum alloys, crystal structure and phases observed .....28(T)
Chromium oxides..... 30, 204
in exothermic atmosphere scale 144
Chromium plating..... 209
of forming tools..... 110
Chromium sulfide (Cr_2S_3) 143
Chromizing.....313, 316(T)
Circular patch test 156
Cleaning .....203–209(T), 210
chemical 178–179
problems and solutions 210
Cleanliness
for brazing 181–182
for brazing surfaces 178–179
of broached workpieces..... 197
determining ESR and VAR electrode quality ...58
diffusion bonded surfaces 174

© 2002 ASM International. All Rights Reserved.
Superalloys: A Technical Guide (#06128G)
www.asminternational.org

Climb milling.....201
Closed-die blocker-type forgings.....94
Closed-die finish forgings.....94
Closed-die forging.....96, 97(F), 114
Coarsening process.....348
Coated carbides, as turning tools for superalloys.....194–195
Coated corrosion resistance.....341
Coating-base alloy system.....310
Coating diffusion.....135
Coating diffusion cycles.....146, 147
Coating diffusion heat treatment.....223
Coating life.....293
Coating residues, mechanical removal plastic deformation from investment casting.....87
Coatings. *See also* Overlay coatings.....8, 209, 304–306(F)
aluminide (diffusion), 304–306(F), 310–316(F,T)
for cast superalloys.....282–283(F)
CoCrAlY, 302(F), 306, 307, 308, 309
development.....349
diffusion.....293, 294
for gas turbine airfoil alloys.....142
information/product sources.....354, 369
lifetimes of alloys.....283
mechanical removal, plastic deformative from investment casting.....87
overlay.....293, 294, 311, 316–319(F)
for oxidation resistance.....142
plasma-sprayed (PS) partially stabilized zirconia.....311
as protection against corrosion.....344
for protection against intergranular oxidation.....142
as protection against oxidation and hot corrosion.....289
reasons for.....310
refurbishment and repair of.....336
for superalloy protection.....309–322(F,T)
test results interpretation.....293
thermal barrier.....311, 319–322(F), 344, 345, 347, 351
and thermal-mechanical fatigue testing.....283
types of.....310
weight gain/loss and performance measured..293
yttrium addition to improve coating life.....30
Cobalt
as addition, effects on nickel-bases superalloys.....239–240(F)
addition preventing carbide formation.....37
addition to NiCrAlY coatings to improve corrosion resistance.....306
as alloying element.....29(T), 30, 106
as brittle phase formation cause.....30
composition ranges as superalloy alloying additions.....29(T)
cost.....8, 239
density.....3
gamma prime coarsening affected to.....240
for increased volume fraction of favorable secondary precipitates.....30
melting temperature.....3
in nickel-base superalloys.....239–240(F)
for precipitation modification in nickel-base superalloys.....31(F)
to retard formation of denuded (depleted) gamma prime zones.....221
as solid-solution element of nickel-base superalloys.....31
Cobalt-base superalloys. *See also* Alloy Index; Cobalt; Superalloys.
aging cycles.....140(T)
aircraft applications.....84, 86(F)
airfoils for low-pressure turbine parts.....89
annealing.....137(T)
applications.....20
brazing.....183, 184(T)
carbide-hardened.....113(F)
carbide-hardened, creep-rupture strength.....20
carbide precipitation.....19, 222–224(F)
carbides for matrix strengthening.....35, 36
castings, ductility.....91
cast, microstructure.....33(F)
chromium content effect on hot corrosion resistance.....303, 304(T)
composition.....4(T), 7(T)
compositional ranges of alloying additions.....29(T)
creep-rupture strength.....20, 241, 243(F)
creep-rupture strength unsatisfactory.....24
crystal structure.....3
crystal structure and phases observed...27–28(T)
density.....3, 22, 246(T), 262(T)
development.....341
ductility.....21
dynamic modulus of elasticity.....245(T), 261(T)
electrical resistivity.....247(T)
electron beam welding.....173
filler metals for.....167
forgeability.....104–105
forgeability rating.....93(T)
forging temperature.....93(T)
friction welding.....175
fusion welding.....164
grain-boundary carbides.....222
heat treatment.....146
hot corrosion.....308
hot corrosion resistance.....289
incipient melting temperature.....3
investment casting.....79, 80
machinability.....189, 190(F), 191(T), 192
mean coefficient of thermal expansion....247(T), 262(T)
melting range.....246(T), 262(T)
mill product availability.....77
minor element effects.....235–236
for orthopedic implants.....133(F)
polycrystalline investment casting.....89
P/M processed, corrosion-resistant applications.....133–134
P/M processed, wear-resistant applications.....133–134

© 2002 ASM International. All Rights Reserved.
Superalloys: A Technical Guide (#06128G)
www.asminternational.org

Cobalt-base superalloys (continued)
repair welding 152
solid-solution-strengthened 211
solution treating cycles ..... 140(T)
specific heat..... 262(T)
specific heat capacity..... 246(T)
strengthening mechanisms.....29
stress relieving ..... 137(T)
stress-rupture strength.. 3(F), 14(T), 18(T), 19(F), 258, 259(F)
stress-rupture strength vs. temperature ..... 21(F)
temperature range..... 8
temperature-strength capability as function of year of availability..... 340(F), 350(F)
tensile elongation ..... 13(T), 17(T)
thermal conductivity..... 247(T), 262(T)
ultimate tensile strength ..... 13(T), 17(T)
welding 150, 151
wrought, fabricability and ductility 91
yield strength (0.2% offset)..... 13(T), 17(T)
Cobalt-chromium alloys, oxidation, gaseous 296–297
Cobalt-chromium-aluminum-yttrium (CoCrAlY) coatings 306
hot corrosion..... 302(F)
hot corrosion resistance.....306, 309
low-temperature hot corrosion.....307
for marine and industrial turbine applications 308
type 2 attack resistance 308
Cobalt-chromium-molybdenum (Co-Cr-Mo) alloys, for orthopedic implants..... 133
Cobalt-chromium-nickel (Co-Cr-Ni) superalloys
annealing ..... 137(T)
stress relieving ..... 137(T)
Cobalt overlay coatings. *See* Coatings; Overlay coatings.
Cobalt oxide 288, 301, 302
Cobalt-tantalum alloys, crystal structure and phases observed.....28(T)
Cobalt-titanium alloys, crystal structure and phases observed.....28(T)
Cobalt-tungsten alloys, crystal structure and phases observed.....28(T)
Coefficient of expansion, of part and fixture ... 145
Cogging (forging)..... 72, 74–75, 92
definition 74
of IN-718 nickel-base superalloy 75–76
modeling of..... 347
Cold forging ..... 117, 118(F)
Cold forming 21–22, 106, 107, 108
Cold rolling 22
of mechanically alloyed ODS alloys 132
Cold shuts..... 163
Cold working.....11, 15, 77
of solution-treated alloys ..... 138–139(F)
Columbium. *See* Niobium.
Columnar grain directional solidification (CGDS) 21, 90
Columnar grain directionally solidified (CGDS) cast superalloys 79
carbide precipitation..... 224
creep strength..... 272(F)
crystal structure 265–266
density 272
development 342
directionality of mechanical properties..... 258
ductility/elongation ..... 278–279(F)
first- and second-generation alloys..... 267
grain size control in products.....82
hafnium addition for ductility 264
incipient melting point..... 348(T)
low-cycle fatigue and fracture..... 280–282(F)
macrostructure..... 38(F), 39
maximum useful temperature..... 348(T)
orientation.....272–278(F,T)
Poisson ratio..... 272
porosity and hot isostatic pressing.... 279–280(F)
processing..... 83, 85(F)
resistant to thermal-mechanical fatigue cracking 332
rhenium effect on creep-rupture properties.....240–241
rupture life vs. specimen thickness ... 231–232(F)
single precipitate size possible 34
stress-rupture strength..... 258, 260(F), 272(F)
temperature capability extended by rhenium alloying 30
tensile and creep-rupture properties.. 268–272(F), 273(T)
thermal-mechanical fatigue..... 280–281, 282(F), 332
tramp element effects ..... 234–235(F), 236(F)
yield strength 239
Columnar grain directionally solidified (CGDS) parts 18, 79
Columnar voids..... 318
Combustor alloys, creep strength ..... 75(F), 76–77
Combustor inner wall, application reason for Haynes 188 .....76(T)
Combustor outer wall, application reason for Haynes 188 .....76(T)
Combustors. *See also* Turbine engines.
as application of superalloy..... 9(T)
nozzles, P/M processed..... 118
superalloy temperature-strength capability vs. year of availability..... 340(F)
turbine, TMF cracking ..... 333–334(F)
Component metal temperatures..... 8
Compositions
cast superalloys .....6–7(T)
determining ESR and VAR electrode quality ...58
wrought superalloys .....4–5(T)
Compressive strength..... 211
Computer-aided design (CAD) 88–89, 99–100
Computer-aided engineering..... 99–100
Computer-aided manufacture 99–100
Computer algorithms.....11, 15
Computer modeling..... 345–347, 348–349
of investment casting.....87–89
Computer programs, for selection of initial charge materials, EAF/AOD process 46
Conduction, to transfer heat away from investment cast shell 82

© 2002 ASM International. All Rights Reserved.
Superalloys: A Technical Guide (#06128G)
www.asminternational.org

Consolidation 118, 119
of mechanical alloying process ..... 130–132(F)
Consolidation by atmospheric pressure (CAP) process 125
Consolidation techniques ..... 124–125, 127(F)
Constricted arc 64
Contaminants 143, 203
of brazing surfaces 178
removal of 204–205
Contamination 142
surface ..... 143(F)
Continuous balance tests 290
Continuous furnaces 145
Continuous oxide barriers 298
Continuous processing furnaces 144
Control-rod drive mechanisms, as application of superalloy ..... 9(T)
Conventional heat transfer process, in investment casting 83
Conventionally cast superalloys
incipient melting point ..... 348(T)
maximum useful temperature ..... 348(T)
Conveyor belts, as application of superalloy ..... 9(T)
Cooling
by air 136
procedures (methods) ..... 139, 140(T), 141(T)
rate 145
to room temperature 135, 136
Copper
cracking contributor 159
as detrimental tramp element in nickel-base superalloys ..... 31(F)
as metallic contaminant of nickel-base superalloys 203
as tramp element ..... 235, 237(T)
Copper plating 209
Core leaching 85–86
Core warping 85–86
Corner and lap joint, joint designs and dimensions for arc welding nickel- and iron-nickel-base superalloys ..... 171(F)
Corner joints ..... 170(F), 171(F), 172(F)
Corner joints and T-joints, joint designs and dimensions, SMAW of solid-solution-strengthened nickel- and iron-nickel-base superalloys ..... 172(F)
Corrosion. *See also* Corrosion resistance; Hot corrosion; Stress-corrosion cracking 8
due to tcp phase formation 30
information sources 369
Corrosion-erosion rig testing ..... 290–292(F)
Corrosion-protective overlay coatings, with thermal barrier coatings 310
Corrosion resistance 8
of cobalt-base P/M superalloys 133–134
Corrosion testing ..... 289–294(F)
Cost 22, 344, 345
of confirmation tests for computer modeling 346–347
Cracking ..... 152–160(F,T), 163
base-metal 163
centerline longitudinal 63
composition effect ..... 156(F)
crater 163
determining ESR and VAR electrode quality 58
heating rate effect ..... 156(F)
hot short 163
during welding 151
Crack propagation
in cast superalloys 282
of P/M disk alloys 127
rate of 22
tests 211
Crack-susceptibility C-curves 156
Creep. *See also* Creep-rupture strength 2, 21, 22
in gas turbine disks 24
in turbine blade ..... 332–333(F)
Creep damage, recovery ..... 334–335(F)
Creep life 341
investment-cast products ..... 87, 89(F)
Creep rate 21, 211
Creep relaxation 255
Creep resistance, of powder metallurgy disk alloys 127
Creep-rupture resistance, zirconium or boron additions to improve 37
Creep-rupture strength 2, 18, 19–20, 22, 211, 341
carbide effects 222
cast superalloys ..... 261, 264(F)
and grain size ..... 227(F)
of powder metallurgy disk alloys 127
of powder metallurgy processed alloys 118
and precipitate size 34
section size effect ..... 228–232(F)
of wrought superalloys ..... 241, 242(F), 243(F)
wrought superalloys, Larson-Miller parametric plot ..... 241, 248(F)
Creep strength 212
of combustor alloys ..... 75(F), 76–77
recovery techniques ..... 334–335(F)
Critical stress-intensity factors 250
Cryogenic applications ..... 9, 15, 283–286(T)
MC carbide formation 37
Cryogenic temperature(s). *See* Cryogenic applications.
Crystal structure ..... 2–3, 25, 26(F)
disordered ..... 26(F)
ordering ..... 25, 26(F)
CTS. *See* Cast-to-size specimens.
Cubic boron nitride, for turning tools for superalloys 195
Cubic crystal structure ..... 27(T), 28(T)
Cutting tool materials ..... 191(T), 192(T)
CVD. *See* Chemical vapor deposition.
Cyclic (fatigue) tests 211

D

DA. *See* Direct aging process.
Damage tolerance, of powder metallurgy disk alloys 127

© 2002 ASM International. All Rights Reserved.
Superalloys: A Technical Guide (#06128G)
www.asminternational.org

Dams 50, 54
definition 54
Dark-field transmission electron microscopy, to examine gamma double-prime phase....27(T)
Databases, property data on superalloys 354
DBTT. *See* Ductile-to-brittle temperature.
DCEN. *See* Direct current electrode negative.
DCEP. *See* Direct current electrode positive.
Dead shorts 61–62
Dead zone .... 97, 98(F)
resulting in porosity 74
Debits, section size effect on creep-rupture strengths .... 228, 230(F)
Deboronization 142, 144
Deep drawability 108
Deep drawing.... 108
Defects
continuous hard 41
of direct-HIP near-net shape 126
lack-of-fusion.... 159, 160, 163
leader 318
and low-cycle fatigue capability 252
melt-related, from electroslag remelting .... 70(F), 71(F)
melt-related, in vacuum arc remelting ....64–66(F), 67(F)
minimization methods for occurrence.... 128(T)
oxide entrapment....159, 160
positive segregation channel 57
positive segregation, formation during static casting 56
positive segregation, in electroslag remelting...71
positive segregation, in vacuum arc remelting 59–60
in P/M superalloy products .... 128–129(T)
solute-lean (negative segregation)....57
weld, in fusion welding.... 163
Defect tolerance.... 120
Deformation, during mechanical alloying....130, 131
Deformation processing 126
Deformation welding.... 175
See also Inertia bonding
Degassing, from vacuum induction melting ..54–55
Degreasing solutions, for brazing areas.... 178
Delta orthorhombic phase....34
Delta phase.... 25, 27(T), 99, 102(F), 105–106(F)
intragranular ....33(F)
macroetching attacking precipitate.... 65, 66(F)
modeling 346
in nickel-base superalloy .... 361(F)
orthorhombic Ni_3Nb intermetallic compounds..25
role in preventing stress-rupture embrittlement....225–226(F)
role in strengthening IN-718.... 225–226(F), 227(T)
Delta precipitate, in nickel- and nickel-iron-base superalloys 35
Delta solvus temperature ...65, 66(F), 105(F), 106
Density 22
cast superalloys ....258, 262(T)
modeling of....346
of SCDS casting alloys ....272, 273(T)
of wrought superalloys.... 246(T)
Dentistry, application of superalloys.... 1, 9(T)
Deoxidation, and vacuum induction melting 50
Descaling ....207–209(T)
in molten salt.... 206
Design, of welded joints ..... 151–152, 170–172(F)
Desulfurization
in EAF/AOD process 45
and vacuum induction melting 50
DFB. *See* Diffusion bonding or welding.
Diamond, for grinding superalloys.... 193
Die chill....97
Die forging 94
categories....94
Diesel engines, glow plugs, of mechanically alloyed ODS alloys.... 133
Differential melting 166
Diffuse arc 64
Diffusion aluminide coatings. *See* Aluminide diffusion coatings.
Diffusion bonding or welding (DFB)..... 149, 150, 173–174
chemical cleaning methods.... 178
welding of.... 151
Diffusion chromium coatings 311, 314
Diffusion chromizing....311, 314
Diffusion coating....209, 304–306(F)
See also Aluminide diffusion coatings; Coatings
Diffusion welding, aircraft applications 174
Dimensional inspection, of investment-cast products 82
Direct aging (DA) process 218
of forged structure to retain grain structure ... 105
of Inconel 718....248–249
Direct current electrode negative (DCEN)..... 165
Direct current electrode positive (DCEP)
for gas metal arc welding 169
for shielded metal arc welding 172
Directional heat transfer processes, in investment casting 83
Directional investment casting....90
Directionally recrystallized (DR) alloys ..131–132
Directionally solidified (DS) castings.....15, 18
aging cycles.... 141(T)
solution treating cycles .... 141(T)
Directional recrystallization (DR) 28, 39, 129
Directional solidification (DS) ..22, 28, 39, 83–84, 85(F), 347
and carbide precipitation 224
development 341–342
polycrystalline castings adapted to.. 83–84, 85(F)
size extension of parts made.... 267
Directional solidification (DS) products 79
Direct powder consolidation 119
Dirt stringers .... 64–65(F)
Dirty white spots .... 64–65(F), 72
Discrete white spots.... 64–65(F), 72
in electroslag remelting product....71
Disks....22

© 2002 ASM International. All Rights Reserved.
Superalloys: A Technical Guide (#06128G)
www.asminternational.org

application of superalloys ..... 9(T), 18
Dislocation bypassing..... 348
Dispersion hardening.....25
Disposable pattern 79
Dissimilar metals
filler metals used for welds 167
welding of..... 151
Double-bevel groove T-joints..... 166, 170(F)
joint designs and dimensions for arc welding nickel- and iron-nickel-base superalloys ..... 171(F)
Double J-groove T-joints..... 170(F)
joint designs and dimensions for arc welding nickel- and iron-nickel-base superalloys ..... 171(F)
Double-melt product.....72
Double U-groove butt joint ..... 170(F)
joint designs and dimensions for arc welding nickel- and iron-nickel-base superalloys ..... 171(F)
Double V-groove butt joint, joint designs and dimensions for arc welding nickel- and iron-nickel-base superalloys..... 170(F)
DR. *See* Directional recrystallization.
Draw forming, speeds for 110(T)
Drawing.....106, 110
Drilling.....197–200(F,T)
cutting fluids..... 199
fixturing for..... 200
hole sizes range for superalloys..... 199(T)
speeds and feeds ..... 198(T)
Drip short frequency (DSF).....60(F), 61(F), 62–63(F)
Drop hammer, heat treatment for formability... 109
Drop hammer forming 110
Dry argon atmosphere 143, 144
Dry hydrogen atmosphere.....143, 144
DS. *See* Directional solidification.
DSF. *See* Drip short frequency.
Dual-alloy turbine wheel concept..... 119
Ductile-to-brittle transition temperature (DBTT)
of aluminum diffusion coatings 322
of coating strain tolerance.....321–322
Ductility.....21
of aluminide diffusion coatings 322
of overlay coatings ..... 321–322(F)
of polycrystalline cast superalloys 263–264
Ducting, as application of superalloy ..... 9(T)
Dynamic modulus of elasticity
cast superalloys .....258, 261(T)
modeling of..... 346
of wrought superalloys.....241, 245(T)
Dynamic oxidation 290
Dynamic recrystallization.....94

E

EAF. *See* Electric arc furnace.
EAF/AOD. *See* Electric arc furnace/ argon oxygen decarburization process.
Earing..... 108
EB. *See* Electron beam evaporation.
EBPVD. *See* Electron beam physical vapor deposition.
EBW. *See* Electron beam welding.
ECM. *See* Electrochemical machining.
Elastic modulus.....22
Electrical conductivity.....22
Electrical resistivity, of wrought superalloys ..... 247(T)
Electric arc furnace (EAF)..... 45–46, 47–48(F)
deslagging operation 47–48
furnace lining cost.....47
operation capacity 47
schematic of .....47(F)
Electric arc furnace (EAF)/argon oxgen decarburization (AOD) process ..... 44–50(F)
alloy composition.....46
charge assembly.....46
cost for superalloys.....45
decarburization cycle.....49
description 45–46
erosion of refractory.....48
melt times for EAF portion of process 48
raw material used.....44
teeming ..... 49–50(F)
and vacuum induction melting compared.....50
Electric arc furnace/argon oxygen decarburization with electroslag remelting (EAF/AOD with ESR), as melt method for selected superalloys .....45(T)
Electrochemical machining (ECM).....189, 190
and fatigue endurance stress capability ..190, 204
Electrode melt rate..... 61, 62(F)
Electrodes
argon oxygen decarburized.....50
for electroslag remelting.....58
quality factors 58
for vacuum arc remelting.....58, 59
vacuum induction melted cast pieces.....51
Electrode wires, compositions..... 168(T)
Electrodischarge machining..... 200
Electrolytic alkaline cleaning 210
Electrolytic nickel plating 182
Electron beam brazing..... 180
Electron beam deposition..... 344
Electron beam (EB) evaporation, for overlay coating of turbine components 317–318
Electron beam physical vapor deposition (EBPVD).....316, 317, 318, 319, 320(F), 321
Electron beam welding (EBW)..... 161–162, 164
aspects 172–173
for fusion welding superalloys 161
modes employed 162
for repair technique.....336, 337
Electron vacancy number (N_v) 329, 357, 358
average value determination .....358(T), 359
calculation schemes 358
reference method for calculation .....358, 359(T)
Electroplating.....209, 314
Electroslag remelting (ESR) ...44, 56, 57–58, 66–71(F), 101, 121(T)
cold start 68

© 2002 ASM International. All Rights Reserved.
Superalloys: A Technical Guide (#06128G)

Electroslag remelting (ESR) (continued)
control of process ..... 68–69(F)
defects, melt-related ..... 70(F), 71(F)
electrode quality factors 58
furnaces ..... 66–68(F)
hot start 68
ingot processing 72
ingot surface ..... 70(F), 71(F)
pool details ..... 70–71(F)
process description 57–58
reactions with aluminum 58
reactions with silicon 58
reactions with sulfur 58
reactions with titanium 58
reactions with zirconium 58
response time to melt current change 69
slag choices 70
and vacuum arc remelting compared ..... 57–58, 59(F)
Electroslag remelting furnace ..... 66–68(F)
Elements. *See* Alloying elements.
Elevated temperature(s). *See also* High temperature; High temperature strength; Overheating; Temperature(s).
creep/stress-rupture at, aircraft applications 24
hot corrosion 301–302
Elevated temperature applications, P/M superalloys 129
Elevated-temperature corrosion attack 287
Elevated-temperature strength 9
Elongation 211
of nickel-base superalloys ..... 284(T)
Emulsion cleaning, procedure for removing scale superalloys ..... 207(T)
Endothermic atmosphere ..... 143(F), 144
Engines. *See* Turbine engines.
ENiCrFe-1, composition of filler metals and electrode wires for arc welding ..... 168(T)
ENiCrFe-2, composition of filler metals and electrode wires for arc welding ..... 168(T)
ENiCrFe-3, composition of filler metals and electrode wires for arc welding ..... 168(T)
ENiCrMo-2, composition of filler metals and electrode wires for arc welding ..... 168(T)
ENiCrMo-3, composition of filler metals and electrode wires for arc welding ..... 168(T)
ENiCrMo-4, composition of filler metals and electrode wires for arc welding ..... 168(T)
ENiCrMo-7, composition of filler metals and electrode wires for arc welding ..... 168(T)
ENiMo-1, composition of filler metals and electrode wires for arc welding ..... 168(T)
ENiMo-3, composition of filler metals and electrode wires for arc welding ..... 168(T)
Environment, effect on fatigue crack growth rate ..... 255, 257(F)
Equilibration, of ingots that were cogged 74
ERNiCr-3
composition of filler metals and electrode wires for arc welding ..... 168(T)
as filler metal, base metals involved 167
ERNiCrFe-5
composition of filler metals and electrode wires for arc welding ..... 168(T)
as filler metal, base metals involved 167
ERNiCrFe-6
composition of filler metals and electrode wires for arc welding ..... 168(T)
as filler metal, base metals involved 167
ERNiCrFe-7
composition of filler metals and electrode wires for arc welding ..... 168(T)
as filler metal, base metals involved 167
ERNiCrMo-2, composition of filler metals and electrode wires for arc welding ..... 168(T)
ERNiCrMo-3
composition of filler metals and electrode wires for arc welding ..... 168(T)
as filler metal, base metals involved 167
ERNiCrMo-4
composition of filler metals and electrode wires for arc welding ..... 168(T)
as filler metal, base metals involved 167
ERNiCrMo-7
composition of filler metals and electrode wires for arc welding ..... 168(T)
as filler metal, base metals involved 167
Erosion
of refractory 48
of vacuum induction furnace lining 52
ESR. *See* Electroslag remelting.
Eta phase ..... 25, 27(T), 141, 221
composition 34
crystal structure .....27(T)
definition 34
descriptive comments .....27(T)
effect on low-cycle fatigue in IN-706 nickel-base superalloy ..... 253(F)
formula .....27(T)
in iron-nickel superalloy ..... 362(F)
lattice parameter .....27(T)
in nickel-base superalloy ..... 363(F)
role in strengthening A-286 225
role in strengthening IN-901 225
Eta phase hexagonal ordered Ni_3Ti ..... 25, 27(T)
Eta phase precipitates 153
Etching
acid 205
to enhance visual appearance for microscopic and macroscopic examination 293
Exhaust cone, contoured ..... 109–110(F)
Exhaust valves, as application of superalloy ... 9(T)
Exothermic atmosphere. *See also* Atmospheres 143–144
Explosive forming ..... 110, 112–113(F)
of cobalt-base superalloys ..... 113(F)
requirements and restrictions 110
Extreme-pressure (EP) lubricants 111
Extrusion 72, 76, 92, 114, 124
effect on fatigue life 252
for powder consolidation 119
preconsolidated 125

© 2002 ASM International. All Rights Reserved.
Superalloys: A Technical Guide (#06128G)
www.asminternational.org

temperatures for P/M superalloys 125
Extrusion forging 94, 95
Extrusion plus isothermal forging, for P/M processing 126
Extrusion ratios, powder metallurgy processing 125

F

Face-centered cubic (fcc) crystal structure ..... 25, 26(F), 27(T)
dissolution of phases 139
MC carbides 37
Face milling ..... 190(F)
Facing plates 164
Failure
definition 323
modes of 323
of superalloy components ..... 330–334(F)
Fatigue
endurance stress capability and electrochemical machining 190, 204
in investment casting, hot isostatic pressing effect ..... 87, 89(F)
investment-cast products ..... 87, 89(F)
Fatigue crack growth curve, of wrought superalloy ..... 253, 255(F)
Fatigue crack growth rate
environment effects ..... 255, 257(F)
factors influencing ..... 254–255, 257(F)
at subzero temperatures 286
Fatigue cracking 224
Fatigue life
factors influencing ..... 254–255, 257(F)
freckled structures 41
Laves phases and carbides effects on 41
of wrought superalloys 250, 251
Fatigue strength, of welds 153
Fatigue testing 211
of consolidated powder blends 124
fcc. *See* Face-centered cubic (fcc) crystal structure.
Ferrochrome
high-carbon, cost of 46
low-carbon, cost of 46
F-15 Eagle fighter 119
F-100 engine for 77
F-404 turbofan engines, P/M superalloy parts 133
Filing 179
Filler metals 149
for brazing ..... 176–178(T)
for brazing cobalt-base alloys 183
for cobalt-base superalloys, welding of 151
compositions ..... 168(T)
for gas tungsten arc welding ..... 167–169(T)
Finishing 209–210
problems and solutions 210
processes for superalloys 209–210
requirement of 203
Finite-element modeling methods 346
Finwall, diffusion welding of 174
Fireside corrosion 299
Fissures. *See* Microfissuring.
Fixtures
as application of superalloy ..... 9(T)
for brazing 180
welding 164
Fixturing
coefficient of expansion of fixture and part 145
degree of contact of part and fixture 145
for drilling 200
during heat treatment 145
restraint type 145
support type 145
Flameholders, application reason for Haynes 188 ..... 76(T)
Flash pickling 111, 205, 206
Flat products 72–73
Fluid die process 125
Fluorescent penetrant inspection (F.P.I.)
of investment-cast products 82, 83
procedures, to find visible surface cracking of welds 153
of weldments 187
Fluxes 181
for brazing 180
Fluxing corrosion ..... 301, 302(F)
F-100 engine. *See* Pratt & Whitney (PW) F-100 engine.
F-101 engine ..... 120(T)
F-119 aircraft engine ..... 8, 9(F)
Forgeability ..... 22, 93–94(T), 96, 102(T), 344
Forged billets. *See* Billets.
Forging ..... 91–106(F,T)
aims of 92–93
application range 93
capability ratings ..... 93–94(T)
closed-die 94, 95, 114
cold ..... 117, 118(F)
cooling practice 98
design guides ..... 95(T)
die design 95
die deterioration rate 94
flat-die 95
forgeability ratings ..... 102(T)
Gatorizing process 114
grain refinement requirements 102
grain refinement to control structure with precipitated phases 105–106
hand 95
heat sources, location of 94
hot-die 101
information/product sources 353, 367–368
isostatic ..... 128(T)
isothermal 95, 99, 101, 114, 119
isothermal, of P/M consolidated products 126
isothermal/superplastic 99, 102
isothermal/superplastic, and in-process annealing 138
machines, drop forge 94
machines, hydraulic presses 101
machines, hydraulic press forges 94
machines, mechanical screw-driven 94
mechanically alloyed ODS alloys 132

© 2002 ASM International. All Rights Reserved.
Superalloys: A Technical Guide (#06128G)
www.asminternational.org

Forging (continued)
methods for superalloys 94
modeling 99, 102–103, 347
near-net 126
objectives for cycle.....92–93
open-die 94, 95
peripheral cracking .....99, 101(F)
P/M billet 126
precision.....99
precision, of mechanically alloyed ODS alloys.....132
precipitation-hardenable superalloys.....92
process control 102–103
proprietary rotary machines.....94
recording of data.....104
recrystallization promoted.....104
reduction to prevent abnormal grain growth 104–105
shape, sonic shape, and final component interrelationships.....98(F)
superplastic ..... 94, 95, 114–115(F), 119
superplastic isothermal..... 99, 102
surface cracking.....99, 100(F)
temperatures .....93(T), 97, 102(T)
Formability 22, 344
Forming..... 21–22, 106–115(F,T)
alloy condition effect on formability 107–108
cold reduction effect on hardness..... 106, 107(F)
deformation modes of sheet metal components 108
ductility of material 108
information/product sources.....353
lubrication.....110–111
mechanically alloyed oxide-dispersion-strengthened alloys ..... 132(T)
methods.....110
processes 106
rarely controlling or developing microstructure of superalloys.....92
rolling direction effect ..... 109–110(F)
by rubber-diaphragm process 112
speed effect on formability..... 110
spinning from a roll forging .....111(F)
tools for 110
Forming limit curves 108
F.P.I. *See* Fluorescent penetrant inspection.
Fracture..... 2.
See also Fatigue; Fracture toughness.
Fracture mechanics 250–251
Fracture toughness
of nickel-base superalloys .....285(T), 286
Freckle grains 86
Freckles.....41(F), 86, 280
in electroslag remelting electrode.....72
formation.....41–44(F)
formation and vacuum arc remelting.....63
formation, conditions for ..... 43–44(F)
self-perpetuating nature 43
Friction welding (FRW)..... 173, 174–175
aircaft applications.....175
FRW. *See* Friction welding.
Fuel oils, with sulfur-bearing compounds.....143
Full annealing ..... 135, 137(T), 138, 146, 147
carbide precipitation upon cooling propensity 146–147
followed by fast cooling.....138
procedure.....139
purpose 139
temperature requirements and results.....139
Full solutioning 268
Furnace atmospheres
for brazing 180–181
and descaling 210
Furnace brazing 175, 176, 182
Furnaces. *See also* Heat treatment.
atmospheres, protective 143–144
belt conveyor.....144
box 144, 145
consumable arc, for investment casting.....80
continuous.....145
continuous processing.....144
double-chamber vacuum induction melting.....53(F)
electric arc ..... 47–48(F)
electron beam, for investment casting.....80
electroslag remelting ..... 66–68(F)
equipment for heat treatment 144–145
fixturing for heat treatment.....145
forging 95
high-frequency induction 80
metallic muffle 180
providing thermal gradients to control grain size 82
for reheating superalloys 80
roller hearth.....144
traditional production investment casting ..... 84, 86(F)
vacuum 144–145
vacuum arc remelting ..... 58–59(F)
vacuum brazing 147
vacuum induction..... 52–53(F)
Furnace spallings.....143
Fusion welding.....149, 151
cobalt-base superalloys.....164
cracking and soundness of welds ...152–160(F,T)
details.....165–173(F,T)
iron-nickel-base superalloys.....164–165
nickel-base superalloys.....164–165
postweld heat treatments .....160–161(T)
practical aspects.....163–165(T)
precipitation-hardenable alloys 165
preweld heat treatments.....160–161(T)
solid-solution superalloys.....165
techniques for superalloys.....161–163
Fusion zone 159

G

Gamma double-prime phase.....212, 218
age hardening of IN-718 and IN-706 superalloys 155
bct-ordered precipitation.....34
carbide precipitation.....33(F), 34–35, 141, 225

© 2002 ASM International. All Rights Reserved.
Superalloys: A Technical Guide (#06128G)
www.asminternational.org

crystal structure ..... 27(T), 31
descriptive comments ..... 27(T)
formula ..... 27(T)
of IN-718 direct-aged forged structure ... 105, 106
lattice parameter ..... 27(T)
in nickel-base superalloys ..... 361(F), 362(F)
for niobium-strengthened nickel-base superalloys 28
as secondary phase 25
as strengthener from niobium alloying 30
Gamma-gamma prime eutectic 34, 216, 359
hafnium contribution to formation of 237
of nickel-base superalloy ..... 360(F)
Gamma prime 212
cuboidal ..... 31, 32, 33(F), 34(F), 35(F)
definition 34
dual size promoted by intermediate heat treatment 221
precipitation, from prior microstructure 34
radial-type ruptures in forgings 93
in rafts 31, 348
spheroidal ..... 31, 32, 33(F), 34(F), 35(F)
strengthening U-500 142
strength (hardness) vs. particle diameter ..... 213, 216(F)
strength loss by coarsening 217
temperature dependence of tensile properties 213
tensile yield strength, solute influence ..... 213, 214(F)
Gamma prime coarsening
cobalt addition effects 240
and refractory metal additions to nickel-base superalloys 240–241
Gamma prime envelopes 221
Gamma prime-hardened nickel-base superalloys, creep-rupture strength ..... 241, 242(F)
Gamma prime hardener, and cracking tendency 154
Gamma prime phase ..... 20, 25, 26(F), 147
alloying element effects 30–31
composition 34
crystal structure ..... 27(T)
definition 34
descriptive comments ..... 27(T)
dissolution of ..... 324(T), 325(T), 326, 327(F)
formula ..... 27(T)
lattice parameter ..... 27(T)
microstructural degradation 328
in nickel-base superalloy ..... 361(F), 362(F)
Gamma prime precipitates 141, 153
airfoil alloys 118
cuboidal 39
in iron-nickel superalloys 26
and postweld heat treat cracking of welds 153
as secondary phase 25
as strengthener from aluminum alloying 30
as strengthener from titanium alloying 30, 154
in volume fraction gamma prime superalloys ..... 214–216(F,T)
volumetric compaction 32
Gamma prime precipitation effect 214
Gamma prime rafts 31, 348
Gamma prime size ..... 277–278(F)
Gamma prime solvus temperature
of cast superalloys ..... 325(T)
of wrought superalloys ..... 324(T)
Gas atomization 119
for producing cobalt-base superalloys 133–134
Gas-induced corrosion 287
Gas metal arc welding (GMAW) 162, 164
aspects of 169
for fusion welding superalloys 161
joint design 166–167, 169
shielding gases for 169
welding techniques for ..... 168(T), 169
Gas phase process ..... 311, 316(T)
Gas sampling tubes 133
Gas tungsten arc welding (GTAW) ..... 162, 163–164(T), 165–169(F,T)
base-metal thickness ..... 164(T)
diameter of filler metal ..... 164(T)
direct current electrode negative (DCEN) 165
electrode diameter ..... 164(T)
of exit nozzle ..... 111–112(F)
filler metals for ..... 165, 167–169(T)
of flame deflector ..... 112–113(F)
for fusion welding superalloys 161
joint design 166–167
for repair technique 336
with resistance seam welding 187
shielding gases for ..... 164(T), 167
shielding gas flow rate ..... 164(T)
tail-pipe ball ..... 113(F)
welding current ..... 164(T)
welding techniques with 169
Gas turbine airfoils 22, 23
Gas turbine engine components, application of superalloys 15, 20
Gas turbine engines. *See* Aerospace applications; Aircraft applications; Turbine engines.
Gatorizing process 114, 128
gcp. *See* Geometrically close-packed phase.
General Electric Aircraft Engines
as-HIP powder metallurgy superalloys used ..... 121(T)
GE 90 engine, number of engine systems produced through 1996 using forged P/M superalloys ..... 120(T)
GE-F-110 engine, number of engine systems produced through 1996 using forged P/M superalloys ..... 120(T)
GE F-404 engine, aerospace application of as-HIP P/M superalloys ..... 120(T)
GE F-404/414 engine, number of engine systems produced through 1996 using forged P/M superalloys ..... 120(T)
GE T-700 engine, aerospace application of as-HIP P/M superalloys ..... 120(T)
GE T-700 engine, number of engine systems produced through 1996 using forged P/M superalloys ..... 120(T)

© 2002 ASM International. All Rights Reserved.
Superalloys: A Technical Guide (#06128G)
www.asminternational.org

General oxidation 287
Geometrically close-packed (gcp) phases 25
GFM rotary forging machines 75
Glass, molten, mechanically alloyed ODS alloy components for production or handling of 133
Glass processing industry applications, mechanically alloyed ODS alloys..... 133
GMAW. *See* Gas metal arc welding.
Gold electroplating..... 314
Grain-aspect ratio.....28
Grain boundaries
absent in single crystal directionally solidified alloys.....80
carbide film formation 102
carbides..... 35–37(F), 218–222
control, alloying elements for 30
Grain-boundary carbides.....35–37(F), 102
in cobalt-base superalloys 222
in nickel-base superalloys ..... 218–222(F)
Grain-boundary hardening ..... 218–220(F)
Grain boundary stabilization against excessive shear.....25
Grain misorientation 86
Grain refinement, and forging 102
Grain size 18
affect on crack growth rate 254
cast superalloys 29
in columnar grain directionally solidified products, control of.....82
control in polycrystalline parts 82
and creep-rupture strength..... 227(F)
effect on fatigue crack growth rate ... 254, 256(F)
effect on weldability and creep resistance..... 151
and liquation cracking ..... 159(F)
modeling of..... 346
in SCDS products, control of.....82
wrought superalloys 29
Grain structure, modeling of..... 346
G-ratio. *See* Grinding ratio.
Greases, unpigmented 111
Green rot.....289, 299
Green shell, in investment casting 83
Grindability index..... 202
Grinding..... 192–193, 201–202(T)
fluids for..... 201–202(T)
grindability, media and speed effects..... 202(T)
for scale removal 206
Grinding fluids..... 201–202(T)
identification and classification of ..... 202(T)
Grinding on component airfoil surface or attachments, plastic deformation from investment casting 87
Grinding ratio (*G*-ratio) ..... 193, 202(T)
Grit blasting 179
before aluminide coating 315
for grit blasting brazing surfaces..... 179
GTAW. *See* Gas tungsten arc welding.
GTCP 331 auxiliary power unit (APU) engine 119
Gun drills .....198, 199(T), 200

H

HAB. *See* High-angle boundaries.
Hafnium
added to CGDS superalloys to reduce cracking 267
addition allowing increased transverse ductility..... 269
as addition to increase ductility in cast nickel-base superalloys.....263–264
as alloying element.....30
alloying element effects in nickel-base superalloys .....29(T)
in base alloy, incorporated in coatings..... 294
content effect on coating/superalloy system 313, 314
content effect on oxidation resistance..... 297
cost..... 8
encouraging inclusions tendency.....86
for grain-boundary strengthening in nickel-base superalloys .....31(F)
improving ductility of grain-boundary regions.....38
in iron-nickel superalloys.....26
mechanical properties improved by addition of .....235–238(T)
in nickel-base superalloys 26
in SCDS alloys..... 224
Hafnium carbides 37
phase observed, crystal structure.....27(T)
Hardening. *See* Work hardening.
Hard facing, application to turbine tips..... 151
HAZ. *See* Heat-affected zone.
HCF. *See* High-cycle fatigue.
hcp. *See* Hexagonal close-packed crystal structure.
Heat-affected zone (HAZ)
contaminants and weld soundness ..... 159(T)
for gas metal arc welding 162
hot cracking..... 156–157(F), 158(F)
hot cracking after fusion welding..... 152(F)
liquation cracking.....157–159(F,T)
postweld heat treatment cracking ..... 152–153(F)
Heat corrosion resistance. *See* Corrosion; Hot corrosion.
Heat flux..... 145
Heat treatment (Heat treating).. 15, 135–147(F,T)
cooling rate 145
definition 135
direct aging process 248–249
economics of manufacturing..... 146
to ensure gamma double-prime precipitation.....35
equipment, as application of superalloy ..... 9(T)
fixtures, of mechanically alloyed ODS alloys..... 133
fixturing 145
furnace equipment 144–145
heating/cooling rates for cast superalloys..... 147
heating/cooling rates for wrought superalloys 146–147
heat-up rate 145
information sources.....368–369

© 2002 ASM International. All Rights Reserved.
Superalloys: A Technical Guide (#06128G)
www.asminternational.org

not obvious or overlooked 135–136
objectives.....135
and orientation of products.....228
of overlay coatings 311
precipitation-hardened alloys for formability 108–109
of precipitation-hardened superalloys.....154
of precipitation-hardened superalloys after welding 150
for precipitation hardening, various product forms.....228, 229(T)
procedures.....139–142(T)
reasons for 135
to reduce liquation cracking susceptibility 160
section size as factor 136
step heat treatments 347
for superalloys, processes used.....135
surface attack and contamination ..... 142–143(F)
Heat treatment fixtures, of mechanically alloyed ODS alloys.....133
Heat treatment industry applications, mechanically alloyed ODS alloys.....133
Heat-up rate 145
Helium. *See also* Atmospheres; Shielding gases.
as detrimental tramp element in nickel-base superalloys .....31(F)
Hexagonal close-packed (hcp) crystal structure ..... 25, 26(F), 27(T)
Hexagonal crystal structure..... 27(T), 28(T)
High-angle boundaries (HAB)..... 271(F), 280
High-cycle fatigue (HCF)
and carbide precipitation 224–225
hot isostatic pressing effect ..... 279–280(F)
of wrought superalloys.....250–253(F,T), 255–258(F,T)
High-cycle fatigue strength, of investment castings ..... 87, 89(F)
High-pressure compressor (HPC).....23
High-pressure turbine (HPT) airfoils.....23, 341, 342
capability growth 347
High-pressure turbine (HPT) sections, application of superalloys.....22
High-speed cobalt tool steels..... 191
High-speed steels
for broaching tools for superalloys 197
for machining tools for superalloys..... 191(T)
for twist drills 199
High temperature, applications, of superalloys 24
High-temperature strength. *See also* Elevated temperature; Fatigue; Fatigue strength; High temperature; Overheating; Strength; Temperature(s); Tensile strength; Thermal fatigue.
of iron-nickel-base superalloys 24
High-titanium alloys, weldability..... 153
HIP. *See* Hot isostatic pressing.
Hold-down bars.....164
Homogenization.....72
of solute distribution in ingots 73–74
temperatures 73
Hot corrosion. *See also* Corrosion; Hot corrosion resistance; Sulfidation.....287, 288–289, 298–309(F,T), 323, 344
chromium content effect on resistance..... 303, 304(T)
chromium diffusion coatings for protection.....313
coatings for protection against.....309
definition 299
as degradation process .....300–301, 302(F)
factors determining stages..... 301(F)
fluxing reactions 300
high-temperature 301–302
high-temperature (type 1) ..... 302–306(F,T), 314
identification of ..... 299–300(F), 301(F)
low-temperature (type 2) .....306–307(F), 308
minimization of attack by coatings use..... 342
overlay coatings for 317
promoted by additives 290
protection against 289
ranking superalloy performance 308–309
salt-induced 309
stages .....299–300, 301(F)
surface protection against 309
of turbine blades 332
type 1 model systems.....302–303
type 1 of superalloys and coatings.....303–306(F,T)
type 2, of superalloys and coatings..... 306, 307–308
Hot corrosion resistance
alloying elements for.....30
alloying elements producing 30
Hot cracking..... 101, 151, 152(F), 156–159(F,T), 164
filler metal choice effect.....167
locations ..... 152(F)
Hot deformation 21–22
Hot-die forging.....101
Hot forming.....106–107
Hot isostatic pressing (HIP).....15, 87, 89, 124
of aircraft P/M superalloy parts 133
creep behavior affected by ..... 335(F)
direct-HIP method 117, 126
effect on high-cycle fatigue behavior of SCDS superalloy ..... 279–280(F)
effect on high-cycle fatigue strength .... 87, 89(F)
followed by hot-working 131
near-net shapes 126
orthopedic implant fully dense materials 133
plus hot forging ..... 117, 118(F)
of polycrystalline alloys 87
of polycrystalline cast superalloys 264–265
for powder metallurgy processing.....117, 118(F), 119, 126
process description 124–125
of single crystal directionally solidified alloys.....87
to upgrade stress-rupture capability..... 114
Hot isostatic pressing/extrusion process..... 124
Hot rolling, and mechanical alloying..... 131

© 2002 ASM International. All Rights Reserved.
Superalloys: A Technical Guide (#06128G)
www.asminternational.org

Hot shear spinning, mechanically alloyed ODS alloys....132
Hot short cracking, in shielded metal arc welded welds....172
Hot sizing, fixtures for....145
Hot tops, for vacuum induction melted electrode....56
Hot working....11, 15, 102, 135
as full annealing step....138
Hot work tools and dies, as application of superalloy....9(T)
HPC. *See* High-pressure compressor.
HPT. *See* High-pressure turbine airfoils.
Hydrogen embrittlement....208

I

IB. *See* Inertia bonding.
IHT. *See* Intermediate heat treatment.
Immersion, as cleaning method before brazing....179
Impact damage, plastic deformation from investment casting....87
Incipient melting....2–3, 139, 146, 147
See also Incipient melting temperatures; Melting; Melting point.
and brazing....150
during friction welding....175
and hot cracking....156–157
and overheating....324–325(T), 326(F)
and precipitation hardening....217(F)
temperature effect on homogenization....216
Incipient melting temperatures. *See also* Incipient melting; Melting; Melting point....2–3, 8, 23
of cast superalloys....325(T)
of wrought superalloys....324(T)
Inclusions....163, 212
investment casting....86
Inconel alloys. *See* Alloy Index.
Induction brazing....175, 180, 182
Industrial applications, mechanically alloyed ODS alloys....132–133
Industrial gas turbine components, as application of superalloy....9(T)
Inert atmosphere, for reducing postweld heat treatment cracking....155
Inert gas atomization....121–122(F)
oxygen contents....122
process description....121–122(F)
process steps in powder production....121(T)
for producing powders for orthopedic implants....133
size range of powders....122
Inertia bonding (IB)....150, 173, 175
aircraft applications....173, 175
Inertia welding. *See* Friction welding.
Information sources....353, 365–369
Infrared brazing....180
Ingode....72
Ingot breakdown....72–73(F)
Inlet air filtration, to reduce hot corrosion levels in stationary turbines....309
In-process (mill) annealing 135, 138–139(F), 147
Inserts....164
Inspectability....22
Interdiffusion zone....313
of overlay coatings....317
Intergranular attack....142–143(F), 295(F)
and cleaning chemicals....204
and descaling procedure....208
showing need for coatings....310
Intergranular corrosion....293
Intergranular cracking....235
and carbide precipitation....226
Intergranular oxidation....142–143(F), 287
of turbine blade....332(F)
Intergranular oxide penetration....295
Intermediate heat treatment (IHT)....226
promoting dual size of gamma prime in an alloy....221
reducing carbon supersaturation....220
requirement for....220
between solution and aging....219(F)
Intermetallic compound precipitation
of nickel-base superalloys....28
of solid-solution-strengthened nickel-base superalloys....28
Intermetallic compounds. *See also* Eta phase; Gamma prime precipitate; Laves phase; Mu phase.
precipitation in fcc matrix....26
solvus temperatures, and setting of forging temperatures....97
Internal oxidation. *See also* Oxidation....288
International Symposium on Structural Stability (in superalloys)....358
Interphase spacing, modeling of....346
Investment casting...11, 73, 79–90(F,T), 344, 346
aircraft applications....79, 80, 83, 84(F)
atmosphere in furnace....79
ceramic shell preparation....82
ceramic shell process, for making molds....80
cobalt-base superalloys....79, 80
description of process....79
dimensional tolerances....79
disposable patterns....79
industry growth....347
information/product sources....353, 368
mold making processes....80
nickel-base superalloys....79, 80
pattern materials....80
polycrystalline products...84, 86(F), 87(F), 88(F)
porosity control....87
postcast processing....82
problem areas....85–89(F)
process improvement and development..347–348
rejection causes....86
shell mold process....82–83, 84(F)
shell mold use....147
solid investment (solid mold) process, for making molds....80
source stock....80

© 2002 ASM International. All Rights Reserved.
Superalloys: A Technical Guide (#06128G)
www.asminternational.org

steps in process ..... 80, 81(F)
traditional production furnace ..... 84, 86(F)
vacuum induction melting heat sizes 80
Iridium, addition effect 347
Iron. *See also* Alloy Index; Iron-chromium-nickel superalloys; Iron-nickel-base superalloys; Iron-nickel-chromium superalloys; Precipitation-strengthened superalloys; Superalloys.
alloying element effects in nickel-base superalloys .....29(T)
composition of freckle vs. matrix .....41(F)
density 3
as joint base element in nickel-base superalloys .....31(F)
melting temperature 3
as solid-solution element of nickel-base superalloys 31
as tramp element..... 235, 237(T)
Iron boride, crystal structure and phases observed .....28(T)
Iron carbides, crystal structure, phases observed .....27(T)
Iron-chromium alloys, crystal structure and phases observed .....28(T)
Iron-chromium-molybdenum alloys, crystal structure and phases observed .....28(T)
Iron-chromium-nickel superalloys, stress-rupture strength ..... 19(F)
Iron grit 179
Iron-molybdenum alloys, crystal structure and phases observed .....28(T)
Iron molybdenum carbides, crystal structure and phases observed .....27(T)
Iron-nickel-base solid-solution-hardened superalloys, shielded metal arc welding .. 169, 172
Iron-nickel-base superalloys. *See also* Alloy Index; Iron; Superalloys.
aging cycles..... 140(T)
annealing ..... 137(T)
boride formation 37
carbide precipitation..... 224–225(F)
casting problems 87
cast, temperature limitations 15
composition ..... 4(T), 5(T)
compositional ranges of alloying additions.....29(T)
cost 8
creep and rupture resistance 24
creep-rupture strength ..... 19–20, 241, 243(F)
crystal structure 25–26
crystal structure and phases observed ..... 25–26, 27–28(T)
density ..... 3, 22, 246(T)
diffusion bonding 173–174
ductility.....21
dynamic modulus of elasticity..... 245(T)
electrical resistivity ..... 247(T)
electron beam welding 173
elevated-temperature applications 91
elevated temperature strength.....92
filler metals for..... 167
forgeability rating.....93(T)
forging .....99(F)
forging temperature.....93(T)
forging temperature range 103
fusion welding.....164–165
gamma prime precipitation.....26
gas metal arc welding..... 169
grain-boundary carbides 222
hot corrosion..... 308
incipient melting temperature..... 3
investment casting not customary.....80
machinability ..... 189, 190(F), 191(T)
mean coefficient of thermal expansion..... 247(T), 262(T)
melting range..... 246(T)
microstructure 32
mill product availability 77
mismatches between precipitate and matrix.....32
precipitates and strength..... 32–37(F)
precipitation..... 3
process effects.....31
repair welding 152
solid-solution-hardened 146
solid-solution-strengthened 211
solution treating cycles ..... 140(T)
specific heat capacity..... 246(T)
stress relieving ..... 137(T)
stress-rupture strength.....3(F), 14(T)
temperature range..... 8
tensile elongation .....13(T)
thermal conductivity..... 247(T)
ultimate tensile strength .....13(T)
welding 150, 151
wrought, aerospace applications.....24
wrought, microstructure.....33(F)
wrought, temperature limitations.....15
yield strength (0.2% offset).....13(T)
Iron-nickel-chromium superalloys
annealing ..... 137(T)
filler metals used for welds 167
stress relieving ..... 137(T)
Iron-niobium alloys, crystal structure and phases observed .....28(T)
Iron-niobium carbides, crystal structure and phases observed .....27(T)
Iron oxide 179
Iron-titanium alloys, crystal structure and phases observed .....28(T)
Iron-tungsten carbides, crystal structure and phases observed .....27(T)
Isostatic forging..... 128(T)
Isothermal forging 28, 93, 99, 101, 114, 119
of P/M consolidated products..... 126
Isothermal hot corrosion testing..... 291–292(F)
Isothermal/superplastic forging 73, 102
and in-process annealing 138
Isothermal superplastic forging/forming.....93

J

Jet engine applications. *See* Aerospace applications; Aircraft applications; turbine engines.

© 2002 ASM International. All Rights Reserved.
Superalloys: A Technical Guide (#06128G)

J-groove design 166
Joining. *See also* Welding ..... 149–187(F,T), 336–337
  information sources..... 368–369
Joints ..... 170–172(F)
JTSD-17R Turbofan engine, aerospace application of as-HIP P/M superalloys ..... 120(T)

K

Kanthal, variant, for overlay coating 316
Kirkendall effects..... 74

L

LAB. *See* Low-angle boundaries.
Land-based gas turbines, application of superalloys 8
Lanthanum, as alloying element .. 29(T), 30, 31(F)
Lap joint..... 170(F)
Lard oil 111
Laser beam welding (LBW) ... 162–163, 164, 337
  for fusion welding superalloys 161
Laser brazing..... 180
Laser fusion..... 351
Laser glazing 318
Launders 53–54, 55
Laves phase..... 26, 32, 157, 357
  alloying elements as cause 30
  crystal structure ..... 28(T)
  descriptive comments ..... 28(T)
  formula ..... 28(T)
  lattice parameter ..... 28(T)
  $MgNi_2$ in nickel-base superalloys 239
  and microstructural degradation 328, 329
  modeling of 346
  in nickel-base superalloy ..... 363(F)
  and solidification..... 41
LBW. *See* Laser beam welding.
LCF. *See* Low-cycle fatigue.
Lead
  alloyed with fixturing metals for VIM 51–52
  cracking contributor 159
  detection of contamination by test solution ..... 204(T)
  as detrimental tramp element in nickel-base superalloys ..... 31(F)
  as metallic contaminant..... 203
  removal through vacuum arc remelting 57
  as source of liquation cracking..... 159
  as tramp element..... 30, 233–237(F,T)
Leak tests, for weldments 163
Leak-up rates..... 54–55
Lime, as sulfur-reducing compound for EAF/AOD process..... 46, 49
Liquation 157
Liquation cracking
  elements as contamination sources 159
  and grain size..... 159(F)
  in heat-affected zone ..... 157–159(F,T)
  impurity limits permissible..... 159(T)
  susceptibility reduction 160
Liquid metal embrittlement..... 159, 181
  of cobalt-base superalloys 183
  of drilled surface..... 200
  by zinc..... 111
Liquid nitriding..... 200
Liquid penetrant inspection
  of forgings 103
  locating cold shuts and surface pits 163
  microfissuring detection 153
Liquidus temperature 43
Load cells..... 61
Localized corrosion 293
Local solidification time (LST), definition..... 43
Long products..... 72–73
Lorentz stirring 63–64
Lost wax investment process. *See* Precision investment casting.
Low angle boundaries (LAB)..... 86, 271, 280
Low-carbon ferritic steel, cold reduction effect on hardness ..... 106, 107(F)
Low-cycle fatigue (LCF) 129, 341
  atmosphere effects ..... 255, 257(F)
  and carbide precipitation 224, 225
  and crack propagation rate 22
  eta phase effect..... 253(F)
  interaction with creep-rupture at high temperatures 255
  iron-nickel-base superalloys..... 24
  of P/M disk alloys..... 127
  of wrought superalloys..... 250–253(F,T)
Low-cycle fatigue (LCF) cracking, of turbine engine disks..... 334(F)
Low-cycle fatigue (LCF) strength 18, 22
  and shot peening 210
Low-cycle fatigue (LCF) testing..... 255
  of consolidated powder blends 124
Low-pressure plasma spraying (LPPS).. 318, 320, 321
Low-pressure turbine (LPT) airfoils..... 23
Low temperature attack ..... 306–307(F)
LPPS. *See* Low-pressure plasma spraying.
LPT. *See* Low-pressure turbine airfoils.
LST. *See* Local solidification time.
Lubricants
  for forming..... 110–111
  removal of 204
  with sulfur-bearing compounds..... 143

M

MA. *See* Mechanical alloying.
Machined from components (MFC) specimens..... 230, 232
Machining ..... 189–202(F,T)
  costs..... 189
  cutting temperatures 192
  cutting tool materials..... 191–192(T)
  factors affecting 189
  information sources..... 368–369
  machinability ..... 189, 190(F)
  manufacturing time ..... 193–194(T)
  methods..... 189

© 2002 ASM International. All Rights Reserved.
Superalloys: A Technical Guide (#06128G)
www.asminternational.org

tool life 191–192
Macroetching
of forged parts 98
Macrosegregation. *See also* Segregation.
eliminated by P/M processing 119
Magnesium
addition counteracting sulfur effect in forging 102
addition to melt in vacuum induction melting 55
as alloying element ..... 30, 31(F)
as desulfurizer 238
dust as safety hazard in vacuum induction melting 55
improving ductility of grain-boundary regions 38
reduction in vacuum arc remelting 57
Magnesium oxide, lining for AOD vessel 48
Magnesium sulfides 30
forming spherical particles during vacuum induction melting 55
Magnetic fields, generated by consumable remelting processes 44
Manganese, as tramp element ..... 235, 237(T)
Manifold, heat treatment for formability 109
Masking 336
before aluminide coating 315–316
Matrix boride (M_3B_2) phase
crystal structure ..... 28(T)
descriptive comments ..... 28(T)
formula ..... 28(T)
lattice parameter ..... 28(T)
Matrix carbides ..... 31, 35–37(F)
MC carbides, 35–37(F), 157
MC carbides, accelerated oxidation of nickel-base superalloys ..... 295, 296(F)
MC carbides, and carbide films in Waspaloy ..... 221–222(F)
MC carbides, crystal structure ..... 27(T)
MC carbides, descriptive comments ..... 27(T)
MC carbides, discontinuous cellular carbides 220
MC carbides, formation with overheating and microstructural degradation ..... 327–330(F)
MC carbides, formula ..... 27(T)
MC carbides, gamma prime-hardened alloys 218
MC carbides, lattice parameter ..... 27(T)
MC carbides, microstructure ..... 36(F)
MC carbides, in nickel- and iron-nickel-base superalloys 224
MC carbides, reactions in nickel-base superalloys ..... 359(T)
MC carbides, in Udimet 500 142
M_6C carbides ..... 35–37(F), 219–220
M_6C carbides, crystal structure, descriptive comments, formula, and lattice parameter ..... 27(T)
M_6C carbides, in nickel- and iron-nickel-base superalloys 224
M_6C carbides, Widmanstätten (acicular) formation 221
M_7C_3 carbides ..... 35–37(F)
M_7C_3 carbides, crystal structure, descriptive comments, formula, and lattice parameter ..... 27(T)
$M_{23}C_6$ carbides ..... 35–37(F)
$M_{23}C_6$ carbides, crystal structure, descriptive comments, formula, and lattice parameter ..... 27(T)
$M_{23}C_6$ carbides, dissolved by solution annealing 160
$M_{23}C_6$ carbides, gamma prime-hardened alloys 218
$M_{23}C_6$ carbides, in nickel- and iron-nickel-base superalloys 224
$M_{23}C_6$ carbides, in Udimet 500 142
Matrix nitrides, crystal structure, descriptive comments, formula, and lattice parameter ..... 28(T)
Maximum inclusion size 122, 123–124
MCR. *See* Minimum creep rate.
MCrAl coatings. *See* Overlay coatings.
MCrAlY coatings. *See* Overlay coatings.
Mean coefficient of thermal expansion
of cast superalloys ..... 258, 262(T)
of wrought superalloys ..... 247(T)
Mechanical alloying (MA) 129
aerospace applications 133
aircraft applications 133
applications for alloys 132–133
composition of selected materials ..... 129(T)
consolidation to produce components ..... 130–132(F)
definition 130
heat treatment industry applications 133
industrial applications 132–133
powder production ..... 130(F), 131(F)
product availability of ODS alloys ..... 132(T)
purpose 129
reduction ratios for nickel-base alloys 131
of superalloys ..... 129–133(F,T)
temperature range for nickel-base alloys 131
Mechanical cleaning 179
See also Cleaning.
Mechanical core removal, plastic deformation from investment casting 87
Mechanical properties 211–212
See also Microstructural degradation.
due to tcp phase formation 30
Mechanical removal methods
for metallic contaminants 204
for oxides 206–207
for scales 206–207
for tarnish 205
Medical applications
biomedical ..... 9, 133(F)
biomedical, P/M superalloys 129
biomedical, requirements for orthopedic implants 133
Medical components, as application of superalloy ..... 9(T)
Melt current, effect on arc gap and drip short frequency ..... 60, 61(F), 62(F)

© 2002 ASM International. All Rights Reserved.
Superalloys: A Technical Guide (#06128G)
www.asminternational.org

Melting. *See also* Incipient melting; Melting point..... 2–3, 139
methods, combinations for frequently used superalloys ..... 44, 45(T)
methods, selection criteria..... 44, 45(T)
Melting/ingot breakdown, information sources..... 367
Melting/ingot production, information/product sources..... 353
Melting point. *See also* Incipient melting; Melting.
overlay vs. diffusion coatings..... 319
Melting-point depressants, in brazing ..... 176, 177(T), 181
Melting range
cast superalloys ..... 258, 262(T)
of wrought superalloys..... 246(T)
Melting temperatures..... 3
Melt-melt-forge-melt process..... 72
Melt-melt-melt process 72
Melt rate..... 62–63(F)
of electrode ..... 61, 62(F)
Melt rate excursions (MREs)..... 61–62
See also *events* 58
Mesh number..... 124
Mesh sizes, of powders 122
Meta-dynamic recrystallization 94
Metal fin..... 71(F)
Metal inert gas welding (MIG). *See* Gas tungsten arc welding (GTAW).
Metallic contaminants..... 203
removal of 204–205
Metallic inclusions, minimization methods for defects ..... 128(T)
Metallic soaps 111
Metallographic examination, microfissure detection..... 153
Metallurgical instabilities..... 323
Metallurgy of superalloys 25–39
strengthening mechanisms..... 25–29
Metal powders. *See* Powder metallurgy (P/M) processing.
Metal processing, as application of superalloy ..... 9(T)
Metal removal methods, for scales..... 207–208
MFC. *See* Machined from components specimens.
Mica, for pigmenting 111
Microcast-X method 82
Microcracking, with grinding..... 201
Microfissuring..... 153, 157–159(F,T)
Microporosity, and crack initiation in cast superalloys 280
Microprobe analysis, tramp element presence determined by 30
Microsegregation defects, modeling of 346
Microstructural degradation. *See also* Mechanical properties; Microstructure ..... 327–330(F)
Microstructure. *See also* Microstructural degradation..... 30–32
control 30
evolution of..... 32, 33(F), 34(F)
grain-boundary strengthening 32
information sources..... 366–367
phases..... 30–32
processing, effects of..... 38–39(F)
structures ..... 38–39(F)
MIG. *See* Metal inert gas welding.
Mill annealing..... 146
carbide precipitation upon cooling propensity 146–147
of solid-solution-strengthened alloys ..... 160(T)
Milling 201
cutter material 201
cutting fluids for 201
Mill products
availability ..... 76(F), 77
condition variability for same compositions 11
information/product sources..... 353
Mineral oils, unpigmented..... 111
Minimum creep rate (MCR), specimen size effect ..... 228, 230(F)
Minipatch welding tests..... 155(F)
Mismatches, matrix-precipitate 34
Missiles. *See* Aerospace applications.
Mixed gas attack ..... 287, 288, 294–298(F)
Modeling..... 345–347, 348–349
for forging 102–103
information sources..... 369
of investment casting..... 87–89
Moderate temperatures. *See* Temperature(s).
Mold cooling, causing plastic deformation from investment casting 87
Molten-salt hot corrosion..... 311
Molybdenum
addition effect on ternary alloys for hot corrosion 303
addition preventing carbide formation 37
as addition to nickel-base superalloys.... 240–241
as alloying element..... 29(T), 30, 106
as brittle phase formation cause..... 30
composition of freckle vs. matrix..... 41(F)
composition ranges as superalloy alloying additions..... 29(T)
compromising hot corrosion resistance of coated alloy..... 314–315
cost..... 8
increasing susceptibility to intergranular attack..... 143
as solid-solution element of nickel-base superalloys 31
for strength..... 30
strengthening element encouraging hot corrosion 303, 304
Molybdenum boride, crystal structure and phases observed..... 28(T)
Molybdenum carbides..... 37
crystal structure and phases observed ..... 27(T)
Molybdenum disulfide, in lubricants, not recommended..... 111
Molybdenum iron boride, crystal structure and phases observed..... 28(T)
Molybdenum oxide, as EAF/AOD process raw material..... 44–45

© 2002 ASM International. All Rights Reserved.
Superalloys: A Technical Guide (#06128G)
www.asminternational.org

Monocrystalloy.....90
MREs. *See* Melt rate excursions.
MTDATA software.....346
Mu (μ) phase.....26, 357
alloying elements as cause.....30
crystal structure, descriptive comments, formula, lattice parameter.....28(T)
and microstructural degradation.....328
"Mushy" zone.....43, 71, 157–159
backfilling from.....160
of vacuum arc remelting.....56–57, 63(F)

N

Nanocrystalline technology.....345
Near-net shape manufacturing.....100, 117
with precision casting.....189
Near-net shapes.....11, 15
of aircraft P/M superalloy parts (René 95).....133
of cobalt-base superalloys for biomedical applications.....133(F)
hot isostatic pressing.....124–125, 126
jet engine first-stage rotor assembly.....134
production ability.....119
Nichrome, development.....339
Nichrome-type alloys.....1
Nickel. *See also* Nickel-base superalloys; Nickel-chromium alloys.
as alloying element.....2, 29(T), 30
in brazing filler metals.....176, 177(T)
composition of freckle vs. matrix.....41(F)
composition ranges as superalloy alloying additions.....29(T)
cost.....8
density.....3
in matrix of mechanically alloyed superalloys.....129
melting temperature.....3
for phase stability.....30
Nickel-aluminide coating, ductility.....318(F)
Nickel-aluminide-type coating.....304, 305(F)
Nickel-aluminum-titanium superalloy, solution treated vs. fully heat treated.....326, 327(F)
Nickel-base superalloys. *See also* Alloy Index; Cast superalloys; Nickel; Precipitation-strengthened alloys; Solution-strengthened alloys; Superalloys; Wrought superalloys.
addition effects on forgeability.....103
aging cycles.....140(T)
aircraft applications.....84, 87(F)
aircraft applications, failure mechanisms.....333–334(F)
alloying elements.....30, 31(F)
annealing.....137(T)
boride formation.....37
brazing.....181–183
brazing surface pretreatment.....179
carbide precipitation.....224–225(F)
carbides in microstructures.....36(F)
cast, density.....22
casting, heat treatments used.....136
casting problems.....87
cast, microstructure.....33(F)
cast precipitation-hardened aging cycles.....141(T)
cast precipitation-hardened, solution treating cycles.....141(T)
cast, temperature limitations.....15
chromium content effect on hot corrosion resistance.....303, 304(T)
composition.....4(T), 5(T), 6(T), 7(T)
compositional ranges of alloying additions.....29(T)
composition ranges as superalloy alloying additions.....29(T)
creep-rupture strength.....20
crystal structure.....25–26
crystal structure and phases.....25–26, 27–28(T)
density.....22, 246(T), 262(T)
diffusion bonding.....174
directional grain-structured aircraft structures.....84–85, 88(F), 89(F)
ductility.....21
dynamic modulus of elasticity.....245(T), 261(T)
electrical resistivity.....247(T)
elevated-temperature applications.....91
elongation.....284(T)
forgeability rating.....93(T)
forging.....96–97(F)
forging, aircraft applications.....99, 100(F)
forging temperature.....93(T)
fracture toughness.....285(T)
friction welding.....175
fusion welding.....164–165
gamma double-prime precipitate.....31
grain-boundary carbides in.....218–222(F)
hot isostatic pressing effect on high-cycle fatigue strength.....87, 89(F)
incipient melting temperatures.....3
inertia bonding.....175
intergranular attack.....295(F)
for investment-cast airfoils.....89
investment casting.....79, 80
joint design.....166
low-cycle fatigue.....251–253(F,T)
machinability.....189, 190(F), 191(T), 192
mean coefficient of thermal expansion.....247(T)
melting range.....246(T), 262(T)
microstructure.....32
microstructure range.....38–39(F)
mill product availability.....77
mismatches between precipitate and matrix.....32
niobium-strengthened.....28
oxidation resistance.....8
oxide-dispersion-strengthened (ODS).....20
polycrystalline investment casting.....89
polycrystalline products.....84, 86(F), 87(F), 88(F)
powder metallurgy processing.....117–134(F,T)
precipitates and strength.....32–37(F)
precipitation.....3
precipitation-strengthened.....20
precipitation-strengthened, creep-rupture strength.....20
process effects.....31

© 2002 ASM International. All Rights Reserved.
Superalloys: A Technical Guide (#06128G)
www.asminternational.org

Nickel-base superalloys (continued)
reduction in area ..... 284(T)
refractory metal addition effects.....240–241
repair welding 152
room-temperature yield strength..... 285(T)
rupture strength vs. temperature..... 264(F)
single-crystal directionally solidified 20
single-crystal directionally solidified aircraft structures .....84–85, 88(F), 89(F)
solid-solution-hardened 146
solid-solution-strengthened 211
solid-solution-strengthened, creep-rupture strength 20
solution treating cycles ..... 140(T)
specific heat..... 246(T), 262(T)
strengthening mechanisms.....26–29
stress relieving ..... 137(T)
stress-rupture strength.. 3(F), 14(T), 18(T), 19(F), 258, 259(F)
temperature range..... 8
temperature-strength capability as function of year of availability.....340(F), 341(F), 343(F), 350(F)
tensile elongation ..... 12(T), 13(T), 16(T), 17(T)
tensile strength ..... 284(T)
thermal conductivity..... 247(T), 262(T)
tramp elements in.....31(F)
transient liquid phase bonding..... 185(F), 186
ultimate tensile strength ..... 12(T), 13(T), 16(T), 17(T)
vacuum arc remelting ..... 63–64(F)
welding 149, 150, 151
wrought, aerospace applications.....24
wrought, temperature limitations.....15
yield strength ..... 284(T)
yield strength (0.2% offset)..... 12(T), 13(T), 16(T), 17(T)
Nickel boride, crystal structure and phases observed.....28(T)
Nickel brazing filler metal, for grit blasting.... 179
Nickel carbides, phases observed, crystal structure .....27(T)
Nickel-chromium alloys
oxidation behavior, groupings ..... 294–295(F), 296(F)
oxidation, gaseous 296–297
Nickel-chromium-aluminum alloys, oxide scale development ..... 288(F)
Nickel-chromium-aluminum-niobium alloys, gamma double-prime phase, precipitation hardening..... 218
Nickel-chromium-aluminum-yttrium (NiCrAlY) coatings, hot corrosion resistance 306
Nickel-chromium-iron-base alloys, filler metals used for welds..... 167
Nickel-chromium-molybdenum alloys, filler metals used for welding of..... 167
Nickel-cobalt carbides, crystal structure and phases observed.....27(T)
NiCoCrAlY coatings, for protection against hot corrosion 309
Nickel flashing.....179, 181
Nickel-iron-base superalloys, gamma double-prime precipitate 31
Nickel-nickel sulfide (Ni-Ni_3S_2) eutectic, melting temperature 143
Nickel niobium (delta)..... 105
crystal structure, descriptive comments, formula, and lattice parameter.....27(T)
Nickel oxide (NiO) 288, 296, 302
formers ..... 288(F)
Nickel plating..... 179, 181, 209
Nickel titanium (Ni_3Ti), alloying element effects in cobalt-base superalloys.....29(T)
Niobium
addition preventing carbide formation 37
as addition to nickel-base superalloys....240–241
as alloying element.....29(T)
composition of freckle vs. matrix.....41(F)
composition ranges as superalloy alloying additions.....29(T)
content in nickel-base superalloy and freckle formation ..... 41–42(F), 43
distribution in homogenized ingot of IN-718 .....73(F)
effects, nickel-base precipitation-strengthened superalloys 31
as gamma prime strengthener..... 154
as precipitate former in nickel-base superalloys .....31(F)
precipitate-forming element for P/M disk alloys..... 128
retained in solution by quenching 139
segregating positively 43
as strengthener forming gamma double-prime precipitates 30
Niobium boride, crystal structure and phases observed.....28(T)
Niobium carbides.....37
crystal structure and phases observed.....27(T)
Niobium carbonitride, crystal structure and phases observed.....28(T)
Nickel cobalt carbides, crystal structure and phases observed.....27(T)
Niobium nitride, crystal structure and phases observed.....28(T)
Niobium oxide, as EAF/AOD process raw material.....44–45
Nitrides 212
Nitrogen
as alloying element..... 29(T), 31(F)
impurity limits permitted to avoid liquation-type hot cracking..... 159(T)
reduction in vacuum induction melting.....51
as source of liquation cracking..... 159
Nitrogen atomization 129
Nitrogen gas, as tramp element.....233–237(F,T)
Nitrogen pickup..... 143(F)
Nitrogen reduction 339
Noble metals, addition effect on DBTT of aluminide coatings..... 322

© 2002 ASM International. All Rights Reserved.
Superalloys: A Technical Guide (#06128G)
www.asminternational.org

Noncarbide formers
effect on carbide formation 225
effect on carbide precipitation 225
Notch-rupture testing ..... 226, 227(T)
Notch sensitivity 34
Nozzle convergent liner, application reason for Haynes 188 ..... 76(T)
Nuclear power systems, as application of superalloy ..... 9(T)
Nucleated grains 86

O

ODS. *See* Oxide-dispersion-strengthened alloys.
Oil-hole drills ..... 198, 199(T), 200
Open-die forgings ..... 94, 96(F), 97(F)
formed with aid of plugs and rings to impart certain shapes 94
Optical pyrometers, to monitor temperatures during vacuum induction melting 55
Orange peel 107
Ordering
of crystal structure ..... 25, 26(F)
of precipitates 32–34
Orientation 28
as process-related microstructural variable 39
Orthopedic implants ..... 133(F)
Orthorhombic crystal structure ..... 27(T)
Osprey Metals 125
Osprey spray process 124, 125
Outgassing
techniques 124
with vacuum induction melting 50
of virgin material in vacuum induction melting 54, 55
Out-of-contact process 311, 314
Overaging 139, 165
Overheating ..... 324–327(F,T)
alloy depletion 325
and coatings 325
and corrosion 325
Overlay coatings. *See also* Coatings ..... 209, 311, 316–319(F)
applications 316
chromium content effect for hot corrosion resistance 307
CoCrAlY ..... 302(F), 306, 307, 308, 309
CoCrAlY (18Cr-9Al), ductility ..... 322(F)
CoCrAlY (23Cr-12Al), ductility ..... 322(F)
CoCrAlY (27Cr-12Al), ductility ..... 322(F)
composition 319
development 342
fabrication processes 316–317
features 317
heat treatment for homogenization 311
MCrAlY-type, hot corrosion resistance ..304–306
melting point 319
NiCrAlY (20Cr-9–11Al), ductility ..... 322(F)
NiCrAlY (38Cr-11Al), ductility ..... 322(F)
overlay thickness consideration in testing 293, 294
structure ..... 316, 317(F)
Oxidation 142, 323, 344
coatings for protection against 309
diffusional transport 297
in EAF/AOD process 45
elevated-temperature 287
forms of 287–288
gaseous, degradation by ..... 294–298(F)
protection against 289
selective 297
of turbine combustion chamber ..... 330, 331(F)
Oxidation attack, of turbine blades .... 332–333(F)
Oxidation/corrosion testing ..... 289–294(F)
Oxidation potential, of thermal barrier coating system 311
Oxidation resistance 8, 33, 204
alloying elements for 30
alloying elements producing 30
alloying elements promoting 30
of precipitation-hardenable superalloys 142
Oxidation/volatilization 297
Oxide-dispersion-strengthened (ODS) superalloys 28, 129
aircraft applications 117, 118, 345
brazing 183
creep-rupture strength ..... 241, 242(F), 250(T)
diffusion welding 173
directional recrystallization 129, 250
electrical resistivity ..... 250(T)
elongation ..... 250(T)
hot corrosion ..... 299, 300(F)
incipient melting point ..... 348(T)
maximum useful temperature ..... 348(T)
mean coefficient of thermal expansion ..... 250(T)
mechanically alloyed product forms ..... 132(T)
mechanical properties ..... 244–245, 250(T)
melting range ..... 250(T)
physical properties ..... 244–245, 250(T)
reduction in area ..... 250(T)
specific heat capacity ..... 250(T)
stress-rupture strength ..... 20–21(F)
thermal conductivity ..... 250(T)
ultimate tensile strength ..... 250(T)
yield strength ..... 250(T)
Oxide entrapment 179
Oxide formers, and diffusion welding 174
Oxide inclusions 46
Oxide-nitride stringers 64, 66
Oxide reduction, before brazing 182
Oxides 163
formation of 205–206
removal of 204, 205–207
Oxide scale 292
development on Ni-Cr-Al alloys ..... 288(F)
formation 295–296
Oxide tarnish films, removal of 205–207
Oxidized carbides 224, 225
Oxygen
as detrimental tramp element in nickel-base superalloys ..... 31(F)
impurity limits permitted to avoid liquation-type hot cracking ..... 159(T)

© 2002 ASM International. All Rights Reserved.
Superalloys: A Technical Guide (#06128G)
www.asminternational.org

Oxygen (continued)
as source of liquation cracking 159
Oxygen "blow" 45
Oxygen gas, as tramp element ..... 233–237(F,T)
Oxygen reduction 339

P

Pack cementation (pack diffusion process) ..... 311–312, 314, 315(F), 316(T)
Pack coating 136
heating of alloy 135
Pack diffusion process (pack cementation) ... 311–312, 314, 315(F), 316(T)
Palladium electroplating 314
Pancakes, of open-die forged products ..... 96, 97(F), 98(F)
Paris' Law ..... 253, 255(F)
PAW. *See* Plasma arc welding.
PC. *See* Polycrystalline.
Petrochemical industries, as application of superalloy ..... 9(T)
PFZ. *See* Precipitate-free zones.
PHACOMP process 358
Phases. *See also* Precipitation-strengthened superalloys 25, 26
boride 32
crystal structure ..... 27(T), 28(T)
dissolution of 139
formula ..... 27(T), 28(T)
intermetallic 34
lattice parameter ..... 27(T), 28(T)
precipitation, strength from 31
secondary 15
of superalloys ..... 25–26, 27(T), 28(T), 29(T), 31–32, 357–363(F)
Phase stability, alloying elements for 30
Phosphorus
alloying element effects in iron-base superalloys ..... 29(T)
as detrimental tramp element in nickel-base superalloys ..... 31(F)
impurity limits permitted to avoid liquation-type hot cracking ..... 159(T)
as melting-point depressant for brazing ..... 176, 177(T)
as source of liquation cracking 159
as tramp element ..... 30, 233–237(F,T)
Pickling 108, 206
before brazing 179
to remove scale from exothermic atmosphere 143–144
after tumbling ..... 207(T)
Piping, as application of superalloy ..... 9(T)
Pitting corrosion, of turbine blade roots and disks 307
Planing 195–196
Plasma arc welding (PAW) 164, 337
for fusion welding superalloys 161
Plasma coating deposition 344
Plasma rotating electrode process (PREP) 123
process steps in powder production ..... 121(T)
Plasma-sprayed (PS) partially stabilized zirconia coatings 311
Plasma spraying (PS) ..... 320(F)
of overlay coatings 317, 318, 319
Plastics, pattern material for investment casting ..80
Plastic-strain ratio (*r*) 108
Plate, mill product availability 77
Plate flashing 179
Platinum
addition effect 347
as creep strengthener for nickel-base superalloys 241
Platinum coatings 304
Platinum electroplating 314
P/M. *See* Powder metallurgy (P/M) processing.
Poisson ratio
of CGDS superalloys 272
of SCDS superalloys 272
Polishing 209–210
Polycrystalline alloys
macrostructure ..... 38(F), 39
macrostructure, carbides present ..... 35, 38(F)
Polycrystalline cast cobalt-base superalloys, aircraft applications 260
Polycrystalline (PC) castings 79
adaptation of directional solidification 83
aircraft applications ..... 84, 86(F), 87(F), 88(F)
hafnium addition for ductility 264
porosity and hot isostatic pressing 264–265
yield strength 239
Polycrystalline (PC)(conventional) castings
aging cycles ..... 141(T)
solution treating cycles ..... 141(T)
Polycrystalline (PC) equiaxed superalloys 23
Polycrystalline investment-cast alloys 89
Polycrystalline investment casting 89–90
Polycrystalline nickel-base superalloys, stress-rupture strength ..... 258, 260(F)
Polycrystalline parts, grain size control methods 82
Polycrystalline superalloys, rupture life vs. specimen thickness ..... 231–232(F)
Polystyrene, pattern material for investment casting 80
Pores, minimization methods for defects ..... 128(T)
Porosity. *See also* Voids.
causes from arc welding 163
definition 163
determining ESR and VAR electrode quality ... 58
with hydrogen gas addition 167
of investment casting 87
Postdeformation processing 115
Postweld heat treatment (PWHT) cracking ..... 151, 152–153(F)
of welds ..... 153–156(F)
Postweld strain-age cracking ..... 152–153(F)
Powder metallurgy (P/M) processing .. 15, 22, 28, 87, 102, 114, 117–134(F,T), 344
advantages compared to wrought alloys 126
as alternative to machining 189
biomedical applications of superalloys 133

© 2002 ASM International. All Rights Reserved.
Superalloys: A Technical Guide (#06128G)
www.asminternational.org

of brazing filler metal wires 178
and carbide precipitation 225
component production techniques..... 126–127
composition of superalloys..... 120(T)
consolidation techniques....119, 124–125, 127(F)
cost savings..... 117
defect tolerance 120
disk components, powder-based..... 125–129(F,T)
engine systems using forged P/M superalloys ..... 120(T)
evaluation and preparation 123–124
extrusion ratios..... 125
as-HIP aerospace applications ..... 120(T)
history 117–119
information sources..... 367–368
inspection of products..... 127(F)
mechanical alloying ..... 129–133(F,T)
nickel-base superalloys, wrought aerospace applications 24
powder consolidation techniques..... 124–125, 127(F)
production techniques..... 120–124(F,T)
sonic inspection of disks ..... 127(F)
and transient liquid phase bonding of superalloys 186
ultrasonic inspection of alloys..... 127(F)
very-high-strength nickel-base superalloys ... 244, 249(T)
weight reductions possible ..... 117, 118(F)
Power-law behavior..... 253, 255(F)
Power spinning..... 111
Power stations, burner hardware 133
PPB. *See* Prior particle boundaries.
Pratt & Whitney PWF-100 aircraft gas turbine engine 119
components and application reason for Haynes 188 use ..... 76(T), 77
number of engine systems produced through 1996 using forged P/M superalloys..... 120(T)
Pratt & Whitney 2000 (PW 2000) engine, number of engine systems produced through 1996 using forged P/M superalloys..... 120(T)
Pratt & Whitney 4000 (PW 4000) engine, number of engine systems produced through 1996 using forged P/M superalloys..... 120(T)
Pratt & Whitney Gatorizing process 128
Prealloyed powders 120–121
for orthopedic implants 133
Precipitate-free zones (PFZ) 212, 221
Precipitate mismatch 347
Precipitates..... 3, 15
and liquation cracking 159
Precipitation age hardening..... 135
Precipitation-hardened nickel-base superalloys
brazing..... 181
welding 151, 166, 167
Precipitation-hardened superalloys
aircraft applications..... 91
brazing..... 181
bright annealing 144
compositions..... 4(T), 5(T)
fusion welding..... 165
gas metal arc welding..... 169
heat treatment 154
inertia bonding 175
overaged condition for welding 155
oxidation resistance..... 142
postweld heat treat cracking 152–153
postweld heat treatments for fusion welding 160–161
preweld heat treatments for fusion welding 160–161
shielded metal arc welding..... 172
welding 150, 151, 166, 167
Precipitation hardening..... 18–19, 101, 212
aspects of..... 213–218(F,T)
factors..... 213
heat treatments for different product forms..... 228, 229(T)
Precipitation-strengthened superalloys 32–34
nickel-base, electron beam welding..... 173
stress-rupture strength..... 3(F)
Precipitation treatments..... 139, 140(T), 141(T)
economic consideration for manufacturing 146
factors influencing selection or number of steps..... 140
procedures..... 139–142
protective atmosphere for 144
for stress relief 139
temperature range..... 140, 146
time duration 146
Precision forging..... 99
as alternative to machining..... 189
mechanically alloyed ODS alloys..... 132
Precision investment castings..... 89
Precracked carbides 224
Preforms..... 126
consolidation techniques..... 124–125
forging of 95–96
powder metallurgy processed 117
spray-formed..... 125
superplastic forging..... 115
PREP. *See* Plasma rotating electrode process.
Press-brake bending ..... 109(F)
Press-brake forming 106, 110
Press cogging 74
Primary dendrites..... 41–43(F)
Primary pipe cavity, of vacuum induction melted electrode..... 56
Prior particle boundaries (PPB) 119
hot isostatic pressing without retaining 125
oxide 128
of P/M processed parts 118–119
Prior particle boundary contamination, minimization methods for defects..... 128(T)
ProCAST software 346
Process annealing..... 165
Processing
information sources..... 367–369
microstructural effects..... 38–39(F)
Process modeling 100, 345–347, 348–349
Process reheating, without full anneal 135

© 2002 ASM International. All Rights Reserved.
Superalloys: A Technical Guide (#06128G)
www.asminternational.org

Properties. *See also* Mechanical properties.
data, sources 354–355
information sources 366
Property reduction, order of 23
Prosthetic devices, as application of superalloy ..... 9(T)
Protective atmospheres 143–144
for aging 145
dry argon 143, 144
dry hydrogen 143, 144
endothermic ..... 143(F), 144
exothermic 143–144
for precipitation treatment 144
vacuum 143, 144
Protective oxide spallation 290
Prototyping, of investment casting 87–89
PS. *See* Plasma spraying.
Pumps, as application of superalloy ..... 9(T)
PW. *See* Pratt & Whitney.
PWHT. *See* Postweld heat treatment.
Pyrometers, optical, for temperature control in vacuum induction melting 55

Q

Quenching ..... 139, 140(T), 142(T)
by air ..... 140(T)
essence of 139
by oil ..... 140(T)

R

Radial forging 74
Radiation, to transfer heat away from investment cast shell 82
Radiography, of investment-cast products 83
Rafted gamma prime structures 348
Rafting 212, 348
Rafts 212
Ramping up, temperature, heat treatment 136
Ram travel, in vacuum arc remelting ..... 62(F)
Rapid omnidirectional compaction (ROC) process. *See* Fluid die process.
Rapid prototyping 88, 117, 347–348
Rapid solidification 118
Rapid solidification rate (RSR) ..... 121(T)
processing 345
Reaction vessels, as application of superalloy 9(T)
Reaming 200
Rebrazing 135
Recoating process 336, 337
Recrystallization 74–75, 86
with annealing 137, 138
of cobalt-base superalloys 104
to control deformation with forging 93
degree of 94
diffusion bonding 174
dynamic 94
meta-dynamic 94
secondary heat treatment in mechanical alloying 130, 131
with solution annealing 146
after solution heat treatment ..... 87, 89(F)
static 94
types 94
Recrystallized grains 280
Recycling, of scrap 46
Reducing agent 167
Reduction in area 211
of nickel-base superalloys ..... 284(T)
of tramp elements' effect ..... 233–234(F)
Reduction phase, of melt 45
Refractory lining, protection of 47
Refractory metals
as additions 22
as addition to nickel-base superalloys 240–241
alloying element effects on hot corrosion 304
Refurbishment of components 161, 336–337
information/product sources 354, 368–369
Reheating 135
Remelt processes 44, 56–58
REP. *See* Rotating electrode process.
Repair of components 161, 336–337
information/product sources 354, 368–369
Repair welding 152
Residual heat, effect on recrystallization 94
Residual stresses
from brazing 181
effect on fatigue properties 162
introduced by machining 204
from welding 163, 165
Resistance brazing 180
Resistance seam welding (RSEW) 162
for fusion welding superalloys 161
with gas tungsten arc welding 187
Resistance spot welding (RSW) 162
for fusion welding superalloys 161
Resistance welding 162, 164
Retort, purge before placement in dry argon atmosphere in furnace 144
Revert material, of vacuum induction melting 51, 52
Rewelding 135
Rhenium 344
addition effect on CGDS and SCDS alloys 270
addition effect on density 347
addition to improve strength 349
as addition to nickel-base superalloys 240–241
as addition to SCDS superalloys 342
as alloying element ..... 29(T), 30
as brittle phase formation cause 30
composition ranges as superalloy alloying additions ..... 29(T)
cost 8
effect on coarsening rate for gamma-prime precipitate 30
effect on density as alloying addition 3
for solid-solution strengthening in nickel-base superalloys ..... 31(F)
for strength 30
Rhodium electroplating 314
Rig testing ..... 290–292(F)

© 2002 ASM International. All Rights Reserved.
Superalloys: A Technical Guide (#06128G)
www.asminternational.org

Ring rolling 94, 95, 96
of P/M billet 126
ROC. *See* Rapid omnidirectional compaction.
Rocket-engine parts. *See also* Aerospace applications.
as application of superalloy ..... 9(T)
Roller hearth furnaces 144
Roll forging 94, 95–96
Rolling 72, 76–77, 92
and mechanical alloying 131
Room-temperature yield strength, of nickel-base superalloys ..... 285(T)
Rotary forging 74, 96
Rotating electrode process (REP) ..... 122–123(F)
process steps in powder production ..... 121(T)
Rotating electrode process atomization 121
RSEW. *See* Resistance seam welding.
RSR. *See* Rapid solidification rate.
RSW. *See* Resistance spot welding.
Rubber-diaphragm forming process 112
Rupture 2
Rupture life 341
and cooling rate compared ..... 233(F)
tramp elements' effect ..... 233–234(F)
Ruthenium, addition effect on density 347

S

Safe ending 166
Salt bath descaling ..... 208–209(T)
Salt bath descaling/pickling, to remove scale from exothermic atmosphere 143–144
Salt baths, and aging 145
Sand, alluvial garnet, and support fixturing 145
SAW. *See* Submerged arc welding.
Saybolt universal seconds (SUS), viscosity unit for cutting fluids 197
Scale 143–144
formation of 206
removal of ..... 204, 206–209(T)
Scale conditioning ..... 207–208(T)
SCDS. *See* Single-crystal directionally solidified (SCDS) cast superalloys.
Scrap
recycling of 46
from vacuum induction melting 50, 51
SD/GS. *See* Specimen diameter to grain diameter ratio.
Sea salt 308
constituents 299
Secondary phases 15
See also Phases.
Secondary pipe cavity, of vacuum induction melted electrode 56
Secondary precipitates, increased volume fraction due to cobalt alloying 30
Second-phase particles 212
Section size, effect on creep-rupture properties ..... 228–232(F)
Seeding ..... 85(F)
Segregation. *See also* Macrosegregation; Microsegregation 15
residual 139
Selected automotive components, as application of superalloy ..... 9(T)
Selective laser sintering 88
Selenium
as metallic contaminant 203
as tramp element ..... 30, 233–237(F,T)
as tramp element in nickel-base superalloys ..... 31(F)
Sensitization 112
Service temperatures 15, 100
Seven Springs Symposium 358
SFE. *See* Stacking fault energy.
Shafts, as application of superalloy ..... 9(T)
Shape, as process-related microstructural variable 39
Shaping 195–196
cutting fluid 196
Shearing 274, 276, 277
Sheet, mill product availability 77
Shelf 64
Shell molds, for casting 147
Shielded metal arc welding (SMAW) 162, 164
aspects of 169, 172
electrodes used ..... 168(T), 172
filler metal for 162
for fusion welding superalloys 161
joint design 166–167
welding conditions ..... 172(F)
Shielding gases
for gas metal arc welding 169
for gas tungsten arc welding 167
for welding atmosphere 150
Shot peening 203, 209–210, 318
and low-cycle fatigue capability 210
Shrinkage, prediction by designer of investment casting 82
Shrinkage cavity, formation during vacuum arc remelting 61
Shrouds, welded ..... 815(F), 186–187
Sigma phase 25, 26, 32, 141, 357
alloying element effects 30, 31
avoidance of 344
crystal structure, descriptive comments, formula, and lattice parameter ..... 28(T)
microstructural degradation 328
in nickel-base superalloys ..... 359(F), 360(F), 362(F)
Silica, amorphous, coating for protection 351
Silicon
as alloying element ..... 29(T), 106–107
composition of freckle vs. matrix ..... 41(F)
content in ESR electrode 58
impurity limits permitted to avoid liquation-type hot cracking ..... 159(T)
incorporation effect on hot corrosion 304
as melting-point depressant for brazing ..... 176, 177(T), 181
as tramp element ..... 30, 234, 236(T)

© 2002 ASM International. All Rights Reserved.
Superalloys: A Technical Guide (#06128G)
www.asminternational.org

Silicon carbide
for grinding superalloys 193
for grit blasting..... 179
Silver
as metallic contaminant..... 203
as tramp element..... 30, 31, 235, 237(T)
Silver plating 209
Single-bevel groove T-joint..... 170(F)
joint designs and dimensions for arc welding nickel- and iron-nickel-base superalloys ..... 171(F)
Single-bevel T-joint..... 166
Single-crystal castings, aging cycles ..... 141(T)
solution treating cycles ..... 141(T)
Single-crystal directionally solidified (SCDS) cast superalloys 79
carbide precipitation..... 224, 225
creep strength..... 272(F)
crystal structure 265–266
density ..... 272, 273(T)
development 342
directionality of mechanical properties..... 258
ductility/elongation ..... 278–279(F)
generations of alloys developed..... 267
grain absence 217
grain boundaries absent..... 80
grain size control in products..... 82
hafnium addition effect 238
high-cycle fatigue..... 274
impact energy vs. temperature..... 279(F)
incipient melting point..... 348(T)
low-cycle fatigue and fracture..... 280–282(F)
macrostructure..... 38(F), 39
maximum useful temperature..... 348(T)
microporosity 280
orientation..... 272–278(F,T)
parts..... 18
Poisson ratio 272
porosity and hot isostatic pressing..... 279–280(F)
processing ..... 23, 83–84, 85(F)
rafted structures 212
resistant to thermal-mechanical fatigue cracking 332
rhenium effect on creep-rupture properties..... 240–241
rupture life vs. specimen thickness ... 231–232(F)
single precipitate size possible 34
stress-rupture strength..... 258, 260(F), 272(F)
temperature capability extended by rhenium alloying..... 30
tensile and creep-rupture properties.. 268–272(F), 273(T)
tension-compression asymmetry..... 274, 277(F)
thermal-mechanical fatigue..... 274, 280–281, 282(F)
yield strength 239
Single crystal (SC) products 79
Single crystal superalloys
first-generation..... 90
second-generation..... 90
Single J-groove T-joint ..... 170(F)
joint designs and dimensions for arc welding nickel- and iron-nickel-base superalloys ..... 171(F)
Single U-groove butt joint, joint designs and dimensions for arc welding nickel- and iron-nickel-base superalloys..... 170(F)
Single V-groove butt joints, joint designs and dimensions, SMAW of solid-solution-strengthened nickel- and iron-nickel-base superalloys ..... 172(F)
Single V-groove butt joint with backing strip or ring, joint designs and dimensions for arc welding nickel- and iron-nickel-base superalloys ..... 170(F)
Single V-groove butt joint with backing weld, joint designs and dimensions for arc welding nickel- and iron-nickel-base superalloys ..... 170(F)
Sintered carbides, for machining superalloys... 192
Size, as process-related microstructural variable ..39
Skittering, electrode positioning on top of molten slag cap..... 68
Slag 57, 143
for electric arc furnace..... 45
entrapment 163
and shielded metal arc welding 172
60/20/20 70
Slivers 86
Slurry electrophoresis 314
Slurry processes..... 314
Slurry "slip packs," 314
Slurry spraying 314
SMAW. *See* Shielded metal arc welding.
Sodium hydride descaling and acid pickling ..... 208–209(T)
Sodium sulfate 299, 301
formation during hot corrosion..... 298
Solidification..... 41–44(F)
modeling of..... 347
Solidification modeling program..... 43(F)
Solidification-nucleated grains, spurious..... 86
Solidification rate..... 43
Solidification white spots ..... 65–66(F), 67(F)
Solid investment (solid mold) process, for investment casting 80
Solid-solution alloys..... 139
composition..... 4(T)
Solid-solution-hardened wrought superalloys
applications 150
welding 150–151
Solid-solution hardening..... 18–19, 26, 212
Solid-solution nickel-base superalloys, electron beam welding..... 173
Solid-solution-strengthened superalloys
creep-rupture strength..... 241, 242(F), 244(F)
fusion welding..... 165
gas metal arc welding..... 169
heat treatment 146
postweld heat treatment for stress relief..... 160
shielded metal arc welding..... 169, 172

© 2002 ASM International. All Rights Reserved.
Superalloys: A Technical Guide (#06128G)
www.asminternational.org

stress-rupture strength ..... 3(F)
welding 150
Solid-solution strengthening 101
Solid-state welding (SSW) 149, 173–175
Solidus temperature 43
Soluble gas process, process steps in powder production ..... 121(T)
Soluble gas process atomization 121
Soluble gas (vacuum) atomization ..... 122, 123(F)
Solution annealing ..... 108, 109, 135, 139, 140(T), 141(T), 146
procedure 139
purpose 139
of solid-solution-strengthened alloys 160
temperature requirements and results 139
of weld 154
before welding to reduce PWHT cracking tendency 154
Solution heat treatment. *See also* Heat treatment 136, 138, 144–145
with brazing 147
of cast superalloys, to develop properties 265
of directionally solidified product 83
economics consideration for manufacturing 146
protective atmospheres for 143–144
time-at-temperature considerations 146
of turbine airfoil, and recrystallization ..... 87, 89(F)
Solvus temperature, for intermetallics, and setting of forging temperatures 97
Sonic-finished shapes 22
Sonic inspectability 73
Soviet superalloys, zirconium addition effects on strength 236
Space shuttle main engine (SSME), hydrogen environment similar to cryogenic conditions 286
Space vehicle components. *See also* Aerospace applications.
as application of superalloy ..... 9(T)
Spallation 290
Spalling 290, 292, 297
of aluminide diffusion coatings 314
coatings for protection against 309
of overlay coatings 319
Specific heat 22
capacity, of wrought superalloys ..... 246(T)
cast superalloys ..... 258, 262(T)
Specimen diameter to grain diameter (SD/GS) ratio 230
Sperm oil 111
SPF. *See* Superplastic forming.
Spinel 288, 296
Spinning 106, 110, 111
backward 111
forward 111
from roll forging ..... 111(F)
Spray forming 15, 125
Springs, as application of superalloy ..... 9(T)
Square-groove butt joint 166
joint designs and dimensions, SMAW of solid-solution-strengthened nickel- and iron-nickel-base superalloys ..... 172(F)
Square-groove butt joint with backing strip or ring, joint designs and dimensions for arc welding nickel- and iron-nickel-base superalloys ..... 170(F)
Square-groove butt joint with backing weld, joint designs and dimensions for arc welding nickel- and iron-nickel-base superalloys ..... 170(F)
SSME. *See* Space shuttle main engine.
SSW. *See* Solid-state welding.
Stable-oxide formers, and bright annealing of superalloys 144
Stack-gas reheaters, as application of superalloy ..... 9(T)
Stacking fault energy (SFE) 212, 241
Stacking faults 37
Stainless steels
cold reduction effect on hardness ..... 106, 107(F)
cold work effect on yield strength ..... 139(F)
face milling ..... 190(F)
for grit blasting 179
hot corrosion ..... 302(F)
machining ..... 190(T), 191
rupture strength 244
stress-rupture strength ..... 19(F)
Stamping of identification marks, plastic deformation from investment casting 87
Static casting ..... 44(F)
definition 56
of product from an AOD vessel 46
Static recrystallization 94
Steam autoclave, in investment casting 83
Steam turbine power plant components, as application of superalloy ..... 9(T)
Steels
face milling ..... 190(F)
friction welding 175
Stellite, development 339
Stereolithography 88
Stinger (ESR) 67
of vacuum arc remelting furnace ..... 59(F)
Stool 56, 68
cooling of 66
of vacuum arc remelting crucible ..... 58–59(F)
Stop-off, during diffusion welding 174
Straightening 336
Strain, in forging regions ..... 97, 98(F)
Strain-age cracking 151, 165
Strain-controlled vs. stress-controlled testing ..... 280, 281(F)
Strain-hardening exponent (*n*-value) 108
Strain range, vs. orientation effect on fatigue life ..... 280, 281(F)
Strength. *See also* Fatigue strength; Stress-rupture strength; Tensile strength.
alloying elements for 30
Stress-controlled vs. strain-controlled testing ..... 280, 281(F)
Stress-corrosion cracking
of cobalt-base superalloys 183
in precipitation-hardenable alloys 182

© 2002 ASM International. All Rights Reserved.
Superalloys: A Technical Guide (#06128G)
www.asminternational.org

Stress decay.....138
Stress-equalizing heat treatment.....165
Stresses
contraction.....87
thermal, and component distortion.....147
Stress raisers.....64–65(F), 166
Stress ratio (*R*).....254
Stress-relief annealing.....108
Stress relieving.....135, 137–138(T), 146, 165
with aging.....145
before brazing.....182
and PWHT cracking.....153
reasons for.....138
of support fixtures that were welded.....145
temperatures.....136, 137
weldments.....138
wrought heat-resisting alloys.....137(T)
Stress-rupture strength.....2, 20(F), 21(F)
See also Creep; Rupture.
cast cobalt-base superalloys.....261, 263(F)
of cobalt-base superalloys.....14(T), 18(T)
of iron-nickel-base superalloys.....14(T)
microfissuring effect on welds.....153
of nickel-base superalloys.....14(T), 18(T)
of P/M disk alloys.....127
and tcp phase formation.....357
temperature effect.....14(T), 18(T), 19(F)
temperature effect on wrought superalloys..14(T)
tramp elements' effect.....223–224(F)
Stress-rupture tests.....211
Stretch forming.....106, 110, 111
Stretching.....108
Stringers.....74
oxide-nitride.....64, 66
Strip, mill product availability.....77
Structural transitions, modeling of.....346
Submerged arc welding (SAW).....162, 164–165
for fusion welding superalloys.....161
Subzero temperatures. *See* Cryogenic applications.
Sulfates.....301
and hot corrosion.....299
Sulfidation. *See also* Hot corrosion.....289, 299, 300(F), 303, 304, 306, 307(F)
Sulfides.....212
Sulfochlorinated oils.....111
Sulfur
alloying element effect on formability.....106, 107
content in ESR electrode.....58
as detrimental tramp element in nickel-base superalloys.....31(F)
impurity limits permitted to avoid liquation-type hot cracking.....159(T)
reduction in slag.....46
as source of liquation cracking.....159
as tramp element.....30, 233–237(F,T)
Sulfur-induced degradation.....302(F)
Sulfurized oils.....111
Sulfurized waxes.....111
Sulfur trioxide.....301
Superalloy(s). *See also* Alloy Index; Cast superalloys; Cobalt-base superalloys; Iron-nickel-base superalloys; Nickel-base superalloys; Oxide-dispersion-strengthened superalloys; Powder metallurgy (P/M) processing; Precipitation-hardened superalloys; Precipitation-strengthened superalloys; Solid-solution-strengthened superalloys; Wrought superalloys.
alloying elements.....29–30(T)
applications.....9(T)
composition ranges of alloying additions....29(T)
drilling, grouping for nominal speeds and feeds.....198(T)
elevated-temperature properties.....2
fabrication methods.....2
fiber-reinforced.....345
history of development.....1
mechanical properties.....2, 8
physical properties.....2, 3, 8, 22
processing.....38–39(F)
product forms.....2, 11
property data sources.....354–355
segregation-prone, vacuum arc remelting process.....57
selection criteria.....20
selection of.....22–24
strengthening.....32–37(F)
stress-rupture strength.....2, 3(F)
temperature range.....2
temperature-strength capability as function of year of availability.....340(F), 350(F)
tramp elements effect on properties.....30, 233–235(F), 236(F,T), 237(F,T)
yield strength advances as function of year of availability.....343(F)
Superalloy castings. *See* Cast superalloys.
Supercooling.....66
Superplastic forging.....114–115(F), 119
Superplastic forming (SPF).....113–115(F)
Superplastic forming/bonding processes.....175–183(F,T)
Superplastic forming/forging.....113–115(F)
Superplastic isothermal forging.....99
Superplasticity.....113–115(F)
Surface alloying, detection by metallographic examination.....204
Surface degradation.....142–143(F)
Surface pits.....163
SUS. *See* Saybolt universal seconds.
Swaging.....94, 96

T

Tail-pipe ball, explosive forming.....113(F)
Tantalum.....344
as addition to nickel-base superalloys....240–241
as alloying element.....29(T), 30
content in base alloy, improving cyclic oxidation with aluminide coating.....314
effect on density as alloying addition.....3

© 2002 ASM International. All Rights Reserved.
Superalloys: A Technical Guide (#06128G)
www.asminternational.org

effects, nickel-base precipitation-strengthened superalloys 31
composition ranges as superalloy alloying additions....29(T)
as precipitate former in nickel-base superalloys ....31(F)
for solid-solution strengthening in nickel-base superalloys ....31(F)
for strength....30
strengthening element innocuous for hot corrosion 303
Tantalum boride, crystal structure and phases observed....28(T)
Tantalum carbides....37
phases observed, crystal structure....27(T)
Tantalum cobalt carbides, phases observed, crystal structure ....27(T)
Tapping 200–201
cutting fluids....200–201
machines for....200
Tarnish....203
removal....205
removal before welding or brazing 203
TBC. *See* Thermal barrier coatings.
tcp phases. *See* Topologically close-packed precipitates.
Teeming....49–50(F)
Teeming vessel. in EAF/AOD process 45
Tellurium, as tramp element ....30, 31(F), 233–237(F,T)
Temperature. *See also* Cryogenic applications; Elevated temperatures.
effect on mechanical properties ....12–13(T)
effect on stress-rupture strengths.... 14(T), 18(T), 19(F)
intermediate, applications....22
mold-metal pour 82
Temperature capability, extended by alloying elements 30
Temperature cycles, economics of manufacturing 146
Temperature gradient 43
Temperature-strength capability .... 340–344(F)
Tensile elongation (%)
of cast cobalt-base superalloys ....17(T)
of cast nickel-base superalloys ....16–17(T)
of nickel-base superalloys....12–13(T)
of wrought cobalt-base superalloys....13(T)
of wrought iron-nickel-base superalloys ....13(T)
Tensile forming, speeds for .... 110(T)
Tensile strength 211, 212, 241, 341
See also Strength; Tensile yield strength.
microfissuring effect on welds....153
of nickel-base superalloys.... 284(T)
and precipitate size 34
Tensile yield strength 19
Tetragonal crystal structure ....28(T)
TF. *See* Thermal fatigue testing.
TFE 731 engine, aerospace application of as-HIP P/M superalloys.... 120(T)
Thallium, as tramp element ... 31(F), 233–237(F,T)
Thermal barrier coatings (TBC)....311, 319–322(F), 344, 345, 347, 351
ceramic ....310, 320(F)
failure in service 321
Thermal buoyancy stirring....63
Thermal conductivity....22
cast superalloys ....258, 262(T)
modeling of....346
of wrought superalloys.... 247(T)
Thermal cycling.... 290, 292, 299
enhanced adherence of oxides....310
Thermal expansion....22
Thermal expansion coefficient, modeling of ...346
Thermal expansion mismatch, as cause of thermal barrier coating failure....321, 322
Thermal fatigue (TF) cracking, overlay coatings for protection against....317
Thermal fatigue (TF) testing, of cast superalloys 280
Thermal-mechanical fatigue (TMF)(thermomechanical) 274, 280
and carbide precipitation 224
definition 280
of PC, CGDS, and SCDS cast nickel-base superalloys compared ....280–281, 282(F)
Thermal-mechanical fatigue (TMF) cracking
of brazed parts 336
in combustion chamber....330, 331(F)
resistance to....344
of turbine airfoil (blade)....331–332(F)
of turbine combustor....333–334(F)
Thermal-mechanical fatigue (TMF) resistance 341
Thermal mechanical fatigue (TMF) strength 22, 23
Thermal-mechanical fatigue (TMF) test (cycle I) ....281, 282(F)
Thermal-mechanical fatigue testing, coatings for cast superalloys....283
Thermal-mechanical stresses....23
Thermal processing industry applications, mechanical alloying ODS alloys 133
Thermal shock test, application to an airfoil ...135
Thermal spraying 151
Thermal stresses, causing component distortion 147
Thermal treatment. *See* Heat treatment.
Thermocouple tubes 133
Thermomechanical processing, of wrought superalloys 252
Thoria
as dispersant for ODS alloys 129
radioactivity....129
Thorium, as alloying element....29(T)
Thorium carbide, phases observed, crystal structure ....27(T)
Threaded fasteners....145
Threading 200
Thread milling 200–201
Three-dimensional (3-D) printing technology...88
Thrust reversers, as application of superalloy .... 9(T)

© 2002 ASM International. All Rights Reserved.
Superalloys: A Technical Guide (#06128G)
www.asminternational.org

Time-temperature-transformation diagram, for precipitates of IN-718 ..... 105(F)
Tin, as tramp element ..... 235, 237(T)
Titanium
as alloying element ..... 20, 29(T), 30, 106
composition of freckle vs. matrix ..... 41(F)
composition ranges as superalloy alloying additions ..... 29(T)
content effect in nickel-chromium alloys 294
content effect on forgeability of nickel-base superalloys ..... 103(T)
content effect on hot cracking susceptibility .. 151
content effect on weldability 149
content in ESR electrode 58
effect on density as alloying addition 3
effects, nickel-base precipitation-strengthened superalloys 31
forming hardening precipitates 30
as gamma prime strengthener 30, 154
hardener content effect on welding problems ..... 154, 155(F)
for hot corrosion resistance 30
intergranular attack 142–143
as precipitate former in nickel-base superalloys ..... 31(F)
precipitate-forming element for P/M disk alloys 128
reduced diffusivity effect on creep strength ... 240
retained in solution by quenching 139
segregating positively 43
as stable-oxide former 144
Titanium boride, crystal structure and phases observed ..... 28(T)
Titanium carbides 37
formation during surface contamination, carbon pickup 143
phases observed ..... 27(T)
Titanium carbide tools 191
Titanium carbonitride, crystal structure and phases observed ..... 28(T)
Titanium nitrides 30
crystal structure and phases observed ..... 28(T)
formation during nitrogen contamination 143
Titanium oxides 180
removal from part to be brazed 182
Titanium-to-aluminum ratio, effect on yield strength 239, 240
T-joints ..... 170(F), 171(F), 172(F)
T-joint with fillet ..... 170(F)
joint designs and dimensions for arc welding nickel-and iron-nickel-base superalloys 171(F)
TLP. *See* Transient liquid phase bonding.
TMF. *See* Thermal-mechanical fatigue.
Tool life 191–192
Tool steels, for machining superalloys ..... 191(T)
Topologically close-packed (tcp) phases .. 26, 141, 153, 212
cobalt addition effect on formation 240
detrimental effects 357
effect on low-cycle fatigue 252–253
formation due to alloying elements 30
formation of 346
formation, resistance estimated ..... 357–363(F)
and microstructural degradation 328
prediction of formation 358
Torch brazing 175, 182
Tramp-elements
control by alloying with carbon, boron, or magnesium 30
detrimental effects 30
in nickel-base superalloys ..... 31(F)
and property degradation .. 233–235(F), 236(F,T), 237(F,T)
Transfer ladle 48
Transient liquid phase bonding (TLP) ..... 173, 183–186(F)
Transition elements 22
Transverse cracking
determining ESR and VAR electrode quality ... 58
of vacuum arc remelted electrodes 62
Trays, as application of superalloy ..... 9(T)
"Tree", investment casting mold 81, 83
Trepanning 195
Triple-melted products 71–72
Tube seamless, mill product availability 77
Tundish ..... 51, 53(F), 54
definition 54
for vacuum induction melting 55, 56
Tungsten
addition effect on ternary alloys for hot corrosion 303
addition preventing carbide formation 37
as addition to nickel-base superalloys 240–241
as alloying element ..... 29(T), 30, 106
in brazing filler metals ..... 176, 177(T)
as brittle phase formation cause 30
composition ranges as superalloy alloying additions ..... 29(T)
compromising hot corrosion resistance of coated alloy 314–315
cost 8
effect on density as alloying addition 3
face milling (93% density) ..... 190(F)
face milling (96% density) ..... 190(F)
as solid-solution element of nickel-base superalloys 31
for solid-solution strengthening in nickel-base superalloys ..... 31(F)
for strength 30
strengthening element encouraging hot corrosion 303, 304
Tungsten carbides 37
crystal structure and phases observed ..... 27(T)
tools 191
Turbine airfoils. *See* Turbine engines, airfoils.
Turbine blades. *See* Turbine engines, blades.
Turbine disks. *See* Turbine engines, disks.
Turbine engines. *See also* Aerospace applications; Aircraft applications.
aircraft gas turbine (AGT) disk ..... 96(F)
airfoil blades, cast test bars not representative of ..... 230, 231(F)

© 2002 ASM International. All Rights Reserved.
Superalloys: A Technical Guide (#06128G)
www.asminternational.org

airfoils
coatings for 142
cobalt addition effects..... 240
cobalt-base superalloys for.....91
columnar grain directionally solidified.....85, 88(F), 89(F)
forging of 95
high-pressure turbine (HPT) 341–342
hot corrosion..... 299, 300(F)
investment cast polycrystalline ..... 84, 86(F)
low-temperature attack..... 306(F)
of ODS alloys 117, 132
of turbine blades, shot peening of 210
precision investment castings.....89
recrystallization after solution heat treatment ..... 87, 89(F)
single crystal directionally solidified .....85, 88(F), 89(F)
wrought superalloys 91
blade alloys, impact energy vs. temperature ..... 279(F)
blade and vane, grain size of P/M products... 127
blades
as application of superalloy..... 9(T), 18
creep causing root failure ..... 332–333(F)
creep damage..... 333(F)
forged 91
forging .....99, 100(F)
hot corrosion..... 307
hot corrosion resistance..... 304, 305(F)
intergranular oxidation attack..... 332(F)
investment-cast .....81, 82(F), 83, 84(F)
macrostructure..... 38(F), 39
of cast superalloys..... 258
oversize, precision-forged, and final machined .....99, 100(F)
oxidation attack ..... 332, 333(F)
root attachments, shear criteria 276, 277
shot peening of..... 210
superalloy temperature-strength capability vs. year of availability ..... 340(F)
thermal-mechanical fatigue cracking ..... 331–332(F)
Waspaloy used..... 228
burner cans, superalloy temperature-strength capability vs. year of availability ..... 340(F)
burner rig testing..... 290–292(T)
casings, forging of.....95, 96
cobalt-base sheet superalloys 76
combustion chamber, failure of ..... 330, 331(F)
combustor nozzles, P/M processed 118
combustors, superalloy temperature-strength capability vs. year of availability ..... 340(F)
combustor, thermal-mechanical fatigue cracking ..... 333–334(F)
complex blades, investment-cast polycrystalline..... 84, 87(F)
component alloy development.....348–349
component temperature-strength capability of superalloys as function of year of availability ..... 340(F)
compressor blades, shot peening of 210
compressor disks, powder metallurgy processed, weight reductions ..... 117, 118(F)
compressors, superalloy temperature-strength capability vs. year of availability ..... 340(F)
conditions affecting surface behavior..... 310
corrosion-resistant coating requirements 310
creep-rupture strength considerations.....242–243
directional investment casting 90
disks..... 22, 23–24(F)
advances in superalloy yield strength as function of year of availability ..... 343(F)
breakage, safety issue 128
creep 24
flat ..... 114(F)
forged ..... 91, 95, 96, 97(F)
hot isostatic pressed 125
inertia welding of.....173, 175
low-cycle fatigue cracks ..... 334(F)
P/M processed..... 119, 125, 127–128
superalloy temperature-strength capability vs. year of availability ..... 340(F)
Waspaloy used..... 228
wrought superalloys 91
elevated-temperature service 243
exhaust mixer nozzle component ..... 114(F)
gas turbine disks..... 23–24(F)
guide vanes and segments, investment-cast polycrystalline..... 84, 86(F)
high-pressure turbine airfoils 341, 342
hollow blades, investment-cast polycrystalline..... 84, 87(F)
hot corrosion..... 298
integral disk-shaft forged ..... 96, 97(F)
integral nozzles, investment-cast polycrystalline..... 84, 88(F)
integral rotors, investment-cast polycrystalline..... 84, 88(F)
investment casting practice.....80
investment cast products.....79, 80
iron-nickel-base (or high-iron-nickel-base) superalloys, cost effective 243
of mechanically alloyed ODS alloys 132–133
nickel-base sheet superalloys 76
noise suppressor assembly ..... 114(F)
oxidation degradation, gaseous ..... 294–295(F), 296(F)
refurbishment of components.....336–337
repair of components.....336–337
section size problems 230
shaft/disk combinations, forging of.....96
shafts, forging of..... 96, 99(F)
shrouds, welded .....185(F), 186–187
single-crystal directionally solidified components 267
stationary, inlet air filtration and periodic washing..... 309
turbine-blade dovetails, shot peening of 210
vanes
broaching of ..... 197(T)
cast cobalt-base superalloys..... 261

© 2002 ASM International. All Rights Reserved.
Superalloys: A Technical Guide (#06128G)
www.asminternational.org

Turbine engines, vanes (continued)
creep causing bowing ..... 331(F)
refurbishment 336
superalloy temperature-strength capability vs. year of availability ..... 340(F)
thermal barrier coated ..... 321, 322(F)
transient-liquid-phase-bonded ..... 185(F), 186
wrought airfoils 76
wrought superalloys, temperature range 242
Turbine vanes. *See* Turbine engines, vanes.
Turbochargers, as application of superalloy ... 9(T)
Turbofan engine 133
aerospace application of as-HIP P/M superalloys ..... 120(T)
Turning 194–195
cutting fluids for 195
tool-holding devices ..... 195(F)
tool materials for superalloys 194
Tuyeres, of argon oxygen decarburization vessel 48
Twin bands 37
Twin ends 37
Twist drills ..... 198–200(T)

U

U-groove design 166
U-groove joints ..... 169, 170(F)
Ultimate strength 211
of P/M alloys 127
Ultimate tensile strength 19, 341
of cast cobalt-base superalloys ..... 17(T)
of cast nickel-base superalloys ..... 16–17(T)
of forgings ..... 232–233(T)
of nickel-base superalloys ..... 12–13(T)
of wrought cobalt-base superalloys ..... 13(T)
of wrought iron-nickel-base superalloys ..... 13(T)
Ultrasonic cleaning 179
Ultrasonic inspection
cogging of IN-718 75–76
of forged parts 98
of investment-cast products 82, 83
of P/M alloys ..... 127(F)
Unbending 108
Undercut in fusion welds 151
Underfill in fusion welds 151
Underwater explosive-forming techniques 112
Uniform oxidation 287
Upset, in solid-state welds 151
Upsetting ..... 94, 95, 97, 98(F), 102
USAF F-111F TF 30-P100 military turbine engine
aerospace application of as-HIP P/M superalloys ..... 120(T)
diffusion welding of Finwall 174
turbine blade damper, cobalt-base P/M superalloy 134

V

Vacuum arc remelting (VAR) ..... 41(F), 42(F), 44, 101, 121, 343–344
control anomalies 61–63
control of process ..... 59–61(F), 62(F)
defects, melt-related ..... 64–66(F), 67(F)
electrode quality factors 58
electrodes 59
and electroslag remelting compared 57–58
furnace ..... 58–59(F)
inherent ring solidification structure of ingots 65–66
melting process applied to electroslag remelted ingot 72
pool details ..... 63–64(F)
process description 56–57
process operation ..... 58–64(F)
Vacuum arc remelting furnace ..... 58–59(F)
Vacuum atmosphere. *See also* Atmospheres 143, 144
for reducing postweld heat treatment cracking 155
for welding atmosphere 150
Vacuum atomization 121
Vacuum brazing 147, 180–181
Vacuum furnaces 144–145
Vacuum induction furnace, for vacuum induction melting ..... 52–53(F)
Vacuum induction melting (VIM) ..... 50–56(F), 121(T)
alloying element control 50
charge 51–52
charge calculation 52
charge materials cost 50
chips from machining processes 51–52
correction factor 51, 52
crucible construction ..... 52–53(F)
crucible size 52
description of process 50–51
and EAF/AOD process compared 50
furnace operation 54–56
heat sizes for investment casting 80
as hybrid secondary melt process with electroslag remelting 71–72
investment cast superalloys 81
mold shapes 51
nitrogen reduction 51
pour time 51
reactive materials 51
remelting stock production 80
revert material 51, 52
slag components 55
vacuum induction furnace ..... 52–53(F)
virgin material 51
wash heats 52
Vacuum induction melting furnaces
launders 53–54
operation 54–56
Vacuum induction melting with electroslag melting, as melt method for selected superalloys ..... 45(T)
Vacuum induction melting with electroslag remelting and vacuum arc remelting, as melt method for selected superalloys ..... 45(T)

© 2002 ASM International. All Rights Reserved.
Superalloys: A Technical Guide (#06128G)
www.asminternational.org

Vacuum induction melting with vacuum arc remelting, as melt method for selected superalloys ..... 45(T)
Vacuum induction remelting, to remove tramp elements 233
Vacuum melting ..... 109, 117, 118(F)
development of technology 339
effect on forgeability 103
Vacuum (soluble gas) atomization ..... 122, 123(F)
process description ..... 122, 123(F)
Valve stems, as application of superalloy ..... 9(T)
Vanadates 289, 298
Vanadium
as addition to nickel-base superalloys 240–241
compromising hot corrosion resistance of coated alloy 314–315
strengthening element encouraging hot corrosion 303, 304
Vanadium boride, crystal structure and phases observed ..... 28(T)
Vanadium oxide (V_2O_5) 289, 301
Vanes. *See* Turbine engines, vanes; Turbine vanes.
Vapor degreasing 205
procedure for removing scale superalloys 207(T)
process 178–179
Vapor honing 206, 209
VAR. *See* Vacuum arc remelting.
Vessels, reaction. *See* Reaction vessels.
V_f. *See* Volume fraction.
V-groove design 166
Vibratory finishing, before aluminide coating .. 315
Vibratory tumbling 206–207
VIM. *See* Vacuum induction melting.
Visual inspection
of investment-cast products 83
locating cold shuts and surface pits 163
Vitrification, of silicate binder, in investment casting 82
Voids. *See also* Porosity.
minimization methods for defects ..... 128(T)
Volume fraction (V_f) of gamma prime (γ') alloys 211, 347
friction welding 173
gamma prime envelopes 221
strength decreasing with particle growth 214–215
strength increasing as Al+Ti content increases ..... 215, 216(F,T)
tensile yield strengths ..... 213, 215(F)

W

Wash heats 52
Water elutriation 124
Waxes, pattern material for investment casting 80, 82–83
Wear resistance, of cobalt-base P/M superalloys 133–134
Weaving, of electrode 172
Weight, of forgings ..... 96, 97(F)
Weight change, in oxidation/corrosion testing ..... 291–292(F), 295
Weirs 50, 54
definition 54
Weldability 2, 22
Weld cracking 151
Weld fusion zone fissuring 159
Welding 135
See also Fusion welding; Solid-state welding; Weldments.
aerospace applications ..... 186(F), 187
carbide-hardened cobalt-base superalloys 151
cobalt-base superalloys 151
cold deformation during mechanical alloying 130
design of joints 151–152
filler metals 149
fixtures 164
grain size effect 151
integrity of joints 151, 152
precipitation-hardenable wrought nickel- and iron-nickel-base superalloys 151
as repair technique 336–337
after solution annealing at 2150°F and quenching 112
soundness of weldments ..... 152–160(F,T)
specifications 161
surface preparation 209
Weldments. *See also* Welding.
elevated temperature service and cracking 156
elongation ..... 284(T)
fracture toughness ..... 285(T)
postweld heat treatment cracking ..... 153–156(F)
reduction in area ..... 284(T)
room-temperature yield strength ..... 285(T)
soundness and contaminants effect ... 159–160(T)
stress relieving 138
tensile strength ..... 284(T)
verification of crack-free assemblies 153
yield strength ..... 284(T)
Weld overlay cladding 151
Weld repair, of cast cobalt-base superalloy airfoils 261
Weld spatter, with gas metal arc welding 169
White lead, in lubricants, not recommended 111
Widmanstätten platelets ..... 362(F)
Widmanstätten precipitation 221
Widmanstätten structure ..... 27(T), 36–37(F), 105–106
Wire, mill product availability 77
Wire brushing 179, 207
Work hardening 18–19, 101
and forming 106
Wrought carbide-hardened cobalt-base superalloys, welding 151
Wrought heat-resisting alloys
aging cycles ..... 140(T)
solution treating cycles ..... 140(T)
Wroughting 11, 15
Wrought nickel-base superalloys, microstructure ..... 33(F)
Wrought precipitation-hardened superalloys, heat treatment 146

© 2002 ASM International. All Rights Reserved.
Superalloys: A Technical Guide (#06128G)
www.asminternational.org

Wrought solid-solution-hardened superalloys, welding 150–151
Wrought superalloys. *See also* Alloy Index; Superalloys.
carbides for grain size control 35
and cast superalloys compared, strengthening mechanisms ..... 226–241(F,T)
compositions ..... 4–5(T)
creep-rupture strength ..... 241, 242(F), 243(F)
density ..... 246(T)
directionality of properties 250
ductility 15
dynamic modulus of elasticity ..... 241, 245(T)
electrical resistivity ..... 247(T)
fatigue and fracture properties ..... 250–258(F,T)
fatigue crack growth rate ..... 253–254(F)
gamma prime solvus temperature ..... 324(T)
grain sizes 29
heating/cooling rates 146–147
incipient melting temperatures ..... 324(T)
mean coefficient of thermal expansion ..... 247(T)
melting range ..... 246(T)
processing operations 92
properties, physical, tensile, and creep-rupture ..... 241–250(F,T), 251(F)
service temperature 15
specific heat capacity ..... 246(T)
stress-rupture characteristics, Larson-Miller parametric plot ..... 241, 248(F)
thermal conductivity ..... 247(T)

X

X-ray diffraction
determining stress decay 138
of investment-cast products 82, 83
microfissuring detection 153
X-ray radiography, of weldments, internal defects 187

Y

Yield strength 18, 211
of combustor alloys ..... 75(F), 76–77
factors influencing 239
of forgings ..... 232, 233(T)
of gamma prime-hardened superalloys 239
of nickel-base superalloys ..... 284(T)
of P/M alloys 127
superalloy advances as function of year of availability ..... 343(F)
Yield strength (0.2% offset)
of cast cobalt-base superalloys ..... 17(T)
of cast nickel-base superalloys ..... 16–17(T)
of nickel-base superalloys ..... 12–13(T)
of wrought cobalt-base superalloys ..... 13(T)
of wrought iron-nickel-base superalloys ..... 13(T)
Yo-yo aging process 141–142, 217
Yttria (Y_2O_3), strengthening mechanically alloyed ODS alloys 132
Yttria-stabilized zirconia ..... 320(F), 321
Yttrium
as alloying element ..... 29(T), 31(F)
as coating addition to improve oxide scale adherence 311
enhancing coating life 30
in overlay coatings, for adherence improvement 317
Yttrium oxide 320

Z

Zero root opening 166
Zinc, as tramp element ..... 235, 237(T)
Zinc compounds, in lubricants, not recommended 111
Zirconium
addition to improve creep-rupture resistance 37
as alloying element ..... 29(T), 30, 31(F)
content in ESR electrode 58
intergranular attack along grain boundaries 143
in iron-nickel superalloys 26
mechanical properties improved by addition of ..... 235–238(T)
in nickel-base superalloys 26
to retard formation of denuded (depleted) gamma prime zones 221
in SCDS alloys 224
as tramp element ..... 235, 237(T)
Zirconium carbide, crystal structure and phases observed ..... 27(T)
Zirconium carbonitride, crystal structure and phases observed ..... 28(T)
Zirconium nitride, crystal structure and phases observed ..... 28(T)
Zirconium oxide ..... 320(F)

ASM International is the society for materials engineers and scientists, a worldwide network dedicated to advancing industry, technology, and applications of metals and materials.

ASM International, Materials Park, Ohio, USA
www.asminternational.org

This publication is copyright © ASM International®. All rights reserved.

Publication title	Product code
Superalloys: A Technical Guide	06128G

To order products from ASM International:

Online Visit www.asminternational.org/bookstore

Telephone 1-800-336-5152 (US) or 1-440-338-5151 (Outside US)

Fax 1-440-338-4634

Mail Customer Service, ASM International
9639 Kinsman Rd, Materials Park, Ohio 44073-0002, USA

Email CustomerService@asminternational.org

In Europe American Technical Publishers Ltd.
27-29 Knowl Piece, Wilbury Way, Hitchin Hertfordshire SG4 0SX, United Kingdom
Telephone: 01462 437933 (account holders), 01462 431525 (credit card)
www.ameritech.co.uk

In Japan Neutrino Inc.
Takahashi Bldg., 44-3 Fuda 1-chome, Chofu-Shi, Tokyo 182 Japan
Telephone: 81 (0) 424 84 5550

Terms of Use. This publication is being made available in PDF format as a benefit to members and customers of ASM International. You may download and print a copy of this publication for your personal use only. Other use and distribution is prohibited without the express written permission of ASM International.

No warranties, express or implied, including, without limitation, warranties of merchantability or fitness for a particular purpose, are given in connection with this publication. Although this information is believed to be accurate by ASM, ASM cannot guarantee that favorable results will be obtained from the use of this publication alone. This publication is intended for use by persons having technical skill, at their sole discretion and risk. Since the conditions of product or material use are outside of ASM's control, ASM assumes no liability or obligation in connection with any use of this information. As with any material, evaluation of the material under end-use conditions prior to specification is essential. Therefore, specific testing under actual conditions is recommended.

Nothing contained in this publication shall be construed as a grant of any right of manufacture, sale, use, or reproduction, in connection with any method, process, apparatus, product, composition, or system, whether or not covered by letters patent, copyright, or trademark, and nothing contained in this publication shall be construed as a defense against any alleged infringement of letters patent, copyright, or trademark, or as a defense against liability for such infringement.